U.PORTO

DOUTORAMENTO

CIÊNCIAS BIOMEDICAS

Bioactive Secondary Metabolites from Marine-Derived Fungi

War War May Zin

D

2017

U.PORTO

War War May Zin. Bioactive Secondary Metabolites from Marine-Derived Fungi

Bioactive Secondary Metabolites from Marine-Derived Fungi
War War May Zin

D.ICBAS **2017**

INSTITUTO DE CIÊNCIAS BIOMÉDICAS ABEL SALAZAR

WAR WAR MAY ZIN

BIOACTIVE SECONDARY METABOLITES FROM MARINE-DERIVED FUNGI

Thesis submitted to Instituto de Ciências Biomédicas Abel Salazar, Universidade do Porto to obtain the degree of Doctor in Biomedical Sciences.

Adviser - Dr. Anake Kijjoa
Category - Full Professor
Affiliation - Instituto de Ciências Biomédicas Abel Salazar da Universidade do Porto

Co-adviser - Dr. Madalena Maria de Magalhães Pinto
Category - Full Professor
Affiliation - Faculdade de Farmácia da Universidade do Porto

This experimental work of this thesis has been carried out in the Departamento de Química, Instituto de Ciências Biomédicas Abel Salazar (ICBAS) da Universidade do Porto. The candidate performed this work with the PhD's scholarship provided by the "Lotus Unlimited Project under the ERASMUS MUNDUS ACTION 2-EU-Asia Mobility Project". This work was partially supported through national funds provided by FCT/MCTS – Foundation for Science and Technology from the Minister of Science, Technology and Higher Education (PIDDAC) and European Regional Development Fund (ERDF) through the COMPETE – Programa Operacional Factores de Competitividade (POFC) programme, under the project PTDC/MAR-BIO/4694/2014 (reference POCI-01-0145-FEDER-016790; Project 3599 – Promover a Produção Cientifica e Desenvolvimento Tecnológico e a Constituição de Redes Temáticas (3599-PPCDT) in the framework of the programme PT2020 as well as by the project INNOVMAR - Innovation and Sustainability in the Management and Exploitation of Marine Resources (reference NORTE-01-0145-FEDER-000035, within Research Line NOVELMAR), supported by North Portugal Regional Operational Programme (NORTE 2020), under the PORTUGAL 2020 Partnership Agreement, through the European Regional Development Fund (ERDF).

STATUS THESIS

The results of the work of this thesis have been published, as original articles, in the following journals.

LIST OF PUBLICATIONS

1. Zin, W. W. M., Buttachon, S., Buaruang, J., Gales, L., Pereira, J. A., Pinto, M. M., Silva, A., and Kijjoa, A. **(2015)**. A new meroditerpene and a new tryptoquivaline analog from the algicolous fungus *Neosartorya takakii* KUFC 7898. *Marine Drugs* **13**, 3776-3790. Doi:10.390/md13063776.
2. Zin, W. W. M., Prompanya, C., Buttachon, S., and Kijjoa, A. **(2016)**. Bioactive secondary metabolites from a Thai collection of soil and marine-derived fungi of the genera *Neosartorya* and *Aspergillus*. *Current Drug Delivery* **13**, 378-388.
3. Zin, W. W. M., Buttachon, S., Dethoup, T., Fernandes, C., Cravo, S., Pinto, M. M., Gales, L., Pereira, J. A., Silva, A., and Sekeroglu, N. **(2016)**. New cyclotetrapeptides and a new diketopiperzine derivative from the marine sponge-associated fungus *Neosartorya glabra* KUFA 0702. *Marine Drugs* **14**, 136. Doi:10.390/md14070136.

4. Zin, W. W. M., Buttachon, S., Dethoup, T., Pereira, J. A., Gales, L., Inácio, Â., Costa, P. M., Lee, M., Sekeroglu, N., and Silva, A. M. **(2017)**. Antibacterial and antibiofilm activities of the metabolites isolated from the culture of the mangrove-derived endophytic fungus *Eurotium chevalieri* KUFA 0006. *Phytochemistry* **141**, 86-97. Doi.org/10.1016/j.phytochem.2017.05.015.

COMMUNICATIONS

Oral presentation

1. War War May Zin, Suradet Buttachon, Tida Dethoup, José A. Pereira and Anake Kijjoa **(2017)**. Bioactive secondary metabolites from the culture of the mangrove-derived endophytic fungus *Eurotium chevalieri* KUFA 0006. Proc. of 10th European Conference on Marine Natural Products 3-7 September, 2017, Kolymbari, Crete, Greece.
2. War War May Zin, Chadaporn Prompanya, Carla Fernandes*, Sara Cravo, Madalena Pinto and Anake Kijjoa **(2017)**. Chiral liquid chromatography in analysis of the stereochemistry of marine natural compounds: Contribution for Medicinal Chemistry. Proc. of 3rd International Electronic Conference on Medicinal Chemistry, 1-30 November, 2017. Sciforum Electronic Conference Series, **3**. Doi:10.3390/ecmc-3-04676.

Posters presentation

1. War War May Zin, Suradet Buttachon, Jamrearn Buaruang and Anake Kijjoa **(2015)**. Indole alkaloids and dihydroisocoumarin from the alga-associated fungus *Neosartorya takakii* KUFC 7898. Proc. of 9th European Conference on Marine Natural Products, 30th August 2015-2nd September 2015, Technology and Innovation Centre, University of Strathclyde, Glasgow, Scotland.

INDEX

FIGURES INDEX

FIGURES INDEX

FIGURES INDEX

TABLES INDEX

ACKNOWLEDGEMENTS

I am indebted to many people who have helped make this work possible. I wish to deeply express my sincere gratitude to my advisor Professor Dr. Anake Kijjoa, Professor and Head of Department of Chemistry, Instituto de Ciências Biomédicas Abel Salazar (ICBAS), Universidade do Porto, for his warm support, kindness, excellent guidance and encouragement with unlimited patience throughout this study. His guidance helped me in all the time of research and writing of this thesis. I could not have imagined having a better advisor and mentor for my Ph.D study.

I am deeply grateful to Professor Dr. Madalena Pinto, my co-supervisor, from the Departamento de Ciências Químicas, Faculdade de Farmácia, Universidade do Porto, for her suggestion, sharing the experience of Natural Products Chemistry research, her kindness and willingness to educate me during my Ph.D course.

My sincere thanks to Professor Dr. Eduardo Rocha, Director of the doctoral program in Biomedical Sciences of Instituto de Ciências Biomédicas Abel Salazar (ICBAS), Universidade do Porto, for accepting me to study in this program.

My special thanks also go to Professor Dr. Hla Ngwe, Prof. Dr. Hnin Hnin Aye, Prof. Dr. Ni NI Than and Associate Professor Dr. Nwet Nwet Win, Department of Chemistry, University of Yangon, Myanmar for their valuable advice, encouragement and continuing support during the work at University of Yangon.

ACKNOWLEDGEMENTS

I am deeply indebted to Professor Dr. Artur M. S. Silva, Department of Chemistry, University of Aveiro, for providing ^{1}H NMR, ^{13}C NMR, COSY, HMBC and NOESY spectra and to Dr. Mick Lee, Department of Chemistry, University of Leicester, UK for measurement of High Resolution Mass Spectra. Many thanks also go to Professor Dr. Luis Gales, Instituto de Ciências Biomédicas Abel Salazar (ICBAS), Universidade do Porto, for his assistance in the X-ray crystallography analysis and to Professor Dr. José Augusto Pereira (ICBAS), Universidade do Porto, for the kind help of ECD spectra calculations and measurement.

I would like to express my sincere thanks to Professor Dr. Carla Fernandes and Dr. Sara Cravo, Departamento de Ciências Químicas, Faculdade de Farmácia, Universidade do Porto, for their valuable discussion and advices on chiral HPLC analysis. I am also thankful to Professor Dr. Paulo Costa (ICBAS), Universidade do Porto and Dr. Ângela Inácio, from Interdisciplinary Centre of Marine and Environmental Research (CIIMAR), for performing antibacterial and antibiofilm assays of the isolated compounds.

I am very grateful to Professor Dr. Tida Dethoup, from Department of Plant Pathology, Kasetsart University, Bangkok, Thailand and Dr. Jamrearn Buaruang, Division of Environmental Science, Faculty of Science, Ramkhamhaeng University, Bangkok, Thailand for providing the fungi materials for this study.

ACKNOWLEDGEMENTS

My sincere thanks to Mrs. Julia Bessa, Ms. Sonia Pereira Santos and Mrs. Isabel Silva for their technical assistance in the isolation of the compounds, encouragement, friendship and informal participation during my works at ICBAS. I also wish to extend my appreciation to my colleagues at University of Yangon, for their constructive contribution and assistance during the course of the work at the University of Porto.

My sincere thanks are also for Prof. Dr. Maria de Fátima Marinho (Vice-Rector of International Relations), Mrs. Barbara Costa (Director of International Relations Office), Ms. Ana Castro Paiva and Ms. Ana Sofia Ferreira of the International Relations Office of Universidade do Porto, for their kind help during my stay in Porto.

My special thanks also go to Dr. Suradet Buttachon, Assistant researcher of the Interdisciplinary Centre of Marine and Environmental Research (CIIMAR), for proofreading, enormous encouragement, and help as well as for being a good friend during my stay in Porto. I also appreciate all of my labmates for their encouragement, understanding and for taking over parts of my work during the time of completion of this thesis and for all the fun we have had in the last four years.

I wish to sincerely thank the Lotus Unlimited Project under the Erasmus Mundus Action 2-EU-Asia Mobility project for the PhD's scholarship during three years to pursue my doctoral study at the University of Porto.

ACKNOWLEDGEMENTS

Last but not the least, I would like to thanks my family: my parents and to my brothers and sisters for providing me with unfailing support and continuous encouragement throughout my years of study and through the process of researching and writing this thesis. This accomplishment would not have been possible without them.

Thanks for all your encouragement!

ABSTRACT

The aim of this thesis was the isolation and structure elucidation of secondary metabolites from marine-derived fungi, collected from the tropical region, and the evaluation of their biological activities. Consequently, we have investigated the secondary metabolites produced by the cultures of marine-derived fungi *Talaromyces helicus* KUFA 0063, *Neosartorya takakii* KUFC 7898, *Neosartorya glabra* KUFA 0702 and *Eurotium chevalieri* KUFA 0006.

The fungal strain *Talaromyces helicus* KUFA 0063, isolated from a cauliflower coral, *Pocillopora verrucosa*, which was collected from Angthong National Marine Park, Amphur Samui, Suratthani Province, Thailand, produced four previously described secondary metabolites: palmitin, acetyl ergosterol 5, 8-endoperoxide, glaucanic acid and glauconic acid.

The ethyl acetate extract of the culture of fungus *Neosartorya takakii* KUFC 7898, which was isolated from the marine macro-alga *Amphiroa sp*., collected from the Samaesarn Island, in the Gulf of Thailand, Chonburi Province, Thailand, furnished a new meroditerpene sartorenol, a new prenylated indole derivative takakiamide and a new tryptoquivaline analog, tryptoquivaline U, in addition to the previously described chevalone B, 6-hydroxymellein, aszonalenin, acetylaszonalenin, aszonapyrone A, tryptoquivalines F, H, L and 3′- (4-oxoquinazolin-3-yl) spiro [1*H*-indole-3,5′-oxolane]-2, 2′-dione. The three new

compounds were evaluated for their antibacterial activity against Gram-positive (*Staphylococcus aureus* ATCC 25923 and *Bacillus subtilis* ATCC 6633), Gram-negative (*Escherichia coli* ATCC 25922 and *Pseudomonas aeruginosa* ATCC 27853) bacteria and multidrug-resistant isolates from the environment as well as for their quorum sensing inhibitory activity, and none of them exhibited antibacterial activity against the tested organisms (MIC > 256 µg/mL) and any quorum sensing inhibition in the screening protocol based on the pigment production by *Chromobacterium violaceum* (ATCC 31532).

Chromatographic fractionation of the crude ethyl acetate extract of the fungus *Neosartorya glabra* KUFA 0702, isolated from the marine sponge *Mycale sp*., which was collected from the coral reef at Samaesarn Island, in the Gulf of Thailand, resulted in isolation of two new cycloteterapeptides: sartoryglabramide A and sartoryglabramide B, and a new analog of fellutanine A together with eight known compounds including ergosta 4,6,8 (14), 22-tetraen-3-one, ergosterol 5,8-endoperoxide, aszonalenin, takakiamide, (11a*S*)-2, 3-dihydro-1*H*-pyrrolo [2,1-c] [1,4] benzodiazepine-5, 11 (10*H*, 11a*H*)-dione, helvolic acid, (3*R*)-3-(1*H*-indole-3-ylmethyl)-3, 4-dihydro-1*H*-1, 4-benzodiazepine-2, 5-dione and fellutanine A. All of the compounds were tested for their antibacterial activity against Gram-positive (*S. aureus* ATCC 25923) and Gram-negative (*E. coli* ATCC 25922) bacteria as well as for their antifungal activity against filamentous (*Aspergillus fumigatus* ATCC 46645), dermatophyte (*Trichophyton ruburm* ATCC FF5) and yeast

(*Candida albicans* ATCC 10231). None of the test compounds exhibited either antibacterial activity (MIC> 256 µg/mL) or antifungal activity against (MIC> 512 µg/mL).

Additionally, we have also investigated a Thai collection of the endophytic fungus *Eurotium chevalieri* KUFA 0006, which was isolated from the inner twig of the mangrove tree *Rhizophora mucronata* Poir. From the culture of this fungus, five previously undescribed secondary metabolites, including the anthraquinone derivative acetylquestinol, two prenylated indole 3-carbaldehyde derivatives, an anthranilic acid derivative, and an isochrome derivative, were isolated together with eleven known compounds: palmitic acid, ergosterol 5, 8-endoperoxide, emodin, physicon, questin, questinol, (11*S*, 14*R*)-cyclo (tryptophylvalyl), preechinulin, neoechinulin E, echinulin and eurocristatine. All the isolated compounds except palmitic acid and ergosterol 5, 8-endoperoxide, were evaluated for their antibacterial activity against two Gram-positive (*S. aureus* ATCC 25923 and *Enterococcus faecalis* ATCC 29212) and two Gram-negative (*E. coli* ATCC 25922 and *P. aeruginosa* ATCC 27853) bacteria, as well as multidrug-resistant isolates from the environment. Only emodin showed antibacterial activity against Gram-positive bacteria *S. aureus* ATCC 25923 and *E. faecalis* ATCC 29212 with MIC values of 32 and 64 µg/mL respectively. None of the test compounds were active against either Gram-negative bacteria or methicillin-resistant *S. aureus* (MRSA) and vancomycin-resistant enterococci (VRE). All the tested compounds showed weak or moderate

synergistic association with vancomycin against VRE enterococci. Some of the tested compounds exhibited antibiofilm activity, depending on the bacterial strains. Emodin not only exhibited antibacterial activity against Gram-positive bacteria but also showed strong synergistic association with oxacillin against MRSA *Staphylococcus aureus*.

Keywords: *Neosartorya takakii*; *Neosartorya glabra*; *Eurotium chevalieri*; *Talaromyces helices* KUFA 0063; meroditerpene; sartorenol; tryptoquivaline U; cyclotetrapeptides; sartoryglabramides A and B; fellutanine A epoxide; prenylated indoles; isochromone; anthraquinones; diketopiperazines; mangrove-derived fungus; antibacterial activity; antibiofilm

RESUMO

O objetivo desta tese foi o isolamento e a elucidação da estrutural de metabolitos secundários de fungos marinhos e avaliação de suas atividades biológicas, nomeadamente produzidos por culturas de *Talaromyces helicus* KUFA 0063, *Neosartorya takakii* KUFC 7898, *Neosartorya glabra* KUFA 0702 e *Eurotium chevalieri* KUFA 0006.

Talaromyces helicus KUFA 0063, isolado do coral *Pocillopora verrucoso*, que foi coletada no Parque Marinho Nacional de Angthong, Amphur Samui, Província de Suratthani, Tailândia, produziu quatro metabolitos secundários descritos anteriormente: palmitina, acetilergosterol 5, 8-endoperóxido, ácido glaucânico e ácido glaucónico.

O extrato de acetato de etilo da cultura do fungo *Neosartorya takakii* KUFC 7898, isolado da macroalga marinha *Amphiroa sp*., coletado na ilha de Samaesarn, no Golfo da Tailândia, Província de Chonburi, Tailândia, forneceu um novo meroditerpeno sartorenol, um novo derivativo de indol prenilado takakiamida e um novo análogo de triptoquivalina (triptoquivalina U), além de chevalona B, 6-hidroximeleína, aszonalenina, acetilaszonalenina, aszonapirona A, triptoquivalinas F, H, L e 3'- (4- oxoquinazolin-3-il) espiro [1H-indol-3,5'-oxolano] -2, 2'-diona. Os três novos compostos foram avaliados quanto à sua atividade antibacteriana contra bactérias de Gram-positivo (*Staphylococcus aureus* ATCC 25923 e *Bacillus subtilis*

ATCC 6633), e de Gram-negativo (*Escherichia coli* ATCC 25922 e *Pseudomonas aeruginosa* ATCC 27853) e também em isolados do ambiente resistentes a múltiplos fármacos, bem como para atividade inibidora de *quorum sensing*. Nenhum deles exibiu atividade antibacteriana contra os organismos testados (MIC> 256 µg / mL) e nem foi observada qualquer inibição de deteção de *quorum sensing* no protocolo de rastreio com base na produção de pigmento por *Chromobacterium violaceum* (ATCC 31532).

O fracionamento cromatográfico do extrato bruto de acetato de etilo do *Neosartorya glabra* KUFA 0702, isolado da esponja marinha *Mycale sp*., que foi coletado do recife de coral na ilha de Samaesarn, no Golfo da Tailândia, resultou no isolamento de dois novos ciclotetrapeptidos: sartoryglabramida A e sartoryglabramida B, e um novo análogo de fellutanina A, juntamente com oito compostos conhecidos incluindo ergosta 4,6,8 (14), 22-tetraen-3-ona, ergosterol 5,8-endoperóxido, aszonalenina, takakiamida, (11a*S*) -2, 3-di-hidro-1*H*-pirrolo [2,1-c] [1,4] benzodiazepina-5, 11 (10*H*, 11a*H*) -diona, ácido helvólico, (3*R*) -3- (1*H*-indol- 3-ilmetil) -3, 4-di-hidro-1*H*-1, 4-benzodiazepina-2, 5-diona e fellutanina A. Todos os compostos foram testados quanto à sua atividade antibacteriana contra microrganismos Gram-positivo (*S. aureus* ATCC 25923) e Gram- negativo (*E. coli* ATCC 25922), bem como para a atividade antifúngica contra o fungo filamentoso (*Aspergillus fumigatus* ATCC 46645), um dermatófito (*Trichophyton ruburm* ATCC FF5) e leveduras (*Candida albicans* ATCC 10231). Nenhum dos compostos exibiu

atividade antibacteriana (MIC> 256 µg / mL) ou atividade antifúngica (MIC> 512 µg / mL).

Além do referido, também foi investigado o fungo endofítico *Eurotium chevalieri* KUFA 0006, que foi isolado do interior dos galhos da planta do manguezal *Rhizophora mucronata* Poir. A partir da cultura deste fungo, cinco metabolitos secundários anteriormente não descritos, incluindo o derivado de antraquinona, acetilquestinol, dois derivados de indol-3-carbaldeído prenilados, um derivado de ácido antranílico e um derivado de isocromona foram isolados juntamente com onze compostos conhecidos: ácido palmítico, ergosterol 5,8-endoperóxido, emodina, physicon, questin, questinol, (11*S*, 14*R*) - ciclo (triptofilvalyl), preechinulina, neoechinulina E, echinulina e eurocristatina. Todos os compostos isolados, exceto o ácido palmítico e o ergosterol 5, 8-endoperóxido, foram avaliados quanto à sua atividade antibacteriana contra dois microrganismos Gram-positivo (*S. aureus* ATCC 25923 e *Enterococcus faecalis* ATCC 29212) e dois Gram-negativo (*E. coli* ATCC 25922 e *P. aeruginosa* ATCC 27853), multirresistentes isolados do meio ambiente. Somente a emodina mostrou atividade antibacteriana contra bactérias Gram-positivo, *S. aureus* ATCC 25923 e *E. faecalis* ATCC 29212, com valores de CIM de 32 e 64 µg / mL, respetivamente. Nenhum dos compostos testados foi ativo contra bactérias de Gram-negativo ou *S. aureus* resistente à meticilina (MRSA) e enterococos resistentes a vancomicina (VRE). Todos os compostos testados apresentaram associação sinérgica fraca ou moderada com a vancomicina contra

enterococos VRE. Alguns dos compostos testados exibiram atividade antibiofilme, dependendo das cepas bacterianas. A emodina não só exibiu atividade antibacteriana contra bactérias de Gram-positivo, mas também mostrou forte associação sinérgica com a oxacilina contra MRSA *Staphylococcus aureus*.

Palavras-chave: *Neosartorya takakii*; *Neosartorya glabra*; *Eurotium chevalieri*; *Talaromyces helicus* KUFA 0063; meroditerpeno; sartorenol; triptoquivalina U; ciclotetrapeptidos; sartoryglabramidas A e B; epóxido de fellutanina A; indois prenilados; isocromona; antraquinonas; dicetopiperazinas; fungo derivado de plantas de manguezal; atividade antibacteriana; antibiofilme.

ABBREVIATION AND SYMBOLS

$[M+H]^+$	Pseudo-molecular ion (Positive ion mode)
$[\alpha]_D^{20}$	Specific optical rotation at 20 ºC for D (sodium) line
$[\alpha]_D^{23}$	Specific optical rotation at 23 ºC for D (sodium) line
$[\alpha]_D^{26}$	Specific optical rotation at 26 ºC for D (sodium) line
®	Register or Trademark
^{13}C NMR	Carbon thirteen Nuclear Magnetic Resonance
1D	One-Dimension
^{1}H NMR	Proton Nuclear Magnetic Resonance
2D	Two-Dimension
Å	Angstrom
A-549	Human lung carcinoma cancer cell line
Ac	Acetyl
Ac_2O	Acetic anhydride
ADC	Antibody Drug Conjugate
AIDS	Acquired Immune Deficiency Syndrome
Ala	Alanine
AMP	Ampicillin

amu	Atomic mass unit
Ara-A	9-β-D-arabinofuranosyladenine
Ara-C	Cytosine Arabinoside
Arg	Arginine
Asp	Aspartic acid
ATCC	American Type Culture Collection
BIC	Biofilm Inhibitory Concentration
brd	Broad doublet
brs	Broad singlet
Calcd.	Calculated
CCDC	Cambridge Crystallographic Data Centre
CD	Cluster of Differentiation
CFU	Colony-Forming Unit
CLSI	Clinical Laboratory Standards Institute
CoA	Coenzyme A
COSY	Correlated Spectroscopy
CTX	Cefotaxime
CYA	Czapek Yeast Autolysate Agar
Cys	Cysteine

CZA	Czapek's Agar
dd	Double doublet
ddd	Double double doublet
DEPT	Distortionless Enhancement by Polarization Transfer
DMSO	Dimethylsulfoxide
DMSO-*d6*	Deuterated dimethylsulfoxide
DMXBA	3-(2,4-Dimethoxybenzylidene)-Anabaseine
DNA	Deoxyribonucleic Acid
DPPH	2, 2-Diphenylpicrylhydrazyl
dq	double quartet
dt	Double triplet
ECD	Electronic Circular Dichroism
EGFR	Epidermal Growth Factor Receptor
EMA	European Medicines Agency
EMEA	European Middle Eastern and African
ESBL	Extended Spectrum Beta-Lactamases
ET	Ecteinascidin
EU	European Union
FDA	Food and Drug Administration

FIC	Fractional Inhibitory Concentration
FTIR	Fourier Transform Infrared Spectroscopy
g	Gram
GABA	Gamma-aminobutyric acid
GI_{50}	Half maximal growth inhibitory concentration
Gly	Glycine
HMBC	Heteronuclear Multiple Bond Correlation
HPLC	High Performance Liquid Chromatography
HRESIMS	High-Resolution Electrospray Ionization Mass Spectrometry
HRMS	High Resolution Mass Spectrometry
HSQC	Heteronuclear Single Quantum Coherence
HSV	Herpes Simplex Virus
HUVEC	Human Umbilical Vein Endothelial Cells
Hz	Hertz
IC_{50}	Half maximal inhibitory concentration
IL-6	Interleukin 6
IR	Infrared
ITS	Internal Transcribed Spacer
J	Coupling constant in Hz

KB cell	Human oral epidermoid carcinoma cell line
KKU	Khon Kaen University
KUFA	Kasetsart University Fungal Agriculture
KUFC	Kasetsart University Fungal Culture
LC	Liquid Chromatography
LC-MS	Liquid Chromatography coupled with Mass Spectrometry
Leu	Leucine
LH-60	Human Promyelocytic Leukemia Cell Line
LN-caP	Prostate Cancer Cell Line
LPS	Lipopolysaccharide
Lys	Lysine
m	Multiplet
m/z	Mass per charge
MAO	Monoamine Oxidase
MBC	Minimum Bactericidal Concentration
MCF-7	Human breast carcinoma cell line
MDA-MB-435	Estrogen-Independent Human Breast Adenocarcinoma Cell Line
Me	Methyl
MEA	Malt Extract Agar

Me_2CO	Acetone
Met	Methionine
MH	Mueller-Hinton Agar
MeOH	Methanol
MHz	Mega hertz
MIC	Minimum Inhibitory Concentration
mm	Millimeter
MMAE	Monomethyl Auristatin E
MMAF	Monomethyl Auristatin F
mp	Melting point in ºC
MRSA	Methicillin-resistant *Staphylococcus aureus*
MS	Mass Spectrometry
NA	Not Available
NAD(P)H	Reduced Nicotinamide Adenine Dinucleotide (Phosphate)
NCBI	National Center for Biotechnology Information
NCE	New Chemical Entities
NCI	National Cancer Institute
NCI-H460	Non-small cell lung cancer cell line
NK-1	Human Neurokinin Receptor 1

nm	Nanometer
NMR	Nuclear Magnetic Resonance
NO	Nitric oxide
NOESY	Nuclear Overhauser Effect Spectroscopy
NSCLC	Non-Small Cell Lung Cancer
ºC	Degree Celsius
ORTEP	Oak Ridge Thermal Ellipsoid Plot
OX	Oxacillin
PDA	Potato Dextrose Agar
PDB	Protein Data Bank
PHVD	Prevention of head and vascular disease
PN/NT	Protection of neurons/ neurotoxicity
ppt	Parts per thousand
PTLC	Preparative Thin Layer Chromatography
q	Quartet
s	Singlet
S	Streptomycin
SEM	Scanning Electron Microscope
Ser	Serine

Si gel	Silica gel
sp.	Species (singular)
spp.	Species (plural)
t	Triplet
Thr	Threonine
TLC	Thin Layer Chromatography
TMV	Tobacco Mosaic Virus
TNF	Tumor Necrosis Factor
Tyr	Tyrosine
UPLC	Ultra Performance Liquid Chromatography
US	United States
UV	Ultraviolet
VAN	Vancomycin
VRE	Vancomycin-resistant Enterococcus
WHO	World Health Organization
δ	Chemical shift value in ppm
ε	Molar absorptivity (molar extinction coefficient)
λ	Wavelength in nanometer
ΣFIC	FIC index

CHAPTER I

INTRODUCTION

1. INTRODUCTION

1.1 Natural Products Drug Discovery and Its Current Status

Natural products are chemical compounds derived from living organisms, such as plants, animals, insects and microorganisms many of which have been used to treat diseases. Plants and microorganisms produce unique bioactive substances, providing access to very different types of lead compounds. Natural products have long been traditional sources of medicines, and are still nowadays considered the most successful supply of potential drug leads with more than one million new chemical entities discovered so far (Carter, 2011; Dias *et al*. 2012). More than 60% of the drugs are in the market derived from natural sources (Molinari, 2009).

Natural products are highly diverse and often provide highly specific biological activities, which have been the basic of the treatment of human diseases and a major source of new drugs. Many successful drugs in the market today were originally synthesized to mimic the action of molecules found in nature (Feher and Schmidt, 2003). The World Health Organization (WHO) estimated in 1985 that approximately 65% population of the world predominately relied on plant-derived traditional medicines for their primary health care, while the plant products also play an important, through more indirect role in the health care systems of the remaining population who mainly reside in developing countries (Farnsworth *et al*., 1985).

Moreover, Natural Products are the most important part of the armamentarium for anticancer and anti-infective agents. More than 60 % of approved and pre-new drug application (NDA) candidates are either natural products or related to them, not including biological such as vaccines and monoclonal antibodies (Cragg *et al*., 1997). Many natural products have reached the market without chemical modification, a testimony to the remarkable ability of microorganisms to produce small, drug-like molecules (Zhang and Demain, 2005). In the modern drug discovery era there are three major sources of new compounds: original natural products, compounds derived semi-synthetically from natural products and combinatorial synthetic compounds based on natural products models (Cragg *et al*., 1997; Feher and Schmidt, 2003; Newman *et al*., 2003). Most natural product research today is due to several reasons such as (i)-unmet medical needs (ii)-remarkable diversity of structures and activities (iii)-utility as biochemical probes, (iv)-novel and sensitive assay methods (v)-improvement in isolation, purification and characterization, and (vi)-new production methods (Clark, 1996). Natural products are the most successful source of drug leads and continue to provide greater structural diversity than standard combinational chemistry, and major opportunities for finding novel molecules. In the modern area of drug discovery, they will continue to be important as targets for production by biotechnological approaches, a source of lead compounds of novel chemical structures, and as the active ingredients of useful treatment derived from traditional systems of medicine (Harvey, 1993).

Many of these natural products have become current drug candidates (Dias *et al*., 2012). They have contributed to identifying and understanding novel chemical pathways and proved to make not only valuable drugs available but also essential tools in biochemistry and molecular cell biology (Grabley and Sattler, 2003).

Natural products have provided many effective drugs. Historical example of early identified natural compound, commercially important drug morphine (**1**) from *Papaver somniferum* L. (opium poppy), was first reported in 1803 (Benyhe 1994; Der Marderosian and Beutler, 2002). Another important example is the antimalarial drug, quinine (**2**) which formed the basis for the synthesis of the commonly used antimalarial drugs chloroquine (**3**) and mefloquine (**4**) (Figure 1). It was originally isolated in 1820 by French pharmacists Caventou and Pelletier from the bark of *Cinchona succirubra Pav.* ex Klotsh, which had been used for centuries for the treatment of malaria, fever, indigestion, mouth and throat diseases and cancer (Kremsner *et al*., 1994). Arteether (**5**) introduced in 2000 as Artemotil® is derived from artemisinin (**6**) (introduced in 1987 as Artemisinin) which was isolated from the plant *Artemisia annua* and are both approved antimalrial drugs (Newman and Cragg, 2007).

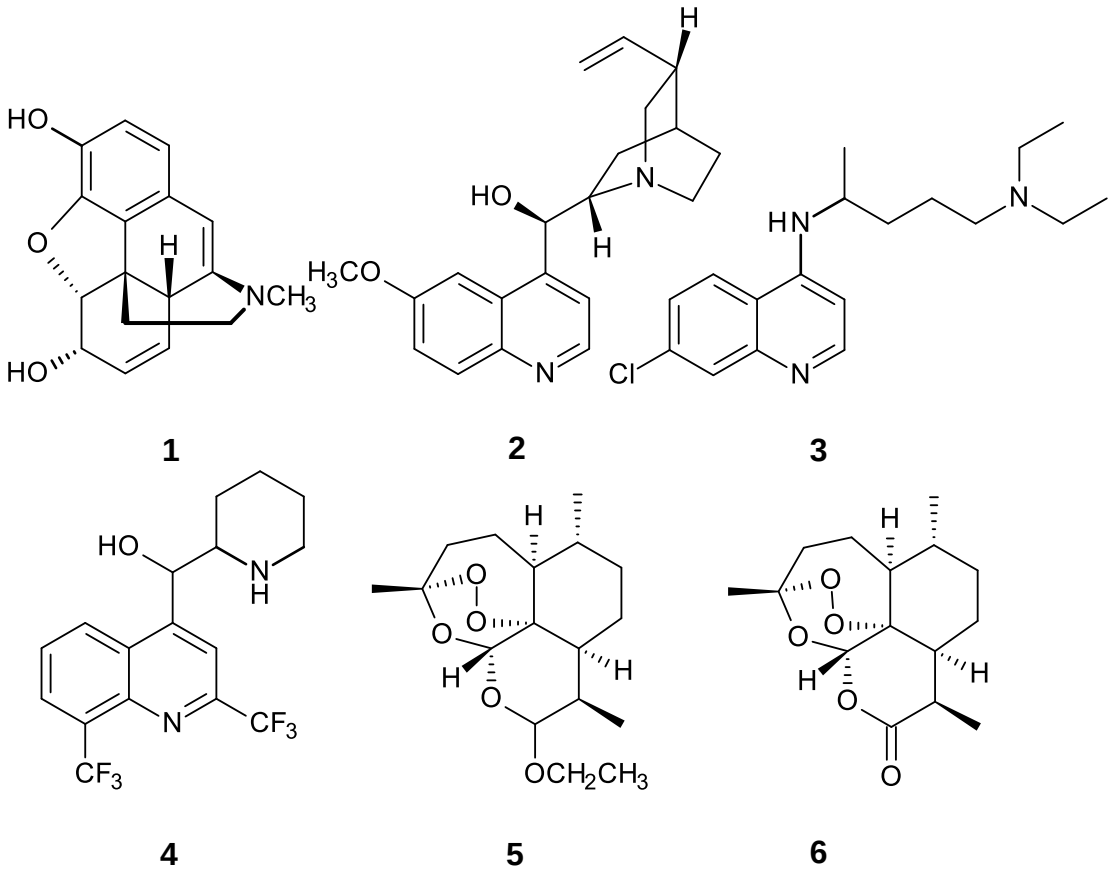

Figure 1. Structures of morphine (**1**), quinine (**2**), chloroquine (**3**), mefloquine (**4**), arteether (**5**) and artemisinin (**6**)

Another example is paclitaxel (Taxol®) (**7**) which was originally isolated from the bark of the Pacfic yew tree *Taxus brevifolia* Nutt. (Taxaceae), collected in Washington State as part of a random collection program for the NCI by the U.S. Department of Agriculture (USDA) (Cragg, 1998; Wani *et al*., 1971). The structure of paclitaxel was elucidated in 1971 and was clinically introduced to the US market in the early 1990s, which was significantly active against ovarian cancer, advanced breast cancer, small and non-small cell lung cancer (Rowinsky *et al*., 1992). Other

examples of plant-derived anticancer drugs are the *bis*-indole alkaloids vinblastine (VLB) (**8**) and vincristine (VCR) (**9**), which were isolated from the Madagascar periwinkle *Catharanthus roseus*. Vinblastine (VLB) and vincristine (VRE) are primarily used in combination with other cancer chemotherapeutic drugs for the treatment of a variety of cancers such as leukemia, lymphomas, advanced testicular, breast and lung cancers, and Kaposi's sarcoma (Cragg and Newman, 2005b).

Among the natural sources, the potential of microorganisms in drug discovery is recently exploited. Many of the drugs especially the antibiotics currently in the pharmaceutical market have been reported from microorganisms. The most famous natural product penicillin which was discovered from a fungus *Penicillium notatum* in 1928 by Fleming along with its re-isolation and commercialization in 1940 initiated a great revolution in drug discovery and research which is often referred to as the "Golden Age of Antibiotics". Penicillin G (**10**) was first used in a large scale during World War II to treat soldiers wounded on battlefields to stave off infections (Hussain *et al*., 2014). Cyclosporine (cyclosporin A, CsA) (**11**) is a cyclic undecapeptide containing a novel amino acid together with several *N*-methylated amino acids and one new amino acid (Petcher *et al*., 1976; Rüegger *et al*., 1976; Zhou *et al*., 2009), which was discovered in 1970s from the fungus *Tolypocladium inflatum* (Kobel and Traber, 1982). This compound was found to have effective immunosuppressive ability in organ transplantations and successfully marketed as an immunosuppressant drug (Borel *et al*., 1977). In addition, cyclosporines have been

established to have anti-inflammatory, antifungal, and antiparasitic properties, and reversing potential for multidrug resistance in several types of cancers (Sallam *et al*., 2005). All of these compounds or derivatives are still in use as drugs today (Butler, 2004).

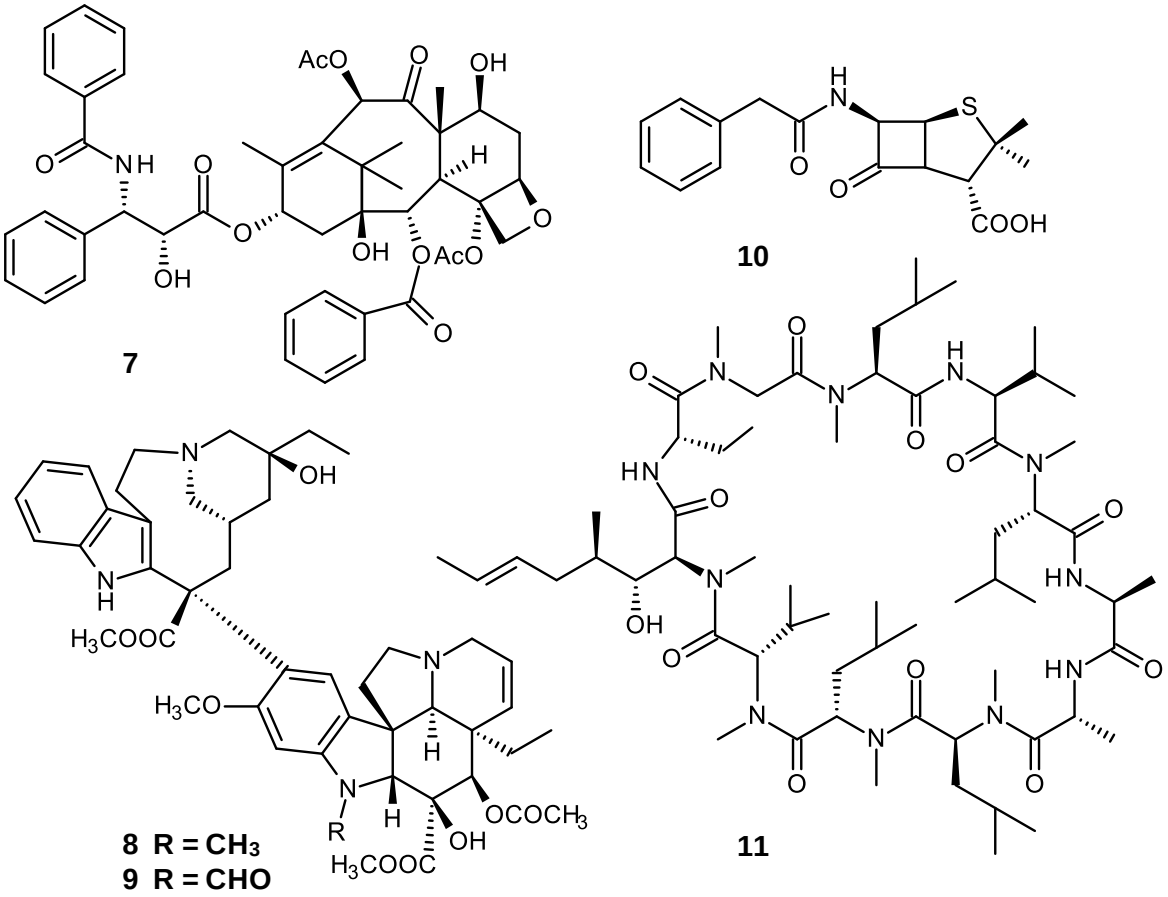

Figure 2. Structures of paclitaxel (Taxol®) (**7**), vinblastine (VLB) (**8**), vincristine (VCR) (**9**), penicillin G (**10**) and cyclosporine (cyclosporin A, CsA) (**11**)

In 2016, Newman and Cragg reported that 77.5% of the small-molecule new chemical entities (NCEs) discovered from 1981 to 2014 were inspired by natural products (Figure 3). These include: 6% natural products (N), 26% semi-synthetically modified natural products (ND), 5% totally synthetic compounds based on a natural product pharmacophore (S*), and 27% synthetic/semisynthetic natural product mimics (S*/NM and S/NM). In addition, over 73% of antibacterial and 83% of anticancer discovered were based on, or derived from natural products (Newman and Cragg, 2016). Moreover, many of the best selling drugs currently on the market in various therapeutic fields such as antibacterial, antifungal, antiparasitic, anticoagulant, immunosuppressant and anticancer were derived from natural products (Newman and Cragg, 2007).

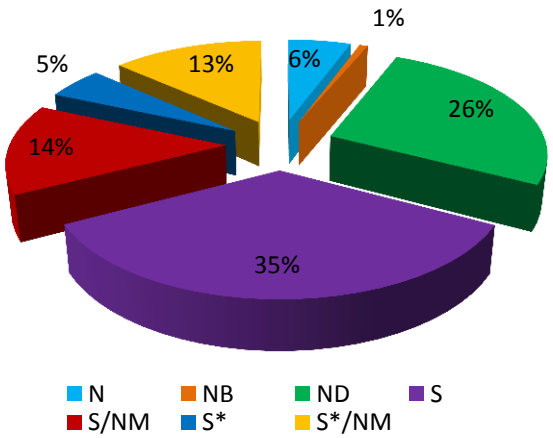

Figure 3. All small-molecules new chemical entities from 1981 to 2014 (Newman and Cragg, 2016)

Today, pharmaceutical companies are under scrutiny due to the gradual decline and pressure to increase the number of new drugs on the market, and as a result in the last decade, many pharmaceutical companies have abandoned their natural products drug discovery programs (Dickson and Gagnon, 2004; McChesney *et al*., 2007).

1.2 Current Status of Marine Natural Products Research

Over 22,000 structurally diverse secondary metabolites have been isolated and characterized from a variety of marine organisms from different marine environments over the last fifty years (Blunt *et al*., 2013; Gerwick and Fenner, 2013; Hill, 2013; Hu *et al*., 2011). In the marine environment, where a different transcriptome, proteasome, and finally a different metabolome which allows organism to survive, one can speculate that different secondary metabolites might be the result of special requirements to adapt to such an extreme environment (Firn and Jones, 2000).

Almost all forms of life in the marine environment have been investigated for their natural products content, representing a valuable source of novel compounds with great potential such as pharmaceuticals, nutritional supplements, cosmetics, agrochemicals and enzymes, many of them with a strong potential market value (Blunt *et al*., 2013; Kijjoa and Sawangwong, 2004). Before the 1980s, marine natural products discovered annually were less than 100, however the number of novel

marine compounds greatly increased after 1985, and then stabilized at about 500 per year in the late 1990s (Hu *et al*., 2015). Figure 4 shows the variation in the number of new marine natural products isolated from 1985-2012 as well as the proportion of the bioacive and non-active compounds for each year. The same authors have also summarized in Figure 5 the activities of the new marine natural products isolated during this period into several groups. It is interesting to observe that compounds with anticancer activity constitute a major group (56%), followed by antibacterial (13%) and antifungal (5%). Moreover, the new marine natural products, although in small percentage, are also found to have other activities such as pest resistance, antiviral, pesticide, prevention of head and vascular diseases, and protection of neuron/neurotoxicity (Hu *et al*., 2015).

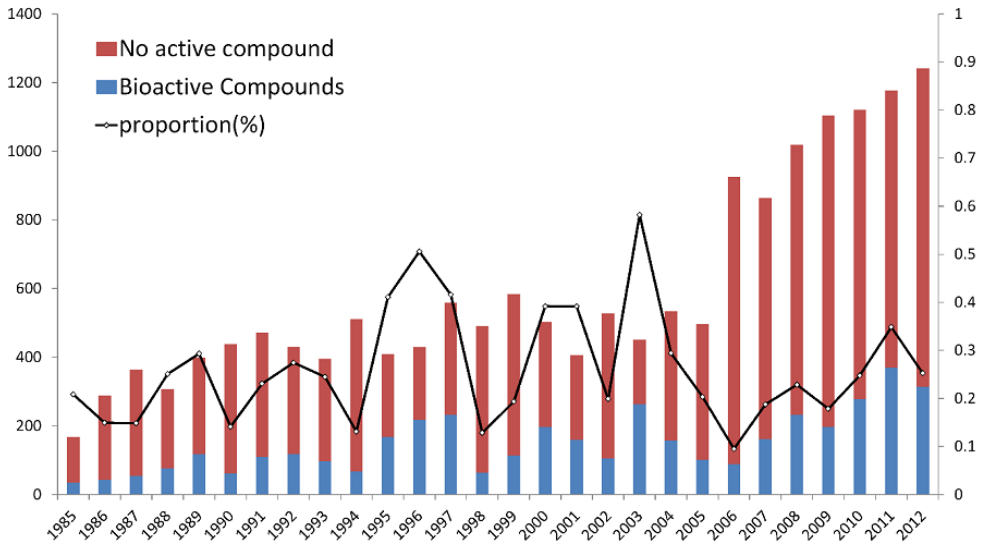

Figure 4. Variation in number of new marine natural products for 1985-2012 (Hu *et al*., 2015)

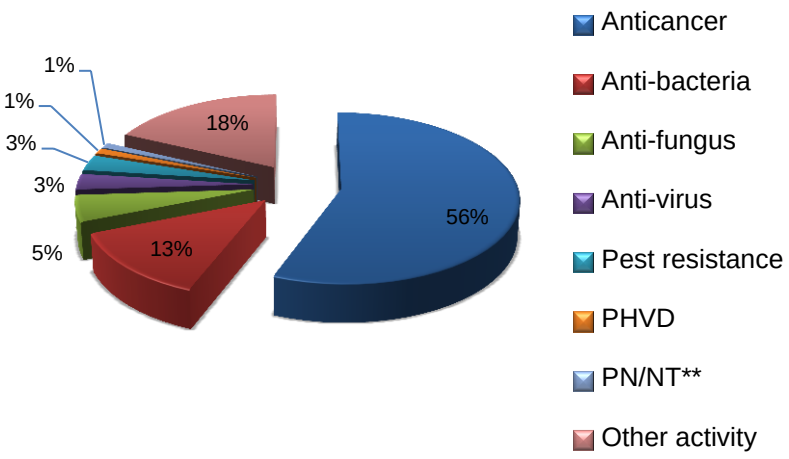

Figure 5. Bioactivity of new marine natural products (*PHVD: Prevention of head and vascular disease, **PN/NT: Protection of neurons/ neutoxicity) (Hu *et al*., 2015)

Although the percentage of marine natural products that can be developed into drugs is still low so far, there are signs that an increasing number of marine bioactive compounds will be approved for the treatment of human diseases (Haefner, 2003; Liu *et al*., 2012; Nastrucci *et al*., 2012). In order to accomplish this objective, more interdisciplinary approaches and innovative manipulations are urgently needed to improve bioactivity studies. Marine natural products exhibit a wide range of biological activities, which play an important role in the discovery of leads for the development of drugs for the treatment of human diseases (Newman and Cragg, 2012), which had become an established sub-discipline of natural products chemistry, and several thousands of compounds have been described (Faulkner, 2000a). Due to their bioactivities such as anti-tumor, anti-microtubule,

anti-proliferative, photoprotective, antibiotic and anti-infective, marine natural products are exceptionally interesting high-value ingredients in the pharmaceutical industry and more and more companies are investing in this field (Berdy, 2005; Mishra and Tiwari, 2011; Molinski *et al*., 2009; Pettit *et al*., 1982; Schumacher *et al*., 2011; Sudek *et al*., 2007).

Approximately 30, 000 structurally diverse natural products with a vast array of bioactivities have been discovered from marine organisms including microbes, algae and invertebrates (Radjasa *et al*., 2011; Salomon *et al*., 2004) and currently available commercial drugs for the treatment of various diseases have been derived from microorganisms (Cragg and Newman, 2005a; Li and Vederas, 2009). In fact, some studies reported that marine organisms provide more bioactive natural products than terrestrial organisms. Concerning marine natural products, it is interesting to verify that most interest has been directed to marine organisms from temperate and tropical areas, while polar organisms are still underexplored (Avila *et al*., 2008; Blunt *et al*., 2014; Lebar *et al*., 2007). The majority of novel compounds from marine organisms, approximately 75% were isolated from invertebrates mainly from the phylum Porifera (sponges) but also from Coelenterate (mostly coral). Additionally, algae and microorganisms are also major sources of novel metabolites (Hu *et al*., 2011). Among marine microorganisms, fungi have gained an important role as a source of new biologically active secondary metabolites with antitumor, antibacterial, antiviral, antifungal, anti-inflammatory and anticancer activities and enzyme inhibitor compounds (Gamal-Eldeen *et al*., 2009; Samuel *et al*., 2017).

1.3 Marine Chemistry and Pharmacology

Marine organisms are producing diverse structural metabolites such as polyketides, alkaloids, peptides, proteins, lipids, glycosides, isoprenoids and hybrids of those metabolites (Mayer *et al*., 2011; Rateb and Ebel, 2011). The first biologically marine natural products sponge-derived arabinosyl nucleosides spongouridine and spongothymidine formally reported in the early 1950s from the Caribbean sponge *Tethya crypta* by Bergmann (Bergmann and Stempien Jr, 1957). In late 1970, it was established that marine plants and animals are genetically and biologically unique. Around 15,000 natural products have been described and among these 30% were from sponges (Murti and Agrawal, 2010). Covering the period from 1981 to 2008, around 68% of all the drugs used to curb infection including antibacterial, antiviral, antiparasitic and antifungal compounds and 63% of anti-cancer drugs were naturally derived (Cragg *et al*., 2009).

Currently there are 13 marine derived compounds in the clinical lineup that are at different stages of clinical trials, with a very large number of marine-derived compounds in the preclinical testing pipeline as well. The three Food and Drug Administartion (FDA) approved marine-derived drugs currently used in the United States are cytarabine (Cytosar-UW, DepocytW), vidarabine (Vira-AW), and ziconotide (PrialtW). **Table 1** showed the marine-derived compounds which have been approved by FDA and different phases of the clinical pipeline http://marinepharmacology.midwestern.edu/clinPipeline.htm (Mayer *et al*., 2010).

Trabectedin (Yondelis®, ET-743) (**12**) (Figure 6) is a tetrahydroisoquinoline alkaloid, originally isolated from the colonial tunicate *Ecteinascidia turbinate*. This compound was the first anticancer agent approved in the EU for the treatment of soft-tissue sarcoma and in relapsed cases of platinum-sensitive ovarian cancer (Verweij, 2009; Yap *et al*., 2009).

Brentuximab vedotin 63 (Adcetris®) (**13**) (Figure 6) is an anticancer agent that is based on a fully synthetic analog of dolastatin 10 molecule. Dolastatin 10 was isolated in 1972 from the sea hare *Dolabella auricularia* (Pettit *et al*., 1987). It is currently the marine drug that successfully enters into the market and was approved for the treatment of Hodgkin and systemic anaplastic large cell lymphoma (Firsova *et al*., 2017).

Eribulin mesylate (Halaven®) (**14**) (Figure 6) is a marine-derived microtubule-targeted agent that was a structurally simplified synthetic analogue of halichondrin B which was originally isolated for the first time in 1986 from the marine sponge *Halichondria okadai* and was found to be highly cytotoxic in murine leukemia cells. This compound was approved by FDA in 2010 and EMEA's in 2011, for metastatic breast cancer (Dumontet and Jordan, 2010; Huyck *et al*., 2011).

Lovaza® (formerly known as omacor) (**15**) (Figure 6) is the brand name for anti-hypertriglyceridemia drug composed of ethyl esters of several omega-3 fatty acids isolated from fish oils. Omega-3 fatty acids of marine origin are proven to reduce triglycerides and low density cholesterols and to increase high density

cholesterols in the blood and are therapeutic in combination with diet and statins (Pettit *et al*., 1987).

Ziconotide (Prialt®) (**16**) (Figure 6) is a synthetic version of ω-conotoxin, a naturally occurring peptide isolated from the cone snail *Conus magus*. This compound was the first intrathecal analgesic drug to be approved after morphine, receiving the FDA approval in 2004 and EMEA approval in 2005 and is currently labeled for the management of severe chronic pain patients with cancer or AIDS (Rauck *et al*., 2009; Staats *et al*., 2004).

Vidarabine (arabinofuranosyladenine or adenine arabinoside, Ara-A) (**17**) (Figure 6) is a synthetic purine nucleoside which was developed from spongouridine, firstly isolated from the Caribbean sponge *Tethya crypta* (Newman *et al*., 2009). Spongouridine is currently obtained from fermentation of *Streptomyces antibioticus* (Hong *et al*., 1986). It is approved by FDA for use in recurrent epithelial keratitis caused by herpes simplex virus type 1 and 2, acute kerato-conjunctivitis, and also for superficial keratitis (Mayer *et al*., 2010).

Cytarabine (arabinosyl cytosine or cytosine arabinoside, Ara-C) (**18**) (Figure 6) a marine-derived anticancer compound which is a synthetic pyrimidine nucleoside developed from spongothymidine which was firstly isolated from a Caribbean sponge *Tethya crypta* (Newman *et al*., 2009). This compound was approved in 1969 and mainly used in different types of leukemia, including acute myelocytic leukemia, lymphocytic leukemia, meningeal leukemia and blast crisis phase of chronic myelogenous leukemia (Absalon and Smith, 2009; Thomas, 2009).

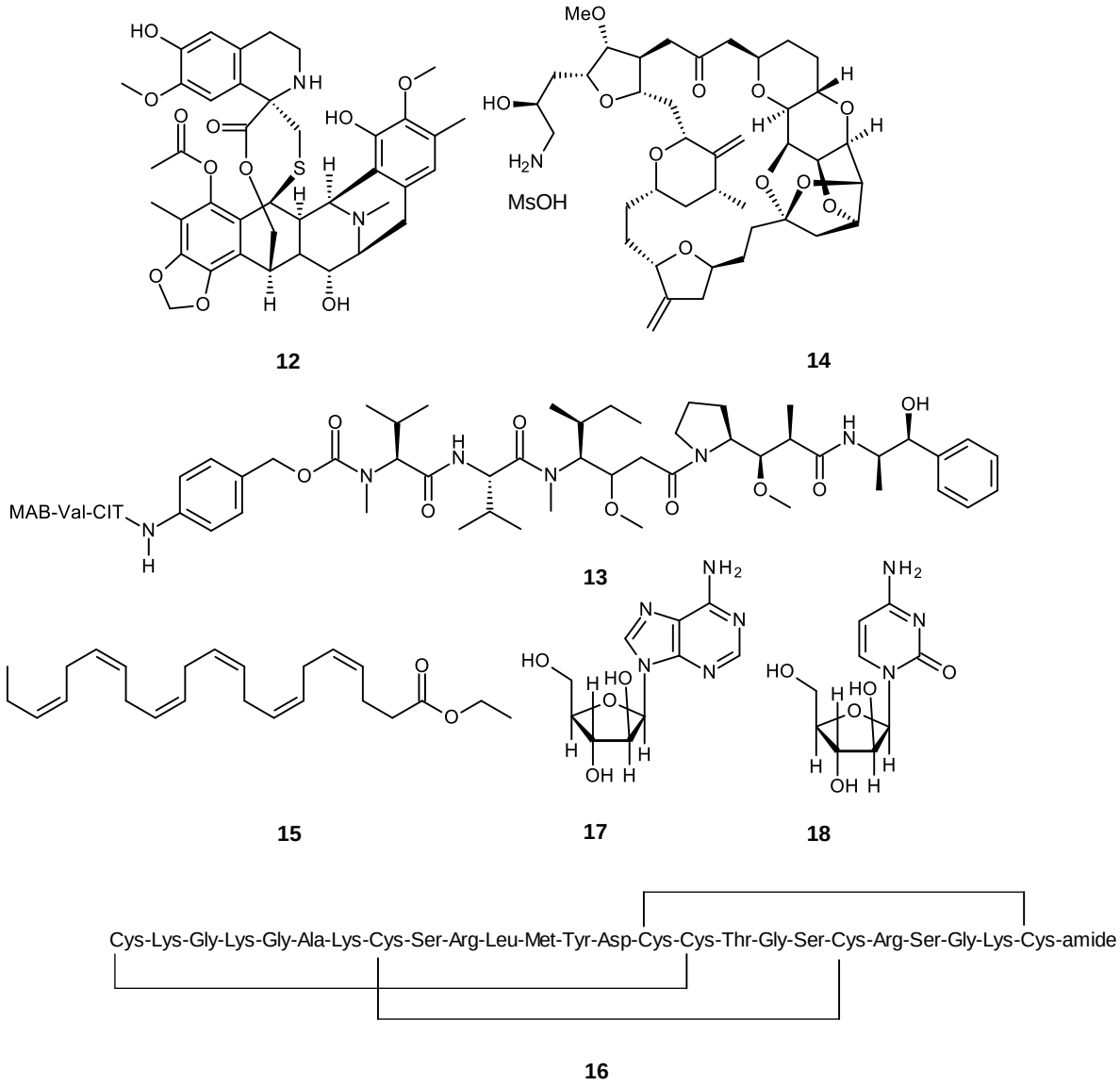

12 **14** **13** **15** **17** **18** **16**

Figure 6. Structures of trabectedin (ET-743) (**12**), brentuximab vedotin (SGN-35) (**13**), eribulin mesylate (E7389) (**14**), omega-3-fatty acid ethyl ester (**15**), ziconotide (**16**), vidarabine (Ara-A) (**17**) and cytarabine (Ara-C) (**18**)

Table 1. A perspective of pipeline of marine drugs

(http://marinepharmacology.midwestern.edu/clinPipeline.htm)

Clinical status	Compound name	Marine organism	Chemical class	Disease area
FDA Approved	Trabectedin (ET-743)	Tunicate	Alkaloid	Cancer
	Brentuximab vedotin (SGN-35)	Mollusk/ cynobacterium	ADC (MMAE)	Cancer, lymphoma
	Eribulin mesylate (E7389)	Sponge	Macrolide	Breast cancer
	Omega-3-fatty acid ethyl esters	Fish	Omega-3-fatty acid	Hypertriglyceridemia
	Ziconotide	Cone snail	Peptide	Pain
	Vidarabine (Ara-A)	Sponge	Nucleoside	Anti-viral
	Cytarabine (Ara-C)	Sponge	Nucleoside	Cancer
Phase III	Pinabulin (NPI-2358)	Fungus	Diketopiperazine	Cancer
	Plitidepsin	Tunicate	Depsipeptide	Cancer
	Squalamine lactate	Dogfish Shark	Aminosterol	Neovascular Diseases
	Tetrodotoxin	Pufferfish	Guanidinium alkaloid	Chronic pain
	Glembatumumab vedotin	Mollusk/cyanobacterium	ADC (MMAE)	Chronic pain

Table 1. A perspective of pipeline of marine drugs (Cont.)

(http://marinepharmacology.midwestern.edu/clinPipeline.htm)

Clinical status	Compound name	Marine organism	Chemical class	Disease area
Phase II	ABT-414 EGFRvIII-MMAF	Mollusk/cyanobacterium	ADC (MMAF)	Cancer
	DMXBA (GTS-21)	Worm	Alkaloid	Schizophrenia, Alzheimer Disease, Attention Deficit Hyperactivity Disorder, Endotoxemia, Sepsis, Vagal Activity
	SGN-CD19A	Mollusk/cyanobacterium	ADC (MMAF)	Cancer
	Lurbinectedin (PMO1183)	Tunicate	Alkaloid	Cancer
	AGS-16C3F	Mollusk/cyanobacterium	ADC (MMAF)	Cancer
	Lifastuzumab vedotin (DNIB0600A)	Mollusk/cyanobacterium	ADC (MMAF)	Cancer
	Pinatuzumab vedotin (DCDT-2980S)	Mollusk/cyanobacterium	ADC (MMAE)	Non-Hodgkin Lymphoma, chronic lymphocytic leukemia
	Polatuzumab vedotin (DCDS-4501A)	Mollusk/cyanobacterium	ADC (MMAE)	Cancer

Table 1. A perspective of pipeline of marine drugs (Cont.)

(http://marinepharmacology.midwestern.edu/clinPipeline.htm)

Clinical status	Compound name	Marine organism	Chemical class	Disease area
Phase I	GSK2857916	Mollusk/cyanobacterium	ADC (MMAF)	Cancer
	ABBV-085	Mollusk/cyanobacterium	ADC (MMAE)	Cancer
	ABBV-399	Mollusk/cyanobacterium	ADC (MMAE)	Cancer
	ABBV-221	Mollusk/cyanobacterium	ADC (MMAE)	Cancer
	ABBV-838	Mollusk/cyanobacterium	ADC (MMAE)	Cancer
	ASG-67E	Mollusk/cyanobacterium	ADC (MMAE)	Cancer
	ASG-15ME	Mollusk/cyanobacterium	ADC (MMAE)	Cancer
	Enfortumab Vedotin ASG-22ME	Mollusk/cyanobacterium	ADC (MMAE)	Cancer
	Bryostatin	Bryozoa	Macrolide lactone	Cancer
	Tisotumab Vedotin	Mollusk/cyanobacterium	ADC (MMAE)	Cancer
	Marizomib (Salinosporamide A; NPI-0052)	Bacterium	Beta-lactone-gamma lactam	Cancer
	MLN-0264	Mollusk/cyanobacterium	ADC (MMAE)	Cancer
	PM060184	Sponge	Polyketide	Cancer
	SGN-LIV1A	Mollusk/cyanobacterium	ADC (MMAE)	Cancer

ADC: Antibody Drug Conjugate; Ara-A: 9-β-D-arabinofuranosyladenine; Ara-C: Cytosine Arabinoside; DMXBA: 3-(2, 4-Dimethoxybenzylidene)-Anabaseine; ET: Ecteinascidin; EGFR: Epidermal Growth Factor Receptor; MMAE: Monomethylauristatin E; MMAF: Monomethylauristatin F

*http://marinepharmacology.midwestern.edu/clinPipeline.htm with permission from Professor Alejandro M.S. Mayer, PhD. (Department of Pharmacology, Chicago College of Osteopathic Medicine Midwestern University).

1.4 Marine-Derived Fungi

The oceans which cover more than 70% of the earth's surface and more than 95% of the earth's biosphere harbor various marine organisms. Because of the special physical and chemical conditions in the marine environment, almost every class of marine organism displays a variety of molecules with structurally unique features. Currently, thousands of structurally unique and biologically active compounds have been reported from marine fungi (Jin *et al*., 2016).

The generally accepted ecological definition of marine fungi is, "Obligate marine fungi are those which grow and sportulate exclusively in a marine or estuarine habitat; facultative marine fungi are those from freshwater or terrestrial milieus able to grow and possibly also to sporulate in the marine environment'' (Kohlmeyer and Kohlmeyer, 1979). Marine-derived fungi are known to produce structurally unique secondary metabolites due to the adaptation to a very distinct set of environmental pressures from marine environment, and since the beginning of the 1990s, a sharp and exponential increase in the number of reported relevant biologically active metabolites occurred (Bhadury *et al*., 2006; Gomes, 2014). The distribution of marine-derived fungi in the tropics has not been explored as thoroughly as in the temperate areas (Blunt *et al*., 2009; Blunt *et al*., 2005; Kohlmeyer, 1984). Nevertheless, inventory data for the marine fungi investigated in several tropical countries such as Thailand (Chaeprasert *et al*., 2010), Palau Islands (Chatmala *et al*., 2004; Kohlmeyer, 1984), Singapore

(Lim and Tan, 1986; Sundari, 2010), Brunei (Hyde, 1988), Malaysia (Alias and Jones, 2000; Jones and Hyde, 1988; Pang *et al*., 2010; Zainuddin *et al*., 2010) and Siargao Island, Philippines (Besitulo *et al*., 2002) are available. However, many tropical regions have been still largely unexplored, such as the Indonesia archipelago.

Recently, Jin *et al*. (2016) reported that about three quarters of all new chemical structures from marine fungi are derived from isolation from living matters, such as marine animals (30.1%), marine plants (42.5%), while the remaining compounds are obtained from non-living sources, most notably sediments (22.9%). Within the individual groups, mangrove habitats (25.5%), alga (14.4%) and sponges (9.2%) are the predominant sources for fungal diversity (Figure 7). According to Bugni and Ireland (2004) marine sponges were the richest source of marine fungi. Several cultivation based studies with marine sponges have shown a vast biological diversity, yielding the greatest taxonomic diversity in comparison with other marine sources. On the other hand, Kelecom (2002) reported that the numbers of compound having antitumor and antibacterial activities isolated from bacteria were the same as those from fungi. However, fungi are found to be a rich source of anticancer rather than antibacterial metabolites. From the number of new compounds published each year, it is evident that the number of natural products from marine-derived fungi continues to be rapidly increasing and still has not reached its climax (Rateb and Ebel, 2011).

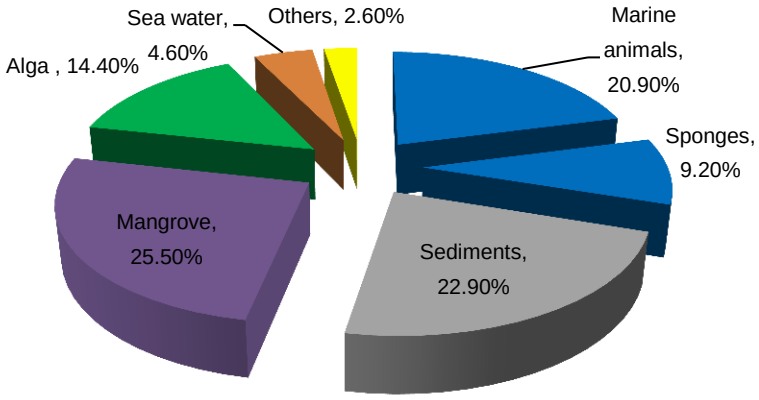

Figure 7. New compounds from marine-derived fungi divided by sources of the fungal strains (Jin *et al*., 2016)

1.4.1 Marine sponges-associated fungi

Marine invertebrates are one of the major groups of organisms that gave a number of secondary metabolites with pharmacological properties and led in the formulation of novel drugs. Among marine invertebrates, sponges became the dominant source of novel bioactive metabolites (Hu *et al*., 2011; Perdicaries *et al*., 2013). When compared to other marine invertebrates, marine sponges (Porifera) are recognized as the richest sources (Mehbub *et al*., 2014; Taylor *et al*., 2007). Figure 8 showed the distribution of new marine natural products from different types of marine sources, including microorganisms and phytoplankton discovered from 2001-2010 (Mehbub *et al*., 2014).

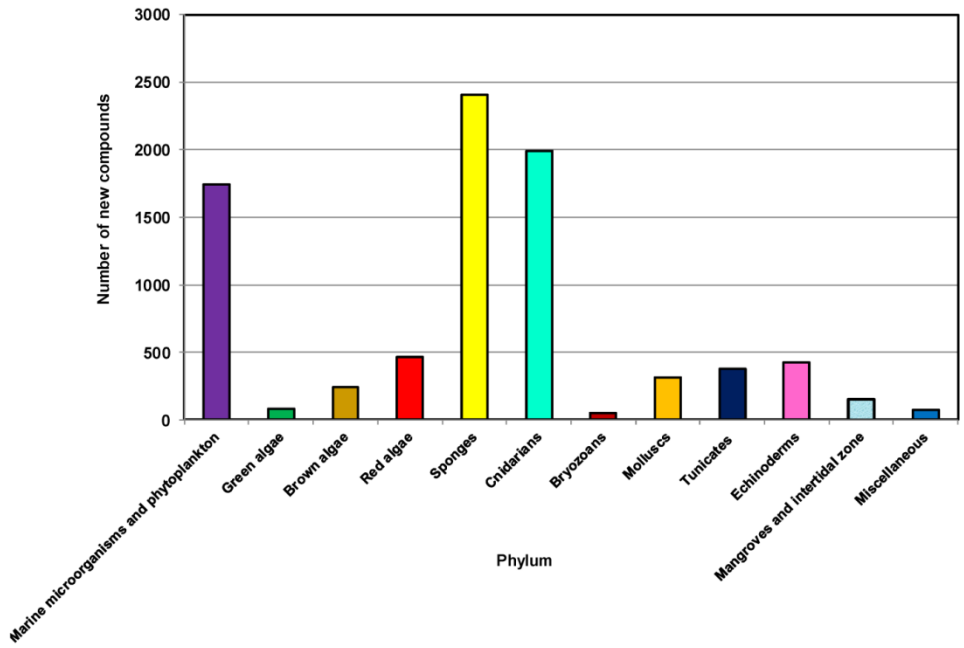

Figure 8. Total number of new compounds isolated from different types of marine sources, 2001-2010 (Mehbub *et al*., 2014)

In particular, sponge-associated fungi have yielded novel metabolites with potent antibacterial and anticancer activities (Jensen and Fenical, 2000). Trichoharzin (**19**), a compound isolated from *Trichoderma harzianum* associated with the sponge *Mycale cecilia,* was the first novel metabolite from sponge-associated fungi (Kobayashi *et al*., 1993), while gymnastatins A (**20a, b**), B (**21**) and C (**22**) were the first novel cytotoxic metabolites from a strain of *Gymnasella dankaliensis*, which was isolated from the sponge *Halichondria japonica* (Amagata *et al*., 1998). Sorbicillactone A (**23**) is yet another antileukemic agent produced by *Penicillium chrysogenum* associated with the marine sponge *Ircinia fasciculata.* Compound **23** is also known to have antiviral and neuroprotective properties

(Bringmann *et al*., 2007), and due to its antileukemic properties, this compound was also qualified for human trials (Thakur and Thakur, 2006). Therefore, marine sponges are considered a rich source of chemical diversity and health benefits for developing drug candidates, cosmetics, nutritional supplements and molecular probes that can be exploited to increase the healthy life span of humans.

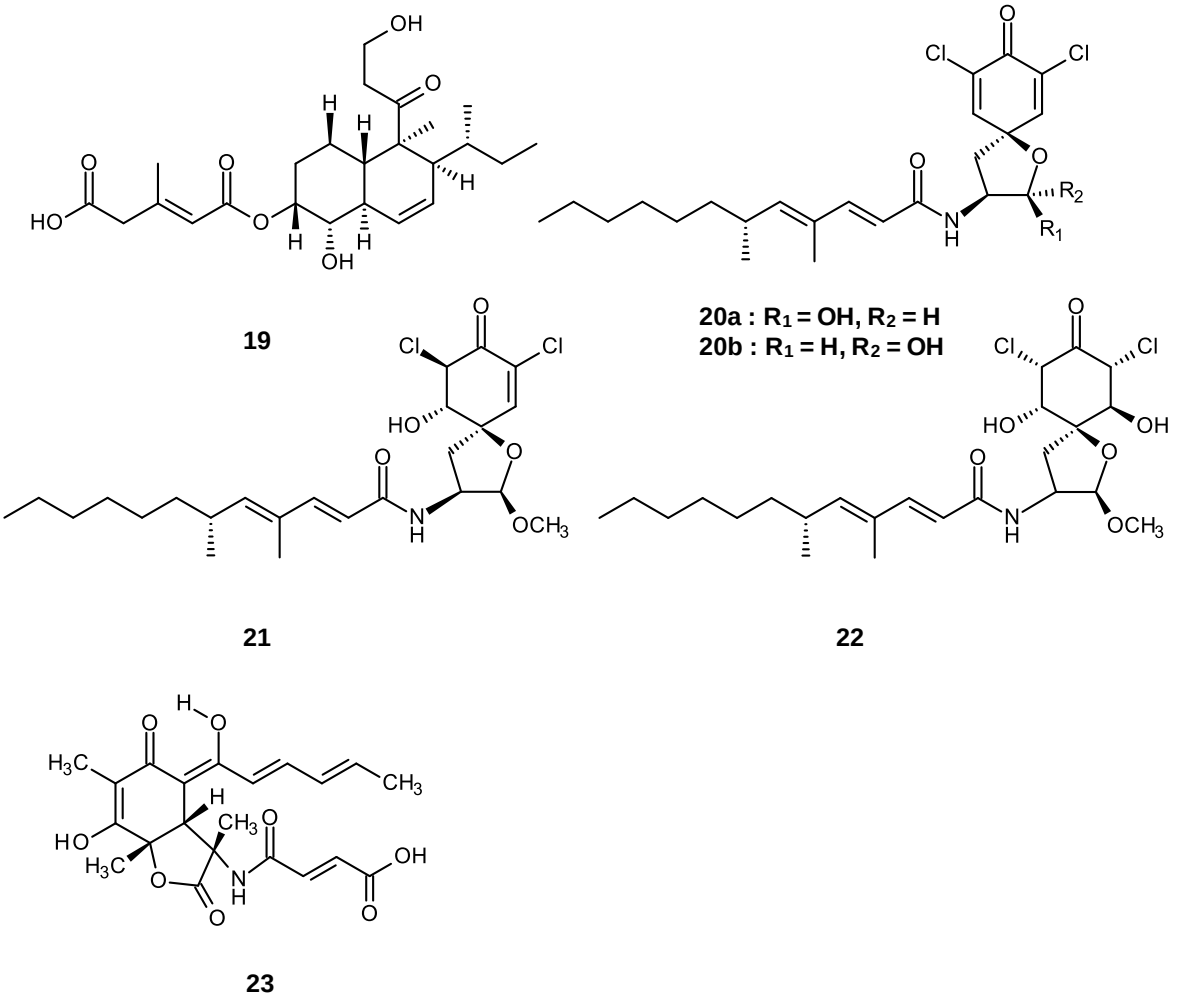

Figure 9. Structures of trichoharzin (**19**), gymnastatins A-C (**20-22**) and sorbicillactone A (**23**)

1.4.2 Marine algae-associated fungi

Algae represent an important source of marine fungi with almost one third of all known higher marine fungi are associated with algae (Bugni and Ireland 2004; Jones and Pang, 2012; Kohlmeyer and Kohlmeyer, 1979). Additionally, algae are one of the most prevalent sources of marine-derived fungi for chemical studies (Rateb and Ebel, 2011). A number of studies have demonstrated that algae-inhabiting fungi were responsible for the production of many bioactive secondary metabolites, which were previously attributed to the host (Flewelling *et al*., 2015; Overy *et al*., 2014). Natural Products isolated from marine algae-derived fungi have been the subject of many chemical reports in the past decades especially during 2002 to mid-2015. A number of new compounds have been isolated and identified, with a wide range of biological properties including anticancer, antibiotic, antiviral, antioxidative and antikinase activities (Zhang *et al*., 2016). An example of bioactive compound is plinabulin (NPI-2358) (**24**), which was isolated from a marine alga-associated *Aspergillus sp*. CNC-139 (Kanoh *et al*., 1997). This compound inhibits tubulin assembly and acts as a vasculature disrupting agent that destabilizes the tumor vascular endothelial architecture and leads to cell damage (Nicholson *et al*., 2006). Another examples is the new meroterpene arisugacin K (**25**), isolated from the fungal strain *Penicillium echinulatum* pt-4, which was isolated from the marine red alga *Chondrus ocellatus*. This compound showed inhibitory activity against *Escherichia coli* with an inhibition diameter 8 mm at 30 µg/disk (Li *et al*., 2014).

A new nitrobenzoyl sequiterpenoid, 6β-9α-dihydroxy-14-*p*-nitrobenzoylcinnamolide (**26**) was isolated from a marine derived fungus *Aspergillus ochraceus* Jcma1F17, which was derived from a marine alga *Coelarthrum sp*. Compound **26** showed significant cytotoxicity against 10 human cancer cell lines (K562, H1975, U937, Molt-4, BGC-823, HL60, MCF-7, A549, Hela, and Huh-7) with IC_{50} values ranging from 1.95 μM to 6.35 μM, in addition to the antiviral activity against the influenza virus A/Hong Kong/8/68 (H3N2) and the human enterovirus 71 (EV71) (Fang *et al*., 2014). Two new oxepine-containing diketopiperazine alkaloids: varioloids A (**27**) and B (**28**) from the fungus *Paecilomyces variotii* EN-291, which was isolated from the marine red alga *Grateloupia turuturu* were found to exhibit potent inhibitory activity against the pathogenic fungus *Fusarium graminearum* with MIC values of 8 and 4 μg/mL, respectively (Zhang *et al*., 2015).

Moreover, a structurally unique 3*H*-oxepine-containing alkaloid, varioxepine A (**29**), which was isolated from the marine alga-derived endophytic fungus *Paecilomyces variotii* showed antimicrobial activity against several human- and aqua-pathogenic bacteria *Aeromonas hydrophila*, *Staphylococcus aureus*, *Vibrio anguillarum*, *E. coli*, *Micrococcus luteus*, *Vibrio harveyi* and *Vibrio parahemolyticus* with MIC values ranging from 16 to 64 μg/mL as well as plant pathogenic fungus *Fusarium graminearum* with an MIC value 4 μg/mL (Zhang *et al*., 2014). Compounds **24-29** are not well represented in the pipelines of drugs and none of them currently is on the market. Only pinabulin (**24**), a synthetic cyclic peptide analog of halimide, is in

phase II clinical trial for treatment of non-small cell lung cancer (Bhatnagar and Kim, 2010; Jin *et al*., 2016)

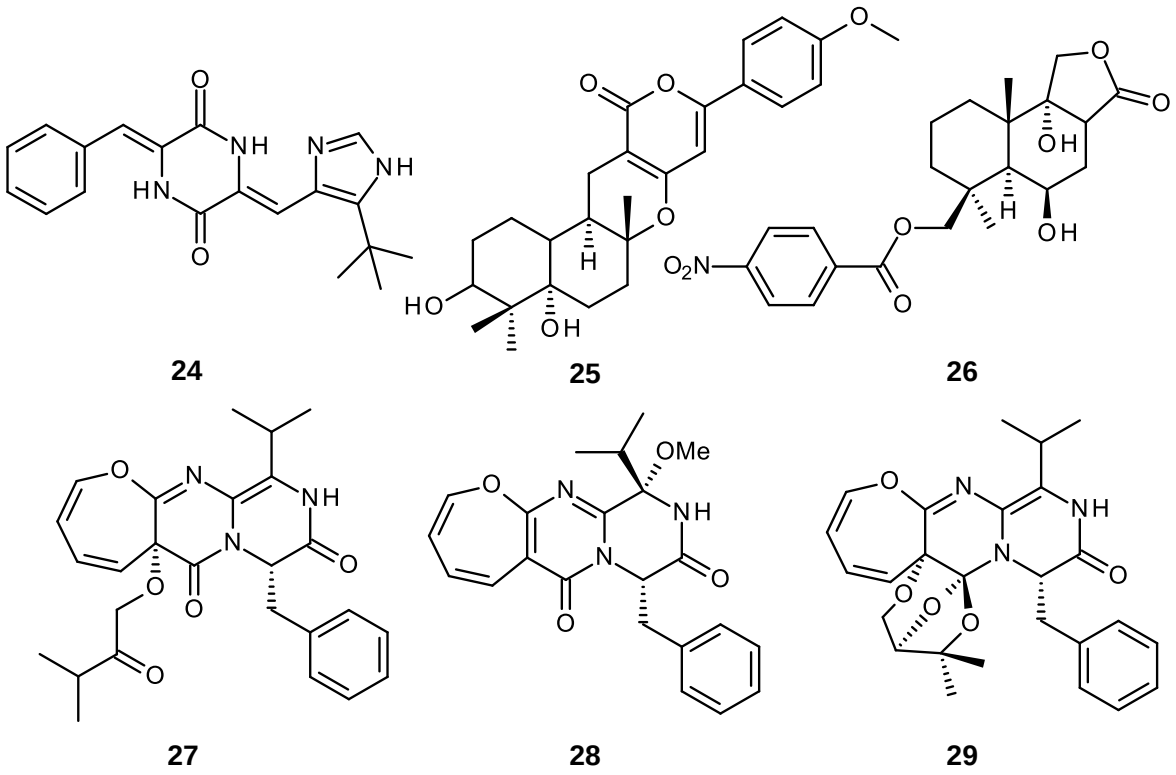

Figure 10. Structures of plinabulin (**24**), arisugacin K (**25**), 6β-9α-dihydroxy-14-*p*-nitrobenzoylcinnamolide (**26**), varioloids A and B (**27** and **28**) and varioxepine A (**29**)

1.4.3 Marine coral-associated fungi

Corals are sessile marine invertebrates which are generally categorized into hard, soft or gorgonian type organisms. Marine soft corals are known to produce a wide array of secondary metabolites, particularly diterpenoids and steroids, which are often characterized by uncommon structural features and potent bioactivities (Putra and Murniasih, 2016). The diterpene glycosides pseudopterosins A-D (**30-33**) (Figure 11) isolated from the Caribbean gorgonial coral *Pseudopterogorgia elisabethae*, showed anti-inflammatory activity and are in phase II of clinical trial (Faulkner, 2000b; Mayer *et al*., 2010; Newberger *et al*., 2006; Newman and Cragg, 2004; Rouhi, 1995; Yauan *et al*., 2006). In addition, these compounds are effective in preventing sun damage to the skin and have a nourishing property to the skin. Due to their excellent anti-inflammatory and analgesic activities, pseudoterosins A-D (**30-33**) are currently incorporated into skin care preparations (Pomponi, 1999).

Interestingly, the presence of the fungi associated with corals suggests that beneficial interactions between fungi and corals are accumulating and current challenges include the elucidation of the metabolites (Yarden, 2014). The structurally unique metabolites with biological and pharmacological activities oxalicumones D and E (**34** and **35**) were isolated from a culture broth of marine gorgonian-associated fungus *Penicillium oxalicum* SCSGAF 0023. Compounds **34** and **35** showed significant cytotoxicity against several carcinoma cell lines with IC_{50} less than 10 µM (Bao *et al*., 2014). The fungal strain *Aspergillus terreus* SCSGAF0162, which was

isolated from the gorgonian coral *Echinogorgia aurantiaca* produced three lactones including the territrem derivativies, territrem D (**36**), territrem E (**37**), 11α, dehydroxyisoterreulactone A (**38**) and isobutyrolactone II (**39**). Compounds **36** and **37** showed strong inhibitory activity against acetylcholinesterase with IC_{50} 4.2 ± 0.6 and 4.5 ± 0.6 µM, respectively. While compounds **38** and **39** showed antiviral activity towards HSV-1 with IC_{50} 16.4 ± 0.6 and 21.8 ± 0.8 µg/mL, respectively, compound **36** exhibited potent antifouling activity with EC_{50} 12.9 ± 0.5 µg/mL toward barnacle *Balanus Amphitrite* larvae (Nong *et al*., 2014). Therefore, numerous compounds isolated from different species of marine coral-associated fungi can be exploited in various applications due to their different biological and pharmacological properties.

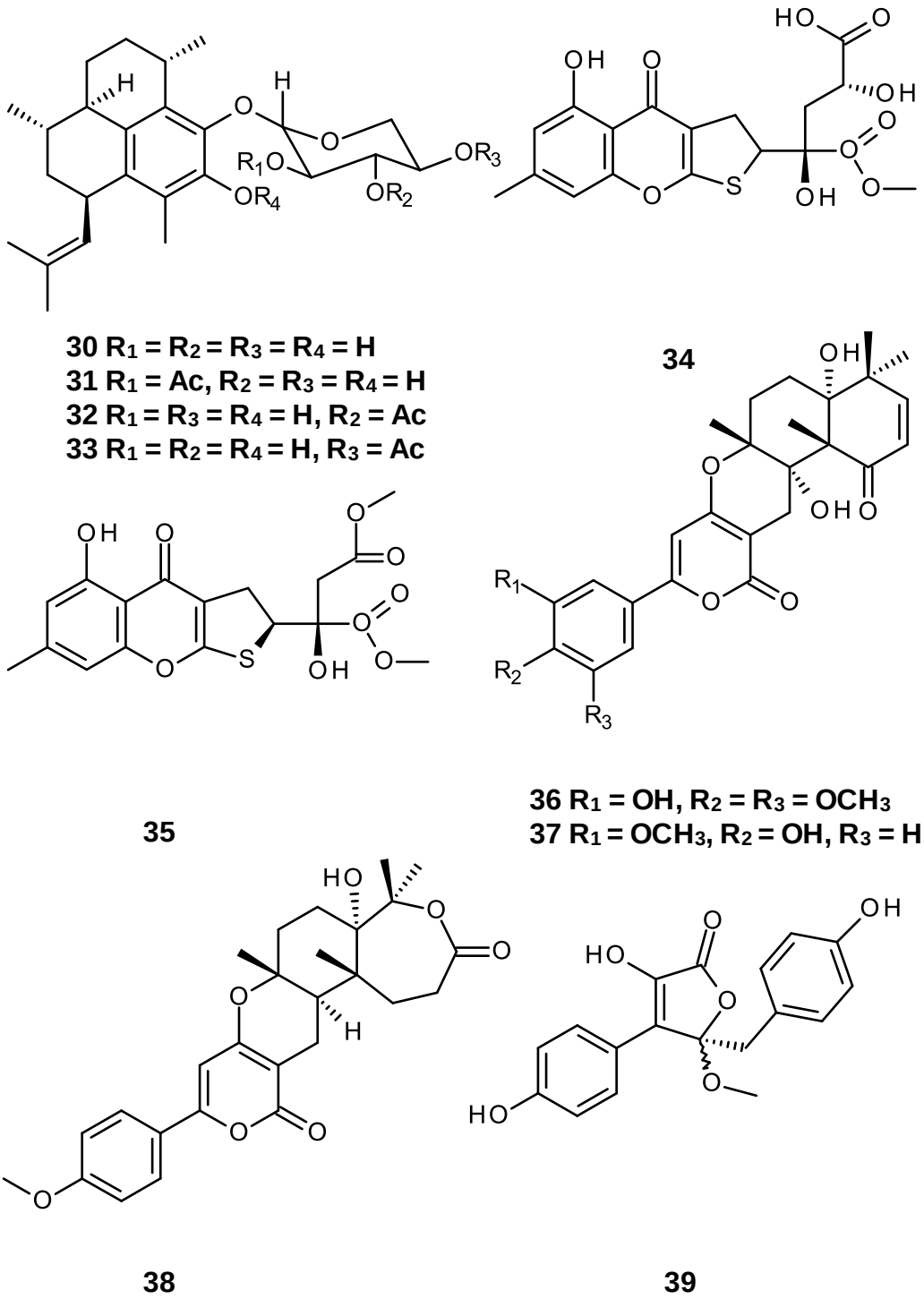

Figure 11. Structures of pseudopterosins A-D (**30-33**), oxalicumones D and E (**34** and **35**), territrems D and E (**36** and **37**), 11α, dehydroxyisoterreulactone A (**38**) and isobutyrolactone II (**39**)

1.4.4 Mangrove-associated endophytic fungi

Mangroves are tropical and subtropical wetlands forest harboring a great diversity of marine fungi (Shearer *et al*., 2007). Mangrove-derived fungi constitute the second largest ecological group of the marine fungi and many of them are new or inadequately described species (Sridhar, 2004). Many mangrove-derived fungi are found to produce chemicals with novel functions and structures (Kobayashi and Tsuda, 2004). Approximately 90% of mangroves are distributed in South-East Asia, America and Africa (Shearer *et al*., 2007). According to Kohlmeyer and Kohlmeyer (1979), the marine fungi found in the mangrove habitat live on roots, stems and twigs submerged in water while their terrestrial counterparts inhabit on lower stem, branches and upper parts of the roots above the water surface. Mangrove-derived fungi can be categorized into saprophytic, parasitic and symbiotic fungi (Cheng *et al*., 2009; Thatoi *et al*., 2013). Among the different groups of mangrove-derived fungi, mangrove endophytic fungi are considered to have a great potential for applications in pharmaceutical and nutraceutical industries to produce antibiotic, antidiabetic, antiviral, anti-inflammatory, anticancer, antioxidant and immunosuppressive drugs and therapeutic agents (Balagurunathan and Radhakrishnan, 2007).

More than twenty years after Taxol (paclitaxel) (**7**) was discovered from the bark of *Taxus brevifolia*, Strobel *et al*. isolated a novel taxol producing endophytic fungus, *Taxomyces andreanae*, from *Taxus brevifolia* (Strobel *et al*., 1993). In the

following years, further endophytic fungi such as *Pestalotiopsis microspore* (Strobel *et al*., 1996), *Seimatoantlerium tepuiense* (Strobel *et al*., 1999), *Periconia sp*. (Li *et al*., 1998), have also been reported to be producers of taxol and their derivatives. A quinoline indole alkaloid, camptothecin (CPT) (**40**), which was commercially exploited as an anticancer agent, was first isolated from the bark and stem of *Camptotheca acuminata*, a plant used in traditional medicine. Later on, camptothecin and its analogs were found to be produced by the cultures of an endophytic fungus of *Camptotheca acuminate* (Kusari *et al*., 2009). A new aromatic amine pestalamine A (**41**), isolated from the mangrove-derived endophytic fungus *Pestalotiopsis vaccinii* showed moderate cytotoxic activity against human cancer cell lines MCF-7 (breast cancer), HeLa (cervical cancer), and HepG2 (hepatic carcinoma) with IC_{50} values of 40.3, 22.0, and 32.8, respectively (Zhou *et al*., 2014). Moreover, a new aromatic butyrolactone, flavipesin A (**42**), isolated from marine-derived endophytic fungus *Aspergillus flavipes* AIL8, which was isolated from the inner leaves of mangrove plant *Acanthus ilicifolius,* displayed significant antibacterial activity against *Staphylococcus aureus* and *Bacillus subtillis* with MIC values of 8.0 and 0.25 µg/mL respectively, and also showed the unique antibiofilm activity by decreasing the number of living cells embed in the biofilm matrix OD values from 390.6 to 97.7 µg/mL ($p<0.01$). Compound **42** could penetrate the biofilm matrix and kill the living bacteria inside the mature *S. aureus* biofilm (Bai *et al*., 2014). Therefore, endophytic fungi can represent an interesting source of new lead structures for pharmaceutical and agrochemical applications.

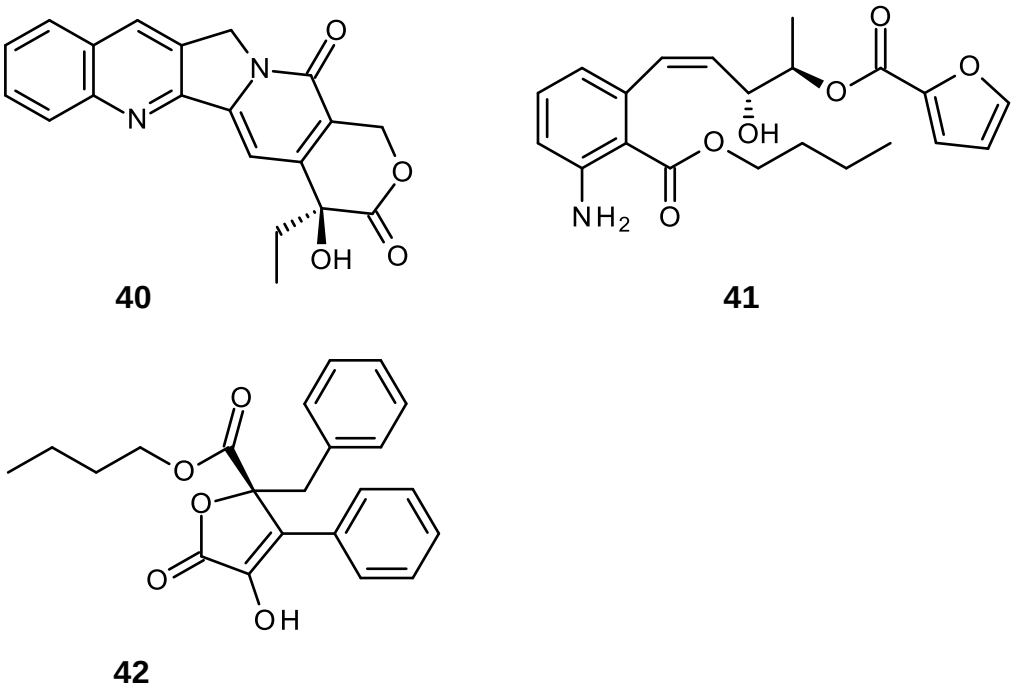

40 **41**

42

Figure 12. Structures of camptothecin (**40**), pestalamine A (**41**) and flavipesin A (**42**)

1.5 Aim and Scope of the Study

The main goal of this study was to isolate and identify new and bioactive natural products from the cultures of marine-derived fungi isolated from marine organisms such as corals, sponges and algae as well as mangrove-derived endophytic fungi. To achieve this aim four fungal strains belonging to the genera *Talaromyces*, *Neosartorya* and *Eurotium* which were isolated from soft coral, marine sponge and mangrove, were taxonomically identified and cultured in cooked-rice medium to produce secondary metabolites for this study.

1.5.1 Isolation and chemical investigation of selected fungal strains

In order to isolate the secondary metabolites, the crude extracts were prepared from the cultures of the marine-associated fungi on solid media (cooked rice) and fractionated by column chromatography. The constituents of the extracts were isolated and purified by crystallization and also by different chromatographic techniques. The structures of the compounds were elucidated by extensive analysis of the 1D and 2D NMR spectra, IR and HRMS. The absolute configurations of the stereogenic carbons of the new compounds were established by X-ray analysis when the compounds were obtained as suitable crystals otherwise the comparison of the experimental and calculated ECD spectra or chiral HPLC were used.

1.5.2 Biological evaluation of the isolated pure compounds

The pure compounds were evaluated by different bioassays for their biological activities. Antibacterial, antifungal and antibiofilm assays were performed using Gram-positive and Gram-negative bacteria, as well as multidrug-resistant isolates from the environment.

CHAPTER II

CHEMISTRY OF THE GENERA

TALAROMYCES, *NEOSARTORYA* AND *EUROTIUM*

2. An Overview of Secondary Metabolites and Biological Activities

The marine-derived fungi selected for the study in this thesis belong to three distinct genera, namely *Talaromyces* (*Talaromyces helicus* KUFA 0063), *Neosartorya* (*Neosartorya takakii* KUFC 7898 and *Neosartorya glabra* KUFA 0702) and *Eurotium* (*Eurotium chevalieri* KUFA 0006).

While the genus *Talaromyces* is a sexual state of *Penicillium*, the genera *Neosartorya* and *Eurotium* are sexual state of *Aspergillus*. According to Visagie *et al*. (2014), *Aspergillus*, *Penicillium* and *Talaromyces* are among the most chemically inventive of all fungi, producing a wide array of secondary metabolites.

Talaromyces species are commonly isolated from soil, indoor environment, humans with penicilliosis and food products (Yilmaz *et al*., 2014). Several bioactive secondary metabolites including alkaloids, peptides, lactones, polyketides, and compounds with miscellaneous structural types were reported from members of this genus (Zhai *et al*., 2016). On the other hand, *Aspergillus* sections include many important species because they can be pathogenic or allergenic to man as well as causing food spoilage and producing mycotoxins. A large number of novel compounds, including alkaloids, peptides, polyketides, terpenes, sterols, and cerebroside analogues, have been isolated from this genus and most of the compounds exhibit interesting biological properties (Lee *et al*., 2013). Consequently,

the following literature review focuses on novel chemical structures reported for members of the genera *Talaromyces* and *Aspergillus* reported with references to their biological activities.

2.1 *Talaromyces* Species

The genus *Talaromyces* (Family Trichocomaceae) was introduced by Benjamin (1955) as a sexual state of *Penicillium* that produces soft walled ascomata covered with interwoven hyphae, which was re-defined by Stolk and Samson (1972) and was restricted to species producing asci borne in chains. The genus *Talaromyces* is an important fungal genus because of its ubiquity and as rich sources of biologically active novel compound (Liu *et al*., 2010). They have a worldwide distribution, being recorded from soil, indoor, food, and waste (Pitt and Hocking, 1997; Samson and Pitt, 2000). The present review covers the secondary metabolites of *Talaromyces* section which includes five species, namely *T. flavus*, *T. wortmannii*, *T. thailandiasis*, *T. helicus* and *T. stipitatus*, as well as unspecified species. Many of these metabolites showed biological activities.

2.1.1 *Talaromyces flavus*

A new antibiotic, fosfonochlorin (**43**) (Figure 13) was isolated from the strain *Talaromyces flavus* SANK 15680, which was isolated from a soil sample collected at Taga-cho, Inugami-gun, Shiga Prefecture, Japan. Fosfonochlorin (**43**) was active against *Proteus mirabilis* and *Proteus vulgaris* and weakly active against *Salmonella enteritidis*, *Klebsiella pneumonia* and *Providencia rettgeri* but inactive against other bacteria tested at a concentration of 200 µg/mL (Takeuchi *et al*., 1989).

Seven new compounds including 4, 6-dihydroxy-5-methylphthalide (**44**), methyl 4-carboxy-5-hydroxyphthalaldehydate (**45**), 7-hydroxy-2, 5-dimethylchromone (**46**), 3-hydroxymethyl-6, 8-dimethoxycoumarin (**47**), desmethyldehydroaltenusin (**48**), talaroflavone (**49**) and deoxytalaroflavone (**50**) (Figure 13) were isolated from the soil fungus *T. flavus* (Ayer and Racok, 1990).

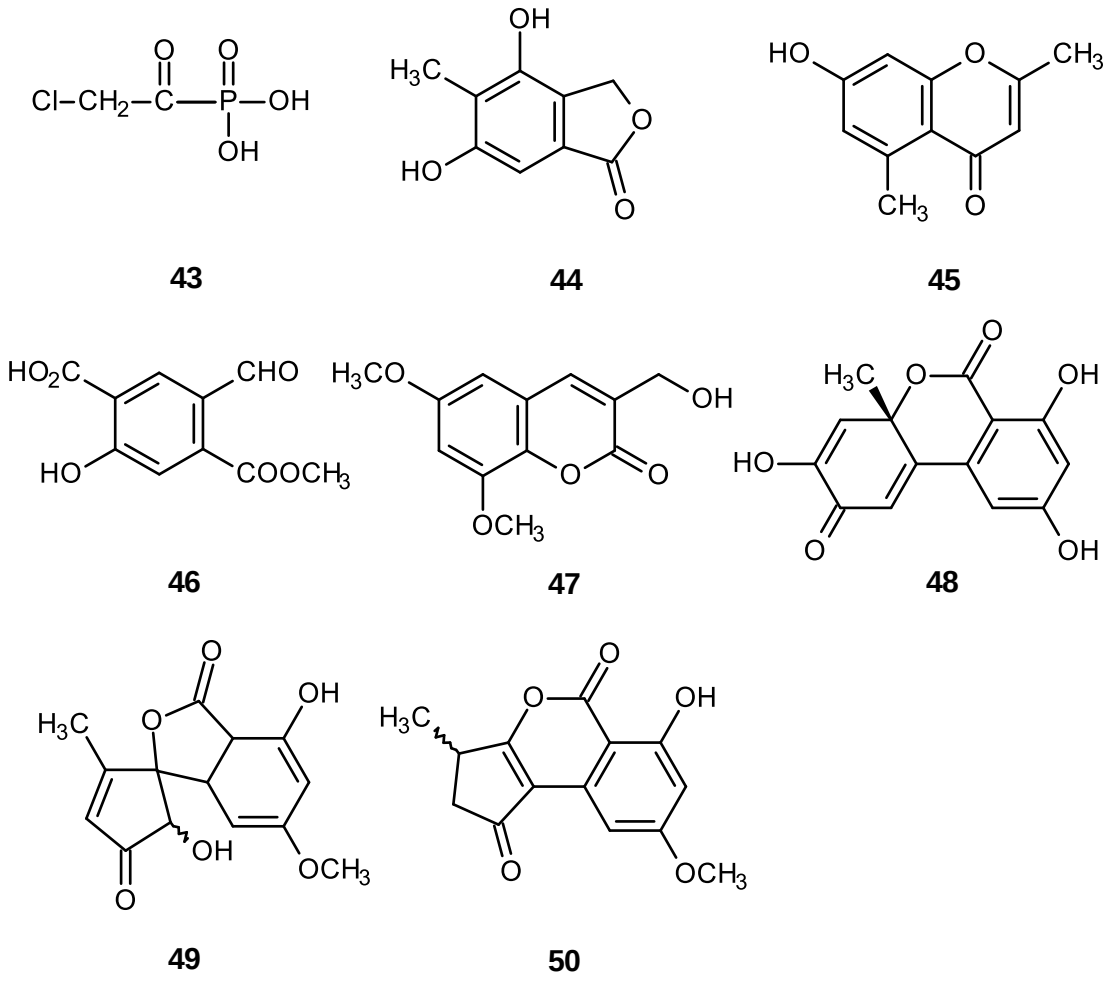

43 **44** **45**

46 **47** **48**

49 **50**

Figure 13. Secondary metabolites isolated from *Talaromyces flavus* (**43-50**)

Tabata *et al*. (1999) reported the isolation of a new azaphilone-type metabolite, diazaphilonic acid (**51**) (Figure 14) was produced by a fermentation of *T. flavus* PF 1195. Compound **51** inhibited DNA amplification by polymerase chain reaction (PCR) with DNA polymerase with the IC_{50} value of 2.6 µg/mL. This

compound also inhibited the telomerase activity of human leukemia MT1 showing almost complete inhibition at 50 µM. On the contrary, compound **51** displayed no antimicrobial activity against Gram positive bacteria *Bacillus subtilis* ATCC 6633, *Micrococcus luteus* ATCC 9341, *Staphylococcus aureus* 209P and Gram negative bacteria *Escherichia coli* NIHJ, as well as several kinds of yeast *Saccharomyces cerevisiae* SHY3, *Candida albicans* M9001, *Candida pseudotropicalis* M9035, *Cryptococcus neoformans* M9010, *Debaryomyces hansenii* M9011, *Trigonopsis variabilis* M9031, *Schizosacchromyces pombe* M9025 and *Hansenula schneggi* IAM4269.

A novel metabolite, funicone-related compound actofunicone (**52**) (Figure 14) was isolated from the culture broth of *T. flavus* FKI-0076 which was isolated from the soil sample. Compound **52** showed no effect on the growth of *Candida albicans* up to 300 µM; however, this compound became inhibitory when administered in association with myconazole (Arai *et al*., 2002).

Another funicone derivative, 9, 14-epoxy-11-deoxyfunicone (**53**) (Figure 14) was isolated from the ethyl acetate extract of *T. flavus* IFM52668. Compound (**53**) exhibited the weak antifungal activity against *Aspergillus niger* with an 10 mm inhibition zone at 200 µg/disc (Komai *et al*., 2004).

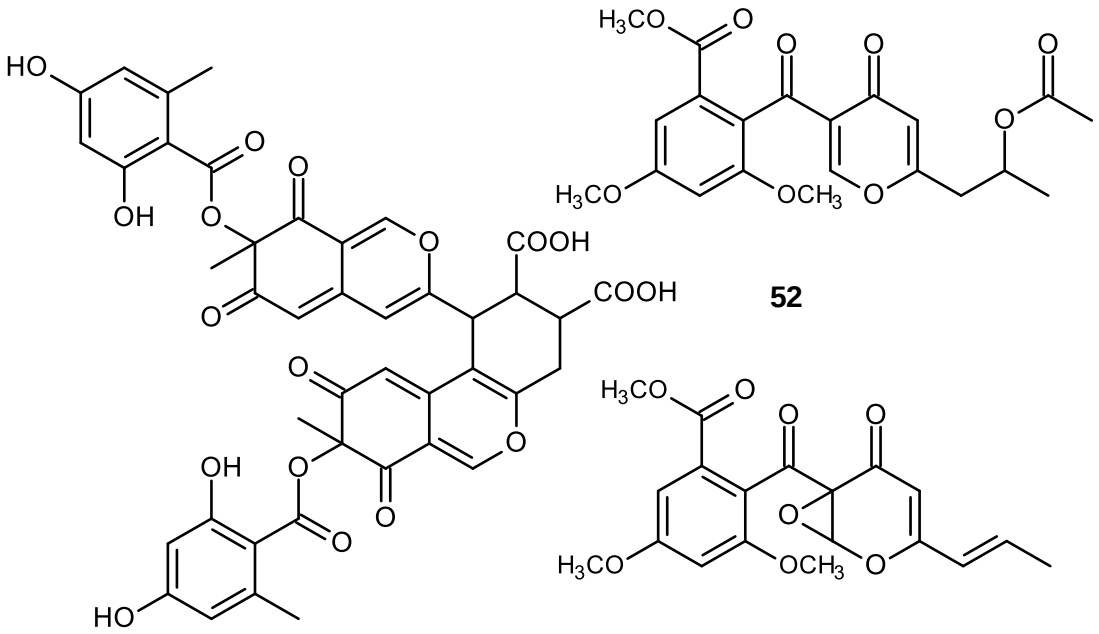

51 **52** **53**

Figure 14. Structures of diazaphilonic acid (**51**) actofunicone (**52**) and 9, 14-epoxy-11-deoxyfunicone (**53**)

Four new norsesquiterpene peroxides, talaperoxides A-D (**54-57**) (Figure 15) were isolated from the mangrove endophytic fungus, *T. flavus*. Compounds **55** and **57** showed cytotoxic activity against human breast cancer cell lines MCF-7 and MDA-MB-435, human hepatoma cell line HepG2, human cervical cancer cell line HeLa and human prostatic cancer cell line PC-3 with IC_{50} values between 0.70 and 2.78 μg/mL. However, none of the compounds showed antimicrobial activity against *Staphylococcus aureus* ATCC 27154, *Escherichia coli* ATCC 25922, *Sarcina*

ventriculi ATCC 29068, *Pseudomonas aeruginosa* ATCC 25668, *Candida albicans* ATCC 10231 or *Aspergillus niger* ATCC 13496 at a concentration of 50 µg/mL. All norsesquiterpene peroxides **54-57** exhibited lethal activity against brine shrimp *Artemia salina* with LD_{50} < 10 ppm (Li *et al*., 2011b).

A new nardosinane-type sesquiterpene, talaflavuterpenoid A (**58**) (He *et al*., 2014a) and two new coumarines, talacoumarins A and B (**59** and **60**) (He *et al*., 2014c) were isolated from the wetland soil-derived fungus *T. flavus* BYD07-13. These three compounds **58-60** exhibited no cytotoxic effects on five human tumor cell lines: HL-60 (human myeloid leukemia), SMMC-7721 (hepatocellular carcinoma), A-549 (lung cancer), MCF-7 (breast carcinoma) and SW480 (colon cancer) with IC_{50} > 40 µM as compared to cisplatin and also antimicrobial activity against *Escherichia coli*, *Staphylococcus aureus*, *Candida albicans*, and *Aspergillus niger* with MIC > 1.0 mg/mL. Compounds **59** and **60** showed moderate anti-$A\beta_{42}$ aggregation activity, with relative inhibitory rates of 49.33 ± 3.16 % and 44.99 ± 3.64 % at the concentration of 100 µM (He *et al*., 2014a; He *et al*., 2014c).

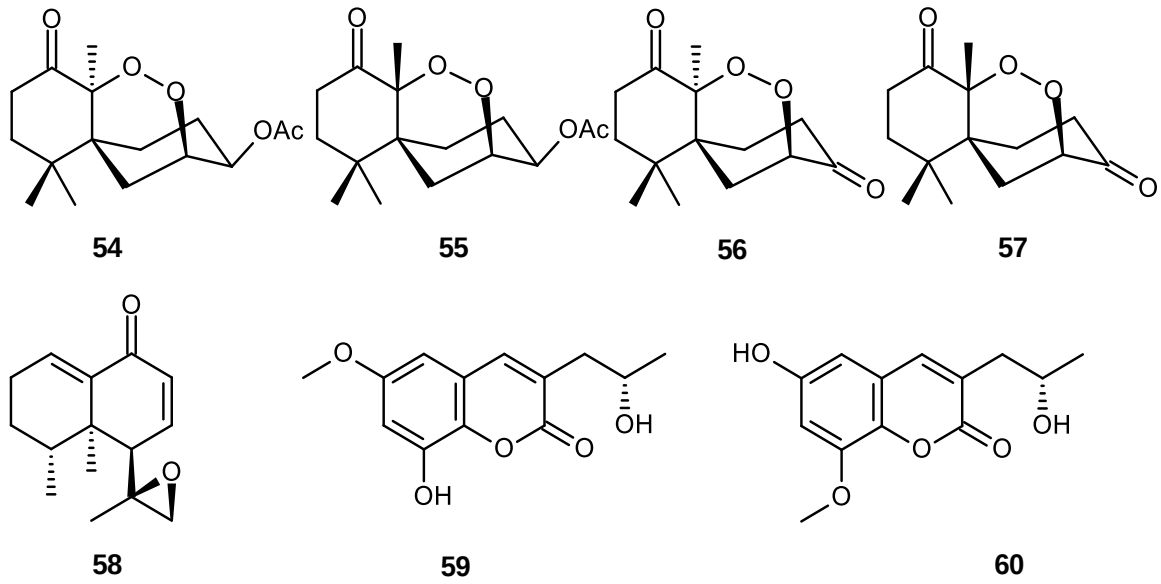

Figure 15. Structure of talaperoxides A-D (**54-57**), talaflavuterpenoid A (**58**) and talacoumarins A and B (**59** and **60**)

Additionally, six new polyesters, talapolyesters A-F (**61-66**) (Figure 16) were obtained from the soil-derived fungus *T. flavus* BYD07-13. Compound **65** and **66** exhibited cytotoxic activity against five human tumor cell lines: HL-60 (myeloid leukemia), SMMC-7721 (hepatocellular carcinoma), A-549 (lung cancer), MCF-7 (breast cancer) and SW480 (colon cancer) with IC_{50} 14.81, 18.39, 17.66, 14.59, 26.62 and 13.62, 15.74, 11.09, 15.96, 15.54 μM, respectively. However, compounds **61-64** showed no cytotoxic activity against five tumor cell lines with IC_{50} > 40 μM as compared to cisplatin (He *et al*., 2014b).

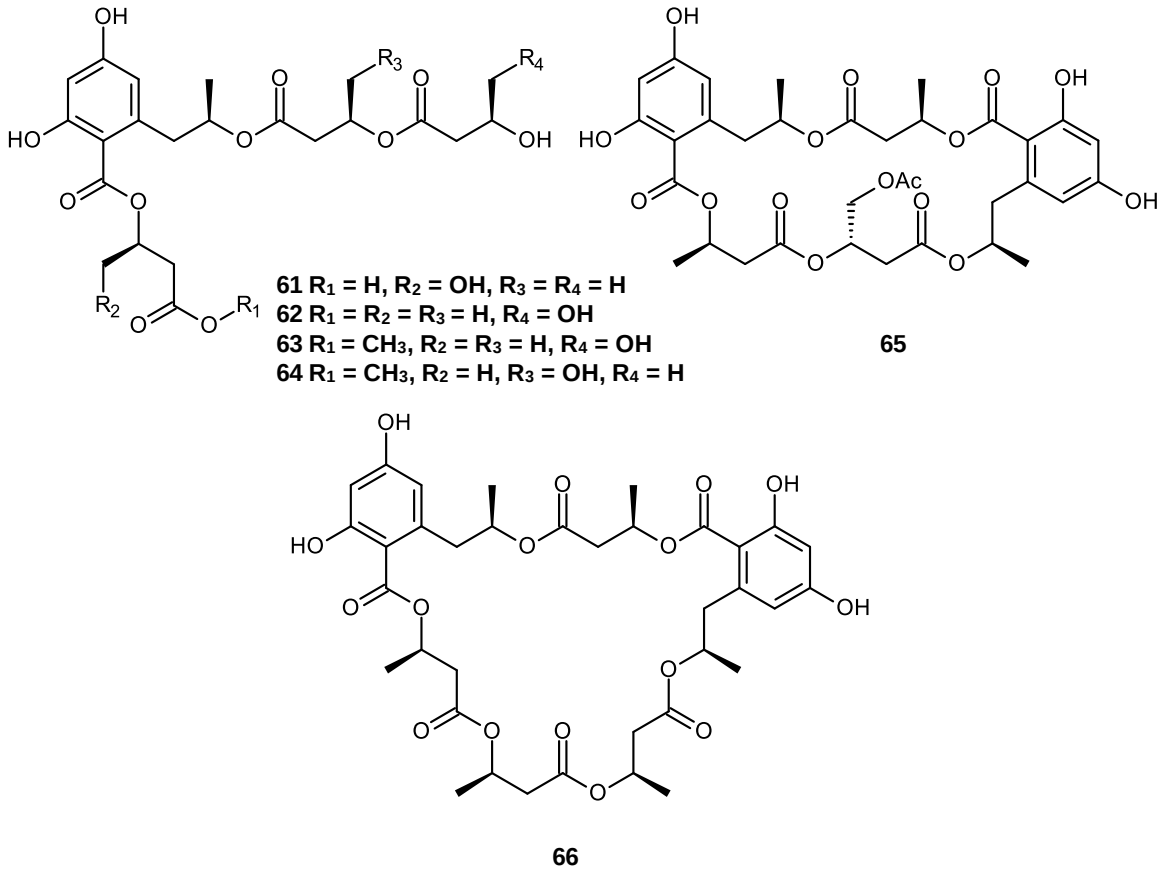

Figure 16. Structures of talapolyesters A-F (**61-66**)

A wetland soil-derived fungus *T. flavus* AHK07-3 produced three pairs of new isopentenyl dibenzo [*b*, *e*] oxepinone enantiomers (+)-(5*S*)-arugosin K (**67**), (−)-(5*R*)-arugosin K (**68**), (+)-(5*S*)-arugosin L (**69**), (−)-(5*R*)-arugosin L (**70**), (+)-(5*S*) arugosin M (**71**), (−)-(5*R*)-arugosin M (**72**) and a new isopentenyl dibenzo [b, e] oxepinone, arugosin N (**73**) (Figure 17) (Sun *et al*., 2016). Later on, the same authors (Sun *et al*., 2017) have described isolation of four stereoisomers of sequoiatones (**74-77**) by chiral HPLC (Figure 17) from the same fungus.

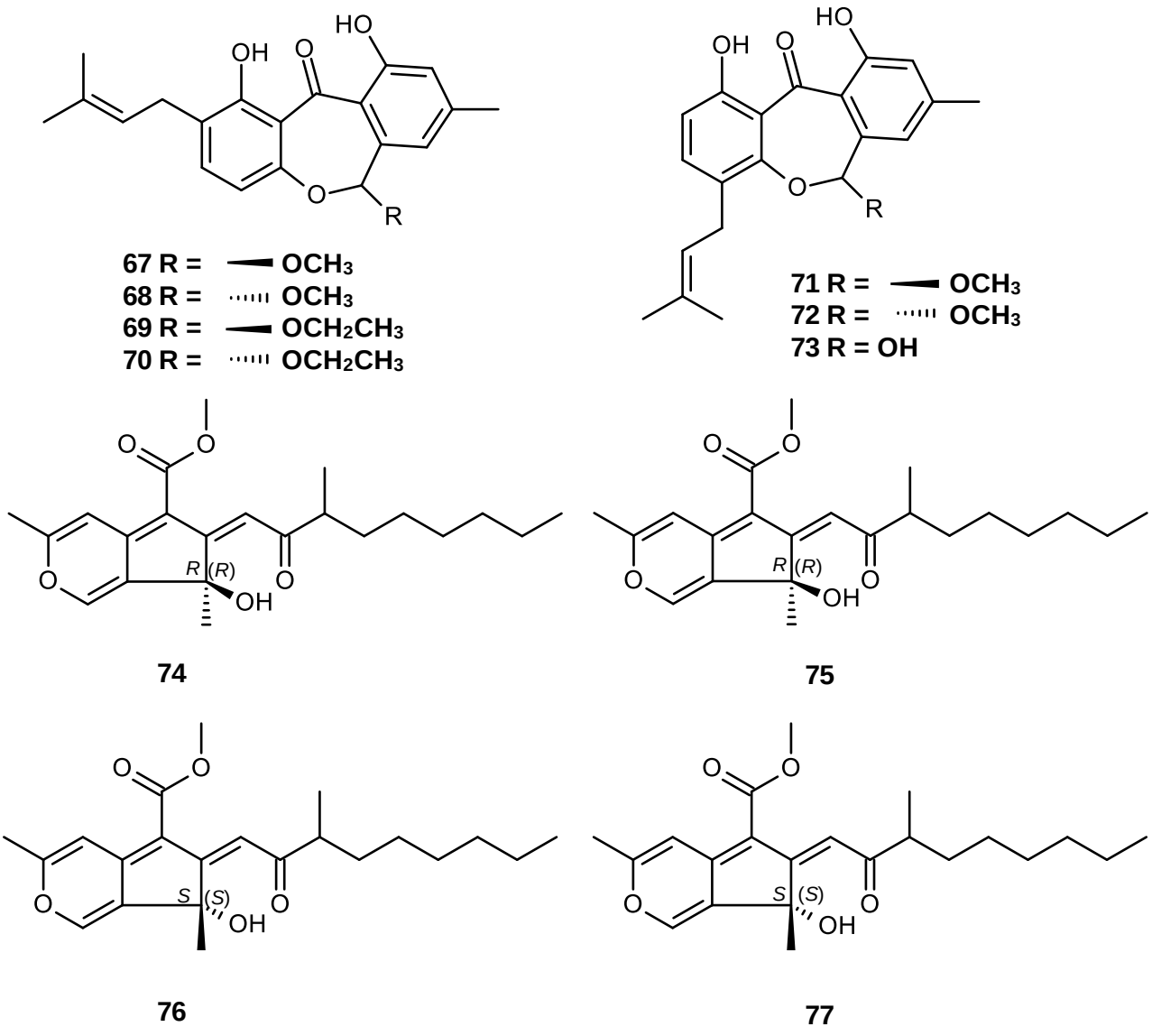

Figure 17. Secondary metabolites isolated form *Talaromyces flavus* AHKO7-3 (**67-77**)

2.1.2 *Talaromyces wortmannii*

Talaromyces wortmannii, isolated from a soil sample collected in China's Yunnan province, produced wortmannilactones A-D (**78-81**) (Figure 18). Compounds **78-81** exhibited in vitro cytotoxic activity against a panel of human cancer cell lines HCT-5 and HCT-115 (colon cancer), A549 (lung cancer), MDA-MB-231 (breast cancer) and K562 (leucocythemia) with the IC_{50} values ranging from 28.7 to 130.5 µM (Dong *et al*., 2006). In 2009, four new secondary metabolites, wortmannilactones E-H (**82-85**), (Figure 18) were isolated from the culture of the soil-derived *T. wormannii*. Compounds **82-85** exhibited inhibitory activities against cathepsin B with IC_{50} values of 4.3, 6.5, 13.0 and 6.0 µM, respectively (Dong *et al*., 2009).

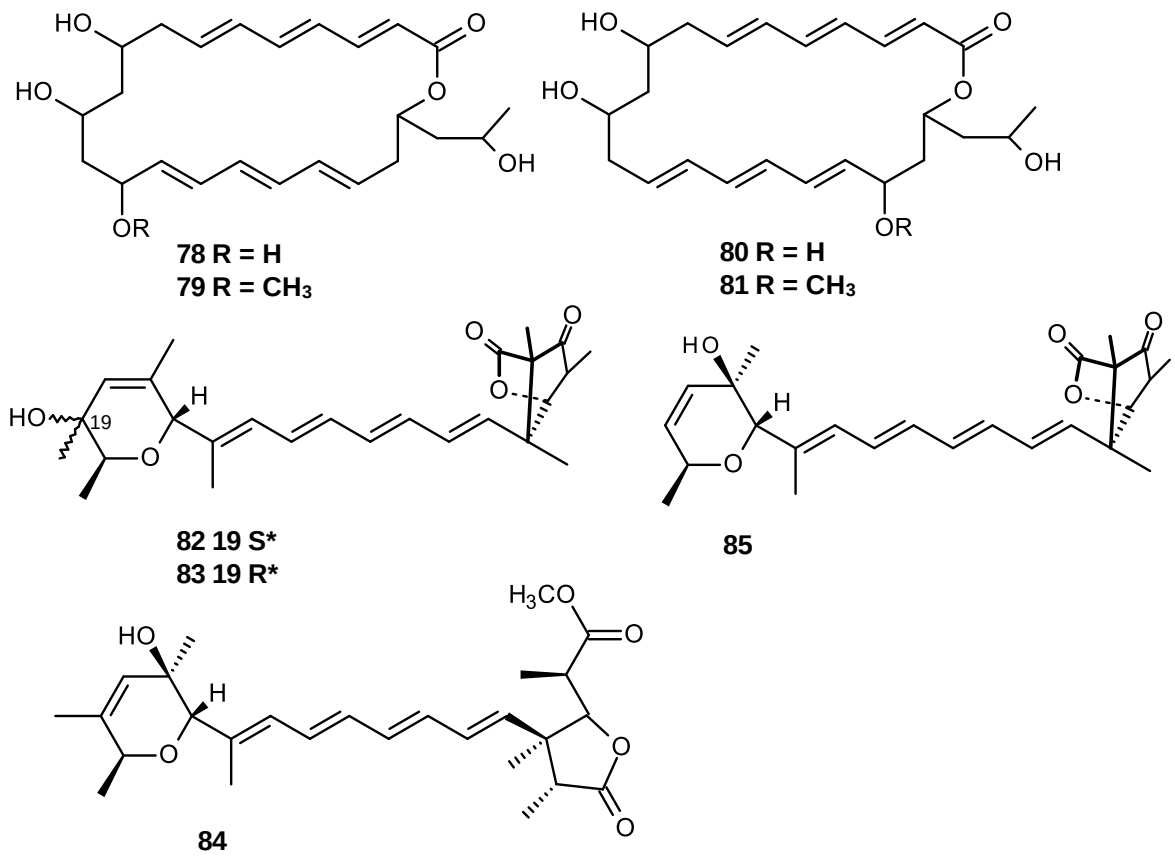

Figure 18. Secondary metabolites isolated from *Talaromyces wortmannii* (**78-85**)

The entophytic fungus *T. wormannii*, which was isolated form *Aloe vera*, produced two new cyclic peptides, talaromins A and B (**86** and **87**) (Bara *et al*., 2013b), in addition to, wortmannin B (**88**) and biemodin (**89**) (Bara *et al*., 2013a) shown in Figure 19. While talaromins A and B (**86-87**) showed neither cytotoxicity against L5178Y (mouse lymphoma cells) nor antibacterial activity against *Staphylococcus aureus* ATCC 29213, *Streptococcus pneumoniae* ATCC 49619, *Escherichia coli* ATCC 25922 and *Klebsiella pneumoniae* ATCC 27799 up to a

concentration of 64 µg/mL, biemodin **89** displayed a strong antibacterial activity against Gram positive bacteria *Staphylococcus epidermidis*, *Streptococcus pneumonia* and *Enterococcus faecalis* with MIC values of 16 µg/mL, especially against Methicillin-resistant *Staphylococcus aureus* MRSA with MIC values of 8 µg/mL (Bara *et al*., 2013a).

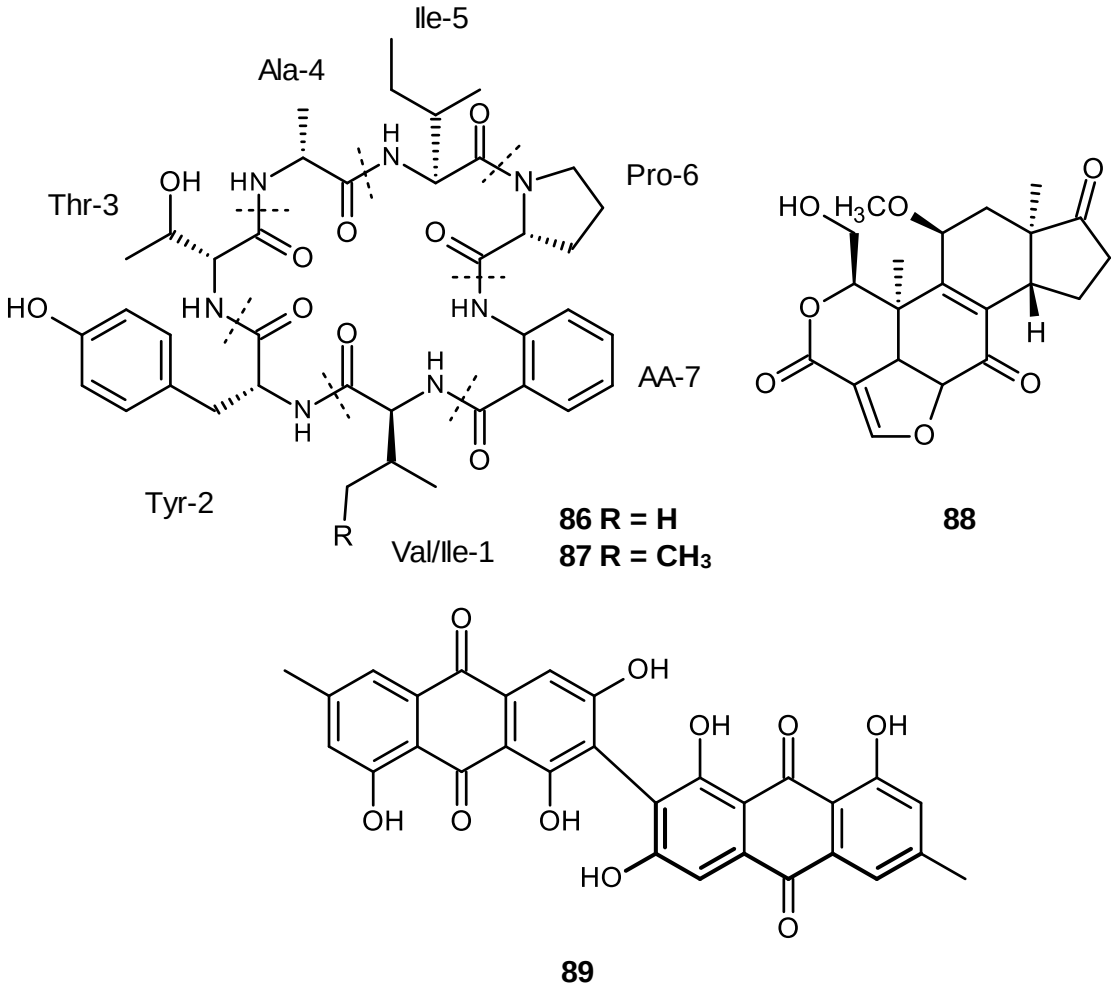

Figure 19. Structures of talaromins A and B (**86** and **87**), wortmannin B (**88**) and biemodin (**89**)

Two previously unreported bisdihydroanthracenones atropodiasteromeric pairs, flavomannins A and B (**90** and **91**), two new unsymmetrical dimers flavomannins C-D (**92-93**) and two new mixed dihydroanthracenone/anthraquinone dimers talaromannin A and B (**94** and **95**) (Figure 20) were isolated from the endophytic fungus *T. wormannii* (Bara *et al*., 2013c). Compounds **90-95** exhibited antibacterial activity against *Staphylococcus aureus*, including (multi) drug-resistant clinical isolates and were predominantly active against *Staphylococci* with the MIC values from 4-8 µg/mL. Reporter gene analyses indicated induction of the SOS response for some of the derivatives, suggesting interference with DNA structure or metabolism. The compounds **90-95** showed no cytotoxic activity against THP-1 human leukemic monocyte cells and BALB/3T3 mouse embryonic fibroblast cells, encouraging their further evaluation as potential starting points for antibacterial drug development.

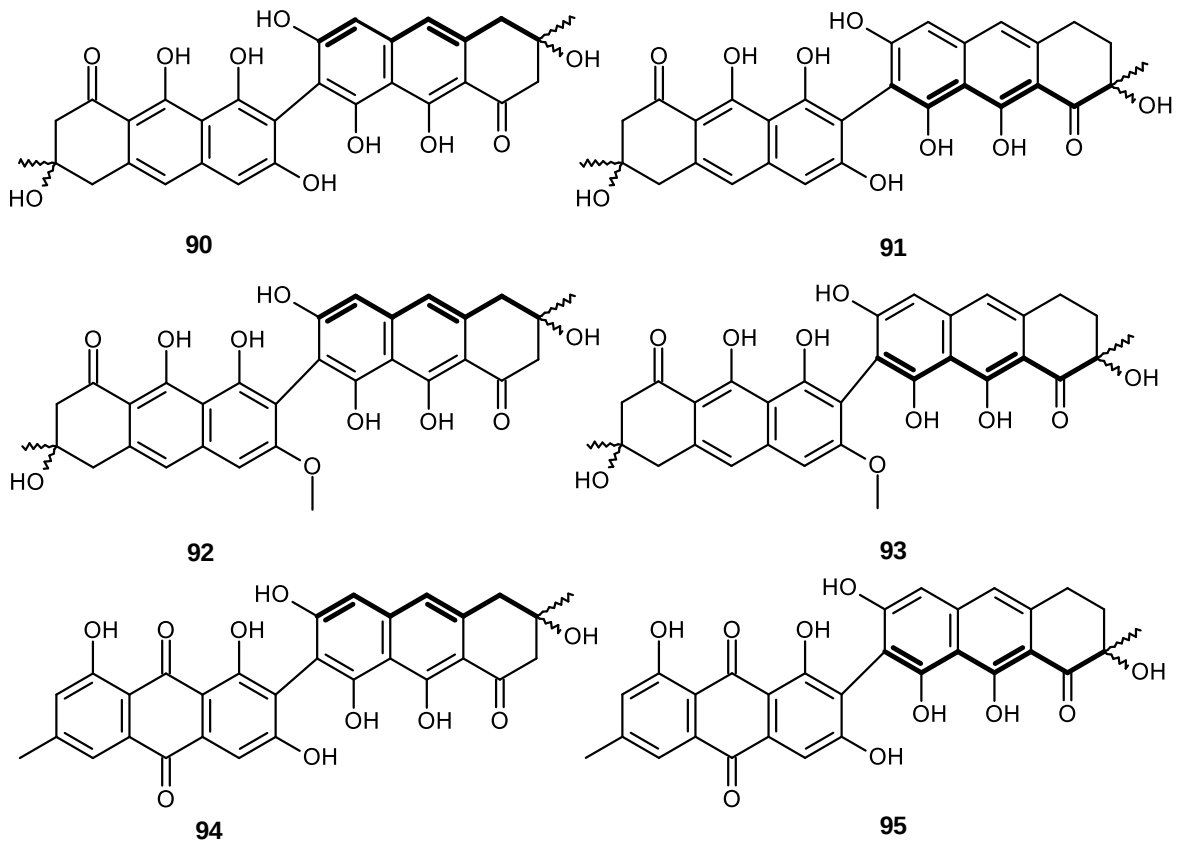

Figure 20. Structures of flavomannins A-D (**90-93**) and talaromannins A and B (**94** and **95**)

A new furanosteroid, secovironolide (**96**) and a new epoxide containing viridian derivative, epoxyvirone (**97**) (Figure 21) were isolated from the culture broth of an endophytic fungus *T. wormannii* LGT-4, which was isolated from the Chinese medicinal plant *Tripterygium wilfordii*. Compound **96** was found to possess a weak monoamine oxidase MAO inhibitory activity with IC_{50} 91.22 µg/mL. However, the

crude extract from the endophytic fungus *Talaromyces wortmannii* LG-4 inhibited the MAO with IC_{50} 50.3 µg/mL (Ding *et al*., 2015).

Fu *et al*. (2016a) have recently isolated two new azaphilones, deacetylisowortmin A (**98**) and deacetylisowortmin B (**99**) (Figure 21) from *T. wortmannii* LGT-4. Both compounds were evaluated for the monoamine oxidase (MAO) and acetylcholinesterase (AChE) activities and they showed neither of these activities. Nearly simultaneously, the same group also isolated four new wortmannin derivatives, wortmannines A-D (**100-103**) (Figure 21) together with other previously described compounds from the zeistic culture of *T. wortmannii* LGT-4. At 10 µg/mL concentration, compounds **100-103** displayed no cytotoxic activity against anti-HL60 Human promyelocytic leukemia (Fu *et al*., 2016b).

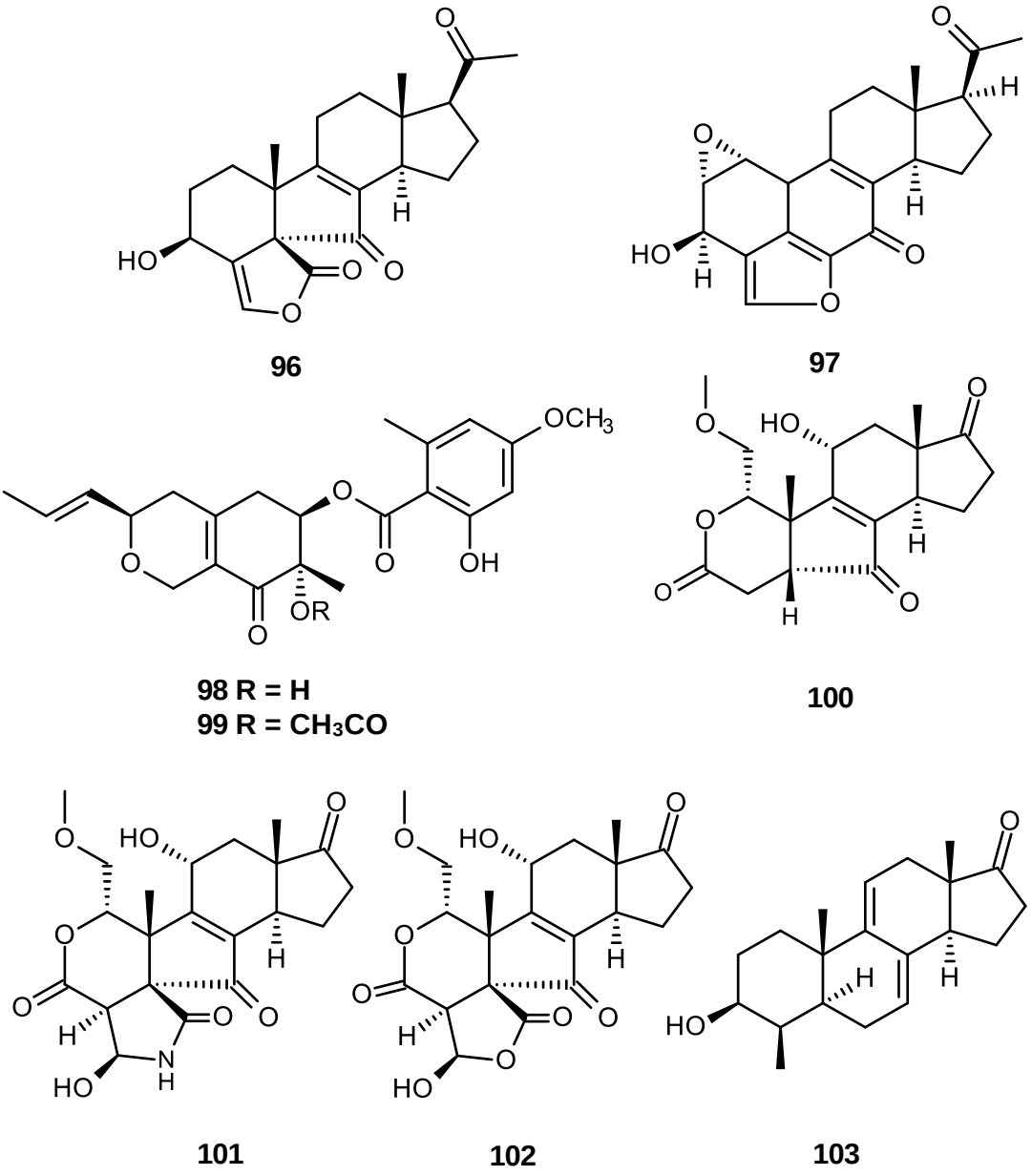

Figure 21. Structures of secovironolide (**96**), epoxyvirone (**97**), deacetylisowortmins A and B (**98** and **99**) and wortmannines A-D (**100-103**)

Liu *et al*. (2016a) described isolation of four new wortmannilactones derivatives, wortmannilactones I-L (**104-107**) (Figure 22) from the *T. wortmannii* treated with the epigenome regulatory agent suberoylanilide hydroxamic acid. Compounds **104-107** showed potent inhibitory activity against NADH-fumarate reductase with the IC_{50} values ranging from 0.84 to 1.35 µM. NADH-fumarate reductase is considered as specific target for treating helminthiasis and cancer.

Using the One strain Many Compounds (OSMAC) strategy, (Liu *et al*., 2016b) were able to isolate three new polyketides, wortmannilactone I1 (**108**), wortmannilactone I2 (**109**) and wortmannilactone I3 (**110**) (Figure 22) from the culture of *T. wortmannii.* Compounds **108-110** exhibited selective inhibitory activity against NADH-fumarate reductase with IC_{50} of 8.8, 11 and 13 µM, respectively.

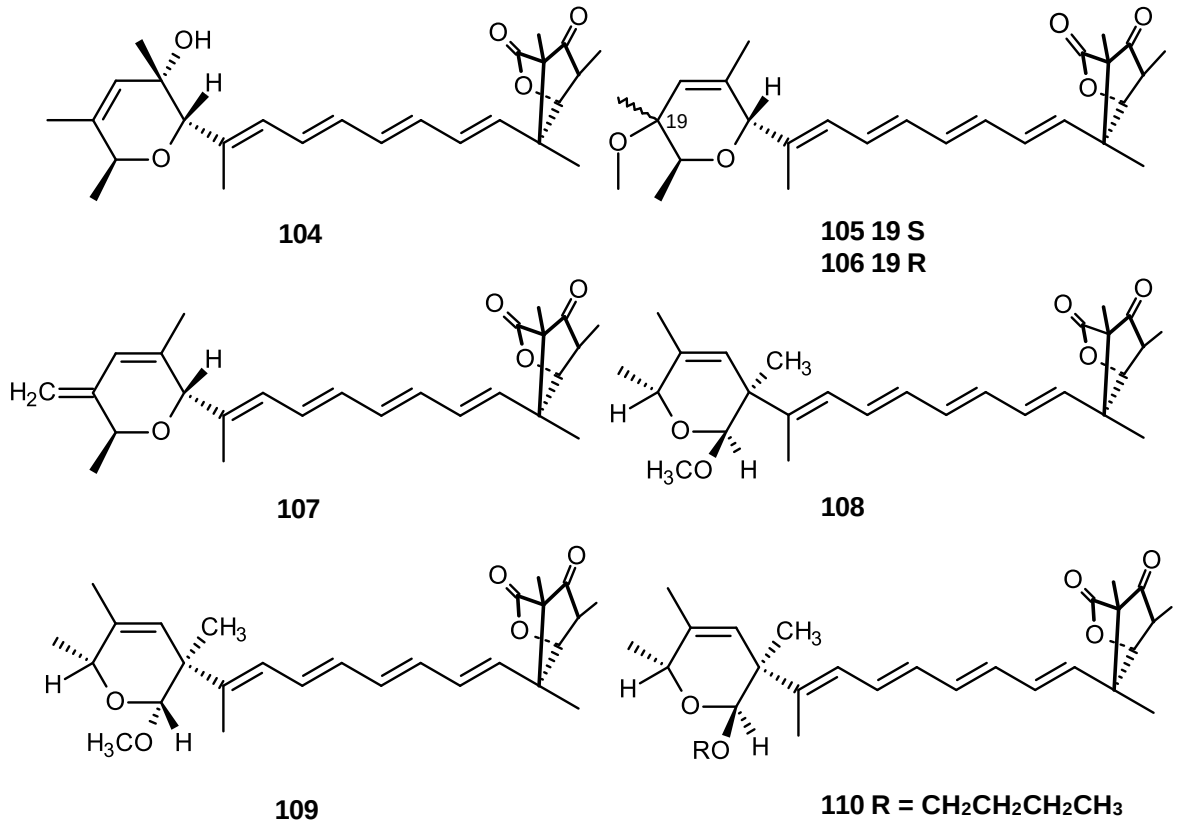

Figure 22. Structures of wortmannilactones I-L (**104-107**) and I1-I3 (**108-110**)

2.1.3 *Talaromyces thailandiasis*

Two previously undescribed meroditerpenes, thailandolides A and B (**111** and **112**) and 3-methyl-6-hydrohyl-8-methoxy-3, 4-dihydroisocoumarin (**113**) (Figure 23) were isolated from the fungus *Talaromyces thailandiasis*, which was isolated from a soil sample collected in Trat Province, Southern Thailand (Dethoup *et al*., 2007).

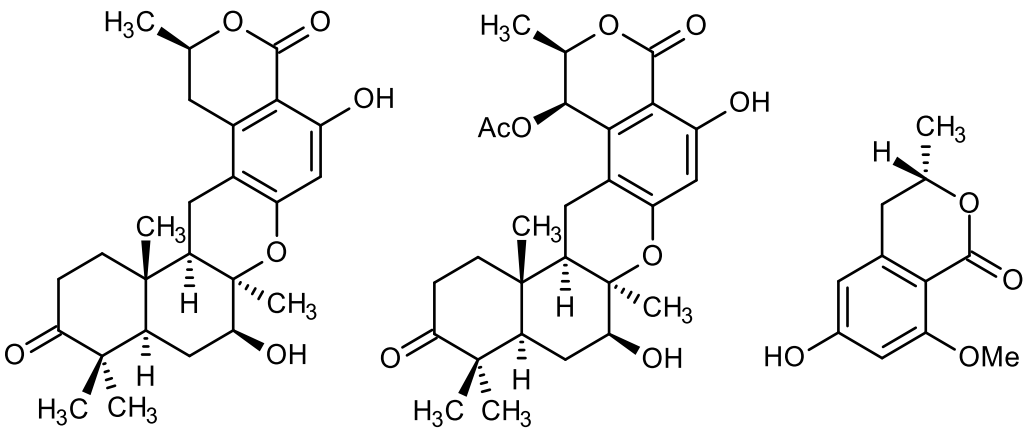

111 **112** **113**

Figure 23. Structures of thailandolides A and B (**111** and **112**) and 3-methyl-6-hydrohyl-8-methoxy-3, 4-dihydroisocoumarin (**113**)

2.1.4 *Talaromyces helicus*

Four chlorinated azaphilones, helicusins A-D (**114-117**) (Figure 24) were isolated from the culture of *T. helicus* IFM 42241. All of the four compounds (**114-117**) showed weak inhibitory effects on monoamine oxidase MAO (Yoshida *et al*., 1995).

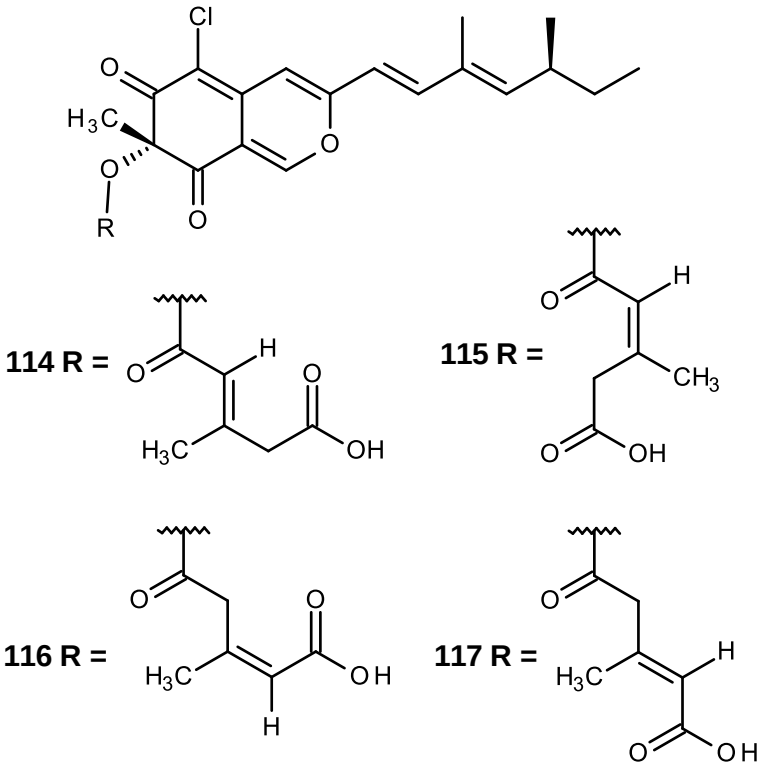

Figure 24. Structures of helicusins A (**114**), B (**115**), C (**116**) and D (**117**)

2.1.5 *Talaromyces stipitatus*

Lynn *et al*. (1982) reported the isolation of a new spiroketal talaromycins talaromycins A and B (**118** and **119**) (Figure 25) from the fungus *Talaromyces stipitatus*, which was isolated from a wood-shavings-based chicken litter. Later on, Phillips *et al*. (1987) have described four novel spiroketal talaromycins, talaromycins C-F (**120-123**) (Figure 25) from the same fungus. Four previously undescribed secondary metabolites talaroenamines B-E (**124-127**) and a new linear polyester,

talapolyester G (**128**) (Figure 25) were isolated from the fungus *T. stipitatus* ATCC10500. Compounds **124-127** were evaluated for their antiplasmodial activity. Only compound **126** showed a modest inhibition activity against chloroquine-resistant *Plasmodium falciparum* chloroquine-resistant *Plasmodium falciparum* with IC_{50} 19 µM without noticeable toxicity on HeLa and pre-adipose cell lines (Zang *et al*., 2015).

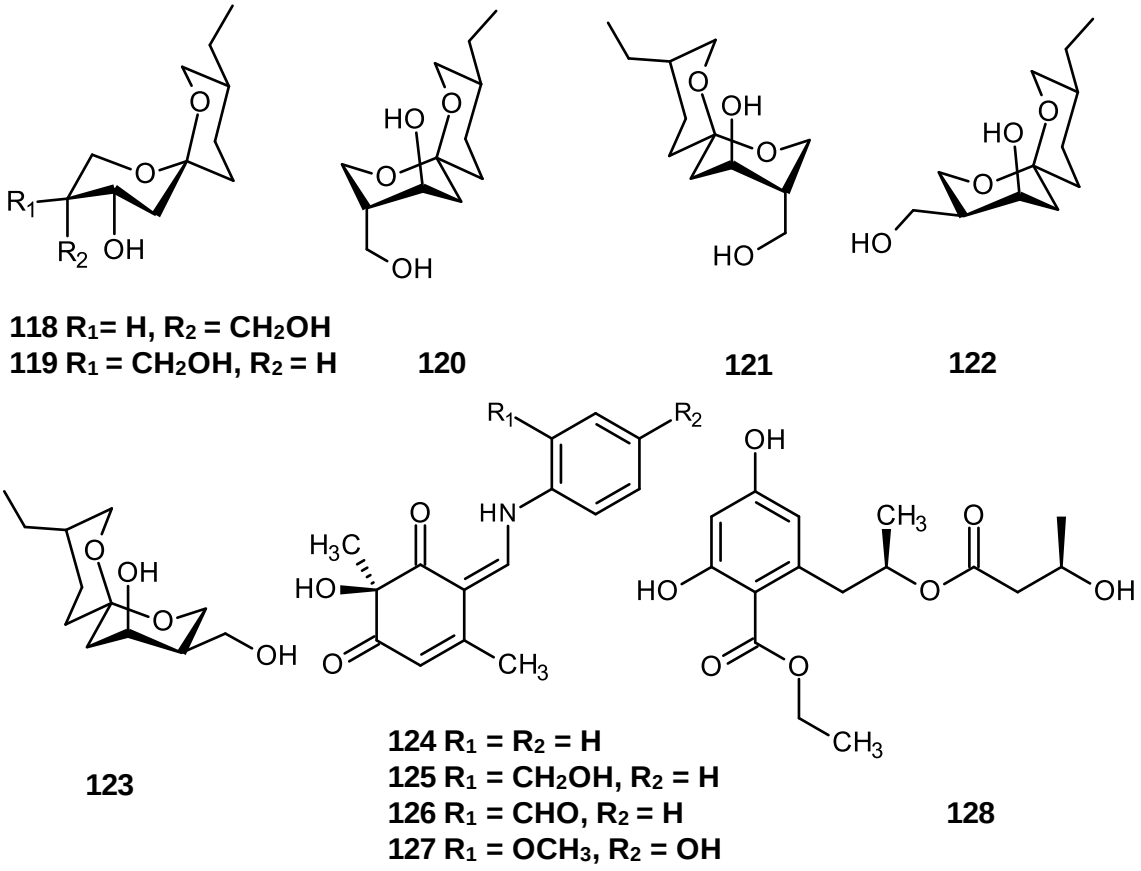

Figure 25. Structures of talaromycins A-F (**118-123**), talaroenamines B-E (**124-127**) and tatapolyester G (**128**)

Zang *et al*. (2016) reported the isolation of four new polyketide-derived oligophenalenone dimers, 9a-*epi*-bacillisporin E (**129**) and bacillisporins F-H (**130-132**), (Figure 26) from the fungus *T. stipitatus*. Bacillisporin H **132** exhibited antimicrobial activity against *Staphylococcus aureus* with a MIC value of 5.0 µM and a modest cytotoxic activity against the HeLa cell line with IC_{50} > 50 µg/mL. A new ergosterol analog, talarosterone (**133**) and a new *bis*-anthraquinone derivative, *bis* (1, 4, 5-trihydroxy-7-methylanthraquinone (**134**) were isolated from the culture of marine sponge-associated fungus *Talaromyces stipitatus* KUFA 0207 (Noinart *et al*., 2017).

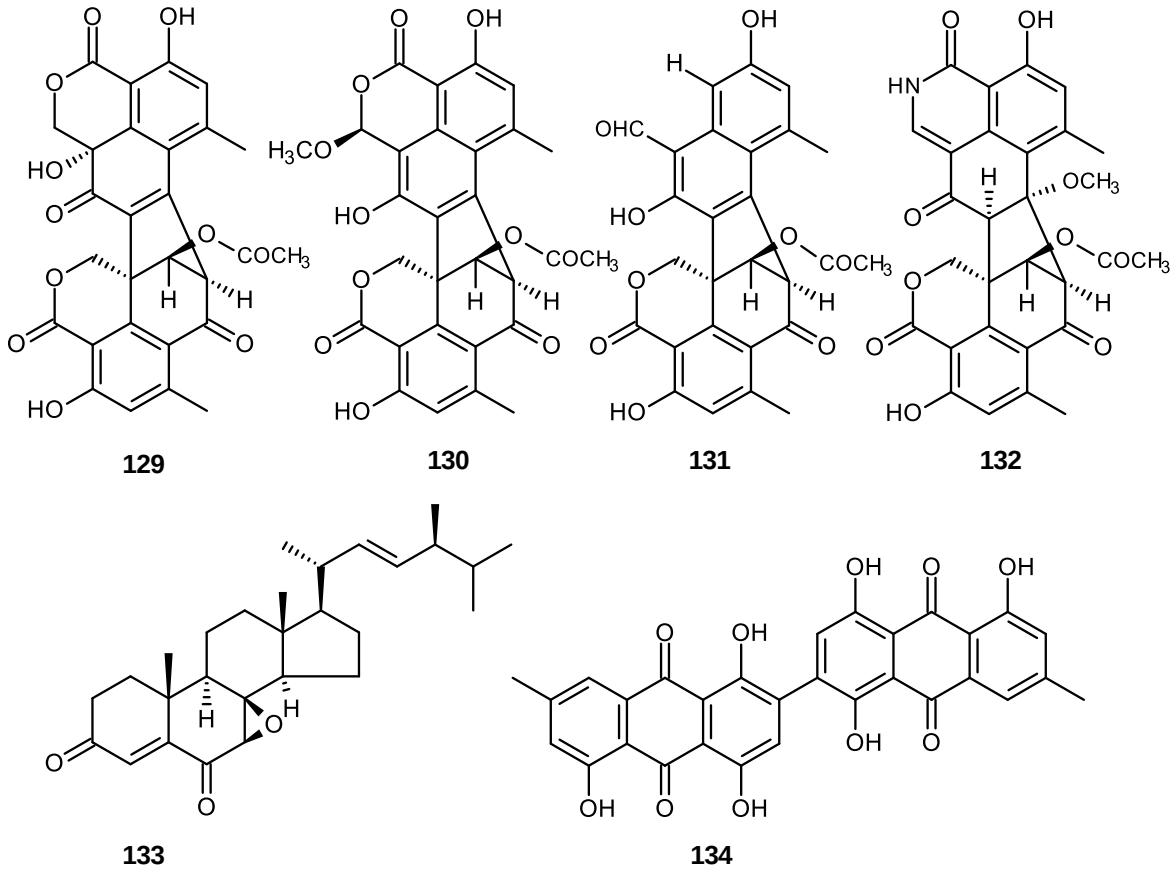

Figure 26. Structures of 9a-*epi*-bacillisporin E (**129**), bacillisporins F-H (**130-132**), talarosterone (**133**) and *bis* (1, 4, 5-trihydroxy-7-methylanthraquinone (**134**)

2.1.6 Unspecified *Talaromyces sp*.

NK 374200 (**135**) (Figure 27) was isolated from the culture broth of the soil-derived fungus *Talaromyces sp*. and was found to have the anti-mosquito larval activity. However, this compound showed no cytotoxicity against HeLa cell at 100 µg/mL, and also no acute toxicity with mice at 160 mg/kg (Morino *et al*., 1995). Tomikawa *et al*. (2000) described isolation of rasfonin (**136**) (Figure 27) from the fermented mycelium of *Talaromyces sp*. 3656-A1. Rasfonin (**136**) was shown to induce cell death in Ba/F3-V12 cells in an IL-3-free medium containing Dex (2×10^{-7} M) with IC_{50} 0.16 µg/mL.

Kimura *et al*. (2008) isolated two previously undescribed azaphilones which they have named kasanosins A and B (**137** and **138**) (Figure 27) from the cultures of the seaweed-derived *Talaromyces sp*. Both compounds **137** and **138** selectively inhibited the activities of eukaryotic DNA polymerases β and λ (pols beta and lambda) in family X of pols, kasanosin A (**137**) was a stronger inhibitor than kasanosin B (**138**). Compounds **137** and **138** showed on the rat pol β with IC_{50} values of 27.3 and 60.1 µM and human pol λ with IC_{50} 35.0 and 72.9 µM, respectively. A new kasanosin analog, kasanosin C (**139**) was later isolated from the solid fermentation of *Talaromyces sp*. T1BF which was isolated from the old bast tissue of *Taxus yunnanensis* (Li *et al*., 2010b).

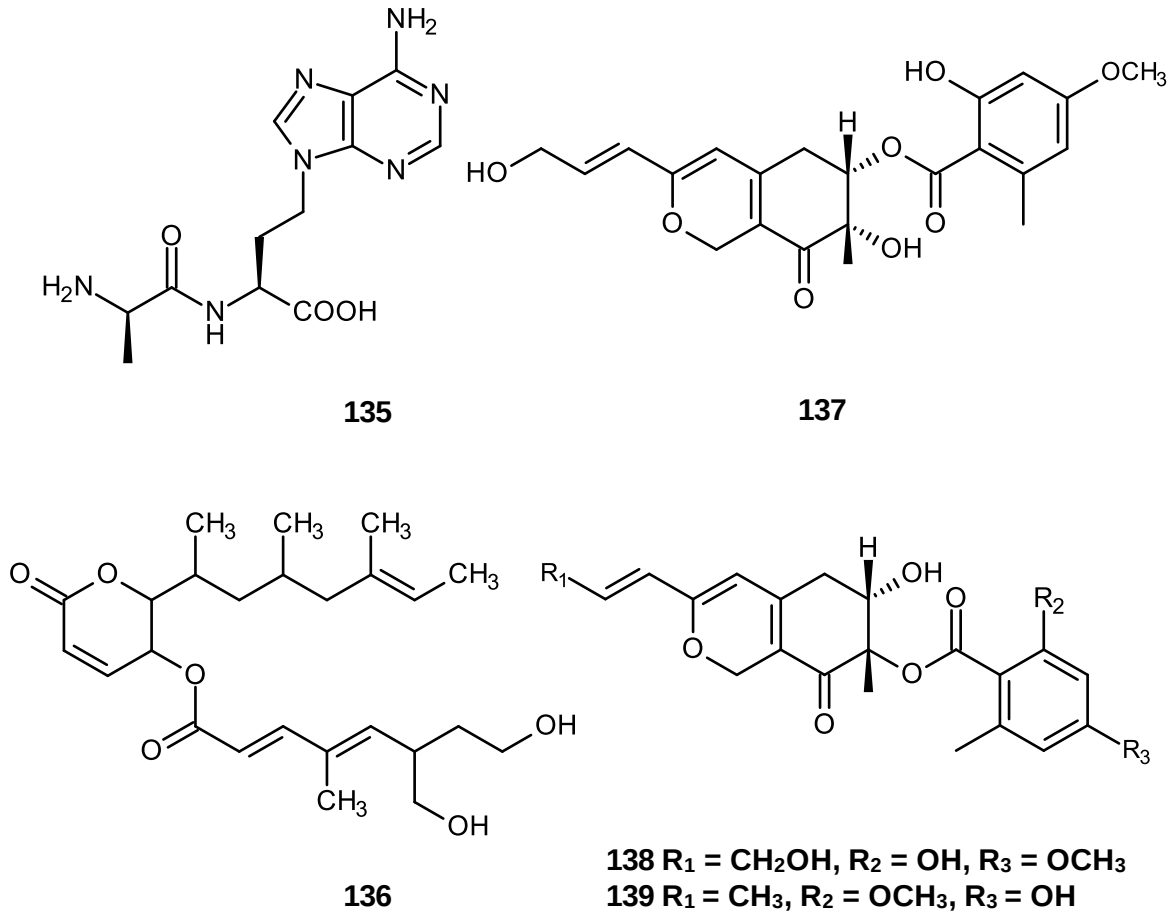

135 **137**

136

138 R_1 = CH_2OH, R_2 = OH, R_3 = OCH_3
139 R_1 = CH_3, R_2 = OCH_3, R_3 = OH

Figure 27. Structures of NK 374200 (**135**), rasfonin (**136**), kasanosins A and B (**137** and **138**) and kasanosin C (**139**)

Two new diphenyl ether derivatives, tenelates A and B (**140** and **141**) (Figure 28) were isolated from the mangrove endophytic fungus *Talaromyces sp*. (SBE 14), from a South China Sea (Liu *et al*., 2009). In 2010, two new metabolites 7-epiaustdiol (**142**) and 8-O-methylepiaustdiol (**143**) (Figure 28) were isolated from the

mangrove-endophytic fungus *Talaromyces sp*. ZH-154. Compound **142** displayed significant inhibitory antimicrobial activity against *Pseudomonas aeruginosa* ATCC 25668 with MIC values of 6.25 µg/mL. Compounds **142** and **143** showed moderate cytotoxicity against KB and KB*v* 200 (human epidermoid carcinoma) cell lines with IC_{50} 20.04, 19.32 µg/mL and 16.37, 37.16 µg/mL, respectively (Liu *et al*., 2010).

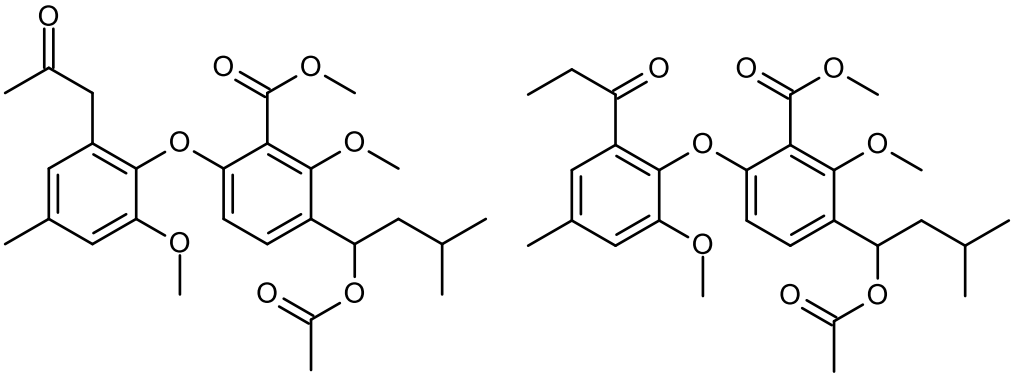

140 **141**

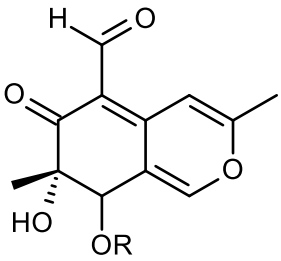

142 R = H
143 R = CH_3

Figure 28. Structures of tenelates A and B (**140** and **141**), 7-epiaustdiol (**142**) and 8-O-methylepiaustdiol (**143**)

New meroterpenoids, chrodrimanins C-G (**144-148**) (Figure 29) were isolated from the YO-2 strain of *Talaromyces sp*. which was isolated form the soil sample. However, compounds **145-147** displayed insecticidal activity against silkworms with the LD_{50} values of 20, 10 and 50 µg/g of diet, respectively (Hayashi *et al*., 2012a, b).

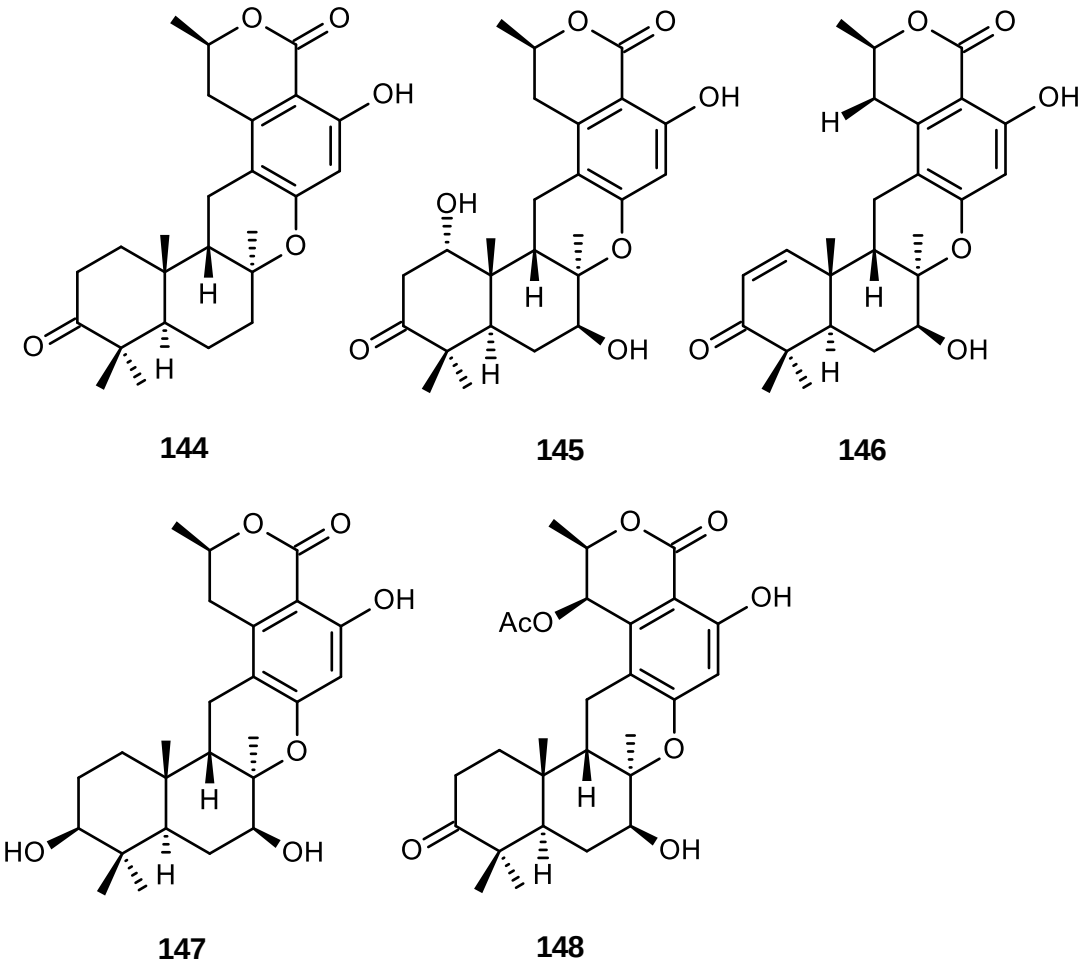

Figure 29. Structures of chrodrimanins C-G (**144-148**)

While, a new xanthone dimer, talaroxanthone (**149**) (Figure 30) was isolated from the endophytic fungus *Talaromyces sp*. DgCr22.1b (Koolen *et al*., 2013), two new metabolites (3*S*, 4a*R*, 7*S*)-7, 8-dihydroxy-3-methyl-3, 4, 10, 5, 6, 7-hexahydro-1*H*-isochromen-1-one (**150**) and (1*S*, 3*R*, 5*R*)-3-methyl-2-oxabicyclo [3.3.1] nonan-7-one (**151**) (Figure 30) were isolated from an endophytic fungus, a close relative of *Talaromyces sp*. Compounds **150** and **151** displayed a range of cytotoxicities against the human cancer cell lines, HCT-116 (colon carcinoma), A-549 (lung), HEP-1 liver, THP-1 (leukemia) and PC-3 (prostatic) at 50 µM and induced apoptosis in HL-60 cells (Kumar *et al*., 2013).

A new penicillic acid derivative, coculnol (**152**) (Figure 30) was isolated from the co-culture broth of *Fusarium solani* FKI-6853 and *Talaromyces sp*. FKA-65. Coculnol **152** displayed anti-influenza virus activity against the strain A/PR/8/34 (H1N1) with IC_{50} values of 283 µg/mL, and weak cytotoxic activity against Madin-Darby canine kidney (MDCK) cells with IC_{50} 781 µg/mL (Nonaka *et al*., 2015). More recently, Kaifuchi *et al*. (2015a) described the isolation of ukulactone C (**153**) (Figure 30) from *Talaromyces sp*. FKI-6713. Ukulactone C (**153**) showed an in vitro inhibitory activity with the IC_{50} values of 62 µM against NADH-fumarate reductase of the roundworm *Ascaris suum*.

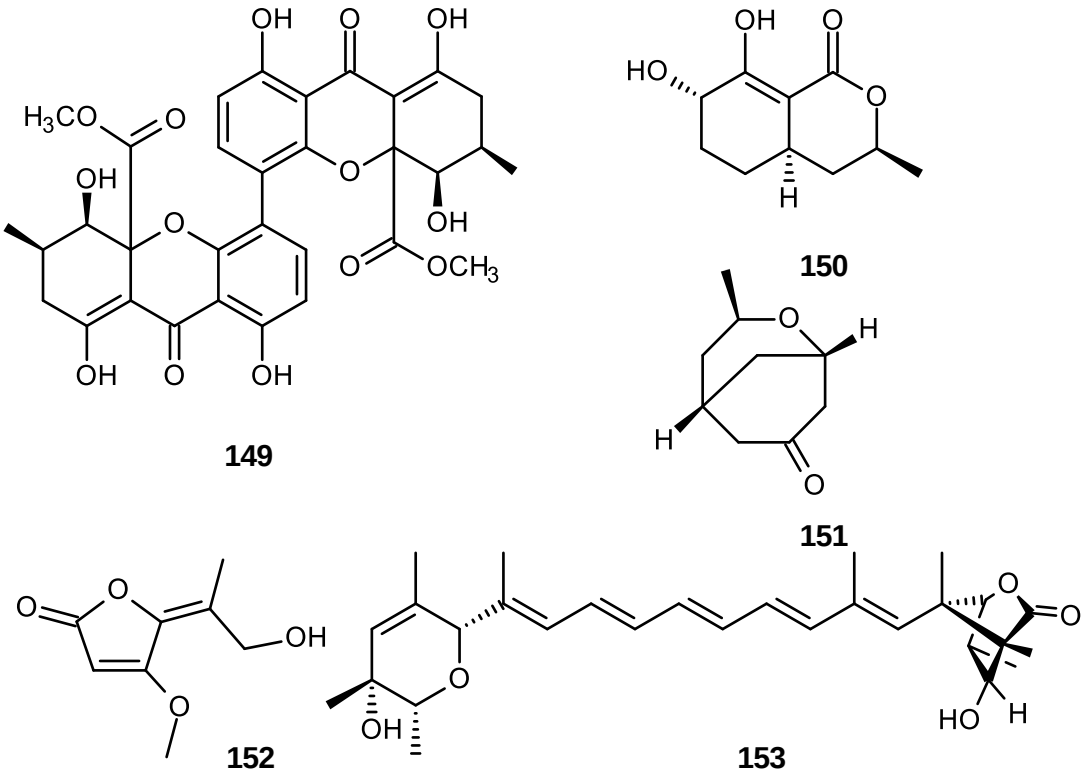

Figure 30. Structures of talaroxanthone (**149**), (3*S*, 4a*R*, 7*S*)-7, 8-Dihydroxy-3-methyl-3, 4, 10, 5, 6, 7-hexahydro-1*H*-isochromen-1-one (**150**), (1*S*, 3*R*, 5*R*)-3-Methyl-2-oxabicyclo [3.3.1] nonan-7-one (**151**), coculnol (**152**) and ukulactone C (**153**)

The diphenyl ether derivatives, talaromycins A-C (**154-156**) (Figure 31) were isolated from a gorgonian-derived fungus, *Talaromyces sp*. Compounds **154-156** showed no cytotoxic activity against human cancer cell lines, HepG2 and Hep3B (hepatoma), MCF-7/ADR (breast), PC-3 (prostatic) and HCT-116 (colon carcinoma). However, compound **156** showed antifouling activity against the larval settlement of the barnacle *Balanus Amphitrite* with EC_{50} values of 2.8 ± 0.2 µg/mL (Chen *et al*., 2015).

Five new metabolites, including two tricyclic polypeptides: vanitaracins A and B (**157** and **158**), 3, 5-dihydroxy-2-(2-(2-hydroxy-6-methylphenyl)-2-oxoethyl)-4-methylbenzaldehyde (**159**), 2-chromone derivatives, 7-hydroxy-5-methyl-2-(2-oxobutyl)-4*H*-chromen-4-one (**160**) and 2, 7-dihydroxy-5-methyl-2-(2-oxobutyl)chroman-4-one (**161**) (Figure 31) were isolated from a culture broth of *Talaromyces sp*. Only compound **157** showed the strongest anti-hepatitis B virus HBV activity against using HBV-susceptible HepG2-hNTCP-C4 cells with an IC_{50} 10.5 µM. While compounds **158-161** exhibited weak anti-HBV activity with an IC_{50} 91.2, 51.4, 72.4 and 52.1 µM, which suggested that the substituents at C-9 in compound **157** are likely to be important for its antiviral activity (Matsunaga *et al*., 2015).

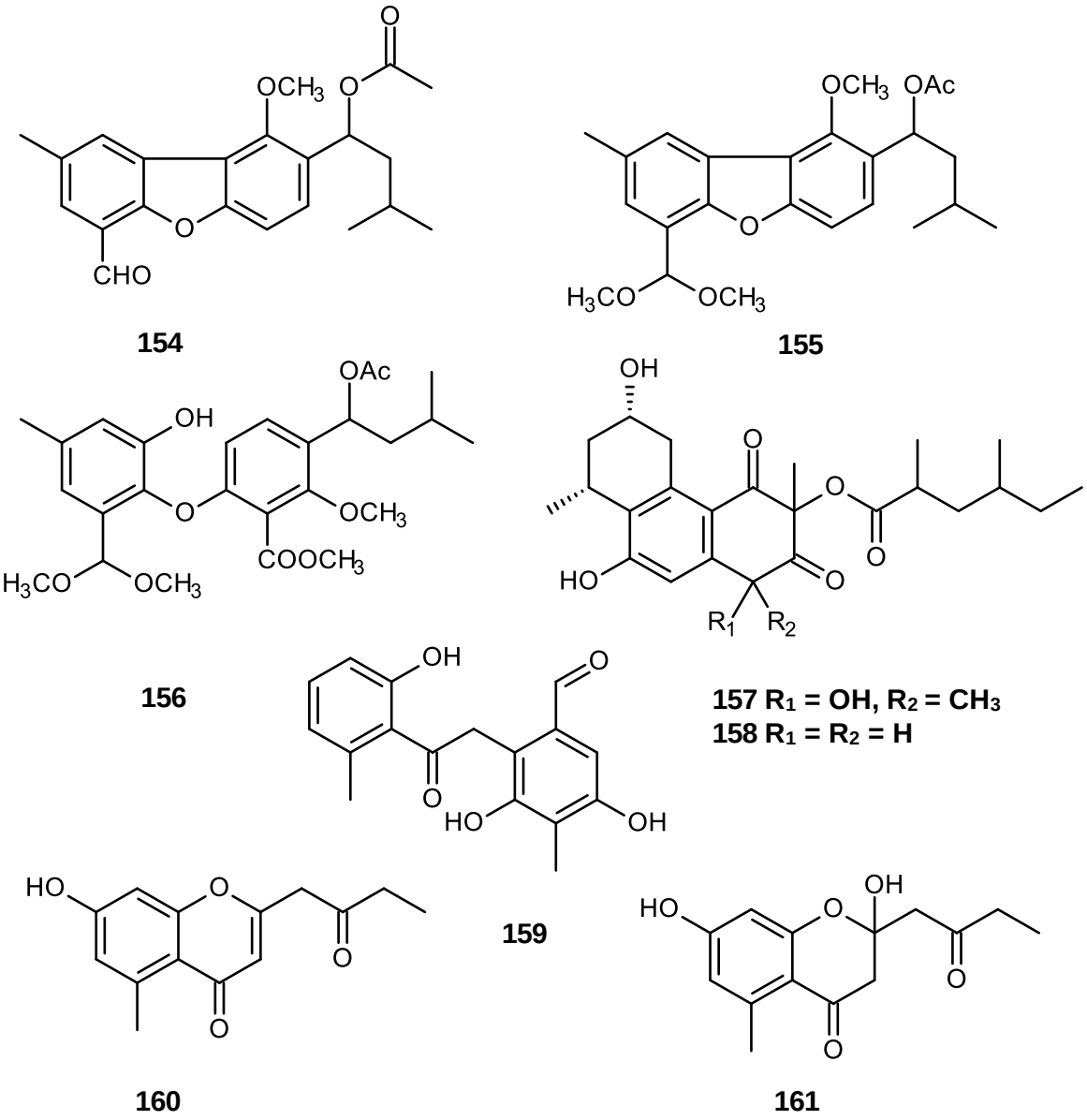

Figure 31. Structures of talaromycins A-C (**154-156**), vanitaracins A-B (**157-158**), 3,5-dihydroxy-2-(2-(2-hydroxy-6-methylphenyl)-2-oxoethyl)-4-methylbenzaldehyde (**159**), 7-hydroxy-5-methyl-2-(2-oxobutyl)-4*H*-chromen-4-one (**160**) and 2, 7-dihydroxy-5-methyl-2-(2-oxobutyl)chroman-4-one (**161**)

Two new oxaphenalenone dimers: Talaromycesones A (**162**) and B (**163**) and a new isopentenyl xanthenone: talaroxanthenone (**164**) (Figure 32) were isolated from the culture broth and mycelia of a marine fungus *Talaromyces sp* strain LF458. Talaromycesones A (**162**) and B (**163**) showed antibacterial activity against human pathogenic *Staphylococcus epidermidis* strains with IC_{50} 3.70 and 17.36 µM, while compounds **162** and **164** exhibited *acetylcholinesterase* AchE inhibitory activity with IC_{50} 7.49 and 1.61 µM, respectively. Interestingly, compound **164** inhibited *phosphodiesterase* PDE-4B2 with IC_{50} 7.25 µM (Wu *et al*., 2015).

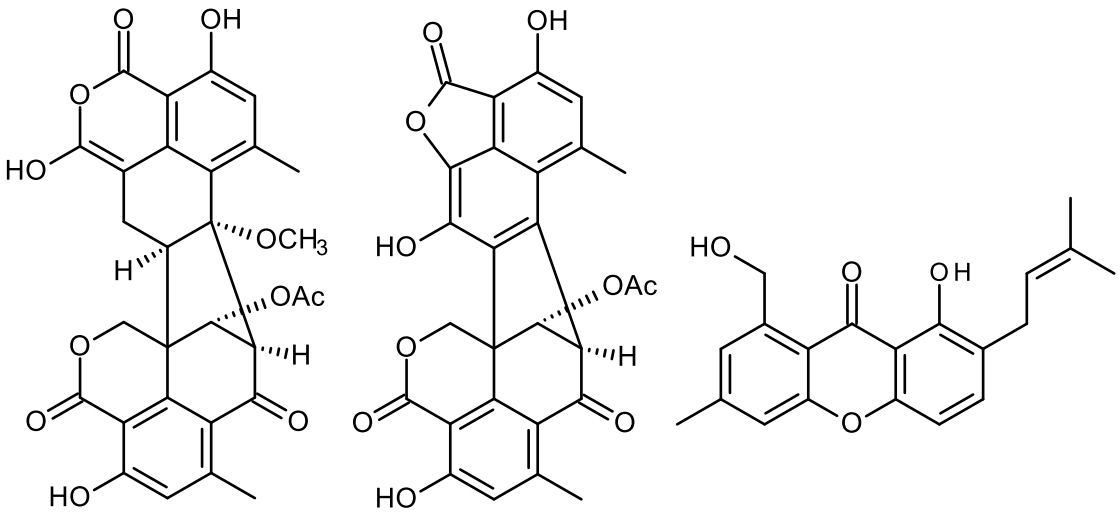

162 **163** **164**

Figure 32. Structures of talaromycesones A and B (**162** and **163**) and talaroxanthenone (**164**)

A new unsymmetrical dimeric anthraquinone, 3-demethyl-3-(2-hydroxypropyl)-skyrin (**165**) (Figure 33) from the solid-state fermentation extract of an endophytic fungal strain *Talaromyces sp*. YE 3016. Compound **165** showed moderate cytotoxic activity against MCF-7 breast adenocarcinoma with IC_{50} 20.76 ± 3.41 µg/mL (Xie *et al*., 2016). A new analog of wortmannin, wortmannolol (**166**) (Figure 33) was isolated from an endophytic fungus *Talaromyces sp*. LGT-4 of the plant *Triptergium wilfordii*. This compound exhibited weak monoamine oxidase inhibitory activity at the final concentration of 25 µg/mL (inhibitory rate was 30%) (Zhi *et al*., 2016). Moreover, [2-(*S*)-hydroxy (phenyl) methyl]-3-methylquinazolin-4(3*H*)-one (**167**) and 2-[(*R*)-hydroxy (phenyl) methyl]-3-methylquinazolin-4(3*H*)-one (**168**) (Figure 33) were isolated from the fungus *Talaromyces sp*. cf-16. Compounds **167** and **168** showed similar toxicity to brine shrimp *Artemia salina* with LC_{50} of 97.8 and 106.4 µg/mL but inactive antibacterial activity against *Staphylococcus aureus* and *Escherichia coli* bacteria (Haibin *et al*., 2016).

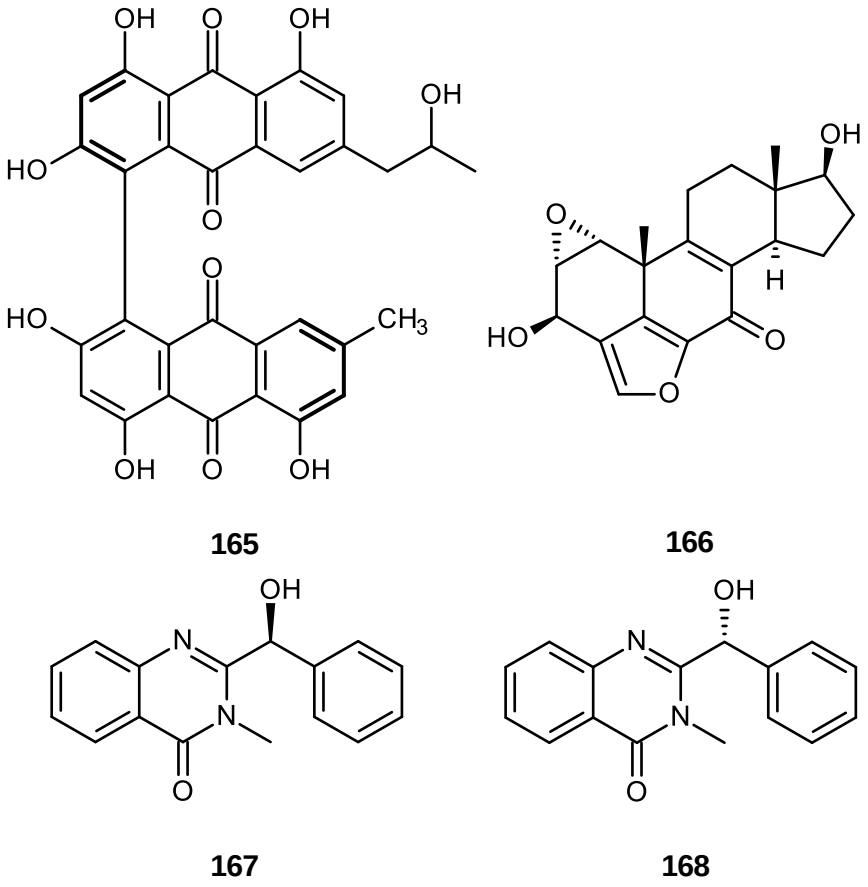

165 **166**

167 **168**

Figure 33. Structures of 3-demethyl-3-(2-hydroxypropyl)-skyrin (**165**), wortmannolol (**166**), 2-(*S*)-hydroxy (phenyl) methyl]-3-methylquinazolin-4(3*H*)-one (**167**) and 2-(*R*)-hydroxy (phenyl) methyl]-3-methylquinazolin-4(3*H*)-one (**168**)

Kalansuriya *et al*. (2017) reported the isolation of five new coprogen siderophores; talarazines A-E (**169-173**) (Figure 34) from a mud dauber wasp-associated fungus, *Talaromyces sp*. (CMB-W045). Talarazine A (**169**) and talarazines C-E (**171-173**) displayed no growth inhibition against Gram-positive bacteria *Staphylococcus aureus* ATCC 25923, the Gram-negative bacteria *Escherichia coli* ATCC 25922, *Pseudomonas aeruginosa* ATCC 27853 and the fungus *Candida albicans* ATCC 90028 with IC_{50} > 30 µM and also no cytotoxic activity against human large cell lung carcinoma NCI-H460, human colorectal adenocarcinoma SW620 and cervical carcinoma KB3-1 cell lines.

A cyclic heptapetide, talarolide A (**174**) was (Figure 34) isolated from an Australian marine tunicate-associated fungus, *Talaromyces sp*. (CMB-TU011). Talarolide A **174** showed neither cytotoxic activity against NCI-H460, SW620, KB3-1 and human hepatocellular carcinoma HepG2cell lines with IC_{50} > 30 µM nor antimicrobial activity against Gram-positive bacteria *S. aureus* ATCC 25923 and ATCC 9144, *B. subtilis* ATCC 6633 and ATCC 6051 and Gram-negative bacteria *E. coli* ATCC 11775 and *P. aeruginosa* ATCC 10145, and the fungus *C. albicans* ATCC 90028 with IC_{50} >30 µM (Dewapriya *et al*., 2017).

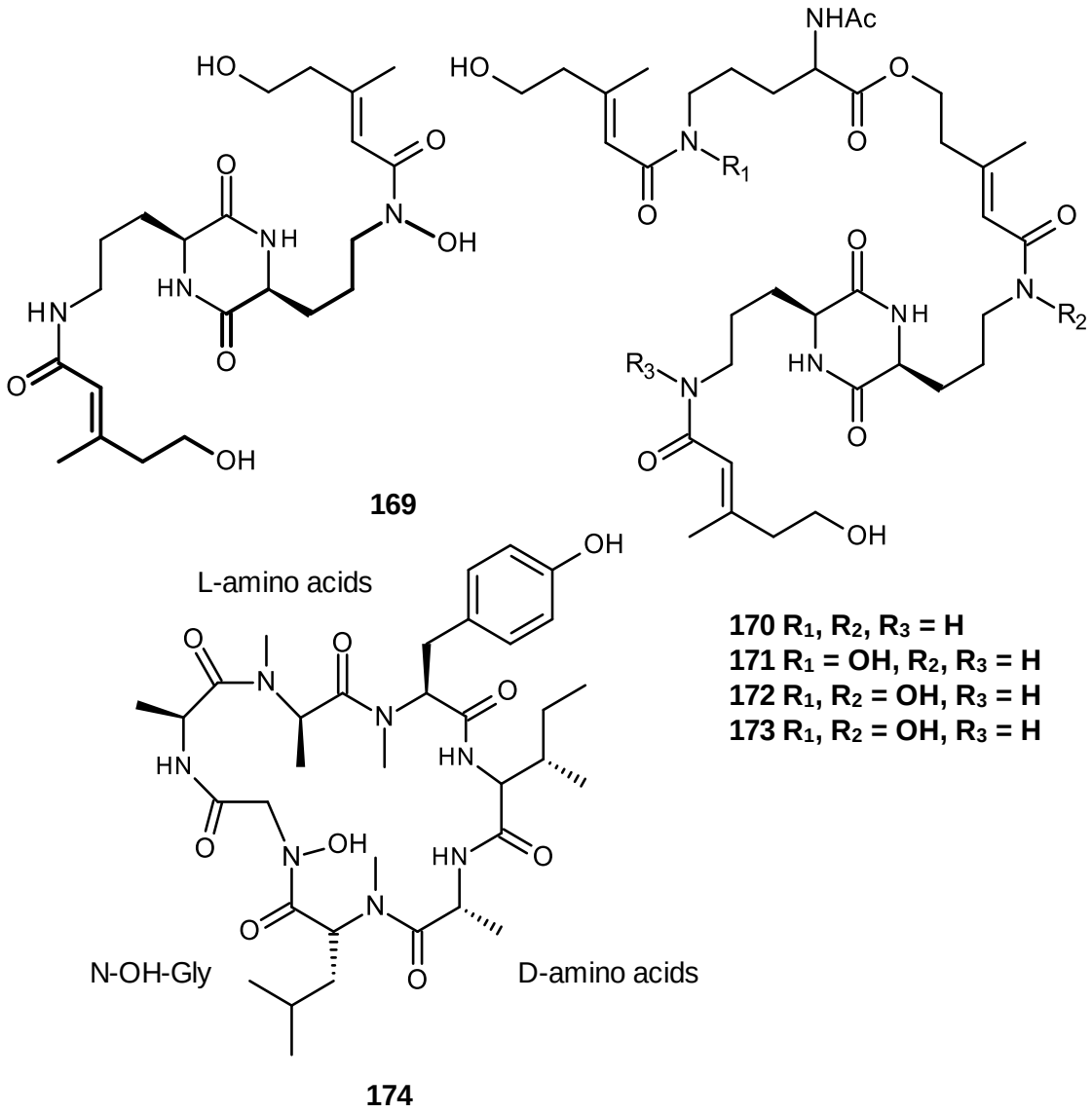

Figure 34. Structures of talarazines A-E (**169-173**) and talarolide A (**174**)

2.2 *Neosartorya* species

Neosartorya species are the sexual state of the *Aspergillus* species, especially of the *Fumigati* section, which belong to the family Trichocomaceae and are distributed in soil worldwide (Samson *et al*., 2007). *Neosartorya* species produced both a sexual state with ascospores and an asexual state with conidiospores (Frisvad *et al*., 2009), which included many important species because they can be pathogenic or allergenic to man (Brakhage and Langfelder, 2002), as well as causing food spoilage and producing mycotoxins (Cole and Cox, 1981).

Many species of *Neosartorya* produce novel bioactive secondary metabolites, which have potential for pharmaceutical (Jayasuriya *et al*., 2009; Kijjoa *et al*., 2011) and agricultural use including biodegradation, bioinsecticide and bioherbicide (Chaillan *et al*., 2004; Ozoe *et al*., 2004; Phattanawasin *et al*., 2007). The present literature survey focuses on the novel metabolites from the species of *Neosartorya* reported with their biological activities.

2.2.1 *Neosartorya fischeri*

Three novel metabolites, fiscalins A-C (**175-177**) (Figure 35) were isolated from the culture broth of *Neosartorya fischeri*, which was isolated from a plant rhizosphere. Compounds **175-177** inhibited the binding of ^{125}I-Bolton-Hunter-substance P ligand to human neurokinin (NK-1) receptor, with Ki values of 57, 174, and 68 µM, respectively (Wong *et al*., 1993).

Three previously undescribed secondary metabolites, NK372135s A-C (**178-180**), (Figure 35) were isolated from the culture broth of the fungus, *N. fischeri var. glabra* IFO9857. Compounds **178-180** displayed strong *in vitro* growth antifungal activity against *Candida albicans* with IC_{50} = 2.12, 0.53 and 0.27 µg/mL. Among them, compound **180** showed the most potent antifungal activity (Morino *et al*., 1994). Proksa *et al*. (1998) reported the isolation of an asymmetric ergochrome, neosartorin (**181**) (Figure 35) from the mycelium of *N. fischeri* grown on the glucose/glycerol medium, while two new cyclopentanone derivatives, isoterrein (**182**) and terrein (**183**) were isolated from *Neosartorya fischeri* IFM52672 (Wakana *et al*., 2006).

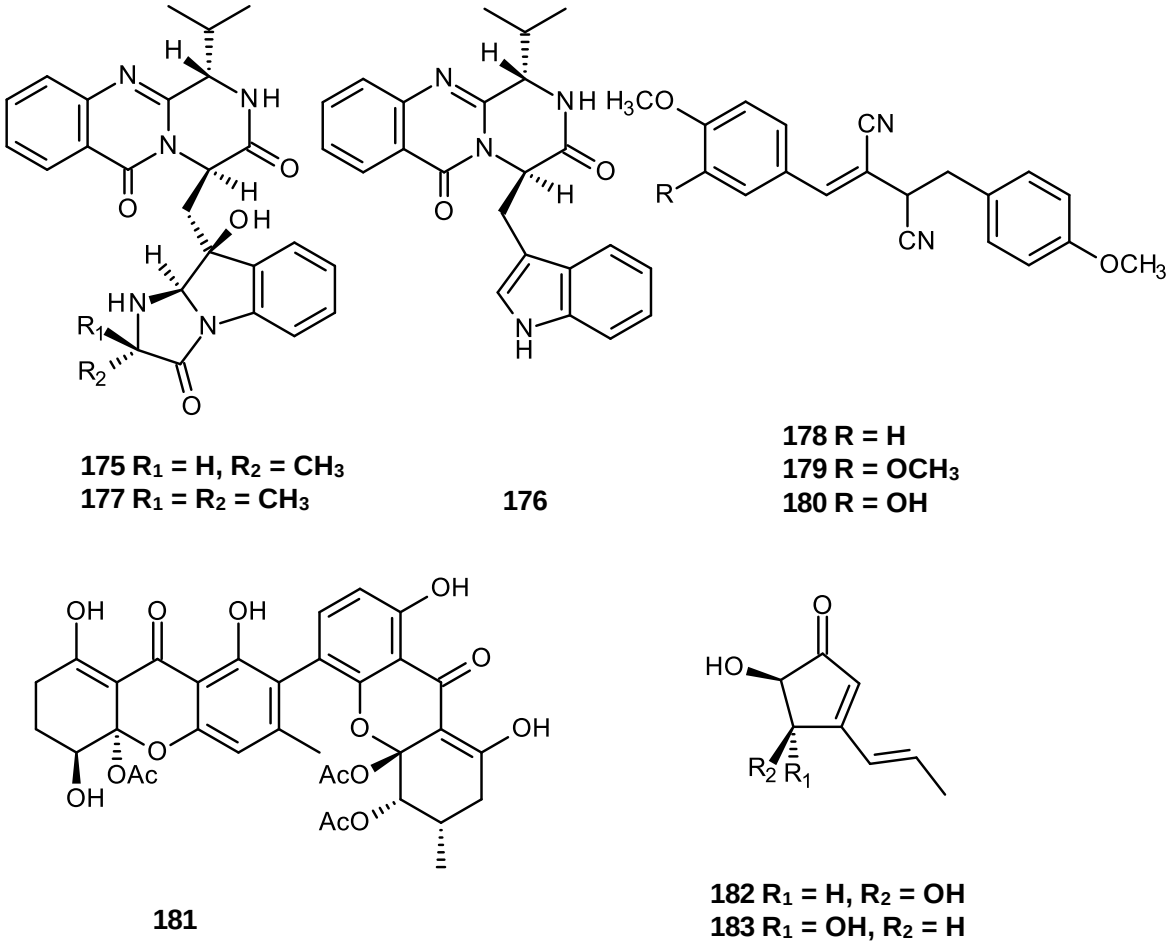

Figure 35. Secondary metabolites isolated from *Neosartorya fischeri* (**175-183**)

In 2012, Tan *et al*. reported isolation of fischeacid (**184**) and fischexanthone (**185**) from the marine-derived fungus *Neosartorya* strain 1008F$_1$. Compounds **184-185** displayed no cytotoxic effect on human gastric cancer cell line SGC-7901, hepatic cancer cells BEL-7404 and antiphytoviral effect on tobacco mosaic virus (TMV) under the concentration of 200 µg/mL (Tan *et al*., 2012). The activation of the polycyclic polyketide prenyltransferases (pcPTase) in transformant T2 *N. fischeri* produced new metabolite, neosartoricin (**186**) (Figure 36). Compound **186** showed neither antibacterial activity against Gram positive and Gram negative bacteria nor antifungal activity against yeasts *Saccharomyces cerevisiae* and *Candida albicans* (> 64 µg/mL), however neosartoricin **186** exhibited antiproliferative activity on anti-CD3/CD28 activated murine spleenic T-cells with IC_{50} = 2.99 µM but was less cytotoxic against human foreskin fibroblast HFF and HeLa cells at the concentration up to 50 µM, which suggested its physiological role as an immunosuppressive agent (Chooi *et al*., 2013).

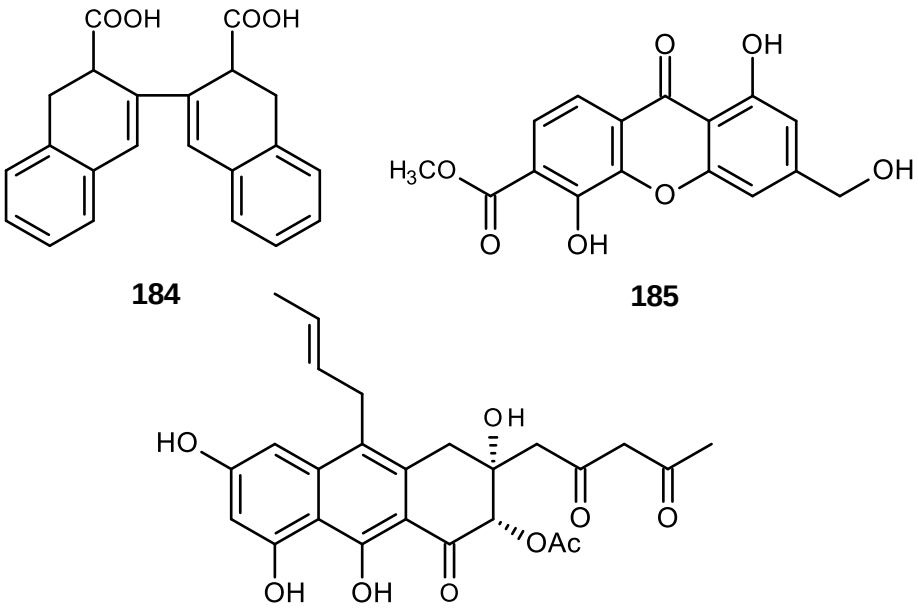

184 **185**

186

Figure 36. Structures of fischeacid (**184**), fischexanthone (**185**) and neosartoricin (**186**)

New meroditerpene, sartorypyrone A (**187**) and a new aszonalenin analogue, 1-formyl-5-hydroxyaszonalenin (**188**) were isolated from the soil fungus *N. fischeri* KUFC 6344. Only compound **187** showed an *in vitro* growth inhibitory activity against three human tumor cell lines, A375-C5 melanoma with GI_{50} 21.5 ± 1.9 µM, but less activity against MCF-7 breast adenocarcinoma with GI_{50} 46.3 ± 7.6 µM and NCI-H460 non-small cell lung cancer with GI_{50} 37.3 ± 4.0 µM (Eamvijarn *et al*., 2013). In addition, compound **187** exhibited antibacterial activity against Gram-positive

bacteria *Staphylococcus aureus* and *Bacillus subtilis* with MIC values of 32 and 64 µg/mL, respectively and also was found to inhibit the biofilm formation in both reference strains *S. aureus* ATCC 25923, *B. subtilis* ATCC 6633 and the multi-drug resistant isolates *S. aureus* B1 and *E. faecalis* W1, at the 2× MIC and MIC (Gomes *et al*., 2014).

Strain of *N. fischeri* FO-5897 isolated from a soil sample collected in Funabashi city, Chiba, Japan, produced sartorypyrone D (**189**) (Figue 37). Compound **189** displayed antibacterial activities against all tested Gram-positive bacteria, *Bacillus subtilis*, *Kocuria rhizopila* and *Mycobacterium smegmatis* with IC_{50} 8.0, 9.0 and 10.0 µg/mL, and also inhibited NADH-fumarate reductase NFRD and mammalian NADH oxidase with IC_{50} 1.7 and 3.0 µM, respectively (Kaifuchi *et al*., 2015b). Shan *et al*. (2014) described isolation of a new aszonalenin analogue, 6-hydroxyaszonalenin (**190**) (Figure 37) from the culture of *N. fischeri* CGMCC 3.5378, Later on, the new prenylated diketopiperazine alkaloids, neofipiperazines A-C (**191-193**) (Zheng *et al*., 2014) and neofipiperazine D (**194**) (Chen *et al*., 2014) were isolated from the same fungus. Compound **194** was evaluated for cytotoxic activity against four human cancer cell lines MCF-7 (breast carcinoma), H1299 (lung carcinoma), HUVEC (human umbilical vein endothelial cells), MDA-MB-231 (breast carcinoma) and showed no significant activity at the concentration of 20 µM (Chen *et al*., 2014).

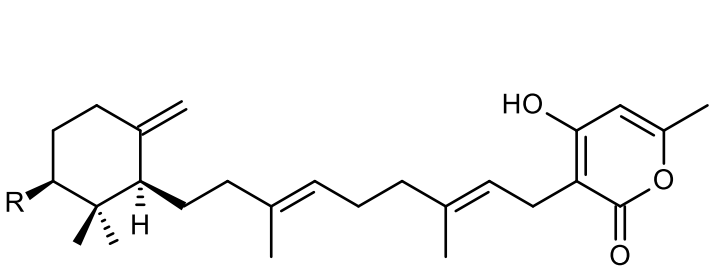

187 R = OAc
189 R = OH

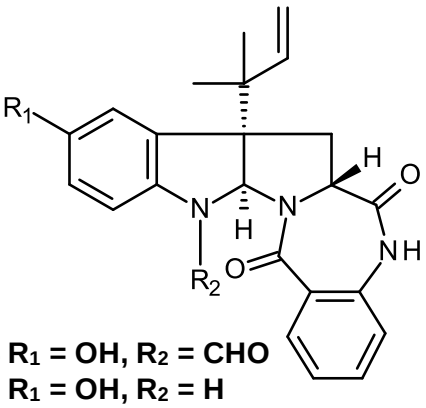

188 R_1 = OH, R_2 = CHO
190 R_1 = OH, R_2 = H

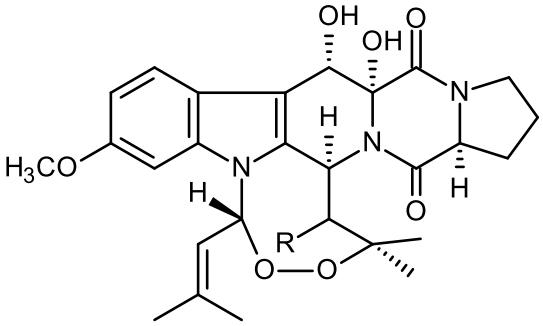

191 R = α-OH
192 R = β-OH

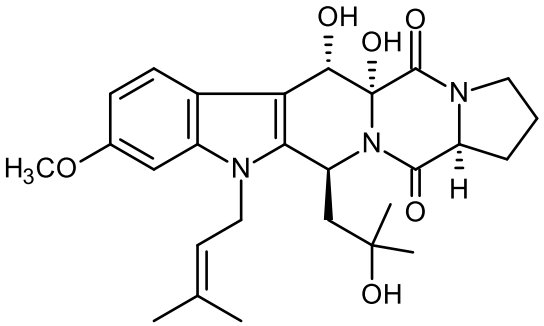

193

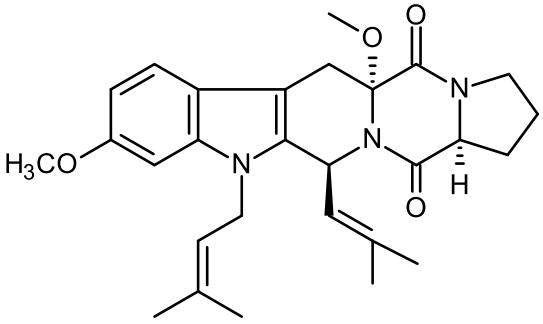

194

Figure 37. Structures of sartorypyrone A (**187**), 1-formyl-5-hydroxyaszonalenin (**188**), sartorypyrone D (**189**), 6-hydroxyaszonalenin (**190**), neofipiperazines A-D (**191-194**)

2.2.2 *Neosartorya quadricincta*

A new prenylated dihydroisocoumarin derivative, PF 1223 (**195**) (Figure 38) was isolated from the culture of *Neosartorya quadricincta* PF 1223. Compound **195** inhibited [^{3}H] ethynylbicycloorthobenzoate (EBOB) binding by 65% with IC_{50} 2.2 µM and inhibited the binding for the insect GABA receptor and proved to be a lead compound for the improvement of novel insecticides (Ozoe *et al*., 2004).

Prompanya *et al*. (2016) reported isolation of two new polyketide derivatives, quadricinctones A and C (**196** and **197**), and seven new benzoic acid derivatives including quadricinctapyrans A and B (**198** and **199**), quadricinctoxepine (**200**) quadricinctone B (**201**), quadricinctafurans A and B (**202** and **203**) and quadricinctone D (**204**) (Figure 38) from the culture of the marine sponge-associated fungus *N. quadricincta* KUFA 0061. Compounds **196-204** did not exhibit either antibacterial activity against Gram-positive and Gram-negative bacteria, as well as multidrug-resistant isolates from the environment (MIC > 256 µg/mL), or antifungal activity against yeast *Candida albicans* ATCC 10231, filamentous fungus *Aspergillus fumigatus* ATCC 46645 and dermatophyte *Trichophyton rubrum* FF5 with MIC > 512 µg/mL. They also showed no *in vitro* growth inhibitory activity against MCF-7 breast adenocarcinoma, NCI-H460 non-small cell lung cancer and A375-C-5 melanoma cell lines (GI_{50} > 150 µM).

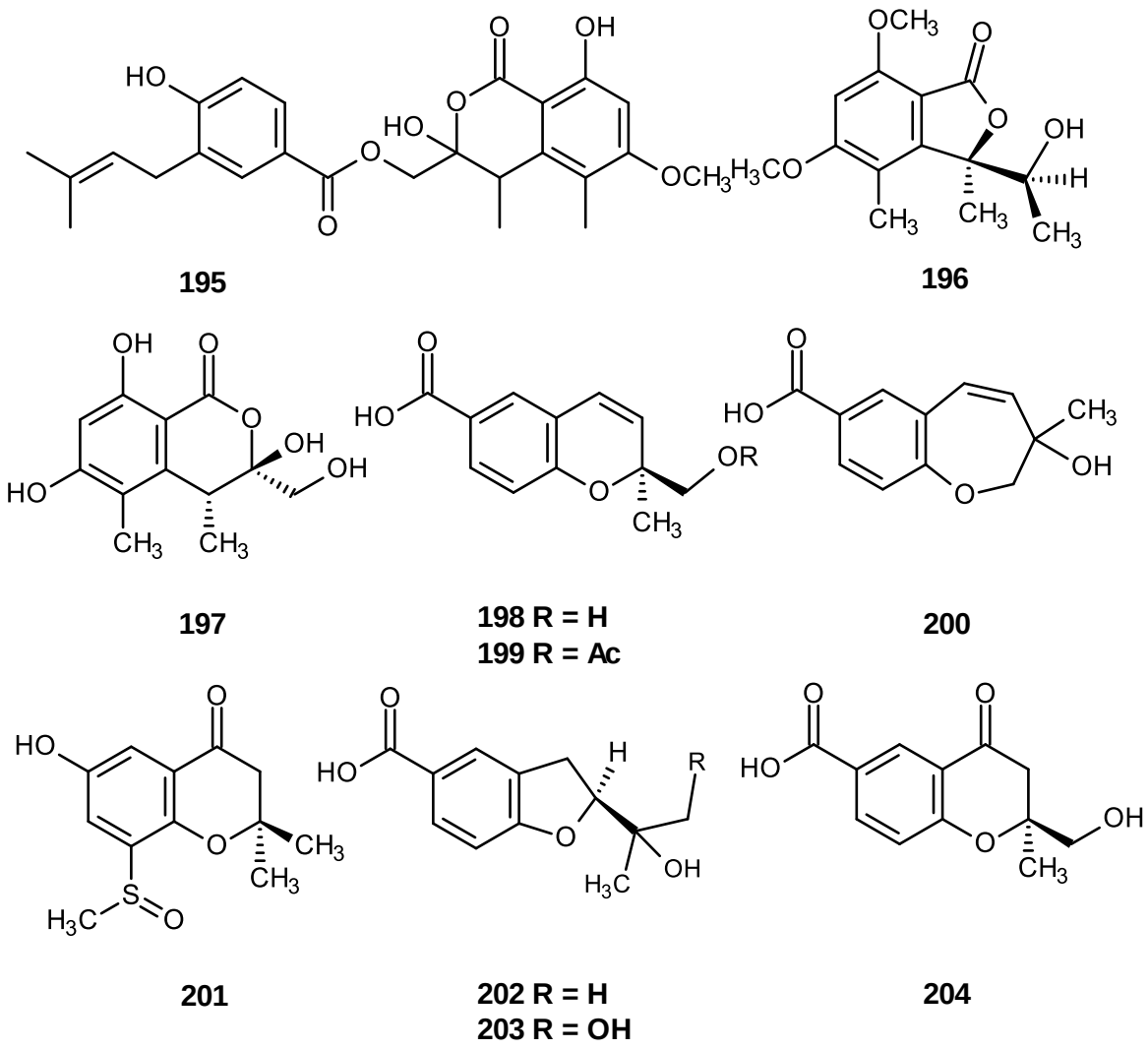

Figure 38. Secondary metabolites isolated from *Neosartorya quadricincta* (**195-204**)

2.2.3 *Neosartorya pseudofischeri*

Three new metabolites, including 1, 4-diacetyl-2, 5-dibenzylpiperazine derivatives, 3, 8-diacetyl-4-(3-methoxy-4, 5-methylenedioxy) benzyl-7-phenyl-6-oxa-3, 8-diazabicyclo [3.2.1] octane (**205a, b**), a quinazolinone-containing indole derivative pseudofischerine (**206**) and a new ester of 2,4-dihydroxy-6-methylbenzoic acid, 3-hydroxy-5-methylphenyl 2, 4-dihydroxy-6-methylbenzoate (**207**) (Figure 39) were isolated form the culture of *N. pseudofisheri* KUFC 6422. Compounds **205-207** showed no cytotoxic activity against six human cancer cell lines: Hs683 (glioblastoma), A549 (non-small cell lung cancer), MCF-7 (breast cancer), OE21 (esophageal), U373 (glioblastoma) and SKMEL-28 (melomana) at the highest concentration tested (IC_{50} > 100 µM) (Eamvijarn *et al*., 2012). Masi *et al*. (2013) described isolation of the previously undescribed pyrroloindole terpenoid, fischerindoline (**208**) (Figure 39) from solid and liquid cultures of *N. pseudofischeri*. Fischerindoline (**208**) showed *in vitro* growth inhibitory activity against six human cancer cell lines: A549 (non-small cell lung cancer), Hs683 (oligodendroglioma), MCF-7 (breast cancer), SKMEL28 (melanoma), U373 (glioblastoma) and mouse cancer cell lines B16F10 with IC_{50} 29, 32, 25, 32, 37 and 27 µM respectively.

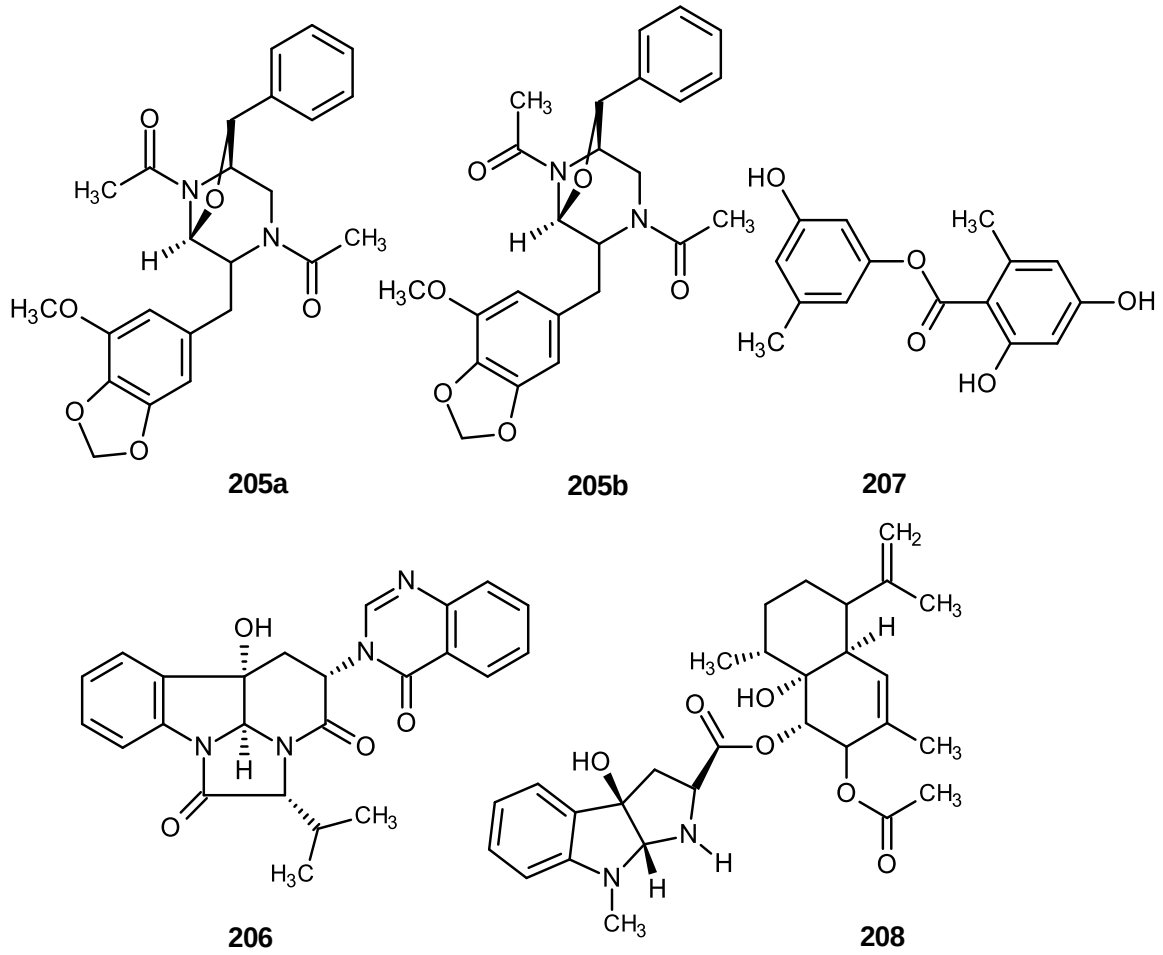

Figure 39. Structures of 3, 8-diacetyl-4 (3-methoxy-4, 5-methylenedioxy) benzyl-7-phenyl-6-oxa-3, 8-diazabicyclo [3.2.1] octane (**205a, b**), pseudofischerine (**206**), 3-hydroxy-5-methylphenyl 2, 4-dihydroxy-6-methylbenzoate (**207**) and fischerindoline (**208**)

The extract from the GlyPY (glycerol-peptone-yeast extract) and GluPY (glucose-peptone-yeast extract) culture broth of the marine-derived fungus *N. pseudofischeri*, which was isolated from the inner tissue of starfish *Acanthaster planci*, furnished two novel diketopiperazines, neosartins A and B (**209** and **210**) and a new alkaloid, neosartin C (**211**) (Figure 40) (Liang *et al*., 2014). Compounds **210** and **211** were evaluated for their antibacterial activity against three multidrug-resistant bacteria; Gram-positive *Staphylococcus aureus* ATCC29213, Methicillin-resistant *Staphylococcus aureus* R3708 and Gram-negative *Escherichia coli* ATCC25922 but showed no activity against all these tested organisms with MIC > 256 µg/mL.

Five new metabolites including deacetylsesquiterpene (**212**), 5-formyl-6-hydroxy-8-isopropyl-2-naphthoic acid (**213**), 6, 8-dihydroxy-3-(1*E*, 3*E*)-penta-1, 3-dien-1-yl) isochroman-1-one (**214**), 5-olefin phenylpyropene A (**215**) and 13-dehydroxylpyripyropene A (**216**) (Figure 40) were obtained from the mycelium of the marine fungus *N. pseudofischeri*, which was isolated from *Acanthaster planci* from the South China Sea. Compounds **212-216** showed significant cytotoxicity against the insect cell line Sf9 (*Spodoptera frugiperda*) with the cell growth inhibitory rates 98.68, 90.97, 61.67, 85.24 and 85.37 %, after 48 h of the treatment at the concentration of 50 mg/L (Lan *et al*., 2016).

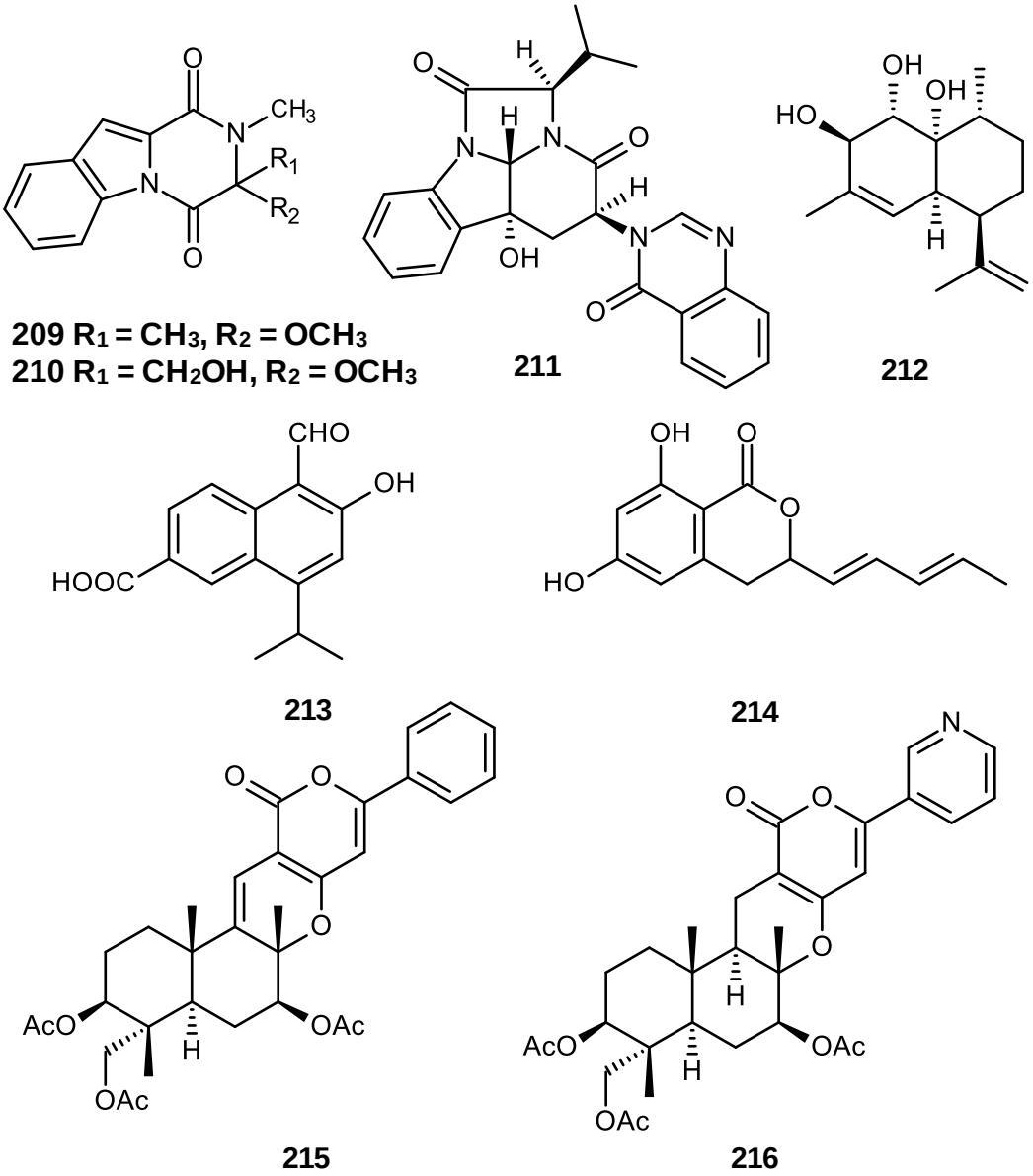

Figure 40. Structures of neosartins A-C (**209-211**), deacetylsesquiterpene (**212**), 5-formyl-6-hydroxy-8-isopropyl-2-naphthoic acid (**213**), 6, 8-dihydroxy-3-(1*E*, 3*E*)-penta-1, 3-dien-1-yl) isochroman-1-one (**214**), 5-olefin phenylpyropene A (**215**) and 13-dehydroxylpyripyropene A (**216**)

2.2.4 *Neosratorya spinosa*

Rajachan *et al*. (2016) reported isolation of two ester epimers, 2*S*, 4*S*-spinosate (**217**), 2*S*, 4*R*-spinosate (**218**) and four meroterpenoids, 1-hydroxychevalone C (**219**), 1-acetoxychevalone C (**220**) 1,11-dihydroxychevalone C (**221**) and 11-hydroxychevalone C (**222**) (Figure 41) from the culture broth of the soil-derived fungus *Neosartorya spinosa* KKU-1NK1.

Compound **219** showed antimycobacterial activity against *Mycobacterium tuberculosis* with MIC value of 26.5 µM, while compound **220** exhibited weak antimalarial activity against *Plasmodium falciparu*m with IC_{50} values of 6.67 µM. In addition compounds **219-221** displayed cytotoxic activity against three human cancer cell lines, epidermoid carcinoma KB, breast adenocarcinoma MCF-7 and small cell lung cancer NCI-H187 with IC_{50} values in the range of 32.7-100.7 µM, as well as against Vero cell lines with IC_{50} in the range of 28.9-78.2 µM, respectively (Rajachan *et al*., 2016).

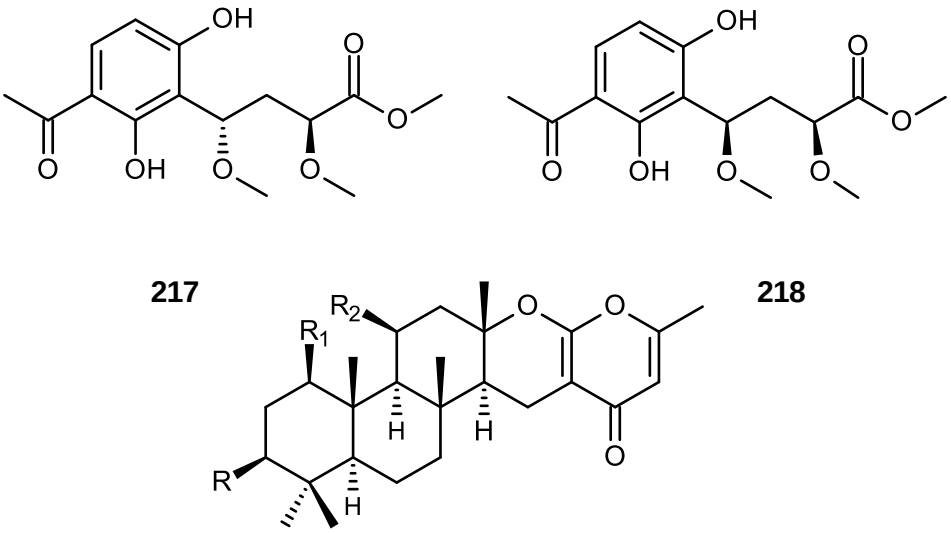

219 R = OAc, R_1 = OH, R_2 = H
220 R = R_1 = OAc, R_2 = H
221 R = OAc, R_1 = R_2 = OH
222 R = OAc, R_1 = H, R_2 = OH

Figure 41. Secondary metabolites isolated from *Neosartorya spinosa* KKU-1NK1 (**217-222**)

2.2.5 *Neosartorya siamensis*

Seven new indole alkaloids including a new indoloazepinone derivative sartorymensin (**223**), two new quinazolinone derivatives: tryptoquivaline O (**224**), 3′-(4-oxoquinazolin-3-yl) spiro [1*H*-indole-3, 5′-oxolane]-2, 2′-dione (**225**) and four new pyrazinoquinazolinone derivatives: *epi*-fiscalin A (**226**), *epi*-fiscalin C (**227**), neofiscalin A (**228**) and *epi*-neofiscalin A (**229**) (Figure 42) were isolated from the previously undescribed soil fungus *N. siamensis* KUFC 6349. Only compound **223**

displayed a moderate *in vitro* growth inhibitory activity against the human U373 and Hs683 (glioblastoma), A549 (non-small cell lung cancer), MCF-7 (breast cancer) and SKMEL-28 (melanoma) cancer cell lines with IC_{50} 44, 50, 39, 43 and 73 µM respectively (Buttachon *et al*., 2012).

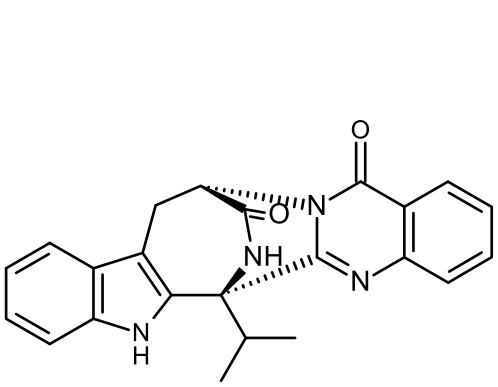

223

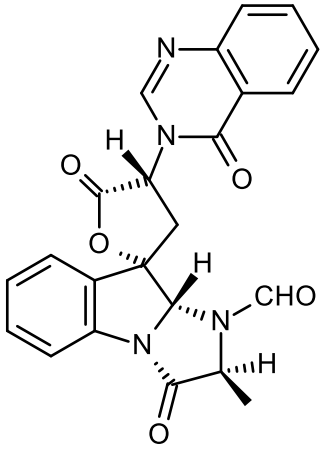

224

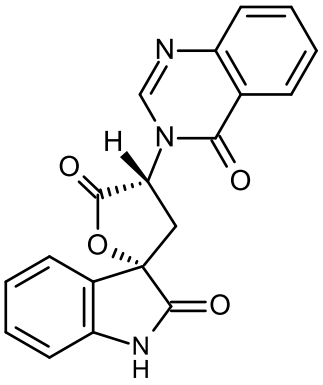

225

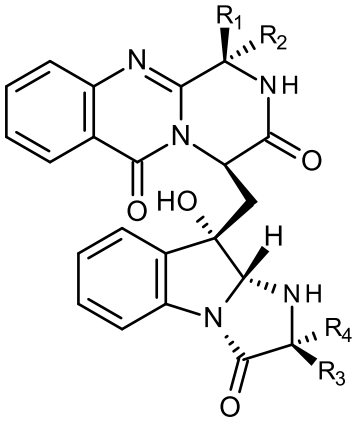

226 R_1 = CH $(CH_3)_2$, R_2 = R_4 = H, R_3 = Me
227 R_1 = CH $(CH_3)_2$, R_2 = H, R_3 = R_4 = Me
228 R_1 = R_3 = H, R_2 = CH $(CH_3)_2$, R_4 = Me
229 R_1 = CH $(CH_3)_2$, R_2 = R_3 = H, R_4 = Me

Figure 42. Structures of sartorymensin (**223**), tryptoquivaline O (**224**), 3′-(4-oxoquinazolin-3-yl) spiro [1*H*-indole-3, 5′-oxolane]-2, 2′-dione (**225**), *epi*-fiscalin A (**226**), *epi*-fiscalin C (**227**), neofiscalin A (**228**) and *epi*-neofiscalin A (**229**)

New chevalone derivative, chevalone E (**230**), two new isocoumarin derivatives 6, 8-dihydroxy-3, 7-dimethylisocoumarin (**231**) and 5-hydroxy-8-methyl-2*H*, 6*H*-pyrano [3,4-*g*]-chromen-2, 6-dione (**232**) and a new pyripyropene named pyripyropene S (**233**) (Figure 43) were isolated from the marine sponge-associated fungus *Aspergillus similanesis* KUFA 0013. Compounds **230-233** showed no antimicrobial activity against Gram-positive bacteria: *Staphylococcus aureus* ATCC 25923, *Bacillus subtilis* ATCC 6633 and Gram-negative bacteria: *Escherichia coli* ATCC 25922, *Pseudomonans aeruginosa* ATCC 27853, as well as multidrug-resistant isolates from the environment with MIC > 256 µg/mL. The compounds also did not inhibit an in vitro growth of the yeast *Candida albicans* ATCC 10231, at the highest concentration used. However, chevalone E (**230**) was found to exhibit potential synergy with the antibiotic oxacillin (OX) and ampicillin (AMP) against methicillin-resistant *Staphylococcus aureus* (MRSA) strain (Prompanya *et al*., 2014).

Later on, the same authors Prompanya *et al*. (2015) have described isolation of a new isocoumarin derivative**,** similanpyrone C (**234**), a new pyripyropene derivative, pyripyropene T (**235**) and a new cyclohexapeptide similanamide (**236**), (Figure 43) from the same fungus. Compounds **235** and **236** were evaluated for their antibacterial and cytotoxic activities. Similanamide (**236**) exhibited a weak *in vitro* growth inhibitory activity against three human cancer cell lines, MCF-7 (breast adenocarcinoma), NCI-H460 (non-small cell lung cancer) and A373 (melanoma) with GI_{50} 125 ± 0, 117.50 ± 3.55 and 115 ± 7.07, respectively. However, neither of them showed antibacterial activity against four reference strains *Staphylococcus aureus*

ATCC 25923, *Bacillus subtilis* ATCC 6633, *Escherichia coli* ATCC 25922 and *Pseudomonans aeruginosa* ATCC 27853, as well as MRSA and VRE multidrug-resistant isolates from the environment (MIC > 256 µg/mL).

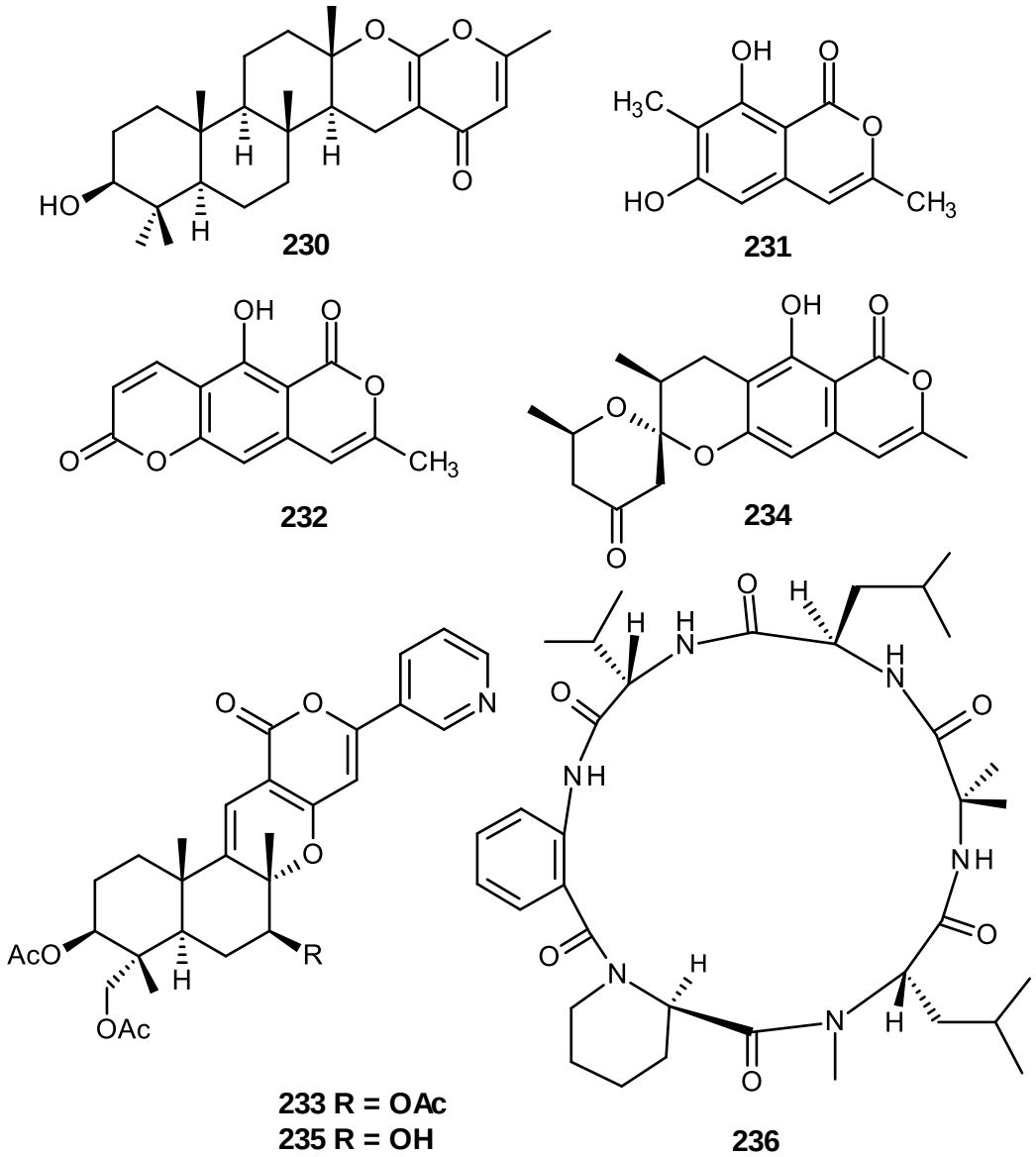

Figure 43. Structures of chevalone E (**230**), 6, 8-dihydroxy-3, 7-dimethylisocoumarin (**231**), 5-hydroxy-8-methyl-2*H*, 6*H*-pyrano [3,4-*g*]-chromen-2, 6-dione (**232**), pyripyropenes S and T (**233** and **235**), similanpyrone C (**234**) and similanamide (**236**)

2.2.6 *Neosartorya glabra*

Three new bicyclic lactones, glabramycins A-C (**237-239**) (Figure 44) were isolated from a *Neosartorya glabra* strain, which was isolated from a soil sample collected from Candamia, Spain. Compound **239** exhibited strong antibacterial activity against *Streptococcus pneumonia* with MIC 2 µg/mL, modest antibiotic activity against *Staphylococcus aureus* and *Bacillus subtilis* with MIC 16 µg/mL but weak activity against *Enterococcus faecalis* with MIC > 32 µg/mL. Compounds **237** and **238** showed weak activity against *Streptococcus pneumonia* with MIC values of 32 and 64 µg/mL, respectively (Jayasuriya *et al*., 2009).

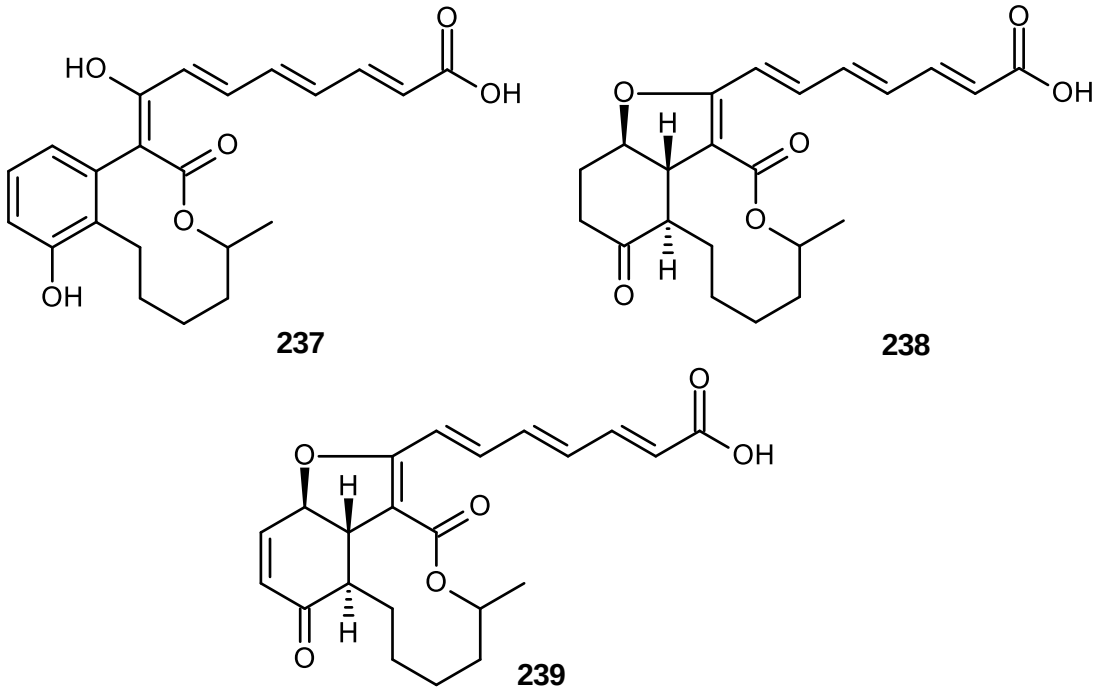

Figure 44. Structures of glabramycins A (**237**), B (**238**) and C (**239**)

The culture of *N. glabra* KUFC 6311 produced the ardeemin analogs, sartoryglabrins A-C (**240-242**) (Figure 45). Compound **240** showed a strong growth inhibitory activity against MCF-7 (breast adenocarcinoma) cell line with GI_{50} 27.0 ± 0.57 µM and a weak activity against NCI-H460 (non-small cell lung cancer) cell line with GI_{50} 84.0 ± 2.1 µM but inactive against the A375-C5 (melanoma cell line) at the highest concentration tested with GI_{50} > 150 µM. Compound **241** displayed a moderate growth inhibitory activity against MCF-7 cell line with GI_{50} 53.0 ± 4.7 µM but inactive against both NCI-H460 and A-375-C5 cell lines with GI_{50} > 150 µM. Compound **242** displayed moderate growth inhibitory activity against MCF-7 cell line with GI_{50} 44.0 ± 7.2 µM and weak inhibitory activity against NCI-H460 and A375-C5 cells with GI_{50} 82.3 ± 5.6 µM and 108.0 ± 7.7 µM respectively (Kijjoa *et al*., 2011)

Liu *et al*. (2015) described isolation of two new polyketides, neosarphenols A-B (**243-244**) (Figure 45) from *N. glabra* CGMCC 32286 and both of the compounds were evaluated for their cytotoxic activity against human breast cancer cells MCF-7, MDA-MB-231 and human pancreatic cancer cell PANC-1. Only neosarphenol A (**243**) showed selective but moderate cytotoxic activity against PANC-1 cell line with IC_{50} values of 14.38 µM.

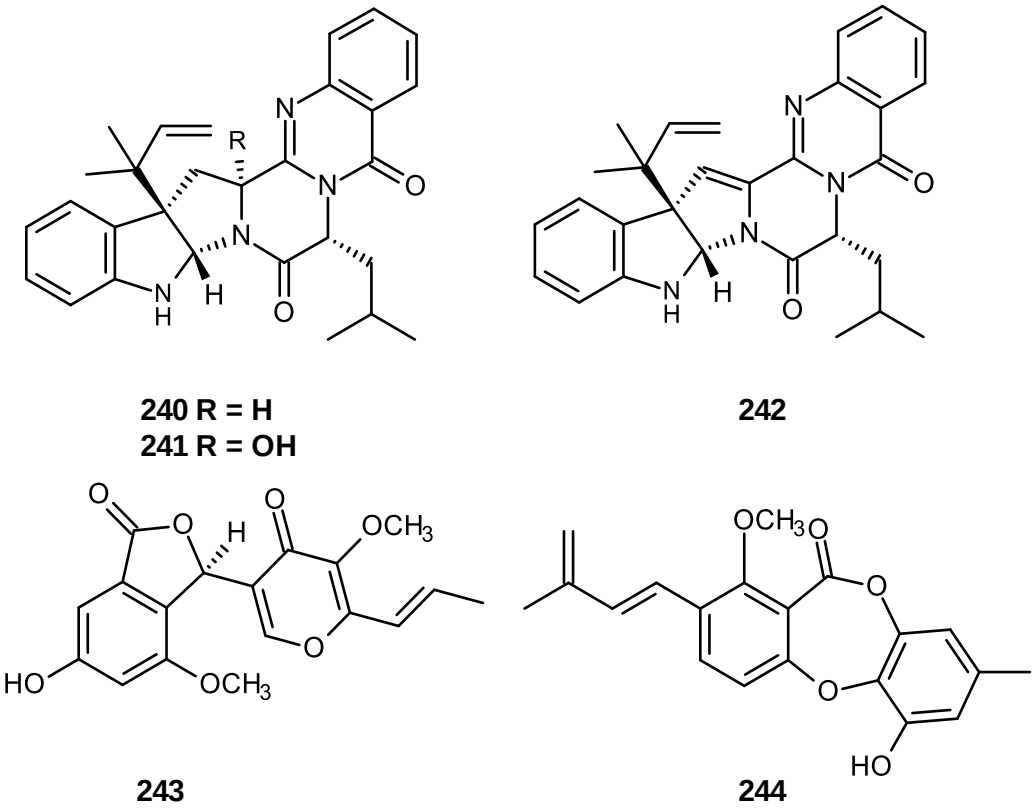

240 R = H
241 R = OH

242

243

244

Figure 45. Structures of sartoryglabrins A-C (**240-242**) and neosarphenols A and B (**243** and **244**)

2.2.7 *Neosartorya udagawae*

Four new quinazoline-containing indole alkaloids, neosartoryadins A and B (**245** and **246**) and fiscalins E and F (**247** and **248**) (Figure 46) were isolated from the endophytic fungus *Neosartorya udagawae* HDN 13-313. Compounds **245-248** showed no cytotoxic activity against human myeloid leukemia HL-60 cancer cell line with IC_{50} >50 μM. However, compounds **245** and **246** showed antiviral activity against influenza virus A (H1N1) with IC_{50} values of 66 and 58 μM, respectively (Yu *et al*., 2016).

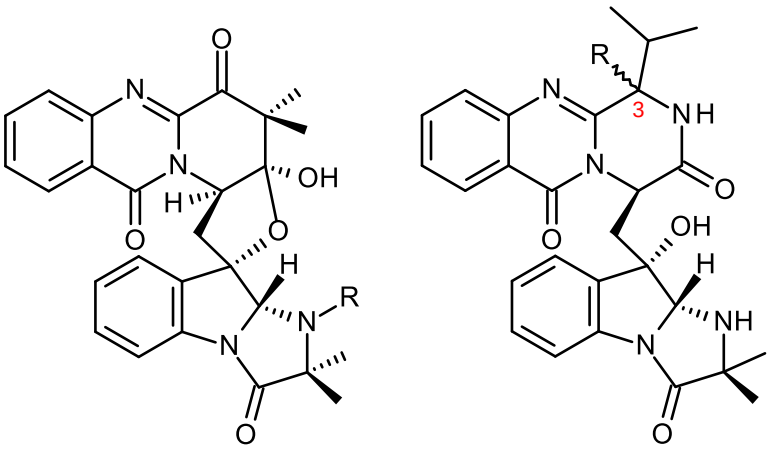

245 R = H
246 R = OH

247 R = OCH_3, 3*R*
248 R = OCH_3, 3*S*

Figure 46. Structures of neosartoryadins A and B (**245** and **246**) and fiscalins E and F (**247** and **248**)

2.2.8 *Neosartorya tsunodae*

A new chevalone analog, sartorypyrone B (**249**) (Figure 47), was isolated from the culture of the marine sponge-associated fungus *N. tsunodae* KUFC 9213. Compound **249** showed strong growth inhibitory activity against breast adenocarcinoma (MCF-7), non-small cell lung cancer (NCI-H460) and melanoma (A375-C5) with GI_{50} 17.8 ± 7.4 µM, 20.5 ± 2.4 µM, and 25.0 ± 4.4 µM, respectively (Eamvijarn *et al*., 2013).

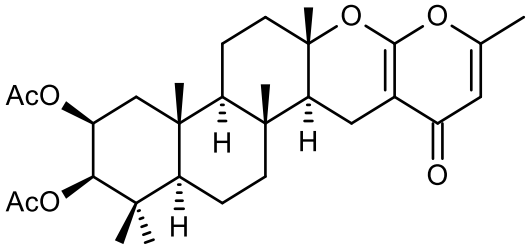

249

Figure 47. Structure of sartorypyrone B (**249**)

2.2.9 *Neosartorya paulistensis*

A new aszonapyrone analog, sartorypyrone C (**250**) (Figure 48) was isolated from the culture of *N. paulistensis* KUFC 7897, which was isolated from the marine sponge *Chondrilla australiensis*, collected from the Gulf of Thailand. Compound **250** displayed no antibacterial activity against four reference strains

Staphylococcus aureus ATCC 25923, *Bacillus subtilis* ATCC 6533, *Escherichia coli* ATCC 25922, and *Pseudomonas aeruginosa* ATCC 27853, as well as the environmental multidrug-resistant isolates (Gomes *et al*., 2014).

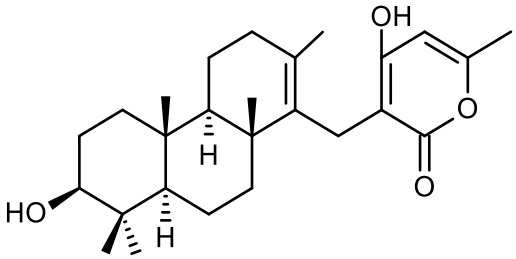

250

Figure 48. Structure of sartorypyrone C (**250**)

2.3 *Eurotium* species

The fungal genus *Eurotium*, which is the teleomorph of *Aspergillus*, has been proved to be a rich source of novel bioactive metabolites (Ishikawa *et al*., 1984; Li *et al*., 2009; Slack *et al*., 2009). The genus *Eurotium* is an important mycotoxin-producer (Samson and Pitt, 2000), which produces a variety of metabolites, including meroterpenoids, sesquiterpene alkaloids, sesquiterpenes, benzaldehyde derivatives, phenolic compounds, diketopiperazines, hydraquinone pigments and anthraquinones (Al-Julaifi, 2003; Anke *et al*., 1980; Domsch *et al*., 1980; Gould and Raistrick, 1934;

Kanokmedhakul *et al*., 2011; Li *et al*., 2008a; Sáiz-Jiménez and Haider, 1975; Slack *et al*., 2009).

Only few species of *Eurotium* have been investigated for their secondary metabolites and associated biological activities. The present review covers only new secondary metabolites isolated from some *Eurotium* species and their interesting biological activities.

2.3.1 *Eurotium cristatum*

Four new indole alkaloids cristatumins A-D (**251-254**) (Figure 49) were isolated from the marine-derived entophytic fungus *Eurotium cristatum* EN-220. Compound **251** displayed moderate antibacterial activity against *Escherichia coli* with the MIC 64 µg/mL, while compound **254** exhibited weak activity against *Staphylococcus aureus* with an inhibititon zone of 8 mm at 100 µg/disk. Compound **252** showed moderate lethal activity against brine shrimp (*Artemia salina*) with the LD_{50} 74.4 µg/mL (Du *et al*., 2012).

Gomes *et al*., (2012) described isolation of eurocristatine, a new diketopiperazine dimer (**255**) (Figure 49) from the culture of the marine sponge-associated fungus *E. cristatum* KUFC 7356. Compound **255** showed no *in vitro* growth inhibitory activity against breast adenocarcinoma (MCF-7), non-small lung

cancer (NCI-H-460) and melanoma (A375-C5) at the highest concentration tested (150 µM). Moreover they did not exhibit either antifungal activity against yeast *Candida albicans*, filamentous fungus *Aspergillus fumigatus* and dermatophyte *Trichophyton rubrum* or antibacterial activity against *Staphylococcus aureus*, *Escherichia coli* and *Pseudomonas aeruginosa*.

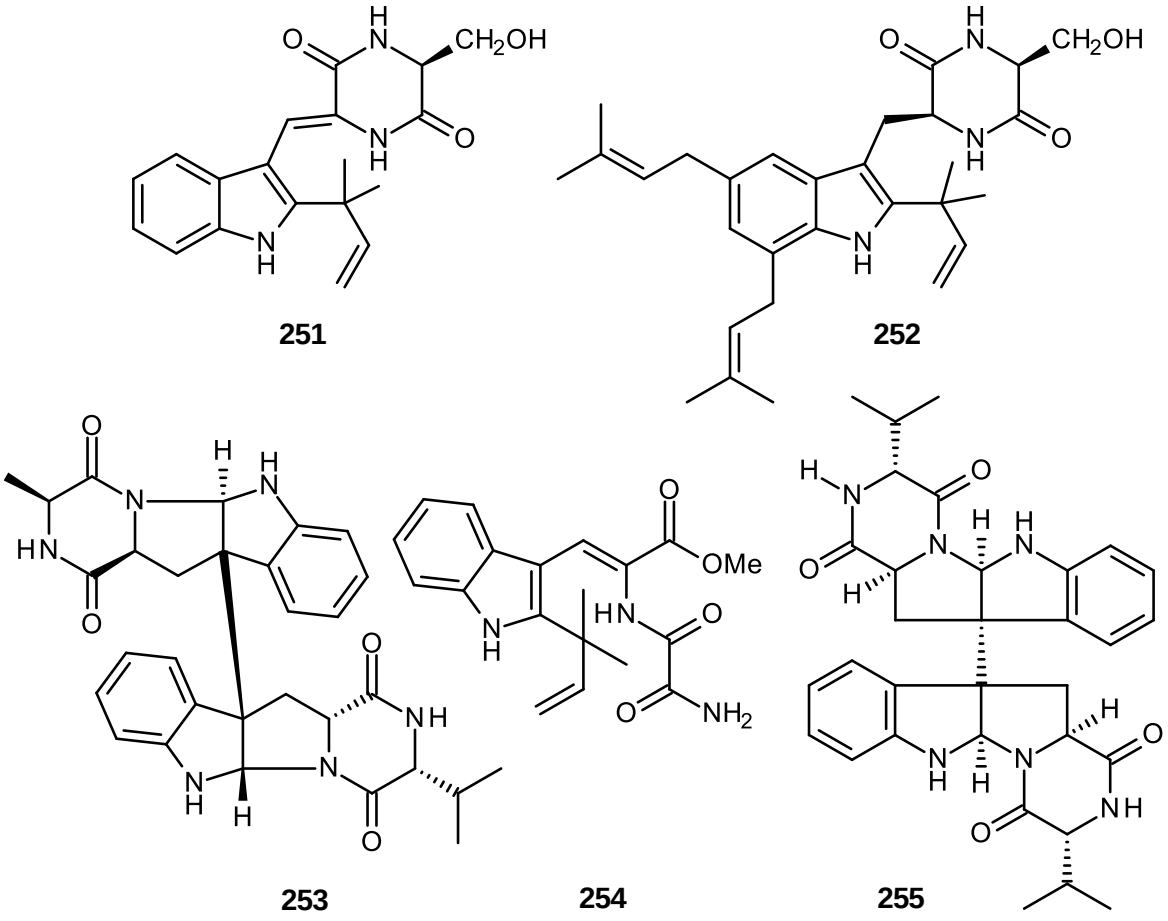

Figure 49. Structures of cristatumins A-D (**251-254**) and eurocristatine (**255**)

A new prenylated indole diketopiperazine alkaloid, cristatumin F (**256**) (Figure 50) was isolated from the fungus *E. cristatum*, which was isolated from a sample of fuzhuan brick tea, and cultured on a solid-substrate fermentation. Compound **256** exhibited a modest radical scavenging activity against DPPH (1, 1-diphenyl-2-picrylhydrazyl) radical with an IC_{50} value of 53.6 μM and exhibited marginal cell prolification inhibition (20.6 % inhibition) against 3T3L1 pre-adipocytes at 200 μM (Zou *et al*., 2014).

Marine alga-derived endophytic fungus *E. cristatum* EN-220 produced a new anthraquinone glycoside, 3-*O*-(α-D-ribofuranosyl) questinol (**257**) and a new orsellinic acid ester, cristatumside A (**258**) (Figure 50). Compounds **257** and **258** showed neither antibacterial activity against *Staphylococcus aureus* and *Escherichia coli*, nor antifungal activities against *Physalospora obtuse*, *Alternaria brassicae*, *Valsa mali*, *Alternaria solania* and *Sclerotinia miyabeana*. They did not exhibit any lethality activity against brine shrimp *Artemia salina* (Du *et al*., 2014).

Four new indolediketopiperazine derivatives, *N*-(4′-hydroxyprenyl)-cyclo (alanyltryptophyl) (**259**), isovariecolorin I (**260**), 30-hydroxyechinulin (**261**) and 29-hydroxyechinulin (**262**) (Figure 50) were isolated from the endophytic fungus *E. cristatum* EN-220 which was isolated from the marine alga *Sargassum thunbergii*. Compound **260** showed lethal activity against brine shrimp *Artemia salina* with

LD_{50} 19.4 μg/mL, while compounds **261** and **262** exhibited weak lethal activity with LD_{50} 138.1 and 140.6 μg/mL. Compound **260** not only displayed weak nematicidal activity against *Panagrellus redivivus* (nematode) with LD_{50} 110.3 μg/mL but also showed a moderate antioxidative activity against DPPH with IC_{50} 20.6 μg/mL. However, compounds **259-262** exhibited no antimicrobial activity against six pathogenic bacteria *Escherichia coli*, *Staphylococcus aureus*, *Bacillus subtilis*, *Micrococcus luteus*, *Salmonella enterica* and *Bacillus pumilus* and nine plant-pathogenic fungi *Alternaria brassicae*, *Valsa mali*, *Physalospora obtusa*, *Alternaria solania*, *Sclerotinia miyabeana*, *Magnaporthe grisea*, *Fusarium oxysporum*, *Botryosphaeria dothidea* and *Colletotrichum gloeosporioides* (Du *et al*., 2017).

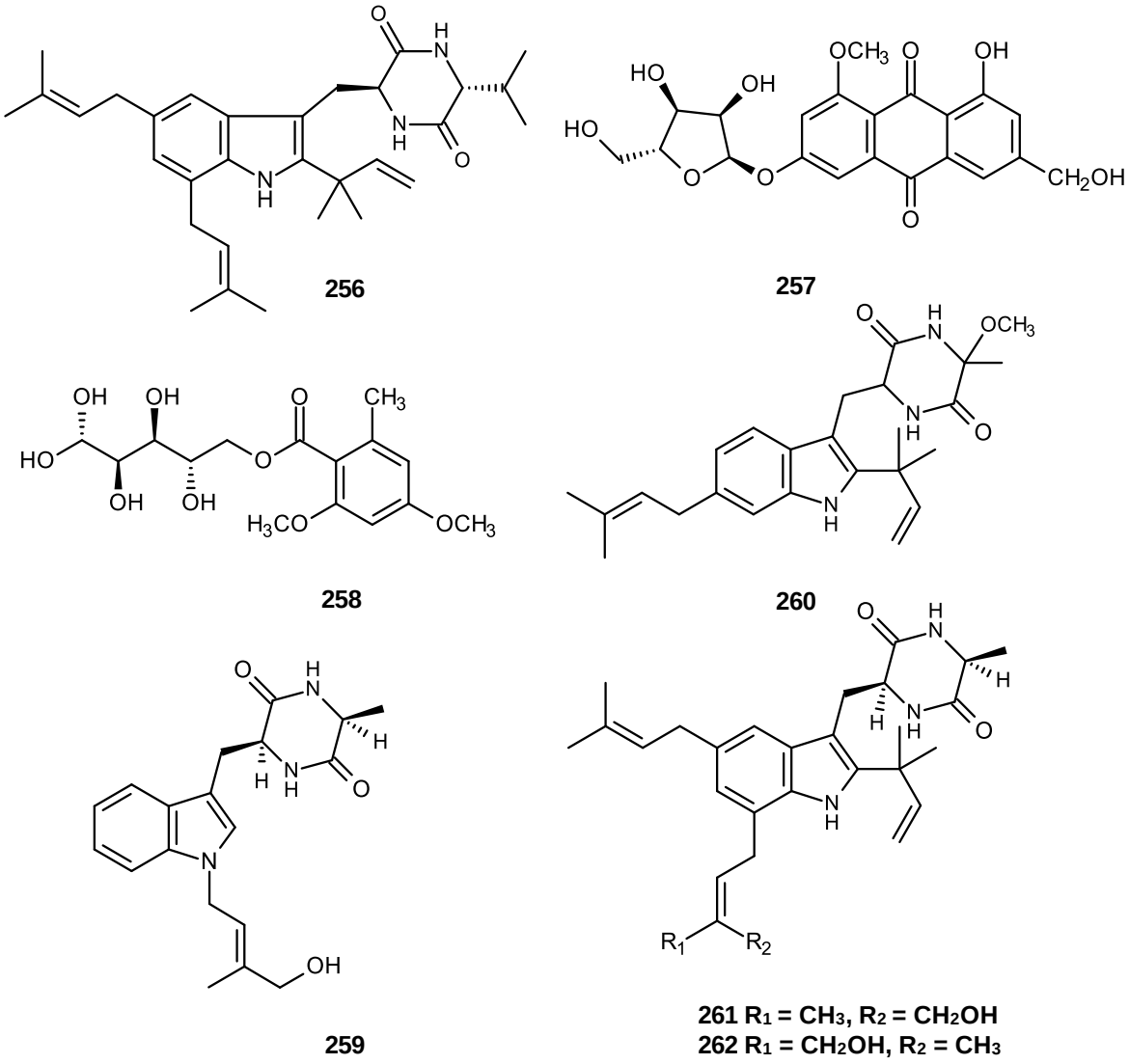

Figure 50. Structures of cristatumin F (**256**), 3-*O*-(α-D-ribofuranosyl) questinol (**257**), cristatumside A (**258**), *N*-(4′-hydroxyprenyl)-cyclo (alanyltryptophyl) (**259**), isovariecolorin I (**260**), 30-hydroxyechinulin (**261**) and 29-hydroxyechinulin (**262**)

2.3.2 *Eurotium rubrum*

Four new benzaldehyde derivatives, eurotirumin (**263**), 2-(2′, 3-epoxy-1′-heptenyl)-6-hydroxyl-5-(3″-methyl-2″-butenyl) benzaldehyde (**264**), 2-(1′, 5′-heptadienyl)-3, 6-dihydroxy-5-(3″-methyl-2″-butenyl) benzaldehyde (**265**) and (*E*)-6-hydroxy-7-(3-methyl-2-butenyl)-2-(3-oxobut-1-enyl) chroman-5-carbaldehyde (**266**) (Figure 51) were isolated from the liquid fermentation cultures of an endophytic fungus *Eurotium rubrum*, which was isolated from the inner tissue of stems of the mangrove plant *Hibiscus tiliaceus* (Li *et al*., 2008a). None of the compounds showed cytotoxic activity against any of the four cell lines: mouse leukemai P-388, human leukemia K-562, human promyelocytic leukemia HL-60 and human pulmonary epithelial A-549 with IC_{50} > 10 µg/mL (Li *et al*., 2008a). Later on, the same authors (Li *et al*., 2008b) have described isolation of two new dioxopiperazine derivatives, dehydrovariecolorin L (**267**) and dehydroechinulin (**268**) from the same fungus. Compounds **267** and **268** showed neither 1, 1-diphenyl-2-picrylhydrazyl (DPPH) radical-scavenging activity (IC_{50} > 160 µM) nor cytotoxic activity against three cancer cell lines: P-388, HL-60 and A-549.

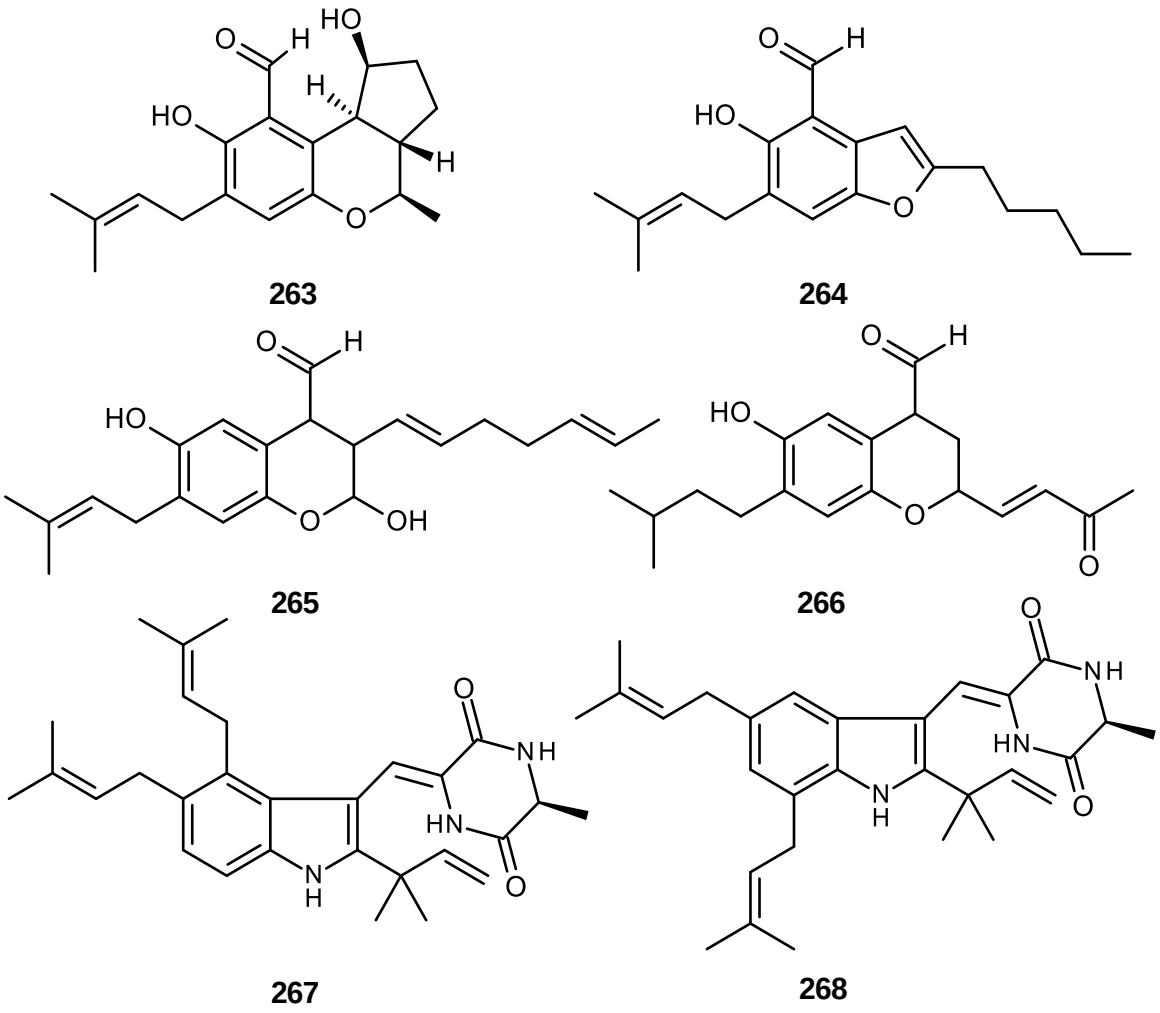

Figure 51. Secondary metabolites isolated form *Eurotium rubrum* (**263-268**)

Marine mangrove plant-derived endophytic fungus *Eurotium rubrum* produced four new metabolites including bisdihydroanthracenone derivative, eurorubrin (**269**), two *seco*-anthraquinone derivatives, 2-*O*-methyl-9-dehydroxyeurotinone (**270**), 2-*O*-methyl-4-*O*-(α-D-ribofuranosyl)-9-dehydroxyeurotinone (**271**) and anthraquinone glycoside, 3-*O*-(α-D-ribofuranosyl)-questin (**272**) (Figure 52). Compound **269** showed strong DPPH (1, 1-diphenyl-2-picrylhydrazyl) radical scavenging activity with IC_{50} 44.0 µM. However, compounds **270**, **271** and **272** showed weak or moderate DPPH radical scavenging activity (Li *et al*., 2009). A new spirocyclic diketopiperazine alkaloid, 7-*O*-methylvariecolortide A (**273**) was also isolated from the marine mangrove-derived endophytic fungus *E. rubrum* which was isolated from the inner tissue of the stems of the mangrove plant *Hibiscus tiliaceus* (Li *et al*., 2010a).

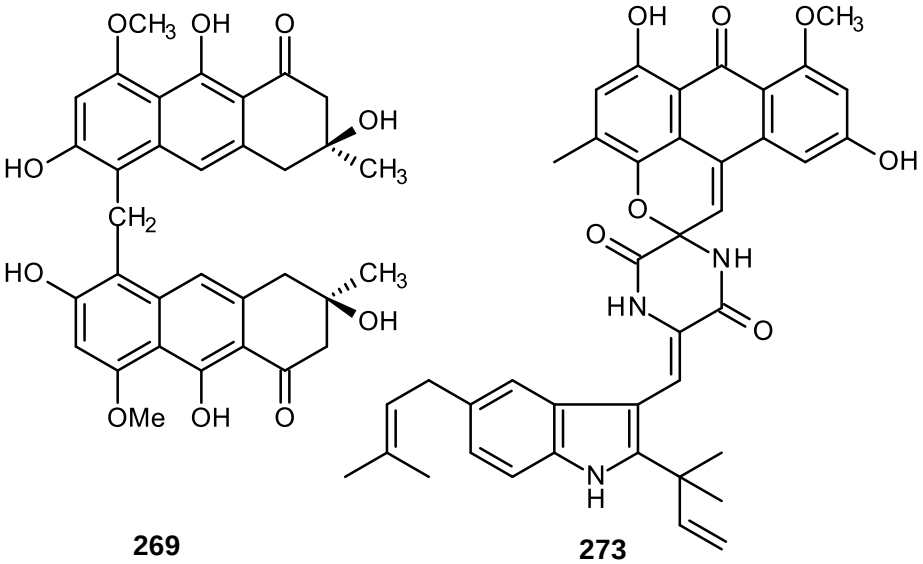

269 **273**

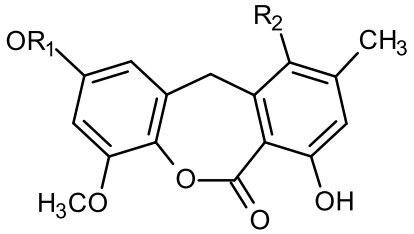

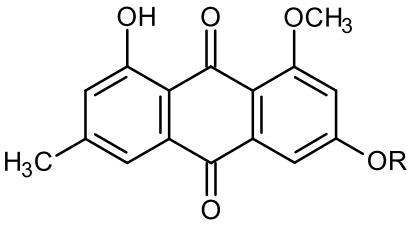

270 R_1 = R_2 = H
271 R_1 = α-D-ribofuranosyl **272 R = α-D-ribofuranosyl**

Figure 52. Structures of eurorubrin (**269**), 2-*O*-methyl-9-dehydroxyeurotinone (**270**), 2-*O*-methyl-4-*O*-(α-D-ribofuranosyl)-9-dehydroxyeurotinone (**271**), 3-*O*-(α-D-ribofuranosyl)-questin (**272**) and 7-*O*-methylvariecolortide A (**273**)

New diketopiperazine alkaloid, 12-demethyl-12-oxo-eurotechinulin B (**274**) and anthraquinone derivative, 9-dehydroxyeurotinone (**275**) (Figure 53) were isolated from an endophytic fungus *E. rubrum*. Compound **274** displayed cytotoxic activity against human hepatoma cell line SMMC-7721 with the IC_{50} 30 µg/mL, while compound **275** showed weak antibacterial activity against *Escherichia coli* with an inhibition zone of 7.0 mm at 100 µg/disk and also showed weak cytotoxic activity against human-cholangiocarcinoma cell line SW1990 with IC_{50} 25 µg/mL (Yan *et al*., 2012).

Two new sulfur-containing benzofuran derivatives eurothiocin A and B (**276** and **277**) (Figure 53) were isolated from the soft coral-derived fungus *E. rubrum* SH-823. Compounds **276-277** exhibited more potent inhibitory effects against α-glucosidase activity with IC_{50} 17.1 and 42.6 µM than the α-glucosidase inhibitor acarbose with IC_{50} 376.7 µM (Liu *et al*., 2014b).

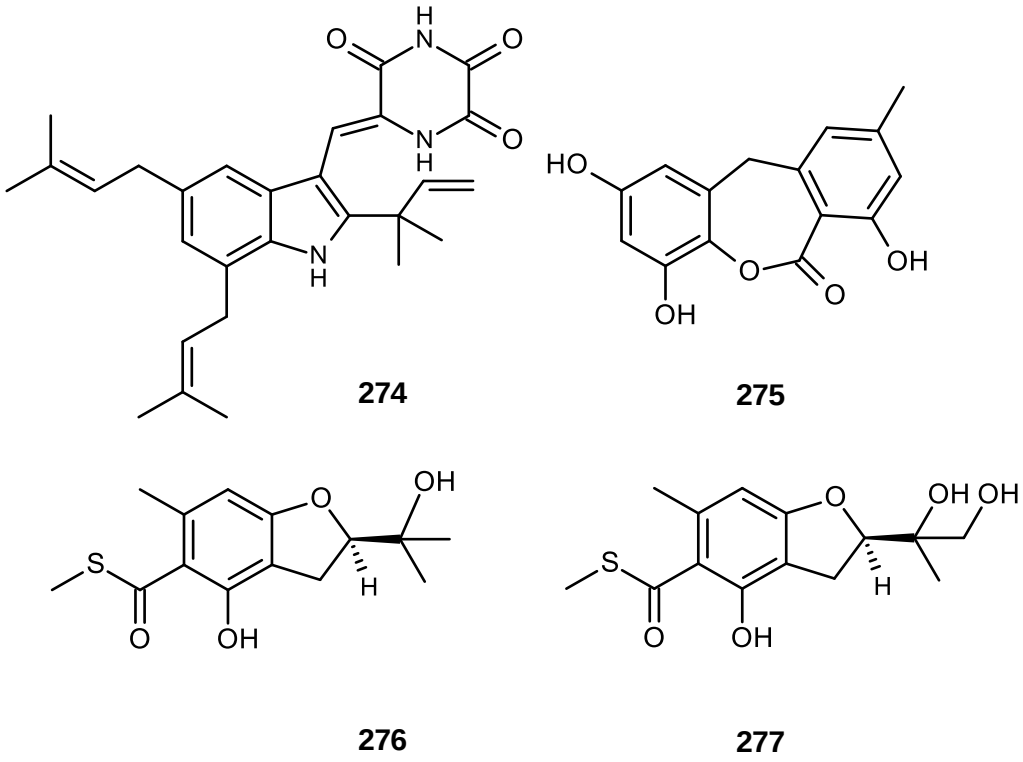

274 **275**

276 **277**

Figure 53. Structures of 12-demethyl-12-oxo-eurotechinulin B (**274**), 9-dehydroxyeurotinone (**275**) and eurothiocins A and B (**276** and **277**)

The strain *E. rubrum* MA-150 which was isolated form the mangrove-derived rhizospheric soil, collected from the Andaman Sea coastline, Thailand produced three new indolediketopiperazine alkaloids, rubrumazines A-C (**278-280**). Compounds **278** and **280** displayed moderate activity in brine shrimp lethal activity assay against *Artemia salina* with LD_{50} 29.8 and 16.5 µM, while compound **279** showed potent lethal activity with LD_{50} 2.4 µM. However, compounds **278-280**

displayed no antibacterial activity against *Escherichia coli*, *Staphylococcus aureus*, *Micrococcus luteus*, *Vibrio alginolyticus* and *Vibro anguillarum* (Meng *et al*., 2015).

In 2016, Meng *et al*. (2016) described isolation of a chiral 2-benzofuran-1 (3*H*)-one derivative (±)-europhenol A (**281**) (Figure 54) from the same fungus. Compound **281** exhibited potent DPPH radical scavenging activity with IC_{50} 1.23 µg/mL but weak antibacterial activity against *Vibrio anguillarum* with MIC 32 µg/mL. Recently, Kamauchi *et al*. (2016) isolated a new dikeopiperazine, isoechinulin D (**282**) (Figure 54) from the marine-derived fungus *Eurotium rubrum* MPUC136, which was cultured on the wheat medium. Compound **282** was found to inhibit melanogenesis using theophylline-stimulated B16 melanoma 4A5 cells with IC_{50} 60 µM.

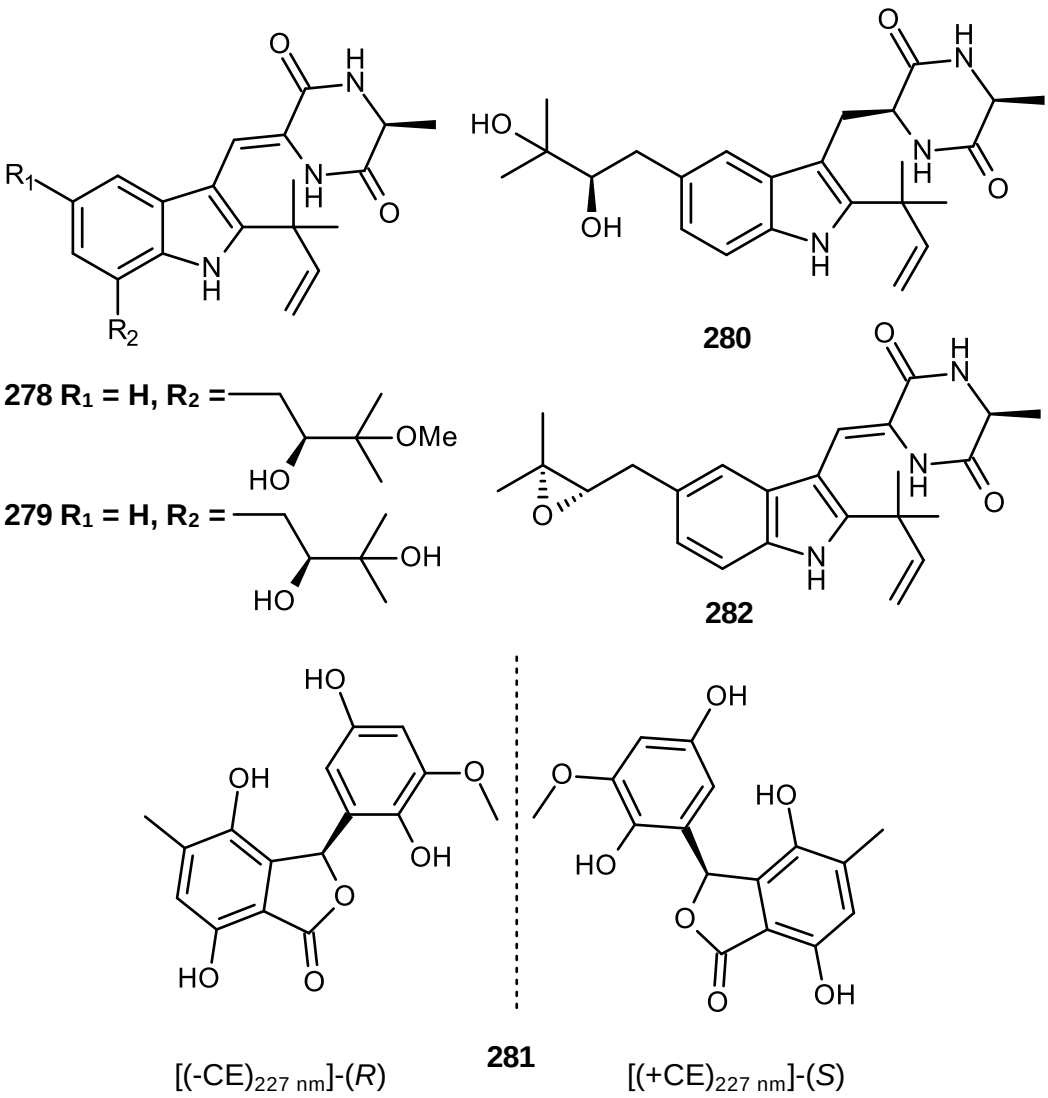

Figure 54. Structures of rubrumazines A-C (**278-280**), (±)-europhenol A (**281**) and isoechinulin D (**282**)

2.3.3 *Eurotium repens*

Two new benzyl derivatives, (*E*)-2-(hept-1-enyl)-3-(hydroxymethyl)-5-(3-methylbut-2-enyl) benzene-1, 4-diol (**283**) and (*E*)-4-(hept-1-enyl)-7-(3-methylbut-2-enyl)-2, 3-dihydrobenzofuran-2, 5-diol (**284**) (Figure 55), were isolated from the bioassay-guided fractionation of the fungus *Eurotium repens*. Compounds **283** and **284** showed good binding affinity for human opioid with IC_{50} 5.4 and 32.4 µM (Gao *et al*., 2011).

Compound **283** showed both active antibacterial activity against methicillin-resistant *Staphylococcus aureus* (MRSA) with IC_{50} 11.97 µg/mL and antifungal activity against *Candida glabrata* with IC_{50} 7.17 µg/mL. Moreover, compound **283** also exhibited antimalarial activity against both chloroquine-sensitive and chloroquine-resistant strains of *Plasmodium falciparum* with IC_{50} 3.0 and 2.8 µg/mL as well as active antileishmanial activity against *Leishmania donovani* promastigotes with IC_{50} 19 µg/mL. However compounds **283** did not show any cytotoxic activity against the mammalian kidney fibroblasts VERO cells (Gao *et al*., 2012).

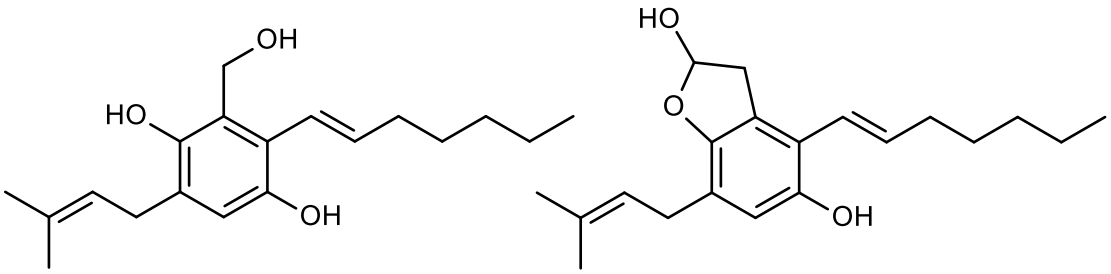

283 **284**

Figure 55. Structures of (*E*)-2-(hept-1-enyl)-3-(hydroxymethyl)-5-(3-methylbut-2-enyl) benzene-1, 4-diol (**283**) and (*E*)-4-(hept-1-enyl)-7-(3-methylbut-2-enyl)-2, 3-dihydrobenzofuran-2, 5-diol (**284**)

2.3.4 *Eurotium amstelodami*

Five new prenylated indole metabolites, including neoechinulins A-E (**285-289**), (Figure 56) were isolated from the mycelium of *Aspergillus amstelodami* (Dossena *et al*., 1974; Dossena *et al*., 1975; Marchelli *et al*., 1977). Parshikov *et al*. (2006) described isolation of 5β-hydroxyartemisinin (**290**), a biotransformation product of artemisinin by *Eurotium amstelodami*. Later on, Yang *et al*. (2014) reported isolation of the anthraquinone derivative, questinol (**291**) (Figure 56) from the marine-derived fungus *E. amstelodami*. Compound **291** showed no cytotoxic activity against lipopolysaccharide (LPS)-stimulated macrophage cell line (RAW 264.7) at the concentration up to 200 μM. Additionally, compound **291** also significantly inhibited nitric oxide (NO) and prostaglandin E_2 (PGE_2) production in a

concentration-dependent manner in RAW 264.7 cells, but showed a weak effect on the down-regulation of cyclooxygenase (COX-2) at the concentration of 200 μM. Interestingly, compound **291** significantly inhibited the production of pro-inflammatory cytokines, tumor necrosis factor-α (TNF-α), interleukin (IL-1β) and IL-6 production in RAW 264.7 cells (Yang *et al*., 2014).

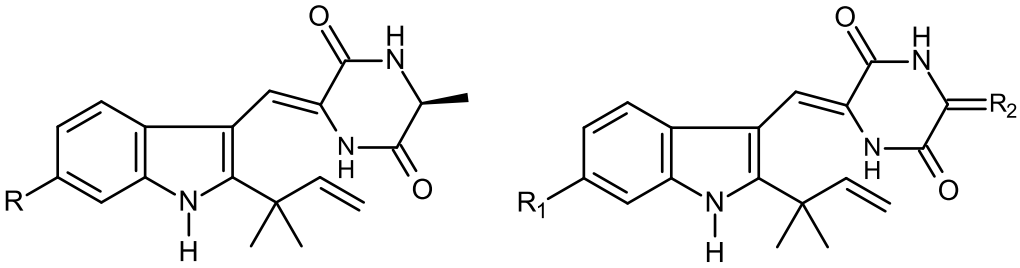

285 R = H

288 R = 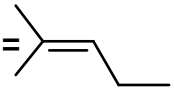

286 R_1 = H, R_2 = CH_2

287 R_1 = 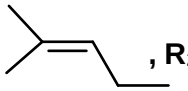 **, R_2 = CH_2**

289 R_1 = H, R_2 = O

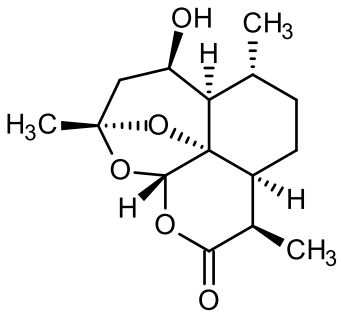

290

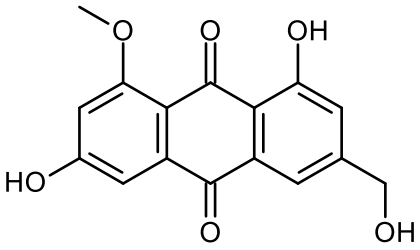

291

Figure 56. Structures of neoechinulins A-E (**285-289**), 5β-hydroxyartemisinin (**290**), questinol (**291**)

2.3.5 *Eurotium herbariorum*

A new pyrrolidinoindoline diketopiperazine dimer, cristatumin E (**292**) (Figure 57) was isolated from the fermentation broth of the algicolous fungus *Eurotium herbariorum* HT-2. Compound **292** displayed moderate cytotoxic activity against human leukemic cell line K562 with IC_{50} 8.3 μM but inactive against breast cancer cell line MCF-7 with IC_{50} > 50 μM. This compound also exhibited weak antibacterial activity against *Bacillus aerogenes* and *Escherichia coli*, both with MIC values 44.0 μM (Li *et al*., 2013).

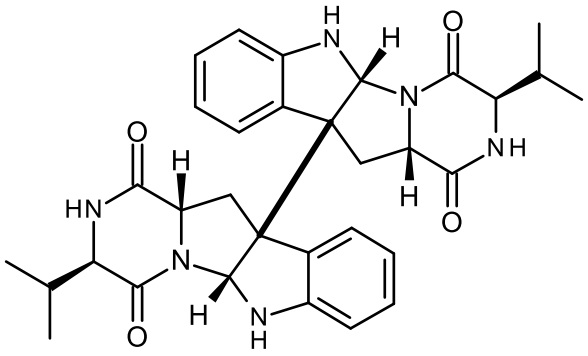

292

Figure 57. Structure of cristatumin E (**292**)

2.3.6 *Eurotium chevalieri*

Five new meroterpenoids, chevalones A-D (**293-296**), aszonapyrone B (**297**) and a new sequiterpene alkaloid, eurochevalierine (**298**) (Figure 58), were isolated from *Eurotium chevalieri*, which was collected from rhizosphere soil of para rubber tree at Surathari Province, Thailand (Kanokmedhakul *et al*., 2011).

Compounds **296** and **298** exhibited antimalarial activity against *Plasmodium falciparum* with IC_{50} 3.1 and 3.4 µg/mL respectively, while compound **295** and **298** showed antimycobacterial activity against *Mycobacterium tuberculosis* with IC_{50} 6.3 and 50.0 µg/mL respectively. Compounds **295**, **296** and **298** also showed cytotoxic activity against human breast cancer BC1 cell lines with IC_{50} of 8.7, 7.8 and 5.9 µg/mL, whereas compound **294** and **298** showed cytotoxicity against two cancer cell lines: human epidermoid carcinoma KB and small cell lung cancer NCI-H187. While the IC_{50} values of **294** against KB and NCI-H187 were 2.9 and 9.8 µg/mL, those for **298** were 3.9 and 9.2 µg/mL, respectively (Kanokmedhakul *et al*., 2011).

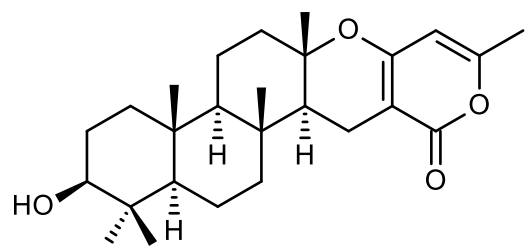

293

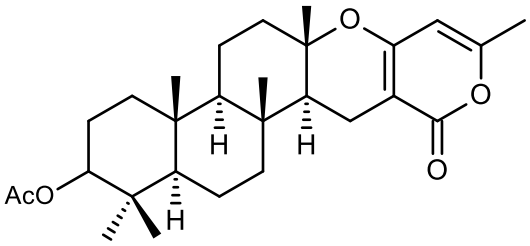

294

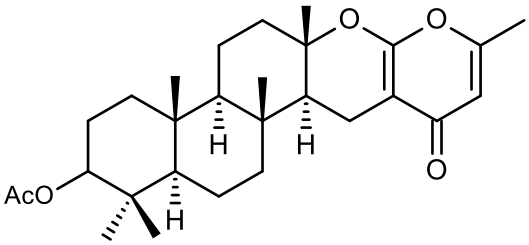

295

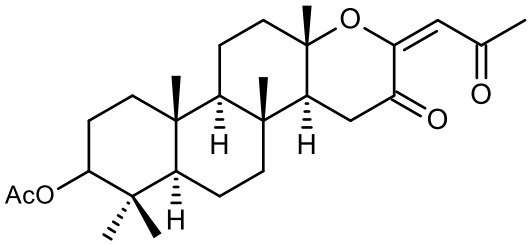

296

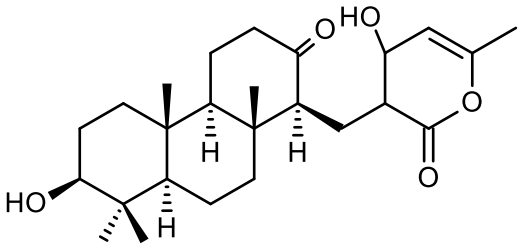

297

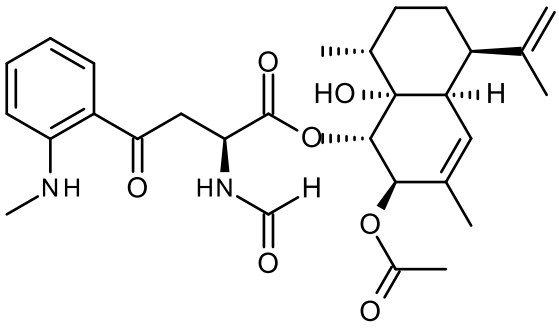

298

Figure 58. Structures of chevalones A-D (**293-296**), aszonapyrone B (**297**) and eurochevalierine (**298**)

CHAPTER II. CHEMISTRY OF THE GENERA *TALAROMYCES*, *NEOSARTORYA* AND *EUROTIUM*

CHAPTER III

RESULTS AND DISCUSSIONS

3.1 Chemical Investigation of Marine-Derived Fungi and Mangrove-Derived Fungus

Chromatographic fractionation, followed by several purification procedures, of the crude ethyl acetate of the marine-derived fungus *Talaromyces helicus* KUFA 0063, resulted in isolation of four previously reported secondary metabolites: palmitin (**TH 1**), acetyl ergosterol 5, 8-endoperoxide (**TH 2**), glaucanic acid (**TH 3**) and glauconic acid (**TH 4**) (Figure 59).

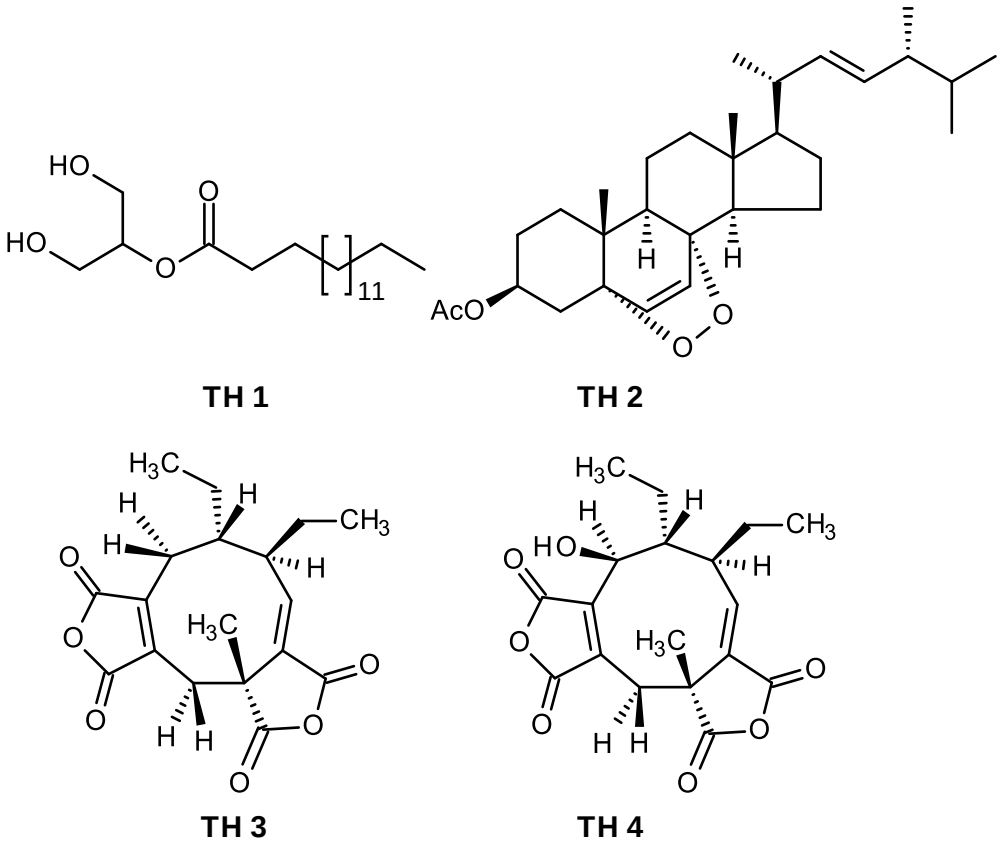

TH 1 **TH 2**

TH 3 **TH 4**

Figure 59. Secondary metabolites isolated from *Talaromyces helicus* KUFA 0063

Two marine-derived fungi *Neosartorya* species were investigated namely, the marine alga-assiociated fungus *Neosartorya takakii* KUFC 7898 and the marine sponge-associated fungus *Neosartorya glabra* KUFA 0702.

Chromatographic separation of the crude ethyl acetate extract of the marine-derived fungus *N. takakii* KUFC 7898, resulted in the isolation of nine known compounds: 6-hydroxymellein (**NTK 1**), aszonalenin (**NTK 2**), acetylaszonalenin (**NTK 3**), 3′-(4-oxoquinazolin-3-yl) spiro [1*H*-indole-3, 5′-oxolane]-2, 2′-dione (**NTK 5**), tryptoquivaline F (**NTK 6**), tryptoquivaline H (**NTK 7**), tryptoquivaline L (**NTK 8**), chevalone B (**NTK 10**), aszonapyrone A (**NTK 11**), together with three new compounds including takakiamide (**NTK 4**), tryptoquivaline U (**NTK 9**) and a new meroditerpene sartorenol (**NTK 12**) (Figure 60).

Three new secondary metabolites including two new cyclotetrapeptides, sartoryglabramide A (**NG 8**) and sartoryglabramide B (**NG 9**), and a new analog of fellutanine A: fellutanine A 2′, 3′-epoxide (**NG 11**), were isolated together with eight known compounds including ergosta-4, 6, 8 (14), 22-tetraen-3-one (**NG 1**), ergosterol 5, 8-endoperoxide (**NG 2**), helvolic acid (**NG 3**), aszonalenin (**NG 4**), (3*R*)-3-(1*H*-indol-3-ylmethyl)-3,4-dihydro-1*H*-1,4-benzodiazepine-2,5-dione (**NG 5**), (11a*S*)-2,3-dihydro-1*H*-pyrrolo [2,1-c] [1,4] benzodiazepine-5, 11 (10a*H*, 11a*H*)-dione (**NG 6**), takakiamide (**NG 7**) and fellutanine A (**NG 10**) from the ethyl acetate extract of the culture of the marine sponge-associated fungus *N. glabra* KUFA 0702 (Figure 61).

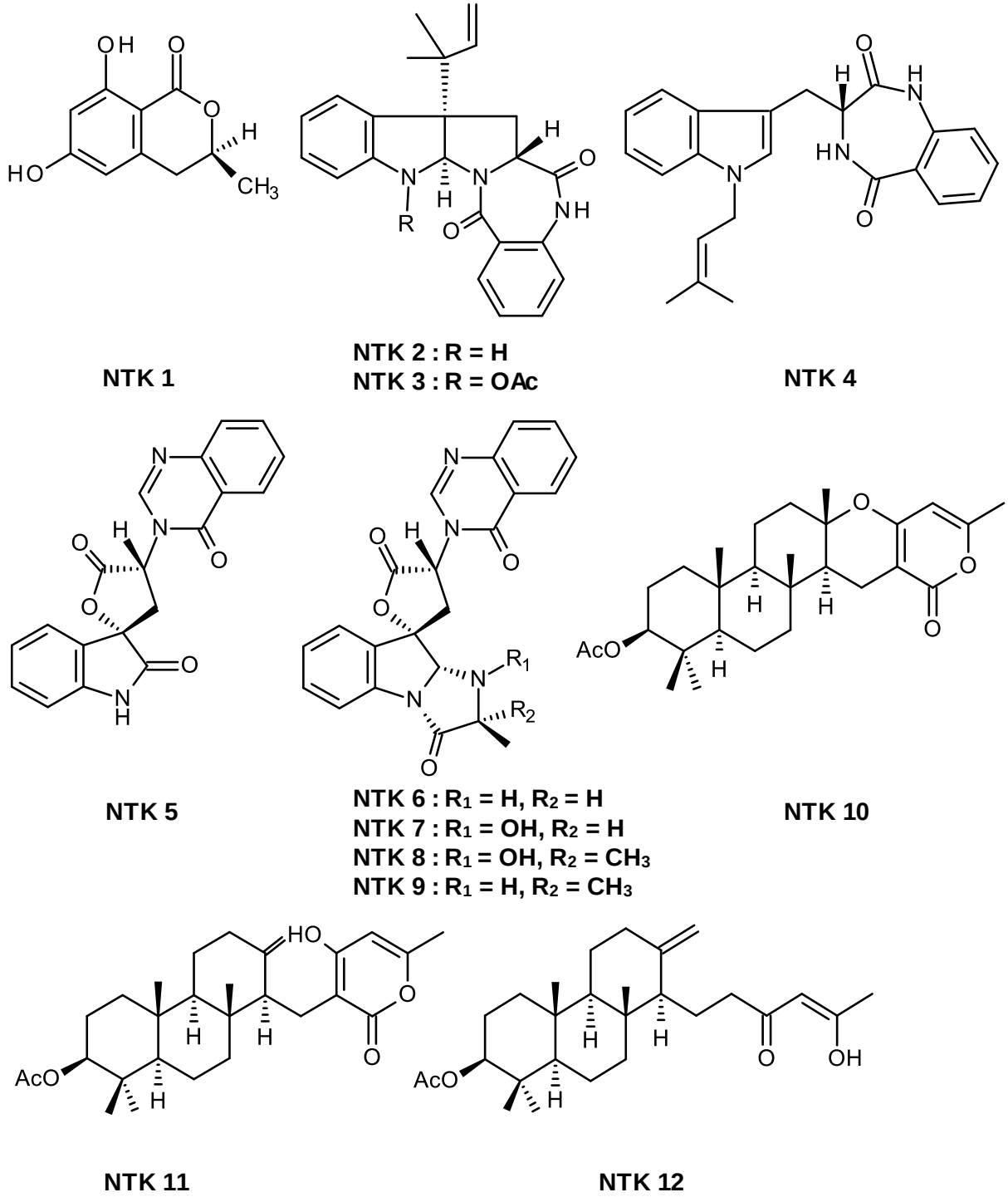

Figure 60. Secondary metabolites isolated from *Neosartorya takakii* KUFC 7898

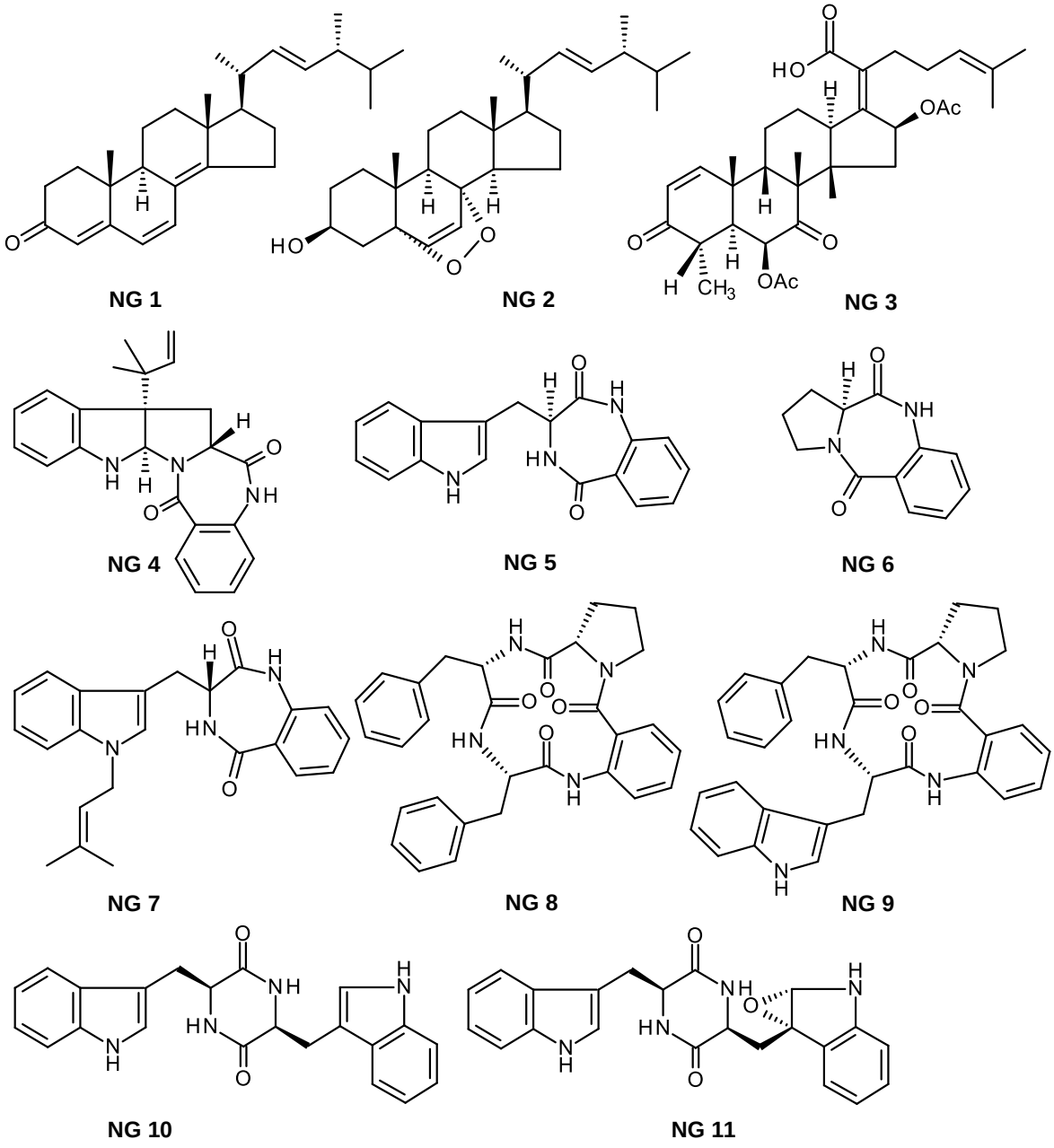

Figure 61. Secondary metabolites isolated from *Neosartorya glabra* KUFA 0702

The ethyl acetate extract from the culture of the endophytic fungus *Eurotium chevalieri* KUFA 0006 furnished five new metabolites, including a new anthraquinone derivative acetylquestinol (**EC 7**), two prenylated indole 3-carbaldehyde derivatives 2-(2-methyl-3-en-2yl)-1*H*-indole-3-carbaldehyde (**EC 8**), (2, 2-dimethylcyclopropyl)-1*H*-indole-3-carbaldehyde (**EC 9**), an anthranilic acid derivative 2-(2, 2-dimethylbut-3-enoyl) amino-benzoic acid (**EC 10**) and an isochromone derivative: 6, 8-dihydroxy-3-(2*R*-hydroxypropyl)-7-methyl-1*H*-isochromen-1-one (**EC 11**), together with eleven known metabolites: palmitic acid (**EC 1**), ergosterol 5, 8-endoperoxide (**EC 2**), emodin (**EC 3**), physcion (**EC 4**), questin (**EC 5**), questinol (**EC 6**), (11*S*, 14*R*)-3-(1*H*-indol-3-ylmethyl)-6-isopropyl-2,5-piperazinedione (**EC 12**), preechinulin (**EC 13**), neoechinulin E (**EC 14**), echinulin (**EC 15**) and eurocristatine (**EC 16**) (Figure 62).

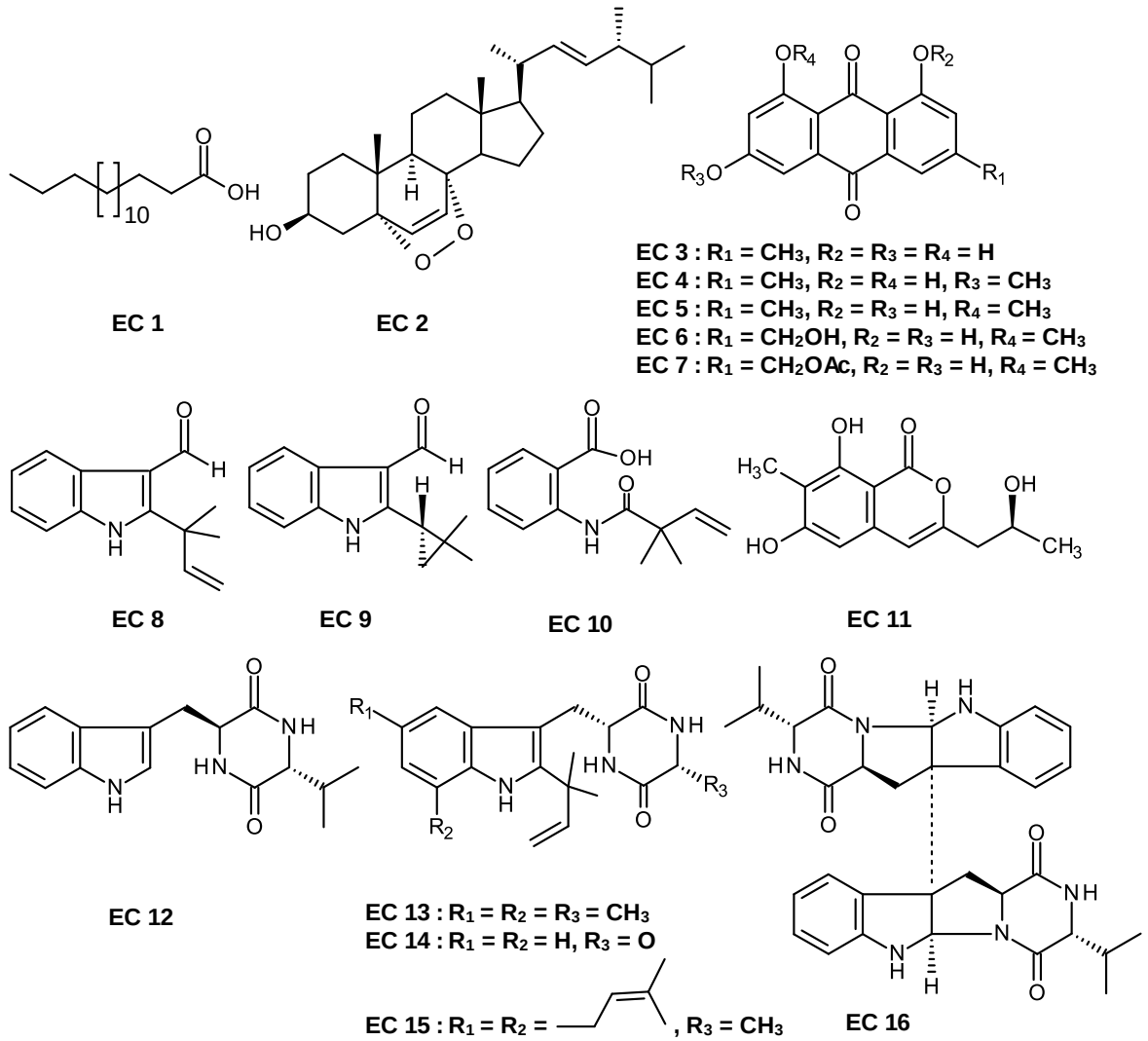

Figure 62. Secondary metabolites isolated from *Eurotium chevalieri* KUFA 0006

3.1.1 Structure Elucidation of Fatty Acids

3.1.1.1. Palmitic acid (EC 1)

EC 1 was isolated as a white solid (mp, 62-63 ºC). The ^{1}H and ^{13}C NMR spectral feature of **EC 1** revealed that it was a fatty acid.

The ^{13}C NMR, DEPTs and HSQC spectra (Table 2) revealed the signals of one carboxyl carbonyl at δ_C 180.6, the methylene carbons (δ_C 34.1, 31.9, 24.7 and 22.7), a cluster of peaks of methylene carbons (δ_C 29.7, 29.6, 29.4, 29.3 and 29.1) and one methyl (δ_C 14.1) carbons.

The ^{1}H NMR spectrum (Table 2) showed, in addition to a board singlet of the hydroxyl proton at δ_H 10.81 and a triplet of the methyl protons at δ_H 0.89 (J = 6.7 Hz), a triplet of methylene protons at δ_H 2.35 (J = 6.7 Hz), a multiplet of methylene protons at δ_H 1.64 and a broad singlet of several methylene protons at δ_H 1.26.

Since the (+)-HRESIMS of **EC 1** exhibited the $[M+H]^+$ peak at *m/z* 257.2484 (calculated 257.2481), corresponding to $C_{16}H_{33}O_2$, the molecular formula of **EC 1** was $C_{16}H_{32}O_2$. Combining the molecular formula and the NMR data, **EC 1** was identified as palmitic acid (Figure 63).

Table 2. ^{1}H and ^{13}C NMR ($CDCl_3$, 300.13 and 75.47 MHz) assignment for **EC 1**

Position	δ_C, type	δ_H, (*J* in Hz)
1	180.6, CO	-
2	34.1, CH_2	2.35, *t* (7.5)
3	24.7, CH_2	1.64, *m*
4-8	29.7, CH_2	1.26, *m*
9	29.6, CH_2	1.26, *m*
10	29.4, CH_2	1.26, *m*
11	29.3, CH_2	1.26, *m*
12	29.1, CH_2	1.26, *m*
13	-, CH_2	1.26, *m*
14	31.9, CH_2	1.26, *m*
15	22.7, CH_2	1.26, *m*
16	14.1, CH_3	0.89, *t* (6.7)
OH	-	10. 81, *brs*

Palmitic acid has been previously reported from several sources including from the root bark of plant *Terminalia glaucescens* (Barton *et al*., 1965b; Bulama *et al*., 2014), brown alga *Sargussum muticum* (Bazes *et al*., 2009) and marine sponge-associated fungus *Talaromyces stipitatus* KUFA 0207, which was collected from coral reef at Samaesarn Island in the Gulf of Thailand (Noinart *et al*., 2017).

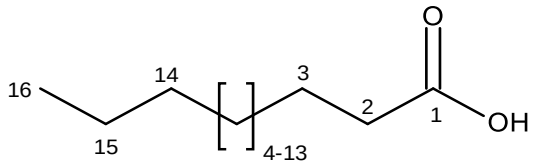

Figure 63. Structure of palmitic acid (**EC 1**)

3.1.1.2. Palmitin (TH 1)

TH 1 was isolated as a white solid (mp, 65-66 ºC) and the ^{13}C NMR, DEPTs and HSQC spectra (Table 3) showed the signals of one ester carbonyl (δ_C 174.4), twelve methylene sp^3 (δ_C 65.1, 63.4, 34.2, 31.9, 29.7, 29.6, 29.5, 29.4, 29.3, 29.1, 24.9 and 22.7), one oxymethine sp^3 (δ_C 70.2) and one methyl (δ_C 14.1) carbons.

The ^{1}H NMR spectrum, in combination with HSQC spectrum, (Table 3) showed the presence of three double doublets (one proton each) at δ_H 4.13 (J = 5.5, 1.9 Hz), δ_H 3.67 (J = 11.6, 3.8 Hz), δ_H 3.56 (J = 11.6, 6.0 Hz), a triplet at δ_H 2.32 (J = 7.4 Hz), a broad singlet of several protons at δ_H 1.23, a multiplet of one methine sp^3 proton at δ_H 3.90 and triplet of one methyl protons at δ_H 0.86 (J = 6.4 Hz).

Table 3. ^{1}H and ^{13}C NMR ($CDCl_3$, 300.13 and 75.47 MHz) and HMBC assignment for **TH 1**

Position	δ_C, type	δ_H, (*J* in Hz)	COSY	HMBC
1a	63.4, CH_2	3.67, *dd* (11.6, 3.8)	H-2	C-2, 3
b		3.56, *dd* (11.6, 6.0)	-	-
2	70.2, CH	3.90, *m*	H-1, 3	C-3
3	65.1, CH_2	4.13, *dd* (5.5, 1.9)	H-2	C-1, 1′, 2
1′	174.4, CO	-	-	-
2′	34.2, CH_2	2.32, *t* (7.4)	H-3′	C-1′, 3′
3′	24.9, CH_2	1.58, *m*	H-2′	-
4′	31.9, CH_2	1.23, *brs*	-	-
5′	29.7, CH_2	1.23, *brs*	-	-
6′	29.6, CH_2	1.23, *brs*	-	-
7′	29.5, CH_2	1.23, *brs*	-	-
8′	29.4, CH_2	1.23, *brs*	-	-
9′	29.3, CH_2	1.23, *brs*	-	-
10′	29.1, CH_2	1.23, *brs*	-	-
11′	-, CH_2	1.23, *brs*	-	-
12′	-, CH_2	1.23, *brs*	-	-
13′	-, CH_2	1.23, *brs*	-	-
14′	-, CH_2	1.23, *brs*	-	-
15′	22.7, CH_2	1.23, *brs*	H-16′	-
16′	14.1, CH_3	0.86, *t* (6.4)	H-15′	C-15′

The COSY spectrum (Table 3) showed cross peaks from the multiplet at δ_H 3.90 (δ_C 70.2) to the doublets at δ_H 4.13 (*J* = 5.5, 1.9 Hz; δ_C 65.1), 3.56 (*J* = 11.6, 6.0 Hz; δ_C 63.4) and 3.67 (*J* = 11.6, 3.8 Hz; δ_C 63.4), in addition to cross peaks between the doublets at δ_H 3.56 (*J* = 11.6, 6.0 Hz) and 3.67 (*J* = 11.6, 3.8 Hz). Moreover, the

COSY spectrum also showed correlations from the methyl triplet at δ_H 0.86 (*J* = 6.4 Hz; δ_C 14.1) to the *brs* at δ_H 1.23 (δ_C 22.7) as well as from a methylene triplet at δ_H 2.32 (*J* = 7.4 Hz; δ_C 34.2) to a multiplet at δ_H 1.58 (δ_C 24.9). The ^{1}H and ^{13}C NMR spectral features of **TH 1** revealed that it contained a fatty acid moiety.

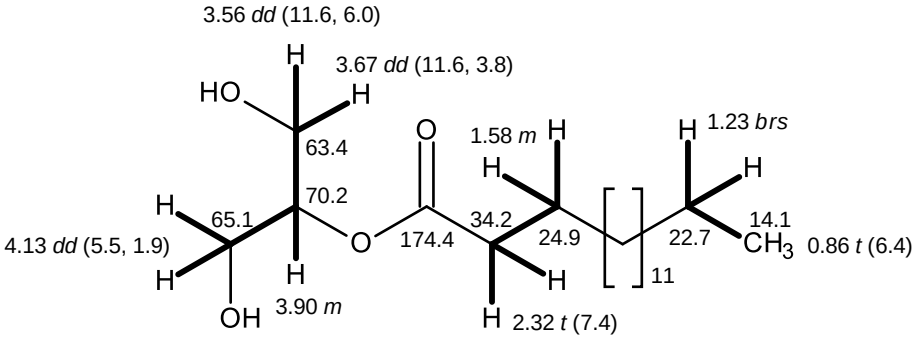

That **TH 1** was 2-alkanoylglycerol was evidenced by the HMBC correlations from the doublet doublet at δ_H 3.67 (*J* = 11.6, 3.8 Hz; δ_C 63.4, H-1a) to the oxymethine sp^3 carbon at δ_C 70.2 (C-2) and oxymethylene carbon at δ_C 65.1 (C-3), from the multiplet at δ_H 3.90 (δ_C 70.2, H-2) to the methylene carbon at δ_C 65.1 (C-3), from the doublet doublet at δ_H 4.13 (*J* = 5.5, 1.9 Hz; δ_C 65.1, H-3) to the oxymethylene carbon at δ_C 63.4 (C-1), ester carbonyl carbon at δ_C 174.4 (C-1′) and methine carbon at δ_C 70.2 (C-2), from the triplet at δ_H 2.32 (*J* = 7.4 Hz; δ_C 34.2, H-2′) to the ester carbonyl carbon at δ_C 174.4 (C-1′) and methylene carbon at δ_C 24.9 (C-3′), from the triplet at δ_H 0.86 (*J* = 6.4 Hz; δ_C 14.1, H-16′) to the methylene carbon at δ_C 22.7 (C-15′).

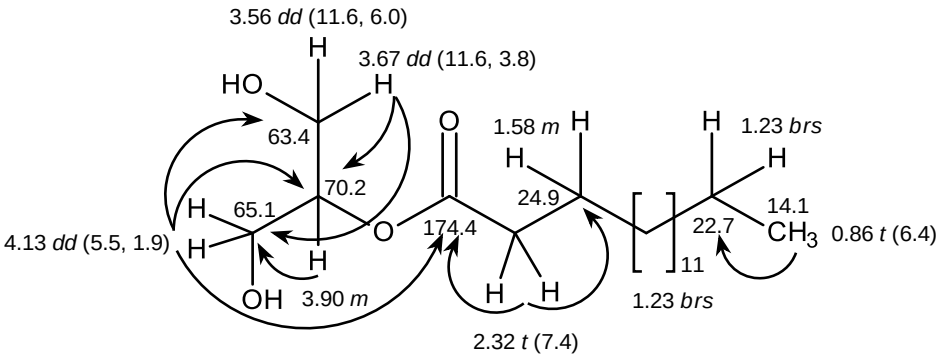

Since the (+)-HRESIMS exhibited the $[M+H]^+$ at *m/z* 331.2814 (calculated 331.2848), the molecular formula of **TH 1** was identified as $C_{19}H_{38}O_4$. Therefore, **TH 1** was established as 2-palmitoylglycerol which is commonly known as palmitin (Figure 64). Palmitin which has been isolated from several natural sources including the mangrove-endophytic fungus *Penicillium thomi*, which was isolated from the root of *Bruguiera gymnorrhia* (Chen *et al*., 2007).

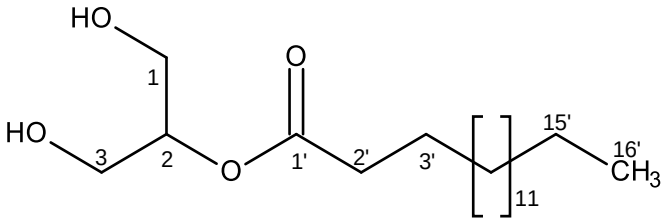

Figure 64. Structure of palmitin (**TH 1**)

3.1.2 Structure Elucidation of Glaucanic acid and Glauconic acid

3.1.2.1. Glaucanic acid (TH 3)

TH 3 was isolated as a white solid (mp, 188-189 ºC) and its molecular formula $C_{18}H_{20}O_6$ was established on the basis of the (+)-HRESIMS *m/z* 333.1311 $[M+H]^+$ (calculated 333.1338), indicating nine degrees of unsaturation.

The ^{13}C NMR, DEPTs and HSQC spectra (Table 4) revealed the presence of four ester carbonyls (δ_C 173.8, 165.3, 164.5 and 163.7), three quaternary sp^2 (δ_C 148.4, 140.5 and 131.9), one methine sp^2 (δ_C 150.1), one quaternary sp^3 (δ_C 48.6), two methine sp^2 (δ_C 48.1 and 43.9), four methylene sp^3 (δ_C 31.7, 28.4, 26.0 and 21.4) and three methyl (δ_C 20.3, 12.9 and 12.4) groups.

The ^1H NMR spectrum, in combination with HSQC spectrum, exhibited besides, a doublet at δ_H 6.99 (*J* = 12.1 Hz) of one olefinic proton (δ_C 150.1) and two doublets of geminally coupled protons at δ_H 3.27 (*J* = 13.5 Hz) and 2.67 (*J* = 13.4 Hz) (δ_C 31.7), two methyl triplets at δ_H 1.07 (*J* = 7.1 Hz, δ_C 12.4) and 0.81 (*J* = 7.4 Hz, δ_C 12.9), a methyl singlet at δ_H 1.49 (δ_C 20.3), a doublet doublet at δ_H 2.87 (*J* = 11.9, 2.8 Hz, δ_C 28.4), and multiplets at δ_H 2.10 (δ_C 48.1), 2.08 (δ_C 43.9), 2.00 (δ_C 28.4), 1.85 (δ_C 21.4), 1.65 (δ_C 26.0), 1.52 (δ_C 26.0), 1.18 (δ_C 21.4).

Table 4. ^{1}H and ^{13}C NMR ($CDCl_3$, 300.13 and 75.47 MHz) and HMBC assignment for **TH 3**

Position	δ_C, type	δ_H, (*J* in Hz)	COSY	HMBC
1	140.5, C	-	-	-
2	148.4, C	-	-	-
3a	31.7, CH_2	3.27, *d* (13.5)	H-3a	C-1, 2, 4, 5, 12, 13
b		2.67, *d* (13.4)	H-3b	-
4	48.6, C	-	-	-
5	131.9, C	-	-	-
6	150.1, CH	6.99, *d* (12.1)	H-7	C-4, 8, 15
7	43.9, CH	2.08, *m*	H-6, 8	-
8	48.1, CH	2.10, *m*	H-7, 9a, b	-
9a	28.4, CH_2	2.87, *dd* (11.9, 2.8)	H-8, 9b	-
b		2.00, *m*	H-9a	-
10	164.5, CO	-	-	-
12	165.3, CO	-	-	-
13	173.8, CO	-	-	-
15	163.7, CO	-	-	-
16a	26.0, CH_2	1.65, *m*	H-15b, 17	-
b		1.52, *m*	H-15a, 17	-
17	12.9, CH_3	0.81, *t* (7.4)	H-16a, b	C-7, 16
18a	21.4, CH_2	1.85, *m*	H-18b, 19	-
b		1.18, *m*	H-18a, 19	-
19	12.4, CH_3	1.07, *t* (7.1)	H-18a, b	C-8, 18
20	20.3, CH_3	1.49, *s*	-	C-3, 4, 5, 13

The COSY spectrum exhibited correlations from the olefin proton at δ_H 6.99 (*J* = 12.1 Hz, δ_C 150.1, H-6) to the multiplet at δ_H 2.08 (δ_C 43.9, H-7), from the doublet doublet at δ_H 2.87 (*J* = 11.9, 2.8 Hz, δ_C 28.4, H-9a) to the multiplets at δ_H 2.10 (δ_C 48.1, H-8) and δ_H 2.00 (δ_C 28.4, H-9b). The multiplet at δ_H 2.10 (δ_C 48.1, H-8) also gave cross peaks to H-7 and H-9.

Similarly, the multiplets at δ_H1.65 (δ_C 26.0, H-16a) and 1.52 (δ_C 26.0, H-16b) to the triplet at δ_H 0.81 (*J* = 7.4 Hz, δ_C 12.9, H-17), from the multiplets at δ_H 1.85 (δ_C 21.4, H-18a) and 1.18 (δ_C 21.4, H-18b) to the triplet at δ_H 1.07 (J = 7.1 Hz, δ_C 12.4, H-19). The COSY correlations confirmed the coupling system of CH-6-CH-7, CH_2-16 and CH_3-17 and CH_2-9-CH-8, CH_2-18 and CH_3-19. That C-6 was connected to C-8 was corroborated by the HMBC cross peaks from H-6 at δ_H 6.99, *d* (*J* = 12.1 Hz; δ_C 150.1) to the C-4 (δ_C 48.6) and C-8 (δ_C 48.1). Moreover, H-3 at δ_H 3.27, *d* (*J* = 13.5 Hz) also showed HMBC cross peaks to the C-4 (δ_C 48.6) and C-5 (δ_C 131.9).

That the methyl group at δ_H 1.49, *s* (δ_C 20.3) was on C-4 was evidenced by the HMBC cross peaks of the methyl singlet at δ_H 1.49 (δ_C 20.3, H-20) to the carbon at δ_C 48.6 (C-4). Moreover, this methyl signal also gave cross peaks to C-5 (δ_C 131.9) and methylene carbon at δ_C 31.7 (C-3). In turn, the methylene proton at δ_H 3.27, *d* (*J* = 13.5 Hz) exhibited cross peaks to the carbonyls at δ_C 173.8 (C-13), 165.3 (C-12) as well as to C-4 and C-5. Taking these HMBC correlations into account, the coupling system of C-3 was connected to C-1 was substantiated by the

HMBC correlations from H-3 to C-1 (δ_C 140.5) and C-2 (δ_C 148.4), thus forming a cyclononene portion.

That the dihydrofuran-2, 5-dione was on C-4 and C-5, and the furan-2, 5-dione was on C-1 and C-2 was substantiated by the HMBC cross peaks (Table 4), from H-6 (δ_H 6.99, *d*, *J* = 12.1 Hz) to C-15 (δ_C 163.7), from Me-20 (δ_H 1.49, *s*) to C-13 (δ_C 173.8), as well as from H-3 (δ_H 3.27, *d*, *J* = 13.5 Hz) to C-13 (δ_C 173.8) and C-12 (δ_C 165.3).

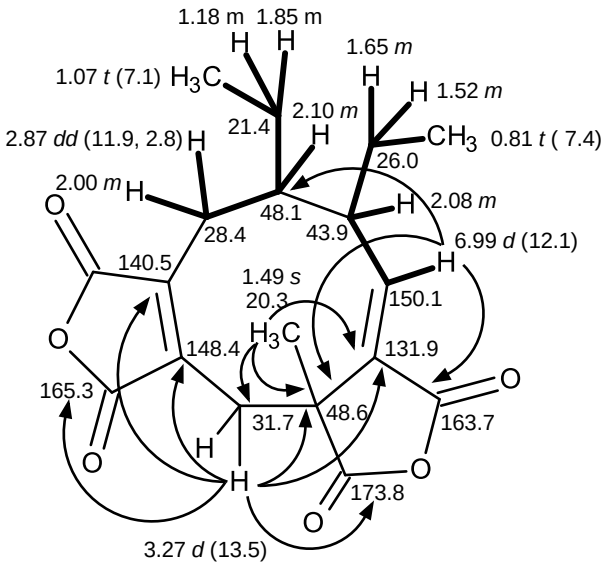

Literature search revealed that the structure of **TH 3** corresponded to that of glaucanic acid (Figure 65). Since **TH 3** has three stereogenic centers, i.e. C-4, C-7 and C-8, it was necessary to establish the absolute configurations of these carbons. Comparison of ^{1}H and ^{13}C chemical shift values of H-4/C-4, H-7/C-7 and H-8/C-8 and the optical rotation of **TH 3** ($[\alpha]_D^{20}$ = +185) were agreement with those of glaucanic acid, whose absolute configuration of 4*R*, 7*R*, 8*S* respectively. It was

concluded that they are the same compound. Glaucanic acid has been previously isolated by Wijkman in 1931 from a fungus *Penicillium glaucum* (Wijkman, 1931) and in 1934 by Yuill from a *Penicillium purpurogenum* species (Yuill, 1934), as well as from the marine-sponge associated fungus *Talaromyces trachyspermus* KUFA 0021 (Kuml *et al*., 2014).

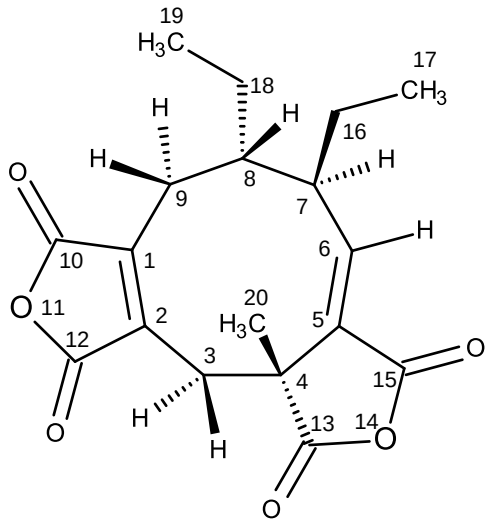

Figure 65. Structure of glaucanic acid (**TH 3**)

3.1.2.2. Glauconic acid (TH 4)

TH 4 was isolated as a white solid (mp, 199-200 ºC) and its molecular formula $C_{18}H_{20}O_7$ was established on the basis of the (+) HRESIMS *m/z* 349.1293 $[M+H]^+$ (calculated 349.1287), indicating nine degrees of unsaturation. The general feature of the ^{1}H and ^{13}C NMR spectra of **TH 4** closely resembled that of **TH 3**.

The ^{13}C NMR, DEPTs and HSQC spectra (Table 5) revealed the presence of four ester carbonyls (δ_C 173.9, 164.6, 164.4 and 163.3), three quaternary sp^2 (δ_C 146.1, 143.3 and 129.3), one methine sp^2 (δ_C 150.2), one quaternary sp^3 (δ_C 47.4), one oxymethine sp^3 (δ_C 65.6), two methine sp^3 (δ_C 53.0 and 37.7), three methylene sp^3 (δ_C 31.8, 27.7 and 19.6) and three methyl (δ_C 26.5, 13.0 and 12.5) carbons.

The ^1H NMR spectrum (Table 5), in combination with HSQC spectrum exhibited besides, a doublet at δ_H 6.89 (J = 11.8 Hz) of olefinic proton (δ_C 150.2) and singlet at δ_H 5.11 (δ_C 65.6) of an oxymethine proton, two doublets of the geminally coupled methylene protons at δ_H 3.77 (J = 13.0 Hz, δ_C 31.8) and 3.47 (J = 12.8 Hz, δ_C 31.8), triplets of methyl protons at δ_H 1.16 (J = 7.4 Hz, δ_C 13.0), a broad signal of methyl proton at δ_H 0.92 (δ_C 12.5), a methyl singlet at δ_H 1.72 (δ_C 26.5), two multiplets at δ_H 1.66 (δ_C 27.7, 19.6) and broad singlet at δ_H 2.12 (δ_C 53.0) as well as a broad singal of one proton at δ_H 3.06 (δ_C 37.7).

Table 5. ^{1}H and ^{13}C NMR ($CDCl_3$, 500.13 and 125.77 MHz) and HMBC assignment for **TH 4**

Position	δ_C, type	δ_H, (*J* in Hz)	COSY	HMBC
1	143.3, C	-	-	-
2	146.1, C	-	-	-
3a	31.8, CH_2	3.77, *d* (13.0)	H-3b	C-1, 4, 5
b		3.47, *d* (12.8)	H-3a	C-1, 13
4	47.4, C	-	-	-
5	129.3, C	-	-	-
6	150.2, CH	6.89, *d* (11.8)	-	C-15
7	37.7, CH	3.06, *brs*	-	C-16, 17
8	53.0, CH	2.12, *brs*	H-9	-
9	65.6, CH	5.11, *s*	H-8	-
10	164.4, CO	-	-	-
12	164.6, CO	-	-	-
13	173.9, CO	-	-	-
15	163.3, CO	-	-	-
16	27.7, CH_2	1.66, *m*	H-17	C-6, 7, 8, 17
17	12.5, CH_3	0.92, *brs*	H-16	C-7, 16
18	19.6, CH_2	1.66, *m*	-	C-6, 7, 8, 17
19	13.0, CH_3	1.16, *t* (7.4)	-	C-8, 18
20	26.5, CH_3	1.72, *s*	-	C-3, 4, 5, 13

The COSY spectrum showed cross peaks between the protons at δ_H 3.77, *d* (*J* = 13.0 Hz, δ_C 31.8, H-3a) and δ_H 3.47, *d* (*J* = 12.8 Hz, δ_C 31.8, H-3b), between δ_H 1.66, *m* (δ_C H-16) and δ_H 0.92, *brs* (H-17), between δ_H 5.11, *s* (δ_C 65.6, H-9) and δ_H 2.12, *brs* (δ_C 53.0, H-8), thus confirming the coupling system of C-7 through C-17 and C-8 through C-19. This was confirmed by the HMBC cross peaks from Me-17

(δ_H 0.92, *brs*, δ_C 12.5) to C-7 (δ_C 37.7) and C-16 (δ_C 27.7), from Me-19 (δ_H 1.16, *t*, *J* = 7.4 Hz, δ_C 13.0) to C-8 (δ_C 53.0) and C-18 (δ_C 19.6). That C-7 was connected to C-8 was evidenced by the HMBC cross peaks from H-16 (δ_H 1.66, *m*, δ_C 19.6) to C-7 (δ_C 37.7) and C-8 (δ_C 53.0).

Furthermore, the HMBC spectrum also showed correlations from H-16 to methine sp^2 carbon at δ_C 150.2 (C-6), H-6 also exhibited HMBC cross peaks to the carbonyl carbon at δ_C 163.3 (C-15), while methylene protons at δ_H 3.77, *d* (*J* = 13.0 Hz, H-3) showed correlations to the quaternary sp^3 carbon at δ_C 47.4 (C-4), quaternary sp^2 carbons at δ_C 143.3 (C-1) and δ_C 129.3 (C-5). Another H-3 signal at δ_H 3.47, *d* (*J* = 12.8 Hz, δ_C 31.8) also gave HMBC cross peaks to C-1 (δ_C 143.3) and carbonyl carbon at δ_C 173.9 (C-13), thus confirming the coupling system of C-1 through C-6. That the methyl group at δ_H 1.72, *s* (δ_C 26.5) was on C-4, this was supported by the HMBC cross peaks of the singlet at δ_H 1.72 (δ_C 26.5, H-20) to C-3 (δ_C 31.8), C-4 (δ_C 47.4), C-5 (δ_C 129.3) and C-13 (δ_C 173.9).

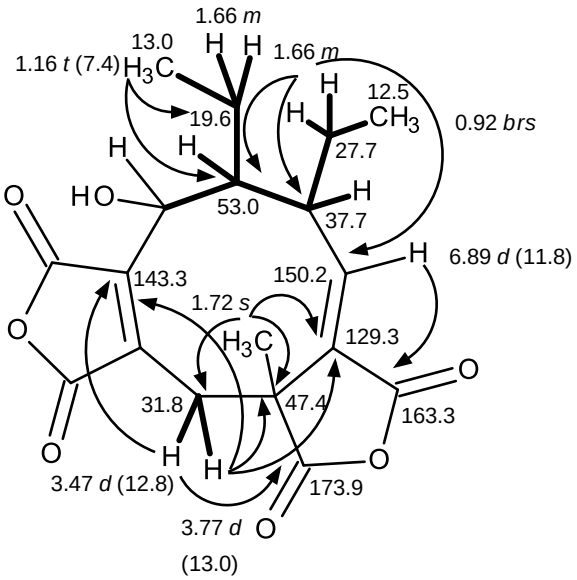

Taking together the NMR spectra data, molecular formula and the degree of unsaturation, the structure of **TH 4** should contain the cyclooctanonene ring, four carbonyls, and another two rings. The structure of **TH 4** (Figure 66) was compatible with those of glauconic acid, a fungal metabolites previously isolated from *Penicillium purpurogenum* IMI 090178 (Barton *et al*. 1965a; Barton *et al*. 1965b; Barton and Sutherland 1965), as well as from the several sources including the fungal strain *Talaromyces atroroseus* (Frisvad *et al*., 2013) and marine-sponge associated fungus *Talaromyces trachyspermus* KUFA 0021 (Kuml *et al*., 2014).

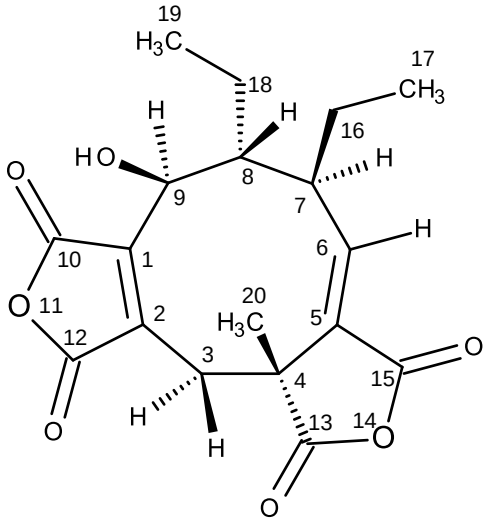

Figure 66. Structure of glauconic acid (**TH 4**)

3.1.3 Structure Elucidation of Ergosterol Derivatives

3.1.3.1. Ergosta-4, 6, 8 (14), 22-tetraen-3-one (NG 1)

NG 1 was isolated as yellow viscous mass, the ^{13}C NMR spectrum exhibited twenty eight carbon signals, which based on DEPTs and HSQC spectra (Table 6), can be classified as one ketone carbonyl (δ_C 199.6), three quaternary sp^2 (δ_C 164.6, 156.2 and 124.4), two quaternary sp^3 (δ_C 43.9 and 36.8), five methine sp^2 (δ_C 135.0, 134.1, 132.5, 124.5 and 123.0), five methine sp^3 (δ_C 55.7, 44.3, 42.9, 39.3 and 33.1), six methylene (δ_C 35.6, 34.1 (2C), 27.7, 25.4 and 19.0) and six methyl (δ_C 21.2, 20.0, 19.7, 19.0, 17.7 and 16.7) carbons.

Table 6. ^{1}H and ^{13}C NMR ($CDCl_3$, 300.13 and 75.47 MHz) and HMBC assignment for **NG 1**

Position	δ_C, type	δ_H, (*J* in Hz)	COSY	HMBC
1a	34.1, CH_2	2.49, *m*	H-1b, 2a	-
b		2.00, *m*	H-1a, 2a	-
2a	34.1, CH_2	1.80, *m*	H-1a, b	-
		2.35, *m*		
3	199.6, CO	-	-	-
4	123.0, CH	5.74, *s*	-	C-1, 2, 6, 10
5	164.6, C	-	-	-
6	134.1, CH	6.61, *d* (9.5)	H-7	C-8
7	124.5, CH	6.03, *d* (9.5)	H-6	C-5
8	124.4, C	-	-	-
9	44.3, CH	2.11, *m*	-	-
10	36.8, C	-	-	-
11a	19.0, CH_2	1.68, *m*	H-9	-
b		1.59, *m*	-	-
12a	35.6, CH_2	2.06, *m*	-	-
b		1.30, *m*		-
13	43.9, C	-	-	-
14	156.2, C	-	-	-
15a	25.4, CH_2	2.43, *m*	H-16a, b	-
b		2.63, *m*	-	-
16a	27.7, CH_2	2.90, *dd* (13.1, 2.9)	-	-
b		1.84, *m*	H-15a	-
17	55.7, CH	1.26, *m*	H-20	C-16
18	19.0, CH_3	0.96, *s*	-	C-12, 13, 14, 17
19	16.7, CH_3	1.00, *s*	-	C-1, 2, 5, 9, 10
20	39.3, CH	2.14, *m*	H-21	-
21	21.2, CH_3	1.06, *d* (6.7)	H-20	C-17, 20, 22
22	135.0, CH	5.20, *dd* (15.0, 7.5)	H-23	-
23	132.5, CH	5.27, *dd* (15.2, 6.8)	H-22	-
24	42.9, CH	1.87, *m*	H-26	-
25	33.1, CH	1.48, *m*	H-27, 28	-
26	17.7, CH_3	0.93, *d* (6.8)	H-24	C-23, 24, 25
27	19.7, CH_3	0.83, *d* (6.8)	H-25	C-24, 25, 28
28	20.0, CH_3	0.85, *d* (6.7)	H-25	C-24, 25, 27

The ^{1}H NMR spectrum, in combination with HSQC spectrum (Table 6) displayed the signals of five olefinic protons at δ_H 6.61, *d* (*J* = 9.5 Hz), δ_H 6.03, *d* (*J* = 9.5 Hz), δ_H 5.27, *dd* (*J* = 15.2, 6.8 Hz), δ_H 5.20, *dd* (*J* = 15.0, 7.5 Hz) and a singlet at δ_H 5.74, six methyl protons at δ_H 1.06, *d* (*J* = 6.7 Hz), 0.93, *d* (*J* = 6.8 Hz), 0.85, *d* (*J* = 6.7 Hz), 0.83, *d* (*J* = 6.8 Hz), and the singlets at δ_H 1.00 and δ_H 0.96.

The COSY spectrum showed cross peaks from the multiplet at δ_H 2.49 (δ_C 34.1) to the multiplets at δ_H 2.00 (δ_C 34.1) and δ_H 1.80 (δ_C 34.1), from the multiplet at δ_H 2.00 to the multiplets at δ_H 2.49 and 1.80, from the multiplet at δ_H 1.80 to the multiplets at δ_H 2.49 and 2.00, from the multiplet at δ_H 1.68 (δ_C 19.0) to the multiplet at δ_H 2.11 (δ_C 44.3), from the multiplet at δ_H 2.43 (δ_C 25.4) to the doublet doublet at δ_H 2.90 (*J* = 13.1, 2.9 Hz, δ_C 27.7) and multiplet at δ_H 1.84 (δ_C 25.4), from the multiplet at δ_H 1.84 to the multiplet at δ_H 2.43, from the multiplet at δ_H 1.26 (δ_C 55.7) to the multiplet at δ_H 2.14 (δ_C 39.3), as well as between the doublets at δ_H 6.03 (*J* = 9.5 Hz, δ_C 124.5) and δ_H 6.61 (*J* = 9.5 Hz, δ_C 134.1).

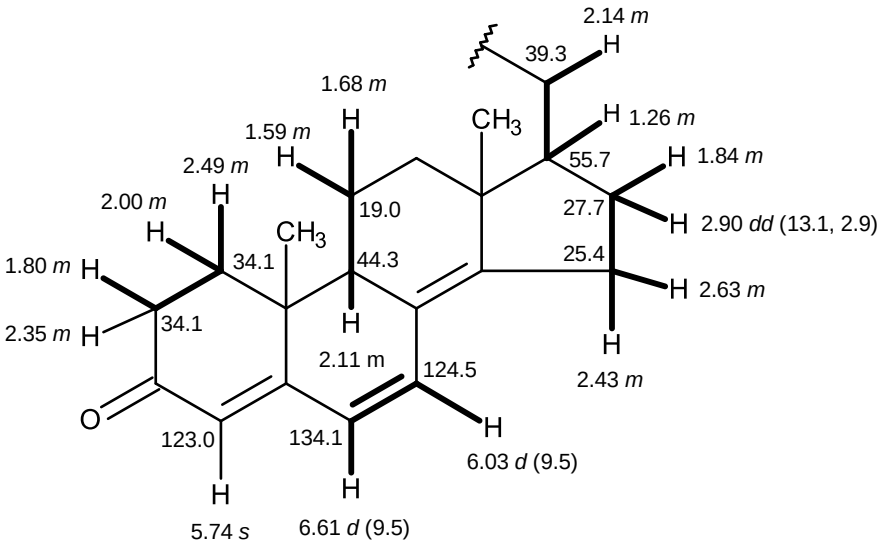

That **NG 1** consisted of a 10, 13-dimethylcyclopentanoperhydrophenanthrene ring system with the ketone carbonyl on C-3 and three conjugated double bonds on C-4/C5, C-6/C-7 and C-8/C-14 (fragment A) was supported by the HMBC correlations from the doublet at δ_H 6.61 (*J* = 9.5 Hz; δ_C 134.1, H-6) to the quaternary sp^2 carbon at δ_C 124.4 (C-8), from the doublet at δ_H 6.03 (*J* = 9.5 Hz; δ_C 134.1, H-7) to the quaternary sp^2 carbon at δ_C 164.6 (C-5), from the singlet at δ_H 5.74 (δ_C 123.0, H-4) to the two methylene carbons at δ_C 34.1 (C-1/C-2), methine sp^2 carbon at δ_C 134.1 (C-6) and the quaternary sp^3 carbon at δ_C 36.8 (C-10), from the methyl singlet at δ_H 1.00 (δ_C 16.7, H-19) to the two methylene carbons at δ_C 34.1 (C-1/C-2), the quaternary sp^2 carbon at δ_C 164.6 (C-5), the methine sp^3 carbon at δ_C 44.3 (C-9) and the quaternary sp^3 carbon at δ_C 36.8 (C-10), from the multiplet at δ_H 1.26 (δ_C 55.7, H-17) to the carbon at δ_C 27.7 (C-16), from the methyl singlet at δ_H 0.96 (δ_C 19.0, H-18) to the carbons at δ_C 35.6 (C-12), 43.9 (C-13), 156.2 (C-14) and 55.7 (C-17).

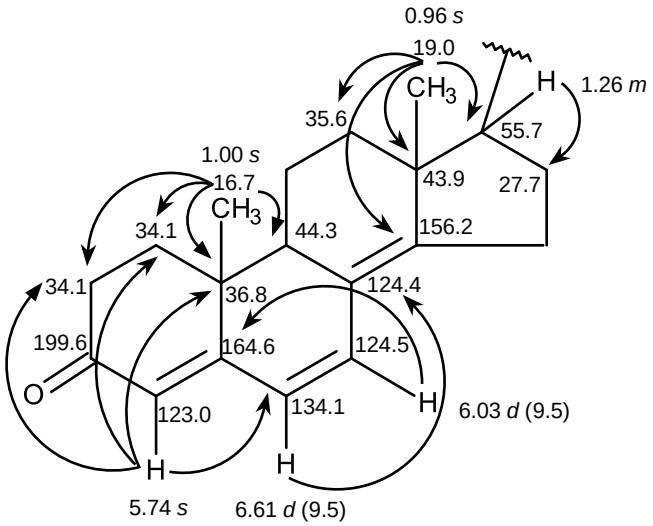

Fragment A

The existence of the (3*E*)-5, 6-dimethylhept-3-en-2-yl side chain was based on the COSY correlations between the multiplet at δ_H 2.14 (H-20, δ_C 39.3) and the methyl doublet at δ_H 1.06 (*J* = 6.7 Hz, H-21, δ_C 21.2), between the doublet doublet at δ_H 5.20 (*J* = 15.0, 7.5 Hz, H-22, δ_C 135.0) and the doublet doublet at δ_H 5.27 (*J* = 15.2, 6.8 Hz, H-23, δ_C 132.5), between the doublet at δ_H 0.93 (*J* = 6.8 Hz, H-26, δ_C 17.7) and a multiplet at δ_H 1.87 (H-24, δ_C 42.9), as well as from the multiplet at δ_H 1.48 (H-25, δ_C 33.1) to the doublet at δ_H 0.83 (*J* = 6.8 Hz, H-27, δ_C 19.7) and the doublet at δ_H 0.85 (*J* = 6.7 Hz, H-28, δ_C 20.0), from the two doublets at δ_H 0.83 (*J* = 6.8 Hz, H-27, δ_C 19.7) and δ_H 0.85 (*J* = 6.7 Hz, H-28, δ_C 20.0) to the multiplet at δ_H 1.48 (H-25).

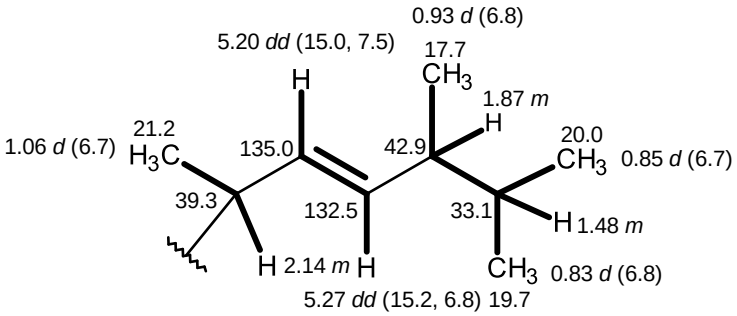

This was confirmed by the HMBC correlations from H-21 (δ_H 1.06, *d*, *J* = 6.67 Hz; δ_C 21.2) to the carbons at δ_C 39.3 (C-20) and 135.0 (C-22), from Me-26 (δ_H 0.93, *d*, *J* = 6.8 Hz; δ_C 17.7) to the carbons at δ_C 132.5 (C-23), 42.9 (C-24) and 33.1 (C-25), from Me-27 (δ_H 0.83, *d*, *J* = 6.8 Hz; δ_C 19.7) to the C-24, C-25 and C-28 (δ_C 20.0), from Me-28 (δ_H 0.85, *d*, *J* = 6.7 Hz; δ_C 20.0) to the C-24, C-25 and C-27 (δ_C 19.7), respectively.

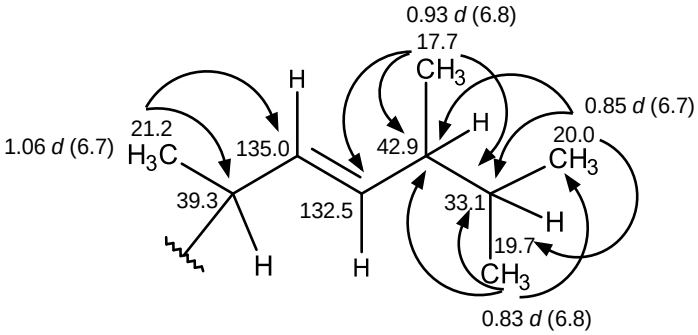

That the (3*E*)-5, 6-dimethylhept-3-en-2-yl side chain was connected to the fragment **A** was supported by the HMBC correlations from the methyl doublet at δ_H 1.06 (*J* = 6.7 Hz; δ_C 21.2, H-21) to the carbons at δ_C 55.7 (C-17).

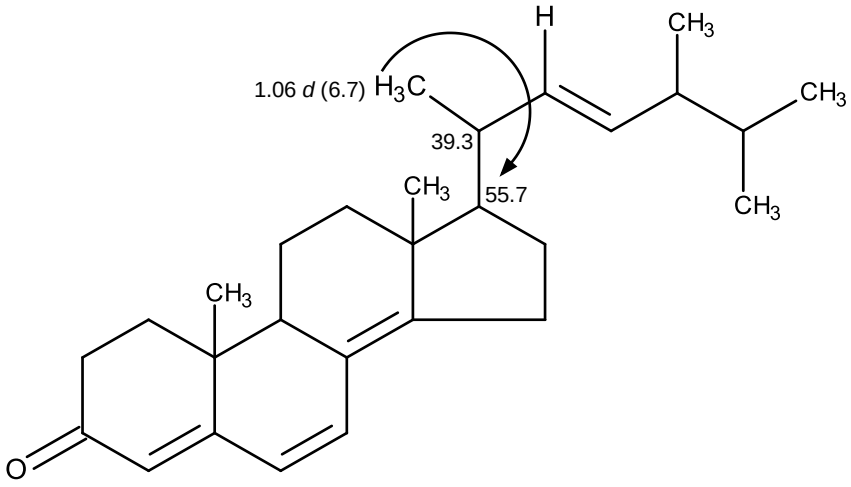

From the above evidence, the structure of **NG 1** was established as ergosta-4, 6, 8-(14), 22-tetraen-3-one (Figure 67) and was previously isolated from the sclerotia of *Polyporus umbellatus*, an edible species of mushroom, which is widely used anti-aldosteronic diuretic in Traditional Chinese medicine (Lee *et al*., 2005; Zhao *et al*., 2009). Moreover, this compound was also reported from the marine sponge-associated fungi *Talaromyces stipitatus* KUFA 0207 (Noinart *et al*., 2017), and *Talaromyces trachyspermus* KUFA 0021 (Kuml *et al*., 2014), as well as from an endophytic fungus *Exophiala oligosperma* EN-21, was isolated from the inner tissue of the marine red alga *Laurencia similis* (Li *et al*., 2011).

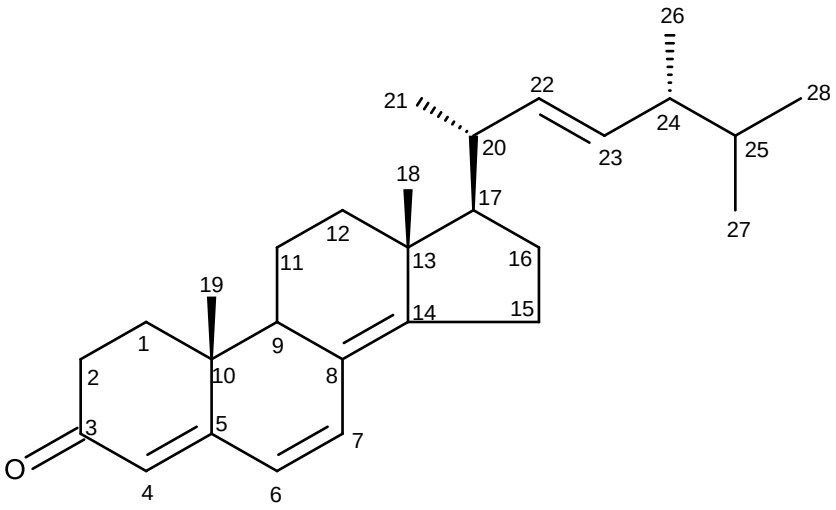

Figure 67. Structure of ergosta-4, 6, 8 (14), 22-tetraen-3-one (**NG 1**)

3.1.3.2. Ergosterol 5, 8-endoperoxide (NG 2/EC 2)

The **NG 2/EC 2** was isolated as a white solid (mp, 182-183 ºC), the ^{13}C NMR spectrum of **NG 2/EC 2** (Table 7) showed twenty eight carbon signals, which through DEPTs and HSQC spectra, can be categorized as four methine sp^2 (δ_C 135.4, 135.2, 132.3 and 130.7), two oxyquaternary sp^3 (δ_C 82.2 and 79.4), one oxymethine sp^3 (δ_C 66.4), six methine sp^3 (δ_C 56.2, 51.7, 51.1, 42.8, 39.7 and 33.1), two quaternary sp^3 (δ_C 44.6 and 37.0), seven methylene sp^3 [(δ_C 39.3, 36.9, 34.7, 30.1, 28.7, 23.4 and 20.6)] and six methyl (δ_C 20.9, 20.0, 19.6, 18.2, 17.6 and 12.9) groups.

The ^{1}H NMR spectrum together with HSQC spectrum (Table 7) showed the signals of two olefinic protons of a *cis* double bond at δ_H 6.50, *d* (*J* = 8.5 Hz) and 6.24, *d* (*J* = 8.5 Hz), two olefinic protons of a *trans* double bond at δ_H 5.23, *dd* (*J* = 15.2, 7.1 Hz) and 5.14, *dd* (*J* = 15.2, 7.8 Hz), an oxymethine proton at δ_H 3.97, *sept* (*J* = 5.2 Hz), the multiplets at δ_H 2.02, 1.95, 1.93, 1.90, 1.85, 1.84, 1.74, 1.69, 1.58, 1.56, 1.53, 1.50, 1.47, 1.40, 1.38, 1.24, 1.23 and *ddd* at δ_H 2.11 (*J* = 13.8, 5.1, 1.8 Hz), two methyl singlet at δ_H 0.88 (δ_C 18.2) and δ_H 0.82 (δ_C 12.9), four methyl doublets at δ_H 1.00 (*J* = 6.6 Hz, δ_C 20.9), δ_H 0.91 (*J* = 6.8 Hz, δ_C 17.6), δ_H 0.83 (*J* = 6.8 Hz, δ_C 20.0) and δ_H 0.82 (*J* = 6.8 Hz, δ_C 19.6) and a singlet of the hydroxyl proton at δ_H 7.27.

The HMBC correlations from the doublet doublet doublet at δ_H 2.11 (*J* = 13.8, 5.1, 1.8 Hz, H-4; δ_C 36.9) to the carbons at δ_C 66.4 (C-3) and δ_C 82.2 (C-5), from the doublet at δ_H 6.24 (*J* = 8.5 Hz, H-6; δ_C 135.4) to C-4 (δ_C 36.9), C-5, C-7 (δ_C 130.7), C-8 (δ_C 79.4) and C-10 (δ_C 37.0), from the doublet at δ_H 6.50 (*J* = 8.5 Hz, H-7; δ_C 130.7) to C-5 and C-6 (δ_C 135.4), C-8 and C-9 (δ_C 51.1), from the methyl singlet at δ_H 0.88 (δ_C 18.2, Me-19) to C-1 (δ_C 34.7), C-5, C-9 and C-10, from the methyl singlet at δ_H 0.82 (δ_C 12.8, Me-18) to C-12 (δ_C 39.3), C-13 (δ_C 44.6), C-14 (δ_C 51.7) and to the carbon at δ_C 56.2 (C-17), indicated the presence of perhydrocyclopentanophenanthrene moiety.

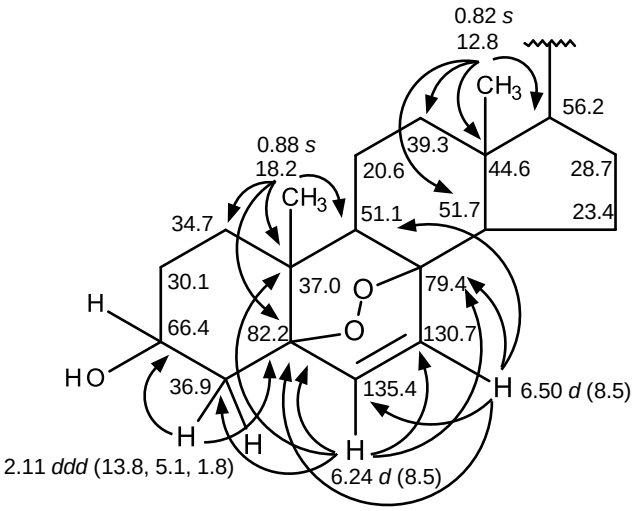

Moreover, the COSY cross peaks from H-20 (δ_H 2.02, *m*) to H-21 (δ_H 1.00, *d*, *J* = 6.6 Hz) and H-22 (δ_H 5.14, *dd*, *J* = 15.2, 7.8 Hz), from H-21 to H-20, from H-22 to H-20 and H-23 (δ_H 5.23, *dd*, *J* = 15.2, 7.1 Hz), from H-23 to the H-22 and H-24 (1.84, *m*), from H-24 to the H-23, from H-25 (δ_H 1.47, *m*) to H-27 (δ_H 0.82, *d*, *J* = 6.8 Hz) and H-28 (δ_H 0.83, *d*, *J* = 6.8 Hz), from H-26 (δ_H 0.91, *d*, *J* = 6.8 Hz) to H-24, from H-27 and H-28 to H-25, indicating the presence (3*E*)-5, 6-dimethylhept-3-en-2-yl moiety.

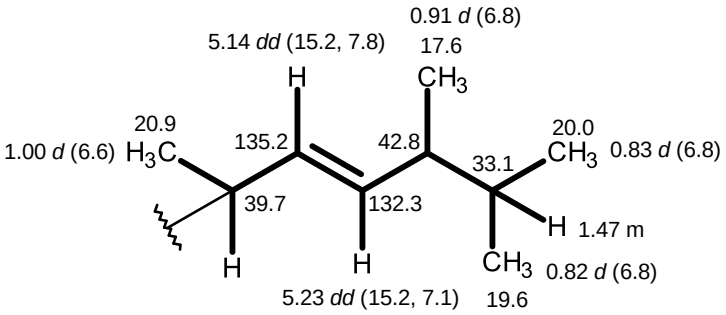

This connectivity was confirmed by the HMBC correlations from H-22 (δ_H 5.14, *dd*, *J* = 15.2, 7.8 Hz; δ_C 135.2) to C-20 (δ_C 39.7) and C-24 (δ_C 42.8), from H-23 (δ_H 5.23, *dd*, *J* = 15.2, 7.1 Hz; δ_C 132.3) to C-24 and C-26 (δ_C 17.6), from H-26 (δ_H 0.91, *d*, *J* = 6.8 Hz; δ_C 17.6) to C-23 (δ_C 132.3), C-24 and C-25, from H-27 (δ_H 0.82, *d*, *J* = 6.8 Hz; δ_C 19.6) and H-28 (δ_H 0.83, *d*, *J* = 6.8 Hz; δ_C 20.0) to C-24 and C-25 respectively.

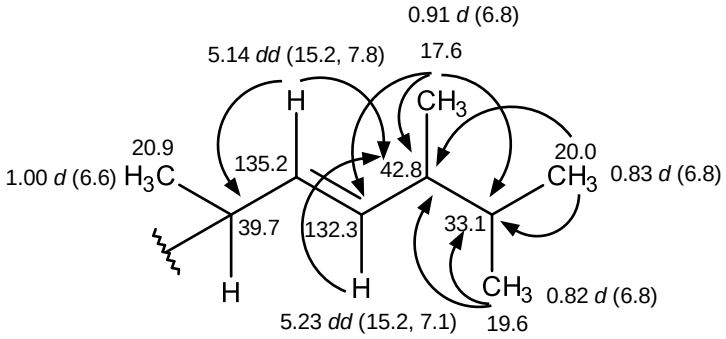

That the (3*E*)-5, 6-dimethylhept-3-en-2-yl moiety was linked to the perhydrocyclopentanophenanthrene moiety was confirmed by the HMBC correlations from H-21 (δ_H 1.00, *d*, *J* = 6.8 Hz; δ_C 20.9) to the carbons at C-17 (δ_C 56.2), C-20 (δ_C 39.7), C-22 (δ_C 135.2). Therefore, the complete structure was:

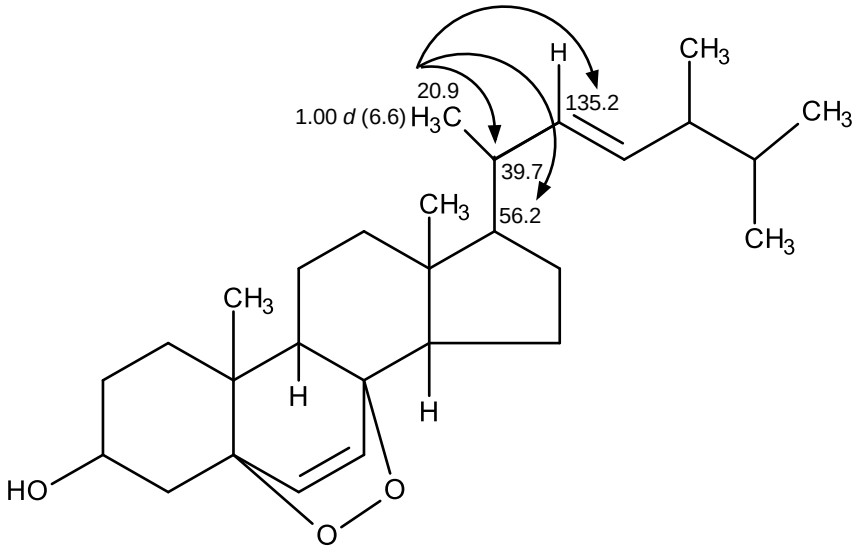

The structure of **NG 2/EC 2** corresponds to ergosterol-5, 8-endoperoxide which was previously isolated from the culture of several sources such as flowers of *Erigeron annuus* L. (Kim *et al*., 2005), pathogenic fungus *Sporothrix schenckii* which was isolated from yeast (Sgarbi *et al*., 1997), entomopathogenic fungus *Paecilomyces tenuipes* (Nam *et al*., 2001), an endophytic fungus *Verticillium sp*. which was isolated from root of wild *Rehmannia glutinosa* (You *et al*., 2009), as well as from the fruiting bodies of a basidiomycete fungus *Lactarius hatsudake* (Zhang *et al*., 2007), and algicolous strain *Aspergillus ustus*, was isolated from the marine green alga *Codium fragile* (Liu *et al*., 2014a).

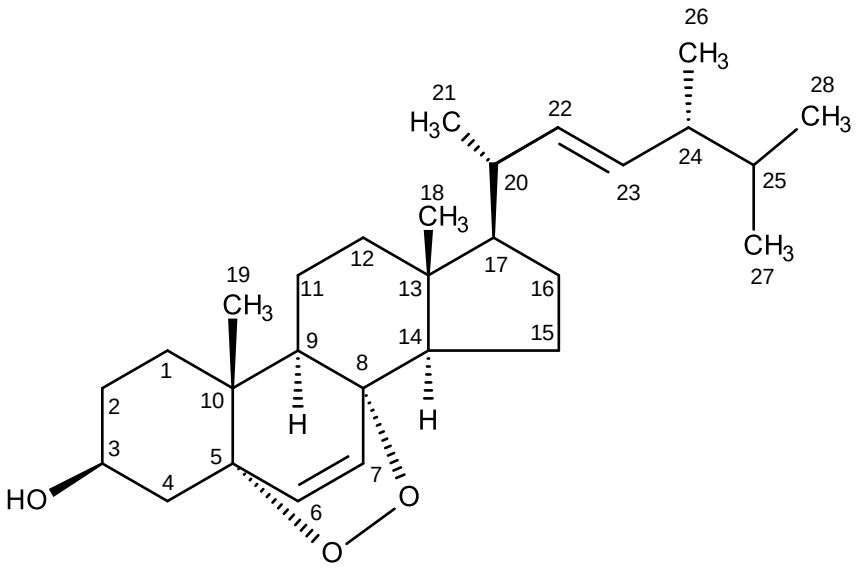

Figure 68. Structure of ergosterol 5, 8-endoperoxide (**NG 2/EC 2**)

3.1.3.3. Acetyl ergosterol-5, 8-endoperoxide (TH 2)

Compound **TH 2** was isolated as a white amorphous solid. The general features of the ^{1}H and ^{13}C NMR spectra of **TH 2** were very similar to those of ergosterol-5, 8-endoperoxide **NG 2/EC 2**. The ^{13}C NMR, DEPTs and HSQC spectra (Table 7) revealed in addition to the acetoxyl group (δ_C 170.2 and δ_C 21.4, δ_H 2.02, *s*), the 28 carbon signals of ergosterol 5, 8-endoperoxide. Since H-3 and C-3 of **TH 2** appeared at higher frequencies (ca. 1 ppm for H-3 and 3 ppm for C-3) than the corresponding proton and carbon of ergosterol-5, 8-endoperoxide, the structure of **TH 2** was elucidated as acetyl ergosterol 5, 8-endoperoxide. Acetyl ergosterol 5, 8-endoperoxide has been previously reported from several sources including from an

aerial parts of *Ajuga remota* Benth. (Cantrell *et al*., 1999) and the marine-sponge associated fungus *Talaromyces trachyspermus* KUFA 0021 (Kuml *et al*., 2014).

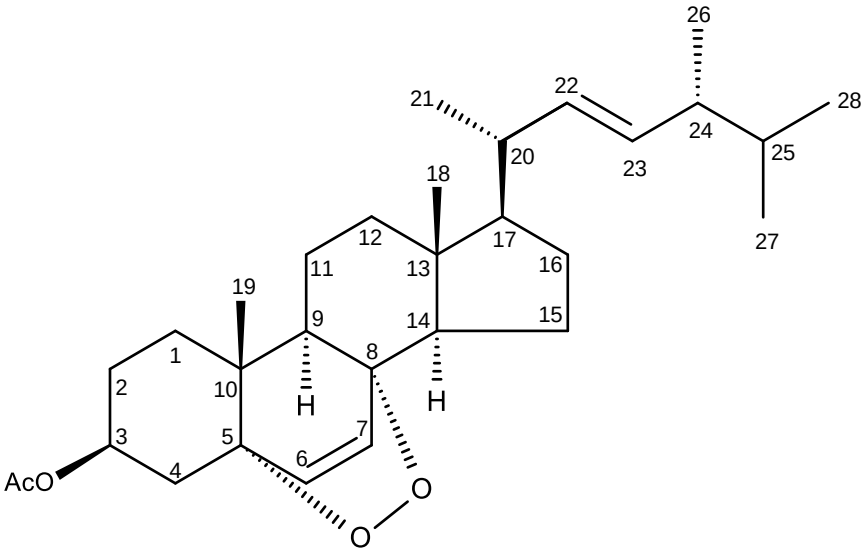

Figure 69. Structure of acetyl ergosterol-5, 8-endoperoxide (**TH 2**)

Table 7. Comparison of ^{1}H and ^{13}C NMR ($CDCl_3$, 300.13 and 75.47 MHz) assignment for **NG 2/EC 2** and **TH 2**

Position	NG 2/ EC 2		TH 2	
	δ_C, type	**δ_H, (*J* in Hz)**	**δ_C, type**	**δ_H, (*J* in Hz)**
1	34.7, CH_2	1.69, *m*/ 1.93, *m*	34.3, CH_2	1.70, *m*/ 1.97, *m*
2	30.1, CH_2	1.53, *m*/ 1.85, *m*	26.3, CH_2	1.55, *m*/ 1.95, *m*
3	66.4, CH	3.97, *sept* (5.2)	69.5, CH	4.99, *sept* (5.6)
4	36.9, CH_2	2.11, *ddd* (13.8, 5.1, 1.8)	33.2, CH_2	2.14, *ddd* (13.7, 5.3, 1.8)
		1.90, *m*		1.91, *m*
5	82.2, C	-	79.4, C	-
6	135.4, CH	6.24, *d* (8.5)	135.1, CH	6.23, *d* (8.5)
7	130.7, CH	6.50, *d* (8.5)	130.9, CH	6.51, *d* (8.5)
8	79.4, C	-	81.7, C	-
9	51.1, CH	1.50, *m*	51.0, CH	1.51, *m*
10	37.0, C	-	37.0, C	-
11	20.6, CH_2	1.40, *m*/ 1.58, *m*	20.6, CH_2	1.40, *m*/ 1.60, *m*
12	39.3, CH_2	1.95, *m*/ 1.23, *m*	39.3, CH_2	1.95, *m*/ 1.24, *m*
13	44.6, C	-	44.6, C	-
14	51.7, CH	1.56, *m*	51.6, CH	1.58, *m*
15	23.4, CH_2	1.50, *m*/ 1.23, *m*	23.4, CH_2	1.51, *m*/ 1.25, *m*
16	28.7, CH_2	1.74, *m*/ 1.38, *m*	28.7, CH_2	1.74, *m*/ 1.33, *m*
17	56.2, CH	1.24, *m*	56.2, CH	1.23, *m*
18	12.9, CH_3	0.82, *s*	12.9, CH_3	0.81, *s*
19	18.2, CH_3	0.88, *s*	18.1, CH_3	0.90, *s*
20	39.7, CH	2.02, *m*	39.8, CH	2.01, *m*
21	20.9, CH_3	1.00, *d* (6.6)	21.0, CH_3	1.00, *d* (6.6)
22	135.2, CH	5.14, *dd* (15.2, 7.8)	135.2, CH	5.15, *dd* (15.3, 8.2)
23	132.3, CH	5.23, *dd* (15.2, 7.1)	132.3, CH	5.22, *dd* (15.3, 7.6)
24	42.8, CH	1.84, *m*	42.8, CH	1.85, *m*
25	33.1, CH	1.47, *m*	33.1, CH	1.47, *m*
26	17.6, CH_3	0.91, *d* (6.8)	17.6, CH_3	0.91, *d* (6.8)
27	19.6, CH_3	0.82, *d* (6.8)	19.7, CH_3	0.82, *d* (6.8)
28	20.0,CH_3	0.83, *d* (6.8)	20.0, CH_3	0.84, *d* (6.8)
OH-3	-	7.27, *s*	-	-
OAc	-	-	170.2, CO	-
			21.4, CH_3	2.02, *s*

3.1.4 Structure Elucidation of Tetracyclic Triterpenoid

3.1.4.1. Helvolic acid (NG 3)

NG 3 was isolated as a white solid (mp, 217-218 ºC), the ^{13}C NMR spectrum (Table 8) displayed 33 carbon signals which, through DETPs and HSQC spectra, can be categorized as two ketone carbonyls (δ_C 208.8 and 201.4), one carboxylic acid (δ_C 174.0), two ester carbonyls (δ_C 170.2 and 168.9), three quaternary sp^2 (δ_C 147.8, 132.9 and 130.4), three methine sp^2 (δ_C 157.3, 127.8 and 122.8), two oxymethine sp^3 (δ_C 73.8 and 73.5), four methine sp^3 (δ_C 49.4, 47.2, 41.7 and 40.4), three quaternary sp^3 (δ_C 52.7, 46.6 and 38.2), five methylene sp^3 (δ_C 40.6, 28.6, 28.3, 25.9 and 23.9) and eight methyl (δ_C 27.5, 25.7, 20.7, 20.5, 18.3, 17.9, 17.8 and 13.1) carbons.

The ^{1}H NMR spectrum (Table 8), in combination with HSQC spectrum, exhibited signals of a pair of *cis*-coupled olefinic protons at δ_H 7.31, *d* (*J* = 10.1 Hz) and 5.87, *d* (*J* = 10.0 Hz), an olefinic proton of the trisubstituted double bond at δ_H 5.11, *dd* (*J* = 7.7, 6.6 Hz), two oxymethine protons at δ_H 5.88, *d* (*J* = 8.3 Hz), 5.24, *d* (*J* = 0.5 Hz), as well as several aliphatic proton signals at δ_H 2.78, *dq* (*J* = 6.7 Hz), 2.62, *dd* (*J* = 11.6, 2.4 Hz), 2.58, *d* (*J* = 10.1 Hz), 2.27, *d* (*J* = 11.3 Hz), 2.48, *m*, 2.40, *m*, 2.20, *m* and 1.92, *d* (*J* = 16.7 Hz), 2.08, *m*, 1.98, *m*, in addition to seven methyl singlets at δ_H 2.11, 1.95, 1.69, 1.61, 1.45, 1.18, 0.93 and a methyl doublet at δ_H 1.28 (*J* = 6.8 Hz).

Table 8. ^{1}H and ^{13}C NMR ($CDCl_3$, 300.13 and 75.47 MHz) and HMBC assignment for **NG 3**

Position	δ_C, type	δ_H, (*J* in Hz)	COSY	HMBC
1	157.3, CH	7.31, *d* (10.1)	H-2	C-3, 5, 9, 10
2	127.8, CH	5.87, *d* (10.0)	-	-
3	201.4, CO	-	-	-
4	40.4, CH	2.78, *dq* (6.7)	H-5, 28	C-3, 18, 28
5	47.2, CH	2.27, *d* (11.3)	-	C-1, 3, 4, 10
6	73.8, CH	5.24, *d* (0.5)	-	C-5, 7, 8, 10, OAc-6
7	208.8, CO	-	-	-
8	52.7, C	-	-	-
9	41.7, CH	2.62, *dd* (11.6, 2.4)	-	-
10	38.2, C	-	-	-
11	23.9, CH_2	1.98, *m*	-	-
12	25.9, CH_2	2.40, *m*	H-13	-
13	49.4, CH	2.58, *d* (10.1)	H-12	-
14	46.6, C	-	-	-
15a	40.6, CH_2	2.20, *m*	H-15b, 16, 29	-
b		1.92, *d* (16.7)	-	C-13, 14, 16, 17
16	73.5, CH	5.88, *d* (8.3)	H-15a, b	C-14, 17, 20, CO (Ac-16)
17	147.8, C	-	-	-
18	27.5, CH_3	1.45, *s*	-	C-1, 5, 9, 10
19	18.3, CH_3	1.18, *s*	-	C-7, 8, 9, 14
20	130.4, C	-	-	-
21	174.0, CO	-	-	-
22	28.6, CH_2	2.48, *m*	-	-
23	28.3, CH_2	2.08, *m*	-	-
24	122.8, CH	5.11, *dd* (7.7, 6.6)	H-26, 27	-
25	132.9, C	-	-	-
26	25.7, CH_3	1.69, *s*	-	C-24, 25, 27
27	17.8, CH_3	1.61, *s*	-	C-24, 25, 26
28	13.1, CH_3	1.28, *d* (6.8)	-	C-3, 4, 5
29	17.9, CH_3	0.93, *s*	-	C-8, 13, 14, 15
OAc-6	168.9, CO	-	-	-
	20.7, CH_3	2.11, *s*	-	CO (Ac-6)
OAc-16	170.2, CO	-	-	-
	20.5, CH_3	1.95, *s*	-	CO (Ac-16)

The COSY spectrum (Table 8) showed the correlations from the olefinic protons at δ_H 7.31, *d* (*J* = 10.1 Hz, H-1) to δ_H 5.87, *d* (*J* = 10.0 Hz, H-2), as well as from the double quartet at δ_H 2.78 (*J* = 6.7 Hz, H-4) to the doublet at δ_H 2.27 (*J* = 11.3 Hz, H-5) and the methyl doublet at δ_H 1.28 (*J* = 6.8 Hz, H-28). The HMBC spectrum (Table 8) showed correlations from the olefinic proton at δ_H 7.31, *d* (*J* = 10.1 Hz; δ_C 157.3, H-1) to the carbonyl carbon at δ_C 201.4 (C-3), the methine carbon at δ_C 47.2 (C-5), 41.7 (C-9) and the quaternary carbons at δ_C 38.2 (C-10), from the doublet at δ_H 2.27 (*J* = 11.3 Hz; δ_C 47.2, H-5) to the carbon at δ_C 157.3 (C-1), the carbonyl carbon at δ_C 201.4 (C-3), the methine sp^3 carbon at δ_C 40.4 (C-4) and the quaternary carbon at δ_C 38.2 (C-10), from the methyl doublet at δ_H 1.28 (*J* = 6.8 Hz; δ_C 13.1, H-28) to the carbonyl carbon at δ_C 201.4 (C-3), the methine sp^3 carbons at δ_C 40.4 (C-4) and 47.2 (C-5), from the methyl singlet at δ_H 1.45 (δ_C 27.5, H-18) to the carbons at δ_C 157.3 (C-1), 47.2 (C-5), 41.7 (C-9) and 38.2 (C-10).

Moreover, the HMBC spectrum showed correlations from the doublet of oxymethine proton at δ_H 5.24 (*J* = 0.5 Hz; δ_C 73.8, H-6) to the carbons at δ_C 47.2 (C-5), 168.9 (C-6), 208.8 (C-7), 52.7 (C-8) and 38.2 (C-10), and from the methyl singlet at δ_H 2.11 (δ_C 20.7) to the ester carbonyl at δ_C 168.9. Therefore, the acetoxy group should be on C-6. Moreover, the methyl singlet at δ_H 1.18 (δ_C 18.3, H-19) showed HMBC cross peaks to the quaternary carbons at δ_C 52.7 (C-8) and 46.6 (C-14), as well as to the ketone carbonyl at δ_C 208.8 (C-7) and the methine carbon at δ_C 41.7 (C-9). These correlations indicated that the methyl substituent was on the quaternary

carbon at δ_C 52.7 (C-8). Taking together the COSY and HMBC correlations, the structure of **NG 3** must have the following moiety.

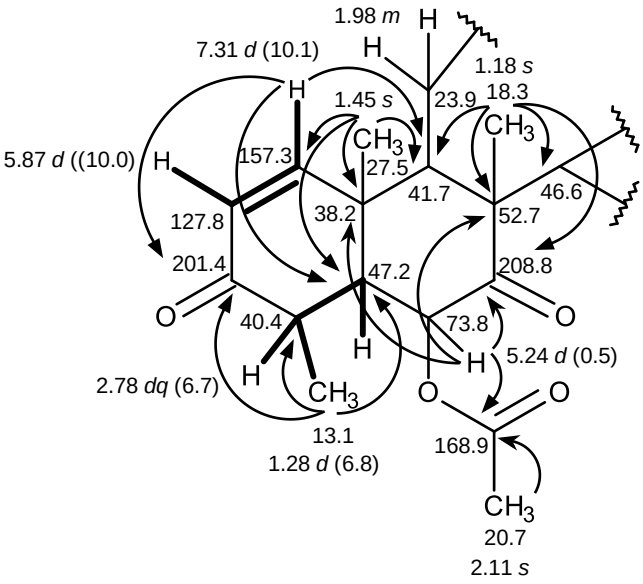

The existence of a 1-methyl-4-acetoxy-1, 2, 3, 4-tetrasubstituted cyclopentane was supported by the COSY correlations from the doublet of the oxymethine proton at δ_H 5.88 (*J* = 8.3 Hz, H-16; δ_C 73.5) to the doublet at δ_H 1.92 (*J* = 16.7 Hz, H-15; δ_C 40.6) and a multiplet at δ_H 2.20 of the methylene protons (H-15, δ_C 40.6) as well as by the HMBC correlations from H-16 to the carbons at δ_C 46.6 (C-14), from the doublet at δ_H 1.92 (*J* = 16.7 Hz, H-15) to C-13, C-14 and C-16, from the methyl singlet at δ_H 0.93 (δ_C 17.9; CH_3-29) to the carbons at δ_C 46.6 (C-14), δ_C 49.4 (C-13) and δ_C 40.6 (C-15) as well as from the methyl singlet at δ_H 1.95 (δ_C 20.5, CH_3-OAc) and H-16 to the carbonyl carbon at δ_C 170.2.

That the 1-methyl-4-acetoxy-1, 2, 3, 4-tetrasubstituted cyclopentane moiety was fused with the cyclohexane ring of the perhydrophenanthrene portion was

supported by the HMBC correlations from the methyl singlet at δ_H 0.93 (δ_C 17.9; CH_3-29) to C-8 (δ_C 52.7) as well as by the COSY correlation between the doublet at δ_H 2.58 (J = 10.1 Hz) to the multiplet at δ_H 2.40 (H-12, δ_C 25.9).

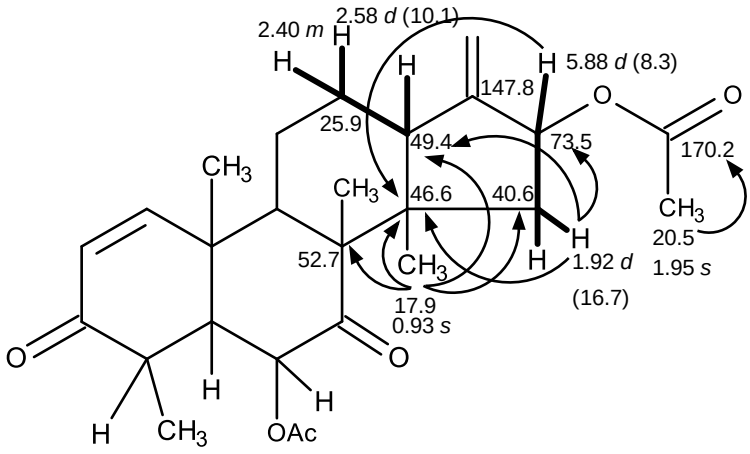

That the cyclopentanoperhydrophenanthrene moiety linked to the 6-methylhept-5-enoic acid through a double bond between C-17 of the former and C-2 of the latter was supported by the HMBC correlations from the methyl singlets at δ_H 1.69 (δ_C 25.7, H-26) and 1.61 (δ_C 17.8, H-27) to the quaternary sp^2 carbon at δ_C 132.9 (C-25) and the methine sp^2 carbon at δ_C 122.8 (C-24), from H-16 to the quatermnary sp^2 carbons at δ_C 147.8 (C-17) and 130.4 (C-20) as well as from presence of the conjugated carboxyl group at δ_C 170.2.

Taking together the ^1H and ^{13}C NMR chemical shifts and the COSY and HMBC correlations, the structure of **NG 3** was proposed as helvolic acid.

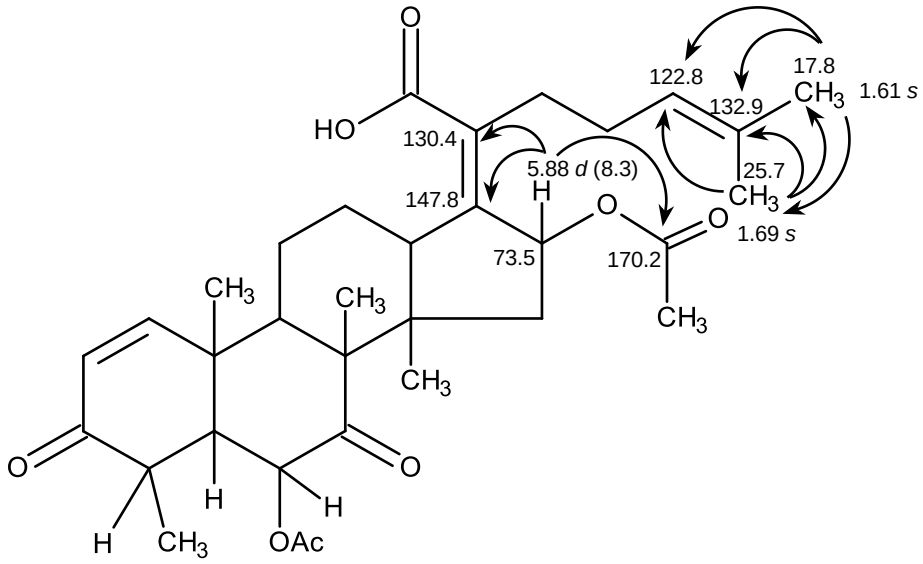

This was confirmed by comparison of the ^{1}H and ^{13}C NMR data of **NG 3** with those reported in the literature (Fujimoto *et al*., 1996). Helvolic acid has been widely isolated from both terrestrial and marine-derived fungi such as from an Ascomycete, *Corynascus setosus* (Fujimoto *et al*., 1996), marine-derived fungus *Aspergillus sydowi* PFW1-13, which was isolated from a driftwood sample (Zhang *et al*., 2008), marine sponge-associated fungus *Emericellopsis minima* (Pinheiro *et al*., 2012), an endophytic fungus *Aspergillus fumigates* strain LN-4, was isolated form the healthy stem bark of *Melia azedarach* L. (Li *et al*., 2012) and the soil fungus *Neosartorya Fischeri* KUFA 6344 (Eamvijarn *et al*., 2013).

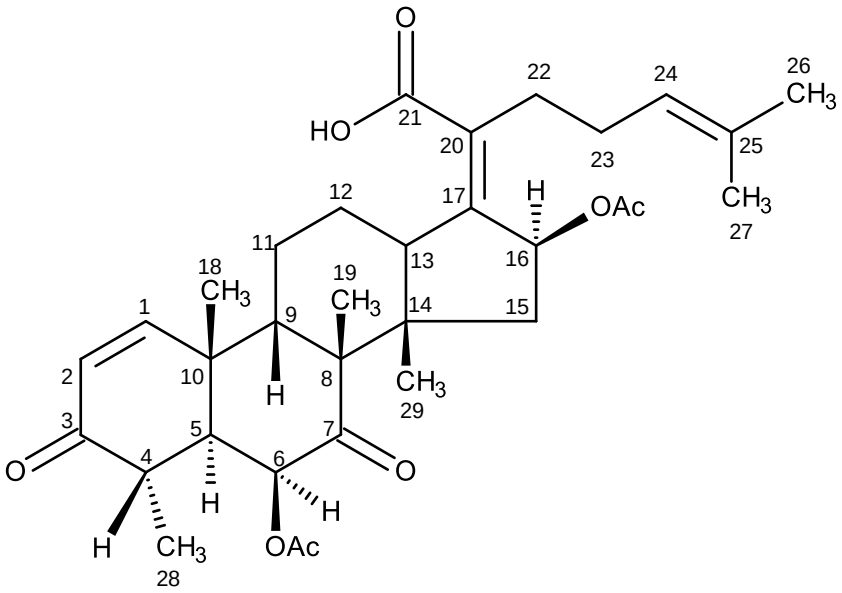

Figure 70. Structure of helvolic acid (**NG 3**)

3.1.5 Structure Elucidation of Meroditerpenes

3.1.5.1. Chevalone B (NTK 10)

NTK 10 was isolated as a white solid (mp, 163-164 ºC), the ^{13}C NMR spectrum, and in combination with DEPTs and HSQC, (Table 9) revealed the presence of one ester carbonyl (δ_C 171.0), one conjugated ester carbonyl (δ_C 165.4), three quaternary sp^2 (δ_C 163.3, 159.7 and 97.8), one methine sp^2 (δ_C 100.6), one oxymethine sp^3 (δ_C 80.6), three methine sp^3 (δ_C 60.2, 55.4 and 51.9), one oxyquaternary sp^3 (δ_C 80.5), three quaternary sp^3 (δ_C 37.8, 37.2 and 37.0), seven

methylene sp^3 (δ_C 40.8, 40.2, 38.0, 23.5, 18.6, 17.8 and 16.8), seven methyl (δ_C 27.9, 21.3, 20.5, 19.7, 16.4, 16.3 and 16.1) carbons.

The ^1H NMR spectrum, in combination with HSQC spectrum, (Table 9) displayed the singlet of one olefinic proton at δ_H 5.69 (δ_C 100.6), one oxymethine proton at δ_H 4.46, *dd* (*J* = 11.0, 5.1 Hz, δ_C 80.6), three methine protons at δ_H 1.45, *dd* (*J* = 12.8, 4.8 Hz, δ_C 51.9), 0.93, *dd* (*J* = 11.6, 1.7 Hz, δ_C 60.2) and 0.88, *m* (δ_C 55.4), seven methylene groups at δ_H [(1.73, *m* and 1.06, *m*, δ_C 38.0) (1.70, *m* and 1.35, *dd*, *J* = 12.4, 3.2 Hz, δ_C 18.6), (1.57, *m* and 1.47, *m*, δ_C 17.8), (2.06, *dd*, *J* = 15.7, 4.3 Hz and 1.59, *dd*, *J* = 12.9, 3.3 Hz, δ_C 40.2), (2.43, *dd*, *J* = 16.8, 4.9 Hz and 2.14, *dd*, *J* = 17.4, 4.1 Hz, δ_C 16.8), (1.85, *dt*, *J* = 12.7, 3.0 Hz and 1.04, *m*, δ_C 40.8) and (1.69, *m*, δ_C 23.5)], seven methyl singlets at δ_H 0.87 (δ_C 16.4), 0.88 (δ_C 16.3), 0.86 (δ_C 27.9), 0.90 (δ_C 16.1), 1.18 (δ_C 20.5), 2.04 (δ_C 21.3) and 2.18 (δ_C 19.7).

Table 9. ^{1}H and ^{13}C NMR ($CDCl_3$, 300.13 and 75.47 MHz) and HMBC assignment for **NTK 10**

Position	δ_C, type	δ_H, (*J* in Hz)	COSY	HMBC
1a	38.0, CH_2	1.73, *m*	H-1b, 2	C-3, 5, 10
b		1.06, *m*	H-1a, 2	-
2	23.5, CH_2	1.69, *m*	H-3	C-3
3	80.6, CH	4.46, *dd* (11.0, 5.1)	H-2	C-22, 23, Ac-3
4	37.8, C	-	-	-
5	55.4, CH	0.88, *m*	H-6	C-1, 9, 10
6a	17.8, CH_2	1.57, *m*	H-5	C-4, 8, 10
b		1.47, *m*	H-5	-
7a	40.8, CH_2	1.85, *dt* (12.7, 3.0)	H-7b	-
b		1.04, *m*	H-7a	-
8	37.0, C	-	-	-
9	60.2, CH	0.93, *dd* (11.6, 1.7)	H-11	C-8, 10
10	37.2, C	-	-	-
11a	18.6, CH_2	1.70, *m*	H-9, 12b	-
b		1.35, *dd* (12.4, 3.2)	H-9, 12b	-
12a	40.2, CH_2	2.06, *dd* (15.7, 4.3)	H-11	C-9, 13, 14
b		1.59, *dd* (12.9, 3.3)	H-11	C-8, 10, 13
13	80.5, C	-	-	-
14	51.9, CH	1.45, *dd* (12.8, 4.8)	H-15	C-8, 13, 25
15a	16.8, CH_2	2.43, *dd* (16.8, 4.9)	H-14, 15b	C-14, 16, 17
b		2.14, *dd* (17.4, 4.1)	H-14, 15a	C-13, 14, 16, 17, 21
16	97.8, C	-	-	-
17	163.3, C	-	-	-
18	100.6, CH	5.69, *s*	H-20	C-16, 17, 19, 20
19	159.7, C	-	-	-
20	19.7, CH_3	2.18, *s*	H-18	C-17, 18, 19
21	165.4, CO	-	-	-
22	27.9, CH_3	0.86, *s*	-	C-3, 4, 5, 23
23	16.1, CH_3	0.90, *s*	-	C-3, 4, 5, 22
24	16.3, CH_3	0.88, *s*	-	C-1, 5, 9, 10
25	16.4, CH_3	0.87, *s*	-	C-7, 8, 9, 14
26	20.5, CH_3	1.18, *s*	-	C-12, 13, 14
Ac-3	171.0, CO	-	-	-
	21.3, CH_3	2.04, *s*	-	CO (Ac)

The COSY spectrum exhibited cross peaks between the protons at δ_H 1.73, *m* (H-1a)/1.06, *m* (H-1b, δ_C 38.0) and δ_H 1.69, *m* (H-2, δ_C 23.5), between δ_H 1.69, *m* (H-2) and δ_H 4.46, *dd* (*J* = 11.0, 5.1 Hz, H-3, δ_C 80.6), indicating the coupling system from H-1 through H-3. The HMBC spectrum exhibited correlations from the protons at δ_H 1.73, *m* (δ_C 38.0, H-1a) to the carbons at δ_C 80.6 (C-3), 55.4 (C-5) and 37.2 (C-10), from the proton at δ_H 1.69, *m* (δ_C 23.5, H-2) to the carbons at δ_C 80.6 (C-3), from the proton at δ_H 4.46, *dd* (*J* = 11.0, 5.1 Hz; δ_C 80.6, H-3) to the carbons at δ_C 171.0 (CO; OAc-3), 16.1 (CH_3-23) and 27.9 (CH_3-22), as well as from the methyl singlets at δ_H 0.86 (δ_C 27.9) and 0.90 (δ_C 16.1) to the quaternary carbon at δ_C 55.4 (C-5) and C-3, and from the methyl proton at δ_H 2.04, *s* (δ_C 21.3, OAc) to the carbonyl carbon at δ_C 171.0 (Ac-3). These correlations suggested the presence of a 3, 3-dimethyl-4-acetoxy-1, 2, 3, 4-substituted cyclohexyl moiety.

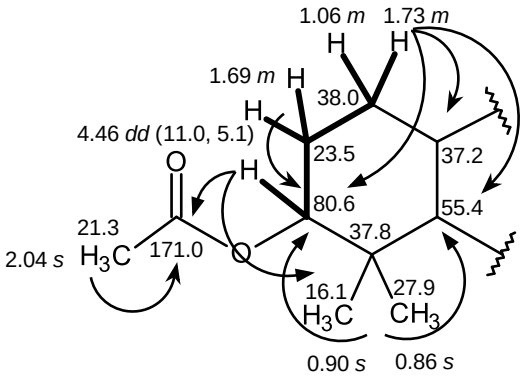

Moreover, HMBC spectrum showed the correlations from the methyl singlet at δ_H 0.88 (CH_3-24, δ_C 16.3) to C-1, C-5, C-9 and C-10, and from H-6 (1.57 *m*, δ_H 17.8) to C-4, C-8 and C-10. The existence of the perhydrophenthrene ring system was supported by the HMBC correlations from H-14 (δ_H 1.45, *dd*, *J* = 12.8, 4.8 Hz;

δ_C 51.9) to C-8 (δ_C 37.0), C-13 (δ_C 80.5) and CH_3-25 (δ_C 16.4) as well as from H_3-25 (δ_H 0.87, *s*) to C-7 (δ_C 40.8), C-8 (δ_C 37.0), C-9 (δ_C 60.2) and C-14 (δ_C 51.9).

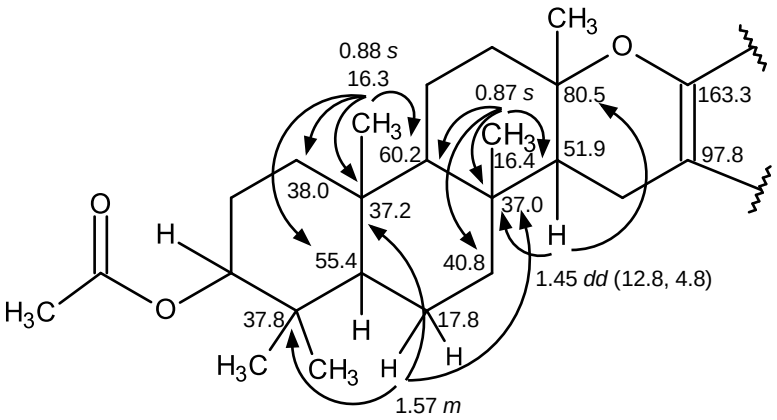

The presence of the 6-methyl-2*H*-pyran-2-one portion was confirmed by the HMBC correlations from the singlet at δ_H 5.69 (δ_C 100.6, H-18) to the carbons at δ_C 97.8 (C-16), 163.3 (C-17), 159.7 (C-19) and 19.7 (C-20), from the methyl singlet at δ_H 2.18 (δ_C 19.7, H-20) to C-17, C-18 and C-19. That the 6-methyl-2*H*-pyran-2-one portion was fused to the perhydrophenanthrene ring system, through the pyran ring, was corroborated by the HMBC correlation from the *dd* at δ_H 2.43, (*J* = 16.8, 4.9 Hz, H-15) to C-14, C-16 and C-17 as well as from the *dd* at δ_H 2.14 (*J* = 17.4, 4.1) to C-13, C- 14, C-16, C-17, and C-21.

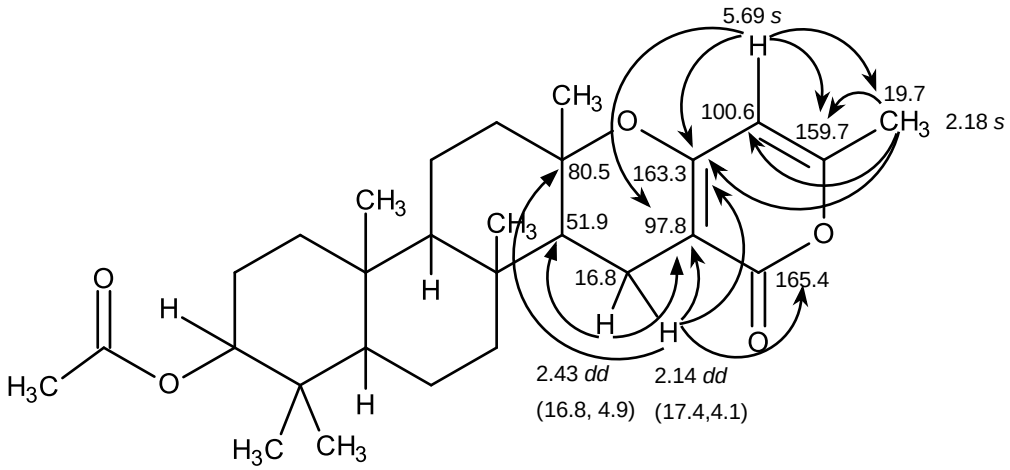

All of the ^{1}H and ^{13}C NMR data together with the COSY and HMBC correlations allowed the formulation of the structure of **NTK 10** as chevalone B (Figure 71). Chevalone B has been previously reported from several fungi including the soil fungi *Eurotium chevalieri* (Kanokmedhakul *et al*., 2011) and *Neosartorya spinosa* KKU-1NK1 (Rajachan *et al*., 2016), coral-derived fungus *Neosartorya laciniosa* KUFC 7896 (Gomes *et al*., 2014) and marine sponge-associated fungus *Aspergillus similanensis* sp. nov. KUFA 0013 (Prompanya *et al*., 2014).

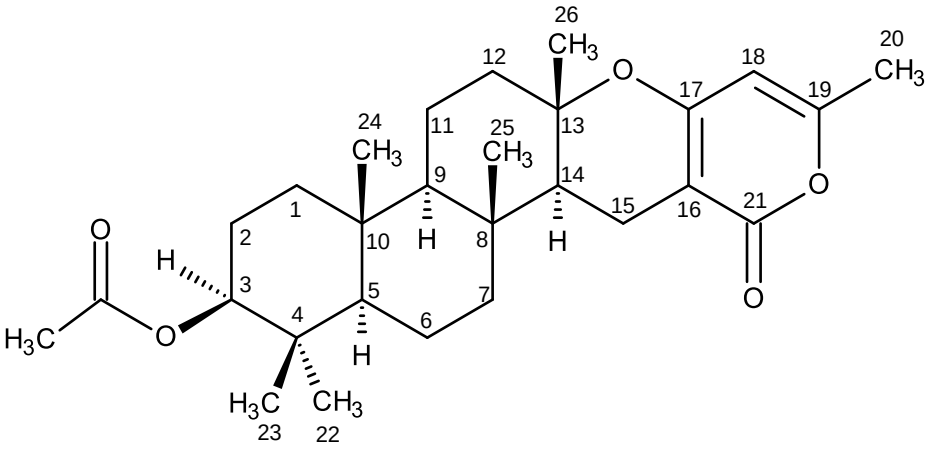

Figure 71. Structure of chevalone B (**NTK 10**)

3.1.5.2. Aszonapyrone A (NTK 11)

NTK 11 was isolated as a white solid (mp, 242-243 ºC). The ^{1}H and ^{13}C NMR features of **NTK 11** resembled those of **NTK 10**.

The ^{13}C NMR spectrum (Table 10) exhibited twenty eight carbon signals which in combination with DEPTs and HSQC, was categorized as one ester carbonyl (δ_C 170.1), one conjugated ester carbonyl (δ_C 164.6), four quaternary sp^2 (δ_C 164.5, 159.4, 148.2 and 101.0), one methylene sp^2 (δ_C 106.4), one methine sp^2 (δ_C 99.8), three quaternary sp^3 (δ_C 36.9 (2C) and 37.3), one oxymethine sp^3 (δ_C 79.8), three methine sp^3 (δ_C 59.1, 54.6 and 52.9), seven methylene sp^3 (δ_C 39.4, 37.6, 37.5, 23.3, 22.8, 18.3 and 18.2), and six methyl (δ_C 27.7, 20.9, 19.1, 16.3, 15.9 and 14.8) carbons.

Table 10. ^{1}H and ^{13}C NMR (DMSO, 300.13 and 75.47 MHz) and HMBC assignment for **NTK 11**

Position	δ_C, type	δ_H, (*J* in Hz)	COSY	HMBC
1a	37.5, CH_2	1.01, *m*	H-1b	C-24
b		1.62, *m*	H-1a	C-22, 24
2	22.8, CH_2	1.62, *m*	H-3	-
3	79.8, CH	4.39, *dd* (10.1, 5.9)	H-2	C-23, 24, Ac-3
4	37.3, C	-	-	-
5	54.6, CH	0.92, *d* (9.1)	H-6b	-
6a	18.3, CH_2	1.54, *m*	H-6b	-
b		1.40, *m*	H-5	-
7a	39.4, CH_2	1.39, *m*	H-7b	-
b		1.87, *m*	H-7a	-
8	36.9, C	-	-	-
9	59.1, CH	1.07, *d* (12.0)	H-11a	-
10	36.9, C	-	-	-
11a	23.3, CH_2	1.26, *m*	H-9	-
b		1.57, *m*	-	-
12a	37.6, CH_2	1.86, *m*	H-12b	-
b		2.22, *m*	H-12a	-
13	148.2, C	-	-	-
14	52.9, CH	2.44, *d* (3.1)	H-15a, b	C-7, 13
15a	18.2, CH_2	2.47, *d* (14.2)	H-14, 15b	C-13, 16, 21
b		2.30, *d* (11.8)	H-14, 15a	C-13, 16, 21
16	101.0, C	-	-	-
17	164.5, C	-	-	-
18	99.8, CH	5.93, *d* (0.8)	H-20	C-16, 19, 20
19	159.4, C	-	-	-
20	19.1, CH_3	2.11, *s*	H-18	C-18, 19
21	164.6, CO	-	-	-
22	27.7, CH_3	0.83, *s*	-	C-3, 4, 5, 23
23	15.9, CH_3	0.81, *s*	-	C-3, 4, 5, 22
24	16.3, CH_3	0.79, *s*	-	C-1, 5, 9, 10
25	14.8, CH_3	0.69, *s*	-	C-7, 9, 14
26a	106.4, CH_2	4.83, *s*	H-26b	C-12, 14
b		4.60, *s*	H-14, 26a	C-12, 14
Ac-3	170.1, CO	-	-	-
	20.9, CH_3	2.00, *s*	-	CO (Ac-3)

The ^{1}H NMR spectrum, together with the HSQC spectrum, (Table 10) exhibited the signals of an olefinic proton at δ_H 5.93, *d* (*J* = 0.8 Hz, δ_C 99.8), an oxymethine proton at δ_H 4.39, *dd* (*J* = 10.1, 5.9 Hz, δ_C 79.8), two singlets of the exocyclic olefinic protons at δ_H 4.83 and 4.60 (δ_C 106.4), and six methyl siglets at 2.11 (δ_C 19.1), 2.00 (δ_C 20.9), 0.83 (δ_C 27.7), 0.81 (δ_C 15.9), 0.79 (δ_C 16.3) and 0.69 (δ_C 14.8). That **NTK 11** contained the 3-acetoxy-4, 4, 8, 10-tetramethylperhydrophenanthrene moiety was substantiated by the HMBC correlations from the doublet doublet at δ_H 4.39 (*J* = 10.1, 5.9 Hz; δ_C 79.8, H-3) to the methyl carbons at δ_C 15.9 (C-23), 16.3 (C-24) and 20.9 (OAc), from the methyl singlet at δ_H 2.00 (δ_C 20.9, Ac) to the carbonyl carbon at δ_C 170.1 (Ac), from the methyl singlet at δ_H 0.83 (δ_C 27.7, H-22) to the carbons at δ_C 79.8 (C-3), 37.3 (C-4), 54.6 (C-5) and 15.9 (C-23), from the methyl singlet at δ_H 0.81 (δ_C 15.9, H-23) to the carbons at δ_C 79.8 (C-3), 37.3 (C-4), 54.6 (C-5) and 27.7 (C-22), from the methyl singlet at δ_H 0.79 (δ_C 16.3, H-24) to the carbons at δ_C 37.5 (C-1), 36.9 (C-10), 54.6 (C-5) and 59.1 (C-9), from the methyl singlet at δ_H 0.69 (δ_C 14.8, H-25) to the carbons at δ_C 39.4 (C-7), 59.1 (C-9) and 52.9 (C-14).

However, the presence of the exocyclic double bond on C-13, instead of the pyran oxygen and the methyl group as in chevalone B, was supported by the HMBC correlations from the exocyclic olefinic protons at δ_H 4.60 and 4.83 (δ_C 106.4, H-26) to the carbons at δ_C 37.6 (C-12) and 52.9 (C-14).

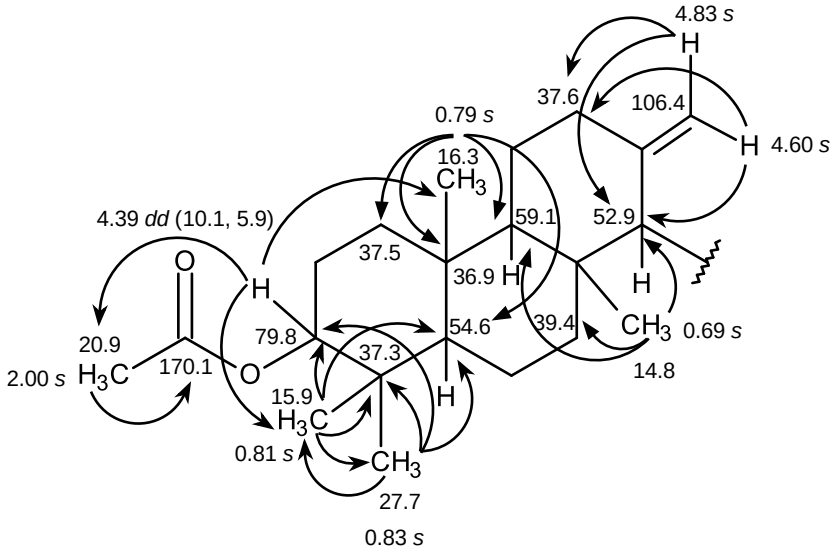

Similar to **NTK 10**, the existence of 6-methyl-2*H*-pyran-2-one was evidenced by the presence of the singlet of olefinic proton at δ_H 5.93, *d* (*J* = 0.8, δ_C 99.8), the methyl singlet at δ_H 2.11 (δ_C 19.1), the conjugated carbonyl carbon at δ_C 164.6, as well as by the HMBC correlations from the doublet at δ_H 5.93 (*J* = 0.8 Hz; δ_C 99.8, H-18) to the carbons at δ_C 101.0 (C-16), 159.4 (C-19) and 19.1 (C-20), from the methyl singlet at δ_H 2.11 (δ_C 19.1, H-20) to the carbons at δ_C 99.8 (C-18) and 159.4 (C-19).

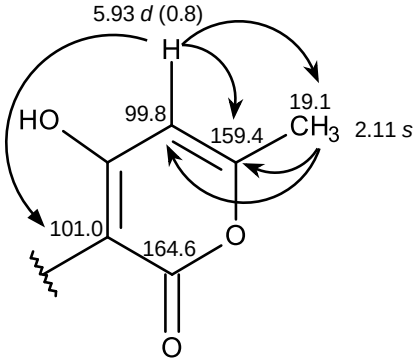

That the 6-methyl-2*H*-pyran-2-one was linked to the perhydrophenanthrene portion, was evidenced by the HMBC correlations from the doublets at δ_H 2.47, *d* (*J* = 14.2 Hz; δ_C 18.2, H-15a) and 2.30, *d* (*J* = 11.8 Hz; δ_C 18.2, H-15b) to the carbons at δ_C 148.2 (C-13), 101.0 (C-16), and 164.6 (C-21).

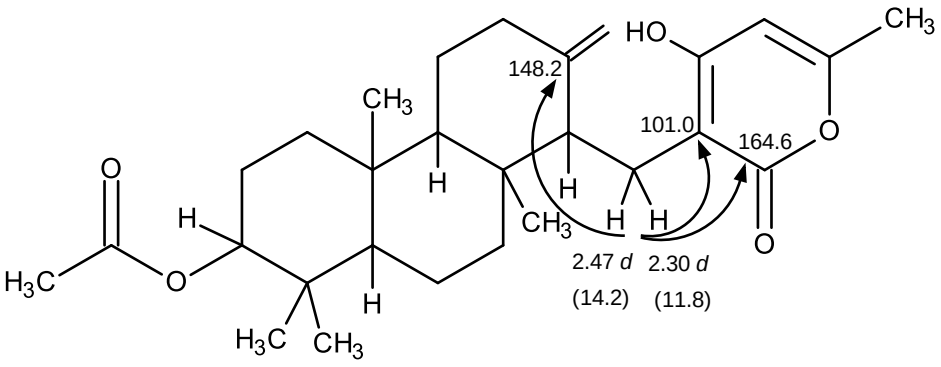

Therefore, the structure of **NTK 11** was established as aszonapyrone A (Figure 72). Aszonapyrone A was first isolated from *Aspergillus zonatus* IFO 8817 (Kimura *et al*., 1982a) and was later reported from the cultures of several soil fungi including *Neosartorya fischeri* KUFC 6344 (Eamvijarn *et al*., 2013), *Eurotium chevalieri* (Kanokmedhakul *et al*., 2011) and *Neosartorya tatenoi* KKU-2NK23 (Yim *et al*., 2014), as well as marine-derived fungi *Neosartorya Laciniosa* (Gomes *et al*., 2014).

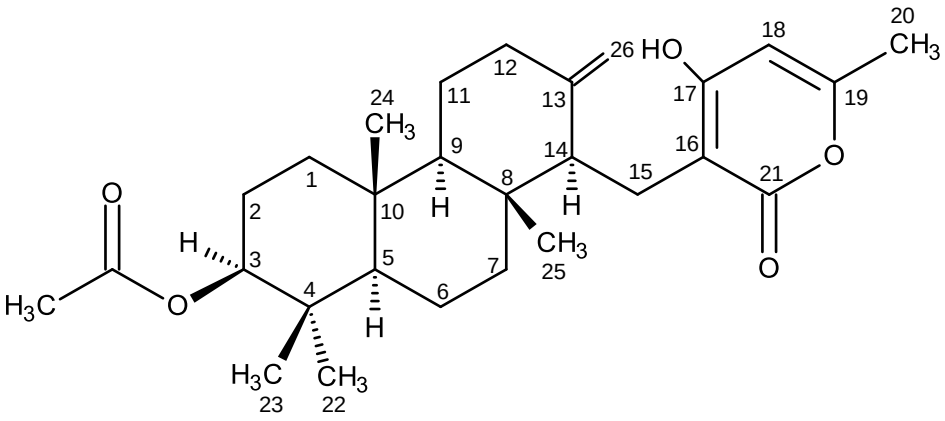

Figure 72. Structure of aszonapyrone A (**NTK 11**)

3.1.5.3. Sartorenol (NTK 12)

NTK 12 was isolated as white crystals (mp, 122-123 ºC) and its molecular formula $C_{27}H_{42}O_4$ was established on the basic of the (+)-HRESIMS *m/z* 431.3175 $[M+H]^+$ (calculated 431.3161), indicating seven degrees of unsaturation. The IR spectrum showed absorptions bands for hydroxyl (3393 cm^{-1}), conjugated ketone carbonyl (1645 cm^{-1}), ester carbonyl (1728 cm^{-1}), and olefin (1558, 1540 cm^{-1}) groups.

The ^{13}NMR, DEPTs and HSQC spectra (Table 11) displayed the signals of one conjugated ketone carbonyl (δ_C 194.7), one ester carbonyl (δ_C 171.0), two quaternary sp^2 (δ_C 147.7 and 191.1), one methine sp^2 (δ_C 99.9), one methylene sp^2 (δ_C 106.4), three quaternary sp^3 (δ_C 39.8, 37.8 and 37.4), one oxymethine sp^3 (δ_C 80.8), three methine sp^3 (δ_C 59.8, 56.4 and 55.4), eight methylene sp^3 (δ_C 40.5, 38.2, 38.0, 37.2, 23.6, 23.3, 19.6 and 18.7) and six methyl sp^3 (δ_C 28.0, 24.9, 21.3, 16.4, 16.3 and 15.3) carbons.

The ^{1}H NMR spectrum (Table 11) revealed the presence of, besides the hydrogen-bonded hydroxyl group of an enol at δ_H 15.47, *s*, two exocyclic methylene protons at δ_H 4.84, *brs*, 4.50, *brs*, one olefinic proton at δ_H 5.45, *s*, and the protons of six methyl group at 0.69, *s*, 0.83, *s*, 0.84, *s*, 0.86, *s*, 2.05, *s* (2 CH_3). The ^{1}H and ^{13}C NMR data of **NTK 12** revealed the presence of the 3-acetoxy-4, 4, 8, 10-tetramethylperhydrophenanthrene moiety similar to that of aszonapyrone A (**NTK 11**), however, there were no proton and carbon signals of the pyran-2-one portion but the signals of an olefinic proton of a trisubstituted double bond (δ_H 5.45, *s*) and enolic proton (δ_C 15.47, *s*) and a conjugated ketone carbonyl (δ_C 194.7).

Table 11. ^{1}H and ^{13}C NMR ($CDCl_3$, 300.13 and 75.47 MHz) and HMBC assignment for **NTK 12**

Position	δ_C, type	δ_H, (*J* in Hz)	COSY	HMBC
1	38.2, CH_2	1.05, *m*	H-2	-
2a	23.3, CH_2	1.65, *m*	H-1, 3	-
b		1.33, *dd* (12.9, 4.2)	H-1, 3	C-4
3	80.8, CH	4.48, *dd* (10.9, 4.6)	H-2	C-1, 4, 21, 22
4	37.8, C	-	-	-
5	55.4, CH	0.91, *dd* (12.0, 2.2)	H-6	-
6a	18.7, CH_2	1.62, *m*	H-5	-
b		1.14, *m*	-	-
7a	40.5, CH_2	1.18, *dd* (12.5, 3.6)	-	-
b		1.88, *m*	-	-
8	39.8, C	-	-	-
9	59.8, CH	1.02, *dd* (12.3, 2.6)	-	-
10	37.4, C	-	-	-
11	23.6, CH_2	1.70, *m*	-	-
12a	38.0, CH_2	2.38, *m*	-	-
b		1.92, *m*	-	C-14, 25
13	147.7, C	-	-	-
14	56.4, CH	1.59, *m*	H-15	-
15	19.6, CH_2	1.86, *m*	H-14, 16	C-13
16	37.2, CH_2	2.08, *m*	H-15	-
17	194.7, CO	-	-	-
18	99.9, CH	5.45, *s*	-	C-16, 17, 19, 20
19	191.1, C	-	-	-
20	24.9, CH_3	2.05, *s*	-	C-18, 19
21	16.3, CH_3	0.83, *s*	-	C-3, 4, 5, 22
22	28.0, CH_3	0.86, *s*	-	C-3, 4, 5, 21
23	16.4, CH_3	0.84, *s*	-	C-1, 5, 9, 10
24	15.3, CH_3	0.69, *s*	-	C-7, 8, 9, 14
25a	106.4, CH_2	4.84, *brs*	-	C-12, 14
b		4.50, *brs*	-	C-12, 13, 14
26	171.0, CO	-	-	-
27	21.3, CH_3	2.05, *s*	-	C-26
OH-19	-	15.47, *s*	-	-

The presence of the 3-acetoxy-4,4, 8, 10-tetramethyl perhydrophenanthrene moiety was supported by the HMBC cross peaks from the doublet doublet at δ_H 4.48 (*J* = 10.9, 4.6 Hz; δ_C 80.8) to the carbons at δ_C 38.2 (C-1), 37.8 (C-4), 16.3 (C-21) and 28.0 (C-22), from the methyl singlet of the acetoxy group at δ_H 2.05 (δ_C 21.3) to the carbonyl at δ_C 171.0, from the methyl singlet at δ_H 0.83 (δ_C 16.3, H-21) to the carbons at δ_C 80.8 (C-3), 37.8 (C-4), 55.4 (C-5) and 28.0 (C-22), from the methyl singlet at δ_H 0.86 (δ_C 28.0, H-22) to the carbons at δ_C 80.8 (C-3), 37.8 (C-4), 55.4 (C-5) and 16.3 (C-21), from the methyl singlet at δ_H 0.84 (δ_C 16.4, H-23) to the carbons at δ_C 38.2 (C-1), 55.4 (C-5), 59.8 (C-9) and 37.4 (C-10).

As well as, from the singlet at δ_H 0.69 (δ_C 15.3, H-24) to the carbons at δ_C 40.5 (C-7), 39.8 (C-8), 59.8 (C-9) and 56.4 (C-14). The position of the methylidene group on C-13 was confirmed by the HMBC correlations from the broad singlet at δ_H 4.84 (δ_C 106.4, H-25a) to the carbons at δ_C 38.0 (C-12) and 56.4 (C-14), from the broad singlet at δ_H 4.50 (δ_C 106.4, H-25b) to the carbons at δ_C 38.0 (C-12), 147.7 (C-13) and 56.4 (C-14). Like azsonapyrone A (**NTK 11**), the acetoxyl group on C-3 of **NTK 12** was beta due to the coupling constants of H-3 were 10.9 and 4.6 Hz.

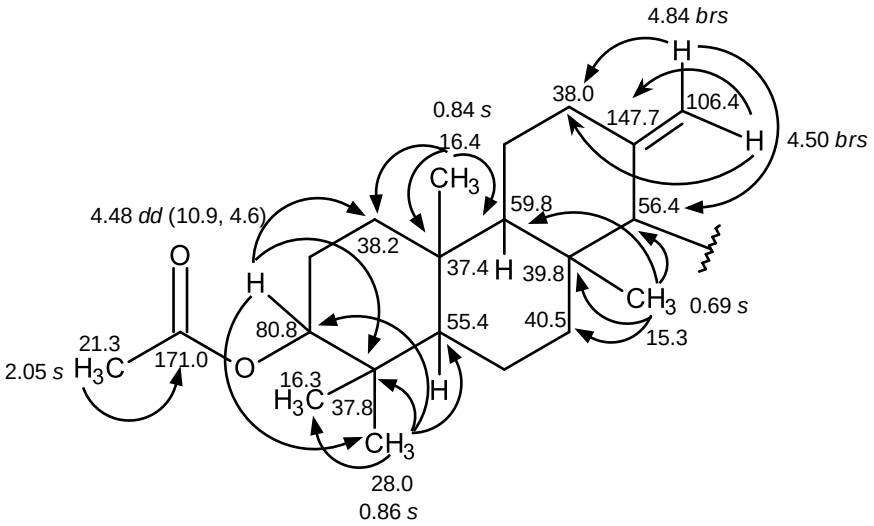

The presence of the (4*Z*)-5-hydroxy-3-oxohex-4-enyl group was substantiated by the COSY cross peaks between the multiplets at δ_H 2.08, *m* (δ_C 37.2, H-16) and δ_H 1.86, *m* (δ_C 19.6, H-15), as well as by the HMBC correlations from the olefinic proton at δ_H 5.45, *s* (δ_C 99.9, H-18) to the methylene carbon at δ_C 37.2 (C-16), the ketone carbon at δ_C 194.7 (C-17), the quaternary sp^2 carbon at δ_C 191.1 (C-19) and methyl carbon at δ_C 24.9 (C-20), from the methyl singlet at δ_H 2.05 (δ_C 24.9, H-20) to the methine sp^2 carbon at δ_C 99.9 (C-18) and the quaternary sp^2 carbon at δ_C 191.1 (C-19).

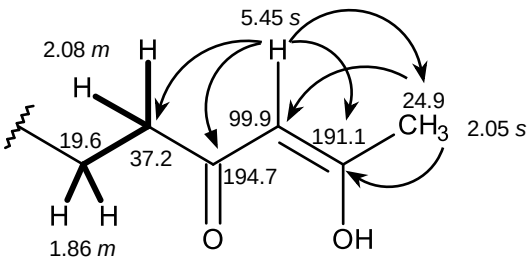

That the (4*Z*)-5-hydroxy-3-oxohex-4-enyl group was connected to the perhydrophenanthrene moiety through the methylene carbon at δ_C 19.6 (C-15) of the former and the methine carbon at δ_C 56.1 (C-14) of the latter was supported by the HMBC correlations from the methylene proton at δ_H 1.86, *m* (δ_C 19.6, H-15) to the quaternary sp^2 carbon at δ_C 147.7 (C-13). Therefore, the complete structure of **NTK 12** was:

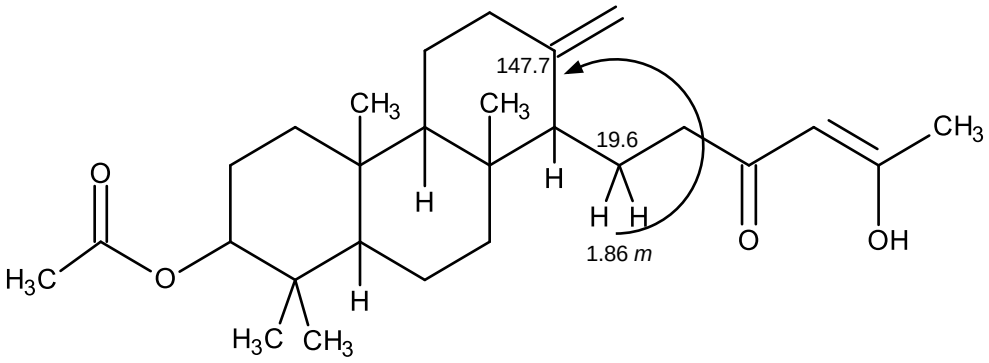

Since **NTK 12** was obtained as a suitable crystal the X-ray diffraction was performed to confirm the structure as well as to establish the absolute configurations of its stereogenic carbons. The ORTEP view showed in Figure 73 revealed that the absolute configurations of C-3, C-5, C-8, C-9, C-10 and C-14 are 3*S*, 5*R*, 8*R*, 9*R*, 10*R* and 14*S*.

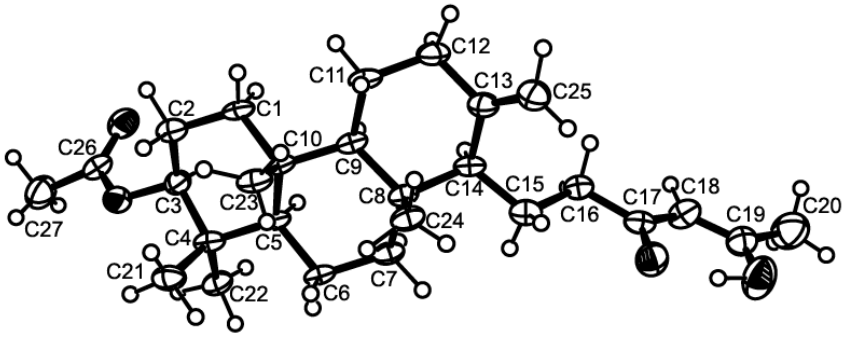

Figure 73. ORTEP view of **NTK 12**

Taking together with ^{1}H and ^{13}C NMR and X-ray data, the structure of **NTK 12** was established as:

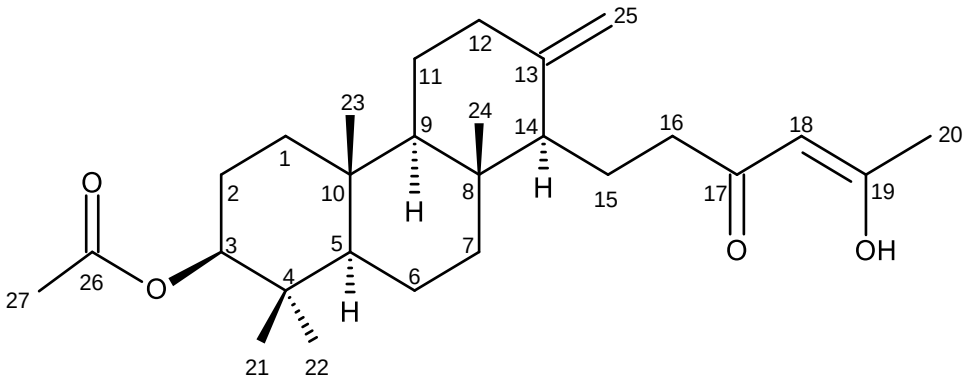

Literature search revealed that the structure of **NTK 12** has never been reported previously. Therefore we have named it sartorenol.

The biosynthesis pathway of sartorenol should resemble those proposed for aszonapyrone A and sartorypyone A, which is hypothesized as originating from a reaction of triketide derivative (**II**) with GPP oxide (**III**) to form the meroditerpene intermediate (**IV**). Cyclization, hydrolysis of the CoA ester and enolization of the side chain give the intermediate (**V**). Decarboxylation of the side chain and acetylation of

the hydroxyl group of the perhydrophenanthrene moiety would finally lead to the formation of sartorenol (Figure 74).

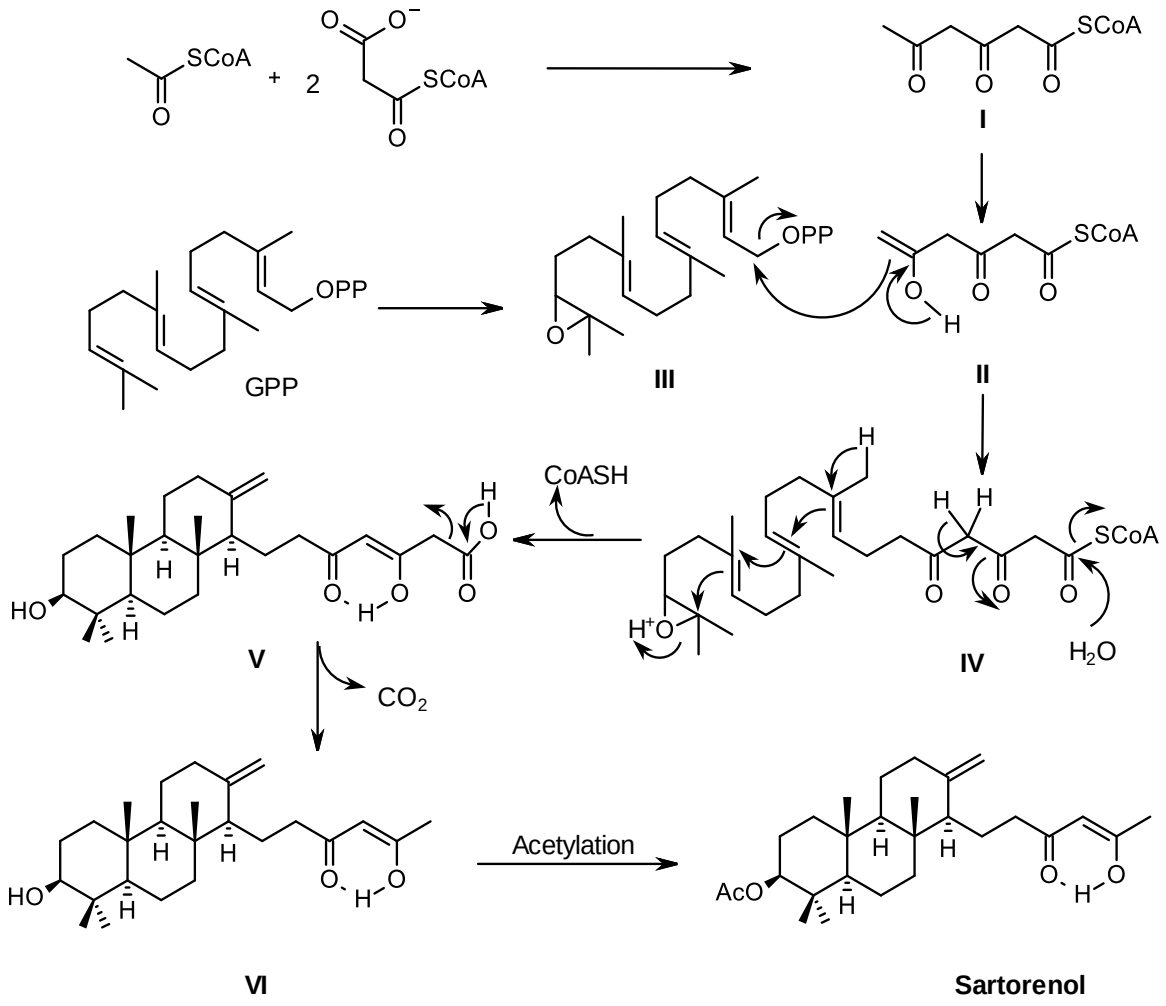

Figure 74. Proposed biogenesis of sartorenol (**NTK 12**)

3.1.6 Structure Elucidation of Isocoumarins

3.1.6.1. 6-hydroxymellein (NTK 1)

NTK 1 was isolated as white solid (mp, 201-202 ºC). The ^{13}C NMR, DEPTs and HSQC spectra (Table 12) displayed the signals of one conjugated ester carbonyl (δ_C 169.5), two oxyquaternary sp^2 (δ_C 163.4 and 164.5), two quaternary sp^2 (δ_C 100.1 and 142.3), two methine sp^2 (δ_C 106.8 and 100.9), one oxymethine sp^3 (δ_C 75.4), one methylene sp^3 (δ_C 33.8) and one methyl (δ_C 20.3) carbons.

The ^{1}H NMR spectrum, in combination with the HSQC spectrum (Table 12), revealed the signals of two *meta*-coupled aromatic protons at δ_H 6.24, *d* (*J* = 2.1 Hz; δ_C 106.8) and 6.19, *d* (*J* = 2.1 Hz; δ_C 100.9), a multiplet of the oxymethine proton at δ_H 4.59, two geminally coupled methylene protons at δ_H 2.93, *dd* (*J* = 16.6, 3.5 Hz; δ_C 33.8) and 2.80, *dd* (*J* = 16.6, 11.1 Hz; δ_C 33.8), one methyl (3H) at δ_H 1.39, *d* (*J* = 6.3 Hz; δ_C 20.3), a singlet of a hydrogen-bonding phenolic hydroxyl proton δ_H 11.13 and a broad singlet of the phenolic hydroxyl proton at δ_H 10.64.

Table 12. ^{1}H and ^{13}C NMR (DMSO, 300.13 and 75.47 MHz) and HMBC assignment for **NTK 1**

Position	δ_C, type	δ_H, (*J* in Hz)	COSY	HMBC
1	169.5, CO	-	-	-
3	75.4, CH	4.59, *m*	H-3, 4	-
4α	33.8, CH_2	2.80, *dd* (16.6, 11.1)	-	C-3
β		2.93, *dd* (16.6, 3.5)	-	C-3, 5, 4, 8a
4a	142.3, C	-	-	-
5	106.8, CH	6.24, *d* (2.1)	H-7	C-6, 7, 8a
6	164.5, C	-	-	-
7	100.9, CH	6.19, *d* (2.1)	H-5	C-5, 6, 8, 8a
8	163.4, C	-	-	-
8a	100.1, C	-	-	-
CH_3-3	20.3, CH_3	1.39, *d* (6.3)	-	C-3, 4
OH-6	-	10.64, *brs*	-	-
OH-8	-	11.13, *s*	-	C-7, 8

The presence of the 6, 8-dihydroxy tetrasubstituted benzene ring was supported by the COSY correlation from the doublet at δ_H 6.19 (*J* = 2.1 Hz, H-7) to the doublet at δ_H 6.24 (*J* = 2.1 Hz, H-5) as well as by the HMBC correlation from the doublet at δ_H 6.24 (*J* = 2.1 Hz; δ_C 106.8, H-5) to the quaternary sp^2 carbon at δ_C 164.5 (C-6), 100.1 (C-8a) and methine sp^2 carbon at δ_C 100.9 (C-7), from the doublet at δ_H 6.19 (*J* = 2.1 Hz; δ_C 100.9, H-7) to C-5, C-6, C-8 (δ_C 163.4) and C-8a, from a singlet at δ_H 11.13 (H-8) to C-7 and C-8.

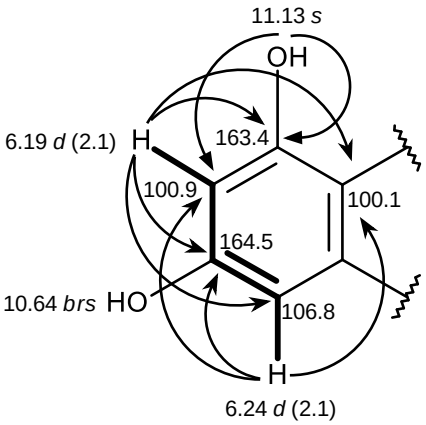

The presence of the 6-methyl-3, 4, 6-trisubstituted pyran-2-one moiety was evidenced by the COSY correlations from the multiplet at δ_H 4.59 (H-3) to the methyl doublet at δ_H 1.39 (*J* = 6.3 Hz; δ_C 20.3), 2.80, *dd* (*J* = 16.6, 11.1 Hz, H-4) and δ_H 2.93, *dd* (*J* = 16.6, 3.5 Hz, H-4) as well as by the HMBC correlations from the methyl doublet at δ_H 1.39 (*J* = 6.3 Hz) to the carbons at δ_C 75.4 (C-3) and 33.8 (C-4), from the doublet doublet at δ_H 2.80 (*J* = 16.6, 11.1 Hz; δ_C 33.8, H-4) to the methyl carbon at δ_C 20.3, and from the doublet doublet at δ_H 2.93 (*J* = 16.6, 3.5 Hz; δ_C 33.8, H-4) to C-3 and C-4.

That the 6, 8-dihydroxy tetrasubstituted benzene ring, was fused to the 6-methylpyran-2-one ring through C-4a and C-8a was confirmed by the HMBC correlations from H-4 to C-4a, C-5 and C-8a. Therefore the planar structure of **NTK 1** was elucidated as 6, 8-dihydroxy-3-methyl-3, 4-dihydro-1*H*-isochromen-1-one.

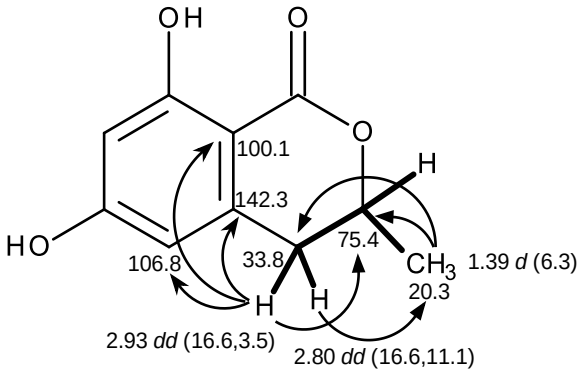

Since the optical rotation of **NTK 1** was ($[\alpha]_D^{26}$ = – 51), its structure was established as 6-hydroxymellein (Figure 75), a secondary metabolites previously reported from the *Ceratocystis minor* which was associated with blue stain disease of pine (Ayer *et al*., 1987). This compound was also reported from an inhibitor of pollen development in *Arabidopsis thaliana*, isolated from the fungus *Aspergillus terreus* (Shimada *et al*., 2002), as well as from the scale insect pathogenic fungus *Torrubiella tenuis* BCC 12732 (Kornsakulkarn *et al*., 2009).

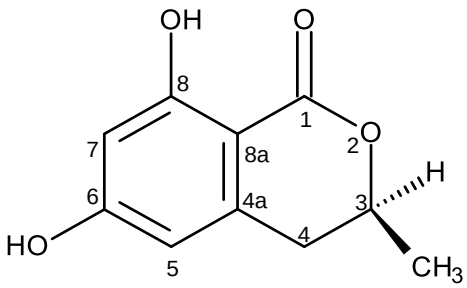

Figure 75. Structure of 6-hydroxymellein (**NTK 1**)

3.1.6.2. 6, 8-Dihydroxy-3-(2*R*-hydroxypropyl)-7-methyl-1*H*-isochromen-1-one (EC 11)

EC 11 was isolated as yellow viscous liquid and its molecular formula $C_{13}H_{14}O_5$ was determined based on the (+)-HRESIMS *m/z* 251.0900 $[M+H]^+$ (calculated 251.0919), indicating seven degrees of unsaturation. The IR spectrum showed absorption bands for hydroxyl (3443 cm^{-1}), a conjugated ester carbonyl (1671 cm^{-1}), aromatic (1540, 1507 cm^{-1}) and olefin (1623 cm^{-1}) groups.

The ^{13}C NMR spectrum (Table 13) exhibited thirteen carbon signals which can be categorized, according to DEPTs and HSQC spectra, into one conjugated ester carbonyl (δ_C 166.2), six quaternary sp^2 (δ_C 163.6, 159.9, 154.5, 136.4, 109.7 and 97.8), three of which are oxygen bearing, two methine sp^2 (δ_C 105.3 and 101.5), one oxygen bearing methine sp^3 (δ_C 64.0), one methylene sp^3 (δ_C 42.6), and two methyl (δ_C 23.4 and 8.0) groups.

The ^1H NMR spectrum revealed the presence of two phenolic hydroxyl groups (δ_H 11.31, *s* and 10.83, *brs*), one of which is hydrogen-bonded (δ_H 11.31, *s*), one aromatic (δ_H 6.44, *s*; δ_C 101.5), one olefinic (δ_H 6.48, *s*; δ_C 105.3), one secondary hydroxyl (δ_H 4.80, *d*, *J* = 4.5 Hz), one oxygen-bearing methine multiplet (δ_H 3.98; δ_C 64.0), one methylene multiplet (δ_H 2.52; δ_C 42.6), one tertiary methyl (δ_H 2.01, *s*; δ_C 8.0) and one secondary methyl (δ_H 1.13, *d*, *J* = 6.2 Hz; δ_C 23.4) group.

Table 13. ^{1}H and ^{13}C NMR (DMSO, 300.13 and 75.47 MHz) and HMBC assignment for **EC 11**

Position	δ_C, type	δ_H, (*J* in Hz)	COSY	HMBC
1	166.2, CO	-	-	-
3	154.5, C	-	-	-
4	105.3, CH	6.48, *s*	-	C-3, 5, 8a, 1′
4a	136.4, C	-	-	-
5	101.5, CH	6.44, *s*	-	C-4, 6, 7, 8a
6	163.6, C	-	-	-
7	109.7, C	-	-	-
8	159.9, C	-	-	-
8a	97.8, C	-	-	-
9	8.0, CH_3	2.01, *s*	-	C-6, 7, 8
1′	42.6, CH_2	2.52, *m*	-	C-3, 4, 2′
2′	64.0, CH	3.98, *m*	OH-2′, H-3′	-
3′	23.4, CH_3	1.13, *d* (6.2)	H-2′	C-1′, 2′
OH-2′	-	4.80, *d* (4.5)	H-2′	C-1′, 2′, 3′
OH-6	-	10.83, *brs*	-	C-6, 7
OH-8	-	11.31, *s*	-	C-7, 8, 8a

That **EC 11** was a 6, 8-dihydroxy-7-methyl isochromone derivative was corroborated by HMBC correlations from the hydrogen-bonded phenolic hydroxyl at δ_H 11.31, *s* (OH-8) to the aromatic carbons at δ_C 109.7 (C-7), 159.9 (C-8) and 97.8 (C-8a), from the tertiary methyl singlet at δ_H 2.01 (CH_3-9) to C-7, C-8 and C-6 (δ_C 163.6), from the singlet at δ_H 6.44 (H-5) to C-6, C-7, C-8a and C-4 (δ_C 105.3), and from the singlet at δ_H 6.48 (H-4) to C-3 (δ_C154.5), C-5 (δ_C101.5) and C-8a.

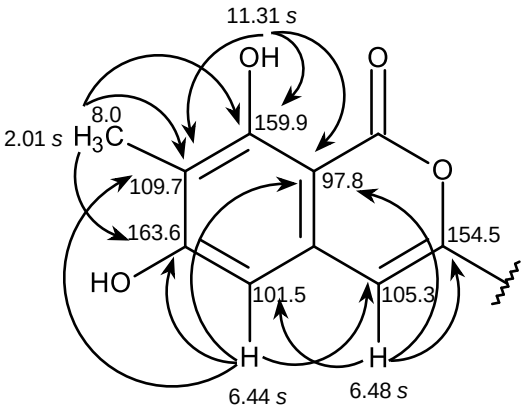

The presence of the 2-hydroxypropyl moiety was substantiated by COSY correlations from the methylene multiplet at δ_H 2.52 (H_2-1′) to the hydroxymethine multiplet at δ_H 3.98 (H-2′), from the secondary methyl doublet at δ_H 1.13 (*J* = 6.2 Hz, H_3-3′) to H-2′, as well as by the HMBC correlations from the hydroxyl doublet at δ_H 4.80, *d* (*J* = 4.5 Hz, OH-2′) to C-1′ (δ_C 42.6), C-2′ (δ_C 64.0), CH_3-3′ (δ_C 23.4), from H_3-3′ to C-1′ and C-2′, from H-1′ to C-2′. That the 2-hydroxypropyl substituent was on C-3 of the isochromone nucleus was supported by the HMBC correlations from H-4 to C-1′, as well as from H-1′ to C-3 and C-4.

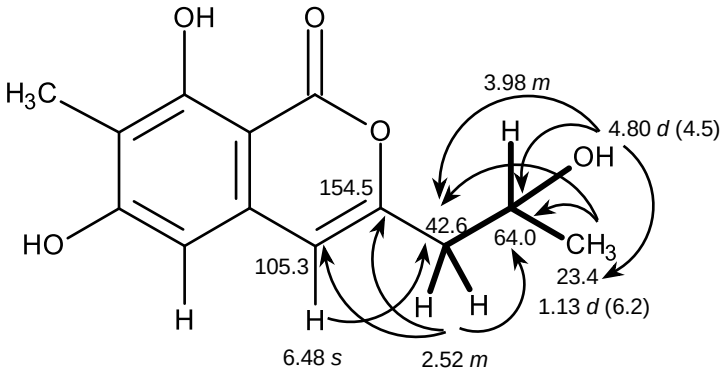

Therefore, the structure of **EC 11** was established as 6, 8-dihydroxy-3-(2-hydroxypropyl)-7-methyl-1*H*-isochromen-1-one.

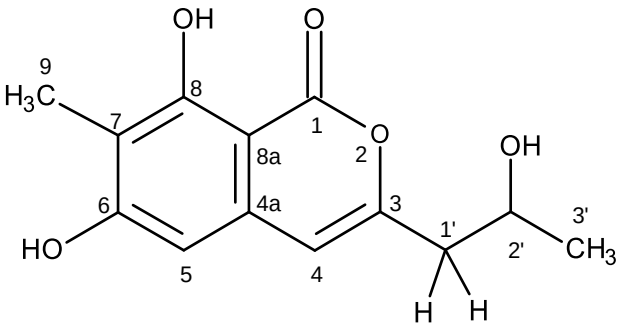

Since compound **EC 11** could not be obtained as a suitable crystal, the stereochemistry of the stereogenic carbon (C-2′) could not be established by X-ray crystallographic analysis. Therefore, comparison of the calculated and experimental ECD spectra was used to determine the absolute configuration of C-2′ of **EC 11**. Conformational analysis of **EC 11** by dihedral driver search and MM2 minimization resulted in eighteen main conformations, and the most populated conformation is represented in Figure 76. The other seventeen conformations resulted from rotating the C-3′/C-2′ bond by 180 degrees steps, the C-1′/C-2′ by 120 degrees steps and the C-2′/OH also by 120 degrees steps. Each was energetically optimized in Gaussian software using APFD/6-311+G (2d, p) model chemistry and IEFPCM model of solvation for methanol. The Gibbs energies thereby obtained were used to determine the populations of each conformation by Boltzmann weighing of the energies at 298 K (Mori *et al*., 2006). The electronic circular dichroism (ECD) transitions for each conformation were calculated also in Gaussian using the same

model chemistry as the energy minimization but with the time-dependent (TD) method. Line broadening was performed for the 18 sets of transitions and a weighted sum enabled to obtain the calculated spectrum in Figure 77. As can be seen, the experimentally obtained ECD spectrum, with negative Cotton effects (217 nm, $\Delta\varepsilon$ = – 2.3 M^{-1} cm^{-1}), also in Figure 77, fits well the calculated spectrum. Therefore, it was concluded that the absolute configuration of C-2′ is 2′*S* and the structure of **EC 11** was establish as 6,8-dihydroxy-3-(2*R*-hydroxypropyl)-7-methyl-1*H*-isochromen-1-one. To the best of our knowledge, **EC 11** is a new natural product.

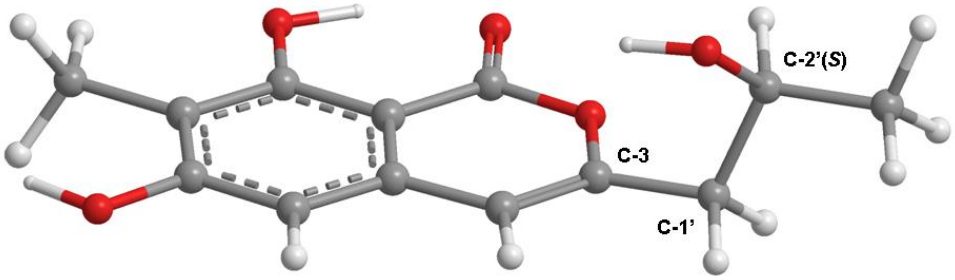

Figure 76. Most stable conformation of **EC 11** (C-2′*S*), representing a fraction of around 35% of all the 18 conformations considered. The next most stable conformation represents a fraction of around 13% of all conformations and is obtained by rotating the hydroxyl group in C-2′ 120 degrees towards the viewer. In this visualization, the carbonyl group points away from the viewer and the rings are viewed diagonally from above.

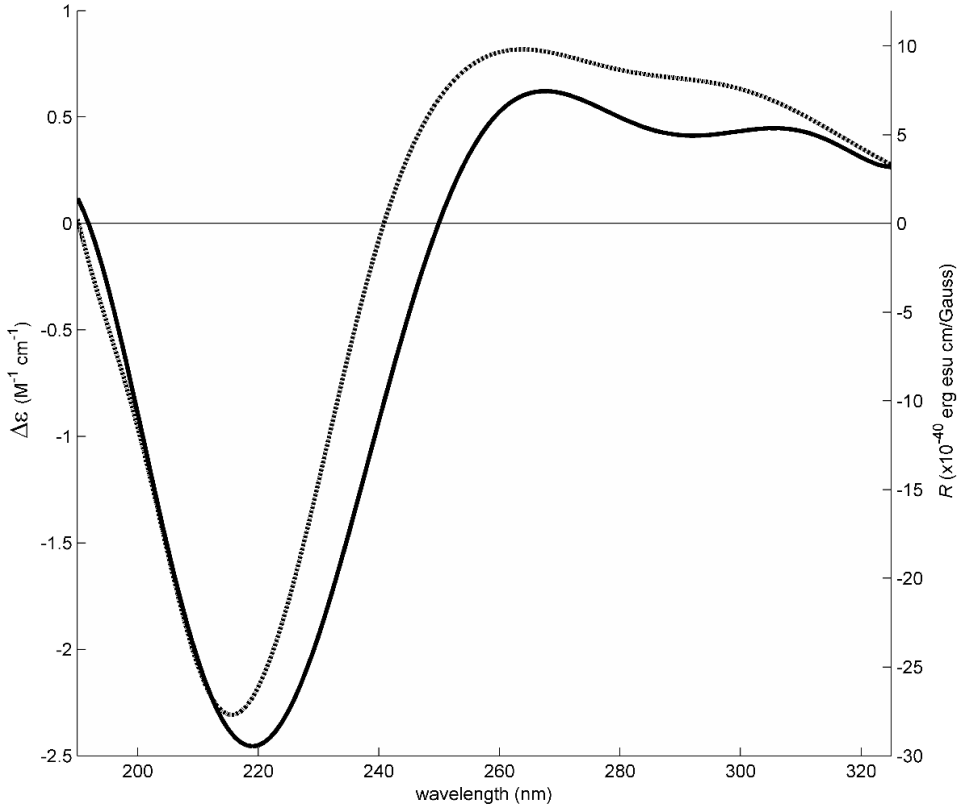

Figure 77. Experimental (solid) and simulated (dotted) ECD spectra of **EC 11** (C-2′*S*) in methanol. The calculated spectral line results from the Boltzmann weighing of rotatory strengths of all 18 conformations of the compound with a gaussian line broadening of 0.3 eV. The experimental data exhibit a negative, deep minimum at 217 nm ($\Delta\varepsilon$ = – 2.3 M^{-1} cm^{-1}) and two smaller positive maxima at 260 nm ($\Delta\varepsilon$ = 0.8 M^{-1} cm^{-1}) and 295 nm ($\Delta\varepsilon$ = 0.7 M^{-1} cm^{-1}) that are well matched by the calculated data.

Therefore, the structure of **EC 11** was established as 6, 8-dihydroxy-3-(2*R*-hydroxypropyl)-7-methyl-1*H*-isochromen-1-one (Figure 78). To the best of our knowledge, **EC 11** has never been reported previously. Therefore, it is a new compound.

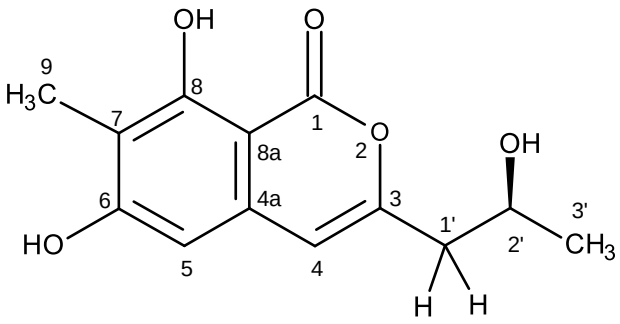

Figure 78. Structure of 6, 8-dihydroxy-3-(2*R*-hydroxypropyl)-7-methyl-1*H*-isochromen-1-one (**EC 11**)

From a biosynthetic point of view, the structure of **EC 11** can be hypothesized to derive from the acetate pathway, which is summarized in Figure 79. Condensation of acetyl CoA (**I**) with five units of malonyl CoA (**II**) gives a hexaketide intermediate (**III**) which, after cyclization and methylation (by SAM), forms an intermediate **IV**. Enolization of **IV** leads to a formation of an isochromone (**V**) which, after stereospecific reduction of the ketone function in the side chain, gives rise to **EC 11**.

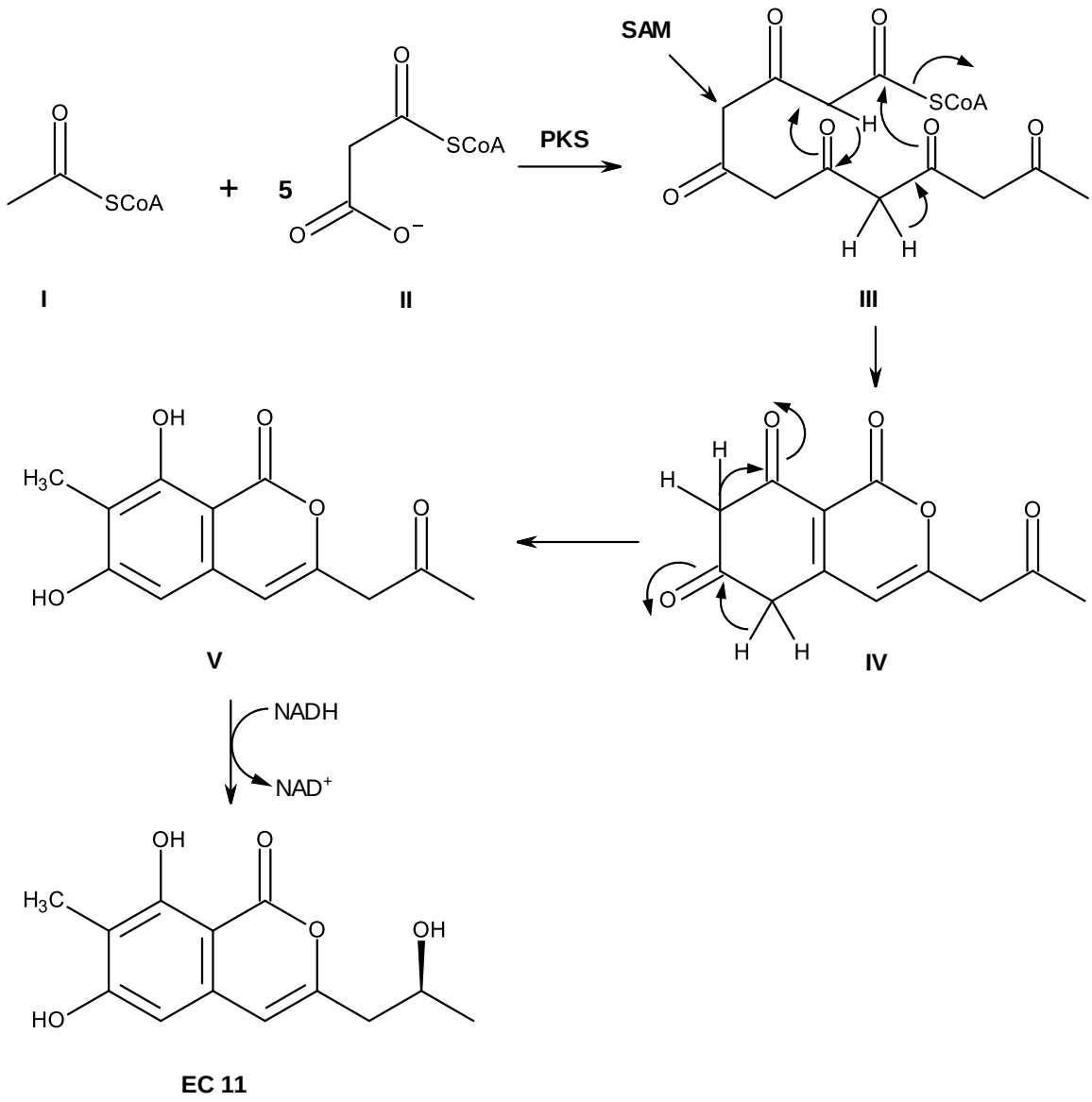

Figure 79. Proposed biogenesis of **EC 11**

3.1.7 Structure Elucidation of Anthraquinones

3.1.7.1. Emodin (EC 3)

EC 3 was isolated as a yellow amorphous solid (mp, 256-257 ºC), its molecular formula $C_{15}H_{10}O_5$ was established on the basis of the (+)-HRESIMS *m/z* 271.0594 $[M+H]^+$ (calculated 271.0606), indicating eleven degrees of unsaturation. The ^{13}C NMR spectrum (Table 14) displayed only thirteen carbon signals which, together with DEPTs and HSQC spectra, were classified as two conjugated ketone carbonyls (δ_C 181.6 and 189.7), six quaternary sp^2 (δ_C 164.6, 161.4, 147.9, 134.9, 132.8 and 113.4), four methine sp^2 (δ_C 124.0, 120.3, 109.7 and 108.1) and one methyl (δ_C 21.5) groups.

The ^1H NMR spectrum (Table 15), together with the COSY spectrum, exhibited two singlets of the aromatic protons at δ_H 7.12 and δ_H 7.44, two doublets of the *meta*-coupled aromatic protons at δ_H 6.51 (*J* = 2.2 Hz) and 7.06 (*J* = 2.2 Hz), in addition to a broad signal of two phenolic hydroxyl protons at δ_H 12.08 and a methyl singlet at δ_H 2.39.

The presence of the aromatic protons/carbons, phenolic hydroxyl groups and the conjugated carbonyl carbons at δ_C 189.7 and 181.6, suggested the existence of the 1, 8-dihydroxyanthraquinone nucleus. This was supported by the HMBC correlations of the singlet at δ_H 7.44 (H-4) and δ_H 7.06, *d* (*J* = 2.2 Hz, H-5) to the carbonyl carbon at δ_C 181.6 (C-10). The methyl group was placed on C-3 was

confirmed by the HMBC correlations from H-2 (7.12, *s*) and H-4 to the methyl carbon at δ_C 21.5 (CH_3-11) as well as from the singlet at δ_H 2.39 (CH_3-11) to the carbons at δ_C 120.3 (C-4) and δ_C124.0 (C-2). That another benzene ring has the hydroxyl group on C-5 and C-7 was supported by the presence of the low frequency aromatic proton at 6.51, *d* (*J* = 2.2 Hz, H-7) and the higher frequency aromatic proton H-5, as well as by the HMBC correlation from H-7 to the oxyquaternary sp^2 carbon at δ_C 164.6 (C-6) and methine sp^2 carbon at δ_C 109.7 (C-5).

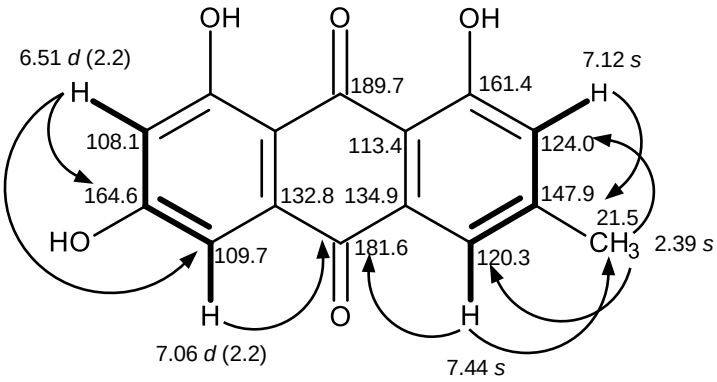

The molecular formula and the ^1H and ^{13}C NMR data of **EC 3** was in agreement with emodin. Emodin has been previously reported from several sources, including from the plant *Rhamnus triquerta* wall (Goel *et al*., 1991), Chinese medicinal plant *Polygonum cuspidatum* (Polygonaceae) (Jayasuriya *et al*., 1992), *Cassia obtusifolia* (Leguminosae) seeds (Yang *et al*., 2003), and marine lichen-derived fungus *Gliocladium sp*. T31 (Ren *et al*., 2006), an endophytic fungus *Aspergillus versicolor*, was isolated from the inner tissue of Red sea green alga *Halimeda opuntia* (Hawas *et al*., 2012), marine-derived fungus *Monodictys sp*., from

the sea urchin *Anthocidaris crassispina,* collected in Toyama Bay in the Sea of Japan (El-Beih *et al*., 2007), an endophytic fungus *Eurotium rubrum*, isolated from the inner tissue of semi-mangrove plant (Yan *et al*., 2012) and marine gorgonian coral-associated fungus *Penicillium sp*. SCSGAF 0023 (Bao *et al*., 2013).

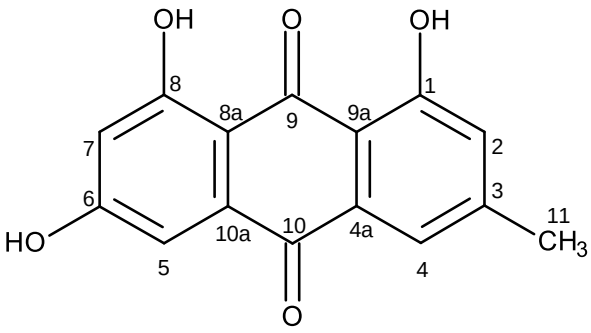

Figure 80. Structure of emodin (**EC 3**)

3.1.7.2. Physcion (EC 4)

EC 4 was isolated as red crystals (mp, 207-208 ºC). The general features of the ^{1}H and ^{13}C NMR spectra of **EC 4** resemble those of **EC 3**, except for the presence of the proton and carbon signals of methoxyl group in the ^{1}H and ^{13}C NMR spectra of **EC 4**.

The ^{13}C NMR spectrum (Table 14) displayed sixteen carbon signals which were classified, based on DEPTs and HSQC spectra, as two ketone carbonyls (δ_C 190.8 and 182.0), three oxygenated quaternary sp^2 carbon (δ_C 166.5, 165.2 and

162.5), five quaternary sp^2 (δ_C 148.5, 135.2, 133.2, 113.7 and 110.2), four methine sp^2 (δ_C 124.5, 121.3, 108.2 and 106.8), one methoxy (δ_C 56.1) and one methyl (δ_C 22.2) carbons.

The ^{1}H NMR spectrum (Table 15), together with COSY spectrum, showed two pairs of *meta*-coupled aromatic protons at δ_H 7.62, *dd* (*J* = 1.4, 0.4 Hz)/ 7.08, *dd* (*J* = 1.6, 0.8 Hz) and δ_H 7.36, *d* (*J* = 2.6 Hz)/ 6.68, *d* (*J* = 2.6 Hz), a singlet of methoxy protons at δ_H 3.94, a singlet of methyl protons at δ_H 2.45 and two singlets of the hydrogen-bonded phenolic hydroxyl protons at δ_H 12.31 and 12.11. That the hydroxyl group was on C-1 and the methyl group was on C-3, in emodin, was confirmed by the COSY correlations from the doublet doublet at δ_H 7.08 (*J* = 1.6, 0.8 Hz, H-2) to the doublet doublet at δ_H 7.62 (*J* = 1.4, 0.4 Hz, H-4), as well as by the HMBC correlations from H-2 to the carbons at δ_C 162.5 (C-1), 121.3 (C-4), quaternary carbon at δ_C 113.7 (C-9a), from H-4 to C-9a and to the carbons at δ_C 124.5 (C-2) and 182.0 (C-10), from the methyl singlet at δ_H 2.45 (δ_C 22.2, H_3-11) to C-2 and C-4 and quaternary carbon at δ_C 148.5 (C-3), from the singlet of hydrogen-bonded hydroxyl proton at δ_H 12.11 (OH-1) to C-1, C-2 and C-9a. That the hydroxyl group was on C-8 and the methoxyl group was on C-6 was confirmed by the HMBC correlations from another hydrogen-bonded hydroxyl singlet at δ_H 12.31 to the carbons at δ_C 165.2 (C-8), 110.2 (C-8a) and 106.8 (C-7) as well as from the singlet of the methoxyl protons at δ_H 3.94 to the carbon at δ_C 166.5.

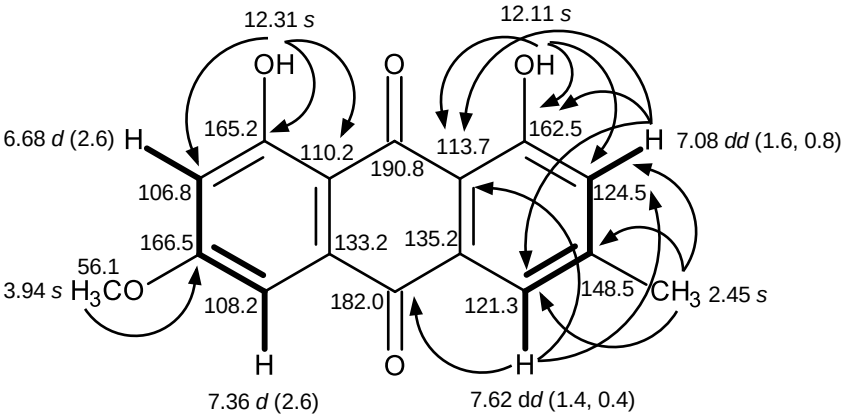

Consequently, the structure of **EC 4** was established as physcion (Figure 81). Physcion has been previously reported from the culture of several fungi including three species of the Lichen genus *Xanthoria* (*X. fallax*, *X. elegans*, *X. policarpa*) (Manojlovic *et al*., 2000), the halotolerant fungus *Aspergillus variecolor* B-17, isolated from the sediments (Wang *et al*., 2007b), *Aspergillus glaucus,* was obtained from marine sediment surrounding mangrove roots (Du *et al*., 2008), *Aspergillus terreus,* isolated as an epiphyte from a soft coral *Sinulariakavarattiensis* (Parvatkar *et al*., 2009), marine sponge-associated fungus *Eurotium cristatum* (Gomes *et al*., 2012) and marine-derived fungus *Microsporum sp*., was isolated from the surface of a marine red alga *Lomentaria catenata* (Wijesekara *et al*., 2014).

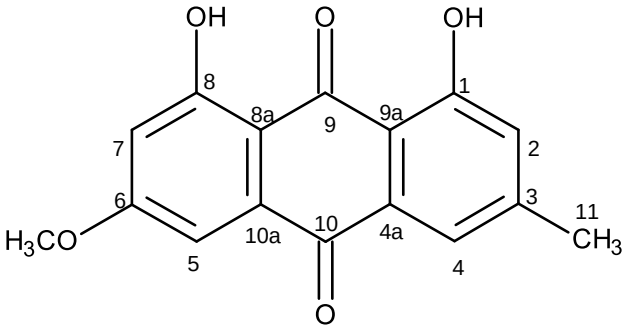

Figure 81. Structure of physcion (**EC 4**)

3.1.7.3. Questin (EC 5)

EC 5 was isolated as a yellow solid (mp 298-299 ºC). The ^{1}H and ^{13}C NMR spectra of **EC 5** were similar to those of **EC 4**. The ^{13}C NMR spectrum (Table 14) showed fifteen carbon signals which were categorized, based on DEPTs and HSQC spectra, as two conjugated ketone carbonyls (δ_C 185.9 and 182.6), two oxygen bearing quaternary sp^2 (δ_C 163.6 and 161.7), five quaternary sp^2 (δ_C 146.3, 136.7, 132.1, 114.5 and 112.5), four methine sp^2 (δ_C 124.1, 118.9, 108.0 and 105.4), one methoxy (δ_C 56.1) and one methyl (δ_C 21.4) groups. The ^{1}H NMR spectrum (Table 15), together with the COSY spectrum, displayed two pairs of *meta*-coupled aromatic protons at δ_H 7.40, *d* (*J* = 1.2 Hz)/ 7.10, *brs* and 7.15, *d* (*J* = 2.0 Hz)/ 6.79, *d* (*J* = 2.1 Hz), one methoxy singlet at δ_H 3.87, a methyl singlet at δ_H 2.38 and a singlet of a hydrogen-bonded hydroxyl proton at δ_H 13.39.

Like **EC 4**, the existence of 1-hydroxy-3-methylpenyl moiety was corroborated by the COSY correlations from the methyl singlet at δ_H 2.38 to a broad singlet at δ_H 7.10 (H-2) and a doublet at 7.40 (*J* = 1.2 Hz, H-4), as well as by the HMBC correlation of H-2 to the carbons at δ_C 161.7 (C-1), 114.5 (C-9a), 118.9 (C-4) and the methyl carbon at δ_C 21.4 (C-3), from H-4 to the carbons at δ_C 124.1 (C-2), (C-9a), the methyl carbon at δ_C 21.4 (C-3) and the ketone carbonyl carbon at δ_C 182.6 (C-10), from the methyl singlet at δ_H 2.38 (δ_C 21.4) to C-2, C-4 and the quaternary sp^2 carbon at δ_C 146.3 (C-3).

Contrary to **EC 4** (physcion), the methoxyl group was on C-8 as was confirmed by the HMBC correlations from the doublet at δ_H 7.15 (*J* = 2.0 Hz; δ_C 108.0, H-5) to the quaternary carbon at δ_C 112.5 (C-8a) and the ketone carbonyl at δ_C 182.6 (C-10), from the doublet at δ_H 6.79 (*J* = 2.1 Hz; δ_C 105.4, H-7) to the quaternary carbons at δ_C 163.6 (C-8) and 112.5 (C-8a).

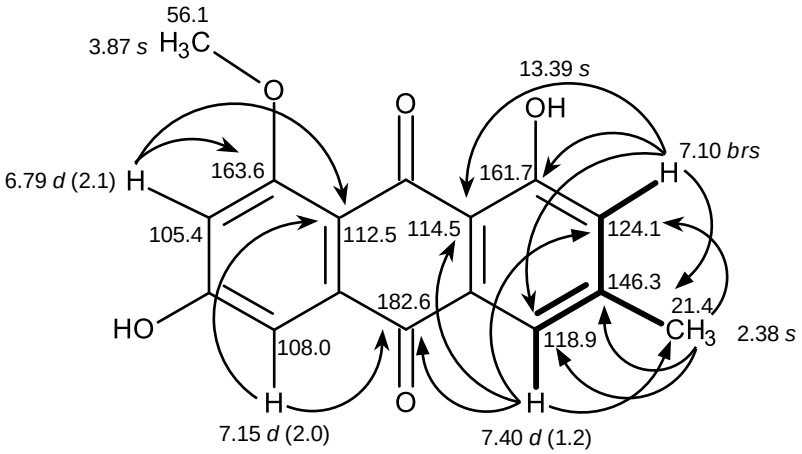

Therefore, the structure of **EC 5** was established as 1, 6-dihydroxy-8-methoxy-3-methyl anthracene-9, 10-dione, commonly known as questin (Figure 82). Questin was previously isolated from several fungal species including the fungus *Penicillium frequentans* Westling (Mahmoodian and Stickings, 1964), marine-derived fungus *Aspergillus sp*. B-F-2 (Liu *et al*., 2006), the halotolerant fungus *Aspergillus variecolor* B-17, was isolated from the sediments (Wang *et al*., 2007b) and mangrove-derived endophytic fungus *Eurotium rubrum* (Li *et al*., 2009).

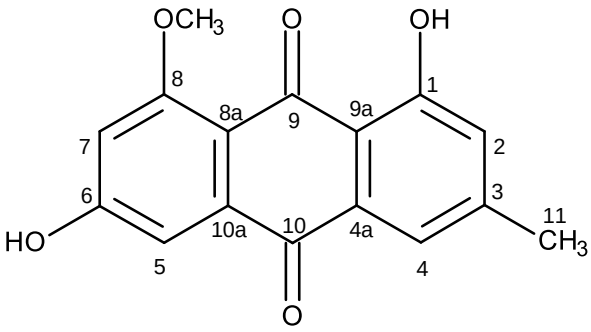

Figure 82. Structure of questin (**EC 5**)

3.1.7.4. Questinol (EC 6)

EC 6 was isolated as yellow crystals (mp 281-282 ºC), its molecular formula $C_{16}H_{12}O_{6,}$ was established on the basis of the (+)-HRESIMS *m/z* 301.0713 $[M+H]^+$ (calculated 301.0712), indicating eleven degrees of unsaturation. The ^{1}H and ^{13}C NMR spectra of **EC 6** resembled those of **EC 5**.

The ^{13}C NMR spectrum (Table 14) showed only fourteen carbon signals and in conjunction with DEPTs and HSQC spectra, they were classified as two ketone conjugated carbonyls (δ_C 185.8 and 182.8), six quaternary sp^2 (δ_C 163.8, 161.8, 150.9, 136.6, 132.3 and 115.3), four methine sp^2 (δ_C 120.8, 115.6, 107.2 and 105.8), one hydroxymethyl (δ_C 62.1) and one methoxy (δ_C 56.1) carbons.

The ^{1}H NMR (Table 15), in combination with HSQC spectrum, exhibited four singlets of the aromatic protons at δ_H 7.55, 7.18, 7.14 and 6.78, a singlet of hydroxymethylene protons (2H) at δ_H 4.57, a methoxy singlet at δ_H 3.86, in addition to a singlet of the hydrogen-bonded hydroxyl proton at δ_H 13.54 and a hydroxyl proton at δ_H 8.30, *d* (*J* = 4.4 Hz).

The COSY spectrum revealed cross peaks from the singlet at δ_H 7.55 (H-4) to the singlet at δ_H 7.18 (H-2) and the singlet at δ_H 4.57 (H_2-11), from H-2 to H-4 and H-11, suggesting that the methyl group on C-3 in **EC 5** (questin) was replaced by a hydroxymethyl group in **EC 6**. This was supported by the HMBC correlations from H-4 to the carbons at δ_C 120.8 (C-2) and 115.3 (C-9a), as well as from H_2-11 to C-2 and C-4 and the quaternary carbon at δ_C 150.9 (C-3). Like **EC 5** (questin), the hydroxyl and methoxyl groups were on C-6 and C-8 of another benzene ring of **EC 6** was supported by COSY correlations between the broad singlets at δ_H 7.14 (H-5) and δ_H 6.78 (H-7) as well as by HMBC correlations from the singlet of methoxy proton at δ_H 3.86 (δ_C 56.1, OCH_3-8) to the quaternary carbon at δ_C 163.8 (C-8).

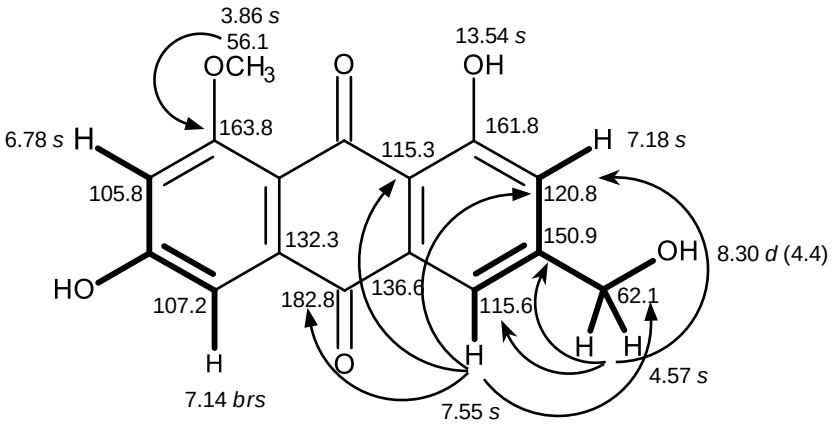

The ^{1}H and ^{13}C NMR data, in conjunction with the molecular formula, of **EC 6** allowed to establish the structure of **EC 6** as questinol. Questinol has been previously isolated from several fungi, including an endophytic fungus *Penicillium glabrum*, was isolated from pomegranate fruits (*Punica granatum*) (Hammerschmidt *et al*., 2012), filamentous fungus *Eurotium herbariorum* NU-2 from Karebushi (a katsuobushi), marine-derived fungus *Eurotium amstelodami* (Yang *et al*., 2014), an endophytic fungus isolated from *Catharanthus roseus*, was collected from the river banks of Amassoma in Southern Nigeira (Akpotu *et al*., 2017), crinoid-derived fungus *Aspergillus ruber* 1017 (Li *et al*., 2017) and marine sponge-associated fungus *Talaromyces stipitatus* KUFA 0207 (Noinart *et al*., 2017).

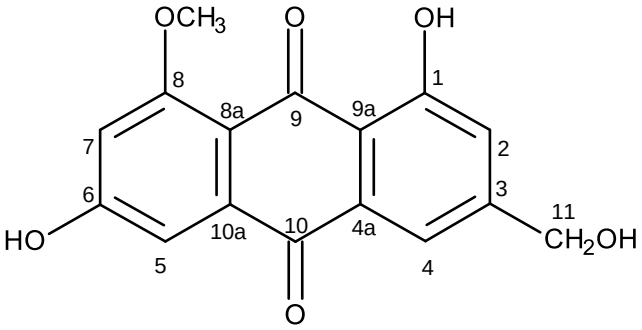

Figure 83. Structure of questinol (**EC 6**)

3.1.7.5. Acetylquestinol (EC 7)

EC 7 was isolated as yellow crystals (mp, 101-103 ºC), and its molecular formula was determined as $C_{18}H_{14}O_7$, based on the (+)-HRESIMS m/z 343.0814 $[M+H]^+$ (calculated 343.0818), indicating twelve degrees of unsaturation. The IR spectrum showed absorption bands for hydroxyl (3442 cm^{-1}), ester (1749 cm^{-1}) and conjugated carbonyl (1631 cm^{-1}) and aromatic (1588 cm^{-1}) groups.

The ^{1}H and ^{13}C NMR spectra of **EC 7** are similar to those of **EC 6** (questin), except for the presence of one ester carbonyl and one extra methyl carbon in the ^{13}C NMR spectrum. The ^{13}C NMR spectrum (Table 14) exhibited eighteen carbon signals which, based on DEPTs and HSQC spectra, can be classified as two conjugated ketone carbonyls (δ_C 186.0 and 182.2), one ester carbonyl (δ_C 170.2), eight quaternary sp^2 [δ_C 163.6, 161.7 (2C), 144.2, 136.7, 132.5, 116.0 and 111.8], four

methine sp^2 (δ_C 122.3, 116.6, 107.5 and 105.3), one methylene sp^3 (δ_C 64.3), one methoxy (δ_C 56.3) and one methyl (δ_C 20.6) groups.

The ^{1}H NMR spectrum (Table 15), together with the COSY spectrum, exhibited two pairs of *meta*-coupled aromatic protons at δ_H 7.54, *d* (*J* = 1.5 Hz)/ δ_H 7.24, *d* (*J* = 1.5 Hz) and δ_H 7.17, *d* (*J* = 2.2 Hz)/ δ_H 6.81, *d* (*J* = 2.2 Hz); a broad singlet of a hydrogen-bonded phenolic hydroxyl at δ_H 13.38, an aromatic methoxy singlet at δ_H 3.89, a singlet of two magnetically equivalent oxymethylene protons at δ_H 5.15 and a methyl singlet at δ_H 2.13. The ^{1}H and ^{13}C NMR general features of compound **EC 7** suggested that it is a 1, 3, 6, 8-tetrasubsituted 9,10-anthraquinone, similar to questin (**EC 5**) (Li *et al*., 2009) and questinol (**EC 6**) (Bao *et al*., 2013).

That the hydroxyl group was on C-1 and the oxygenated methylene substituent as on C-3, was substantiated by the HMBC correlations from H-2 (δ_H 7.24, *d*, *J* = 1.5 Hz) to C-1 (δ_C 161.7), C-4 (δ_C 116.6), C-9a (δ_C 116.0), C-11 (δ_C 64.3), from H-4 (δ_H 7.54, *d*, *J* = 1.5 Hz) to C-2 (δ_C 122.3), C-9a, C-10 (δ_C 182.2) and C-11. Since both H_2-11 (δ_H 5.15, *s*) and the methyl singlet at δ_H 2.13 exhibited HMBC correlations with the carbonyl carbon at δ_C 170.2 (Ac), the substituent on C-3 was acetoxymethyl.

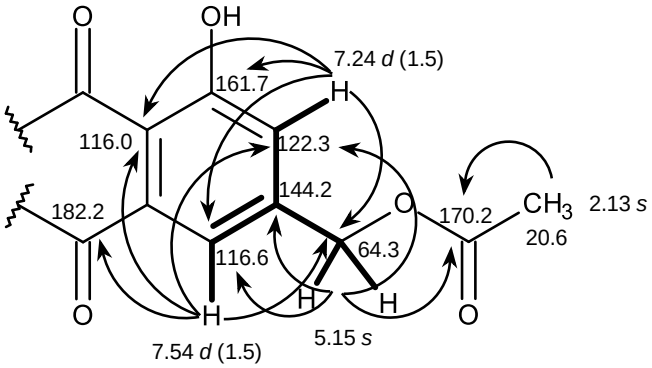

That the hydroxyl and methoxyl groups were on C-6 and C-8 of another aromatic ring was supported by the COSY correlation between H-7 (δ_H 6.81, *d*, *J* = 2.2 Hz) and the methoxyl singlet. This was confirmed by the HMBC correlation of H-7 to C-5 (δ_C 107.5), C-8 (δ_C 163.6), and C-8a (δ_C 111.8) as well as from H-5 (δ_H 7.17, *d*, *J* = 2.2 Hz) to C-7 (δ_C 105.3), C-8a (δ_C 111.8) and C-10 (δ_C 182.2).

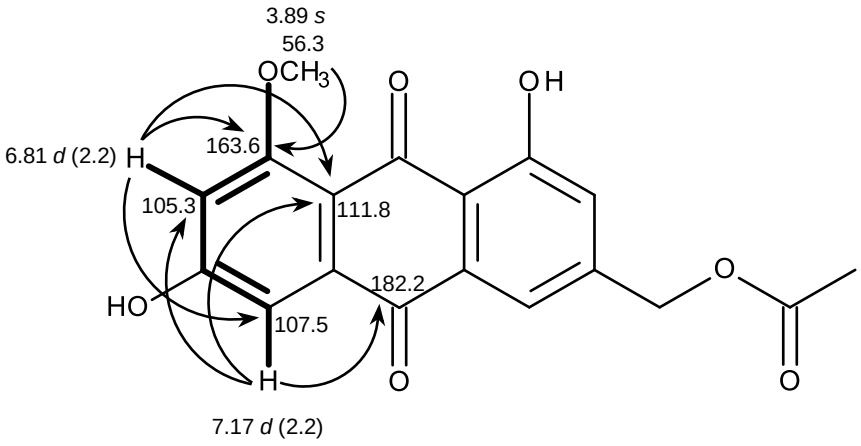

Therefore, the structure of compound **EC 7** was determined as acetylquestinol, which was confirmed by the X-ray analysis as shown in the ORTEP view (Figure 84).

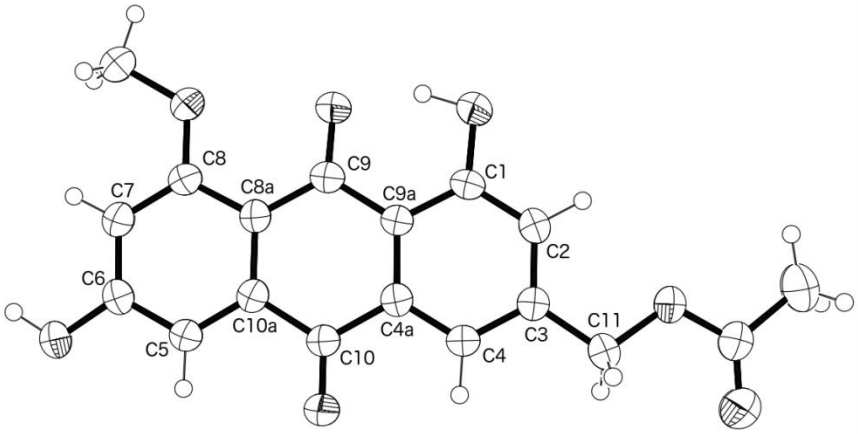

Figure 84. ORTEP view of acetylquestinol

Literature search revealed that although questinol was isolated from several sources (Bao *et al*., 2013; Yang *et al*., 2014), however this is the first report on isolation of acetylquestinol (Figure 85). Therefore, compound **EC 7** is a new natural product.

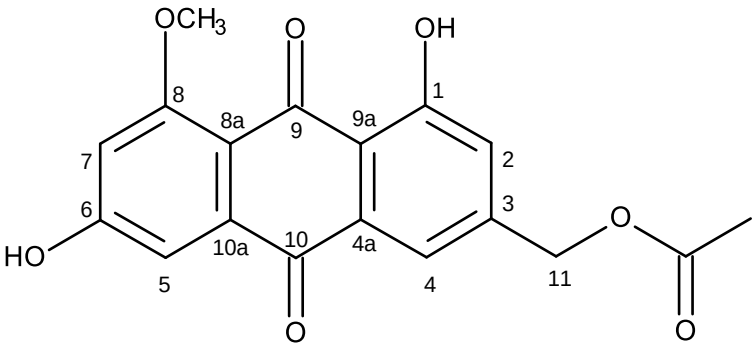

Figure 85. Structure of acetylquestinol (**EC 7**)

Table 14. Comparison of the ^{13}C NMR (300.13 and 75.47 MHz) assignment for **EC 3** (DMSO-d_6), **EC 4** ($CDCl_3$), **EC 5** (DMSO-d_6), **EC 6** (DMSO-d_6), and **EC 7** (DMSO-d_6)

Position	**EC 3**	**EC 4**	**EC 5**	**EC 6**	**EC 7**
	δ_C, type	**δ_C, type**	**δ_C, type**	**δ_C, type**	**δ_C, type**
1	161.4, C	162.5, C	161.7, C	161.8, C	161.7, C
2	124.0, CH	124.5, CH	124.1, CH	120.8, CH	122.3, CH
3	147.9, C	148.5, C	146.3, C	150.9, C	144.2, C
4	120.3, CH	121.3, CH	118.9, CH	115.6, CH	116.6, CH
4a	134.9, C	135.2, C	136.7, C	136.6, C	136.7, C
5	109.7, CH	108.2, CH	108.0, CH	107.2, CH	107.5, CH
6	164.6, C	166.5, C	-	-	161.7, C
7	108.1, CH	106.8, CH	105.4, CH	105.8, CH	105.3, CH
8	-	165.2, C	163.6, C	163.8, C	163.6, C
8a	-	110.2, C	112.5, C	-	111.8, C
9	189.7, CO	190.8, CO	185.9, CO	185.8, CO	186.0, CO
9a	113.4, C	113.7, C	114.5, C	115.3, C	116.0, C
10	181.6, CO	182.0, CO	182.6, CO	182.8, CO	182.2, CO
10a	132.8, C	133.2, C	132.1, C	132.3, C	132.5, C
11	21.5, CH_3	22.2, CH_3	21.4, CH_3	-	-
CH_2-11	-	-	-	62.1, CH_2	64.3, CH_2
OCH_3-6	-	56.1, CH_3	-	-	-
OCH_3-8	-	-	56.1, CH_3	56.1, CH_3	56.3, CH_3
Ac	-	-	-	-	170.2, CO
					20.6, CH_3

Table 15. Comparison of the ^{1}H NMR (300.13 and 75.47 MHz) assignment for **EC 3** (DMSO-d_6), **EC** 4 ($CDCl_3$), **EC 5** (DMSO-d_6), **EC 6** (DMSO-d_6), and **EC 7** (DMSO-d_6)

Position	EC 3	EC 4	EC 5	EC 6	EC 7
	δ_H, (*J* in Hz)	**δ_H, (*J* in Hz)**	**δ_H, (*J* in Hz)**	**δ_H, (*J* in Hz)**	**δ_H, (*J* in Hz)**
1	-	-	-		-
2	7.12, *s*	7.08, *dd* (1.6, 0.8)	7.10, *brs*	7.18, *s*	7.24, *d* (1.5)
3	-	-	-	-	-
4	7.44, *s*	7.62, *dd* (1.4, 0.4)	7.40, *d* (1.2)	7.55, *s*	7.54, *d* (1.5)
4a	-	-	-	-	-
5	7.06, *d* (2.2)	7.36, *d* (2.6)	7.15, *d* (2.0)	7.14, *brs*	7.17, *d* (2.2)
6	-	-	-	-	-
7	6.51, *d* (2.2)	6.68, *d* (2.6)	6.79, *d* (2.1)	6.78, *s*	6.81, *d* (2.2)
8	-	-	-	-	-
8a	-	-	-	-	-
9	-	-	-	-	-
9a	-	-	-	-	-
10	-	-	-	-	-
10a	-	-	-	-	-
CH_3-3	2.39, *s*	2.45, *s*	2.38, *s*	-	-
CH_2-11	-	3.94, *s*	-	4.57, *s*	5.15, *s*
OCH_3-6	-	-	-	-	-
OCH_3-8	-	-	3.87, *s*	3.86, *s*	3.89, *s*
OH-1	12.08, *brs*	12.11, *s*	13.39, *s*	13.54, *s*	13.38, *brs*
OH-6	-	-	-	-	-
OH-8	-	12.31, *s*	-	-	-
OH-11	-	-	-	8.30, *d* (4.4)	-
Ac	-	-	-	-	2.13, *s*

3.1.8 Structure Elucidation of prenylated 1-*H* indole-3-carbaldehydes

3.1.8.1. 2-(2-Methyl-3-en-2yl)-1*H*-indole-3-carbaldehyde (EC 8)

Compound **EC 8** was isolated as yellow crystal (mp, 162-164 ºC) and its molecular formula $C_{14}H_{15}NO$ was determined based on the (+)-HRESIMS *m/z* 214.1236 $[M+H]^+$ (calculated 214.1232), indicating eight degrees of unsaturation. The IR spectrum showed absorption bands for amine (3242 cm^{-1}), carbonyl (1735 cm^{-1}), aromatic (1583 cm^{-1}) and olefin (1622 cm^{-1}) groups.

The ^{13}C NMR spectrum (Table 16) exhibited thirteen carbon signals which, in combination with DEPTs and HSQC spectra, can be categorized as one aldehyde carbonyl (δ_C 186.6), four quaternary sp^2 (δ_C 155.0, 133.9, 127.2 and 113.9), five methine sp^2 (δ_C 145.0, 123.5, 123.1, 122.0 and 111.0), one methylene sp^2 (δ_C 114.0), one quaternary sp^3 (δ_C 39.8) and two methyl (δ_C 28.9) carbons.

The ^1H NMR and COSY spectrum (Table 16), revealed the presence of four aromatic protons of a 1, 2-disubstituted benzene ring at δ_H 8.37, *dd* (*J* = 7.4, 2.0 Hz, H-4), δ_H 7.38, *dd* (*J* = 7.4, 2.0 Hz, H-7), δ_H 7.27, *ddd* (*J* = 7.4, 7.4, 2.0 Hz, H-5) and δ_H 7.24, *ddd* (*J* = 7.4, 7.4, 2.0 Hz, H-6), three olefinic protons of the vinyl group at δ_H 6.24, *dd* (*J* = 17.5, 11.0 Hz, H-12), 5.27, *d* (*J* = 11.0 Hz) and 5.28, *d* (*J* = 17.5, Hz, H-13), in addition to a singlet of an aldehyde proton at δ_H 10.49 (H-10), a broad singlet of NH group at δ_H 8.96 and a singlet of two methyl groups at δ_H 1.68.

Table 16. ^{1}H and ^{13}C NMR ($CDCl_3$, 300.13 and 75.47 MHz) and HMBC assignment for **EC 8**

Position	δ_C, type	δ_H, (*J* in Hz)	COSY	HMBC
2	155.0, C	-	-	-
3	113.9, C	-	-	-
4	122.0, CH	8.37, *dd* (7.4, 2.0)	H-5	C-6, 8
5	123.1, CH	7.27, *ddd* (7.4, 7.4, 2.0)	H-4, 6	C-7, 9
6	123.5, CH	7.24, *ddd* (7.4, 7.4, 2.0)	H-5, 7	C-4, 8
7	111.0, CH	7.38, *dd* (7.4, 2.0)	H-6	C-5, 9
8	133.9, C	-	-	-
9	127.2, C	-	-	-
10	186.6, CHO	10.49, *s*	-	C-3, 9
11	39.8, C	-	-	-
12	145.0, CH	6.24, *dd* (17.5, 11.0)	H-13a, 13b	C-2, 11
13a	114.0, CH_2	5.28, *d* (17.5)	H-12	C-11, 12
b		5.27, *d* (11.0)	H-12	C-11, 12
14	28.9, CH_3	1.68, *s*	-	C-2, 11, 12, 15
15	28.9, CH_3	1.68, *s*	-	C-2, 11, 12, 14
NH-1		8.96, *brs*	-	-

The HMBC spectrum (Table 16) showed correlations from the proton signal at δ_H 8.37, *dd* (*J* = 7.4, 2.0 Hz, H-4) to the carbons at δ_C 123.5 (C-6) and δ_C 133.9 (C-8), from δ_H 7.38, *dd*, *J* = 7.4, 2.0 Hz (H-7) to the carbons at δ_C 123.1 (C-5) and δ_C 127.2 (C-9), from δ_H 7.27, *ddd*, *J* = 7.4, 7.4, 2.0 Hz (H-5) to the carbons at δ_C 111.0 (C-7) and (C-9), from δ_H 7.24, *ddd*, *J* = 7.4, 7.4, 2.0 Hz (H-6) to the carbon at δ_C 122.0 (C-4) and δ_C 133.9 (C-8) as well as from the aldehyde proton (H-10) to the carbon δ_C 113.9 (C-3) and (C-9), suggesting the existence of a 3-carbaldehyde indole moiety.

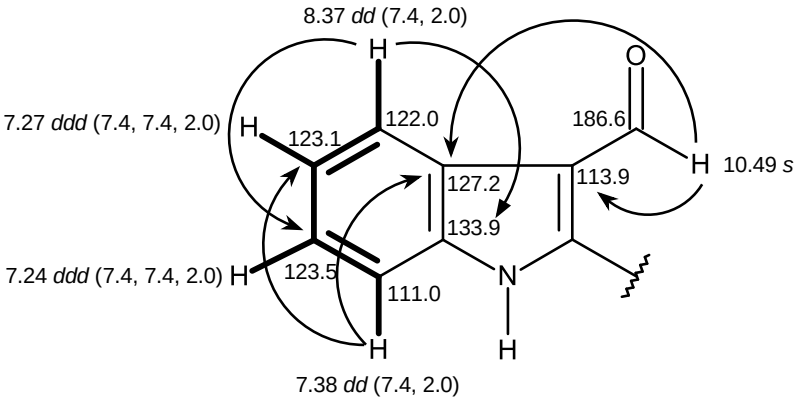

Moreover, the HMBC spectrum (Table 16) also showed correlations from the proton signal at δ_H 6.24, *dd*, *J* = 17.5 Hz, 11.0 Hz (H-12) to the carbon at δ_C 39.8 (C-11), from δ_H 5.28, *d*, *J* = 17.5 Hz (H-13a) and δ_H 5.27, *d*, *J* = 11.0 Hz (H-13b) to C-11 and the carbon at δ_C 145.0 (C-12), and from the methyl signal at δ_H 1.68 (H_3-14/15) to C-11 and C-12, indicating the presence of the 2-methyl-3-en-2-yl substituent. As both H-12 and H_3-14/15 also showed HMBC cross peaks to the carbon at δ_C 155.0 (C-2), the 2-methyl-3-en-2-yl substituent was placed on C-2.

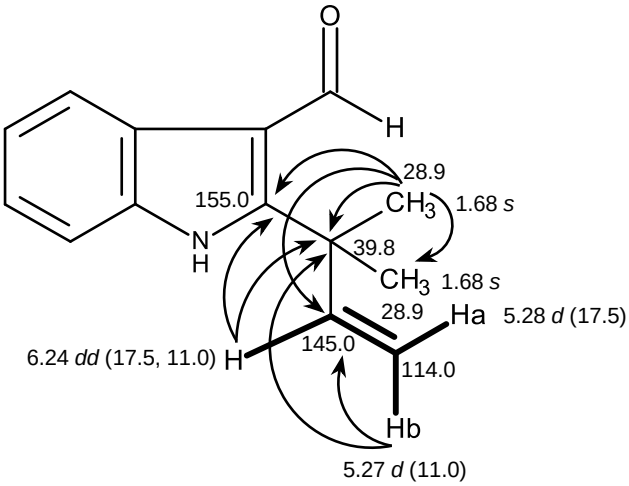

Taking into account the ^{1}H and ^{13}C chemical shift values and their correlations, the structure of **EC 8** (Figure 86) was established as 2-(2-methyl-3-en-2-yl)-1*H*-indole-3-carbaldehyde, extensive literature search revealed that this compound has never been previously reported and therefore it is a new compound.

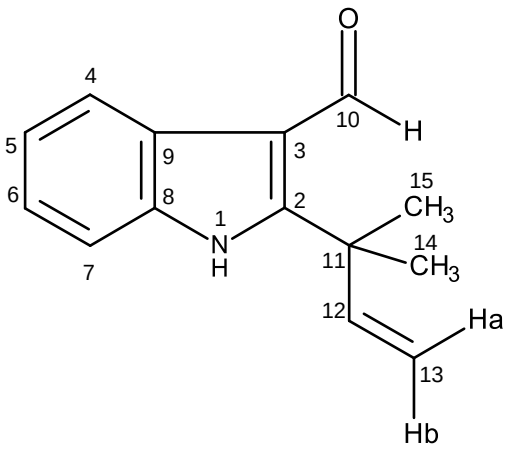

Figure 86. Structure of 2-(2-methyl-3-en-2-yl)-1*H*-indole-3-carbaldehyde (**EC 8**)

3.1.8.2. 2-(2, 2-Dimethylcyclopropyl)-1*H*-indole-3-carbaldehyde (EC 9)

The (+)-HRESIMS of **EC 9** (*m/z* 214.1239 $[M+H]^{+}$, calculated 214.1232), revealed that it has the same molecular formula ($C_{14}H_{15}NO$) as compound **EC 8**. Therefore, compound **EC 9** is an isomer of compound **EC 8**.

The IR spectrum showed absorption bands for amine (3252 cm^{-1}), carbonyl (1768 cm^{-1}), aromatic (1583, 1558 cm^{-1}), and olefin (1633 cm^{-1}) groups. The general

features of the ^{1}H and ^{13}C NMR spectra (Table 17) of compound **EC 9** resemble those of **EC 8**, revealing the presence of a 1*H*-indole-3-carbaldehyde moiety.

Table 17. ^{1}H and ^{13}C NMR ($CDCl_3$, 300.13 and 75.47 MHz) and HMBC assignment for **EC 9**

Position	δ_C, type	δ_H, (*J* in Hz)	COSY	HMBC
2	150.6, C	-	-	-
3	116.7, C	-	-	-
4	121.2, CH	8.26, *dd* (7.5, 2.0)	H-5	C-6, 8
5	122.9, CH	7.26, *ddd* (7.5, 7.5, 2.0)	H-4, 6	C-7,9
6	123.5, CH	7.23, *ddd* (7.5, 7.5, 2.0)	H-5, 7	C-4, 8
7	111.0, CH	7.35, *dd* (7.5, 2.0)	H-6	C-5, 9
8	134.8, C	-	-	-
9	126.2, C	-	-	-
10	185.4, CHO	10.19, *s*	-	C-3, 9
11	21.0, CH	2.25, *dd* (8.4, 5.9)	H-12a, 12b	C-13, 14
12a	19.4, CH_2	1.12, *dd* (8.4, 5.1)	-	C-2, 11
b		1.05, *dd* (5.7, 5.7)	-	C-2, 11, 14
13	20.8, C	-	-	-
14	26.2, CH_3	1.32, *s*	-	C-11, 15
15	21.3, CH_3	0.92, *s*	-	C-11, 15
NH-1	-	8.91, *brs*	-	-

This was supported by the HMBC correlations from the singlet of the aldehyde proton at δ_H 10.19 (H-10) to the quaternary sp^2 carbons at δ_C 116.7 (C-3) and 126.2 (C-9), from the *dd* at δ_H 8.26 (*J* = 7.5, 2.0 Hz, H-4) to the carbons at δ_C 123.5 (C-6) and 134.8 (C-8), from the *dd* at δ_H 7.35 (*J* = 7.5, 2.0 Hz, H-7) to the carbons at

δ_C 122.9 (C-5) and 126.2 (C-9), from the *ddd* at δ_H 7.26 (*J* = 7.5, 7.5, 2.0 Hz, H-5) to the carbon at δ_C 111.0 (C-7) and 126.2 (C-9), and from the *ddd* at δ_H 7.23 (*J* = 7.5, 7.5, 2.0 Hz, H-6) to the carbon at δ_C 121.2 (C-4) and 134.8 (C-8).

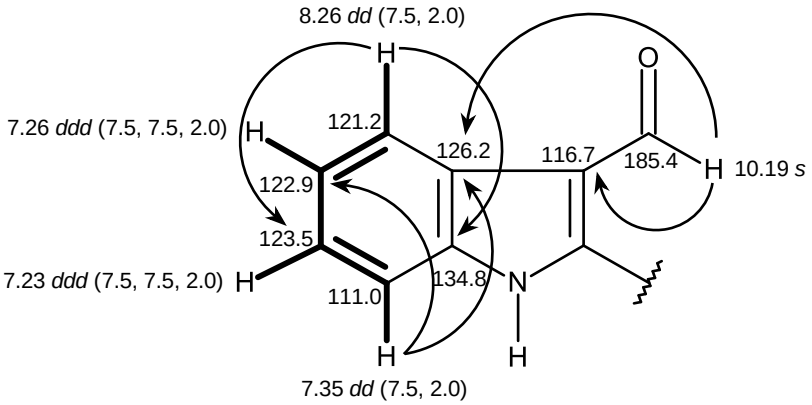

That the substituent on C-2 was the 2, 2-dimethylcyclopropyl group, was substantiated by the presence of two tertiary methyl (δ_H 1.32, *s*/ δ_C 26.2, H_3-14 and δ_H 0.92, *s*/ δ_C 21.3, H_3-15), one sp^3 methylene (δ_H 1.05, *dd*, *J* = 5.7, 5.7 Hz and 1.12, *dd*, *J* = 8.4, 5.1 Hz / δ_C 19.4, H_2-12), one methine (δ_H 2.25, *dd*, *J* = 8.4, 5.9 Hz/δ_C 21.0, H-11) and one sp^3 quaternary carbon (δ_C 20.8, H-13) as well as by the HMBC correlations from H_3-14 and H_3-15 to C-11, from H_2-12 to C-2, C-11 and C-14, as well as from H-11 to C-13 and C-14.

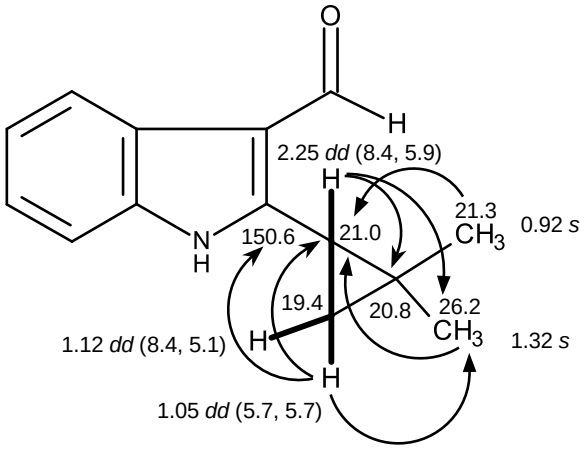

Therefore, the structure of **EC 9** (Figure 87) was established as (2, 2-dimethylcyclopropyl)-1*H*-indole-3-carbaldehyde.

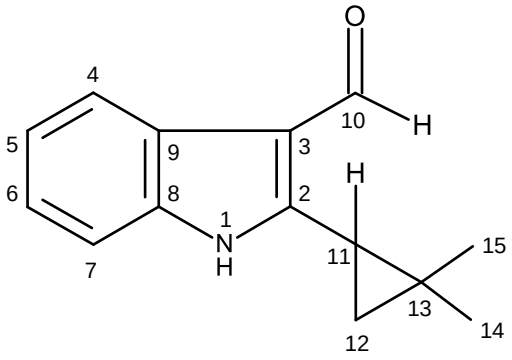

Figure 87. Structure of (2, 2-dimethylcyclopropyl)-1*H*-indole-3-carbaldehyde (**EC 9**)

Examination of the structure of **EC 9** revealed that C-11 of its cyclopropane ring is stereogenic. Therefore, it was necessary to determine the configuration of this carbon. Since compound **EC 9** was isolated as a yellowish viscous mass, the stereochemistry of C-11 could not be determined by X-ray analysis. Therefore, the

absolute configuration of C-11 of **EC 9** was determined by comparison of experimental electronic circular dichroism (ECD) with the calculated ECD. In order to perform ECD calculations, conformational analysis by dihedral driver search and MM2 minimization was carried out which resulted in four main conformations, of which the most populated is represented in Figure 88 (11*S* enantiomer). The other three conformations resulted from rotating the aldehyde and/or the C-2/C-11 bond by 180º. Each conformation was energetically optimized using APFD/6-311+G (2d, p) model chemistry and an IEFPCM model of solvation for chloroform. The Gibbs energies thereby obtained were used to determine the populations of each conformation by Boltzmann weighing at 298 K.

The conformation shown in Figure 88 represents 89.5% of all conformers and was therefore solely used to calculate ECD spectra (Figure 89) for the C-11*S* enantiomer, which superimposed on the experimental spectrum. ECD transitions calculations used the same model chemistry as the energy minimization but with the time-dependent (TD) method. The experimentally observed negative Cotton effects (242 nm, $\Delta\varepsilon$ = – 1.4 M^{-1} cm^{-1} and 280 nm, $\Delta\varepsilon$ = – 0.7 M^{-1} cm^{-1}) fit well the calculated spectrum. Therefore the absolute configuration of C-11 is *S*. To the best of our knowledge, the structure of compound **EC 9** has not yet been reported so far.

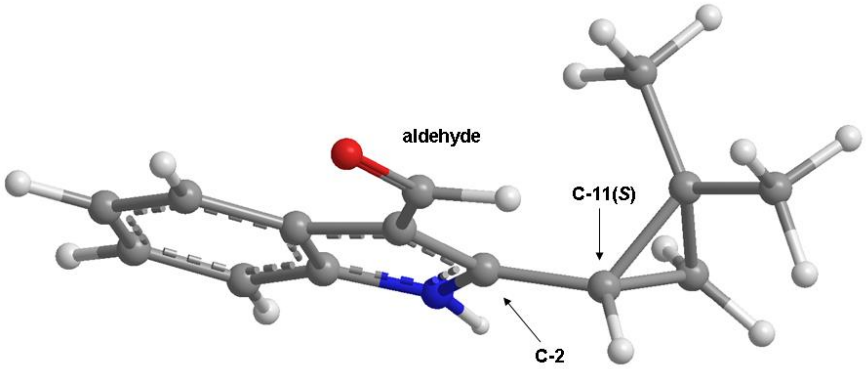

Figure 88. Most stable conformation of **EC 9** (C-11*S*), representing a fraction of around 90% of all four main conformations. In this visualization, the aldehyde is the nearest group and the rings are viewed from below.

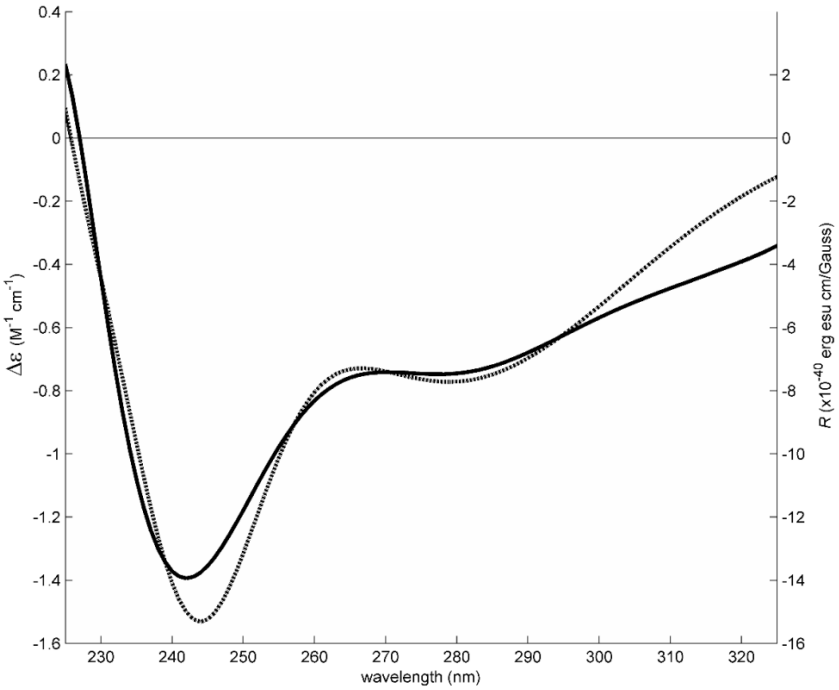

Figure 89. Experimental (solid, left axis) and simulated (dotted, right axis) ECD spectra of **EC 9** (C-11*S*) in chloroform. A line broadening of 0.4 eV was applied to calculated rotatory strengths. The experimental data exhibits two minima around 242 nm ($\Delta\varepsilon$ = – 1.4 M^{-1} cm^{-1}) and 280 nm ($\Delta\varepsilon$ = – 0.7 M^{-1} cm^{-1}) that are well matched by the calculated data.

Structurally, the biosynthesis of **EC 8** and **EC 9** can be proposed to derive from L-tryptophan (L-Trp). Oxiadtive deamination of L-Trp produces indole pyruvic acid (**I**) which, after oxidative decarboxylation, gives rise to indole acetaldehyde (**II**). Oxidation of indole acetaldehyde (**II**) gives indole acetic acid (**III**) which, after oxidative decarboxylation, leads to a formation of indole 3-carbaldehyde (**IV**). Prenylation of **IV** by different prenyltransferase enzymes gives rise to the reverse prenylated indole 3-carbaldehyde **EC 8** and the prenylated 3-carbaldehyde (**V**). Cyclization of the prenyl sidechain of (**V)** leads to a formation of **EC 9**.

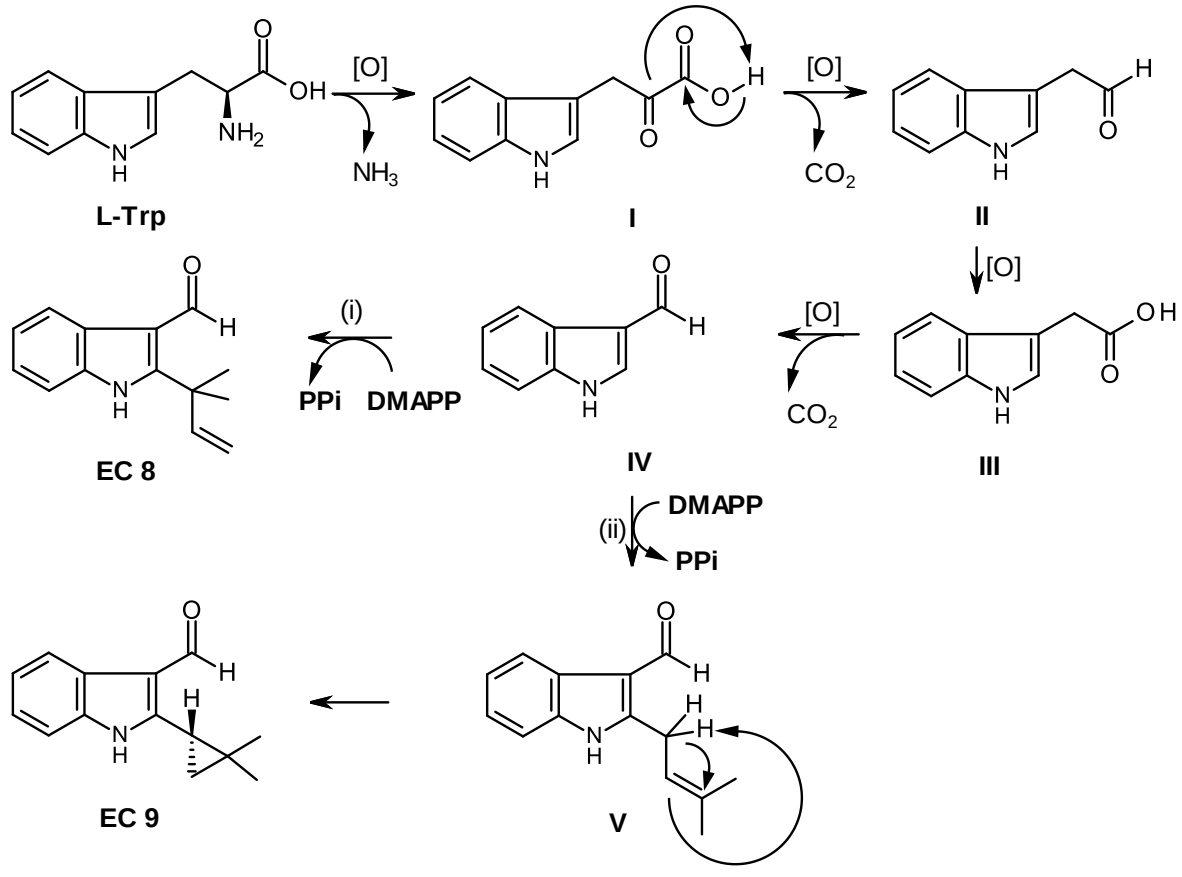

Figure 90. Proposed biosynthetic pathways for **EC 8** and **EC 9**

3.1.9 Structure Elucidation of indolylmethyl 1, 4-bezodiazepen-2, 5-dione

3.1.9.1. Aszonalenin (NTK 2/NG 4)

NTK 2/NG 4 was isolated as a white solid (mp, 249-250 ºC). The ^{13}C NMR spectrum (Table 18) displayed twenty three carbon signals which can classified, according to DEPTs and HSQC spectra, as two amide carbonyls (δ_C 169.9 and 166.8), four quaternary sp^2 (δ_C 149.1, 134.1, 131.3 and 126.8), nine methine sp^2 (δ_C 143.8, 132.6, 131.1, 128.6, 125.3, 125.0, 120.5, 118.4 and 109.2), one methylene sp^2 (δ_C 114.3), two quaternary sp^3 (δ_C 60.7 and 41.5), two methine sp^3 (δ_C 81.7 and 57.1), one methylene sp^3 (δ_C 33.4) and two methyl (δ_C 22.7 and 22.5) groups.

The ^{1}H NMR spectrum, in combination with HSQC spectrum (Table 18) showed the presence of eight aromatic protons at δ_H 7.83, *dd* (*J* = 7.9, 1.4 Hz), 7.44, *ddd* (*J* = 7.7, 7.7, 1.6 Hz), 7.22, *ddd* (*J* = 7.6, 7.6, 1.1 Hz), 7.15, *d* (*J* = 7.4 Hz), 7.08, *ddd* (*J* = 7.6, 7.6, 1.2 Hz), 6.92, *dd* (*J* = 8.0, 0.8 Hz), 6.72, *ddd* (*J* = 7.4, 7.4, 1.0 Hz) and 6.62, *d* (*J* = 7.7 Hz), methine sp^2 proton at δ_H 6.11, *dd* (*J* = 17.3, 10.7 Hz, δ_C 143.8), methylene sp^2 proton at δ_H 5.10, *dd* (*J* = 17.3, 1.2 Hz)/ 5.13, *dd* (*J* = 10.9, 1.2 Hz, δ_C 114.3), two methine sp^3 proton at δ_H 4.00, *dd* (*J* = 8.9, 7.6 Hz, δ_C 57.1), 5.58, *s*, methylene sp^3 proton at δ_H 3.47, *dd* (*J* = 13.9, 7.5 Hz)/ 2.41, *dd* (*J* = 13.9, 9.0 Hz, δ_C 33.4), two methyl singlet at δ_H 1.14, 1.06 and a singlet of NH group at δ_H 6.15 and 8.11.

The COSY spectrum (Table 18) exhibited the cross peaks from the *dd* at δ_H 6.92 (*J* = 8.0, 0.8 Hz, H-18) to the *ddd* at δ_H 7.44 (*J* = 7.7, 7.7, 1.6, H-19), from the *ddd* at δ_H 7.22 (*J* = 7.6, 7.6, 1.1 Hz, H-20) to the *dd* at δ_H 7.83 (*J* = 7.9, 1.4 Hz, H-21) and also by the H-19 and H-20 indicating the presence of the 1, 2-disubstituted benzene ring. This was confirmed by the HMBC correlation from the H-21 to the carbons at δ_C 134.1 (C-15) and 132.6 (C-19), from H-19 to C-15 and the carbon at δ_C 131.1 (C-21), from H-20 to the carbon at δ_C 126.8 (C-14) and 120.5 (C-18), from H-18 to C-14. That this 1, 2-disubstituted benzene ring was fused to the 1, 4-bezodiazepen-2, 5-dione ring through C-14 and C-15 was evidence by the HMBC correlation of H-21 to the amide carbonyl at δ_C 166.8.

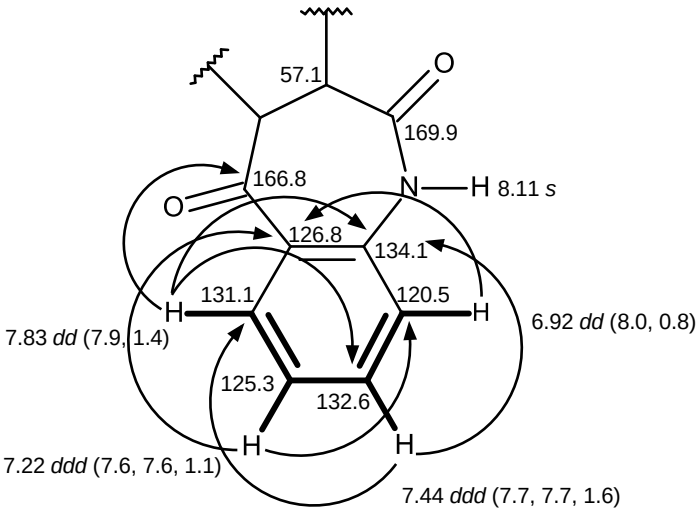

That the second 1, 2-disubstituted benzene ring was part of the 2,3-dihydro-1*H*-indole moiety was confirmed by the COSY correlations from the doublet at δ_H 7.15 (*J* = 7.4 Hz, H-4) to the *ddd* at δ_H 6.72 (*J* = 7.4, 7.4, 1.0 Hz, H-5), from the doublet at δ_H 6.62 (*J* = 7.7 Hz, H-7) to the *ddd* at δ_H 7.08 (*J* = 7.6, 7.6, 1.2 Hz, H-6),

as well as from H-5 to H-4 and H-6, and H-6 to H-5 and H-7. This was confirmed by the HMBC correlations from H-4 to the carbons at δ_C 128.6 (C-6) and 149.1 (C.8), from H-7 to the carbons at δ_C 118.4 (C-5) and 131.3 (C-9), from H-5 to the carbons at δ_C 109.2 (C-7) and C-9, as well as from H-6 to the carbon at δ_C 125.0 (C-4) and C-8, from the amine singlet at δ_H 6.15 (NH-1) to C-8, C-9 and the quaternary carbon at δ_C 60.7, as well as from the singlet at δ_C 5.58 (H-2) to C-8 and C-9.

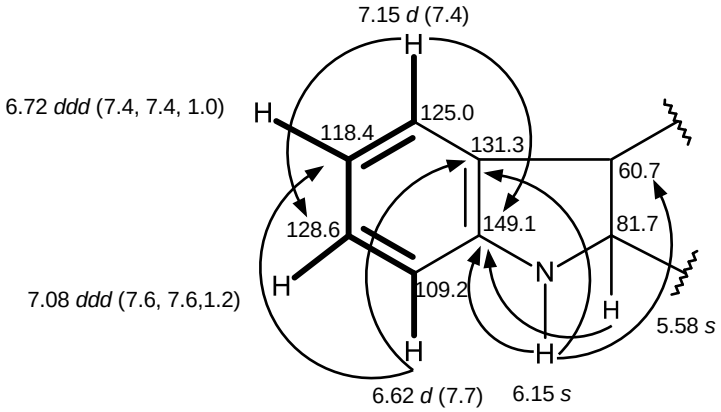

That the 2, 3-dihydro-1*H*-indole and the 3, 4-dihydro-1*H*-1, 4-benzodiazepen-2, 5-dione portions were linked together through a pyrrolidine ring, was corroborated by the HMBC cross peaks from the *dd* at δ_H 3.47 (*J* = 13.9, 7.5 Hz; δ_C 33.4, H-10a) to the carbons at δ_C 60.7 (C-3) and 57.1 (C-11), from the *dd* at δ_H 2.41 (*J* = 13.9, 9.0 Hz, δ_C 33.4, H-10b) to C-11.

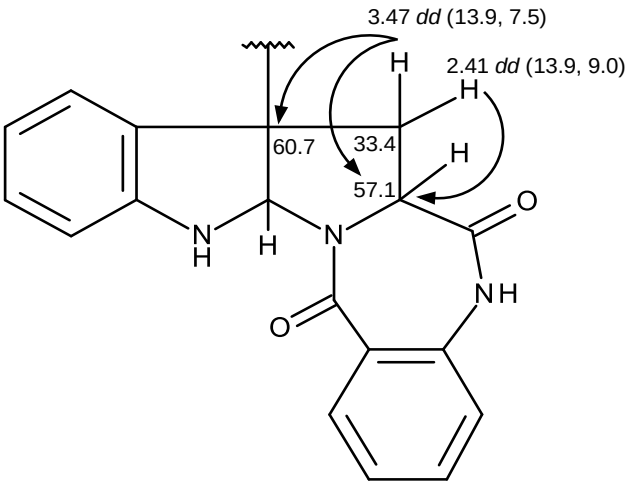

That the 2-methylbut-3-en-2-yl substituent was on C-3 was substantiated by the COSY correlations from the *dd* at δ_H 6.11 (*J* = 17.3, 10.7, H-2′, δ_C 143.8) to the double doublets at δ_H 5.13 (*J* = 10.9, 1.2, H-1′b; δ_C 114.3) and 5.10 (*J* = 17.3, 1.2 Hz, H-1′a; δ_C 114.3) as well as by the HMBC correlations from the methyl singlets at δ_H 1.06 (δ_C 22.5, Me-4′) and δ_H 1.14 (δ_C 22.7, Me-5′) to the quaternary carbon at δ_C 41.5 (C-3′), C-3 and C-2′, and from H-2 to C-3′.

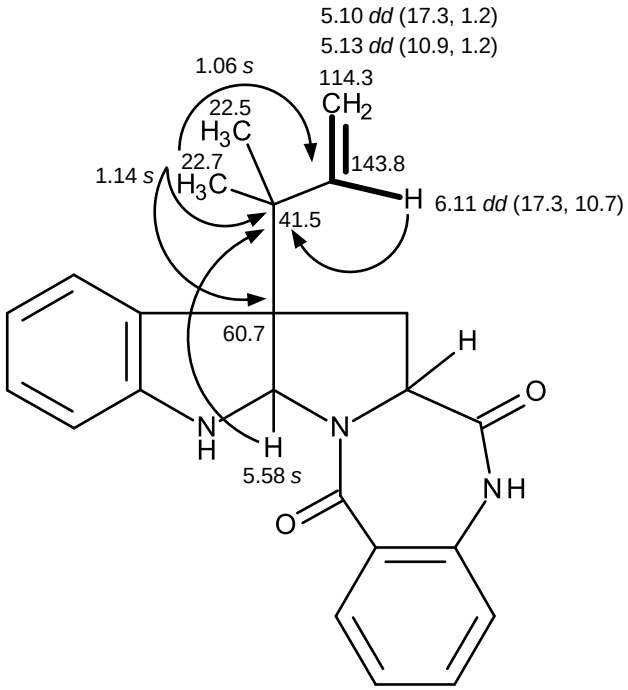

The ^{1}H and ^{13}C NMR data of **NTK 2/NG 4** are compatible with those of aszonalenin. However, the concrete prove of it identity was based on the optical rotation of **NTK 2/NG 4** ($[\alpha]_D^{20}$ = – 27.0) which is compatible with those of aszonalenin.

Aszonalenin is well known fungal metabolites have been isolated from several fungi including *Aspergillus zonatus* (Kimura *et al*., 1982b), *Neosartorya Fischeri* IFM 52672 (Wakana *et al*., 2006) and *Neosartorya fischeri* CGMCC 3.53781 (Shan *et al*., 2014). This compound was also reported from the marine-derived fungus *Aspergillus carneus* which was isolated from an estuarine sediment (Capon *et al*., 2003), as well as from the soil fungi *Neosartorya fischeri* KUFC 6344 (Eamvijarn *et al*., 2013) and *Neosartorya tatenoi* KKU-2NK23 (Yim *et al*., 2014).

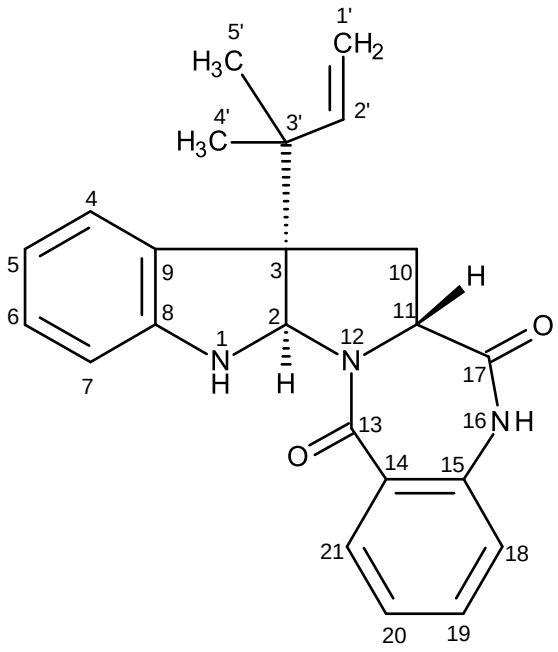

Figure 91. Structure of aszonalenin (**NTK 2/NG 4**)

3.1.9.2. Acetylaszonalenin (NTK 3)

NTK 3 was isolated as a white solid (mp, 237-239 ºC). The general features of the ^{1}H and ^{13}C NMR spectra (Table 18) **NTK 3** were very similar to those of **NTK 2/NG 4** except for the appearance of the signals of the ester carbonyl (δ_C 170.7) and methyl carbons (δ_C 24.2) in the ^{13}C NMR spectrum and an additional methyl singlet at δ_H 2.59 in the ^{1}H NMR spectrum.

That the acetyl group (δ_C 170.7, 24.2; δ_H 2.59, *s*) was on the nitrogen of the indole moiety (N-1) was corroborated by the lower frequencies of C-8 (δ_C 142.0) when compared to the corresponding carbon of **NTK 2/NG 4** (δ_C 149.1) while the

frequencies of H-7 and C-7 increased from δ_H 6.62, *d* (*J* = 7.7 Hz)/ δ_C 109.2 in **NTK 2/NG 4** to δ_H 8.00, *d* (*J* = 7.9 Hz)/ δ_C 119.2, respectively. Therefore the structure of **NTK 3** was proposed to be acetylaszonalenin which was confirmed by the ^{1}H and ^{13}C NMR values and the sign of the rotation from the literature.

Acetylaszonalenin was frequently isolated from many fungi such as *Neosartorya fischeri* KUFC 6344 (Eamvijarn *et al*., 2013), *Neosartorya fischeri* CGMCC 3.53781 (Shan *et al*., 2014) and marine-derived fungus *Aspergillus terreus* (You *et al*., 2015) and normally occurred together with aszonalenin.

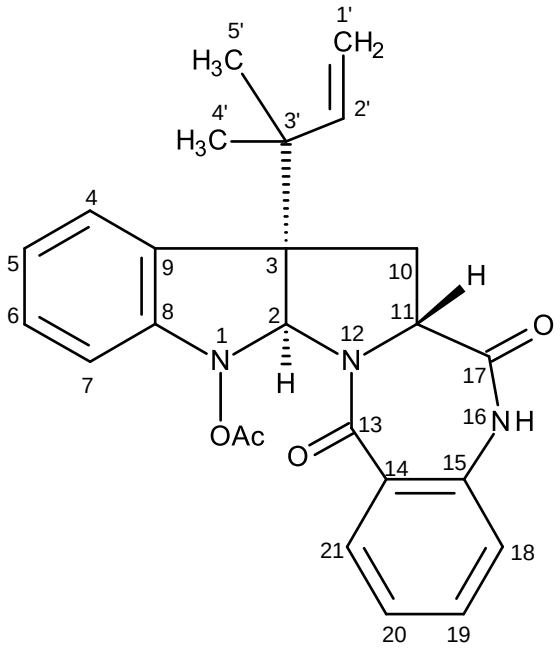

Figure 92. Structure of acetylaszonalenin (**NTK 3**)

Table 18. Comparison of ^{1}H and ^{13}C NMR ($CDCl_3$, 300.13 and 75.47 MHz) assignment for **NTK 2/NG 4** and **NTK 3**

Position	**NTK 2/NG 4**		**NTK 3**	
	δ_C, type	**δ_H, (*J* in Hz)**	**δ_C, type**	**δ_H, (*J* in Hz)**
2	81.7, CH	5.58, *s*	82.1, CH	5.92, *s*
3	60.7, C	-	60.2, C	-
4	125.0, CH	7.15, *d* (7.4)	124.3, CH	7.23, *d* (7.6)
5	118.4, CH	6.72, *ddd* (7.4, 7.4, 1.0)	124.1, CH	7.05, *dd* (7.5, 7.5)
6	128.6, CH	7.08, *ddd* (7.6, 7.6, 1.2)	128.9, CH	7.25, *dd* (7.4, 7.4)
7	109.2, CH	6.62, *d* (7.7)	119.2, CH	8.00, *d* (7.9)
8	149.1, C	-	142.0, C	-
9	131.3, C	-	133.9, C	-
10a	33.4, CH_2	3.47, *dd* (13.9, 7.5)	30.6, CH_2	3.38, *dd* (13.8, 8.4)
b		2.41, *dd* (13.9, 9.0)		2.42, *dd* (13.4, 8.0)
11	57.1, CH	4.00, *dd* (8.9, 7.6)	56.6, CH	3.89, *t* (8.3)
13	166.8, CO	-	166.7, CO	-
14	126.8, C	-	127.4, C	-
15	134.1, C	-	133.8, C	-
17	169.9, CO	-	169.6, CO	-
18	120.5, CH	6.92, *dd* (8.0, 0.8)	120.7, CH	6.98, *d* (7.9)
19	132.6, CH	7.44, *ddd* (7.7, 7.7, 1.6)	132.3, CH	7.36, *ddd* (7.7, 7.7, 1.4)
20	125.3, CH	7.22, *ddd* (7.6, 7.6, 1.1)	125.3, CH	7.10, *dd* (7.4, 7.4, 0.8)
21	131.1, CH	7.83, *dd* (7.9, 1.4)	130.9, CH	7.61, *d* (7.7)
1′a	114.3, CH_2	5.10, *dd* (17.3, 1.2)	114.2, CH_2	5.08, *d* (16.2)
b		5.13, *dd* (10.9, 1.2)		5.07, *d* (11.6)
2′	143.8, CH	6.11, *dd* (17.3, 10.7)	143.3, CH	5.85, *dd* (17.5, 10.7)
3′	41.5, C	-	40.7, C	-
4′	22.7, CH_3	1.06, *s*	22.9, CH_3	0.96, *s*
5′	22.5, CH_3	1.14, *s*	22.5, CH_3	1.16, *s*
NH-1	-	6.15, *s*	-	9.45, *s*
NH-16	-	8.11, *s*	170.7, CO	-
			24.2, CH_3	2.59, *s*

3.1.9.3. Takakiamide (NTK 4/ NG 7)

NTK 4/ NG 7 was isolated as a white solid (mp, 182-183°C), and its molecular formula $C_{23}H_{23}N_3O_2$ was established on the basis of the (+)-HRESIMS *m/z* 374.1876 $[M+H]^+$ (calculated 374.1869), indicating fourteen degrees of unsaturation. The IR spectrum showed absorption bands for amine (3214 cm^{-1}), amide carbonyls (1688, 1654 cm^{-1}), aromatic (3057, 1579 cm^{-1}) and olefin (1607, 1468 cm^{-1}).

The ^1H and ^{13}C NMR spectra of **NTK 4/ NG 7** resembled those of **NTK 2/NG 4** (aszonalenin), but with some slight differences. The ^{13}C NMR spectrum (Table 19), displayed twenty three carbon signals which can be categorized, based on DEPTs and HSQC spectra, as two amide carbonyls (δ_C 172.0 and 168.9), six quaternary sp^2 (δ_C 136.4, 136.3, 135.7, 127.9, 125.5 and 108.0), ten methine sp^2 (δ_C 133.1, 131.4, 127.3, 125.2, 121.7, 121.0, 119.9, 119.2, 118.4 and 109.9), one methine sp^3 (δ_C 52.4), two methylene sp^3 (δ_C 44.2 and 22.4) and two methyl (δ_C 25.6 and 18.1) groups.

The ^1H NMR and HSQC spectra (Table 19) revealed eight aromatic protons at δ_H 7.91, *dd* (*J* = 8.0, 1.5 Hz), 7.54, *d* (*J* = 7.8 Hz), 7.50, *ddd* (*J* = 8.0, 8.0, 1.5 Hz), 7.31, *d* (*J* = 7.8 Hz), 7.24, *dd* (*J* = 8.0, 8.0 Hz), 7.20, *ddd* (*J* = 7.8, 7.8, 0.7 Hz), 7.08, *ddd* (*J* = 7.8, 7.8, 0.7 Hz), 7.06, *d* (*J* = 8.0 Hz), two methine sp^2 proton at δ_H 7.15, *s* and 5.35, *m*, one methine proton at δ_H 4.12, *dt* (*J* = 8.3, 5.5 Hz), two methylene

protons at δ_H 4.63, *d* (*J* = 6.8 Hz), 3.57, *dd* (*J* = 15.2, 5.5 Hz) and 3.26, *dd* (*J* = 15.2, 8.3 Hz), two methyl singlets at δ_H 1.80 and 1.74.

Similar to **NTK 2/NG 4** (aszonalenin), **NTK 4/ NG 7** also consists of the indole ring system which was corroborated by the COSY correlations from the doublet at δ_H 7.54 (*J* = 7.8 Hz; H-4) through the *ddd* at δ_H 7.08 (*J* = 7.8, 7.8, 0.7 Hz; H-5), a *ddd* at δ_H 7.20 (*J* = 7.8 7.8, 0.7 Hz; H-6) and a doublet at δ_H 7.31 (*J* = 8.2 Hz; H-7), as well as the HMBC correlations from H-4 to the carbons at δ_C 121.7 (C-6) ,127.9 (C-9), and 108.0 (C-3), from H-7 to the carbons at δ_C 119.2 (C-5) and C-9, from H-6 to the carbon at δ_C 118.4 (C-4) and 136.3 (C-8), and from the singlet at δ_C 7.15 (H-2) to C-3, C-8 and C-9.

Contrary to **NTK 2/NG 4** (aszonalenin), **NTK 4/ NG 7** has the 3-methylbuten-2-yl substituent on the nitrogen atom of the indole nucleus as was supported by the COSY correlation from the doublet at δ_H 4.63 (*J* = 6.8 Hz, H-1′; δ_C 44.2) though the multiplet at δ_H 5.35 (H-2′; δ_C 119.9) and two methyl singlets at δ_H 1.74 (Me-5′; δ_C 25.6) and 1.80 (Me-4′; δ_C 18.1) as well as the HMBC correlation from H-1′ to C-2, C-2′ and the carbon at δ_C 136.4 (C-3′).

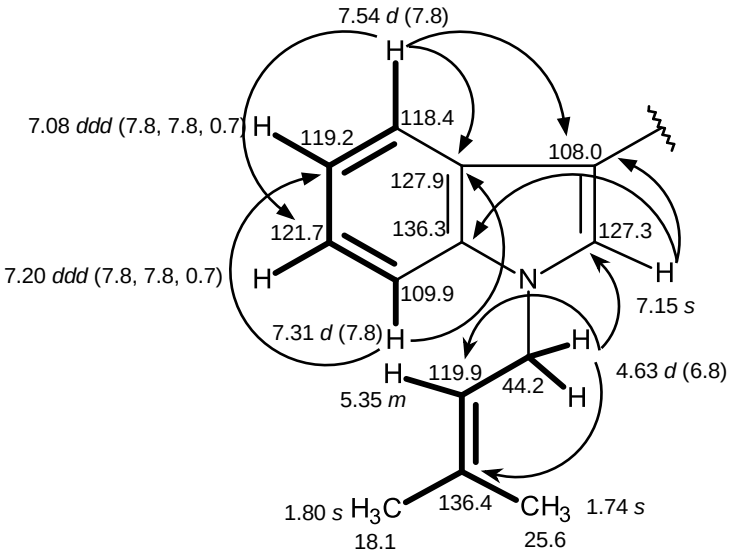

Like aszonalenin (**NTK 2/NG 4**), another part of the molecule consist of 3,4-dihydro-1*H*-1,4-benzodiazepine-2,5-dione based on the COSY correlations from the *dd* at δ_H 7.91 (*J* = 8.0, 1.5, H-21; δ_C 131.4) through the *dd* at δ_H 7.24 (*J* = 8.0, 8.0 Hz; H-20; δ_C 125.2), a *ddd* at δ_H 7.50 (*J* = 8.0, 8.0, 1.5 Hz, H-19; δ_C 133.1) and a doublet at δ_H 7.06 (*J* = 8.0 Hz, H-18; δ_C 121.0), as well as from the HMBC correlations of the amide proton singlet at δ_H 9.03, *s* (NH-16) to the carbons at δ_C 125.5 (C-14) and 52.4 (C-11), from H-21 to the carbons at δ_C 135.7 (C-15), 133.1 (C-19) and 168.9 (CO-13).

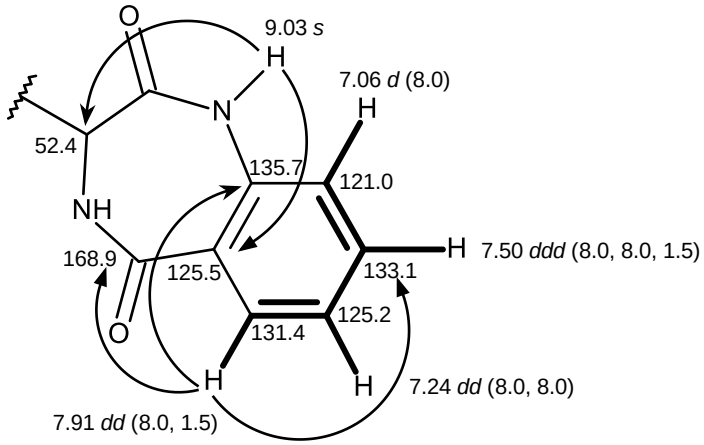

That the *N*-prenylated 3, 4-dihydro-1*H*-1, 4-benzodiazepine-2,5-dione was linked to the indole moiety through a methylene bridge, was evidenced by the COSY correlations from the doublet doublet at δ_H 3.57 (*J* = 15.2, 5.5 Hz, H-10a) and doublet doublet at δ_H 3.26 (*J* = 15.2, 8.3 Hz, H-10b) to the doublet triplet at δ_H 4.12 (*J* = 8.3, 5.5 Hz, H-11), as well as by the HMBC correlations from H-10a and H-10b to C-2, C-3, C-11 and the amide carbonyl at δ_C 172.0 (C-17). Therefore, the flat structure of **NTK4/ NG 7** was proposed as below:

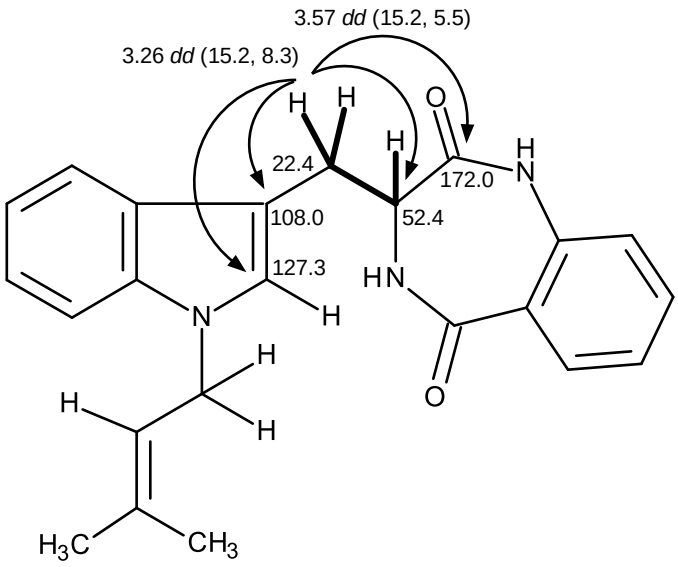

A literature survey revealed that the compound 3*S*)-3[1-(3-methylbut-2-enyl) indol-3-yl]-3,4-dihydro-1*H*-1,4-benzodiazepine-2,5-dione (PubChem SID 185030170), whose flat structure is the same as that of compound **NTK 4/NG 7**, was reported as a product of Angene Chemical (AGN-PC-069E9V) (http://pubchem.ncbi.nlm.nih.gov/substance/185030170).

Although the absolute configuration of its C-11 is reported as *S*, there is neither ^{1}H and ^{13}C NMR nor optical rotation data available for this compound in the PubChem Substance website. Since compound **NTK 4/NG 7** did not provide suitable crystals for X-ray diffraction, it was not possible to determine the absolute configuration of C-11 with certainty. Thus, an attempt was made to combine the data from the NOESY spectrum, scalar coupling constants and molecular mechanics simulations.

The NOESY spectrum exhibited correlations of H-11 to H-4, NH-12 and NH-16. A stochastic conformational search using MMFF force field models of the C-11 stereoisomers of compound **NTK 4/NG 7**, performed with ChemBio3D Ultra 14.0 using the MMFF force field with application's default parameters (Halgren, 1996) showed a somewhat flat energy landscape concerning the spatial relative positions of the two cyclic regions of the molecule. The rotational freedom around the two carbon-carbon single bonds of C-10, on which compound **NTK 4/NG 7** whole conformations hinge, precludes any clear differentiation between the two stereoisomers since both C-11*R* and C-11*S* stereoisomers yield lowest energy

conformations that explain the observed NOESY cross-peaks as well as the ^{1}H scalar coupling constants measured. Regardless of the stereoisomer, the gas-phase least energetic conformers of compound **NTK 4/NG 7** show almost equal steric energy for the two major conformations (half-chair) of the amide ring. Figure 93 shows the C-11*R* stereoisomer as an example: (a) H-11 is in the equatorial and (b) H-11 is in the axial position. The major difference resides in the dihedral angle between H-11 and NH-12, which is approximately 0° for the equatorial and 110° for the axial position of H-11 relative to the ring. The observed scalar coupling of 5.5 Hz between the two protons may be interpreted as an average value between their extreme relative positions, suggesting that the two conformations exchange rapidly at room temperature. The observed NOESY correlation between H-11 and NH-16 does not allow us to positively decide for any of the two amide ring conformations since the distances between the two protons in the molecular mechanics models are very close, *i.e.*, 4.0 Å for the equatorial H-11, and 3.6 Å for the axial H-11. Therefore, the constant exchange between the two conformations of the amide ring is the most probable case.

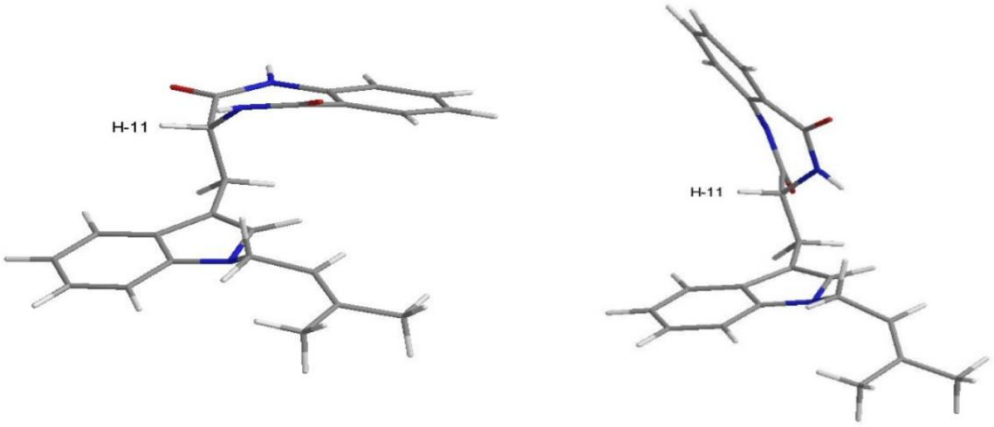

Figure 93. Conformations of C-11 *R* stereoisomer of compound **NTK 4/NG 7** obtained by simulation performed with ChemBio Ultra 14.0; (a) conformer with H-11 in equatorial position; (b) conformer with H-11 in axial position.

NTK 4/NG 7 was isolated together with aszonalenin (**NTK 2/NG 4**) and acetylaszonalenin (**NTK 3**), suggested that they should be derived from the same biosynthetic pathways. It is probable that the absolute configuration of C-11 of **NTK 4/NG 7** is the same as that of the corresponding carbon of aszonalenin (**NTK 2/NG 4**) and acetylaszonalenin (**NTK 3**) *i.e*., C-11 is *R*. Taking together with ^{1}H and ^{13}C NMR, NOESY and conformational analysis, the compound **NTK 4/NG 7** (Figure 94) is a new natural product, which we have named it takakiamide.

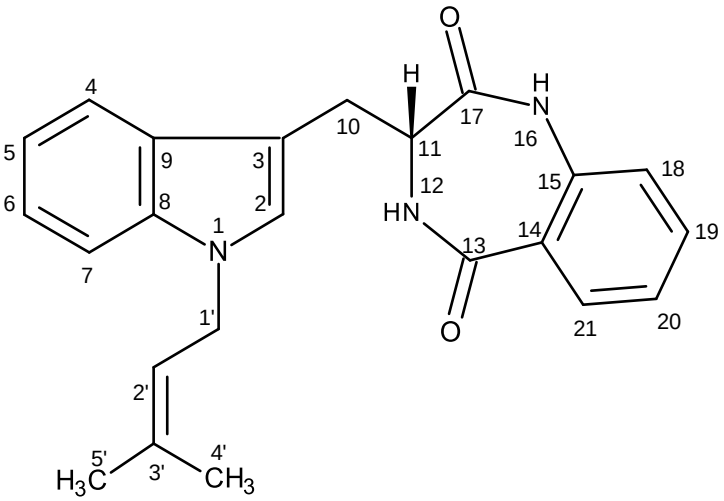

Figure 94. Structure of takakiamide (**NTK 4/NG 7)**

3.1.9.4. (3*R*)-3-(1*H*-indol-3ylmethyl)-3, 4-dihydro-1*H*-1, 4-benzodiazepine-2, 5-dione (NG 5)

NG 5 was isolated as a yellow viscous mass and its molecular formula $C_{18}H_{15}N_3O_2$ was established on the basis of the (+)-HRESIMS m/z 306.1256 $[M+H]^+$ (calculated 306.1243), indicating thirteen degrees of unsaturation. The general feature of the ^1H and ^{13}C NMR spectra of **NG 5** resembled those of **NTK 4/NG 7** (takakiamide) except for the absence of the prenyl substituents.

The ^{13}C NMR spectrum exhibited the presence of 18 carbon signals which, in combination with DEPTs and HSQC spectra (Table 19), can be classified as two amide carbonyls (δ_C 172.1 and 169.2), five quaternary sp^2 (δ_C 136.2, 135.9, 127.2,

125.5 and 109.8), nine methine sp^2 (δ_C 133.1, 131.3, 125.1, 124.0, 122.2, 121.2, 119.6, 118.3 and 111.4), one methine sp^3 (δ_C 52.4) and one methylene (δ_C 24.2) carbons.

The ^{1}H NMR, COSY, HSQC and HMBC spectra displayed the presence of two 1,2-disubstituted benzene rings, one of which belonged to the indole moiety: δ_H 8.17, *d* (*J* = 1.3 Hz, NH-1), δ_H 7.14, *d* (*J* = 1.3 Hz; H-2; δ_C 124.0), δ_H 7.53, *d* (*J* = 7.8 Hz, H-4; δ_C 118.3), δ_H 7.08, *ddd* (*J* = 7.5, 7.5, 1.0 Hz, H-5, δ_C 119.6), δ_H 7.18, *ddd* (*J* = 8.1, 8.1, 1.0 Hz, H-6; δ_C 122.2) and δ_H 7.33, *d* (*J* = 8.1 Hz, H-7; δ_C 111.4).

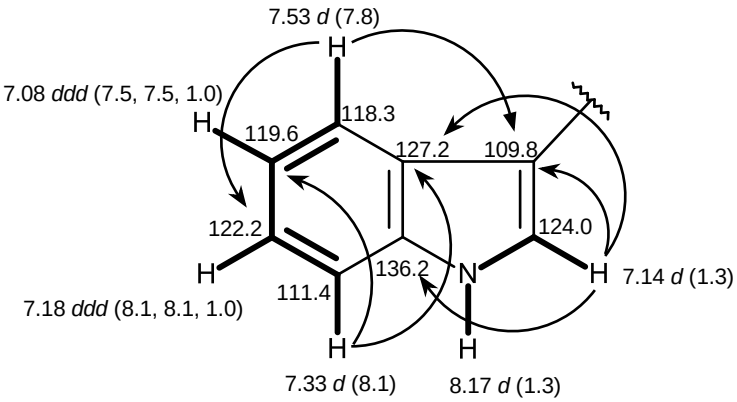

While another belonged to the 1,4-benzodiazepen-2,5-dione moiety: δ_H 7.03, *d* (*J* = 7.5 Hz, H-18; δ_C 121.2), δ_H 7.46, *ddd* (*J* = 7.7, 7.7, 1.6 Hz, H-19; δ_C 133.1), δ_H 7.21, *ddd* (*J* = 7.9, 7.9, 1.6 Hz, H-20; δ_C 125.1), δ_H 7.88, *dd* (*J* = 7.9, 1.6 Hz, H-21; δ_C 131.3), δ_H 4.11, *dt* (*J* = 8.3, 5.6 Hz, H-11; δ_C 52.4), δ_H 9.12, *s* (NH-16), δ_H 7.30, *brd* (*J* = 6.6 Hz, NH-12), δ_C 169.2 (CO-13), δ_C 172.1 (C-17).

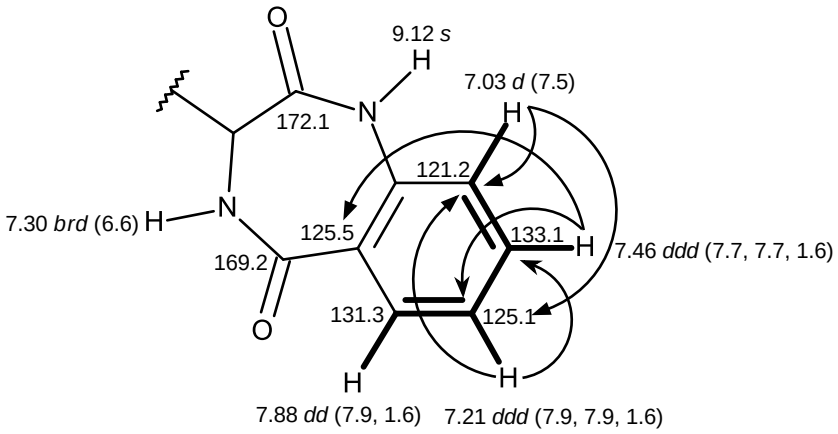

That the 3, 4-dihydro-1*H*-1, 4-benzodiazepine -2, 5-dione moiety was linked to the indole ring by a methylene bridge, was evidenced by the HMBC correlations from the *dd* at δ_H 3.54 (*J* = 15.2, 5.8 Hz; δ_C 24.2, H-10a) and the *dd* at δ_H 3.25 (*J* = 15.2, 8.4 Hz; δ_C 24.2, H-10b) to the carbons at δ_C 124.0 (C-2), 109.8 (C-3), 52.4 (C-11), and 172.1 (C-17), from the broad doublet of imine proton at δ_H 7.30 (*J* = 6.6 Hz; NH-12) to the carbon at δ_C 125.5 (C-14), from NH-16 (9.12, *s*) to C-11 and C-17, as well as the coupling system of (H-10a), (H-10b) and (H-11) were observed in the COSY spectrum.

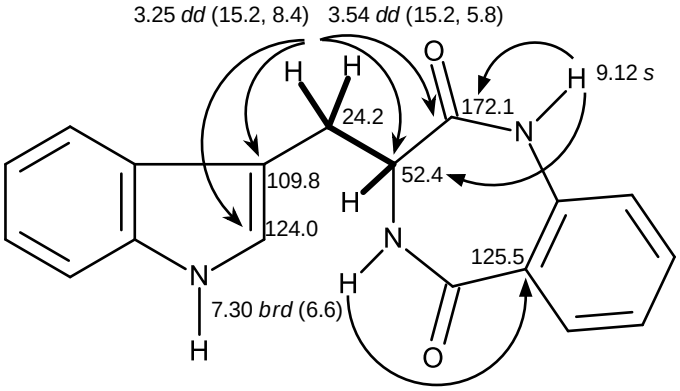

Therefore, the structure of **NG 5** was proposed as 3-(1*H*-indol-3-ylmethyl)-3, 4-dihydro-1*H*-1,4-benzodiazepine-2,5-dione. Comparison of the ^{1}H and ^{13}C chemical shift values and the optical rotation of **NG 5** ($[\alpha]_D^{20}$ = + 96.00) were agreement with those of (3*R*)-3-(1*H*-indol-3-ylmethyl)-3,4-dihydro-1*H*-1,4-benzodiazepine-2,5-dione, whose absolute configuration of C-11 is *S*. This compound has previously reported from the soil fungus *Aspergillus flavipes* (Barrow and Sun, 1994), and also synthesized by the condensation of L-tryptophan and anthranilic acid catalyzed by the non-ribosomal peptide synthetase AnaPS has been already described by Yin *et al*. (2009).

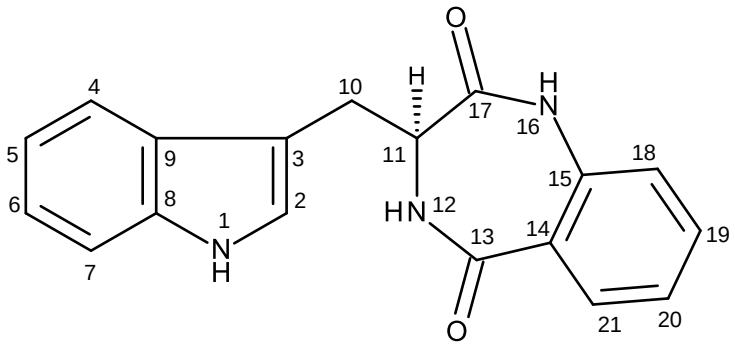

Figure 95. Structure of (3*R*)-3-(1*H*-indol-3-ylmethyl)-3, 4-dihydro-1*H*-1, 4-benzodiazepine-2, 5-dione (**NG 5**)

Table 19. Comparison of ^{1}H and ^{13}C NMR ($CDCl_3$, 300.13 and 75.47 MHz) assignment for **NTK 4/NG 7** and **NG 5**

Position	NTK 4/ NG 7		NG 5	
	δ_C, type	**δ_H, (*J* in Hz)**	**δ_C, type**	**δ_H, (*J* in Hz)**
2	127.3, CH	7.15, *s*	124.0, CH	7.14, *d* (1.3)
3	108.0, C	-	109.8, C	-
4	118.4, CH	7.54, *d* (7.8)	118.3, CH	7.53, *d* (7.8)
5	119.2, CH	7.08, *ddd* (7.8, 7.8, 0.7)	119.6, CH	7.08, *ddd* (7.5, 7.5, 1.0)
6	121.7, CH	7.20, *ddd* (7.8, 7.8, 0.7)	122.2, CH	7.18, *ddd* (8.1, 8.1, 1.0)
7	109.9, CH	7.31, *d* (7.8)	111.4, CH	7.33, *d* (8.1)
8	136.3, C	-	136.2, C	-
9	127.9, C	-	127.2, C	-
10a	22.4, CH_2	3.57, *dd* (15.2, 5.5)	24.2, CH_2	3.54, *dd* (15.2, 5.8)
b		3.26, *dd* (15.2, 8.3)		3.25, *dd* (15.2, 8.4)
11	52.4, CH	4.12, *dt* (8.3, 5.5)	52.4, CH	4.11, *dt* (8.3, 5.6)
13	168.9, CO	-	169.2, CO	-
14	125.5, C	-	125.5, C	-
15	135.7, C	-	135.9, C	-
17	172.0, CO	-	172.1, CO	-
18	121.0, CH	7.06, *d* (8.0)	121.2, CH	7.03, *d* (7.5)
19	133.1, CH	7.50, *ddd* (8.0, 8.0, 1.5)	133.1, CH	7.46, *ddd* (7.7, 7.7, 1.6)
20	125.2, CH	7.24, *dd* (8.0, 8.0)	125.1, CH	7.21, *ddd* (7.9, 7.9, 1.6)
21	131.4, CH	7.91, *dd* (8.0, 1.5)	131.3, CH	7.88, *dd* (7.9, 1.6)
1′	44.2, CH_2	4.63, *d* (6.8)	-	-
2′	119.9, CH	5.35, *m*	-	-
3′	136.4, C	-	-	-
4′	25.6, CH_3	1.74, *s*	-	-
5′	18.1, CH_3	1.80, *s*	-	-
NH-1	-	-	-	8.17, *d* (1.3)
NH-12	-	7.03, *d* (5.5)	-	7.30, *brd* (6.6)
NH-16	-	9.03, *s*	-	9.12, *s*

3.1.9.5. (11 a*S*)-2, 3-dihydro-1*H*-pyrrolo [2, 1-*c*] [1, 4] benzodiazepine-5, 11 (10 *H*, 11 a*H*)-dione (NG 6)

NG 6 was isolated as a yellow viscous mass and its molecular formula $C_{12}H_{12}N_2O_2$ was established on the basis of the (+)-HRESIMS *m/z* 217.0992 $[M+H]^+$ (calculated 217.0977), indicating eight degrees of unsaturation. The ^{13}C NMR spectrum (Table 20) exhibited 12 carbon signals which, through DEPTs and HSQC spectra, can be classified as two amide carbonyls (δ_C 170.8 and 164.6), two quaternary sp^2 (δ_C 136.4 and 126.6), four methine sp^2 (δ_C 132.1, 130.3, 123.9 and 121.3), one methine sp^3 (δ_C 56.2) and three methylene (δ_C 46.9, 25.8 and 23.1) carbons.

The ^1H NMR spectrum together with HSQC spectrum (Table 20) showed the proton signals at δ_H 7.78, *dd* (*J* = 7.9, 1.6 Hz), 7.51, *ddd* (*J* = 8.0, 7.3, 1.7 Hz), 7.22, *ddd* (*J* = 7.8, 7.8, 1.1 Hz), 7.13, *dd* (*J* = 8.1, 0.8 Hz), δ_H 4.11, *dd* (*J* = 7.2, 2.1 Hz), multiplets at δ_H 3.60, 3.45, 2.50, 1.96, 1.93, 1.82 and a singlet of amide proton at δ_H 10.50.

Table 20. ^{1}H and ^{13}C NMR (DMSO, 300.13 and 75.47 MHz) and HMBC assignment for **NG 6**

Position	δ_C, type	δ_H, (*J* in Hz)	COSY	HMBC
1	121.3, CH	7.13, *dd* (8.1, 0.8)	H-2	C-3, 5, 6
2	132.1, CH	7.51, *ddd* (8.0, 7.3, 1.7)	H-1, 3	C-2, 4
3	123.9, CH	7.22, *ddd* (7.8, 7.8, 1.1)	H-2, 4	C-1, 5
4	130.3, CH	7.78, *dd* (7.9, 1.6)	H-3	C-2, 6, 14
5	126.6, C	-	-	-
6	164.6, CO	-	-	-
8a	46.9, CH_2	3.60, *m*	H-9	-
b		3.45, *m*	-	C-9
9a	23.1, CH_2	1.93, *m*	H-8, 10	-
b		1.82, *m*	-	C-10
10a	25.8, CH_2	2.50, *m*	H-11	-
b		1.96, *m*	-	C-9
11	56.2, CH	4.11, *dd* (7.2, 2.1)	H-10	C-9, 10
12	170.8, CO	-	-	-
14	136.4, C	-	-	-
NH-13	-	10.50, *s*	-	C-1, 5, 11, 12

Similar to **NG 5**, the presence of the 3,4-dihydro-1*H*-1,4-benzodiazepine-2,5-dione was evidenced by the COSY correlations from the *dd* at δ_H 7.13 (*J* = 8.1, 0.8 Hz, H-1; δ_C 121.3) through the *ddd* at δ_H 7.51 (*J* = 8.0, 7.3, 1.7 Hz, H-2; δ_C 132.1), the *ddd* at δ_H 7.22 (*J* = 7.8, 7.8, 1,1 Hz, H-3; δ_C 123.9) to the *dd* at δ_H 7.78 (*J* = 7.9, 1.6 Hz, H-4; δ_C 130.3) and by the HMBC correlations from the singlet of the amide group (N13-H) at δ_H 10.50 to the carbonyl carbon at δ_C 170.8 (C-12), the quaternary sp^2 carbon at δ_C 126.6 (C-5), the methine sp^3 carbon at δ_C 56.2 (C-11) and C-1 as

well as from H-4 to the carbonyl carbon at δ_C 164.6 (C-6), the sp^2 quaternary carbon at δ_C 136.4 (C-14) and C-2.

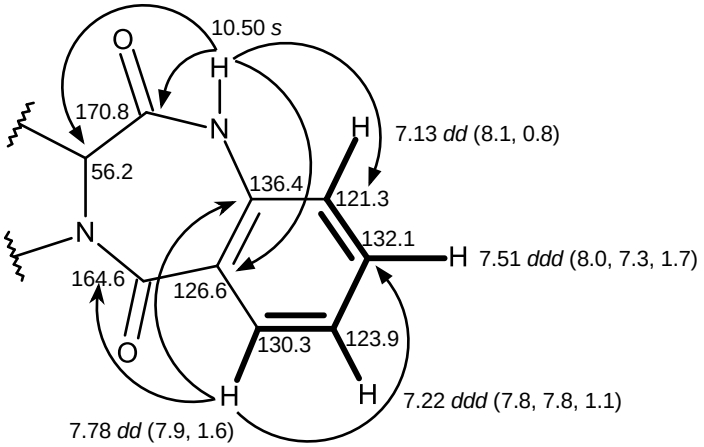

Contrary to **NG 5**, the ^{1}H NMR spectrum of **NG 6** did not display the proton signals of the indole moiety. Instead, it exhibited several multiplets of aliphatic protons belonging to four methylene groups. The COSY spectrum revealed correlations from the mutually coupled multiplets at δ_H 3.45 and 3.60 (H_2-8; δ_C 46.9) through the mutually coupled multiplets at δ_H 1.82 and 1.93 (H_2-9; δ_C 23.1) and the mutually coupled multiplets at δ_H 1.96 and 2.50 (H-10; δ_C 25.8) to the *dd* at δ_H 4.11 (*J* = 7.2, 2.1 Hz, H-11; δ_C 56.2). Taking into account the COSY correlation and the chemical shift value of C-8 (δ_C 46.9), another part portion of **NG 6** was a 1, 2-disubstituted pyrrolidine.

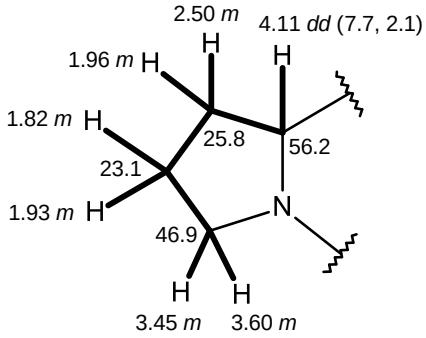

That the pyrrolidine ring was fused to 3,4-dihydro-1*H*-1,4-benzodiazepine-2,5-dione moiety through C-11 and N-7, was confirmed by the HMBC correlation from H-11 to C-9 and C-10 as well as by the lack of proton on N-7.

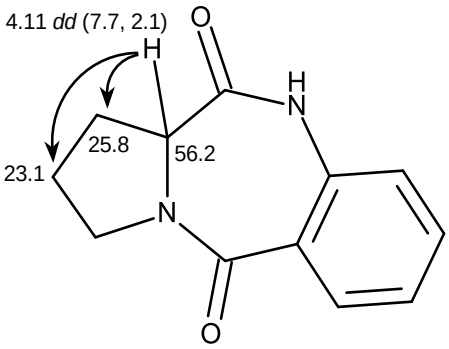

The HRMS, ^{1}H and ^{13}C NMR data of **NG 6** were compatible with the structure of 2, 3-dihydro-1*H*-pyrrolo [2,1-c][1,4] benzodiazepine-5,11(10*H*,11a*H*)-dione. However, the compound called (11a*S*)-2, 3-dihydro-1*H*-pyrrolo [2,1-c] [1,4] benzodiazepine-5,11(10*H*, 11a*H*)-dione, whose absolute configuration of C-11 is *S*, was obtained by cyclocondensation of L-proline with isatoic acid anhydride has been already described by Sorra *et al*. (2012) (Molecules 17, 8762-8772, 2012).

In order to verify if **NG 6** was the same compound as that reported by Sorra *et al*. (2012), the optical rotation of **NG 6** ($[\alpha]_D^{20}$ = + 205.88) was measured. Since both **NG 6** and (11a*S*)-2, 3-dihydro-1*H*-pyrrolo [2, 1-c] [1, 4] benzodiazepine-5, 11 (10*H*, 11a*H*)-dione were dextrorotatory, we concluded that they are the same compound, i.e. the absolute configuration of C-11 is *S*. This compound was also isolated from the fungus *Myrothecium verrucaria*, which was collected from lake water of Chenghai, China (Zhang *et al*., 2017).

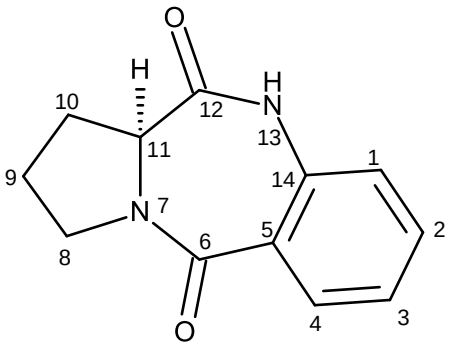

Figure 96. Structure of (11 a*S*) 2, 3-dihydro-1*H*-pyrrolo [2,1-*c*] [1,4] benzodiazepine-5,11 (10 *H*, 11a *H*)-dione (**NG 6**)

3.1.10 Structure Elucidation of Indolyl Quinazolinone Alkaloids

3.1.10.1. 3′-(4-oxoquinazolin-3-yl) [1*H*-indole-3, 5′-oxolone]-2, 2′-dione (NTK 5)

NTK 5 was isolated as a white solid (mp, 266-268 ºC) and its molecular formula $C_{19}H_{13}N_3O_4$, was established based on the (+) HRESIMS m/z 348.0968 $[M+H]^+$ peak indicating fifteen degrees of unsaturation. The ^{13}C NMR spectra (Table 21), in combination with DEPTs and HSQC spectra, revealed the presence of nineteen carbon signals, which were categorized as three carbonyls (δ_C 175.2, 171.7 and 159.7), four quaternary sp^2 (δ_C 147.5, 142.6, 126.2 and 121.2), nine methine sp^2 (δ_C 147.6, 135.0, 131.5, 127.5, 127.3, 126.0, 125.1, 122.9 and 110.6), one quaternary sp^3 (δ_C 80.7), one methine sp^3 (δ_C 56.3) and one methylene sp^3 (δ_C 33.3).

The ^1H NMR spectrum together with the HSQC spectrum (Table 21) displayed the signals for eight aromatic protons at δ_H 8.24, *dd* (*J* = 8.0, 1.2 Hz), 7.92, *ddd* (*J* = 7.7, 7.6, 1.5 Hz), 7.76, *d* (*J* = 7.7 Hz), 7.66, *d* (*J* = 6.8 Hz), 7.64, *ddd* (*J* = 7.5, 7.5, 1.1 Hz), 7.41, *ddd* (*J* = 7.7, 7.7, 1.3 Hz), 7.18, *ddd* (*J* = 7.5, 7.5, 0.9 Hz), 6.96, *d* (*J* = 7.7 Hz), methine sp^2 proton at δ_H 8.63, *s*, methine sp^3 proton at δ_H 5.86, *t* (*J* = 10.1 Hz) and methylene proton at δ_H 3.01, *d* (*J* = 10.4 Hz).

Table 21. ^{1}H and ^{13}C NMR (DMSO, 300.13 and 75.47 MHz) and HMBC assignment for **NTK 5**

Position	δ_C, type	δ_H, (*J* in Hz)	COSY	HMBC
2	175.2, CO	-	-	-
3	80.7, C	-	-	-
3a	126.2, C	-	-	-
4	125.1, CH	7.66, *d* (6.8)	H-5	C-6, 7a
5	122.9, CH	7.18, *ddd* (7.5, 7.5, 0.9)	H-4, 6	C-3a, 7
6	131.5, CH	7.41, *ddd* (7.7, 7.7, 1.3)	H-5, 7	C-4, 7a
7	110.6, CH	6.96, *d* (7.7)	H-6	C-3a, 5
7a	142.6, C	-	-	-
2′	171.7, CO	-	-	-
3′	56.3, CH	5.86, *t* (10.1)	H-4	C-2′, 2″, 4′, 4″
4′	33.3, CH_2	3.01, *d* (10.4)	H-3′	C-2, 2′, 3, 3′, 3a
2″	147.6, CH	8.63, *s*	-	C-3′, 4″, 8″a
4″	159.7, CO	-	-	-
4″a	121.2, C	-	-	-
5″	126.0, CH	8.24, *dd* (8.0, 1.2)	H-6″	C-4″, 7″, 8″a
6″	127.5, CH	7.64, *ddd* (7.5, 7.5, 1.1)	H-5″, H-7″	C-4″a, 8″
7″	135.0, CH	7.92, *ddd* (7.7, 7.6, 1.5)	H-6″	C-5″, 8″a
8″	127.3, CH	7.76, *d* (7.7)	H-7″	C-4″a, 6″
8″a	147.5, C	-	-	-
NH-1	-	10.90, *s*	-	C-2, 3, 3a, 7a

That **NTK 5** contained a 1, 3-dihydro-2*H*-indol-2-one ring system was substantiated by the COSY correlations from the doublet at δ_H 7.66 (*J* = 6.8 Hz, H-4; δ_C 125.1) through the *dd* at δ_H 7.18 (*J* = 7.5, 7.5, 0.9, H-5; δ_C 122.9), the *ddd* at δ_H 7.41 (*J* = 7.7, 7.7, 1.3 Hz; H-6; δ_C 131.5) and the *d* at δ_H 6.96 (*J* = 7.7 Hz, H-7,

δ_C 110.6) as well as the HMBC correlations from H-4 to C-6 and the carbon at δ_C 142.6 (C-7a), from H-5 to C-7 and the carbons at δ_C 126.2 (C-3a), and from the singlet of the amine proton at δ_H 10.90 (NH-1) to C-7a, the carbonyl carbon at δ_C 175.2 (C-2) and the oxyquaternary carbon at 80.7 (C-3) and C-3a, indicated that the 1, 2-disubstituted benzene ring was part of the indole moiety.

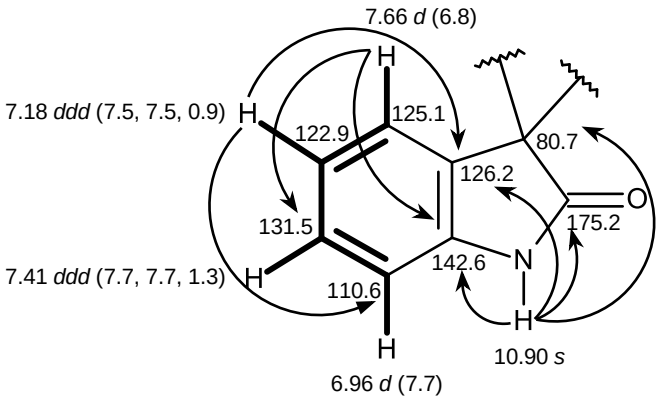

That another of the molecule was a substituted quinazolin-4(3*H*)-one was supported by the existence of the 1, 2 disubstituted benzene ring was evidenced by COSY relations from the *dd* at δ_H 8.24 (*J* = 8.0, 1.2, H-5′′, δ_C 126.0) through the *ddd* at δ_H 7.64 (*J* = 7.5, 7.5, 1.1 Hz, H-6′′, δ_H 127.5), a *ddd* at δ_H 7.92 (*J* = 7.7, 7.6, 1.5 Hz, H-7′′; δ_C 135.0) and a doublet at δ_H 7.76 (*J* = 7.7 Hz; H-8′′; δ_C 127.3) as well as the HMBC correlations from H-5′′ to the carbonyl carbon at δ_C 159.7 (C-4′′) and the quaternary sp^2 carbon at δ_C 147.5 (C-8′′a), and from the singlet of the imine proton at δ_H 8.63 (H-2′′) to C-4′′ and C-8′′a.

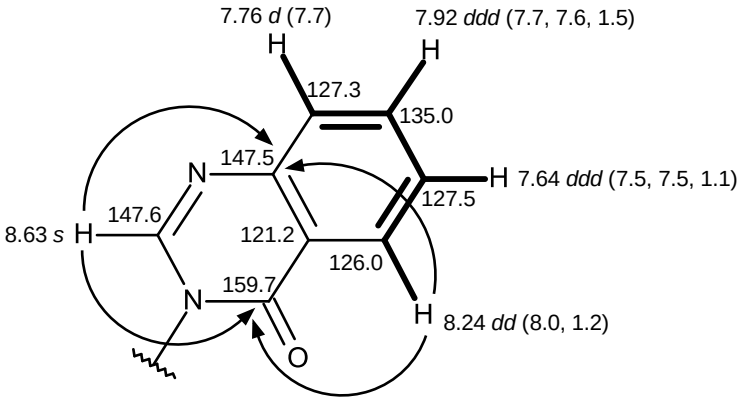

That the *N*-substituted quinazolin-4-one moiety was connected to the 1,3-dihydro-2*H*-indol-2-one ring system, through the spirolactone ring was based not only on the COSY correlation from the triplet at δ_H 5.86 (*J* = 10 Hz, H-3′, δ_C 56.5) to the multiplet at δ_H 3.01 (H_2-4′, δ_C 33.3) but also on the HMBC correlations from H-3′ to C-2′′, C-4′′, C-4′ and the lactone carbonyl at δ_C 171.7 (C-2′), as well as from H-4′ to C-2, C-3a.

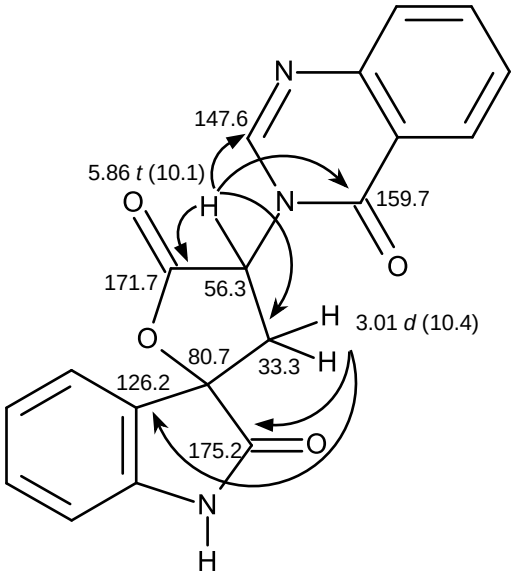

Extensive literature search revealed that the ^{1}H and ^{13}C NMR, chemical shift values and the optical rotation of **NTK 5** ($[\alpha]_D^{20}$ = + 19.7) were compatible with those reported for 3′-(4-oxoquinazolin-3-yl) [1*H*-indole-3,5′-oxolone]-2, 2′-dione, a new natural products previously reported from the soil fungus *Neosartorya siamensis* KUFC 6349 (Buttachon *et al*., 2012), coral-derived fungus *Neosartorya laciniosa* (Eamvijarn *et al*., 2013) and marine sponge-associated fungus Neosartorya paulistensis KUFC 7897 (Gomes *et al*., 2014).

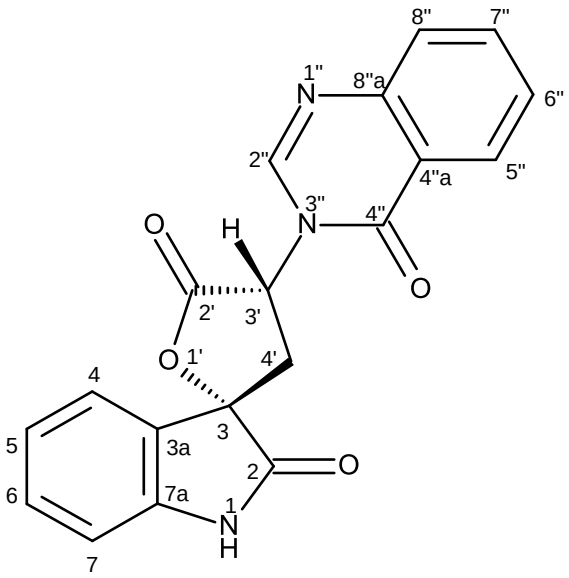

Figure 97. Structure of 3′-(4-oxoquinazolin-3-yl) [1*H*-indole-3, 5′-oxolone]-2, 2′-dione (**NTK 5**)

3.1.10.2. Tryptoquivaline F (NTK 6)

NTK 6 was isolated as a white solid (mp, 278-280 ºC) and its molecular formula $C_{22}H_{18}N_4O_4$, established on the basis of the (+)-HRESIMS m/z 403.1399 $[M+H]^+$ (calculated 403.1406) indicating the sixteen degrees of unsaturation.

The ^{13}C NMR (Table 22) displayed twenty seven carbons signals which was classified, according to DEPTs and HSQC spectra, as three carbonyls (δ_C 176.7, 170.7 and 159.6), four quaternary sp^2 (δ_C 147.5, 140.7, 131.7 and 121.3), nine methine sp^2 (δ_C 147.5, 134.9, 131.5, 127.5, 127.3, 126.0, 125.8, 125.3 and 116.9), three methine sp^3 (δ_C 84.4, 59.3 and 56.8), one quaternary sp^3 (δ_C 86.1), one methylene sp^3 (δ_C 30.9) and one methyl (δ_C 17.4) carbons.

The ^1H NMR spectrum, in conjunction with the HSQC spectrum revealed the presence of eight aromatic protons at δ_H 8.22, *dd* (*J* = 8.0, 1.1 Hz), 7.92, *ddd* (*J* = 7.7, 7.7, 1.5 Hz), 7.76, *d* (*J* = 8.1 Hz), 7.70, *d* (*J* = 7.3 Hz), 7.63, *ddd* (*J* = 7.6, 7.6, 1.1 Hz), 7.58, *ddd* (*J* = 7.6, 7.6, 1.2 Hz), 7.48, *d* (*J* = 7.3 Hz), 7.39, *ddd* (*J* = 7.5, 7.5, 1.2 Hz) and three methine sp^3 protons at δ_H 5.69, *t* (*J* = 10.0 Hz), 5.51, *d* (*J* = 8.4 Hz), 3.64, *q* (*J* = 7.0 Hz), two methylene protons at δ_H 2.89, *dd* (*J* = 13.1, 9.3 Hz) and 3.43, *dd* (*J* = 13.0, 11.0 Hz), one methyl group (3H) at δ_H 1.39, *d* (*J* = 7.6 Hz), a singlet of imine proton at δ_H 8.56 and the other amine proton at δ_H 3.91, *dd* (*J* = 7.6, 7.6 Hz).

The ^{1}H and ^{13}C NMR spectra of **NTK 6** (Table 22) revealed the presence of the same substituted quinazolin-4(3*H*)-one moiety as that of **NTK 5**, as evidenced by the COSY correlations from the *dd* at δ_H 8.22 (*J* = 8.0, 1.1, H-20; δ_C 126.0) through the *ddd* at δ_H 7.63 (*J* = 7.6, 7.6, 1.1 Hz; H-21, δ_C 127.5), the *ddd* at δ_H 7.92 (*J* = 7.7, 7.7, 1.5 Hz; H-22; δ_C 134.9) and *dd* at δ_H 7.76 (*J* = 8.1 Hz; H-23, δ_C 127.3) as well as the HMBC correlations from H-20 to C-22, the carbons at δ_C 147.5 (C-24) and 159.6 (CO-18), from the imine singlet at δ_H 8.56 to C-24 and C-18.

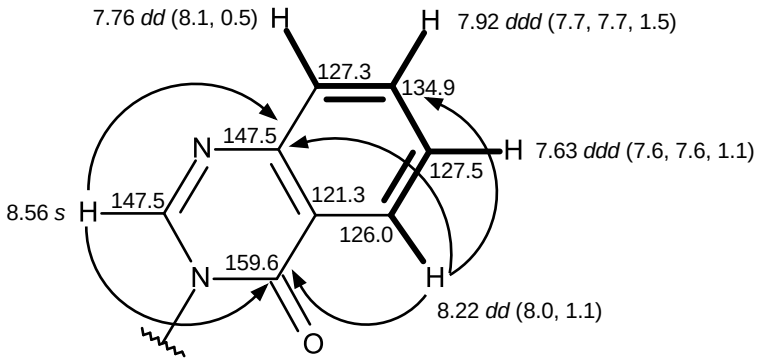

Contrary to **NTK 5**, another 1, 2-disubstituted benzene ring was part of the 6-5-5-2-methyl imidazoindol-3-one ring system. This was supported by the COSY correlations from the *d* at δ_H 7.70 (*J* = 7.3 Hz, H-5; δ_C 125.3) through the *ddd* at δ_H 7.39 (*J* = 7.5, 7.5, 1.2 Hz, H-6; δ_C 125.8), the *ddd* at δ_H 7.58 (*J* = 7.6, 7.6, 1.2 Hz, H-7; δ_C 131.5) and the doublet at δ_H 7.48 (*J* = 7.3 Hz, H-8; δ_C 116.9), from the *dd* of the amine proton of the imidazolone ring at δ_H 3.91 (*J* = 7.6, 7.6 Hz; N16-H) to the a doublet at 5.51 (*J* = 8.4; H-2) and a quartet at δ_H 3.64 (*J* = 7.0 Hz) as well as by the HMBC correlations from H-8 to C-6 and the carbon at δ_C 131.7 (C-4), from H-5 to

C-7 and the carbons at δ_C 140.7 (C-9) and 86.1 (C-3), from H-2 to C-3, the carbons at δ_C 176.7 (C-14) and 59.3 (C-15) and from the methyl doublet at δ_H 1.39 (*J* = 7.6) to C-14 and C-15.

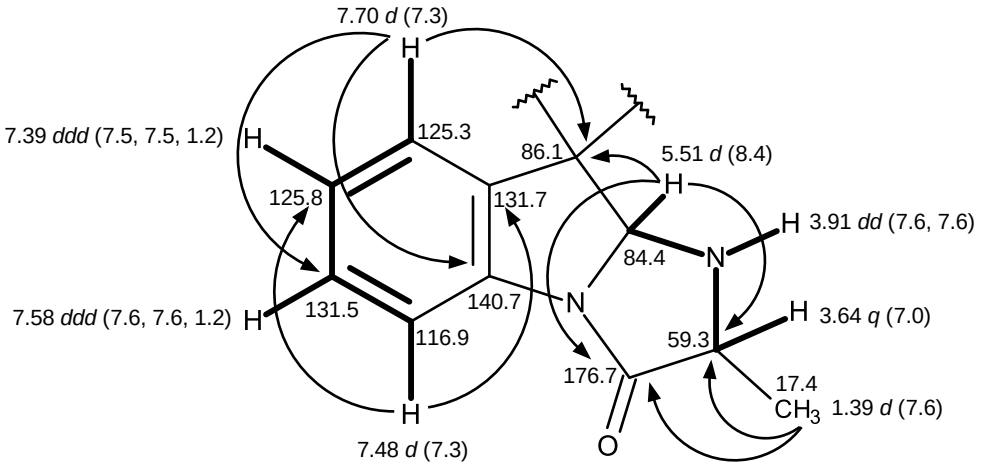

That the 6-5-5-2-methyl imidazoindol-3-one ring system was connected to the substituted quinazolin-4(3*H*)-one moiety through a spirolactone ring was corroborated by the COSY correlations from the triplet at δ_H 5.69 (*J* = 10.0 Hz) to the two methylene doublets at δ_H 2.89 (*J* = 13.1, 9.3 Hz) and 3.43 (*J* = 13.0, 11.0 Hz, δ_C 30.9) as well as the HMBC correlations from H-12 to C-11, C-13 and C-18, from H-16 to C-3, and from H-26 to C-12, C-18 and C-24.

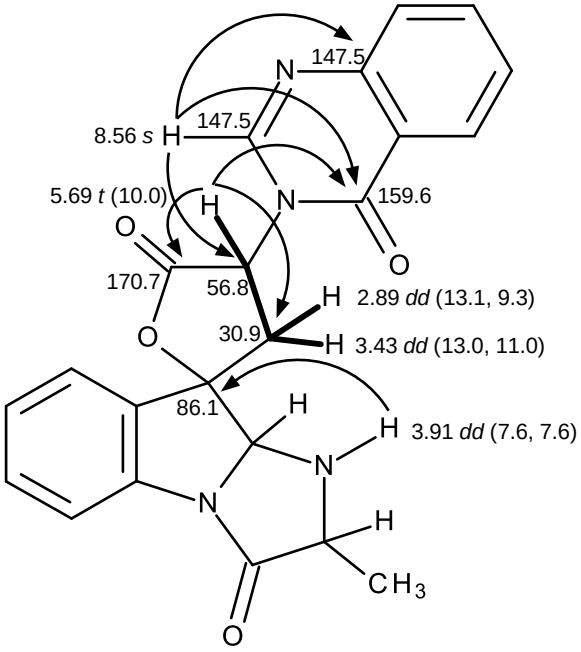

Therefore the flat structure of **NTK 6** was the same as that of tryptoquivaline F. Since, **NTK 6** has four stereogenic centers, i. e. C-2, C-3, C-12 and C-15, it was necessary to establish the absolute configurations of these carbons. Comparison of the ^{1}H and ^{13}C chemical shift values of H-2/C-2, H-3/C-3, H-12/C-12 and H-15/C-15 and the optical rotation of **NTK 6** ($[\alpha]_D^{20}$ = – 120.0) with those of tryptoquivaline F, it was concluded that they are the same compound.

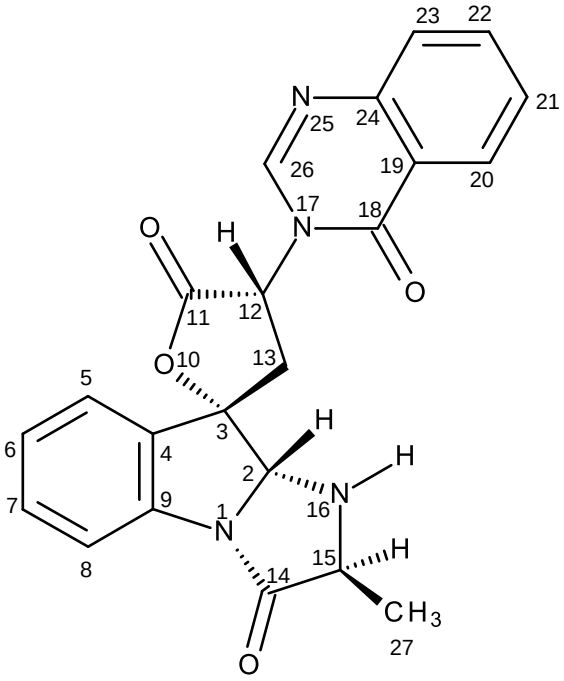

Figure 98. Structure of tryptoquivaline F (**NTK 6**)

3.1.10.3. Tryptoquivaline H (NTK 7)

NTK 7 was isolated as a white solid (mp, 246-248 ºC) and its molecular formula $C_{22}H_{18}N_4O_5$, established on the basis of the (+) HRESIMS *m/z* 419.13496 $[M+H]^+$, indicating sixteen degrees of unsaturation. The general features of the ^1H and ^{13}C NMR of **NTK 7** were very similar to those of **NTK 6**.

However, H-2 of **NTK 7** appeared as a singlet at δ_H 5.43 instead of a doublet at δ_H 5.51 (J = 8.4 Hz). Moreover, CH_3-27 (δ_C 10.6) resonated at lower chemical shift values than the tryptoquivaline F (δ_C 17.4) while C-15 exhibited higher chemical shift

value (δ_C 67.4) than the corresponding carbon (δ_C 59.3) of tryptoquivaline F (Table 22). Thus the different between the **NTK 6** and **NTK 7**, except for only one oxygen atom more than compound **NTK 6**, i.e the N16-OH was replaced by N16-H which was confirmed by the molecular formula of **NTK 7** ($C_{22}H_{18}N_4O_5$).

Analysis of the ^1H, ^{13}C NMR, HSQC and COSY spectra revealed the presence of two 1, 2-disubstituted benzene rings, similar to those found in **NTK 6**. The HMBC correlations between the signals of H-26 (δ_H 8.55, *s*) and C-18 (δ_C 159.8), C-24 (δ_C 147.5) as well as between the signals of H-20 (8.24 *dd*, *J* = 8.0, 1.2 Hz) and C-18, C-22 (δ_C 134.9), C-24, permitted identification of the *N*-substituted quinazolin-4-one. The quinazolinone moiety was connected to the 6-5-5 *gem*-dimethyl imidazoindolone ring system *via* a 5-membered spirolactone, similar to that of tryptoquivaline F (**NTK 6**). Thus, the structure of **NTK 7** could also correspond to the previously reported tryptoquivaline E or H (Yamazaki *et al*., 1978). However, the chemical shift of H-12 (δ_H 5.58, *t*, *J* = 10.0 Hz) of **NTK 7** was more similar to that of H-12 (δ_H 5.69, *t*, *J* = 10.0 Hz) of tryptoquivaline H than H-12 (δ_H 6.20, *t*, *J* = 10 Hz) of tryptoquivaline E.

The flat structure of **NTK 7** was the same as that of tryptoquivaline H. In order to verify if **NTK 7** was the same as tryptoquivaline H, we have measure the optical rotation of **NTK 7** ($[\alpha]_D^{20}$ = – 20.1), which was levoratory like that of tryptoquivaline H. Therefore, **NTK 7** was identified as tryptoquivaline H.

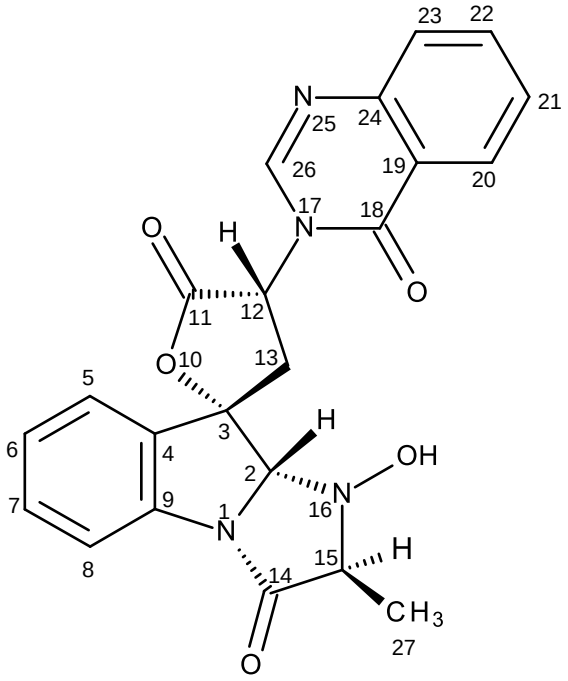

Figure 99. Structure of tryptoquivaline H (**NTK 7**)

3.1.10.4. Tryptoquivaline L (NTK 8)

NTK 8 was isolated as a white solid (mp, 262-264 ºC), exhibited the $[M+H]^+$, peak at *m/z* 433.1509 (HRESIMS), corresponding to $C_{23}H_{21}N_4O_5$, indicating the sixteen degrees of unsaturation. The general features of the ^1H and ^{13}C NMR of **NTK 8** were very similar to those of **NTK 7**, except for the appearance of the signals of the quaternary sp^3 carbon at δ_C 70.3 and methyl carbon at δ_C 22.7 in ^{13}C NMR spectrum and an additional methyl singlet at δ_H 1.26 in ^1H NMR spectrum.

The ^{1}H NMR and COSY spectra (Table 23) revealed the presence of two 1, 2-disubstituted benzene rings of the *gem*-dimethyl imidazoindolone ring system and quinazolin-4 (3*H*)-one moiety as well as the protons of the five-membered spirolactone ring, similar to those of tryptoquivaline H (**NTK 7**). Analysis of the ^{1}H, ^{13}C NMR, COSY, HSQC and HMBC spectra revealed a similarity between the structures of compounds **NTK 7** and **NTK 8**, expect for two methyl substituted groups instead of one methyl group on C-15 of the imidazolone ring in **NTK 7**.

Consequently, it could correspond to the previously reported tryptoquivaline G (Yamazaki *et al*., 1978) or its C-12 epimer, tryptoquivaline L (Yamazaki *et al*., 1979). Comparison of the ^{1}H NMR data of **NTK 8** with those of tryptoquivaline G and L (Yamazaki *et al*., 1978; Yamazaki *et al*., 1979), it was obvious that the chemical shift values of H-12 (δ_H 5.59, *t*, *J* = 10.0 Hz), H_3 -27 (δ_H 1.35, *s*) and H_3-28 (δ_H 1.26, *s*) of compound **NTK 8** were more similar to those of H-12 (δ_H 5.57, *t*, *J* = 10.0 Hz), H_3-27 (δ_H 1.36, *s*) and H_3-28 (δ_H 1.26, *s*) of tryptoquivaline L than those of corresponding protons of tryptoquivaline G (respectively, δ_H 6.16, *t*, *J* = 10 Hz, δ_H 1.35, *s* and δ_H 1.30, *s*). Comparison of the ^{1}H and ^{13}C NMR data, chemical shift values and the optical rotation of **NTK 8** ($[\alpha]_D^{20}$ = – 30.5) which is compatible with those of tryptoquivaline L, it was concluded that they are the same compound.

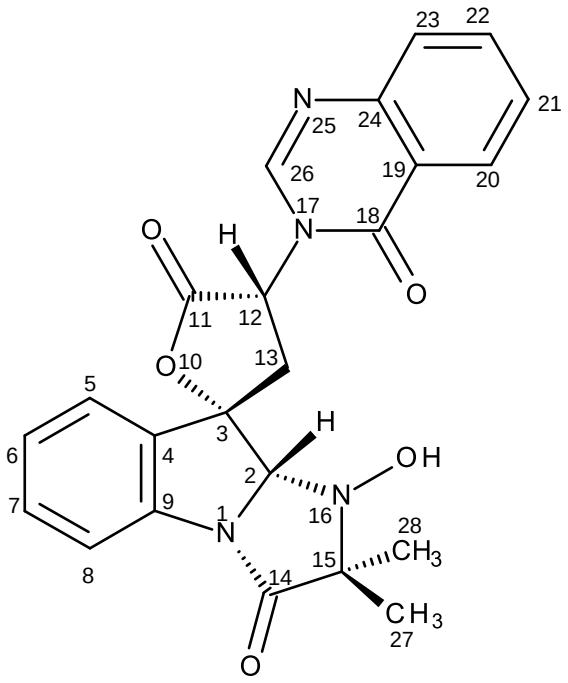

Figure 100. Structure of tryptoquivaline L (**NTK 8**)

Tryptoquivalines, L, H and F have been previously reported from the fungus *Aspergillus fumigatus* (Yamazaki *et al*., 1978; Yamazaki *et al*., 1979). However, Buttachon *et al*. (2012) has isolated tryptoquivaline L, H, F and other analogs from the soil fungus *Neosartorya siamenisis* KUFC 6349 and have corrected the stereochemistry of the stereogenic carbons which were previously incorrectly assigned. Tryptoquivaline L, H and F were also isolated from marine sponge-associated fungus *Neosartorya paulistensis* KUFC 7897 (Gomes *et al*., 2014), as well as tryptoquivaline L, which was isolated from the marine-derived fungus *Neosartorya laciniosa* (KUFC 7896) (Eamvijarn *et al*., 2013).

3.1.10.5. Tryptoquivaline U (NTK 9)

NTK 9 was isolated as white crystals (mp, 208-209 °C), and its molecular formula $C_{23}H_{21}N_4O_4$ was established on the basis of (+)-HRESIMS at *m/z* 417.1563 (calculated 417.1563), indicating sixteen degrees of unsaturation. The ^{1}H and ^{13}C NMR spectra (Table 23) of **NTK 9** resembled those of tryptoquivaline L (**NTK 8**). The ^{13}C NMR, DEPTs and HSQC spectra displayed signals of three carbonlys (δ_C 176.0, 170.7 and 159.6), four quaternary sp^2 (δ_C 147.5, 139.8, 132.0 and 121.4), nine methine sp^2 (δ_C 147.4, 135.0, 131.6, 127.6, 127.3, 126.1, 125.7 (2C) and 116.2), two quaternary sp^3 (δ_C 84.7 and 64.6), two methine sp^3 (δ_C 82.0 and 56.9), one methylene sp^3 (δ_C 31.6) and two methyl (δ_C 26.9 and 26.5) carbons.

The ^{1}H NMR and COSY spectra revealed the presence of two 1, 2-disubstituted benzene rings of the *gem*-dimethyl imidazoindolone ring system and quinazolin-4 (3*H*)-one moiety as well as the protons of the five-membered spirolactone ring, similar to those of tryptoquivaline L (**NTK 8**). However, contrary to tryptoquivaline L, H-2 of **NTK 9** appeared as a doublet at δ_H 5.55 (*J* = 8.4 Hz) instead of a singlet at δ_H 5.25. Moreover, the COSY spectrum exhibited a correlation between H-2 signal and a doublet at δ_H 3.76 (*J* = 8.4 Hz). Consequently, this signal was attributed to NH-16. Interestingly, both CH_3-27 (δ_C 26.5) and CH_3-28 (δ_C 26.9) resonated at higher chemical shift values than their counterparts in tryptoquivaline L (δ_C 16.2 and 22.7) while C-15 exhibited lower chemical shift value (δ_C 64.6) than the corresponding carbon (δ_C 70.0) of tryptoquivaline L. Thus, the only difference

between the structure of **NTK 9** and **NTK 8** is the presence of a hydrogen atom on N-16 instead of a hydroxyl group. This was supported by the molecular formula of **NTK 9** ($C_{23}H_{20}N_4O_4$), which has one oxygen atom less than tryptoquivaline L (**NTK 8**). Since **NTK 9** furnished suitable crystals, an X-ray analysis undertaken. The ORTEP view of **NTK 9** depicted in Figure 101 revealed that the absolute configurations of the stereogenic carbons of C-2, C-3 and C-12 are *S*, *S* and *R*, the same as that of the corresponding carbons of tryptoquivaline L (**NTK 8**).

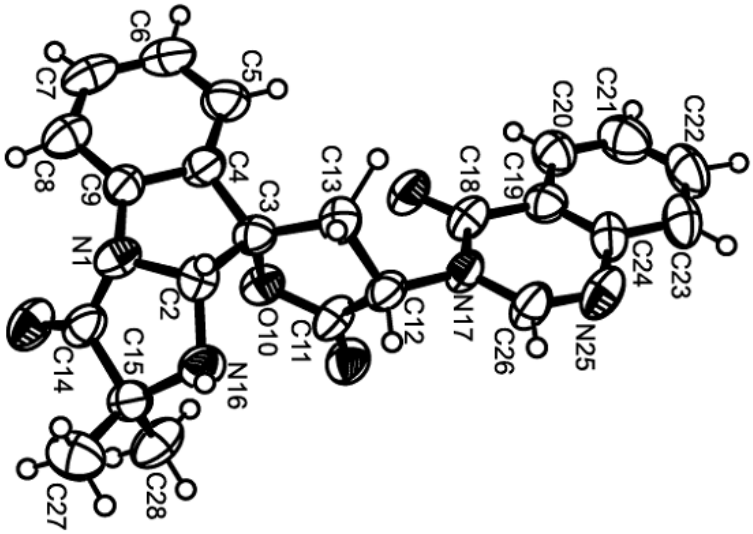

Figure 101. ORTEP view of **NTK 9**

NTK 9 was also levorotatory and it was established as a new analog of tryptoquivalines, which have named tryptoquivaline U.

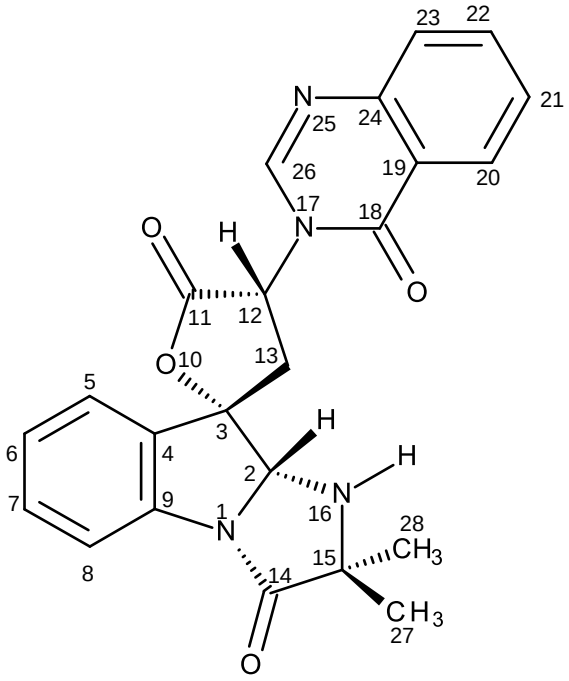

Figure 102. Structure of tryptoquivaline U (**NTK 9**)

Table 22. Comparison of ^{1}H and ^{13}C NMR (DMSO, 300.13 MHz and 75.47 MHz) assignment for **NTK 6** and **NTK 7**

Position	NTK 6		NTK 7	
	δ_C, type	**δ_H, (J in Hz)**	**δ_C, type**	**δ_H, (J in Hz)**
2	84.4, CH	5.51, *d* (8.4)	88.6, CH	5.43, *s*
3	86.1, C	-	83.7, C	-
4	131.7, C	-	132.4, C	-
5	125.3, CH	7.70, *d* (7.3)	126.0, CH	7.81, *d* (7.5)
6	125.8, CH	7.39, *ddd* (7.5, 7.5, 1.2)	125.5, CH	7.37, *ddd* (7.4, 7.4, 1.3)
7	131.5, CH	7.58, *ddd* (7.6, 7.6, 1.2)	131.9, CH	7.57, *ddd* (7.5, 7.5, 1.1)
8	116.9, CH	7.48, *d* (7.3)	114.9, CH	7.51, *d* (7.0)
9	140.7, C	-	138.2, C	-
11	170.7, CO	-	170.7, CO	-
12	56.8, CH	5.69, *t* (10.0)	56.9, CH	5.58, *t* (10.0)
13	30.9, CH_2	2.89, *dd* (13.1, 9.3) 3.43, *dd* (13.0, 11.0)	33.8 CH_2	3.05, *dd* (13.2, 9.3) 3.46, *dd* (13.0, 11.0)
14	176.7, CO	-	169.9, CO	-
15	59.3, CH	3.64, *q* (7.0)	67.4, CH	4.01, *q* (7.0)
18	159.6, CO	-	159.8, CO	-
19	121.3, C	-	121.4, C	-
20	126.0, CH	8.22, *dd* (8.0, 1.1)	126.2, CH	8.24, *dd* (8.0, 1.2)
21	127.5, CH	7.63, *ddd* (7.6, 7.6, 1.1)	127.7, CH	7.64, *ddd* (7.6, 7.6, 1.0)
22	134.9, CH	7.92, *ddd* (7.7, 7.7, 1.5)	135.1, CH	7.92, *ddd* (7.7, 7.7, 1.5)
23	127.3, CH	7.76, *d* (8.1)	127.4, CH	7.77, *d* (7.7)
24	147.5, C	-	147.5, C	-
26	147.5, CH	8.56, *s*	147.6, CH	8.55, *s*
27	17.4, CH_3	1.39, *d* (7.6)	10.6 CH_3	1.44, *d* (7.1)
28	-	-	-	-
NH-16	-	3.91, *dd* (7.6, 7.6)	-	-
OH-16	-	-	-	8.80, *s*

Table 23. Comparison of ^{1}H and ^{13}C NMR (DMSO, 300.13 MHz and 75.47 MHz) assignment for **NTK 8** and **NTK 9**

Position	**NTK 8**		**NTK 9**	
	δ_C, type	**δ_H, (*J* in Hz)**	**δ_C, type**	**δ_H, (*J* in Hz)**
2	86.1, CH	5.25, *s*	82.0, CH	5.55, *d* (8.4)
3	83.4, C	-	84.7, C	-
4	132.3, C	-	132.0, C	-
5	125.9, CH	7.83, *d* (7.5)	125.7, CH	7.71, *d* (7.3)
6	125.2, CH	7.36, *ddd* (7.4, 7.4, 1.4)	125.7, CH	7.38, *ddd* (7.5, 7.5, 1.2)
7	131.7, CH	7.56, *ddd* (7.5, 7.5, 1.4)	131.6, CH	7.57, *ddd* (8.1, 7.7, 1.2)
8	114.7, CH	7.50, *d* (7.8)	116.2, CH	7.49, *d* (7.2)
9	138.2, C	-	139.8, C	-
11	170.6, CO	-	170.7, CO	-
12	56.8, CH	5.59, *t* (10.0)	56.9, CH	5.58, *dd* (10.8, 9.1)
13	34.4, CH_2	3.07, *dd* (13.2, 9.3)	31.6, CH_2	2.86, *dd* (12.9, 9.1)
		3.45, *dd* (13.0, 11.0)		3.45, *dd* (12.7, 11.2)
14	171.2, CO	-	176.0, CO	-
15	70.3, C	-	64.6, C	-
18	159.7, CO	-	159.6, CO	-
19	121.3, C	-	121.4, C	-
20	126.0, CH	8.25, *d* (8.0, 1.2)	126.1, CH	8.23, *dd* (8.0, 1.2)
21	127.5, CH	7.64, *ddd* (7.6, 7.6, 1.1)	127.6, CH	7.63, *ddd* (7.6, 7.6, 1.0)
22	134.9, CH	7.93, *ddd* (7.7, 7.7, 1.5)	135.0, CH	7.92, *ddd* (8.2, 8.2, 1.5)
23	127.3, CH	7.77, *d* (7.7)	127.3, CH	7.76, *d* (7.7)
24	147.4, C	-	147.5, C	-
26	147.5, CH	8.57, *s*	147.4, CH	8.49, *s*
27	16.2, CH_3	1.35, *s*	26.5 CH_3	1.45, *s*
28	22.7, CH_3	1.26, *s*	26.9 CH_3	1.24, *s*
NH-16	-	-	-	3.76, *d* (8.4)
OH-16	-	8.80, *s*	-	-

3.1.11 Structure Elucidation of Diketopiperazine Derivatives

3.1.11.1. Fellutanine A (NG 10)

NG 10 was isolated as a yellow viscous mass and its molecular formula $C_{22}H_{20}N_4O_2$, was established on the basis of the (+)-HRESIMS *m/z* 373.1675 $[M+H]^+$, (calculated for $C_{22}H_{21}N_4O_2$, 373.1665), indicating eighteen degrees of unsaturation. Despite twenty two carbon atoms indicated by the HRMS, the ^{13}C NMR spectrum (Table 24) displayed only 11 signals, which were categorized, according to DEPTs and HSQC spectra, as one carbonyl (δ_C 166.7), three quaternary sp^2 (δ_C 136.0, 127.3 and 108.9), five methine sp^2 (δ_C 124.4, 120.8, 118.5, 118.4 and 111.3), one methine sp^3 (δ_C 55.3) and one methylene sp^3 (δ_C 30.0) carbons. Therefore, the molecule should be symmetrical and each carbon signal must correspond to two carbon atoms.

The ^1H NMR spectrum, in conjunction with the HSQC spectrum (Table 24), exhibited three doublets at δ_H 6.59 (*J* = 2.3 Hz; H-2; δ_C 124.4), δ_H 7.35 (*J* = 7.8 Hz, H-4, δ_C 118.4) and δ_H 7.29 (*J* = 8.0 Hz, H-7; δ_C 111.3), two *ddd* at δ_H 6.95, (*J* = 7.4, 7.4, 1.0, H-5; δ_C 118.5), δ_H 7.04 (*J* = 7.5, 7.5, 1.1 Hz, H-6; δ_C 120.8), two mutually coupled *dd* at δ_H 2.72 (*J* = 14.3, 4.1 Hz; H-10; δ_C 30.0) and 2.17 (*J* = 14.3, 6.7, H-10; δ_C 30.0), in addition to two amine doublets at δ_H 10.85 (*J* = 1.7 Hz) and 7.71 (*J* = 2.5).

Table 24. ^{1}H and ^{13}C NMR (DMSO, 300.13 MHz and 75.47 MHz) and HMBC assignment for **NG 10**

Position	δ_C, type	δ_H, (*J* in Hz)	COSY	HMBC
2	124.4, CH	6.59, *d* (2.3)	-	C-3, 8, 9, 10
3	108.9, C	-	-	-
4	118.4, CH	7.35, *d* (7.8)	H-5	C-6, 8
5	118.5, CH	6.95, *ddd* (7.4, 7.4, 1.0)	H-4	C-7, 9
6	120.8, CH	7.04, *ddd* (7.5, 7.5, 1.1)	H-5, 7	C-4, 8, 9
7	111.3, CH	7.29, *d* (8.0)	H-6	C-4, 5, 9
8	136.0, C	-	-	-
9	127.3, C	-	-	-
10a	30.0, CH_2	2.17, *dd* (14.3, 6.7)	H-10b, 11	C-2, 3, 9, 11, 12
b		2.72, *dd* (14.3, 4.1)	H-10a, 11	C-2, 3, 9, 11, 12
11	55.3, CH	3.87, *q* (3.8)	H-10a, 10b	C-12
12	166.7, CO	-	-	-
NH-1	-	10.85, *d* (1.7)	-	C-2, 3, 8, 9
NH-13′	-	7.71, *d* (2.5)	-	C-11, 12

Similar to **NG 5**, the presence of the indolylmethyl moiety was corroborated by the COSY correlation from H-4 through H-5 and H-6, to H-7 as well by the HMBC correlations from the indole amine doublet at δ_H 10.85 (*J* = 1.7 Hz) to the carbons at δ_C 124.4 (C-2), 108.9 (C-3), 127.3 (C-9) and 136.0 (C-8), from H-4 to C-3, C-6, C-8, from H-7 to C-5 and C-9, from H-2 to C-9 and C-10 and from H_2-10 to C-2, C-3 and C-9.

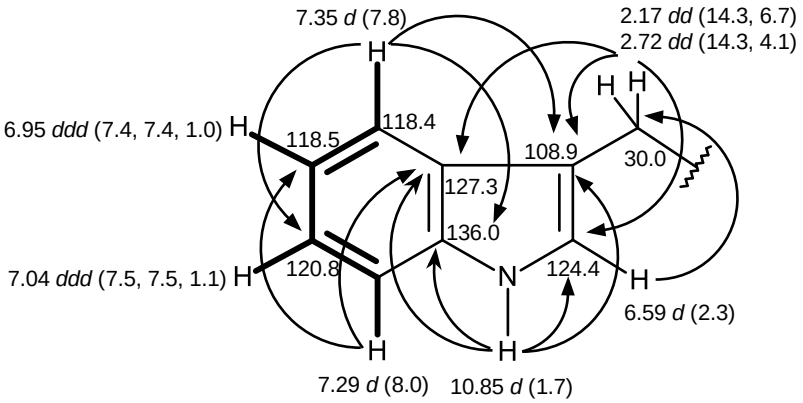

That **NG 10** contained a symmetrical 1, 4-diketopiperazine moiety was corroborated by the coupling system from the doublet of the amide proton (δ_H 7.71, *J* = 2.5 Hz, NH-13′), through the methine quintet at δ_H 3.87 (*J* = 3.8 Hz, H-11; δ_C 55.3) to H_2-10, as observed in the COSY spectrum. This was also supported by the HMBC correlations from NH-13′ to the carbonyl carbon at δ_C 166.7 (C-12) and C-11.

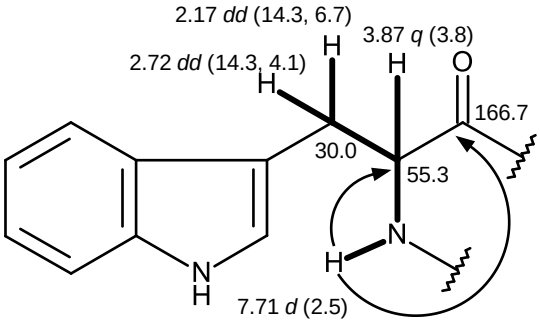

The flat structure of **NG 10** was the same as that of fellutanine A, a secondary metabolite previously reported from *Penicillium fellutanum* by Kozlovsky *et al*. (2000). In order to verify if **NG 10** was the same as fellutanine A, we have measure the optical rotation of **NG 10** ($[\alpha]_D^{20}$ = – 151.5) which as dextrorotatory like that of fellutaine A. Thefore, **NG 10** was identified as fellutanine A or Cyclo (L-Trp-L-Trp).

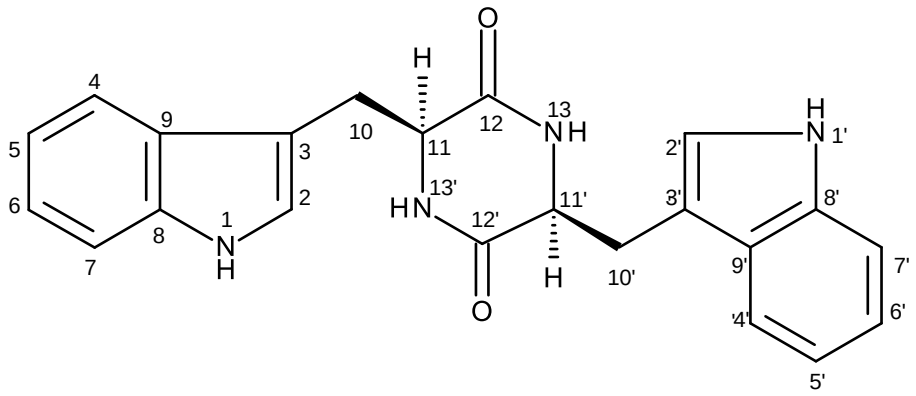

Figure 103. Structure of fellutanine A (**NG 10**)

3.1.11.2. Fellutanine A epoxide (NG 11)

NG 11 was isolated as pale yellow viscous mass, and its molecular formula $C_{22}H_{20}N_4O_3$ was established on the basic of the (+)-HRESIMS *m/z* 389.1626 $[M+H]^+$ (calculated 389.1614), indicating fifteen degrees of unsaturation. The IR spectrum showed absorption bands for amine (3420 cm^{-1}), amide carbonyl (1649 cm^{-1}) and aromatic (1418 cm^{-1}).

The ^{13}C NMR, DEPTs and HSQC spectra (Table 25) revealed the presence of two amide carbonyls (δ_C 169.8 and 167.7), five quaternary sp^2 (δ_C 148.4, 136.0, 131.1, 127.4 and 109.5), nine methine sp^2 (δ_C 128.9, 124.1, 122.5, 120.9, 118.5, 118.3 117.8, 111.3 and 109.8), one oxygen bearing quaternary sp^3 (δ_C 85.9), one oxygen bearing methine sp^3 (δ_C 84.0), two methine sp^3 (δ_C 58.6 and 55.1) and two methylene sp^3 (δ_C 41.3 and 24.7) carbons.

The ^{1}H NMR (Table 25) exhibited, besides four NH signals at δ_H 10.88, *brd* (*J* = 1.4 Hz), 7.72, *brs*, 6.68, *d* (*J* = 4.1 Hz) and 6.05, *s*, and in conjunction with COSY and HSQC spectra, the protons of two 1, 2-disubstituted benzene ring at δ_H 7.60, *d* (*J* = 7.9 Hz, H-4; δ_C 118.5), 7.33, *d* (*J* = 7.9 Hz, H-7; δ_C 111.3), 7.07, *ddd* (*J* = 7.9, 7.9, 1.1 Hz, H-6; δ_C 120.9), 6.99, *ddd* (*J* = 7.9, 7.9, 0.5 Hz, H-5; δ_C 118.3), and at δ_H 7.18, *d* (*J* = 7.4 Hz, H-4′; δ_C 122.5), 7.05, *ddd* (*J* = 7.8, 7.8, 1.3 Hz, H-6′; δ_C 128.9), 6.61, *ddd* (*J* = 7.8, 7.4, 0.5 Hz, H-5′; δ_C 117.8) and 6.54, *d* (*J* = 7.8 Hz, H-7′; δ_C 109.8).

That one of the 1, 2-disubstituted benzene ring was part of the indole moiety was corroborated by the HMBC correlations from H-4 (δ_H 7.60, *d*, *J* = 7.9 Hz) to C-3 (δ_C 109.5), C-6 (δ_C 120.9) and C-8 (δ_C 136.0), from the amine proton at δ_H 10.88 *brd* (*J* = 1.4 Hz, NH-1) to C-2 (δ_C 124.1), C-3, C-8, C-9 (δ_C 127.4) and from H-2 (δ_H 7.25, *d*, *J* = 2.3 Hz) to C-3 and C-9.

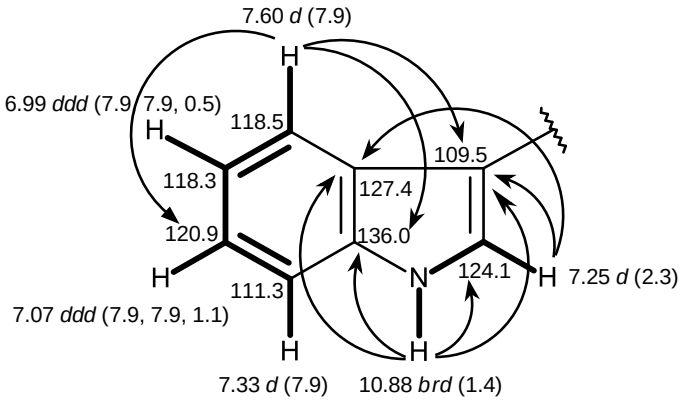

Table 25. ^{1}H and ^{13}C NMR (DMSO, 300.13 and 75.47 MHz), HMBC assignment and NOESY for **NG 11**

Position	**δ_C, type**	**δ_H, (*J* in Hz)**	**COSY**	**HMBC**	**NOESY**
2	124.1, CH	7.25, *d* (2.3)	NH-1	C-3, 9	H-10a, 11 (str), NH-13′
3	109.5, C	-	-	-	-
4	118.5, CH	7.60, *d* (7.9)	H-5	C-3, 6, 8	H-10a, 11 (str)
5	118.3, CH	6.99, *ddd* (7.9, 7.9, 0.5)	H-4, 6	C-7, 9	-
6	120.9, CH	7.07, *ddd* (7.9, 7.9, 1.1)	H-5, 7	C-4, 8	-
7	111.3, CH	7.33, *d* (7.9)	H-6	C-5, 9	-
8	136.0, C	-	-	-	-
9	127.4, C	-	-	-	-
10a	24.7, CH_2	3.06, *dd* (15.7, 6.5)	H-10b, 11	C-3, 9, 11, 12	H-4, 10b, 11, NH-13′
b		3.40, *m*	H-10a, 11	C-3, 9, 11, 12	H-10a
11	55.1, CH	4.46, *t* (5.1)	H-10a, 10b	C-3, 10, 12	H-2, 4, 10a, 11′, NH-13′
12	167.7, CO	-	-	-	-

Table 25. ^{1}H and ^{13}C NMR (DMSO, 300.13 and 75.47 MHz), HMBC assignment and NOESY for **NG 11** (Cont.)

Position	**δ_C, type**	**δ_H, (*J* in Hz)**	**COSY**	**HMBC**	**NOESY**
2′	84.0, CH	5.33, *d* (4.1)	NH-1′	C-3′, 10′	H-11, NH-13, NH-1′(str)
3′	85.9, C	-	-	-	-
4′	122.5, CH	7.18, *d* (7.4)	H-5′	C-6′, 8′	NH-13
5′	117.8, CH	6.61, *ddd* (7.8, 7.4, 0.5)	H-4′, 6′	C-7′, 9′	-
6′	128.9, CH	7.05, *ddd* (7.8, 7.8, 1.3)	H-5′, 7′	C-4′, 8′	-
7′	109.8, CH	6.54, *d* (7.8)	H-6′	C-5′, 9′	-
8′	148.4, C	-	-	-	-
9′	131.1, C	-	-	-	-
10′a	41.3, CH_2	1.83, *dd* (13.0, 11.6)	H-10′b, 11	C-11′, 12′	H-10′b
b		2.43, *dd* (13.6, 6.7)	H-10′a, 11	C-3′	H-10′a, 11
11′	58.6, CH	4.66, *dd* (11.6, 6.7)	H-10′a, 10′b	C-10′, 12′	H-11, 2′, 10′b
12′	169.8, CO	-	-	-	-
NH-1	-	10.88, *brd* (1.4)	H-2	C-2, 3, 8, 9	H-2, 4
NH-1′	-	6.68, *d* (4.1)	H-2′	C-3′, 9′	-
NH-13	-	6.05, *s*	-	C-10′	H-2′, 4′
NH-13′	-	7.72, *brs*	-	C-10, 11, 11′, 12	H-10a (str), 11 (str), H-2

The presence of a 2, 5-disubstituted 1,4-diketopiperazine was supported by the HMBC correlations from a singlet at δ_H 7.72 (NH-13′) to the carbonyl at δ_C 167.7 (C-12), the methine carbon at δ_C 58.6 (C-11′) and 55.1 (C-11) and the methylene carbon at δ_C 24.7 (C-10), and from another singlet at δ_H 6.05 (NH-13) to the methylene carbon at δ_C 41.3 (C-10′), from H-11 (δ_H 4.46, *t*, *J* = 5.1 Hz) to C-10 and C-12, from H-11′ (δ_H 4.66, *dd*, *J* = 11.2, 6.1 Hz) to C-10′ and C-12′, as well as by the COSY correlations from H-11 to H_2-10 (δ_H 3.06, *dd*, *J* = 15.7, 6.5 Hz and 3.40, *m*) and from H-11′ to H_2-10′ (δ_H 1.83, *dd*, *J* = 13.0, 11.6 Hz and 2.43, *dd*, *J* = 13.0, 6.7 Hz). That the indole ring system was connected to the 1, 4-diketopiperazine moiety through CH_2-10 was supported by the HMBC correlations of H-11 to C-3 and H-10 to C-9.

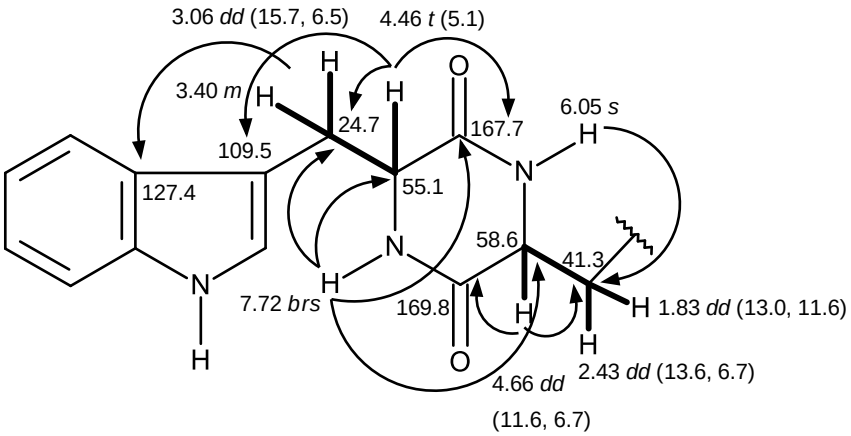

That another 1, 2-disubstituted was part of the 2, 3-disubstituted 2,3-dihydro-1*H*-indole ring system was corroborated by the HMBC correlations of NH-1′ doublet at δ_H 6.68 (*J* = 4.1 Hz) to the oxygenated quaternary carbon at δ_C 85.9 (C-3′) and the quaternary aromatic carbon at δ_C 131.1 (C-9′) as well as of the oxymethine doublet

at δ_H 5.33 (*J* = 4.1 Hz, H-2′) to C-3′. That the 2, 3-disubstituted 2, 3-dihydro-1*H*-indole ring system was linked to the 1, 4-diketopiperazine moiety through CH_2-10′ was evidence by the HMBC correlations of H-2′ to C-10′ and C-11′ as well as of H-10′ to C-3′. As this accounted only for $C_{22}H_{20}N_4O_2$, which is one oxygen atom less than the molecular formula, the epoxide functionality was place between C-2′ and C-3′.

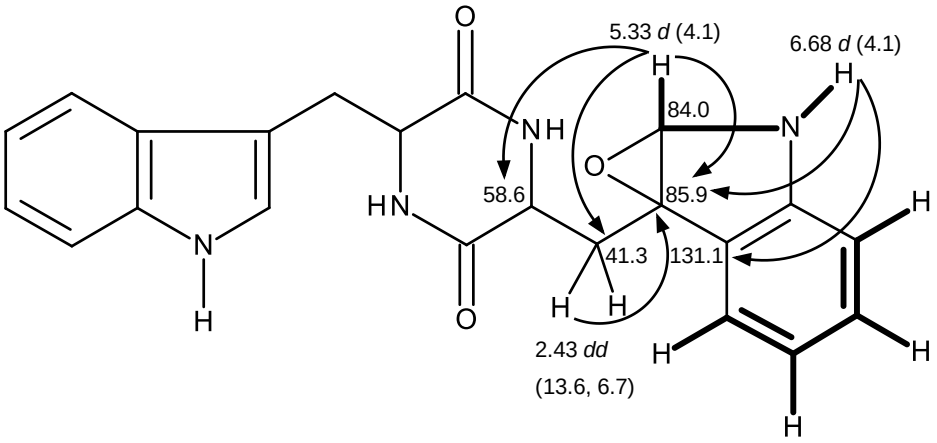

Since **NG 11** was obtained as pale yellow viscous mass, its stereochemistry could not be determined by X-ray crystallography. However, as **NG 11** was isolated together with fellutanine A (**NG 10**), it is legitimate to assume that the stereochemistry of C-11 and C-11′ of both compounds are the same. Like fellutanine A (**NG 10**) and **NG 11** must be derived from the same biosynthetic precursor, i.e. L-tryptophan. Consequently the absolute configurations of C-11 and C-11′ of **NG 10** and **NG 11** are presumed to be *S*. In an effort to unravel the stereochemistry of C-11, C-11′, and the epoxide bearing carbons (C-2′ and C-3′) of **NG 11**, the NOESY

experiments and molecular dynamic simulations were carried out. The NOESY spectrum of **NG 11** exhibited correlations from H-11 to H-2, H-4, H-10a, H-11′, NH-13′, therefore confirming the *cis*-relation between H-11 and H-11′. Since the coupling constant between H-11 and H-10a is 6.5 Hz, H-10a must be in an equatorial and H-11 in axial positions in the major conformation. On the other hand, H-11′ exhibited only correlations to H-11 and H-10′b (δ_H 2.43, *dd*, *J* =13.0, 6.7 Hz), and H-2′, but not with H-10′a (δ_H 1.83, *dd*, *J* =13.0, 11.6 Hz) and NH-13, while H-2′ gave correlations to only H-11′ and NH-13, but not to H-10′a or 10′b. The values of the coupling constants of H-11 to H-10′a (*J* = 11.6 Hz) and to H-10′b (*J* = 6.7 Hz) indicated that H-11′ and H-10′a are in *trans*-diaxial, while H-11′ and H-10′b are in axial-equatorial position. These data indicated that H-2′ is in the same face as H-11′ and points to the opposite direction from H-10′a/ 10′b. However, these correlations do not allow us to determine the stereochemistry of the epoxide. Surprisingly, the NOESY spectrum also shows strong correlation of H-4′ to NH-13.

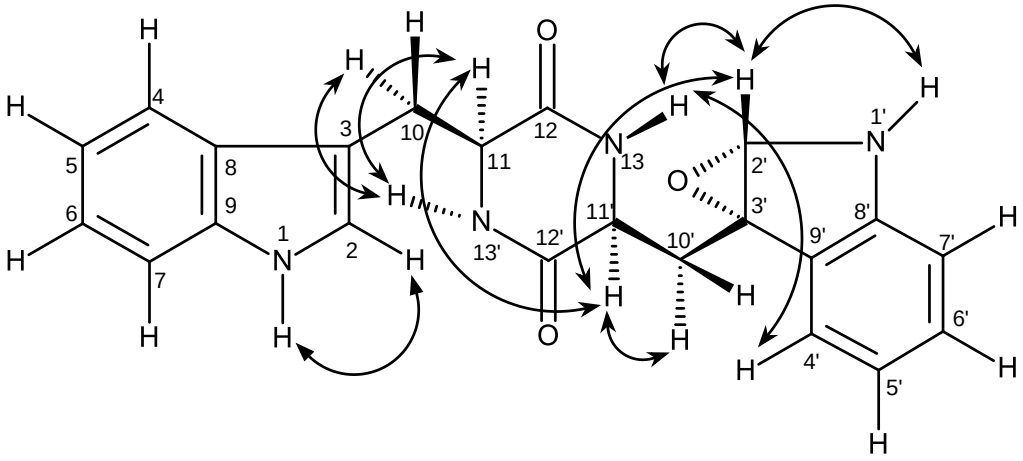

Furthermore, a strong NOESY cross-peak between H-11 and H-11′ of **NG 11**, and in conjunction with conformational search, molecular dynamics and *ab initio* molecular modelling, showed that both amide bonds in the diketopiperazine ring are *cis* and that both amino acids have the same stereochemistry for their α-carbons. This type of six membered ring is thermodynamically stable because resonance compensates for the extra energy of the amide *cis* configurations (Bodanszky, 2012), when compared to the more normal *trans* configuration. Nevertheless, *cis* peptide bonds occur naturally even in linear biological proteins (Jabs *et al*., 1999). NOESY cross-peaks and molecular modeling also aided the assignment of the absolute configurations to the epoxide carbon atoms of **NG 11**. The minimal energy conformations for the *R*/*R* and *S*/*S* models are presented in Figure 104, showing how the epoxide oxygen points outwards in both cases for minimal repulsion. Conformational analysis was based mainly on the combinations of the three staggered conformations for C-10′/C-11′ bond and two for the C-3′/C-10′ bond.

These six conformers differ by less than 7 kcal/mol (RHF/6-21G total energy), independently of the configuration of the epoxide. Of all the conformations, the most stable conformation of the 2′*S*/3′*S* epoxide actually explains simultaneously the observed NOESY correlations of H-4′ to NH-13 and of H-2′ to H-11′ (Table 25 and Figure 104). On the other hand, none of the *R*/*R* conformations justifies the NOESY data without assuming unreasonable spin-diffusion. The assignment of the *S*/*S* isomer for the epoxide carbons of **NG 11** has to assume, however, that there is a

spin-diffusion during the mixing time, otherwise, given the proposed structure for **NG 11**, it would not be possible to explain also the H-2′/H-13 NOESY cross-peak. The proximities H-4′/NH-13 and H-2′/H-11′ are physically incompatible with direct H-2′/H-13 NOE proximity. The fact that H-2′/H-11′/NH-13 forms a coupled dipolar spin system is perhaps an explanation for the very week H-11′/NH-13 NOESY cross-peak (Table 25 and Figure 104), expect to be strong unless some polarization transfer is at play between the three spins.

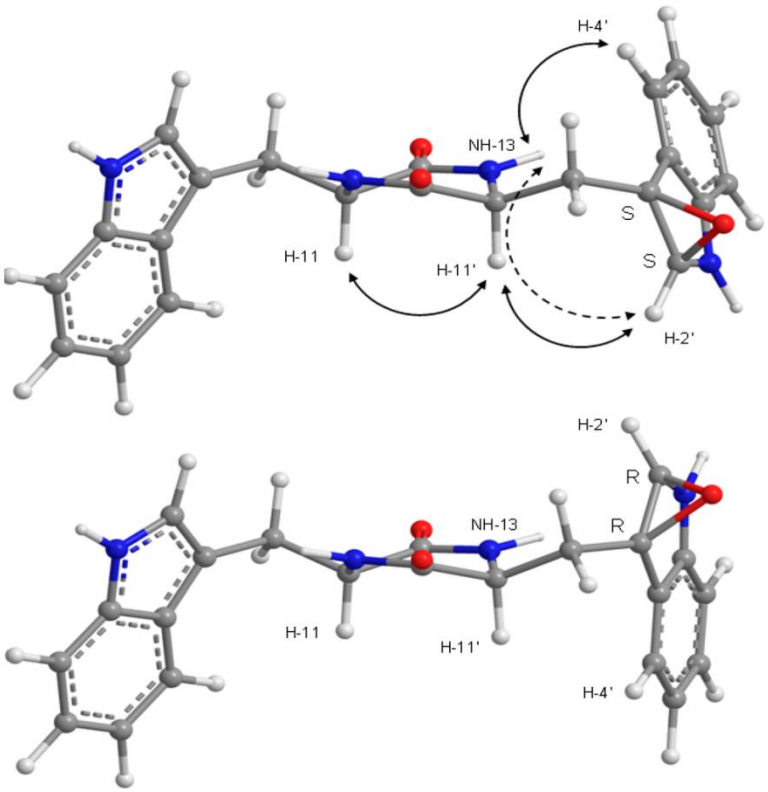

Figure 104. The two possible epoxide configuration for **NG 11** in their lowest RHF/6-21G total energy conformation. Solid lines indicate direct NOESY correlations, explained by the *S*/*S* stereoisomer and not by the *R*/*R*. The discontinuous line shows how spin diffusion gives rise to an H-2′/NH-13 NOESY cross-peak.

Taking together all the evidences, the structure of **NG 11** was proposed as fellutanine A 2′*S*, 3′*S*-epoxide. To the best of our knowledge, compound **NG 11** is a new compound.

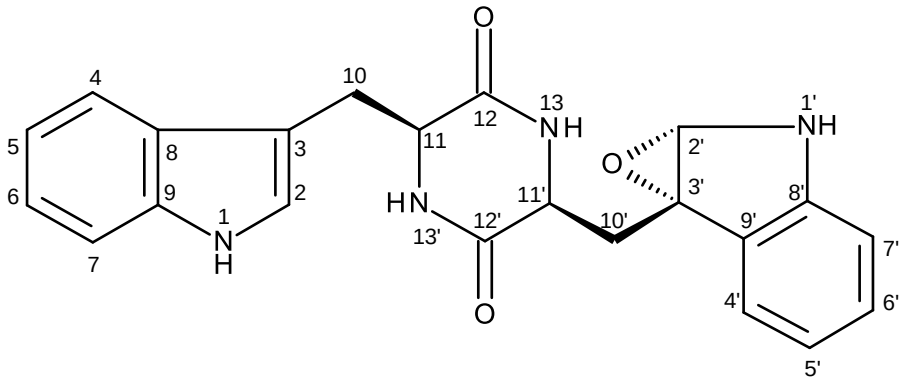

Figure 105. Structure of fellutanine A 2′*S*, 3′*S*- epoxide (**NG 11**)

3.1.11.3. (11*S*, 14 *R*)-3-(1*H*-indol-3-ylmethyl)-6-isopropyl-2, 5-piperazinedione (EC 12)

EC 12 was isolated as white crystals (mp, 270-271 ºC), and its molecular formula $C_{16}H_{19}N_3O_2$ was determined based on the (+)-HRESIMS $[M+H]^+$ peak at *m/z* 286.1555 (calculated for $C_{16}H_{20}N_3O_2$, 286.1556), indicating nine degrees of unsaturation. The ^1H and ^{13}C NMR spectra exhibited characteristic proton and carbon signals of a indolylmethyl diketopiperazine derivative.

The ^{13}C NMR (Table 26) showed the presence of sixteen carbon signals which can be categorized, according to the DEPTs and HSQC spectra, as two amide

carbonyls (δ_C 168.1 and 167.1), three quaternary sp^2 (δ_C 135.8, 127.7 and 108.5), five methine sp^2 (δ_C 124.5, 120.8, 118.9, 118.3 and 111.1), three methine sp^3 (δ_C 59.1, 54.7 and 31.5), one methylene sp^3 (δ_C 28.4) and two methyl (δ_C 18.2 and 16.6) carbons.

Table 26. ^{1}H and ^{13}C NMR (DMSO, 300.13 and 75.47 MHz) and HMBC assignment for **EC 12**

Position	**δ_C, type**	**δ_H, type (*J* in Hz)**	**COSY**	**HMBC**
2	124.5, CH	7.08, *d* (2.3)	-	C-3, 9
3	108.5, C	-	-	-
4	118.9, CH	7.60, *d* (7.9)	H-5	C-3, 6, 8
5	118.3, CH	6.95, *ddd* (7.5, 7.5, 1.4)	H-4, 6	C-8, 9
6	120.8, CH	7.04, *ddd* (7.4, 7.4, 1.1)	H-5, 7	C-4, 7, 8
7	111.1, CH	7.32, *d* (7.1)	H-6	C-5, 9
8	135.8, C	-	-	-
9	127.7, C	-	-	-
10a	28.4, CH_2	3.04, *m*	-	C-2, 3, 9, 11, 12
b		3.23, *dd* (14.5, 4.4)		C-2, 3, 9, 11, 12
11	54.7, CH	4.13, *brt* (3.9)	H-10	C-3, 10, 12
12	168.1, CO	-	-	-
14	59.1, CH	3.04, *m*	-	C-17, 18, 19
15	167.1, CO	-	-	-
17	31.5, CH	2.03, *m*	H-14, 18, 19	-
18	18.2, CH_3	0.77, *d* (6.8)	-	C-14, 17, 19
19	16.6, CH_3	0.82, *d* (7.1)	-	C-14, 17, 18
NH-1	-	10.88, *brs*	H-2	C-3, 8, 9
NH-13	-	7.86, *d* (1.5)	H-14	C-11, 15
NH-16	-	8.03, *brs*	H-11	C-12, 14

Like for **NG 5**, **NG 10** and **NG 11**, the existence of indolylmethyl moiety was evidence by the coupling system of H-4 (δ_H 7.60, *d*, *J* = 7.9 Hz; δ_C 118.9) through H-5 (δ_H 6.95, *ddd*, *J* = 7.5, 7.5, 1.4 Hz; δ_C 118.3) and H-6 (δ_H 7.04, *ddd*, *J* = 7.4, 7.4, 1.1 Hz; δ_C 120.8) to H-7 (δ_H 7.32, *d*, *J* = 7.1 Hz; δ_C 118.9) and from the cross peak from the *brs* of the indole amine proton at 10.88 to the doublet at δ_H 7.08 (*J* = 2.3, H-2; δ_C 124.5) observed in the COSY spectrum. This was also supported by the HMBC correlation from H-4 to C-6, C-3 (δ_C 108.5) and C-8 (δ_C 135.8), from H-7 to C-5 and C-9 (δ_C 127.7), from NH-1 to C-3, C-8, C-9, from H-2 to C-3 and C-9 and from H_2-10 (δ_H 3.04, *m* and 3.23, *dd*, *J* = 14.5, 4.4 Hz; δ_C 28.4) to C-2, C-3 and C-9.

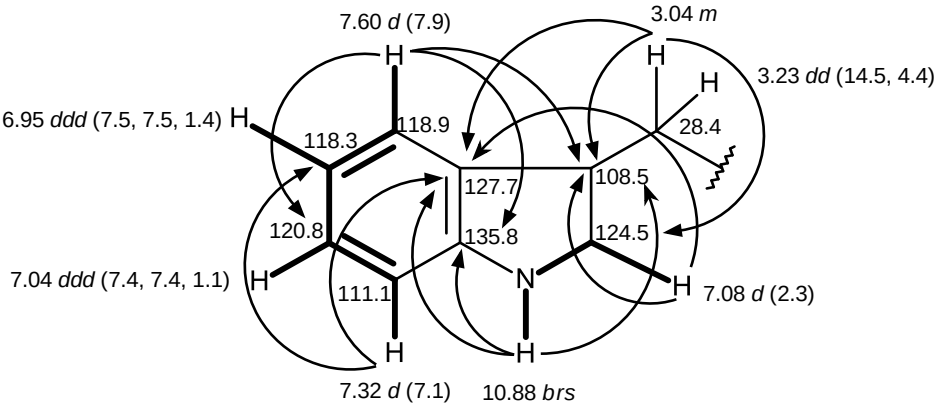

The existence of the 2, 5-diketopiperazine ring was confirmed by the COSY correlations from the amide proton (NH-16) at δ_H 8.03 *brs* to the *brt* at δ_H 4.13 (*J* = 3.9 Hz; H-11; δ_C 54.7) and from another amide proton (NH-13) at δ_H 7.86 (*J* = 1.5 Hz) to a multiplet at δ_H 3.04 (H-14, δ_C 59.1) as well as by the HMBC correlation from NH-16 to carbonyl at δ_C 168.1 (C-12) and C-14 and from NH-13 to the carbonyl at δ_C 167.1 (C-15) and C-11. That the isopropyl group was on C-14 was corroborated by

the COSY correlation from the multiplet at δ_H 2.03 (H-17) to H-14 and the two methyl doublets at δ_H 0.77 (*J* = 6.8 Hz, Me-18; δ_C 18.2) and 0.82 (*J* = 7.1, Me-19; δ_C 16.6) as well as by the HMBC correlations of both Me-17 and Me-18 to C-14.

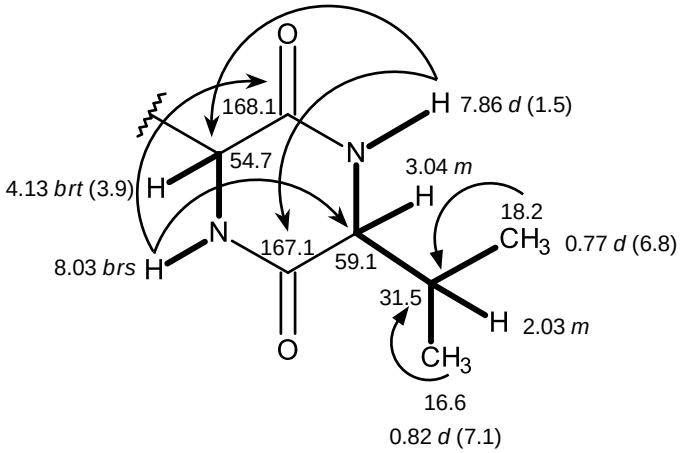

Finally, the isopropyl 1, 4-diketopiperazine ring was linked to the indole moiety through the methyl group was confirmed by the COSY correlation from H_2-10 to H-11 as well as by the HMBC from H-11 to C-3, C-10 and C-12.

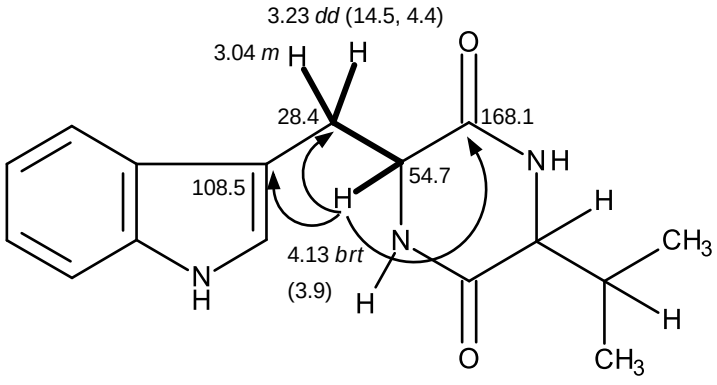

Analysis of the ^{1}H, ^{13}C NMR and (+)-HRESIMS data allowed to establish its structure as 3-(1*H*-indol-3-ylmethyl)-6-isopropyl-2,5-piperazinedione or cyclo (tryptophylvalyl). Literature survey revealed that both 11*S*, 14*R* and 11*S*, 14*S* forms

have been previously reported. While the 11*S*, 14*R* form [mp 278-280ºC; $[\alpha]_D^{20}$ = – 15 (*c* = 1, DMF)] was isolated from *Aspergillus chevalieri*, the 11*S*, 14*S* form [mp 294-298 ºC; $[\alpha]_D^{20}$ = – 98 (*c* = 1, DMF)] was reported from *Phoma linga* (Blunt and Munro, 2007). Since the specific rotation of **EC 12**, determined in acetone, was levorotatory $[\alpha]_D^{20}$ = – 187 (*c* = 0.02, acetone), it was not possible to determine unequivocally the absolute configuration of C-11 and C-14. However, since **EC 12** was obtained in a suitable crystal, an X-ray diffraction was performed. The ORTEP view of **EC 12** (Figure 106) showed clearly that the absolute configuration of C-11 and C-14 are 11*S* and 14*R*, respectively.

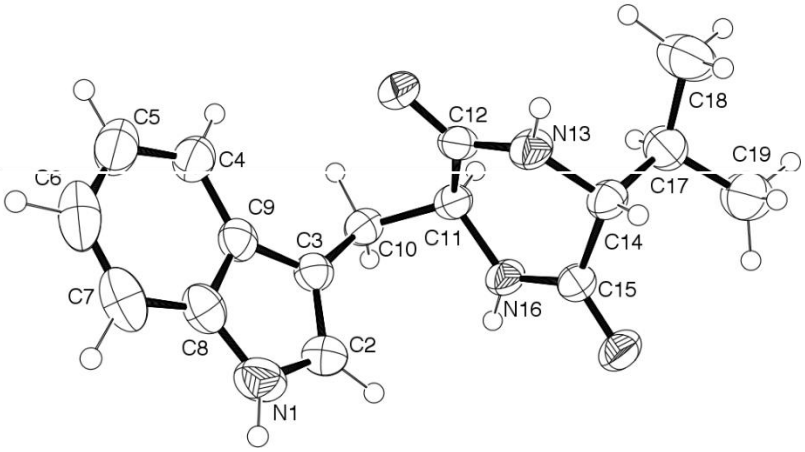

Figure 106. ORTEP view of **EC 12**

Therefore, the structure of **EC 12** (Figure 107) was established as (11*S*, 14*R*) -3-(1*H*-indol-3-ylethyl)-6-isopropyl-2, 5-piperazinedione (Blunt and Munro, 2007).

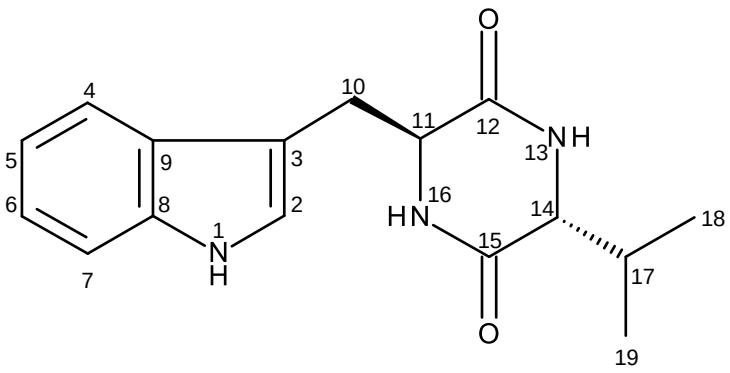

Figure 107. Structure of (11*S*, 14*R*)-3-(1*H*-indol-3-ylethyl)-6-isopropyl-2,5-piperazinedione (**EC 12**)

3.1.11.4. Preechinulin (EC 13)

EC 13 was isolated as a white solid (mp, 251-252 ºC), its molecular formula $C_{19}H_{23}N_3O_2$, was established on the basis of the (+)-HRESIMS *m/z* 326.1873 $[M+H]^+$ (calculated for $C_{19}H_{24}N_3O_2$, 326.1869), indicating ten degrees of unsaturation. The ^{13}C NMR (Table 27), in combination with DEPTs and HSQC spectra, exhibited two amide carbonyls (δ_C 167.9 and 167.3), four quaternary sp^2 (δ_C 141.4, 134.9, 129.0 and 104.7), five methine sp^2 (δ_C 146.5, 120.5, 118.4, 117.9 and 110.8), one quaternary sp^3 (δ_C 39.0), two methine sp^3 (δ_C 55.7 and 50.3), one methylene sp^2 (δ_C 111.1), one methylene sp^3 (δ_C 31.1) and three methyl (δ_C 28.0, 27.9 and 20.7) carbons.

The ^{1}H NMR spectrum, in conjunction with the HSQC spectrum (Table 27) showed the signals of four aromatic protons at δ_H 7.43, *d* (*J* = 7.7 Hz), 7.32, *d* (*J* = 7.9 Hz), 7.03, *ddd* (*J* = 7.5, 7.5, 1.1 Hz) and 6.94, *ddd* (*J* = 7.4, 7.4, 1.0 Hz), one olefinic proton at δ_H 6.19, *dd* (*J* = 17.4, 10.5 Hz), two methine sp^3 protons at δ_H 3.96, *m* and 3.79, *dd* (*J* = 14.1, 7.1, 2.5 Hz), two methylene sp^2 proton at 5.08, *dd* (*J* = 17.5, 1.2 Hz) and 5.02, *dd* (*J* = 10.5, 1.2 Hz), methylene sp^3 proton at δ_H 3.08, *dd* (*J* = 14.4, 8.9 Hz) and 3.33, *dd* (*J* = 14.4, 8.2 Hz), three methyl protons at δ_H 1.50, *s*, 1.49, *s* and 1.23, *d* (*J* = 7.1 Hz), singlet of one amine proton at δ_H 10.55, two doublets of amide protons at δ_H 8.18 (*J* = 2.8 Hz) and 7.53 (*J* = 3.1 Hz). The ^{1}H and ^{13}C NMR spectra of **EC 13** resemble those of **EC 12** exhibiting the presence of the indolylmethyl moiety and the 1, 4-diketopiperazine portion.

Table 27. ^{1}H and ^{13}C NMR (DMSO, 300.13 and 75.47 MHz) and HMBC assignment for **EC 13**

Position	δ_C, type	δ_H, type (*J* in Hz)	COSY	HMBC
2	141.4, C	-	-	-
3	104.7, C	-	-	-
4	117.9, CH	7.43, *d* (7.7)	H-5	C-6, 8
5	118.4, CH	6.94, *ddd* (7.4, 7.4, 1.0)	H-4, 6	C-7, 9
6	120.5, CH	7.03, *ddd* (7.5, 7.5, 1.1)	H-5, 7	C-4, 5, 8
7	110.8, CH	7.32, *d* (7.9)	H-6	C-4, 5, 9
8	134.9, C	-	-	-
9	129.0, C	-	-	-
10a	31.1, CH_2	3.08, *dd* (14.4, 8.9)	H-10b, 11	C-2, 3, 9, 11
b		3.31, *dd* (14.4, 8.2)	H-10a, 11	C-2, 3, 9, 11
11	55.7, CH	3.96, *m*	H-10	C-12, 15
12	167.9, CO	-	-	-
14	50.3, CH	3.79, *ddd* (14.1, 7.1, 2.5)	NH-13, H-17	C-12, 15, 17
15	167.3, CO	-	-	-
17	20.7, CH_3	1.23, *d* (7.1)	H-14	C-12, 14, 15
18	39.0, C	-	-	
19	146.5, CH	6.19, *dd* (17.4, 10.5)	H-20	C-18, 21, 22
20a	111.1, CH_2	5.08, *dd* (17.5, 1.2)	H-19	C-19
b		5.02, *dd* (10.5, 1.2)	H-19	C-19
21	27.9, CH_3	1.49, *s*	H-22	C-2, 19, 22
22	28.0, CH_3	1.50, *s*	H-21	C-2, 19, 21
NH-1	-	10.55, *s*	-	C-2, 3, 9
NH-13	-	8.18, *d* (2.8)	H-14	C-11
NH-16	-	7.53, *d* (3.1)	H-11	C-14

The indole ring system was evidenced by the coupling system, similar to that of **EC 12** as observed in the COSY spectrum, from H-4 (δ_H 7.43, *d*, *J* = 7.7 Hz; δ_C 117.9) through H-5 (δ_H 6.94, *ddd*, *J* = 7.4, 7.4, 1.0 Hz; δ_C 118.4) and H-6 (δ_H 7.03, *ddd*, *J* = 7.5, 7.5, 1.1 Hz; δ_C 120.5) to H-7 (δ_H 7.32, *d*, *J* = 7.9 Hz; δ_C 110.8) as well as by the HMBC correlations from the indole amine proton singlet at δ_H 10.55 to the carbons at δ_C 104.7 (C-3), δ_C 129.0 (C-9) and a quaternary sp^2 carbon at δ_C 141.1 (C-2). The presence of the quaternary sp^2 carbon at δ_C 141.1 and the lack of a proton doublet with a coupling constant ca. 2.5 Hz in the ^{1}H NMR spectrum of **EC 13** led to the conclusion that C-2 of the indole moiety was substituted.

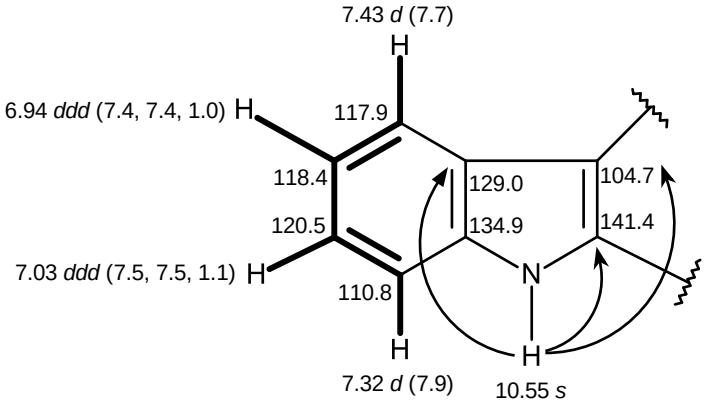

The existence of the 3-methylbut-3-en-2-yl moiety was based on the COSY correlations from the doublet doublet at δ_H 6.19 (*J* = 17.4, 10.5 Hz, H-19; δ_C 146.5) to the two double doublets at 5.08 (*J* = 17.5, 1.2 Hz; H-20a; δ_C 111.1) and 5.02 (*J* = 10.5, 1.2 Hz; H-20b; δ_C 111.1) as well as by the HMBC correlations from H-19 to the quaternary sp^3 carbon at δ_C 39.0 (C-18) and the two methyl singlets at δ_H 1.49 (Me-21, δ_C 27.9) and 1.50 (Me-22; δ_C 28.0). That the 2-methylbut-3-en-2-yl substituent

was on C-2 of the indole moiety was corroborated by the HMBC correlations from Me-21 and Me-22 to C-2.

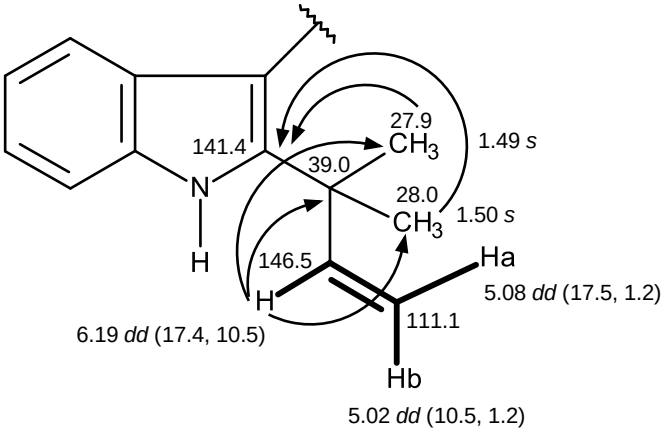

Similar to **EC 12**, the indole portion of **EC 13** was also connected to the 1,4-diketopiperazine moiety by the methylene bridge as evidenced by coupling system, as observed in the COSY spectrum, from the mutually coupled *dd* at δ_H 3.08 (*J* = 14.4, 8.9 Hz, H-10a; δ_C 31.1) and δ_H 3.33 (*J* = 14.4, 8.2 Hz, H-10b; δ_C 31.1) through the multiplet at δ_H 3.96 (H-11; δ_C 55.7) to the doublet of the amide proton at δ_H 7.53 (*J* = 3.1 Hz; NH-16), from NH-16 to the methine sp^3 carbon at δ_C 50.3 (C-14).

Contrary to **EC 12**, the substituent on C-14 of the 1, 4-diketopiperzine ring was a methyl group instead of isopropyl group. This was evident by the COSY correlation from a *ddd* at δ_H 3.79 (*J* = 14.1, 7.1, 2.5 H-14; δ_C 50.3) to the methyl doublet at δ_H 1.23 (*J* = 7.1 Hz, Me-17) as well as the HMBC correlations from H-14 to C-17 and the carbonyl at δ_C 167.9 (C-12).

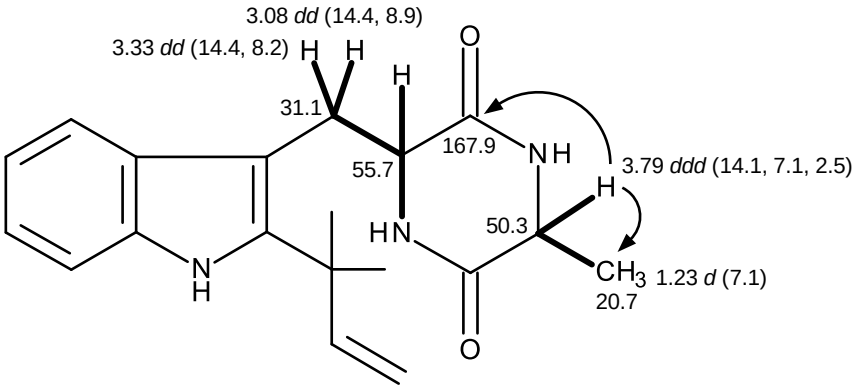

Taking together the ^{1}H and ^{13}C NMR data and their correlations, **EC 13** was identified as 3-Methyl-6-[2-(2-methyl-3-buten-2-yl)-1*H*-indol-3-yl]methyl-2,5-piperazinedione. Since **EC 13** was dextrorotatory ($[\alpha]_D^{20}$ = + 23.4), it was identified as preechinulin (Fugure 108).

Preechinulin was reported from the culture of several fungi such as the fungal strain *Aspergillus chevalieri* (Mangin) Thom *et* Church IFO 4090 (Hamasaki *et al*., 1976), a halotolerant fungus *Aspergillus variecolor* B-17, which was isolated from sediments (Wang *et al*., 2007a), mangrove-derived endophytic fungus *Eurotium rubrum* (Li *et al*., 2008c), sponge-derived fungus *Aspergillus repens* (Chen and GU, 2010), soft coral-derived fungus *Nigrospora oryzae* (Sun *et al*., 2014) and marine-derived fungus *Eurotium rubrum*, which was isolated from the sediments (Chen *et al*., 2015).

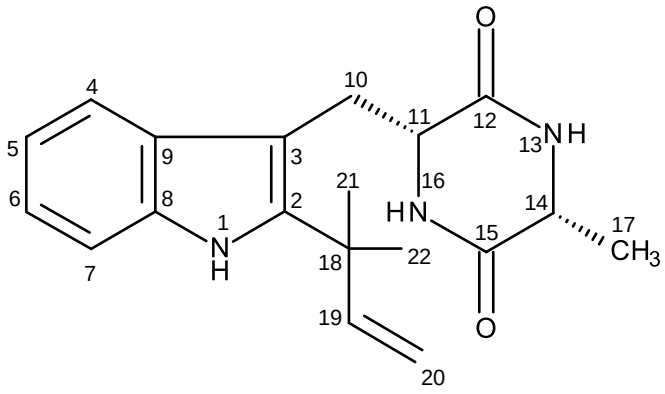

Figure 108. Structure of preechinulin (**EC 13**)

3.1.11.5. Neoechinulin E (EC 14)

EC 14 was isolated as a white solid (mp, 273-275 ºC) and its molecular formula $C_{18}H_{17}N_3O_3$ was determined based on the (+)-HRESIMS *m/z* 324.1347 $[M+H]^+$ (calculated for $C_{18}H_{18}N_3O_3$, 324.1348), indicating twelve degrees of unsaturation. The ^{13}C NMR (Table 28) revealed the presence of eighteen carbon signals which can be categorized, through DEPTs and HSQC spectra as three amide carbonyl (δ_C 160.5, 157.3 and 152.3), five quaternary sp^2 (δ_C 145.6, 135.1, 126.1, 123.4 and 103.7), one quaternary sp^3 (δ_C 39.0), six methine sp^2 (δ_C 144.9, 121.1, 119.7, 119.6, 116.0 and 111.6), one methylene sp^2 (δ_C 112.0) and two methyl [δ_C 27.7 (2C)] carbons.

Like preechinulin, **EC 14** also contained the 2-(2-methylbut-3-en-2-yl)-1*H*-indolemoiety which was supported by the coupling system, as observed in the COSY spectrum, from H-4 (δ_H 7.44, *d*, *J* = 8.0 Hz, δ_C 119.7), through H-5 (δ_H 7.03, *dd*, *J* = 7.6, 7.0 Hz, δ_C 119.7) and H-6 (δ_H 7.12, *dd*, *J* = 7.9, 6.0 Hz, δ_C 121.0) to H-7 (δ_H 7.44, *d*, *J* = 8.0 Hz, δ_C 111.6), from H-18 (δ_H 6.09, *dd*, *J* = 17.3, 10.6 Hz, δ_C 144.9) to H-19a (δ_H 5.07, *d*, *J* = 17.3 Hz, δ_C 112.0) and H-19b (δ_H 5.10, *d*, *J* = 10.6 Hz, δ_C 112.0), as well as by the HMBC correlation from NH-1 (δ_H 11.25, *brs*) to C-2 (δ_C 145.6), C-3 (δ_C 103.7), C-8 (δ_C 135.1) and C-9 (δ_C 126.1), from H-18 to Me-21/Me-22 (δ_C 27.7), C-17 (δ_C 39.0) and C-2.

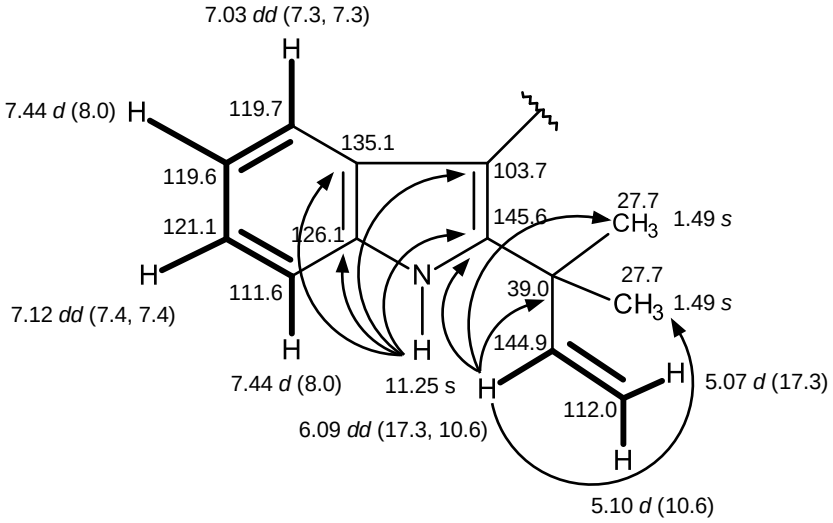

Table 28. ^{1}H and ^{13}C NMR (DMSO, 300.13 and 75.47 MHz) and HMBC assignment for **EC 14**

Position	δ_C, type	δ_H, type (*J* in Hz)	COSY	HMBC
2	145.6, C	-	-	-
3	103.7, C	-	-	-
4	119.7, CH	7.03, *dd* (7.3, 7.3)	H-5	C-7, 8
5	119.6, CH	7.44, *d* (8.0)	H-4, 6	C-4, 8, 9
6	121.1, CH	7.12, *dd* (7.4, 7.4)	H-5, 7	C-4, 5, 9
7	111.6, CH	7.44, *d* (8.0)	H-6	C-4, 5, 8, 9
8	126.1, C	-	-	-
9	135.1, C	-	-	-
10	116.0, CH	7.20, *s*	-	C-2, 3, 8, 12
11	123.4, C	-	-	-
12	160.5, CO	-	-	-
14	152.3, CO	-	-	-
15	157.3, CO	-	-	-
17	39.0, C	-	-	-
18	144.9, CH	6.09, *dd* (17.3, 10.6)	H-19	C-2, 18, 20, 21
19a	112.0, CH_2	5.07, *d* (17.3)	H-18	C-2, 18
b		5.10, *d* (10.6)	H-18	C-2, 18
20	27.7, CH_3	1.49, *s*	-	C-2, 18, 21
21	27.7, CH_3	1.49, *s*	-	C-2, 18, 20
NH-1	-	11.25, *s*	-	C-2, 3, 8, 9
NH-13	-	9.87, *s*	-	-
NH-16	-	12.00, *s*	-	-

The indole ring system was connected to the 1, 4-diketopiperazine moiety, which was revealed by the HMBC correlations from the singlet of methine proton at δ_H 7.20 (δ_C 116.0, H-10) to the quaternary carbons at δ_C 145.6 (C-2), 103.7 (C-3),

126.1 (C-8) and carbonyl carbon at δ_C 160.5 (C-12). Therefore, the complete structure was:

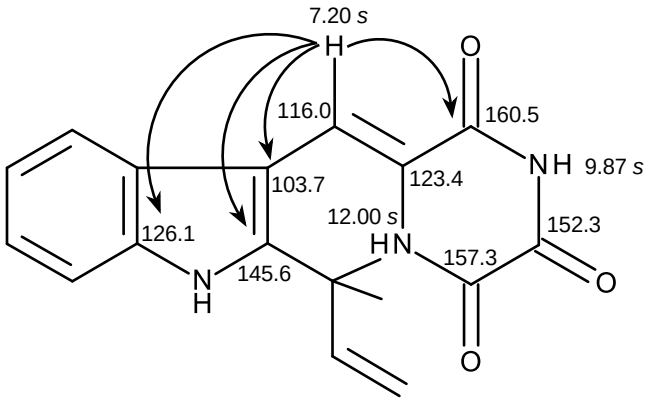

Taking all of the information together, **EC 14** was established as neoechinulin E (Figure 109), previously reported from the fungal strain isolated the mycelium of *Aspergillus amstelodami*, grown on molasses beet cultures (Marchelli *et al*., 1977), mangrove-derived endophytic fungus *Eurotium rubrum* (Li *et al*., 2008c) and marine sponge-associated fungus *Eurotium cristatum* (Gomes *et al*., 2012).

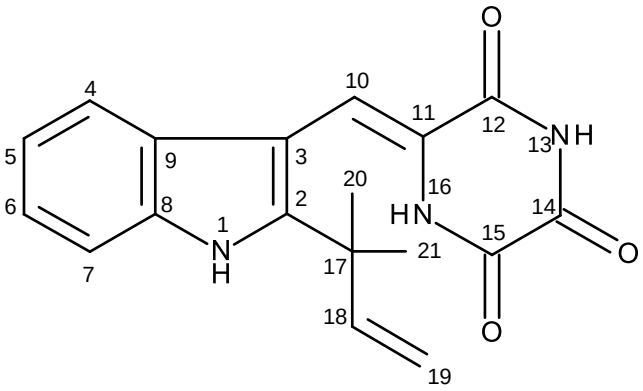

Figure 109. Structure of neoechinulin E (**EC 14**)

3.1.11.6. Echinulin (EC 15)

EC 15 was isolated as a white solid (mp, 226-227 ºC) and the general features of its ^{1}H and ^{13}C NMR spectra revealed that it was an indolylmethyl 1,4-diketopiperazine derivative, similar to **EC 13** (preechinulin), differing only in the substitution pattern of the benzene ring of the indole moiety. The ^{13}C NMR spectrum (Table 29) revealed the presence of 28 carbon signals which can be categorized, according to DEPTs and HSQC spectra, into two amide carbonyl (δ_C 167.9 and 167.4), eight quaternary sp^2 (δ_C 144.4, 132.2, 131.6, 131.5, 130.4, 129.2, 123.6 and 105.1), five methine sp^2 (δ_C 146.8, 124.9, 122.8, 121.0 and 114.6), one methylene sp^2 (δ_C 111.0), one quaternary sp^3 (δ_C 39.0), two methine sp^3 (δ_C 55.6 and 50.3), three methylene sp^3 (δ_C 34.2, 31.3 and 29.0), and seven methyl (δ_C 28.0 (2C), 25.6, 25.5, 20.8, 17.8 and 17.7) carbons.

The ^{1}H NMR spectrum (Table 29) displayed, among others, three amine proton signals at δ_H 9.71, *s*, typical for the indole amine proton, and two doublets at δ_H 8.19 (*J* = 2.6 Hz) and 7.46 (*J* = 3.0 Hz), which were characteristic of the amide protons of a 1,4-diketopiperazine moiety. The existence of a 3-methylpiperazine-2, 5-dione, similar to that of **EC 13** (preechinulin) was evidenced by the coupling system from the amide doublet at δ_H 8.19 (*J* = 2.6 Hz, NH-13) through the *ddd* at δ_H 3.81 (*J* = 14.0, 6.9, 2.8; H-14; δ_C 50.3) to the methyl doublet at δ_H 1.33 (*J* = 7.1 Hz; Me-17; δ_C 20.8), and from the amide doublet at δ_H 7.46 (*J* = 3.0 Hz, NH-16) to the *dt* at δ_H 3.92 (*J* = 9.0, 3.5 Hz; H-11; δ_C 55.6), as observed in the COSY spectrum.

Table 29. ^{1}H and ^{13}C NMR (DMSO, 300.13 and 75.47 MHz) and HMBC assignment for **EC 15**

Position	δ_C, type	δ_H, type (*J* in Hz)	COSY	HMBC
2	144.4, C	-	-	-
3	105.1, C	-	-	-
4	114.6, CH	7.04, *s*	H-6	C-3, 6, 8, 9, 23
5	131.6, C	-	-	-
6	121.0, CH	6.63, *s*	-	C-4, 8, 23, 28
7	123.6, C	-	-	-
8	132.2, C	-	-	-
9	129.2, C	-	-	-
10a	31.3, CH_2	3.31, *m*	-	C-2, 3, 9, 11
b		3.02, *dd* (14.4, 9.5)	H-10a, 11	C-2, 3, 9, 11
11	55.6, CH	3.92, *dt* (9.0, 3.5)	H-10	-
12	167.4, CO	-	-	-
14	50.3, CH	3.81, *ddd* (14.0, 6.9, 2.8)	H-13, 17	C-15, 17
15	167.9, CO	-	-	
17	20.8, CH_3	1.33, *d* (7.1)	H-14	C-14, 15
18	39.0, C	-	-	-
19	146.8, CH	6.22, *dd* (17.5, 10.5)	H-20	C-2, 18, 21, 22
20	111.0, CH_2	5.08, *dd* (17.4, 1.1)	-	C-18, 19
		5.02, *dd* (10.5, 1.2)	-	C-18, 19
21	28.0, CH_3	1.50, *s*	-	C-2, 18, 19, 22
22	28.0, CH_3	1.51, *s*	-	C-2, 18, 19, 21
23	34.2, CH_2	3.29, *d* (6.8)	H-24, 26, 27	C-4, 5, 6, 24, 25
24	124.9, CH	5.30, *dt* (7.3, 1.6)	H-23, 26, 27	-
25	130.4, C	-	-	-
26	25.5, CH_3	1.69, *s*	H-23, 24	C-24, 25, 27
27	17.7, CH_3	1.69, *s*	H-23, 24	C-24, 25, 26
28	29.0, CH_2	3.57, *d* (7.1)	H-29, 31, 32	C-7, 29, 30
29	122.8, CH	5.38, *dt* (7.2, 1.0)	H-28, 31, 32	C-31, 32
30	131.5, C	-	-	-
31	25.6, CH_3	1.74, *s*	H-28, 29	C-29, 30, 32
32	17.8, CH_3	1.74, *s*	H-28, 29	C-29, 30, 31
NH-1	-	9.71, *s*	-	C-2, 3, 8, 9
NH-13	-	8.19, *d* (2.6)	H-14	C-11, 15
NH-16		7.46, *d* (3.0)	H-11	C-12, 14

This was also confirmed by the HMBC correlations from NH-13 to C-11 (δ_C 55.6) and the carbonyl at δ_C 167.9 (C-15), from NH-16 to C-14 (δ_C 50.3) and the carbonyl carbon at δ_C 167.4 (C-12), from Me-17 (δ_H 1.33, *d*, *J* = 7.1 Hz; δ_C 20.8) to C-14 and C-15. Since the COSY spectrum also showed correlation of the mutually coupled methylene protons at δ_H 3.02, *dd* (*J* = 14.4, 9.5 Hz, H-10; δ_C 31.3) to H-11, the 3-methylpiperazine-2, 5-dione ring was connected to the methylene group at C-11.

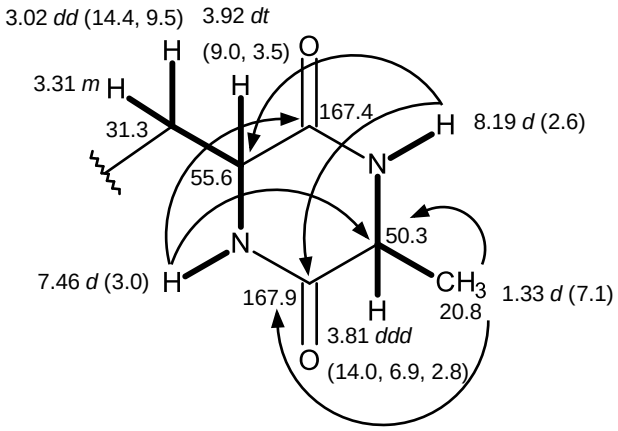

Contrary to **EC 13** (preechinulin), the ^{1}H NMR, COSY and HMBC spectra of **EC 15** (Table 29) also revealed the existence of the 2, 3, 5, 7-tetrasubstituted indole moiety. This hypothesis was confirmed correlations from the proton singlet at δ_H 7.04 (H-4; δ_C 114.6) to another proton singlet at δ_H 6.63 (H-6; δ_C 121.0) as well as the HMBC correlations from H-4 to C-6 (δ_C 121.0), C-3 (δ_C 105.1), C-8 (δ_C 132.2), from H-6 to C-4 (δ_C 114.6) and C-8, from NH-1 (δ_H 9.71, s) to C-3, C-8, C-9 (δ_C 129.2) and C-2 (δ_C 144.4).

Like **EC 13** (preechinulin), the 2-methylbut-3-en-2-yl side chain was on C-2 of the indole moiety which was confirmed by the COSY correlations from a pair of the sp^2 methylene protons at δ_H 5.08, *dd* (*J* = 17.4, 1.1 Hz, H-20a; δ_C 111.0)/5.02, *dd* (*J* = 10.5, 1.2 Hz, H-20b) to the olefinic proton at δ_H 6.22, *dd* (*J* = 17.5, 10.5 Hz, H-19; δ_C 146.8), as well as by the HMBC correlations from H-19 to the methyl carbons at δ_C 28.0 (Me-21 and Me-22), the sp^3 quaternary carbon at δ_C 39.0 (C-18) and C-2, and from the methyl singlets at δ_H 1.50 (Me-21; δ_C 28.0) and 1.51 (Me-20; δ_C 28.0) to C-2, C-18 and C-19.

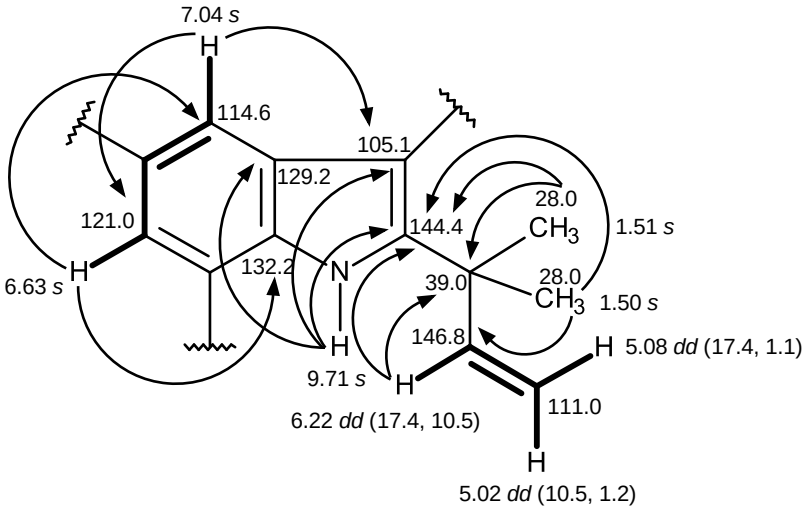

Analysis of the ^1H, ^{13}C NMR, DEPTs, COSY, HSQC and HMBC also revealed the presence of two 3-methylbut-2-en-1-yl (prenyl) groups. The first prenyl group consists of the coupling system, as observed in the COSY spectrum, from the methylene doublet at δ_H 3.29, *d* (*J* = 6.8, H_2-23; δ_C 34.2), through the olefinic proton at δ_H 5.30, *dt* (*J* = 7.3, 1.6 Hz, H-24, δ_C 124.9) to the methyl singlet at δ_H 1.69 (6H, Me-26 and Me-27; δ_C 25.5 and δ_C 17.7).

This system was confirmed by the HMBC correlations from H-23 to C-24 (δ_C 124.9), C-25 (δ_C 130.4), from Me-26/Me-27 (δ_H 1.69, *s*) to C-24 and C-25. Since H-23 showed HMBC correlations to C-4, C-6 and the quaternary sp^2 carbon at δ_C 131.6, this carbon was assigned to C-5. The second group consists of the coupling system from the methylene protons at δ_H 3.57, *d* (*J* = 7.1, H_2-28; δ_C 29.0), through the olefinic proton at δ_H 5.38, *dt* (*J* = 7.2, 1.0 Hz, H-29, δ_C 122.8) to the methyl singlet at δ_H 1.74 (6H, Me-31 and Me-32; δ_C 25.6 and 17.8). This was corroborated by the HMBC correlations from H_2-28 to C-29 (δ_C 122.8), C-30 (δ_C 131.5). Since H_2-28 showed correlation to the quaternary aromatic carbon at δ_C 123.6, this carbon was assigned to C-7.Therefore, the two prenyl substituents were on C-5 and C-7 of the indole moiety.

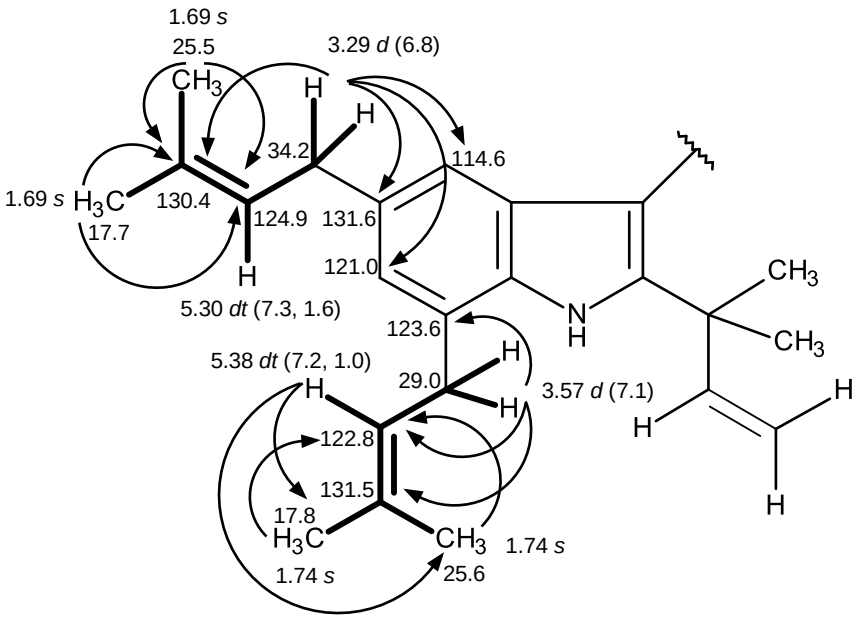

That the prenylated indole moiety was connected to the 3-methylpiperazine-2, 5-dione through the methylene group was confirmed by the HMBC correlation from H_2-10 to C-2, C-3 and C-9. Therefore the complete structure of **EC 15** was elucidated as 3-(2-(1,1-Dimethyl-2-propenyl)-5,7-bis(3-methyl-2-butenyl)-1*H*-indol-3-yl)methyl)-6-methyl-2,5-piperazinedione:

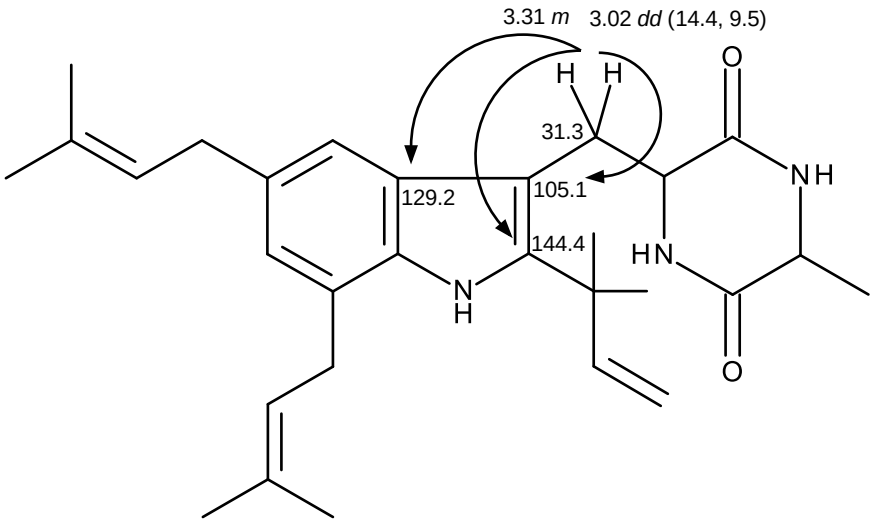

EC 15 was identified as echinulin since its specific rotation ($[\alpha]_D^{20}$ = – 41.7) was compatible with that determined for echinulin (Smetanina *et al*., 2007). Echinulin is a fungal metabolites isolated from various fungal species including the soil fungus *Chaetomium globosum* KMITL-N0802 (Kanokmedhakul *et al*., 2002), *Eurotium repens*, which was isolated from the sponge *Suberites domuncula* (Smetanina *et al*., 2007), a halotolerant fungus *Aspergillus variecolor* B-17 (Wang *et al*., 2007a), mangrove-derived endophytic fungi *Eurotium rubrum* (Li *et al*., 2008b) and *Eurotium cristatum* EN-220 (Du *et al*., 2012), a deep-ocean sediment derived fungus *Penicillium griseofulvum* (Zhou *et al*., 2010), marine sponge-associated fungus

Eurotium cristatum (Gomes *et al*., 2012) and crinoid-derived fungus *Aspergillus rubur* 1017 (Li *et al*., 2017).

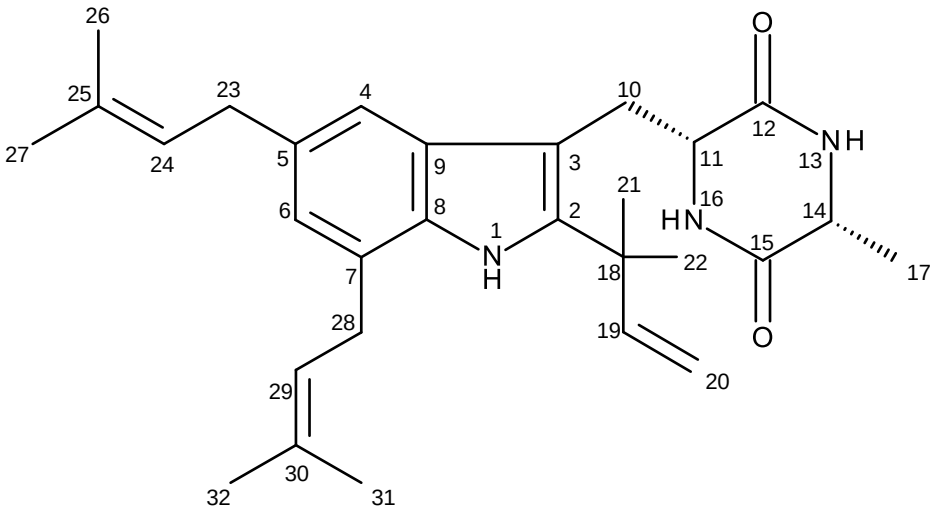

Figure 110. Structure of echinulin (**EC 15**)

3.1.11.7. Eurocristatine (EC 16)

EC 16 was isolated as a white crystal (mp, 243-244 ºC) and its molecular formula was determined as $C_{32}H_{36}N_6O_4$, based on the HRESIMS *m/z* 569.2889 $[M+H]^+$ (calculated for $C_{32}H_{37}N_6O_4$, 569.2876), indicating nineteen degree of unsaturation. However, the ^{13}C NMR spectrum (Table 30) displayed only sixteen carbon signals which was categorized, based on DEPTs and HSQC spectra, as two amide carbonyl (δ_C 168.4 and 167.5), two quaternary sp^2 (δ_C 149.1 and 130.4), four

methine sp^2 (δ_C 128.7, 124.4, 118.0 and 108.9), one quaternary sp^3 (δ_C 59.7), four methine sp^3 (δ_C 78.8, 62.3, 55.7 and 32.1), one methylene sp^2 (δ_C 37.2) and two methyl (δ_C 18.0 and 19.0) carbons. Since the number of the carbon signals displayed by the ^{13}C NMR spectrum was half of the number of the carbon atoms in the molecular formula, **EC 16** was hypothesized to be a symmetrical dimer.

Table 30. ^{1}H and ^{13}C NMR (DMSO, 300.13 and 75.47 MHz) and HMBC assignment for **EC 16**

Position	δ_C, type	δ_H, type (*J* in Hz)	COSY	HMBC
2	78.8, CH	4.90, *brs*	-	-
3	59.7, C	-	-	-
4	124.4, CH	7.39, *d* (7.5)	H-5	C-3, 6, 8
5	118.0, CH	6.64, *dd* (7.5, 7.5)	H-4, 6	C-7, 9
6	128.7, CH	7.03, *dd* (7.6, 7.6)	H-5, 7	C-4, 8
7	108.9, CH	6.60, d (7.3)	H-6	C-5, 9
8	149.1, C	-	-	-
9	130.4, C	-	-	-
10a	37.2, CH_2	3.15, *m*	H-11	C-3
b		2.39, *dd* (14.2, 9.4)	H-11	C-3, 11, 12
11	55.7, CH	4.12, *t* (8.7)	H-10	C-10, 12
12	168.4, CO	-	-	-
14	62.3, CH	3.41, *m*	H-17, NH-13	C-12, 17, 18, 19
15	167.5, CO	-	-	-
17	32.1, CH	1.95, *m*	H-14, 18, 19	C-14, 18, 19
18	19.0, CH_3	0.80, *d* (6.8)	H-17	C-14, 17, 19
19	18.0, CH_3	0.69, *d* (6.7)	H-17	C-14, 17, 18
NH-1	-	6.75, *brs*	-	C-2, 3, 8, 9
NH-13	-	8.28, *d* (4.2)	H-14	C-11, 14, 15

That part of the monomer consisted of 2, 3-dihydro-1*H*-indole was supported by the coupling system, as observed in the COSY spectrum, from H-4 (δ_H 7.39, *d*, *J* = 7.5 Hz; δ_C 124.4), through H-5 (δ_H 6.64, *dd*, *J* = 7.5, 7.5 Hz; δ_C 118.0) and H-6 (δ_H 7.03, *dd*, *J* = 7.6, 7.6 Hz; δ_C 128.7) to H-7 (δ_H 6.60, *d*, *J* = 7.3 Hz; δ_C 108.9) as well as by the HMBC correlations from H-4 to C-6 (δ_C 128.7), C-8 (δ_C 149.1), and a quaternary sp^3 carbon at δ_C 59.7 (C-3), from H-7 to C-5 (δ_C 118.0) and C-9 (δ_C 130.4) and from the *brs* of the amine proton of the 2,3-dihydroindole ring at δ_H 6.75 (NH-1) to C-3, C-8, C-9 and the sp^3 methine carbon at δ_C 78.8 (C-2; δ_H 4.90, *brs*).

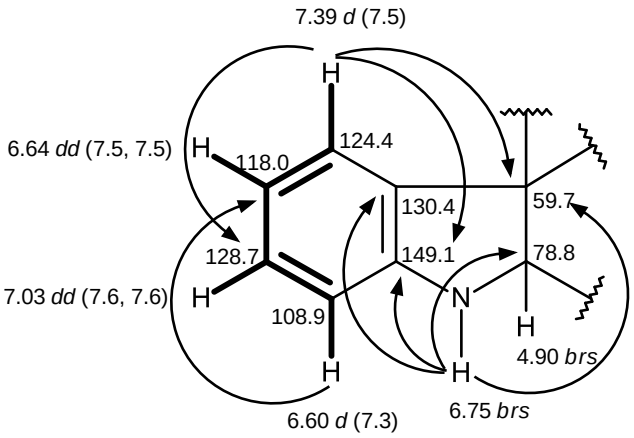

Another part of the monomer was 3-isopropylpiperazine-2, 5-dione, similar to that of **EC 12**, since the COSY spectrum showed correlations from the multiplet at δ_H 1.95 (H-17; δ_C 32.1) to the multiplet at δ_H 3.41 (H-14; δ_C 62.3) and the methyl doublets at δ_H 0.80 (*J* = 6.8 Hz, H-18; δ_C 19.0) and δ_H 0.69 (*J* = 6.7 Hz, H-19; δ_C 18.0) in addition to the HMBC correlations from the doublet of the amide proton at δ_H 8.28 (*J* = 4.2 Hz) to C-11 (δ_C 55.7), C-14 (δ_C 62.3) and the carbonyl at δ_C 167.5

(C-15), from the triplet at δ_H 4.12 (J = 8.7 Hz, H-11, δ_C 55.7) to C-10 (δ_C 37.3) and a weak correlation to the carbonyl at δ_C 168.4 (C-12).

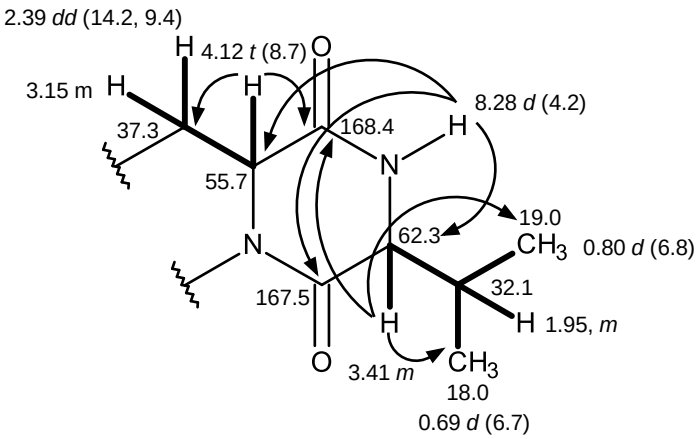

That the 2,3-dihydro-1*H*-indole was connected to the 3-isopropylpiperazine-2, 5-dione between C-3 and C-11, through the methylene group (C-10) as well as between C-2 and N-16, forming an extra pyrrolidine ring between the 2,3-dihydro-1*H*-indole and the 1,4-diketopiperazine ring, was corroborated by the weak HMBC correlation from H_2-10 (δ_H 2.39, *dd*, J = 14.2, 9.4 Hz)/3.15, *m* (δ_C 37.3) to C-3 as well as by COSY correlations from H_2-10 to H-11. Therefore, the structure of the monomer was:

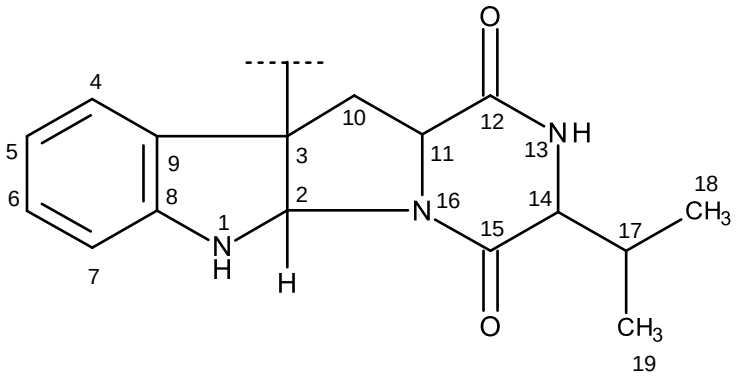

This structure corresponds to a molecular formula $C_{16}H_{18}N_3O_2$ and since there was no substituent on C-3, it was proposed that the two monomers are linked through its C-3. Therefore the molecule of **EC 16** is:

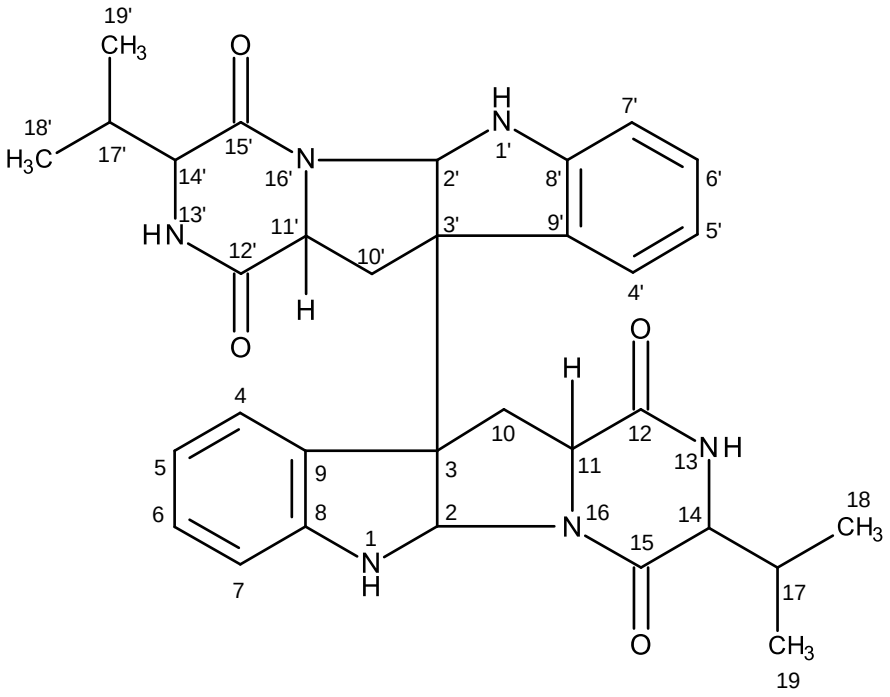

In order to verify the stereochemistry of C-3/C-3′ and C-14/C-14′, the X-ray analysis was performed and the ORTEP view of **EC 16** was shown below:

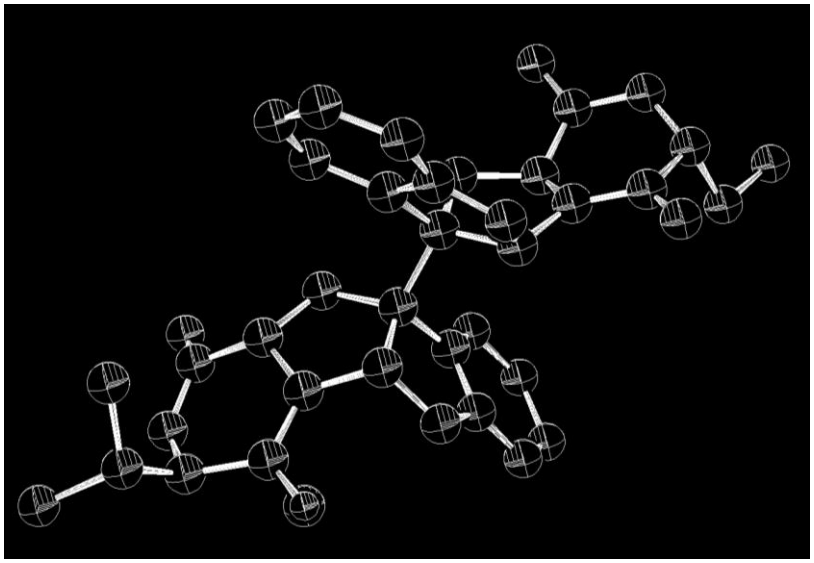

Figure 111. ORTEP view of **EC 16**

From the ORTEP view, it is possible to conclude that the absolute configuration of C-2/2′, C-3/3′, C-11/11′ and C-14/14′, respectively as 2/2′*R*, 3/3′*S*, 11/11′*S* and 14/14′*R*.

Literature search revealed that **EC 16** is eurocristatine, a *bis*-indolylmethyl 1, 4-diketopiperazine previously isolated from marine sponge-associated fungus *Eurotium cristatum* (Gomes *et al*., 2012).

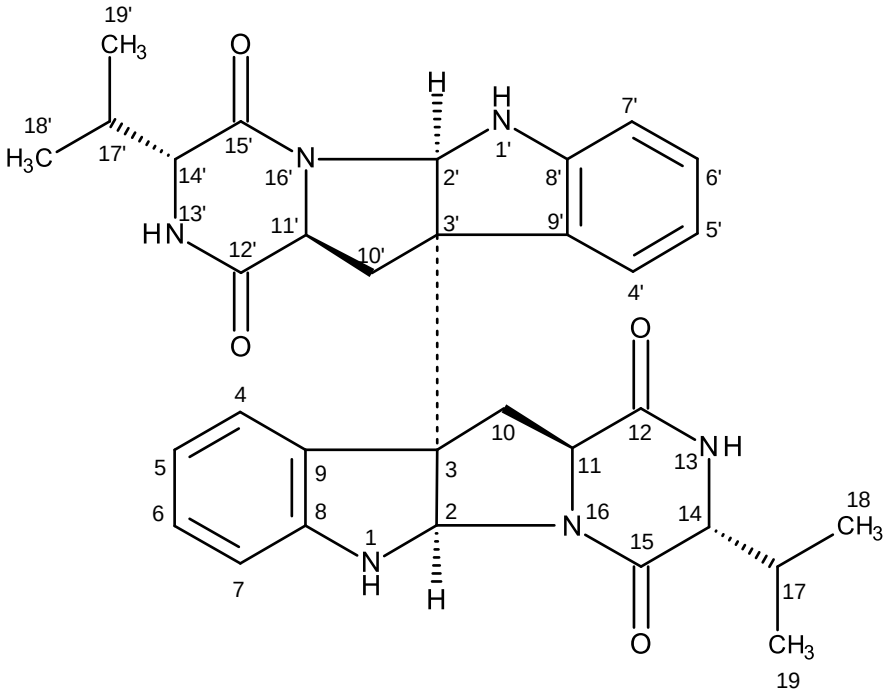

Figure 112. Structure of eurocristatine (**EC 16**)

3.1.12 Structure Elucidation of 2-(2, 2-Dimethylbut-3-enoyl) amino-benzoic acid

3.1.12.1. 2-(2, 2-Dimethylbut-3-enoyl) amino-benzoic acid (EC 10)

EC 10 was isolated as yellow viscous liquid. The (+)-HRESIMS gave the *m/z* at 234.1132 $(M+H)^+$ corresponding to $C_{13}H_{16}NO_3$ (calculated 234.1130). Therefore, the molecular formula of **EC 10** is $C_{13}H_{15}NO_3$, indicating seven degrees of unsaturation. The IR spectrum showed absorption bands for amine (3421 cm^{-1}), hydroxyl (3253 cm^{-1}), conjugated carbonyl (1696 cm^{-1}), amide carbonyl (1670 cm^{-1}), aromatic (1606, 1586 cm^{-1}) and olefin (1636 cm^{-1}) carbons.

The ^{13}C NMR spectrum (Table 31) exhibited thirteen carbon signals which can be classified, according to DEPTs and HSQC spectra, as two carbonyls (δ_C 174.4 and 169.9), two quaternary sp^2 (δ_C 141.2 and 116.4), five methine sp^2 (δ_C 142.5, 133.9, 131.2, 122.4 and 119.4), one methylene sp^2 (δ_C 114.4), one quaternary sp^3 (δ_C 46.3) and two tertiary methyl (δ_C 24.4) groups.

The ^{1}H NMR spectrum, in combination with COSY and HSQC spectra (Table 31), exhibited the signals of aromatic protons of the 1, 2-dissubsituted benzene ring at δ_H 8.60, *d* (*J* = 7.8 Hz; δ_C 119.4), 8.00, *dd* (*J* = 7.8, 1.5 Hz; δ_C 131.2), 7.57, *ddd* (*J* = 7.8, 7.8, 1.5 Hz; δ_C 133.9), 7.13, *ddd* (*J* = 7.8, 7.8, 1.5 Hz; δ_C 112.4), three vinyl proton signals at δ_H 6.09, *dd* (*J* = 17.4, 10.6 Hz; δ_C 142.5), 5.27, *d* (*J* = 17.4 Hz; δ_C 114.4) and 5.22, *d* (*J* = 10.6 Hz; δ_C 114.4) and a methyl singlet at δ_H 1.32 (6H, δ_C 24.4), in addition to a broad singlet of the hydroxyl group at δ_H 11.55.

Table 31. ^{1}H and ^{13}C NMR (DMSO, 300.13 and 75.47 MHz) and HMBC assignment for **EC 10**

Position	δ_C, type	δ_H, type (*J* in Hz)	COSY	HMBC
1	116.4, C	-	-	-
2	141.2, C	-	-	-
3	119.4, CH	8.60, *d* (7.8)	H-4	C-1, 5
4	133.9, CH	7.57, *ddd* (7.8, 7.8, 1.5)	H-3, 5	C-2, 6
5	122.4, CH	7.13, *ddd* (7.8, 7.8, 1.5)	H-4, 6	C-1, 3
6	131.2, CH	8.00, *dd* (7.8, 1.5)	H-5	C-2, 4, 7
7	169.9, CO	-	-	-
1′	174.4, CO	-	-	-
2′	46.3, C	-	-	-
3′	142.5, CH	6.09, *dd* (17.4, 10.6)	H-4′a, 4′b	C-2′, 5′, 6′
4′a	114.4, CH_2	5.27, *d* (17.4)	H-3′	C-2′, 3′
b		5.22, *d* (10.6)	H-3′	C-2′, 3′
5′	24.4, CH_3	1.32, *s*	-	C-1′, 2′, 3′, 6′
6′	24.4, CH_3	1.32, *s*	-	C-1′, 2′, 3′, 5′
OH-7	-	11.55, *brs*	-	-

The HMBC spectrum exhibited correlations from the methyl singlet at δ_H 1.32 (CH_3-5′/6′) to the quaternary sp^3 carbon at δ_C 46.3 (C-2′), the olefinic carbon at δ_C 142.5 (C-3′) and the carbonyl carbon at δ_C 174.4 (C-1′), while the methylene protons at δ_H 5.27, *d* (*J* = 17.4 Hz; H-4′a) and 5.22, *d* (*J* = 10.6 Hz, δ_H H-4′b) exhibited cross peaks to C-2′, C-3′ and the vinylic proton at δ_H 6.09, *dd* (*J* = 17.4, 10.6 Hz; H-3′) showed cross peaks with C-2′ and C-5′/6′, revealing the existence of a 2, 2-dimethylbut-3-enoyl moiety.

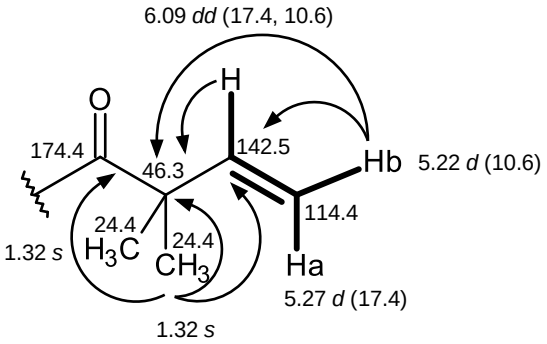

Additionally, the HMBC spectrum also exhibited correlations from the double doublet at δ_H 8.00 (*J* = 7.8, 1.5 Hz, H-6) to the carbons at δ_C 141.2 (C-2), 133.9 (C-4) and 169.9 (CO-7) and from the double at δ_H 8.60 (*J* = 7.8 Hz; H-3) to the carbon at δ_C 116.4 (C-1) and 122.4 (C-5), confirming the presence of the anthranilic acid moiety.

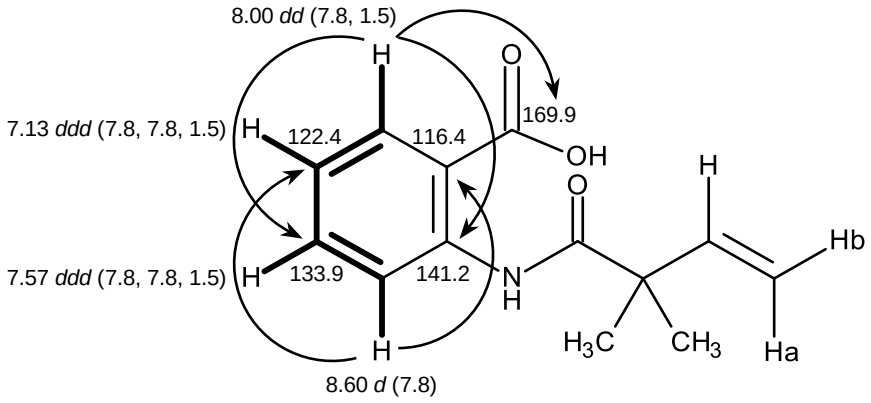

Taking together the NMR data and its molecular formula, the structure of **EC 10** (Figure 113) was established as 2-(2, 2-dimethylbut-3-enoyl) amino-benzoic acid. Extensive literature search revealed that this compound has never been reported previously. Therefore, it is a new compound.

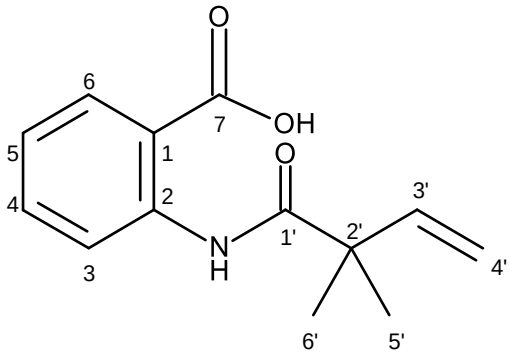

Figure 113. Structure of 2-(2, 2-Dimethylbut-3-enoyl) amino-benzoic acid (**EC 10)**

3.1.13 Structure Elucidation of Cyclopeptides

3.1.13.1. Sartoryglabramide A (NG 8)

NG 8 was isolated as white crystals (mp, 146-148ºC), and its molecular formula $C_{30}H_{30}N_4O_4$ was established on the basis of the (+)-HRESIMS *m/z* 511.2365 $[M+H]^+$, indicating eighteen degrees of unsaturation. The IR spectrum showed absorption bands for amine (3447 cm^{-1}), amide carbonyl (1655 cm^{-1}) and aromatic (1622, 1587, 1526 cm^{-1}).

The ^{13}C NMR, DEPTs and HSQC spectra (Table 32) revealed the presence of four amide carbonyls (δ_C 170.2, 169.9, 168.8 and 166.5), four quaternary sp^2 (δ_C 138.3, 137.3, 136.5 and 124.8), fourteen methine sp^2 [δ_C 130.4, 129.6 (2C), 129.1 (2C), 128.1 (2C), 128.0 (2C), 126.6, 126.3, 126.0, 122.4 and 120.4], three methine

sp^3 (δ_C 62.2, 55.2 and 54.4), and five methylene sp^3 (δ_C 49.4, 37.1, 34.7, 28.3 and 24.6).

The ^{1}H NMR spectrum (Table 32) exhibited, besides three NH signals at δ_H 9.40, *s*, 8.49, *d* (*J* = 7.8 Hz) and 7.41, *d* (*J* = 9.8 Hz), and in conjunction with COSY and HSQC spectrum displayed the signals of four aromatic protons of anthranilic acid at δ_H 8.31, *dd* (*J* =7.9, 0.5 Hz, H-6), 7.55, *dd* (*J* = 7.7, 1.3 Hz, H-3), 7.48, *ddd* (*J* = 7.9, 7.9, 1.4 Hz, H-5) and 7.16, *dd* (*J* = 7.9, 7.7 Hz, H-4). This was supported by the HMBC correlations from NH-8 (δ_H 9.40, *s*) to C-2 (δ_C 124.8), C-6 (δ_C 120.4), from H-3 to C-1 (δ_C 166.5), C-5 (δ_C 130.4) and C-7 (δ_C 136.5), from H-4 to C-2 and C-6.

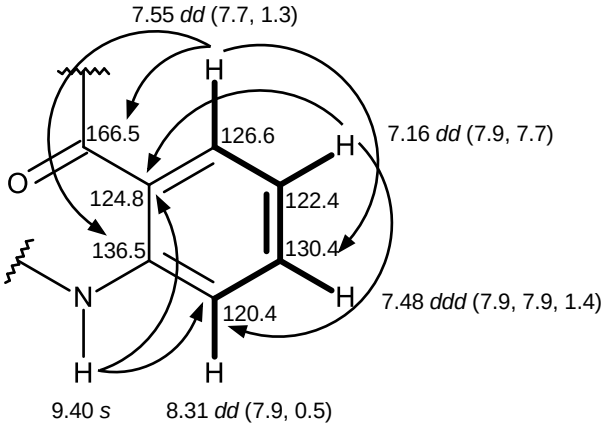

Table 32. ^{1}H and ^{13}C NMR (DMSO, 500.13 MHz and 125.77 MHz) and HMBC assignment for **NG 8**

	Position	**δ_C, type**	**δ_H, (*J* in Hz)**	**COSY**	**HMBC**
Anthranilic acid	1	166.5, CO	-	-	-
	2	124.8, C	-	-	-
	3	126.6, CH	7.55, *dd* (7.7, 1.3)	H-4	C-1, 5, 7
	4	122.4, CH	7.16, *dd* (7.9, 7.7)	H-3, 5	C-2, 6
	5	130.4, CH	7.48, *ddd* (7.9, 7.9, 1.4)	H-4, 6	C-3, 7
	6	120.4, CH	8.31, *dd* (7.9, 0.5)	H-5	C-2, 4
	7	136.5, C	-	-	-
	NH-8	-	9.40, *s*	-	C-2, 6, 9
Phe-I	9	168.8, CO	-	-	-
	10	55.2, CH	4.36, *ddd* (8.4, 7.8, 5.3)	H-11, NH-18	C-9, 11, 12
	11a	34.7, CH_2	2.97, *dd* (13.9, 8.4)	H-10, 11b	C-9, 10, 12, 13, 17
	b		3.23, *dd* (13.9, 5.3)	H-10, 11a	C-9, 10, 12, 13, 17
	12	138.3, C	-	-	-
	13	129.6, CH	7.08, *dd* (7.4, 1.4)	H-14	C-11, 15, 17
	14	128.0, CH	7.19, *dd* (7.4, 7.4)	H-14. 15	C-12, 16
	15	126.0, CH	7.18, *dd* (7.4, 7.4)	H-14, 16	C-13, 17
	16	128.0, CH	7.19, *dd* (7.4, 7.4)	H-15, 17	C-12, 14
	17	129.6, CH	7.08, *dd* (7.4, 1.4)	H-16	C-11, 13, 15
	NH-18	-	8.49, *d* (7.8)	H-10	C-10, 19

Table 32. ^{1}H and ^{13}C NMR (DMSO, 500.13 MHz and 125.77 MHz) and HMBC assignment for **NG 8** (Cont.)

	Position	**δ_C, type**	**δ_H, (*J* in Hz)**	**COSY**	**HMBC**
Phe-II	19	169.9, CO	-	-	-
	20	54.4, CH	4.58, *ddd* (9.8, 8.9, 7.3)	H-21a, b	C-19, 21, 22
	21a	37.1, CH_2	2.71, *dd* (13.5, 8.9)	H-20, 21b	C-19, 20, 22, 23, 27
	b		2.94, *dd* (13.5, 7.3)	H-20, 21a	C-19, 20, 22, 23, 27
	22	137.3, C	-	-	-
	23	129.1, CH	7.14, *dd* (7.4, 1.4)	H-24	C-25, 27
	24	128.1, CH	7.27, *dd* (7.4, 7.4)	H-23, 25	C-22, 26
	25	126.3, CH	7.23, *dd* (7.4, 7.4)	H-24, 26	C-23, 27
	26	128.1, CH	7.27, *dd* (7.4, 7.4)	H-25, 27	C-22, 24
	27	129.1, CH	7.14, *dd* (7.4, 1.4)	H-26	C-23, 25
	NH-28	-	7.41, *d* (9.8)	H-20	C-19, 20, 29
Pro	29	170.2, CO	-	-	-
	30	62.2, CH	4.20, *dd* (9.8, 2.3)	H-31a, b	C-29, 31, 32
	31a	28.3, CH_2	1.54, *m*	H-30, 31b	-
	b		2.12, *m*	H-30, 31a	C-29, 30
	32	24.6, CH_2	1.89, *m*	H-31a, b	-
	33a	49.4, CH_2	3.70, *dd* (17.6, 9.6)	H-32, 33b	C-30, 32
	b		3.63, *m*	H-32, 33a	-
	N-34	-	-	-	-

The existence of phenylalanine residue (Phe I) was based on the HMBC correlations from the *dd* at δ_H 7.08 (*J* = 7.4, 1.4 Hz; δ_C 129.6, H-13) to the carbons at δ_C 34.7 (C-11), 126.0 (C-15), 129.6 (C-17), from the *dd* at δ_H 7.19 (*J* = 7.4, 7.4 Hz; δ_C 128.0, H-14) to the carbons at δ_C 138.3 (C-12) and 128.0 (C-16), from the *dd* at δ_H 7.18 (*J* = 7.4, 7.4 Hz; δ_C 126.0, H-15) to the carbons at δ_C 129.6 (C-13) and C-17, from the *dd* at δ_H 7.19 (*J* = 7.4, 7.4 Hz; δ_C 128.0, H-16) to the C-12 and 128.0 (C-14), from the *dd* at δ_H 7.08 (*J* = 7.4, 1.4 Hz; δC 129.6, H-17) to the C-11, C-13 and 126.0 (C-15). The coupling systems of the aromatic protons of phenylalanine residue as observed in the COSY spectrum (Table 32).

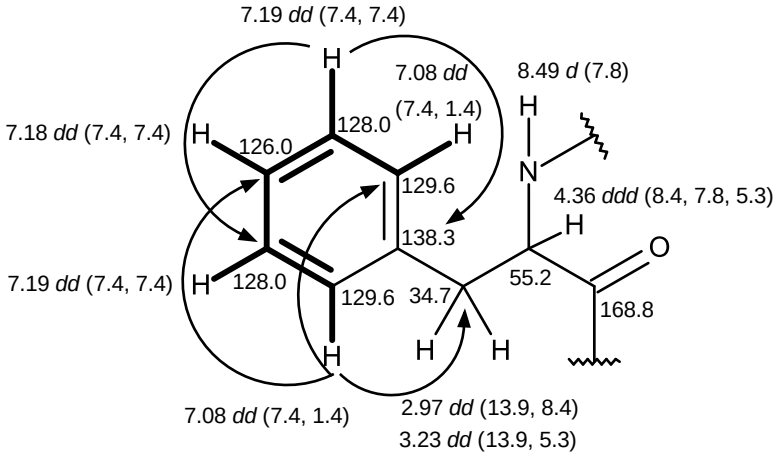

Moreover, the presence of second phenylalanine residue (Phe II) displayed the COSY cross peaks from the *dd* at δ_H 7.14 (*J* = 7.4, 1.4 Hz, H-23) to the *dd* at δ_H 7.27 (*J* = 7.4, 7.4 Hz, H-24), from the *dd* at δ_H 7.14 (*J* = 7.4, 1.4 Hz, H-27) to the *dd* at δ_H 7.27 (*J* = 7.4, 7.4 Hz, H-26), and also by the *dd* at δ_H 7.27 (*J* = 7.4, 7.4 Hz, H-24), *dd* at δ_H 7.23 (*J* = 7.4, 7.4 Hz, H-25) and *dd* at δ_H 7.27 (*J* = 7.4, 7.4 Hz, H-26).

This was confirmed by the HMBC correlations from H-23 to C-25 (δ_C 126.3), C-27 (δ_C 129.1), from H-26 to C-22, C-24 (δ_C 128.1), from H-27 to C-23 and C-25.

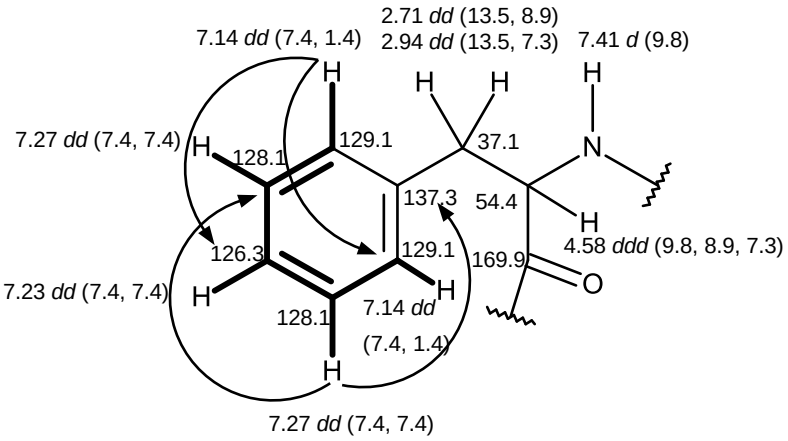

The existence of the proline residue was evidence not only by the COSY correlations from the double doublet at δ_H 4.20 (*J* = 9.8, 2.3 Hz, H-30; δ_C 62.2) to the multiplets at δ_H 1.54 and 2.12 (H_2-31, δ_C 28.3), from the multiplet at δ_H 1.89 (H_2-32; δ_C 24.6) to H_2-31 and the double doublet at δ_H 3.70 (*J* = 17.6, 9.6 Hz, H-33; δ_C 49.4) and a multiplet at δ_H 3.63 (H-33; δ_C 49.4) but also by the HMBC correlations from H-30 to the carbon signals at δ_C 170.2 (CO-29), δ_C 28.3 (C-31) and δ_C 24.6 (C-32), from H_2-33 to C-30 (δ_C 62.2), C-32 and from H_2-31 to C-29 and C-30.

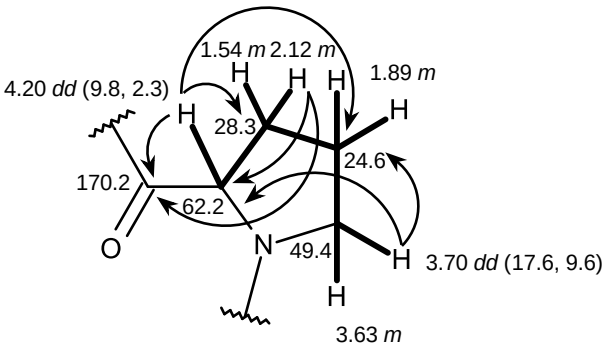

The anthranilic acid residue was linked to the phenylalanine residue, through the amino group of the former and the carboxyl group of the latter, since the HMBC spectrum showed correlations from the NH signal at δ_H 9.40, *s* (NH-8) to the carbonyl carbon at δ_C 168.8 (C-9), from the methine proton at δ_H 4.36, *ddd* (*J* = 8.4, 7.8, 5.3 Hz, H-10) to C-9, C-11 (δ_C 34.7), C-12 (δ_C 138.3), from the methylene protons at δ_H 2.97, *dd* (*J* =13.9, 8.4 Hz, H-11) and 3.23, *dd* (*J* =13.9, 5.3 Hz, H-11) to C-9, C-10 (δ_C 55.2), C-12, C-13/C-17 (δ_C 129.6), as well by the COSY correlation of H-10 and H_2-11.

The phenylalaline residue (Phe-I) was linked to another phenylalanine residue (Phe-II) was corroborated by the COSY correlation of H-10 to the proton doublet at δ_H 8.49, d (*J* = 7.8 Hz, NH-18), as well as by the HMBC correlations of NH-18 to C-10 and the carbonyl carbon at δ_C 169.9 (C-19), from the methine proton signal at δ_H 4.58, *ddd* (*J* = 9.8, 8.9, 7.3, 8.4 Hz, H-20) to C-19, C-21 (δ_C 37.1), C-22 (δ_C 137.3), from the methylene proton (H-21) signals at δ_H 2.71, *dd* (*J* = 13.5, 8.9 Hz)/2.94 *dd* (*J* = 13.5, 7.3 Hz) to C-19, C-20 (δ_C 54.4), and C-23/C-27 (δ_C 129.1), as well as the COSY correlation of H-20 to H_2-21 and the proton doublet at δ_H 7.41 (*J* = 9.8 Hz, NH-28). That the proline residue was connected to the Phe-II residue, through the carbonyl of the former and the amino group of the latter was corroborated by the HMBC correlation of NH-28 to CO-29. Since there are only three NH signals, the nitrogen of the proline residue was linked to the carbonyl group of anthranilic acid.

This was corroborated by the HMBC correlation of H-3 to CO-1 and of NH-8 to C-2 and C-6. Therefore, combining this information, it was possible to conclude that **NG 8** was cyclo (anthranilic acid- Phe- Phe- Pro).

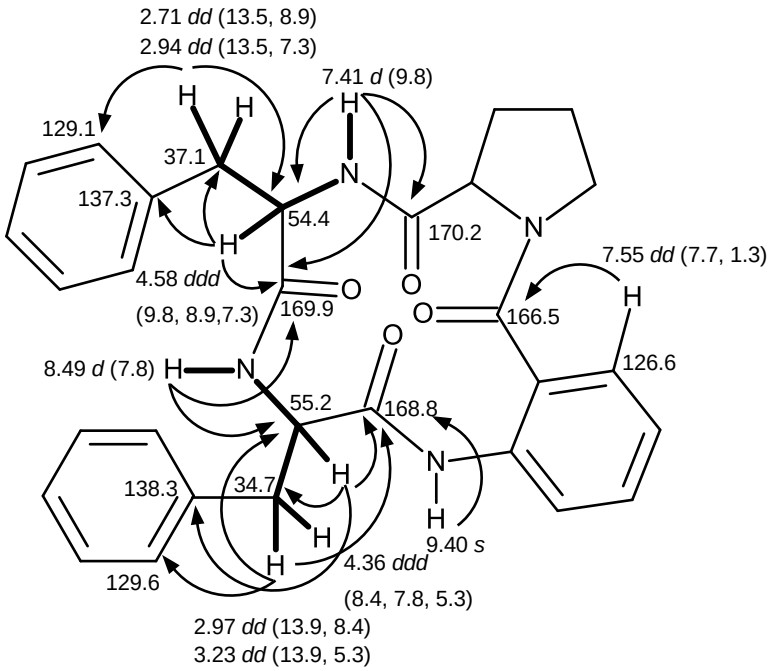

Since **NG 8** could be obtained in a suitable crystal for X-ray diffraction, the stereochemistry of its amino acid residues was tentatively determined by X-ray analysis and the ORTEP view shown in Figure 114 revealed that Phe-I, Phe-II and Pro have the same relative configuration.

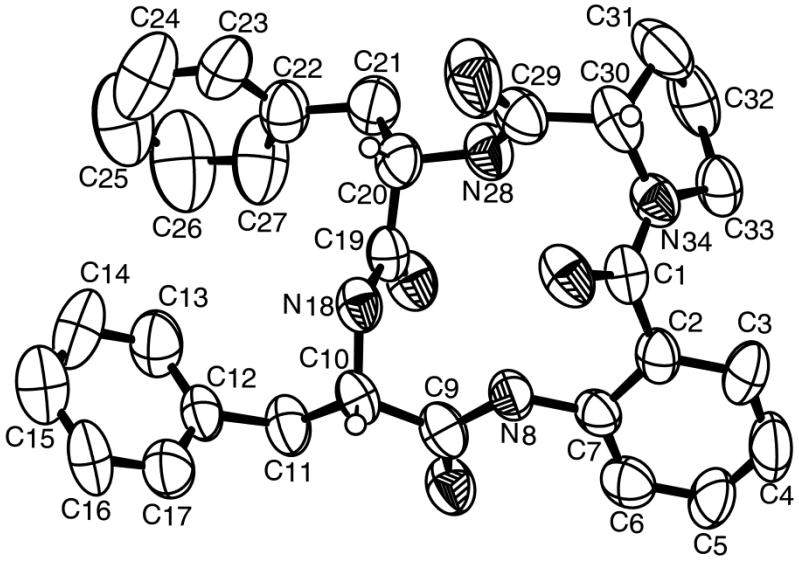

Figure 114. ORTEP view of **NG 8**

However, since the flack *x* parameter value (0.3) did not guarantee the absolute confidence of the absolute configuration, the stereochemistry of the amino acid residues of **NG 8** was confirmed by chiral HPLC analysis of its acidic hydrolysate, using appropriate D- and L- amino acid standards, according to the previously described method (Prompanya *et al*., 2015).

The enantioseparations of the standard amino acids were successfully performed with the Chirobiotic T column under reversed-phase elution conditions (Berthod *et al*., 1996). The elution order of the enantiomers of all the standards amino acids was confirmed by injecting the solutions of the enantiomeric mixtures and then each enantiomer separately at a flow rate of 1mL/min. As predicted, the D-enantiomer was always more strongly retained than the corresponding L-enantiomer on Chirobiotic column (Berthod *et al*., 1996). The retention times (t_R min) for standard

amino acids, using MeOH: H_2O (80:20 v/v) as mobile phase, at a flow rate of 1.0 mL/min, and with UV detection set at 210 nm, were L-Phe (3.8) and D-Phe (5.0), L-Pro (6.7) and D-Pro (20.1) were observed in Table 33 and Figure 115.

Table 33. Chromatographic conditions: column, Chirobiotic T; mobile phase, MeOH: H_2O (80:20 v/v); flow rate, 1.0 mL/min; detection, 210 nm.

Amino Acids	Retention Time (t_R min)
L-Phe	3.81
D-Phe	5.00
L-Pro	6.72
D-Pro	20.10
Anthranilic acid	1.92
Acidic Hydrolysate **NG 8**	1.91, 2.55, 2.86, 3.49, 3.89, 6.79
Acidic Hydrolysate **NG 8** + DL-Phe (coinjection)	1.87, 2.50, 2.89, 3.68, 5.01, 6.82
Acidic Hydrolysate **NG 8** + DL-Pro (coinjection)	1.96, 2.60, 2.96, 3.52, 3.92, 6.70, 21.09

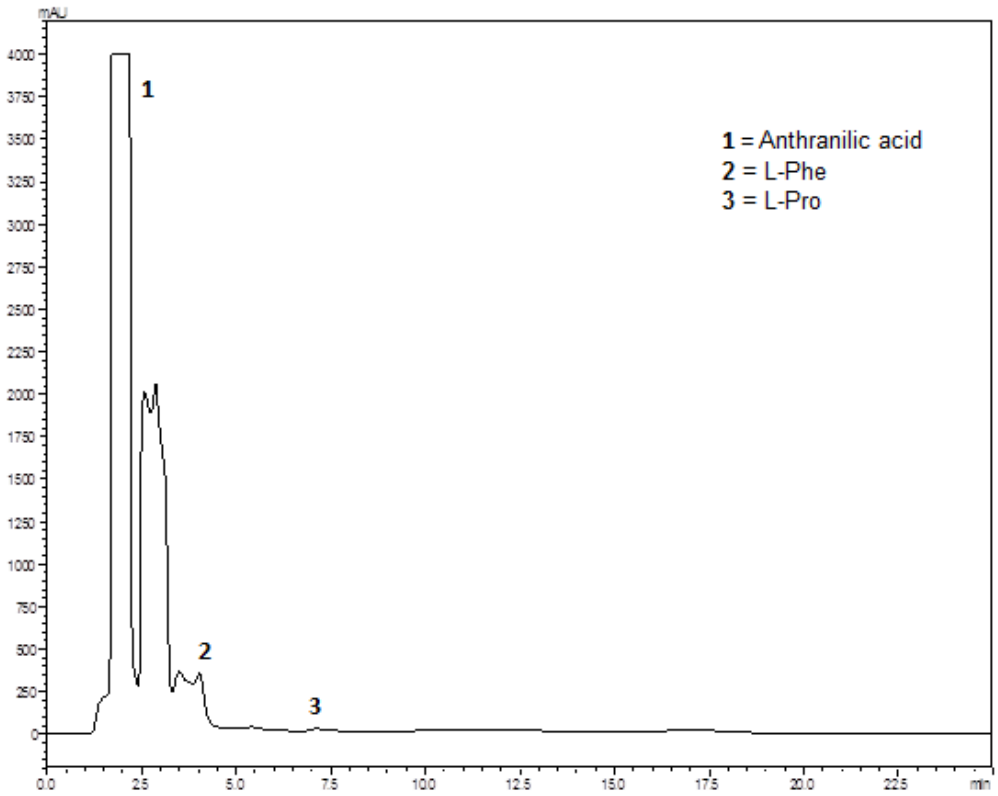

Figure 115. Chromatogram of the acidic hydrolysate of **NG 8**. Chromatographic condition: Chirobiotic T; mobile phase, MeOH: H_2O (80:20 v/v); flow rate, 1.0 mL/min; detection, 210 nm.

Based on mix HPLC analyses of the acidic hydrolysate with standard D- and L-amino acids (co-injection), **NG 8** was elucidated as cyclo (anthranilic acid-L-Phe-L-Phe-L-Pro). Since **NG 8** is a new compound, we have named it sartoryglabramide A.

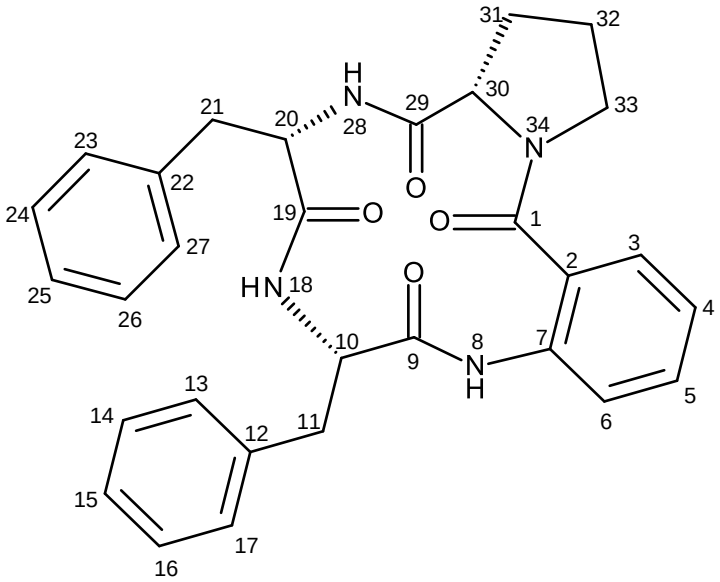

Figure 116. Structure of sartoryglabramide A (**NG 8**)

3.1.13.2. Sartoryglabramide B (NG 9)

Compound **NG 9**, which was also isolated as white solid (mp, 190-192ºC), exhibited the $[M+H]^+$ peak at *m/z* 550.2501 [(+)-HRESIMS], corresponding to $C_{32}H_{32}N_5O_4$ (calculated 550.2454). Like **NG 8**, its IR spectrum showed absorption bands for amine (3417 cm^{-1}), amide carbonyl (1649 cm^{-1}) and aromatic (3058, 1620, 1588, 1526 cm^{-1}). With some exceptions, the general feature of the ^1H and ^{13}C spectra of compound **NG 9** resembled those of **NG 8**.

The ^{13}C NMR, DEPTs and HSQC spectra (Table 34) displayed signals of four carbonyls [δ_C 170.2, 170.1, 169.0 and 166.4], six quaternary sp^2 (δ_C 134.4, 136.3,

136.0, 127.7, 125.2 and 110.2), fourteen methine sp^2 [δ_C 130.4, 129.0 (2C), 128.1 (2C), 126.5, 126.3, 124.0, 122.6, 120.8, 120.7, 118.5, 118.2 and 111.3), three methine sp^3 (δ_C 62.1, 54.6 and 54.3), and five methylene sp^3 (δ_C 49.4, 37.0, 28.3, 24.9 and 24.6).

Unlike **NG 8**, the ^{1}H NMR spectrum (Table 34) exhibited four NH signals at δ_H 10.82, *brs*, 9.25, *s*, 8.42, *d* (*J* = 7.9 Hz) and 7.38, *d* (*J* = 10.0 Hz). Similar to **NG 8**, the presence of the proline residue was corroborated by the presence of the coupling system of the proton signals from H-33 to H_2-36 (δ_H 4.15, *dd*, *J* = 9.0, 1.2 Hz, H-33; δ_C 62.1), δ_H 1.45, *m* and 2.09, *m* (H_2-34; δ_C 28.3), δ_H 1.86, *m* (H_2-35; δ_C 24.6), and δ_H 3.55, *m* and 3.67, *m* (H_2-36; δ_C 49.4) as well as by the HMBC correlation from H-33 to the carbonyl carbon at δ_C 170.2 (C-32) while the existence of the phenylalanine residue was supported by the coupling system from H_2-24 (δ_H 2.66, *dd*, *J* = 13.6, 10.0 Hz, and 2.92, *dd*, *J* = 13.6, 6.4 Hz; δ_C 37.0) through H-23 (δ_H 4.61, *ddd*, *J* = 10.0, 10.0, 6.4 Hz; δ_C 54.6) to NH-31 (δ_H 7.38, *d*, *J* = 10.0 Hz) and by the HMBC correlations from H-23 to C-24 (δ_C 37.0), C-25 (δ_C 134.4) and C-32 (δ_C 170.2), from H_2-24 to C-23 (δ_C 54.6), C-25, C-26/30 (δ_C 129.0).

Table 34. ^{1}H and ^{13}C NMR (DMSO, 500.13 MHz and 125.77 MHz) and HMBC assignment for **NG 9**

	Position	**δ_C, type**	**δ_H, (*J* in Hz)**	**COSY**	**HMBC**
Anthranilic acid	1	166.4, CO	-	-	-
	2	125.2, C	-	-	-
	3	126.5, CH	7.53, *d* (7.6)	H-4	C-1, 5, 7
	4	122.6, CH	7.16, *dd* (7.6, 7.6)	H-3, 5	C-2, 6
	5	130.4, CH	7.48, *ddd* (8.3, 7.6)	H-4, 6	C-3, 7
	6	120.7, CH	8.27, *d* (8.3)	H-5	C-2, 4
	7	136.3, C	-	-	-
	NH-8	-	9.25, *s*	-	C-2, 6, 9
Trp	9	169.0, CO	-	-	-
	10	54.3, CH	4.52, *ddd* (7.9, 6.7, 5.9)	H-11, NH-21	C-9, 11, 12, 22
	11a	24.9, CH_2	3.32, *dd* (14.7, 5.9)	H-10, 11b	C-9, 10, 12, 13, 20
	b		3.14, *dd* (14.7, 6.7)	H-10, 11a	C-9, 10, 12, 13, 20
	12	110.2, C	-	-	-
	13	127.7, C	-	-	-
	14	118.5, CH	7.58, *d* (7.9)	H-15	C-16, 18
	15	118.2, CH	6.98, *dd* (7.9, 7.5	H-14, 16	C-13, 17
	16	120.8, CH	7.06, *dd* (8.0, 7.5)	H-15, 17	C-14, 18
	17	111.3, CH	7.34, *d* (8.0)	H-16	C-13, 15
	18	136.0, C	-	-	-
	NH-19	-	10.82, *brs*	H-20	C-12, 13, 18, 20
	20	124.0, CH	7.04, *d* (1.8)	NH-19	C-13
	NH-21	-	8.42, *d* (7.9)	H-10	C-9, 22

Table 34. ^{1}H and ^{13}C NMR (DMSO, 500.13 MHz and 125.77 MHz) and HMBC assignment for **NG 9** (Cont.)

	Position	**δ_C, type**	**δ_H, (*J* in Hz)**	**COSY**	**HMBC**
Phe	22	170.1, CO	-	-	-
	23	54.6, CH	4.61,*ddd* (10.0, 10.0, 6.4)	H-24a, b	C-24, 25, 32
	24a	37.0, CH_2	2.66, *dd* (13.6, 10.0)	H-23, 24b	C-22, 23, 25, 26, 30
	b		2.92, *dd* (13.6, 6.4)	H-23, 14a	C-22, 23, 25, 26, 30
	25	134.4, C	-	-	-
	26	129.0, CH	7.10, *dd* (7.7, 1.0)	H-27	C-25
	27	128.1, CH	7.20, *m*	H-26, 28	C-25
	28	126.3, CH	7.18, *m*	H-27, 29	-
	29	128.1, CH	7.20, *m*	H-28, 30	C-28
	30	129.0, CH	7.10, *dd* (7.7, 1.0)	H-29	C-25
	NH-31	-	7.38, *d* (10.0)	H-23	C-32
Pro	32	170.2, CO	-	-	-
	33	62.1, CH	4.15, *dd* (9.0, 1.2)	H-34a, b	C-32
	34a	28.3, CH_2	1.45, *m*	H-33, 34b	-
	b		2.09, *m*	H-33, 34a	-
	35	24.6, CH_2	1.86, *m*	H34a, b, 36a,b	-
	36a	49.4, CH_2	3.55, *m*	H-35, 36b	-
	b		3.67, *m*	H-35, 36a	
	N-37	-	-	-	-

Like in **NG 8**, the proline residue was linked to the phenylalanine residue, through the carbonyl of the former and the amine group of the latter, which was supported by the HMBC correlations of the amine proton at δ_H 7.38, *d* (*J* = 10 Hz, NH-31) to C-32, and also to the anthranilic acid residue, through the nitrogen of the pyrrolidine ring of proline and the carbonyl group of carboxylic acid. That the one of the phenyl residues of **NG 8** was replaced by the tryptophan residue was substantiated by the presence of the indole system, as characterized by the coupling system of H-14 (δ_H 7.58, *d*, *J* = 7.9 Hz, δ_C 118.5) through H-17 (δ_H 7.34, *d*, *J* = 8.0 Hz, δ_C 111.3), as observed in the COSY spectrum (Table 34), and also by the HMBC correlations from NH-19 (δ_H 10.82, *brs*) to C-12 (δ_C 110.2), C-13 (δ_C 127.7), C-18 (δ_C 136.0) and C-20 (δ_C 124.0) as well as of the ethylamino moiety, as evidenced by the coupling system from H_2-11 (δ_H 3.14, *dd*, *J* = 14.7, 6.7 Hz and 3.32, *dd*, *J* = 14.7, 5.9 Hz; δ_C 24.9) through H-10 (δ_H 4.52, *ddd*, *J* = 7.9, 6.7, 5.9 Hz; δ_C 54.3) to NH-21 (8.42, *d*, *J* = 7.9 Hz).

That the tryptophan residue was linked to the phenylalanine residue, through the amino group of the former and the carbonyl group of the latter, was corroborated by the HMBC correlations of NH-21 to the carbonyl group at δ_C 170.1 (C-22) and 169.0 (C-9) as well as of H-10 to C-9, C-11, C-12 and C-22. Finally, the amino group of the anthranilic acid residue was linked to the carbonyl group of the tryptophan residue was supported by the HMBC correlations of NH-8 (δ_H 9.25, *s*) to C-2

(δ_C 125.2), C-6 (δ_C 120.7) and C-9. Therefore, **NG 9** was identified as cyclo (anthranilic acid-Trp-Phe-Pro).

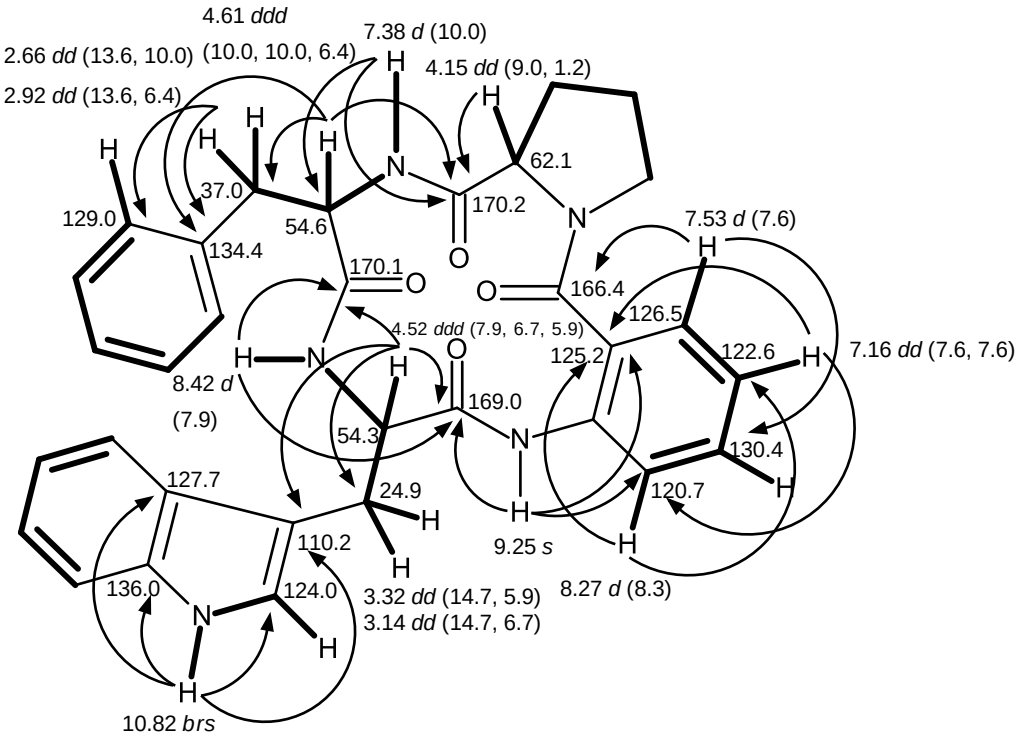

The absolute stereochemistry of the amino acid residues of **NG 9** was also determined by chiral HPLC analysis of its acidic hydrolysate, using appropriate D- and L- amino acids standards. The retention times (t_R min) for standard amino acids, using MeOH: H_2O (80:20 v/v) as mobile phase, at a flow rate of 1.0 mL/min, and with UV detection set at 210 nm, were L-Phe (3.8) and D-Phe (5.0), L-Pro (6.7) and D-Pro (20.1), L-Trp (4.5) and D-Trp (5.2) shown in Table 35 and Figure 117.

Table 35. Chromatographic conditions: column, Chirobiotic T; mobile phase, MeOH: H_2O (80:20 v/v); flow rate, 1.0 mL/min; detection, 210 nm.

Amino Acids	Retention Time (t_R min)
L-Phe	3.81
D-Phe	5.00
L-Pro	6.72
D-Pro	20.10
L-Trp	4.51
D-Trp	5.20
Acidic Hydrolysate **NG 9**	1.93, 3.07, 3.80, 4.29, 4.60, 6.62
Acidic Hydrolysate **NG 9** + DL-Phe (coinjection)	1.90, 3.10, 3.78, 4.39, 5.04, 6.70
Acidic Hydrolysate **NG 9** + DL-Pro (coinjection)	2.04, 3.02, 3.72, 4.30, 4.60, 6.66, 19.40
Acidic Hydrolysate **NG 9** + DL-Trp (coinjection)	1.93, 2.99, 3.70, 4.29, 4.60, 5.07, 6.33

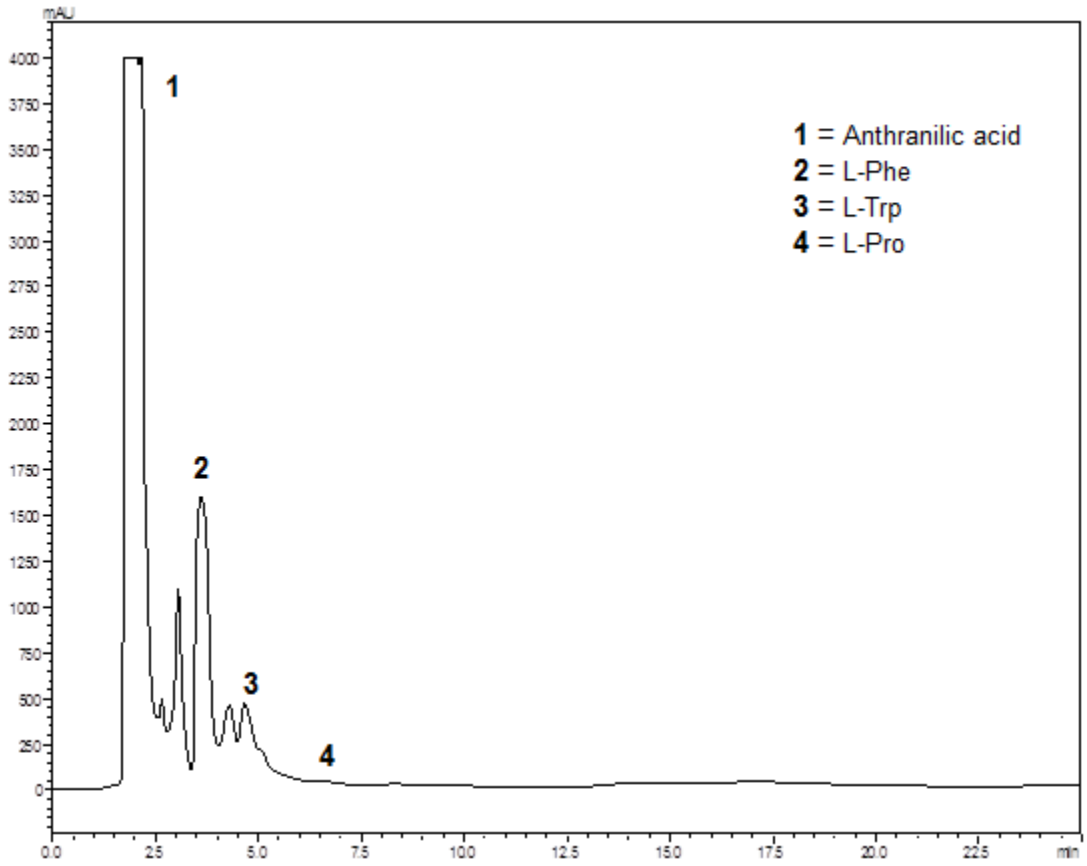

Figure 117. Chromatogram of the acidic hydrolysate of **NG 9**. Chromatographic conditions: column, Chirobiotic T; mobile phase, MeOH: H_2O (80:20 v/v); flow rate, 1.0 mL/min; detection, 210 nm.

Based on mix HPLC analyse of the acidic hydrolysate with standard D- and L-amino acids (co-injection), **NG 9** was elucidated as cyclo (anthranilic acid-L-Trp-L-Phe-L-Pro). Since **NG 9** is a new compound we have named it sartoryglabramide B (Figure 118).

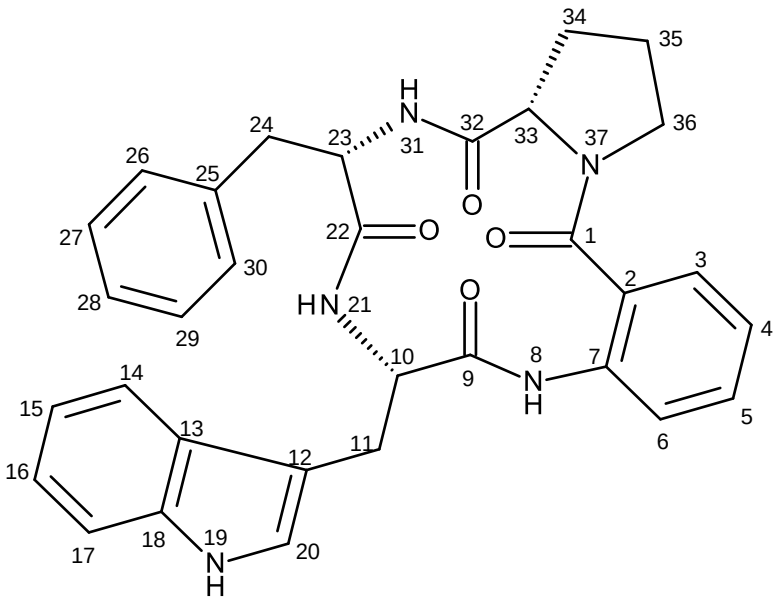

Figure 118. Structure of sartoryglabramide B (**NG 9**)

3.2 Biological Activity Evaluation of Isolated Compounds from Marine-Derived Fungi and Marine Margrove-Derived Fungus

Some of the isolated compounds from the marine alga-associated fungus *Neosartorya takakii* (KUFC 7898), marine sponge-associated fungus *Neosartorya glabra* (KUFA 0702) and marine mangrove-derived endophytic fungus *Eurotium chevalieri* (AKEC 0006) were evaluated for their biological activity.

3.2.1. Antibacterial and Antibiofilm Activity Evaluation

Three new metabolites takakiamide (**NTK 4**), tryptoquivaline U (**NTK 9**) and sartorenol (**NTK 12**) (Figure 119) were isolated form the aligicolous fungus *N. takakii* (KUFC 7898) and evaluated for their antibacterial activity against Gram positive *Staphylococcus aureus* ATCC 25923, *Bacillus subtilis* ATCC 6633 and Gram-negative *Escherichia coli* ATCC 25922, *Pseudomonas aeruginosa* ATCC 27853, as well as methicillin-resistant *S. aureus* (MRSA) and vancomycin-resistant Enterococci (VRE) isolates from the environment. None of the compounds exhibited relevant antibacterial activity against with MIC > 256 µg/mL.

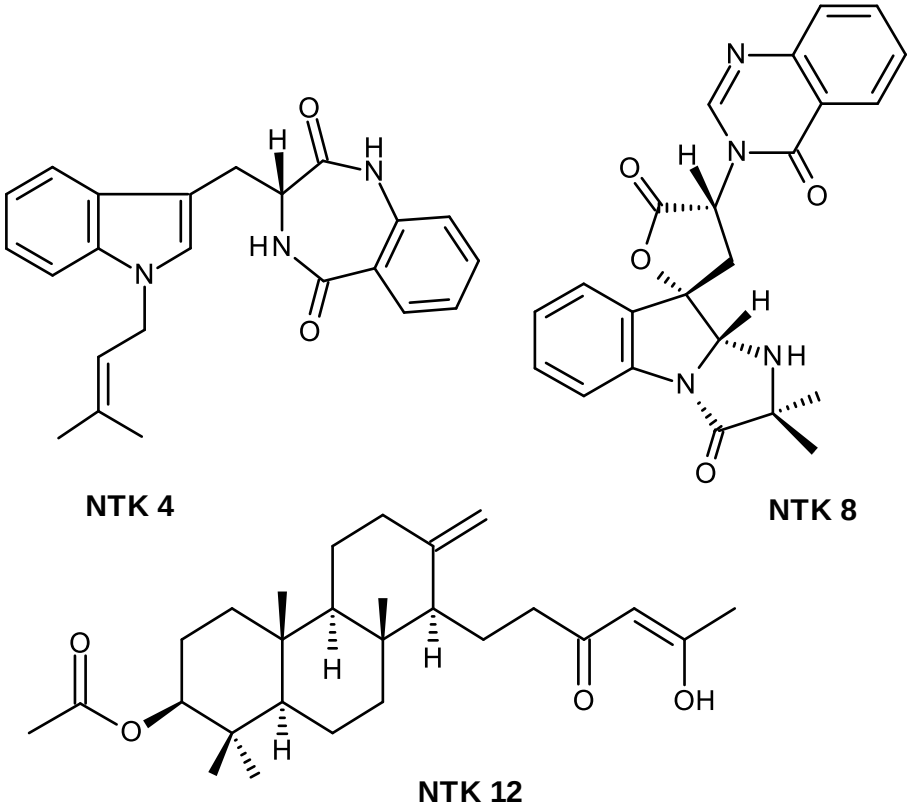

Figure 119. New Secondary metabolites isolated from the ethyl acetate extract of the culture of *N. takakii* KUFC 7898.

As well as, Emodin (**EC 3**), physicon (**EC 4**), questin (**EC 5**), questinol (**EC 6**), acetylquestinol (**EC 7**), (2, 2-dimethyl-3-en-2yl)-1*H*-indole-3-carbaldehyde (**EC 8**), (2, 2-dimethylcyclopropyl)-1*H*-indole-3-carbaldehyde (**EC 9**), 2-(2, 2-dimethylbut-3-enoyl) amino-benzoic acid (**EC 10**), 6, 8-dihydroxy-3-(2-hydroxypropyl)-7-methyl-1*H*-isochrome-1one (**EC 11**), (11*S*, 14*R*)-3-(1*H*-indol-3ylmethyl) 6-isopropyl-2, 5-piperazinedione (**EC 12**), preechinulin (**EC 13**), neoechinulin E (**EC 14**), echinulin (**EC 15**) and eurocristatine (**EC 16**) (Figure 120) were tested for their antibacterial against two Gram-positive *Staphylococcus aureus* ATCC 25923 and *Enterococcus faecalis* ATCC 29212 and two Gram-negative *Escherichia coli* ATCC 25922 and *Pseudomonas aeruginosa* ATCC 27853 bacteria, as well as multidrug-resistant isolates from the environment. The tested compounds were also investigated for their capacity to inhibit biofilm formation in the reference strains of *S. aureus*, *E. faecalis* and *E. coli*. The potential synergism between the tested compounds and the clinically used antibiotics was also evaluated against multidrug-resistant bacteria: methicillin-resistant *S. aureus* (MRSA), vancomycin-resistant enterococci (VRE) and extended-spectrum beta-lactamase *E. coli* (ESBL).

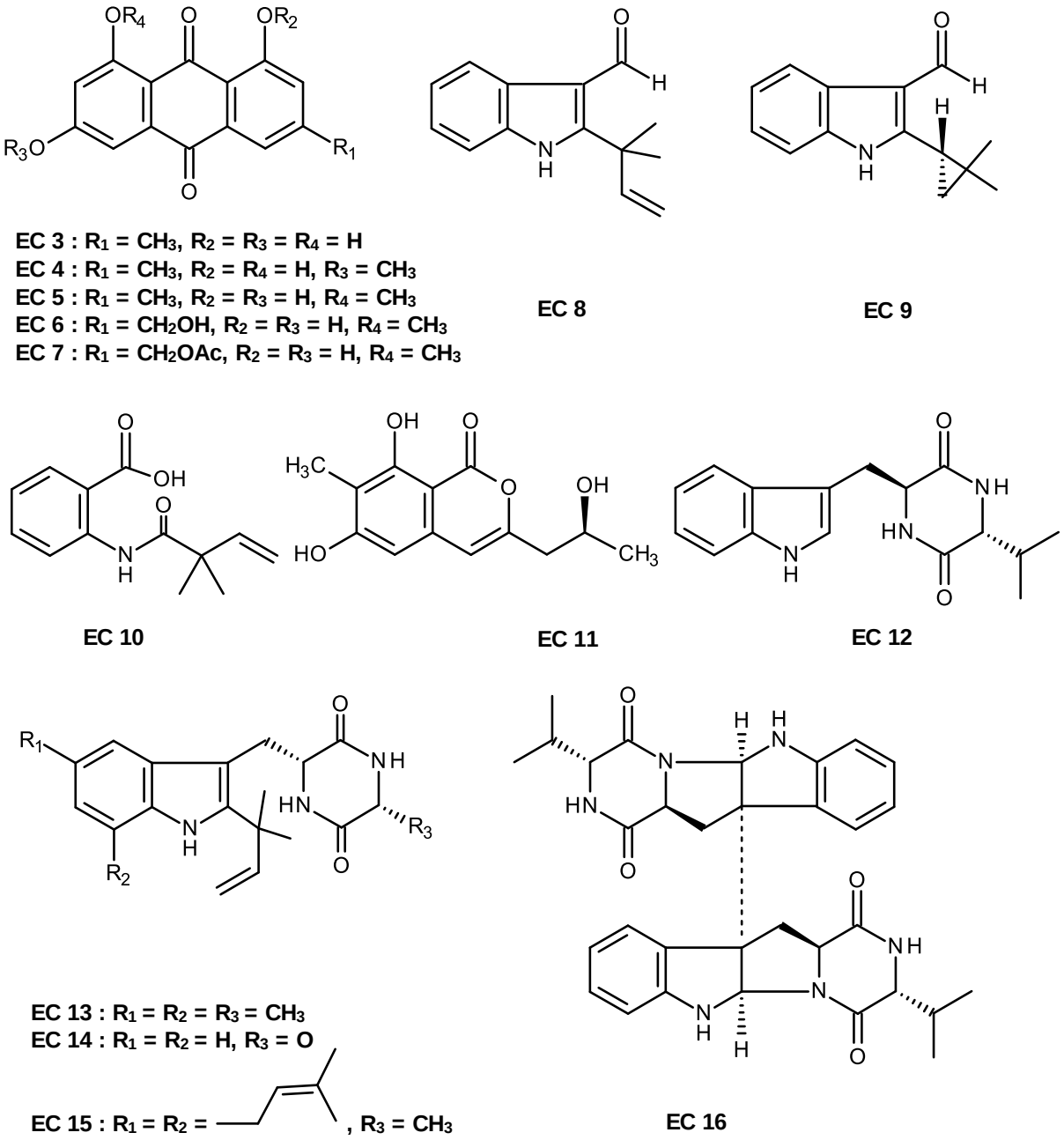

Figure 120. Compounds **EC 3**-**EC 16** evaluated for antibacterial and antibiofilm activities

Based on the results, only **EC 3** (Table 36) showed antibacterial activity against Gram positive bacteria, *S. aureus* ATCC 25923 and *E. faecalis* ATCC 29212 with MIC values of 32 and 64 µg/mL, respectively. However, **EC 3** did not show a bactericidal effect against any of the strains, its MBC was not determined. None of the compounds were inactive against either Gram-negative bacteria or methicillin-resistant *S. aureus* (MRSA) and vancomycin-resistant enterococci (VRE).

Table 36. Antimicrobial activity, expressed in µg/mL, of emodin (**EC 3**) against reference strains and multidrug-resistant isolates

Reference strains	MIC	MBC
E. coli ATCC 25922	>64	>64
P. aeruginosa ATCC 27853	>64	>64
E. faecalis ATCC 29212	64	>64
S. aureus ATCC 25923	32	>64
E. coli SA/2 (ESBL)	>64	>64
E. faecalis B3/101 (VRE)	>64	>64
S. aureus 66/1 (MRSA)	>64	>64

MIC = minimum inhibitory concentration; MBC = minimum bacterial concentration; ESBL = extended spectrum beta-lactamase; VRE = vancomycin-resistant enterococci; MRSA= methicillin-resistant *Staphylococcus aureaus.*

The inhibitory efficacy **EC 3- EC 16** in preventing biofilm formation was also evaluated in the reference strains *S. aureus*, *E. faecalis* and *E. coli*. Compounds that showed a statistically significant reduction (one sample t-test) of biofilm information are shown in Table 37. For emodin (**EC 3**), three concentrations, i.e. 2 x MIC, MIC and ½ x MIC, were tested against *S. aureus* ATCC 25923. For the rest of the compounds, the highest concentration that did not inhibit bacterial growth was used since it was not possible to determine their MIC.

Compounds **EC 6**, **EC 7**, **EC 9**, **EC 10**, **EC 12**, **EC 14** and **EC 16** were found to exhibit a significant reduction in the biofilm production of *E.coli* ATCC 25922. On the other hand, the anthraquinones derivatives, emodin (**EC 3**), physicon (**EC 4**) and two new prenylated indole carbaldehydes (**EC 8** and **EC 9**) showed inhibition of biofilm production in *S. aureus* (ATCC 25923). Emodin (**EC 3)** not only showed maximum inhibitory effects but also interfered with the biofilm production even at the sub-inhibitory concentrations. Interestingly, **EC 9** is the most effective in inhibiting biofilm formation in *E. coli* ATCC 25922, and also causes nearly 80% reduction of the biomass production in *S. aureus* ATCC 25923. Only physicon (**EC 4**) causes a reduction of biofilm formation in *E.faecalis* ATCC 29212 (Table 37).

Table 37. Percentage of biofilm formation for compounds that showed antibiofilm activity, after 24 hr incubation

Compounds	Concentration (µg/mL)	Biofilm biomass (% of control)		
		E. coli ATCC 25922	*E. faecalis* ATCC 29212	*S. aureus* ATCC 25923
CTX	0.31	1.0 ± 1.4*** (MIC)	-	-
EC 3	64	-	-	15.4 ± 20.4* (2 x MIC)
EC 3	32	-	-	21.1 ± 30.2* (MIC)
EC 3	16	-	-	74.5 ± 2.6* (1/2 x MIC)
EC 4	16	-	39.1 ± 16.0*	60.3 ± 27.9*
EC 6	64	56.1 ± 14.3*	-	-
EC 7	64	50.6 ± 17.6*	-	-
EC 8	64	-	-	21.1 ± 11.5*
EC 9	64	23.7 ± 24.8*	-	21.8 ± 18.9*
EC 10	64	57.6 ± 8.1*	-	-
EC 12	64	59.6 ± 16.2*	-	-
EC 14	64	54.0 ± 17.4*	-	-
EC 16	64	67.1 ±10.2*	-	-

Data are shown as Mean ± SD of 3 independent sxperiments. One-sample t test: *p < 0.05 and ** p < 0.001, significantly different from 100 %; MIC = minimum inhibitory concentration.

Additionally, the tested compounds were also investigated for their potential synergy with clinical relevant antibiotics on the multidrug-resistant isolates by a disk diffusion method. It was found that some of the tested compounds exhibited a small to moderate synergistic association with antibiotics depending on the multidrug-resistant strains, as shown in (Table 38).

When tested alone, none of the compounds showed inhibition against the three multidrug-resistant strains. However, in combination with cefotaxime (CTX) in the impregnated disks, **EC 3**, **EC 4**, **EC 6**, **EC 8**, **EC 11**, **EC 14** and **EC 15** produced a small synergistic association as can be seen by a small increase in the inhibition zone when compared with the halo of inhibition produced by CTX alone in the ESBL *E.coli* strain (SA/2). While **EC 7**, **EC 8**, **EC 9**, **EC 12**, **EC 13**, **EC 14**, **EC 15** and **EC 16** induced a moderate increase in the halo of partial inhibition of vancomycin (VAN) in VRE *E. faecalis* B3/101, when compared with VAN alone. Interestingly, only emodin (**EC 3**) produced a synergistic effect with the antibiotic oxacillin (OX) against the MRSA *S. aureus* 66/1, increasing a halo of inhibition zone from zero (when treated with OX alone) to 11 mm when tested in combination.

These results were also confirmed by determining the MICs of each antibiotic for the respective strain, in the presence of a fixed concentration of each compound, which is the highest concentration that did not inhibit the growth of the three multidrug-resistant strains under study. The MICs of antibiotics combined with each compound tested against the three multidrug-resistant strains are shown Table 39.

The combination of CTX with **EC 15** resulted in a four-fold decrease in the MIC of CTX, i.e. from 256 µg/mL of CTX alone to 64 µg/mL of the combination, when tested against ESBL *E. coli* SA/2. The MBC also decrease from >512 µg/mL to 512 µg/mL. Although the rest of the compounds did not show a synergistic effect with CTX in terms of MIC, **EC 3**, **EC 4**, **EC 7**, **EC 8**, **EC 10**, **EC 11**, **EC 15** and **EC 16** reduced the MBC when compared with CTX alone. The combination of VAN with **EC 3**, **EC 4**, **EC 5** and **EC 8** resulted in a four-fold decrease (from 512 µg/mL to 128 µg/mL) in MIC of VAN while **EC 9** reduced the MIC of VAN only by half (from 512 µg/mL to 256 µg/mL) against VRE *E faecalis* B3/101 when compared to VAN alone. The combination of VAN with emodin (**EC 3**) resulted in a four-fold decrease (from 512 µg/mL to 128 µg/mL) in MIC of VAN against VRE *E. faecalis* B3/101 when compared to VAN alone. Contrary to what was observed by the disk diffusion method, the combination of OX with emodin (**EC 3**) against the MRSA *S. aureus* 66/1 did not result in a decrease in the MIC of OX. Therefore, fungal anthraquinones derivatives represent an interesting group of compounds for development as arsenal against multidrug-resistant bacteria.

Table 38. Combined effects of antibiotics with **EC 3-EC 16** against three multidrug-resistant strains by disk diffusion method

Compounds	*E. coli* SA/2	*E. faecalis* B3/101	*S. aureus* 66/1
	CTX	**VAN***	**OX**
Antibiotic + EC 3	+	+	+++
Antibiotic + EC 4	+	+	-
Antibiotic + EC 5	-	+	-
Antibiotic + EC 6	+	+	-
Antibiotic + EC 7	-	++	-
Antibiotic + EC 8	+	++	-
Antibiotic + EC 9	-	++	-
Antibiotic + EC 10	-	+	-
Antibiotic + EC 11	+	+	-
Antibiotic + EC 12	-	++	-
Antibiotic + EC 13	-	++	-
Antibiotic + EC 14	+	++	-
Antibiotic + EC 15	+	++	-
Antibiotic + EC 16	-	++	-

(-) non-effective; (+) slight efficacy-halo of inhibition or additional increase in the halo of inhibition of 1-2.5 mm around the disk; (++) moderate efficacy increase in the halo of inhibition of >2.5-5 mm; (+++) good efficacy-increase in the halo of inhibition of >5-11 mm; CTX = cefotaxime; VAN + vancomycin; OX = oxacillin; *Halo of partial inhibition.

Table 39. Combine effect of antibiotics with **EC 3-EC 16** against three multidrug-resistant strains. MIC and MBC for antibiotics are expressed in µg/mL

Compounds *	*E. coli* SA/2		*E. faecalis* B3/101		*S. aureus* 66/1	
	CTX		VAN		OX	
	MIC	MBC	MIC	MBC	MIC	MBC
Antibiotic	256	>512	512	>1024	64	>256
Antibiotic + EC 3	256	512	128	>1024	64	>256
Antibiotic + EC 4	256	512	128	>1024	64	>256
Antibiotic + EC 5	256	>512	128	>1024	64	>256
Antibiotic + EC 6	256	>512	512	>1024	64	256
Antibiotic + EC 7	256	256	512	>1024	64	>256
Antibiotic + EC 8	256	256	128	>1024	64	>256
Antibiotic + EC 9	512	>512	256	>1024	64	>256
Antibiotic + EC 10	256	256	512	>1024	64	>256
Antibiotic + EC 11	256	512	512	>1024	64	>256
Antibiotic + EC 12	256	>512	512	>1024	64	>256
Antibiotic + EC 13	512	>512	512	>1024	64	>256
Antibiotic + EC 14	256	>512	512	>1024	64	>256
Antibiotic + EC 15	64	512	512	>1024	256	>256
Antibiotic + EC 16	256	512	512	>1024	128	>256

MIC = minimum inhibitory concentration; MBC = minimum bacterial concentration; CTX = cefotaxine; VAN = vancomycin; OX = oxacillin.

*Compound **EC 3** was used a concentration of 16 µg/mL; compounds **EC 4-EC 16** were used at a concentration of 64µg/mL.

3.2.2. Antibacterial and Antifungal Activity Evaluation

Aszonalenin (**NG 4**), (3*R*, 3-(1*H*-indole-3-ylmethyl)-3, 4-dihydro-1*H*-1, 4-benzodiazepine-2, 5-dione (**NG 5**), (11a*S*)-2, 3-dihydro-1*H*-pyrrolo[2,1-c] [1,4] benzodiazepine-5, 11(10*H*, 11a*H*)-dione (**NG 6**), takakiamide (**NG 7**), sartoryglabramide A (**NG 8**), sartoryglabramide B (**NG 9**), fellutanine A (**NG 10**) and fellutanine A epoxide (**NG 11**) were isolated from the ethyl acetate extract of *N.glabra* (KUFA 0702) which were evaluated for their anbacterial activity against Gram-positive *Straphyllococus aureus* ATCC 25923 and Gram-negative *Escherichia coli* ATCC 25922 bacteria, as well as for their antifungal activity against filamentous *Aspergillus fumigatus* ATCC 46645, dermatophyte *Trichophyton rubrum* ATCC FF5, and yeast *Candida albicans* ATCC 10231. Compounds **NG 4-NG 11** displayed no antibacterial activity against with MIC > 256 µg/ mL or antifungal activities MIC > 512 µg/ mL.

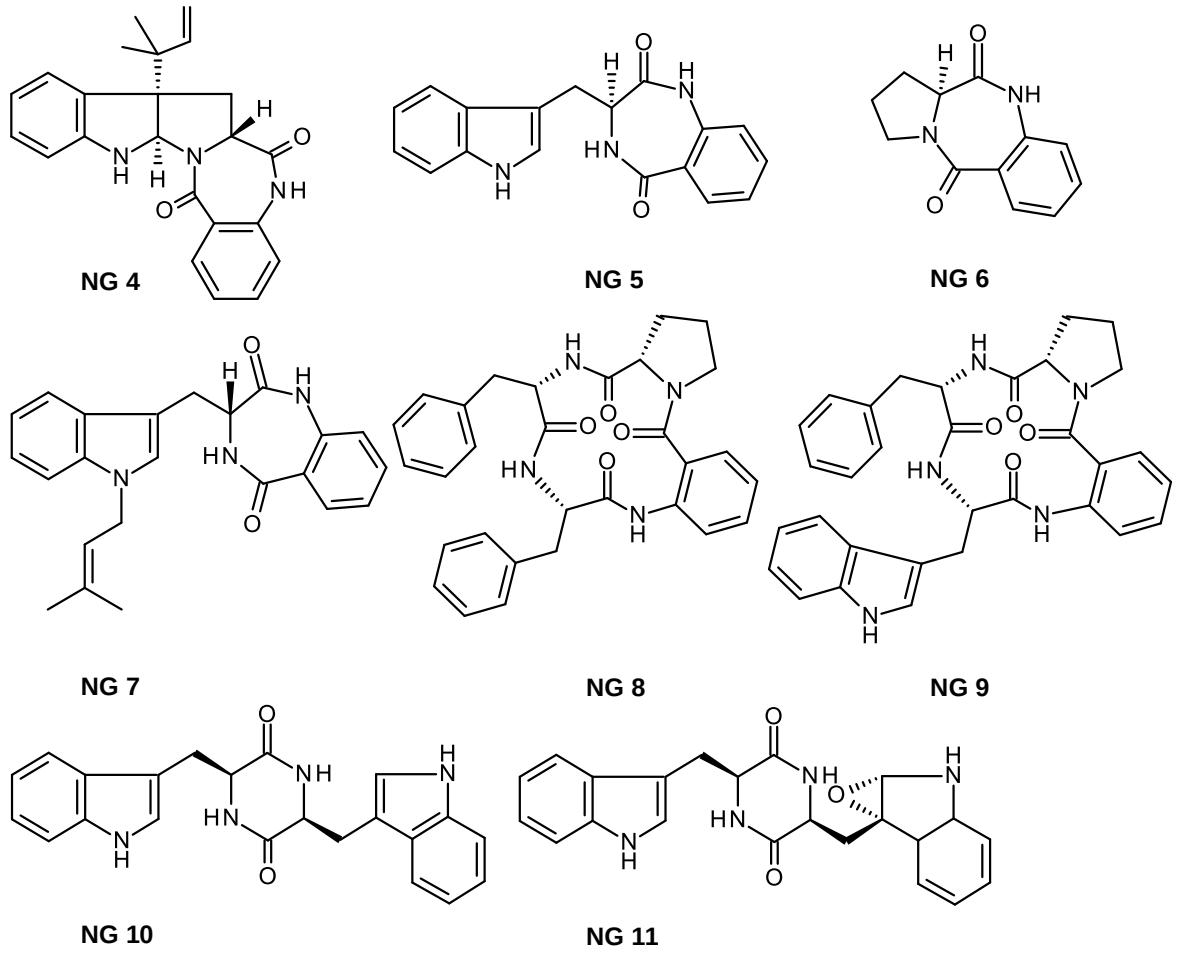

Figure 121. Secondary metabolites isolated from the ethyl acetate extract of the culture of *N. glabra* KUFA 0702.

CHAPTER IV

MATERIALS AND METHODS

4.1 General Experimental Procedures

Merck® silica gel 60 (0.04-0.63 mm), Li Chroprep® Si (40-60 µm) and Sephadex™ LH-20 were used for column chromatography.

Analytical and preparative TLC was performed on silica gel 60 (GF_{254}; Merck, 0.25 mm thickness). The plates were activated at 110ºC in the oven Binder for 4 hours and percolated silica gel sheets, GF_{254} (Macherey-Nagel), ALUGRAM®, Sil G/UV_{254}, 20x20 cm. All TLC plates were visualized under UV_{254} nm and UV_{365} nm or developed with iodine vapor.

^{1}H and ^{13}C NMR spectra were recorded at ambient temperature in $CDCl_3$ or DMSO-d_6 on a Bruker AMC instrument (Bruker Biosciences Corporation, Billerica, MA, USA) operating either at 300.13 and 75.47 MHz or 500.13 MHz and 125.77 MHz, respectively.

High-resolution mass spectra were measured with a Waters Xevo QToF mass spectrometer (Waters Corporations, Milford, MA, USA) coupled to a Waters Aquity UPLC system.

Melting points were determined on a Bock monoscope and are uncorrected.

Optical rotations were measured on an ADP410 Polarimeter (Bellingham + Stanley Ltd., Tunbridge wells, Kent, UK).

UV spectra were taken in $CHCl_3$ and were recorded on a Varian CARY 100 spectrophotometer.

Infrared spectra were recorded in a KBr microplate in a FTIR spectrometer Nicolet iS 10 from Thermo Scientific (Waltham, MA, USA) with smart OMNI-Transmission accessary (Software 188 OMNIC 8.3).

The weight was measured on the analytical balance AND GH-202.

The solvents used were from Merck and Fischer with analytical reagent grade. Solvents were evaporated at reduced pressure, using Büchi Heating Bath B-49, Büchi Rotavapor R-210, Buchi Vacuum Module V-801 EasyVac and Vacuum Pump V-700.

4.2 Isolation and Identification of the Biological Material

4.2.1. *Talaromyces helicus* (KUFA 0063)

Talaromyces helicus (KUFA 0063) was isolated from a cauliflower coral, *Pocillopora verrucosa*, which was collected from Angthong national marine Park, Samui district, Suratthani Province, Thailand. The coral was rinsed 3 times with sterile sea water and let it dry on sterile filter papers. Small pieces of coral tissues (5x5 mm) were placed on plates containing malt extract agar (MEA) with 70% sea

water. The plates were incubated at room temperature for a week and the fungus was transferred onto MEA +70% sea water slant. The fungus was identified based on macro- and microscopic characteristics, observed under light and scanning electron microscopes (SEM). The pure cultures were deposited as KUFA 0063 at Kasetsart University Fungal Collection, Department of Plant Pathology, Faculty of Agriculture, Kasetsart University, Bangkok, Thailand.

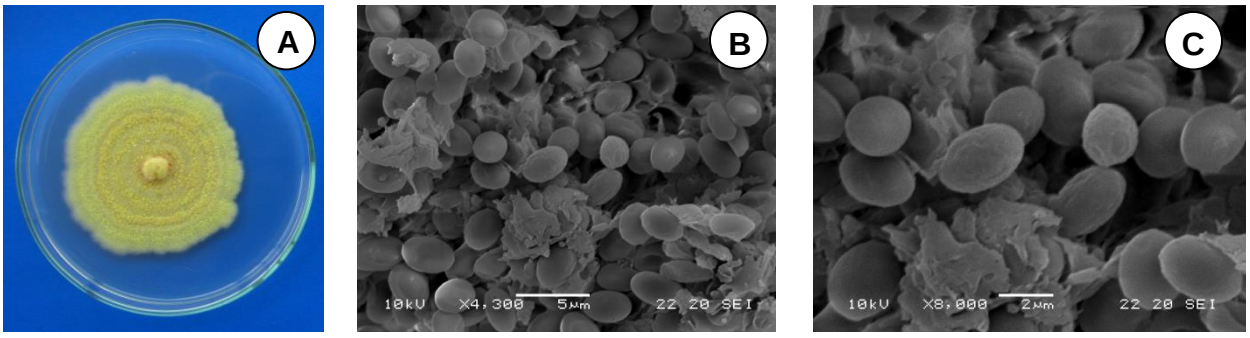

Figure 122. *Talaromyces helicus* (KUFA 0063), colony on PDA 7 days (**A**) and SEM photomicrograph of ascospores (**B** and **C**)

4.2.2. *Neosartorya takakii* (KUFC 7898)

The fungus was isolated from the alga *Amphiora sp*. which was collected from Samaesarn Island, in the Gulf of Thailand, Chonburi Province, in September 2011.

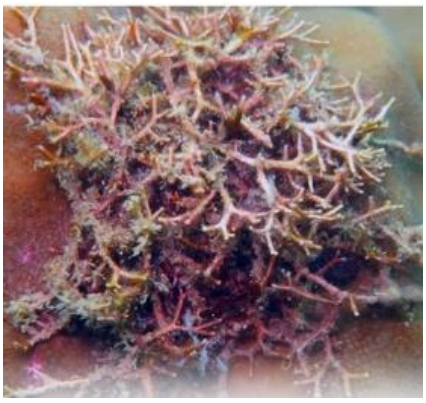

Figure 123. Algae (*Amphiroa sp*)

The alga was washed with 0.06% sodium hypochlorite for 1 min, followed by sterilized sea water for three times. The alga was dried on sterile filter paper and cut into small pieces (5x5 mm) and placed on malt extract agar (MEA) with 70% sea water and incubated at 28ºC for 5-7 days. The fungus was identified as *Neosartorya takakii* by Leka Manoch (Department of Plant Pathology, Faculty of Agriculture, Kasetsart University, Bangkok, Thailand), based on morphological characteristics, such as colony growth rate and growth pattern on standard media namely Czapek's agar (CZA), Czapek yeast autolysate agar (CYA) and malt extract agar (MEA). Microscopic characteristics including size, shape, ornamentation of ascospores and *Aspergillus takakii* anamorph were examined under light and scanning electron microscopes (Horie *et al*., 2001).

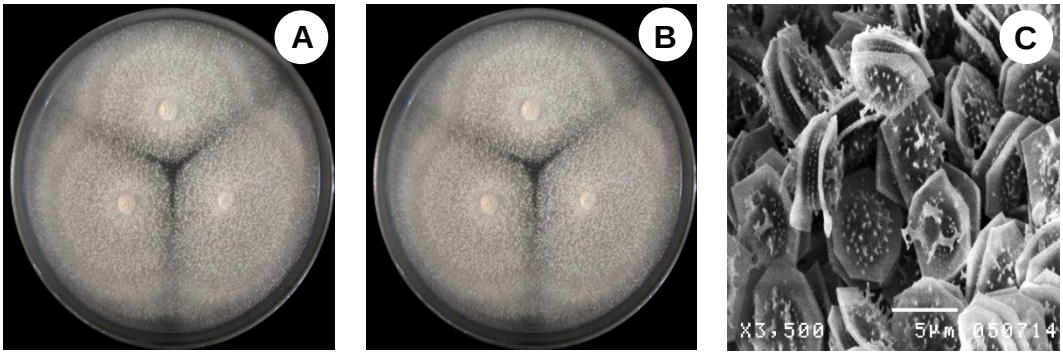

Figure 124. Obverse and reverse views of colonies MEA media, incubated for 7 days at 28ºC (**A** and **B**), and SEM photomicrographs of ascospores (**C**).

This identification was supported by sequence analysis of the β-tubulin, calmodulin and actin genes as described in the previous report (Matsuzawa *et al*., 2014). *Neosartorya takakii* was also confirmed by analysis sequence of the internal transcribed spacer (ITS) gene. Briefly, 2–15 mg of mycelia was ground in liquid nitrogen. DNA was extracted using the DNeasy™ Plant Mini Kit (QIAGEN, Hilden, Germany) according to the manufacturer's instructions. The entire nuclear ITS regions were amplified with the primers: ITS1F-5′ (Gardes and Bruns, 1993) and ITS4-3′ (White *et al*., 1990). PCR reactions were conducted on Thermal Cycler and the amplification process consisted of initial denaturation at 95 °C for 5 min, 34 cycles at 95 °C for 1 min (denaturation), at 55 °C for 1 min (annealing) and at 72 °C for 1.5 min (extension), followed by final extension at 72 °C for 10 min. PCR products were cleaned using QIAquick PCR Purification Kit (QIAGEN, Hilden, Germany), then examined by Agarose gel electrophoresis (1% agarose

with 1× TBE buffer) and visualized under UV light after staining with ethidium bromide. DNA sequencing analyses were carried out by Macrogen Inc. (Seoul, South Korea). The sequences were compared using the NCBI nucleotide BLAST program (http://www.ncbi.nlm.nih.gov/BLAST) for identification (Altschul *et al*., 1997). The pure cultures were deposited as KUFC 7898 at Kasetsart University Fungal Collection, Department of Plant Pathology, Faculty of Agriculture, Kasetsart University, Bangkok, Thailand, and also as MMERU 03 at Microbes Marine Environment Research Unit, Division of Environmental Science, Faculty of Science, Ramkhamhaeng University, Bangkok, Thailand.

4.2.3. *Neosartorya glabra* (Fennell & Raper) Kozak (KUFA 0702)

The strain KUFA 0702 was isolated from the marine sponge *Mycale sp*., which was collected, by scuba diving at a depth of 15-20 m, from the coral reef at Samaesarn Island (12º 34' 36.64'' N 100º 56' 59.69'' E) in the Gulf of Thailand, Chonburi Province, in February 2015. The sponge was washed with 0.06% sodium hypochlorite solution for 1 min, followed by sterilized seawater 3 times, and then dried on sterile filter paper, cut into small pieces (5x5 mm), and placed on malt extract agar (MEA) medium containing 70% sea water and 300 mg/L of streptomycin sulfate. After incubation at 28ºC for 7 days, the hyphal tips were transferred onto a slant MEA and maintained as pure culture for further identification.

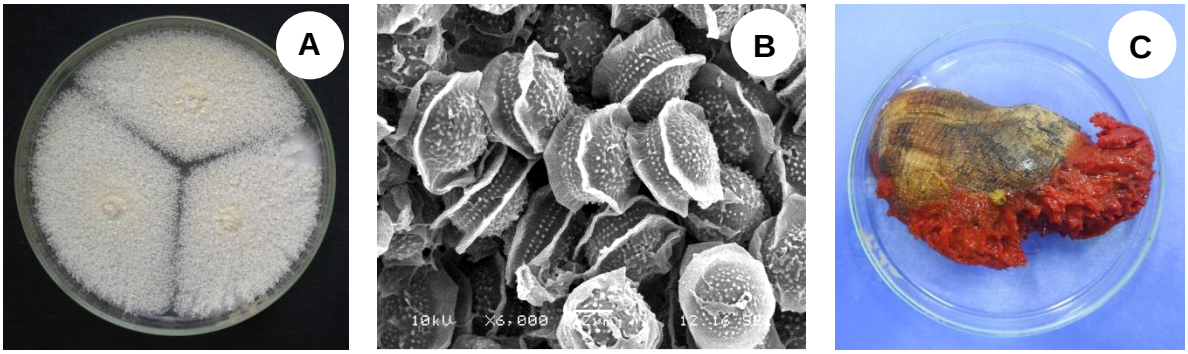

Figure 125. Colony on MEA, 7 days, 28^{o}C obverse (**A**), SEM of ascospores (**B**) and *Mycale sp*. (**C**)

The fungus was identified as *Neosartorya glabra* (Fennell & Raper) Kozak based on morphological characteristics such as colony growth rate and growth pattern on standard media, namely Czapek's agar, Czapek yeast autolysate agar and malt extract agar. Microscopic characteristics including size, shape and ornamentation of ascospores were examined under light and scanning electron microscopes. This identification was supported by sequence analysis of the β-tubulin, calmodulin and actin genes as described in the previous report (Matsuzawa *et al*., 2014). *N. glabra* was also confirmed by sequence analysis of the internal transcribed spacer (ITS) gene, according to the procedure previously described in section 4.2.2. Its gene sequences were deposited in Genbank with accession numbers KU 955860. The pure cultures were deposited as KUFA 0702 at Kasetsart University, Bangkok, Thailand.

4.2.4. *Eurotium Chevalieri* L. Mangin (KUFA 0006)

The fungus was isolated from a healthy twig of *Rhizophora mucronata* Poir, which was collected in Kung Krabaen Bay Royal Development Study Center, Chanthaburi in July 2010. The twig was washed with running tap water and air died in a laminar hood. It was cut to 1 cm long and was surface sterilized with 70% ethanol for 5 min and then rinsed three times in sterile distilled water. The surface sterilized twig was blotted dry on sterilized filter paper under aseptic condition and was transversely cut to 1-2 mm-thick slices using a sterile razor blade, after which were placed in Petri dishes containing potato dextrose agar (PDA) amended streptomycin sulphate (300 mg/L), four pieces per dish. The dishes were incubated at room temperature and the mycelium emerged from plant tissues were observed daily. The hyphal tips of the mycelium emerged from plant were transferred to PDA slants using a sterile needle and maintained as pure culture for further identification.

The strain KUFA 0006 was identified as *Eurotium chevalieri* L. Mangin on the basic of morphological characteristics such as colony growth rate and growth pattern on standard media, namely Czapek's agar, Czapek yeast autolysate agar and malt extract agar as well as microscopic characteristics including size, shape and ornamentation of ascospores were observed under light and scanning electron microscopes.

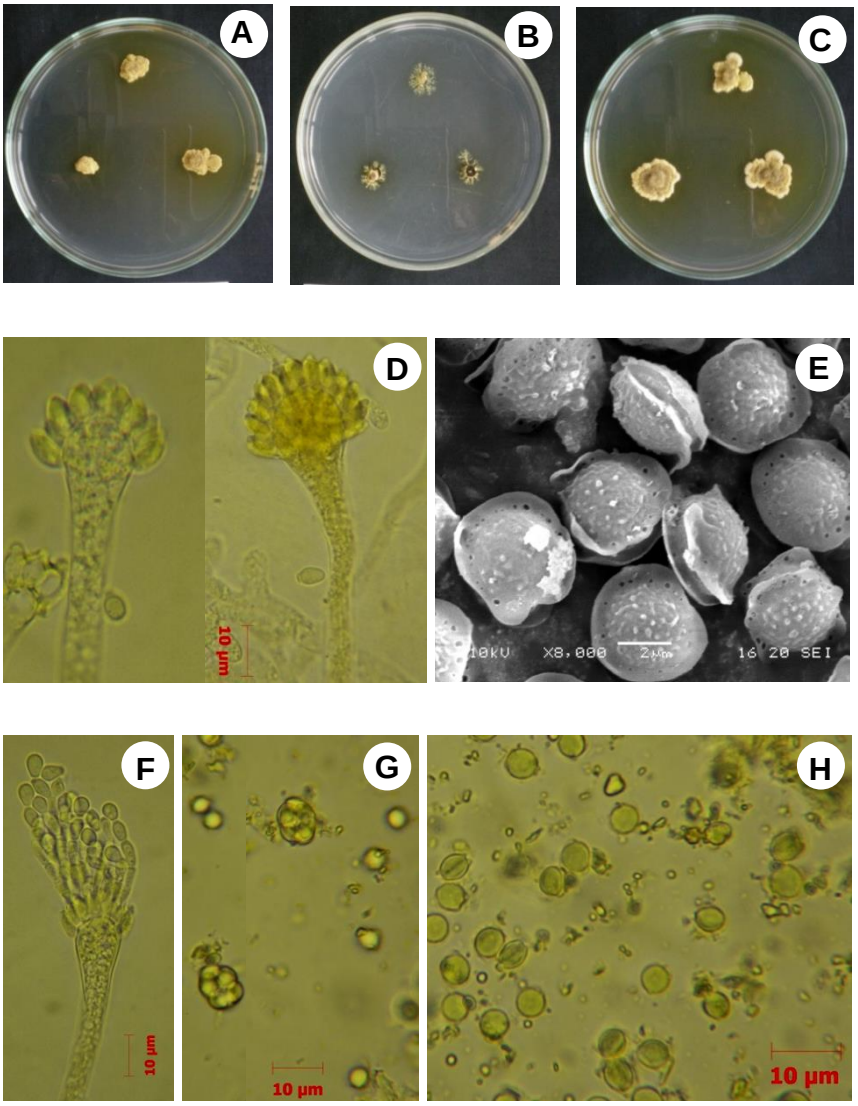

Figure 126. Colony on MEA (**A**), CZA (**B**), CYA(**C**) 7 days, 28°C, *Aspergillia* and spores (**D** and **F**), SEM of ascospores (**E**), ascus and ascospores (**G** and **H**)

The identification also confirmed by molecular techniques. The internal transcribed spacer (ITS) region of rRNA of this fungus was amplified using ITS primers (ITS 1 and ITS 4) as previously described in section 4.2.2. Its gene sequence was deposited in Genbank with accession number, KX 431211. The pure cultures were deposited at Kasetsart University Fungal Collection, Department of Plant Pathology, Faculty of Agriculture, Kasetsart University, Bangkok, Thailand.

4.3. Extraction and Isolation of Metabolites

4.3.1. *Talaromyces helicus* (KUFA 0063)

Talaromyces helicus (KUFA 0063) was cultured for 2 weeks at 28ºC in 10 Petri-dishes (i.d. 90 mm) containing 25 mL per dish of MEA +70% sea water. Fifty-five Erlenmeyer flasks (1,000 mL) containing 200 g of rice, 30 mL water and 70 mL sea water were autoclaved. Each of flasks was inoculated with 5 mycelia plug of this fungus and incubated at 28ºC for 30 days, after which the moldy rice was macerated in ethyl acetate (30 L) for 10 days and filtered. The ethyl acetate solution was evaporated under reduced pressure to give dark brown viscous mass of a crude ethyl acetate extract (96.31 g) which was dissolved in 1000 ml of $CHCl_3$ and then washed with H_2O (3x500 mL). The organic layer were combined and dried with anhydrous Na_2SO_4, filtered and evaporated under reduce pressure to give (47.5 g) of crude chloroform extract.

The crude chloroform extract (40 g) was applied on a column chromatography over a 0.04-0.63 mm Merck® silica gel 60 (350 g) and eluted with mixtures of petrol-$CHCl_3$, $CHCl_3$-Me_2CO and Me_2CO, 250 mL fractions were collected as follows: Fractions 1-26 (petrol-$CHCl_3$, 1:1), 27-48 (petrol-$CHCl_3$, 3:7), 49-160 (petrol-$CHCl_3$, 1:9) and 161-218 ($CHCl_3$-Me_2CO, 9:1), 219-311 ($CHCl_3$-Me_2CO, 7:3). Fractions 107-115 were combined (546 mg) and precipitated in MeOH to give white solid (17.7 mg) of 3-acetyl-ergosterol 5, 8 endoperoxide (**TH 2**).

Fractions 177-206 were combined (2.50 g) and applied on a column chromatography over a 40-60 µm Li Chroprep® silica gel (35 g) and eluted with mixtures of petrol-$CHCl_3$ and $CHCl_3$-Me_2CO and Me_2CO, 100 mL sub-fractions were collected as follows: Sub-fractions 1-34 (petrol-$CHCl_3$, 1:1), 35-170 (petrol-$CHCl_3$, 3:7), 171-223 (petrol-$CHCl_3$, 1:9) and 224-273 ($CHCl_3$-Me_2CO, 9:1), 274-298 ($CHCl_3$-Me_2CO, 7:3), 299-300 (Me_2CO). Sub-fractions 100-138 were combined (206 mg) and precipitated in MeOH to give white solid (9.5 mg) of glaucanic acid (**TH 3**) and sub-fractions 139-195 were combined (443 mg) and precipitated in MeOH to give white solid (34.1 mg) of palmitin (**TH 1**).

Fractions 207-237 were combined (5.676 g) and applied on a column chromatography over a 40-60 µm Li Chroprep® silica gel (35 g) and eluted with mixtures of petrol-$CHCl_3$ and $CHCl_3$-Me_2CO and Me_2CO, 100 mL sub-fractions were collected as follows: Sub-fractions 1-30 (petrol-$CHCl_3$, 1:1), 31-91 (petrol-$CHCl_3$, 3:7), 92-132 (petrol-$CHCl_3$, 1:9) and 133-166 ($CHCl_3$-Me_2CO, 9:1), 167-212

($CHCl_3$-Me_2CO, 7:3), 213-214 (Me_2CO). Sub-fractions 48-51 were combined (241 mg) and precipitated in MeOH to give white solid (10 mg) of glauconic acid (**TH 4**).

4.3.2. *Neosartorya takakii* (KUFC 7898)

Neosartorya takakii (KUFC 7898) was cultured for one week at 28ºC in 10 Petri dishes (i.d. 90 mm) containing 25 mL of MEA with 70% sea water per dish. Fifty 1000 mL Erlenmeyer flasks each containing rice (200 g), water (30 mL) and sea water (70 mL), were autoclaved, inoculated with five mycelia plugs of *N. takakii* and incubated at 28ºC for 30 days, after which the moldy rice was macerated in ethyl acetate (15 L total) for 10 days and then filtered. The two layers were separated using a separating funnel and the ethyl acetate solution was concentrated at a reduced pressure to yield 83.5 g of crude ethyl acetate extract which was dissolved in 1000 mL of $CHCl_3$ and then washed with H_2O (3x500 mL). The organic layers were combined and dried with anhydrous Na_2SO_4, filtered, evaporated under reduced pressure to give 53.8 g of the crude chloroform extract, which was applied on a column chromatography of 0.04-0.63 mm Merck® silica gel 60 (420 g), and eluted with a mixtures of petrol-$CHCl_3$, $CHCl_3$-Me_2CO and Me_2CO, 250 mL fractions were collected as follows: Fractions 1-40 (petrol-$CHCl_3$, 1:1), 41-82 (petrol-$CHCl_3$, 3:7), 83-197 (petrol-$CHCl_3$, 1:9), 198-321 ($CHCl_3$-Me_2CO, 9:1), and 322-460 ($CHCl_3$-Me_2CO, 7:3).

Fractions 198-203 were combined (1.573 g) and applied over a column chromatography of 40-60 µm Li Chroprep® silica gel (35 g) and eluted with a mixtures of petrol-$CHCl_3$ and $CHCl_3$-Me_2CO and Me_2CO, 200 mL sub-fractions were collected as follows: Sub-fractions 1-80 (petrol-$CHCl_3$, 1:1), 81-110 (petrol-$CHCl_3$, 3:7), 111-138 (petrol-$CHCl_3$, 1:9), 139-150 ($CHCl_3$-Me_2CO, 9:1), and 151-154 (Me_2CO). Sub-fractions 27-33 were combined (80.3 mg) and recrystallized in MeOH to give 26.7 mg of sartorenol (**NTK 12**). Sub-fractions 34-70 were combined (498 mg) and purified by TLC (silica gel 60 GF_{254}, $CHCl_3$-Me_2CO-HCO_2H, 9.5:0.5:0.1) to give an additional 18.2 mg of sartorenol (**NTK 12**). Sub-fractions 71-90 were combined (179 mg) and purified by TLC (silica gel 60 GF_{254}, $CHCl_3$-Me_2CO-HCO_2H, 9.5:0.5:0.1) to give (33.6 mg) of chevalone B (**NTK 10**). Sub-fractions 91-112 were combined (78.4 mg) and purified by TLC (silica gel 60 GF_{254}, $CHCl_3$-Me_2CO-HCO_2H, 9.5:0.5:0.1) to yield additional 2.7 mg of chevalone B (**NTK 10**).

Fractions 204-209 were combined (2.08 g) and recrystallized in MeOH to give (586.0 mg) of aszonalenin (**NTK 2/NG 4**) and a mother liquor was combined with fractions 210-212 (1.53 g) and applied over a column chromatography of 40-60 µm Li Chroprep® silica gel (35 g) and eluted with mixture of petrol-$CHCl_3$, $CHCl_3$-Me_2CO and Me_2CO, wherein 200 mL sub-fractions were collected as follows: Sub-fractions 1-25 (petrol-$CHCl_3$, 1:1), 26-120 (petrol-$CHCl_3$, 3:7), 121-164 (petrol-$CHCl_3$, 1:9), 165-179 ($CHCl_3$-Me_2CO, 9:1), 180-189 ($CHCl_3$-Me_2CO, 7:3), 190-191 (Me_2CO). Sub

fractions 69-105 were combined (150.2 mg) and purified by TLC (silica gel 60 GF_{254}, $CHCl_3$-Me_2CO-HCO_2H, 9.5:0.5:0.1) to give (5 mg) of 6-hydroxymellein (**NTK 1**).

Fractions 213-224 were combined (626.0 mg) and crystallized in MeOH to give (230 mg) of aszonapyrone A (**NTK 11**).

Fractions 262-267 were combined (573.4 mg) and purified by TLC (silica gel 60 GF_{254}, $CHCl_3$-Me_2CO-HCO_2H, 8:2:0.1) to give 20.5 mg of takakiamide (**NTK 4/NG 7**) and 91.3 mg of acetylaszonalenin (**NTK 3**).

Fractions 268-283 were combined (1.03 g) and recrystallized in MeOH to give (115.1 mg) of acetylaszonalenin (**NTK 3**).

Fractions 325-334 were combined (2.95 g) and recrystallized in MeOH to give (0.98 g) of tryptoquivaline L (**NTK 8**).

Fractions 335-342 were combined (6.06 g) and recrystallized in MeOH to give (259.5 mg) of tryptoquivaline H (**NTK 7**).

Fractions 343-348 were combined (281 mg) and crystallized in MeOH to give (24.9 mg) of 3′-(4-oxoquinazolin-3-yl) spiro [1*H*-indole -3, 5′-oxolane]-2, 2′-dione (**NTK 5**).

Fractions 356-390 were combined (1.15 g) and purified by TLC (silica gel 60 GF_{254}, $CHCl_3$-Me_2CO-HCO_2H, 7:3:0.1) to give 16.5 mg of tryptoquivaline U (**NTK 9**) and 3.9 mg of tryptoquivaline F (**NTK 6**).

Fractions 391-400 were (125.3 mg) and recrystallized in MeOH to give 8.6 mg of tryptoquivaline F (**NTK 6**).

4.3.3. Neosartorya glabra (KUFA 0702)

Neosartorya glabra (KUFA 0702) was cultured for one week at 28ºC in 5 Petri dishes (i.d. 90 mm) containing 15 mL of potato dextrose agar (PDA). In order to obtain the mycelial suspension, the mycelial plugs were transferred to two 500 mL Erlenmeyer flasks containing 250 mL of potato dextrose broth (PDB), and then incubated on a rotary shaker at 150 rpm at 28ºC for 7 days. Forty 1000 mL Erlenmeyer flasks, each containing 300 g of cooked rice, were autoclaved at 121ºC for 15 min, and then inoculated with 25 mL of mycelial suspension of *N. glabra*, and incubated at 28ºC for 30 days, after which the moldy rice was macerated in ethyl acetate (20 L total) for 7 days, and then filtered with filter paper.

The ethyl acetate solution was concentrated under reduced pressure to yield 98.2 g of crude ethyl acetate extract, which was dissolved in 1000 mL of $CHCl_3$, and then washed with H_2O (3x500 mL). The organic layers were combined and dried with anhydrous Na_2SO_4, filtered and evaporated under reduced pressure to give 71.2 g of the crude chloroform extract, which was applied on a column chromatography of 0.04-0.63 mm Merck® silica gel 60 (420 g), and eluted with mixtures of petrol-$CHCl_3$, $CHCl_3$-Me_2CO and Me_2CO, 250 mL fractions were collected as follows: Fractions

1-80 (petrol-$CHCl_3$, 1:1), 81-144 (petrol-$CHCl_3$, 3:7), 145-201 (petrol-$CHCl_3$, 1:9), 202-356 ($CHCl_3$-Me_2CO, 9:1), 357-398 ($CHCl_3$-Me_2CO, 7:1), and 399-410 (Me_2CO).

Fractions 85-105 were combined (2.04 g) and purified by TLC (silica gel 60 GF_{254}, $CHCl_3$-petrol-EtOAc-HCO_2H, 8:1:1:0.1) to give 11 mg of ergosta-4, 6, 8 (14), 22-tetraen-3-one (**NG 1**).

Fractions 207 (1.14 g) was applied over a column chromatography of Sephadex™ LH-20 (10 g) and eluted with MeOH and a mixture of MeOH: CH_2Cl_2 (1:1), wherein 20 mL sub-fractions were collected as follows: Sub-fractions 1-90 (MeOH), and 91-145 (MeOH: CH_2Cl_2, 1:1). Sub-fractions 53-61 were combined (19.5 mg) and recrystallized in MeOH to give 16.8 mg of ergosterol 5, 8-endoperoxide (**NG 2/EC 2**). Sub-fractions 62-90 were combined (53.2 mg) and purified by TLC (silica gel 60 GF_{254}, $CHCl_3$-Petrol-EtOAc-HCO_2H, 8:1:1:0.1) to give 11.2 mg of aszonalenin (**NG 4/NTK 2**).

Fractions 206-212 were combined (4.88 g) and applied over a column chromatography of 40-60 µm Li Chroprep® silica gel (45 g) and eluted with mixtures of petrol-$CHCl_3$, $CHCl_3$-Me_2CO and Me_2CO, wherein 100 mL sub-fractions were collected as follows: Sub-fractions 1-51 (petrol-$CHCl_3$, 1:1), 52-107 (petrol-$CHCl_3$, 3:7), 108-164 (petrol-$CHCl_3$, 1:9), 165-190 ($CHCl_3$-Me_2CO, 9.5:0.5), 191-310 ($CHCl_3$-Me_2CO, 9:1). Sub-fractions 83-164 were combined (53.4 mg) and recrystallized in MeOH to give 27.6 mg of ergosterol 5, 8-endoperoxide (**NG 2/EC 2**). Sub-fractions

166 (38.8 mg) was recrystallized in Me_2CO to give more 8.7 mg of aszonalenin (**NG 4/NTK 2**).

Fractions 213-245 were combined (3.61 g) and applied over a column chromatography of Sephadex^{TM} LH-20 (10 g) and eluted with MeOH, wherein 60 sub-fractions of 20 mL were collected. Sub-fractions 31-51 were combined and purified by TLC (silica gel 60 GF_{254}, $CHCl_3$-Me_2CO-HCO_2H, 4:1:0.1) to give 9.7 mg of takakiamide (**NG 7/NTK 4**) and 13.1 mg of (11 a*S*)-2, 3-dihydro-1*H*-pyrrolo [2, 1-c] [1, 4] benzodiazepine-5, 11 (10*H*, 11a*H*)-dione (**NG 6**).

Fractions 246-257 were combined (1.44 g) and recrystallized in MeOH to give 23.7 mg of helvolic acid (**NG 3**).

Fractions 273-287 were combined (621.0 mg) and purified by TLC (silica gel 60 GF_{254}, $CHCl_3$-Me_2CO-HCO_2H, 7:3:0.3) to give 12.1 mg of helvolic acid (**NG 3**) and 32.3 mg of sartoryglabramide A (**NG 8**).

Fractions 363-373 were combined (1.26 g) and applied over a column chromatography of Sephadex^{TM} LH-20 (10 g) and eluted with MeOH, wherein 60 sub-fractions of 20 mL were collected. Sub-fractions 22-54 were combined (91.2 mg) and purified by TLC (silica gel 60 GF_{254}, $CHCl_3$-Me_2CO-HCO_2H, 9.5:0.5:0.3) to give 14.7 mg of sartoryglabramide B (**NG 9**) and 10 mg of (3*R*)-3-(1*H*-indol-3ylmethyl)-3, 4-dihydro-1*H*-1, 4-benzodiazepine-2, 5-dione (**NG 5**).

Fractions 374-398 were combined (1.37 g) and purified by TLC (silica gel 60 GF_{254}, $CHCl_3$-Me_2CO-HCO_2H, 3:2:0.3) to give 32.8 mg of fellutanine A epoxide (**NG 11**).

Fractions 403-405 were combined (2.49 g) and applied over a column chromatography of Sephadex^{TM} LH-20 (10 g) and eluted with MeOH, wherein 112 sub-fractions of 20 mL were collected. Sub-fractions 90-112 were combined (24.9 mg) and purified by TLC (silica gel 60 GF_{254}, $CHCl_3$-Me_2CO-HCO_2H, 9.5:0.5:0.3) to give 20.7 mg of fellutanine A (**NG 10**).

4.3.4. *Eurotium chevalieri* L. Mangin (KUFA 0006)

Forty 1000 mL Erlenmeyer flasks, each containing 200 g of cooked white rice and 100 mL of water containing 20% sucrose, were autoclaved at 121ºC for 15 min and then inoculated with ten mycelial plugs of the *E. chevalieri* KUFA 0006, and incubated at 28ºC for 40 days. Each flask of the moldy rice was added 500 mL of ethyl acetate and the content was left to macerate for 7 days and then filtered. The ethyl acetate solution was concentrated under reduced pressure to yield 79 g of dark brown viscous mass of crude ethyl acetate extract which was dissolved in 1000 mL of $CHCl_3$, and then washed with H_2O (3x 500 mL). The organic layer were combined and dried with anhydrous Na_2SO_4, filtered and evaporated under reduced pressure to give 75 g of the crude chloroform extract, which was applied on a column

chromatography of 0.04-0.63 mm Merck® silica gel (770 g), and eluted with mixtures of petrol-$CHCl_3$, $CHCl_3$-Me_2CO, $CHCl_3$-MeOH, Me_2CO and MeOH, 250 mL fractions were collected as follows: Fractions 1-450 (petrol-$CHCl_3$, 1:1), 451-518 (petrol-$CHCl_3$, 3:7), 519-726 (petrol-$CHCl_3$, 1:9), 727-1000 ($CHCl_3$-Me_2CO, 9:1), 1001-1192 ($CHCl_3$-Me_2CO, 7:3), 1193-1311 ($CHCl_3$:MeOH, 9:1), 1312-1328 (Me_2CO) and 1329-1330 (MeOH).

Fractions 72-85 were combined (605.5 mg) and recrystallized in methanol to give 27.3 mg of physcion (**EC 4**).

Fractions 250-294 were combined (919.1 mg) and precipitated in MeOH to give 31.3 mg of palmitic acid (**EC 1**).

Fractions 365-368 were combined (94.3 mg) and precipitated in petroleum ether to give 10.7 mg of 2-(2-methyl-3-en-2yl)-1*H*-indole-3-carbaldehyde (**EC 8**).

Fractions 369-398 were combined (453.6 mg) and purified by TLC (silica gel 60 GF_{254}, $CHCl_3$-Me_2CO-HCO_2H, 9.5:0.5:0.1) to give 10.6 mg of ergosterol 5, 8-endoperoxide (**EC 2/NG 2**).

Fractions 652-708 were combined (157.0 mg) and purified by TLC (silica gel 60 GF_{254}, $CHCl_3$-Me_2CO-HCO_2H, 9.5:0.5:0.1) to give 25.1 mg of 2-(2-dimethyl cyclopropyl)-1*H*-indole-carbaldehyde (**EC 9**).

Fractions 734-738 were combined (166.2 mg) and applied on a Sephadex™ LH-20 column chromatography (10 g) and eluted with MeOH and a mixture with

MeOH:CH_2Cl_2 (1:1), wherein 20 mL sub-fractions were collected as follows: Sub-fractions 1-56 (MeOH) and 57-68 (MeOH:CH_2Cl_2, 1:1). Sub-fractions 48-56 were combined (15.0 mg) and purified by TLC (silica gel 60 GF_{254}, $CHCl_3$-Me_2CO-HCO_2H, 9.5:0.5:0.1) to give 10.2 mg of emodin (**EC 3**).

Fractions 756-770 were combined (155.7 mg) and applied on a Sephadex™ LH-20 column chromatography (10 g) and eluted with MeOH, wherein 60 sub-fractions (20 mL each) were collected. Sub-fractions 42-60 were combined (28.2 mg) and purified by TLC (silica gel 60 GF_{254}, $CHCl_3$-Me_2CO-HCO_2H, 9:1:0.1) to give 23.3 mg of questin (**EC 5**).

Fractions 801-815 were combined (371.5 mg) and applied on a Sephadex™ LH-20 column chromatography (10 g) and eluted with MeOH wherein 68 sub-fractions (20 mL each) were collected. Sub-fractions 34-48 were combined (29.4 mg) and purified by TLC (silica gel 60 GF_{254}, $CHCl_3$-Me_2CO-HCO_2H, 9:1:0.1) to give 23.8 mg of acetyl questinol (**EC 7**).

Fractions 860-874 were combined (59.8 mg) and purified by TLC (silica gel 60 GF_{254}, $CHCl_3$-Me_2CO-HCO_2H, 9:1:0.1) to give 10 mg of 2-(2, 2-dimethylbut-3-enoyl) amino-benzoic acid (**EC 10**), 10.2 mg of echinulin (**EC 15**) and 38.2 mg of neochenulin E (**EC 14**).

Fractions 919-945 were combined (439.1 mg) and purified by TLC (silica gel 60 GF_{254}, $CHCl_3$-Me_2CO-HCO_2H, 9.5:0.5:0.1) to give 10 mg of 6, 8-dihydroxy-3-(2*R*-hydroxylpropyl)-7-methyl-1*H*-isochromen-1-one (**EC 11**).

Fractions 1004-1010 were combined (456.9 mg) and purified by TLC (silica gel 60 GF_{254}, $CHCl_3$-MeOH-HCO_2H, 9.5:0.5:0.1) to give 23.3 mg of questinol (**EC 6**).

Fractions 1032-1049 were combined (1.34 g) and applied on a Sephadex^{TM} LH-20 column chromatography (10 g) and eluted with MeOH:CH_2Cl_2 (1:1), 73 sub-fractions of (20 mL) were collected. Sub-fractions 29-42 were combined (84.4 mg) and purified by TLC (silica gel 60 GF_{254}, $CHCl_3$-MeOH-HCO_2H, 9.5:0.5:0.1) to give (11.9 mg) of eurocristatine (**EC 16**), 15.1 mg of preechinulin (**EC 13**) and 20.3 mg of (11*S*, 14*R*)-3-(1*H*-indol-3ylmethyl)-6-isopropyl-2,5-piperazinedione (**EC 12**).

4.4 Physical Characteristics and Spectroscopic data

Palmitic acid (EC 1): White solid; mp 62-63 ºC; ^1H and ^{13}C NMR (see Table 2); (+)-HRESIMS *m/z* 257.2484 $[M+H]^+$ (calcd. for $C_{16}H_{33}O_2$, 257.2481).

Palmitin (TH 1): White solid; mp 65-66 ºC; ^1H and ^{13}C NMR (see Table 3); (+)-HRESIMS m/z 331.2814 $[M+H]^+$ (calcd. for $C_{19}H_{39}O_4$, 331.2848).

Glaucanic acid (TH 3): White solid; mp 188-189 ºC; $[\alpha]_D^{20}$ = + 185 (c 1.05, $CDCl_3$); ^1H and ^{13}C NMR (see Table 4); (+)-HRESIMS *m/z* 333.1311 $[M+H]^+$ (calcd. for $C_{18}H_{21}O_6$, 333.1338).

Glauconic acid (TH 4): White solid; mp 199-200 ºC; ^1H and ^{13}C NMR (see Table 5); (+)-HRESIMS *m/z* 349.1293 $[M+H]^+$ (calcd. for $C_{18}H_{21}O_7$, 349.1287).

Ergosta-4, 6, 8 (14), 22-tetraen-3-one (NG 1): Yellow viscous mass; ^1H and ^{13}C NMR (see Table 6).

Ergosterol 5, 8-endperoxide (NG 2/EC 2): White solid; mp 182-183 ºC; ^1H and ^{13}C NMR (see Table 7).

Acetyl ergosterol 5, 8-endoperoxide (TH 2): White amorphous solid; ^1H and ^{13}C NMR (see Table 7).

Helvolic acid (NG 3): White solid; mp 216-217 ºC; ^1H and ^{13}C NMR (see Table 8).

Chevalone B (**NTK 10**): White solid; mp 163-164 ºC; ^1H and ^{13}C NMR (see Table 9).

Aszonapyrone A (NTK 11): White solid; mp 242-243 ºC; ^1H and ^{13}C NMR (see Table 10).

Sartorenol (NTK 12): White crystal; mp 122-123ºC (petrol/$CHCl_3$); $[\alpha]_D^{20}$ = – 18 (c 0.02, $CHCl_3$); λmax (log) 228 (4.41), 275 (3.99); IR (KBr) ν_{max} 3393, 2932, 2850, 1728, 1645, 1558, 1540, 1418, 1251 cm^{-1}; ^1H and ^{13}C NMR (see Table 11); (+)-HRESIMS *m/z* 431.3175 $[M+H]^+$ (calcd. for $C_{27}H_{43}O_4$, 431.3161).

6-hydroxymellein (NTK 1): White solid; mp 201-202 ºC; $[\alpha]_D^{26}$ = – 51 (c 0.04, MeOH); ^{1}H and ^{13}C NMR (see Table 12).

6, 8-dihydroxy-3(2*R*-hydroxypropyl)-7-methyl-1*H*-isochromen-1-one (EC 11): Yellow viscous liquid; $[\alpha]_D^{20}$ = –88 (c 0.07, Me_2CO); IR (KBr) ν_{max} 3443, 2921, 2254, 1671, 1623, 1540, 1507, 1455 cm^{-1}; ^{1}H and ^{13}C NMR (see Table 13); (+)-HRESIMS *m/z* 251.0900 $[M+H]^+$ (calcd. for $C_{13}H_{15}O_5$, 251.0919).

Emodin (EC 3): yellow amorphous solid; mp 256-257 ºC; ^{1}H and ^{13}C NMR (see Table 14 and 15); (+)-HRESIMS *m/z* 271.0594 $[M+H]^+$ (calcd. for $C_{15}H_{11}O_5$, 271.0606).

Physcion (EC 4): Red crystal; mp 207-208 ºC; ^{1}H and ^{13}C NMR (see Table 14 and 15).

Questin (EC 5): Yellow solid; mp 298-299 ºC; ^{1}H and ^{13}C NMR (see Table 14 and 15).

Questinol (EC 6): Yellow crystal; mp 281-282 ºC; ^{1}H and ^{13}C NMR (see Table 14 and 15); (+)-HRESIMS *m/z* 301.0713 $[M+H]^+$ (calcd. for $C_{16}H_{13}O_6$, 301.0712).

Acetylquestinol (EC 7): Yellow crystal; mp 101-102ºC; IR (KBr) ν_{max} 3442, 2922, 1749, 1631, 1588, 1466, 1379, 1352, 1264 cm^{-1}; ^{1}H and ^{13}C NMR (see Table 14 and 15); (+)-HRESIMS *m/z* 343.0814 $[M+H]^+$ (calcd. for $C_{18}H_{15}O_7$, 343.0818).

2-(2-Methyl-3-en-2-yl)-1*H*-indole-3-carbaldehyde (EC 8): Yellow crystal; mp 162-164ºC; IR (KBr) ν_{max} 3242 (NH), 2972, 2928, 1735, 1622, 1583, 1453, 1381,

1274 cm^{-1}; ^{1}H and ^{13}C NMR (see Table 16); (+)-HRESIMS *m/z* 214.1236 $[M+H]^+$ (calcd. for $C_{14}H_{16}NO$, 214.1232).

2-(2, 2-dimethylcyclopropyl)-1*H*-indole-3-carbaldehyde (EC 9): Yellow viscous liquid; $[\alpha]_D^{20}$ = + 68 (c 0.04, $CHCl_3$); IR (KBr) ν_{max} 3252 (NH), 2923, 1768, 1633, 1583, 1558, 1463, 1376, 1239 cm^{-1}; ^{1}H and ^{13}C NMR (see Table 17); (+)-HRESIMS *m/z* 214.1239 $[M+H]^+$ (calcd. for $C_{14}H_{16}NO$, 214.1232).

Aszonalenin (NTK 2/NG 4): White solid; mp 249-250 ºC; $[\alpha]_D^{20}$ = – 27.0 (c 0.04, $CDCl_3$); ^{1}H and ^{13}C NMR (see Table 18).

Acetylaszonalenin (NTK 3): White solid; mp 237-239 ºC; ^{1}H and ^{13}C NMR (see Table 18).

Takakiamide (NTK 4/NG 7): White solid; mp 182-183ºC (petrol/$CHCl_3$); $[\alpha]_D^{20}$ = – 213 (c 0.02, $CHCl_3$); IR (KBr) ν_{max} 3214, 3057, 2924, 2851, 1688, 1654, 1607, 1579, 1481, 1334, 1255 cm^{-1}, ^{1}H and ^{13}C NMR (see Table 19); (+)-HRESIMS *m/z* 374.1876 $[M+H]^+$ (calcd. for $C_{23}H_{24}N_3O_2$, 374.1869).

(3*R*)-3-(1*H*-indole-3ylmethyl)-3, 4-dihydro-1*H*-1, 4-benzodiazepine-2, 5-dione (NG 5): Yellow viscous mass; $[\alpha]_D^{20}$ = + 96.00 (c 0.06, $CDCl_3$); ^{1}H and ^{13}C NMR (see Table 19); (+)-HRESIMS *m/z* 306.1256 $[M+H]^+$ (calcd. for $C_{18}H_{16}N_3O_2$, 306.1243).

(11a*S*)-2, 3-dihydro-1*H*-pyrrolo [2, 1-c] [1, 4] benzodiazepine-5, 11 (10*H*, 11 a*H*) (NG 6): Yellow viscous mass; $[\alpha]_D^{20}$ = +205.88 (c 0.03, MeOH); ^{1}H and ^{13}C NMR (see Table 20); (+)-HRESIMS *m/z* 217.0992 $[M+H]^+$ (calcd. for $C_{12}H_{13}N_2O_2$, 217.0977).

3′-(4-oxoquinazolin-3-yl) (1*H*-indole-3, 5′-oxolone]-2, 2′-dione (NTK 5): White solid; mp 266-268 ºC; $[\alpha]_D^{20}$ = + 19.7 (c 0.02, MeOH); ^{1}H and ^{13}C NMR (see Table 21).

Tryptoquivaline F (NTK 6): White solid; mp 278-280 ºC; $[\alpha]_D^{20}$ = – 120.0 (c 0.05, MeOH); ^{1}H and ^{13}C NMR (see Table 22).

Tryptoquivaline H (NTK 7): White solid; mp 246-248 ºC; $[\alpha]_D^{20}$ = – 20.1 (c 0.03, MeOH) ^{1}H and ^{13}C NMR (see Table 22).

Tryptoquivaline L (NTK 8): White solid; mp 262-264 ºC; $[\alpha]_D^{20}$ = – 30.5 (c 0.02, MeOH) ^{1}H and ^{13}C NMR (see Table 23).

Tryptoquivaline U (NTK 9): White crystals; mp 208-209ºC (petrol/$CHCl_3$) ; $[\alpha]_D^{20}$ = − 196 (c 0.01, $CHCl_3$); IR (KBr) ν_{max} 3363, 2924, 2852, 1775, 1710, 1662, 1607, 1473, 1384, 1260, 1199 cm^{-1}; ^{1}H and ^{13}C NMR (see Table 23); (+)-HRESIMS *m/z* 417.1563 $[M+H]^+$ (calcd. for $C_{23}H_{21}N_4O_4$, 417.1563).

Fellutanine A (NG 10): Yellow viscous mass; $[\alpha]_D^{20}$ = − 151.52 (c 0.03, MeOH); ^{1}H and ^{13}C NMR (see Table 24); (+)-HRESIMS *m/z* 373.1675 $[M+H]^+$ (calcd. for $C_{22}H_{21}N_4O_2$, 373.1665).

Fellutanine A epoxide (NG 11): Pale yellow viscous mass; $[\alpha]_D^{20}$ = + 13.9 (c 0.07, Me_2CO); IR (KBr) ν_{max} 3420, 2922, 1649, 1416, 1188, 1047, 1025, 996 cm^{-1}; ^{1}H and ^{13}C NMR (see Table 25); (+)-HRESIMS *m/z* 389.1626 $[M+H]^+$ (calcd. for $C_{22}H_{21}N_4O_3$, 389.1614).

(11*S*, 14*R*)-3-(1*H*-indol-3-ylethyl)-6-isopropyl-2, 5-piperazinedione (EC 12): White crystal; mp 270-271ºC; $[\alpha]_D^{20}$ = − 187 (c 0.02, Me_2CO); ^1H and ^{13}C NMR (see Table 26); (+)-HRESIMS *m/z* 286.1575 $[M+H]^+$ (calcd. for $C_{16}H_{20}N_3O_2$, 286.1556).

Preechinulin (EC 13): White solid; mp 251-252 ºC; $[\alpha]_D^{23}$ = + 23.4 (c 0.09, AcOH); ^1H and ^{13}C NMR (see Table 27); (+)-HRESIMS *m/z* 326.1870 $[M+H]^+$ (calcd. for $C_{19}H_{24}N_3O_2$, 326.1869).

Neoechinulin E (EC 14): White solid; mp 273-275 ºC; ^1H and ^{13}C NMR (see Table 28); (+)-HRESIMS *m/z* 324.1347 $[M+H]^+$ (calcd. for $C_{18}H_{18}N_3O_3$, 324.1348).

Echinulin (EC 15): White solid; mp 226-227 ºC; $[\alpha]_D^{26}$ = – 41.7 (c 0.02, $CDCl_3$); ^1H and ^{13}C NMR (see Table 29).

Eurocristatine (EC 16): White crystal; mp 243-244 ºC; ^1H and ^{13}C NMR (see Table 30); (+)-HRESIMS *m/z* 569.2889 $[M+H]^+$ (calcd. for $C_{32}H_{37}N_6O_4$, 569.2876).

2-(2, 2-dimethylbut-3enoyl) amino-benzoic acid (EC 10): Yellow viscous liquid; IR (KBr) ν_{max} 3421, 3253, 2927, 1696, 1670, 1636, 1606, 1586, 1522, 1448, 1385, 1295, 1259 cm^{-1}; ^1H and ^{13}C NMR (see Table 31); (+)-HRESIMS *m/z* 234.1132 $[M+H]^+$ (calcd. for $C_{13}H_{16}NO_3$, 234.1130).

Sartoryglabramide A (NG 8): White crystal; mp 146-148 ºC ($CHCl_3$-Me_2CO); $[\alpha]_D^{20}$ = + 34.6 (c 0.06, Me_2CO); IR (KBr) ν_{max} 3447, 3060, 3028, 2920, 2850, 1655, 1622, 1587, 1526, 1453, 1415, 1300, 1261, 1173 cm^{-1}; ^1H and ^{13}C NMR (see Table 32); (+)-HRESIMS *m/z* 511.2365 $[M+H]^+$ (calcd. for $C_{30}H_{31}N_4O_4$, 511.2345).

Sartoryglabramide B (NG 9): White solid; mp; 190-192ºC ($CHCl_3$-Me_2CO); $[\alpha]_D^{20}$ = + 42.8 (c 0.05, Me_2CO); IR (KBr) ν_{max} 3417, 3058, 2924, 2852, 1649, 1620, 1588, 1526, 1454, 1418, 1302, 1263, 1101 cm^{-1}; ^1H and ^{13}C NMR (see Table 34); (+)-HRESIMS *m/z* 550.2501 $[M+H]^+$ (calcd. for $C_{32}H_{32}N_5O_4$, 550.2454).

4.5 X-Ray Crystallographic Analysis

4.5.1. X-ray Crystal structure of Sartorenol (NTK 12)

Crystals were orthorhombic, space group $P2_1P2_1P2_1$, cell volume 2449.73 (12) $Å^3$ and unit cell dimensions *a* = 5.99830 (16) Å, *b* = 13.1349 Å and *c* = 31.0931 (11) Å (uncertainties in parentheses). There are four molecules per unit cell with calculated density of 1.170 g/cm^{-3}. Diffraction data were collected at 110 K with a Geminin PX Ultra equipped with CuK_α radiation (λ = 1.54184 Å). The structure was solved by direct methods using SHELXS-97 and refined with SHELXL-97 (Sheldrick, 2008). Carbon and oxygen were refined anisotropically. Hydrogen atoms bound to the carbon atom C-20 were placed at their idealized positions using appropriate HFIX instructions in SHELXL, and included in subsequent refinement cycles. All other hydrogen atoms were directly found from difference Fourier maps and were refined freely with isotropic displacement parameters. The refinement converged to *R* (all data) = 9.51 % and *wR*2 (all data) = 17.76 %. Full details of the data collection

and refinement and tables of atomic coordinates, bond lengths and angles, and torsion angles have been deposited with the Cambridge Crystallographic Data Centre (CCDC 1060934).

4.5.2. X-Ray Crystal Structure of Tryptoquivaline U (NTK 8)

Crystals were triclinic, space group P1, cell volume 501.08 (12) $Å^3$ and unit cell dimensions *a* = 5.3913 (7) Å, *b* = 9.8891 (15) Å and *c* = 9.9063 (13) Å and angles α = 84.939 (11)º, β = 75.732 (11)º and γ = 78.452 (12)º (uncertainties in parentheses). There is one molecule per unit cell with calculated density of 1.380 g/cm^{-3}. Diffraction data were collected at 293 K with a Gemini PX Ultra equipped with CuK_α radiation (λ = 1.54184 Å). The structure was solved by direct methods using SHELXS-97 and refined with SHELXL-97 (Gardes and Bruns, 1993). Carbon and oxygen were refined anisotropically. Hydrogen atoms bound to carbon atoms C-5, C-6, C-20 and C-23 were placed at their idealized positions using appropriate HFIX instructions in SHELXL, and included in subsequent refinement cycles. All other hydrogen atoms were directly found from difference Fourier maps and were refined freely with isotropic displacement parameters. The refinement converged to *R* (all data) = 10.88 % and *wR*2 (all data) = 30.04%. The absolute structure was established with confidence (flask *x* parameter) 0.03 (11). Full details of the data collection and refinement and tables of aromatic coordinates, bond lengths and

angles, and torsion angles have been deposited with the Cambridge Crystallographic Data Centre (CCDC 1060935).

4.5.3. X-Ray Crystal Structure of Sartoryglabramide A (NG 8)

A single crystal of sartoryglabramide A was mounted on a cryoloop using paratone. X-rays diffraction data was collected at room temperature with a Gemini PX Ultra equipped with CuK_{α} radiation (λ = 1.54184 Å). The crystal was orthorhombic, space group $P2_1P2_1P2_1$, cell volume 5459.8 (2) $Å^3$ and unit cell dimensions *a* = 15.1792 (3) Å, *b* = 18.7674 (5) Å and *c* = 19.1659 (3) Å (uncertainties in parentheses). There are two molecular per unit cell with calculated density of 1.242 g/cm^{-3}. The structure was solved by direct methods using SHELXS 97 and refined with SHELXL-97 (Sheldrick, 2008). Carbon, nitrogen and oxygen atoms were refined anisotropically. Hydrogen atoms were either placed at their idealized positions using appropriate HFIX instructions in SHELXL and included in subsequent refinement cycles or were directly found from difference Fourier maps and were refined freely with isotropic displacement parameters. The refinement converged to *R* (all data) = 10.02% and *wR*2 (all data) = 15.26%. The absolute structure could not be established with confidence (flask *x* parameter) 0.3 (4). Full details of the data collection and refinement and tables of atomic coordinates, bond lengths and angles,

and torsion angles have been deposited with the Cambridge Crystallographic Data Centre (CCDC 1483750).

4.5.4. X-Ray Crystal Structure of Acetyquestinol (EC 7) and (11*S*, 14*R*)-3-(1*H*-indol-3ylmethyl)-6-isopropyl-2, 5-piperazinedione (EC 12)

Diffraction data were collected at 293K with a Gemini PX Ultra equipped with CuKα radiation (λ = 1.54184 Å). The structures were solved by direct methods using SHELXS-97 and refinement with SHELXL-97 (Sheldrick, 2008). Carbon, nitrogen and oxygen atoms were refined anisotropically. Hydrogen atoms were directly found from difference Fourier maps and were refined freely with isotropic displacement parameters. Full details of the data collection and refinement and tables of atomic coordinates, bond lengths and angles and torsion angles have been deposited with the Cambridge Crystallographic Data Centre.

Acetyquestinol (**EC 7**): Crystals were monoclinic, space group P21/c, cell volume 1470.45 (19) $Å^3$ and unit cell dimensions *a* = 6.10326 (16) Å, *b* = 29.533 (2) Å and *c* = 11.0898 (9) Å and angle β = 92.503 (7)º (uncertainties in parentheses). The refinement converged to *R* (all data) = 7.65% and *wR*2 (all data) = 14.76%, CCDC 1532709.

(11*S*, 14*R*)-cyclo (tryptophylvalyl) (**EC 12**): Crystals were monoclinic, space group $P2_1$, cell volume 748.51 (4) $Å^3$ and unit cell dimensions *a* = 6.10326 (16) Å,

b = 13.4265 (4) Å and *c* = 9.4770 (3) Å angle β= 105.457 (3)º. The refinement converged to *R* (all data) = 3.32 % and *wR*2 (all data) = 8.01 %. The flask *x* parameter was refined with SHELXL-97 to yield 0.1 (3), CCDC 1532719.

4.6 Amino Acids Analysis of Hydrolysate of Sartoryglabramide A (NG 8) and Sartoryglabramide B (NG 9)

4.6.1. Acid Hydrolysis

The stereochemistry of the amino acids was determined by analysis of the acidic hydrolysate from sartoryglabramide A (**NG 8**) and sartoryglabramide B (**NG 9**) (5.0 mg) was dissolved in 6 N HCl (5 mL) and heated at 110ºC, in a furnace, for 24 h in a sealed glass tube. After cooling to room temperature, the solution was dried under N_2 for 24 h, reconstituted in MeOH or HPLC-MS (200 µL), filtered through a 4 mm PTFE Syringe Filter F2504-4 of 0.2 µm pore size (Thermo Scientific, Mumbai, India), and then analyzed by HPLC equipped with a chiral column.

4.6.2. Chiral HPLC analysis

The HPLC system consisted of Shimadzu LC-20AD pump, equipped with a Shimadzu DGV-20A5 degasser, a Rheodyne 7725i injector fitted with a 20 µL loop,

and a SPD-M20A DAD detector (Kyoto, Japan). Data acquisition was performed using Shimadzu LCMS Lab Solutions software, version 3.50 SP2. The chiral column used in this study was Chirobiotic T (15 cm x 4.6 mm I.D., partical size 5µm) manufactured by ASTEC (Whippany, NJ, USA). The mobile phase composition was MeOH: H_2O (80:20 v/v), all were LC-MS grade solvents obtained from Sigma-Aldrich Co. (St. Louis, MO, USA). The flow rate was 1.0 mL/min and the UV detection wavelength was 210 nm. Analyses were performed at room temperature in an isocratic mode. All standards of pure amino acid enantiomers were purchased from Sigma-Aldrich Co. (St. Louis, MO, USA). The elution order of the enantiomers of all the standards amino acids was confirmed by injecting the solutions of enantiomeric mixtures and then each enantiomer separately. Working solutions of single enantiometric amino acids were prepared by dissolution in MeOH at the concentration of 1 mg/mL (10 µL sample injection), while the enantiometric mixtures were prepared by mixing equal aliquots of each enantiomer (20 µL smaple injection). Mix HPLC analyses of the acidic hydrolysate with standard amino acids (co-injection) confirmed the stereochemistry of the amino acids of sartoryglabramide A (**NG 8**) and sartoryglabramide B (**NG 9**).

4.7 Molecular Mechanics Conformation Analysis of Takakiamide (NTK 4/NG 7) and Fellutanine A Epoxide (NG 11)

Molecular simulations for the structures of takakiamide (**NTK 4/NG 7**) and fellutanine A epoxide (**NG 11**) were carried out in ChemBio3D Ultra 14 (Perkin-Elmerm, Waltham, MA, USA). Stochastic and dihedral driver conformational search, with MMFF force field energy minimization, was done for both *S*/*S* and *R*/*R* isomers of **NTK 4/NG 7** and **NG 11**, followed by *ab* initio RHF/6-21G energy re-minimization of the lowest energy conformations using CSGAMESS interfaced by ChemBio3D. The PCM solvent model for DMSO was used on the *ab* initio minimizations.

4.8 Electronic Circular Dichroism (ECD)

Electronic circular dichroism spectra were obtained in a Jasco J-815 CD spectropolarimeter with a 1mm cuvette; Savitsky-Golay noise reduction was applied when necessary. Dihedral driver and MM2 minimizations were done in Chem3D Ultra (perkin-Elmer Inc.). All other minimizations and spectral calculations were performed with Gaussian (Gaussian Inc.) at the APFD/6-311+G (2d, p) level (Austin *et al*., 2012) with IEFPCM solvation model. The simulated spectral lines were obtained by summation of Gaussian curves, as recommended in Stephan *et al*. (Stephens and Harada, 2010). ECD spectra for all conformations were added using Boltzmann weights derived from its minimal energies (Mori *et al*., 2006).

4.9 Antibacterial Activity Bioassays

4.9.1. Bacterial strains and growth conditions

Two Gram-positive (*Staphylococcus aureus* ATCC 25923 and *Enterococcus faecalis* ATCC 29212) and two Gram-negative (*Escherichia coli* ATCC 25922 and *Pseudomonas aeruginosa* ATCC 27853) reference strains were used. Multidrug-resistant bacterial strains isolated from public buses (MRSCA *S. aureus* 66/1) (Simoes *et al*., 2011), river water (VRE *E. faecalis* B3/101) (Bessa *et al*., 2014) and a clinical isolate (ESBL *E. coli* SA/2) were also used. Frozen stocks of all stains were grown in Mueller-Hinton agar (MH-BioKar diagnostics, Allone, France) at 37ºC. Bacteria were sub-cultured in MH agar and incubated overnight at 37ºC in order to obtain fresh cultures for each assay.

4.9.2. Antimicrobial susceptibility testing

The minimum inhibitory concentration (MIC) for each compound was determined by the broth microdilution method according to the recommendations of the Clinical and Laboratory Standards Institute (CLSI) (CLSI, 2015). With the exception of physcion (**EC 4**), 10 mg/mL stock solutions of each compound were prepared in dimethylsulfoxide (DMSO-Applichem GmbH, Darmstadt, Germany). For physcion (**EC 4**), which was less soluble in DMSO than the other compounds,

a stock solution of 1 mg/mL was prepared. Two-fold serial dilutions of concentrated stock solutions were prepared in Mueller-Hinton broth 2 (MHB2-Sigma-Aldrich, St. Lousis, MO, USA). The range of concentrations tested was 0.016-16 µg/mL in the case of compound physcion (**EC 4**) and 0.062-64 µg/mL for all other compounds. The highest concentrations tested were chosen in order to maintain DMSO in-test concentration below 1% as recommended by the CLSI (CLSI, 2015). At this concentration DMSO did not affect the bacterial growth. Cefotaxime (CTX) ranging from 0.031-16 µg/mL was used as a control. Purity check and colony counts of the inoculum suspensions were also evaluated in order to ensure that the final inoculum density closely approximates the intended at number (5 x 10^5 CFU/mL). The MIC was determined as the lowest concentration at which no visible growth was observed. The minimum bactericidal concentration (MBC) was assessed by spreading 10 µL of culture collected from wells showing no visible growth on MH agar plates. The MBC was determined as the lowest concentration at which no colonies grew after 16-18 hours incubation at 37ºC. These assays were performed in duplicate.

4.9.3. Biofilm formation inhibition assay

The effect of all compounds on biofilm formation was evaluated using crystal violet staining as described previously (Gomes *et al*., 2014). Briefly, the highest

concentration tested in the MIC assay was added to bacterial suspensions of 1 x 10^6 CFU/mL prepared in Tryptic Soy broth (TSB-BioKar diagnostics, Allonne, France). When it was possible to determine a MIC, three concentrations were tested: 2 x MIC, MIC and ½ x MIC. A control without any compound as well as a negative control (TBS alone) was included. CTX was used as a positive control. The stabilized biofilm mass was quantified after 24 hours incubation at 37ºC. The samples were quantified calorimetrically at 595 nm on an iMark™ microplate spectrophotometer (Bio-Rad Laboratories, Hercules, CA, USA). The background absorbance (TBS without inoculum) was subtracted from the absorbance of each sample and the data are presented as percentage of control. Three independent experiments were performed in triplicate for each experimental condition.

4.9.4. Antibiotic synergy testing

In order to evaluate the combined effect of the compounds and clinical relevant antimicrobial drugs, a screening was conducted using the disk diffusion method, as described previously (Bessa *et al*., 2015; Gomes *et al*., 2014). A set of antibiotic disks (Oxoid, Basingstoke, UK) to which the isolates were resistant was selected: cefotaxime (CTX, 30 µg) for *E. coli* SA/2, oxacillin (OX, 1 µg) for *S. aureus* 66/1, and vancomycin (VAN, 30 µg) for *E. faecalis* B3/101. Antibiotic disk alone (controls) and antibiotic disks impregnated with 15 µg of each compound were

placed on MH agar plates seeded with the respective bacteria. Sterile 6 mm blank paper disks (Oxoid, Basingstoke, UK) impregnated with 15 µ of each compound alone was also tested. A blank disk with DMSO was used as a negative control. MH inoculated plates were incubated for 18-20 hours at 37ºC. Potential synergism was recorded when the halo of the antibiotic disk impregnated with a compound was greater than the halo of the antibiotic or compound-impregnated blank disk alone.

The potential synergy between the compounds and clinical relevant antibiotics was also evaluated by determining the antibiotic MIC in the presence of each compound. Briefly, MIC of CTX, OX and VAN (Sigma-Aldrich, St. Louis, MO, USA) for the respective multidrug-resistant strains was determined in the presence of the highest concentration of each compound tested that did not affect bacterial growth when the compound was tested alone. The antibiotic tested was serially diluted whereas the concentration of each compound was fixed. In the case of physcion (**EC 4**), the concentration used was 16 µg/mL. For all other compounds the concentration used was 64 µg/mL. Antibiotic MICs were determined as described above.

CHAPTER V

CONCLUSIONS

CONCLUSIONS

This thesis reports on the secondary metabolites isolated from the marine soft coral-derived fungus *Talaromyces helicus* KUFA 0063, which was collected from Angthong National Marine Park, Thailand, marine alga-assiociated fungus *Neosartorya takakii* KUFC 7898 and marine sponge-associated fungus *Neosartorya glabra* KUFA 0702, collected from the Samaesarn Island in the Gulf of Thailand and the mangrove-derived endophytic fungus *Eurotium chevalieri* KUFA 0006, which was collected in the Eastern Seaboard of Thailand, for the purpose of finding new leads for the discovery of pharmacologically active metabolites.

Totally forty-three secondary metabolites have been successfully isolated in this study which can be classified as fatty acids, nonadrides, ergosterol derivatives, tetracyclic triterpenoid, meroditerpenes, isocoumarins, anthraquinones, prenylated 1*H*-indole 3-carbaldehydes, indolymethyl 1, 4-benzodiazepen 2, 5-dione, indolyl quinazolinone alkaloids, diketopiperazines and cylopeptides. To the best of our knowledge, eleven compounds have never been previously reported.

Four known compounds namely palmitin (**TH 1**), acetyl ergosterol 5, 8-endoperoxide (**TH 2**), glaucanic acid (**TH 3**) and glauconic acid (**TH 4**) were isolated from the marine soft coral-derived fungus *Talaromyces helicus* KUFA 0063. Additionally, the crude ethyl acetate extract of the marine alga-associated fungus *N. takakii* KUFC 7898, produced nine known compounds: 6-hydroxymellein (**NTK 1**),

aszonalenin (**NTK 2/NG 4**), acetylaszonalenin (**NTK 3**), 3′-(4-oxoquinazolin-3-yl) spiro [1*H*-indole-3, 5′-oxolane]-2, 2′-dione (**NTK 5**), tryptoquivaline F (**NTK 6**), tryptoquivaline H (**NTK 7**), tryptoquivaline L (**NTK 8**), chevalone B (**NTK 10**), aszonapyrone A (**NTK 11**), together with three new compounds including takakiamide (**NTK 4**), tryptoquivaline U (**NTK 9**) and a new meroditerpene sartorenol (**NTK 12**).

Two new cyclotetrapeptides, sartoryglabramide A (**NG 8**) and sartoryglabramide B (**NG 9**), and a new analog of fellutanine A: fellutanine A 2′, 3′-epoxide (**NG 11**), were isolated together with eight known compounds including ergosta-4, 6, 8 (14), 22-tetraen-3-one (**NG 1**), ergosterol 5, 8-endoperoxide (**NG 2/EC 2**), helvolic acid (**NG 3**), aszonalenin (**NG 4/NTK 2**), (3*R*)-3-(1*H*-indol-3-ylmethyl)-3,4-dihydro-1*H*-1,4-benzodiazepine-2,5-dione (**NG 5**), (11a*S*)-2,3-dihydro-1*H*-pyrrolo [2,1-c] [1,4] benzodiazepine-5, 11 (10a*H*, 11a*H*)-dione (**NG 6**), takakiamide (**NG 7/NTK 4**) and fellutanine A (**NG 10**) from the ethyl acetate extract of the culture of the marine sponge-associated fungus *N. glabra* KUFA 0702.

The mangrove-derived endophytic fungus *Eurotium chevalieri* KUFA 0006 furnished five new metabolites, including a new anthraquinone derivative acetylquestinol (**EC 7**), two prenylated indole 3-carbaldehyde derivatives 2-(2-methyl-3-en-2-yl)-1*H*-indole-3-carbaldehyde (**EC 8**), (2, 2-dimethylcyclopropyl)-1*H*-indole-3-carbaldehyde (**EC 9**), an anthranilic acid derivative: 2-(2, 2-dimethylbut-3-enoyl) amino-benzoic acid (**EC 10**) and an isochromone derivative:

6, 8-dihydroxy-3-(2*R*-hydroxypropyl)-7-methyl-1*H*-isochromen-1-one (**EC 11**), together with eleven known metabolites: palmitic acid (**EC 1**), ergosterol 5,8-endoperoxide (**EC 2/NG 2**), emodin (**EC 3**), physcion (**EC 4**), questin (**EC 5**), questinol (**EC 6**), (11*S*, 14*R*)-3-(1*H*-indol-3-ylmethyl)-6-isopropyl-2,5-piperazinedione (**EC 12**), preechinulin (**EC 13**), neoechinulin E (**EC 14**), echinulin (**EC 15**) and eurocristatine (**EC 16**).

The structures of the isolated compounds were elucidated by extensive 1D and 2D NMR spectral analysis (^{1}H, ^{13}C NMR, COSY, DEPTs, HSQC, HMBC and NOESY) and High Resolution Mass Spectrometry. The optical rotation used for the comparison of the previously reported compounds. The absolute configurations of the stereogenic carbons of the compounds: tryptoquivaline U (**NTK 8**), sartorenol (**NTK 12**), sartoryglabramide A (**NG 8**), acetylquestinol (**EC 7**) and (11*S*, 14*R*)-3-(1*H*-indol-3-ylmethyl)-6-isopropyl-2,5-piperazinedione (**EC 12**) were determined by X-ray analysis as well as takakiamide (**NG 7/NTK 4**) and fellutanine A epoxide (**NG 11**) were confirmed by molecular mechanics conformation analysis, in addition (2, 2-dimethylcyclopropyl)-1*H*-indole-3-carbaldehyde (**EC 9**) and 6, 8-dihydroxy-3 (2*R*-hydroxypropyl)-7-methyl-1*H*-isochromen-1-one (**EC 11**) were confirmed by comparision of the experimental and calculated electronic circular dichroism (ECD). The absolute stereochemistry of the amino acid constituents of sartoryglabramides **A** and **B** (**NG 8** and **NG 9**) was determined by chiral HPLC analysis of their hydrolysates by co-injection with the D- and L-amino acids standards.

Some of the isolated compounds were screened for antibacterial, antibiofilm and antifungal activities. The result showed that only emodin (**EC 3**), isolated from *E. chevalieiri* KUFA 0006 exhibited moderate antibacterial activity against Gram positive bacteria, *S. aureus* ATCC 25923 and *E. faecalis* ATCC 29212 with MIC values of 32 and 64 µg/mL, respectively, as well as strong synergism with the antibiotic against MRSA *S. aureus* 66/1. All of the metabolites from *Eurotium chevalieri* KUFA 0006 (**EC 3-EC 16**) showed synergistic association with vancomycin against the multidrug-resistant VRE *E. faecalis* B3/101. Emodin (**EC 3**), physicon (**EC 4**) and two new prenylated indole carbaldehydes (**EC 8** and **EC 9**) are found to significantly inhibit the production of biofilm in *S. aureus* ATCC 25923.

Therefore, the anthraquinone derivatives can represent an interesting scaffold to test for their activity against multidrug-resistant bacteria. Interestingly, fungi of the genera *Talaromyces*, *Neosartorya* and *Eurotium* were found to be the most promising genera because of their capacity of producing bioactive compounds. Although many of the secondary metabolites isolated from the fungi of the genus *Neosartorya* did not exhibit antibacterial activity in our assay protocols, it is by no means to conclude that these compounds do not possess any other interesting biological activities. Therefore, it is necessary to test these compounds in more bioassay systems so that their potential can be duly exploited.

These data indicate that the mangrove-derived endophytic fungi are a good source of new antibacterial and antibiofilm compounds and this information will be

benificial for further utilization and development of antibacterial compounds from marine fungi and as lead compounds for pharmaceutical industry in the future.

REFERENCES

References

Absalon, M. J., and Smith, F. O. **(2009)**. Treatment strategies for pediatric acute myeloid leukemia. *Expert Opinion on Pharmacotherapy* **10**, 57-79.

Akpotu, M. O., Eze, P. M., Abba, C. C., Umeokoli, B. O., Nwachukwu, C. U., Okoye, F. B., and Esimone, C. O. **(2017)**. Antimicrobial activities of secondary metabolites of endophytic fungi isolated from *Catharanthus roseus*. *Journal of Health Sciences* **7**, 15-22.

Alias, S. A., and Jones, E. G. **(2000)**. Vertical distribution of marine fungi on *Rhizophora apiculata* at Morib mangrove, Selangor, Malaysia. *Mycoscience* **41**, 431-436.

Al-Julaifi, M. Z. **(2003)**. Ochratoxin A production by *Eurotium amstelodami* and *Eurotium spp*. isolated from locally grown barley in Saudi Arabia. *Kuwait Journal of Science and Engineering* **30**, 59-66.

Altschul, S. F., Madden, T. L., Schäffer, A. A., Zhang, J., Zhang, Z., Miller, W., and Lipman, D. J. **(1997)**. Gapped BLAST and PSI-BLAST: a new generation of protein database search programs. *Nucleic Acids Research* **25**, 3389-3402.

Amagata, T., Doi, M., Ohta, T., Minoura, K., and Numata, A. **(1998)**. Absolute stereostructures of novel cytotoxic metabolites, gymnastatins A–E, from a *Gymnascella* species separated from a *Halichondria* sponge. *Journal of the Chemical Society, Perkin Transactions 1*, 3585-3600.

Anke, H., Kolthoum, I., Zähner, H., and Laatsch, H. **(1980)**. Metabolic products of microorganisms. 185. The anthraquinones of the *Aspergillus glaucus* group. I. Occurrence, isolation, identification and antimicrobial activity. *Archives of Microbiology* **126**, 223-230.

Arai, M., Tomoda, H., Okuda, T., Wang, H., Tabata, N., Masuma, R., Yamaguchi, Y., and Omura, S. **(2002)**. Funicone-related compounds, potentiators of antifungal miconazole activity, produced by *Talaromyces flavus* FKI-0076. *The Journal of Antibiotics* **55**, 172-180.

Austin, A., Petersson, G. A., Frisch, M. J., Dobek, F. J., Scalmani, G., and Throssell, K. **(2012)**. A Density Functional with Spherical Atom Dispersion Terms. *Journal of Chemical Theory and Computation* **8**, 4989-5007.

Avila, C., Taboada, S., and Núñez-Pons, L. **(2008)**. Antarctic marine chemical ecology: what is next? *Marine Ecology* **29**, 1-71.

Ayer, W. A., and Racok, J. S. **(1990)**. The metabolites of *Talaromyces flavus*: Part 1. Metabolites of the organic extracts. *Canadian Journal of Chemistry* **68**, 2085-2094.

Ayer, W. A., Attah-Poku, S. K., Browne, L. M., and Orszanska, H. **(1987)**. The chemistry of the blue stain fungi. Part 3. Some metabolites of *Ceratocystis minor* (Hedgcock) Hunt. *Canadian Journal of Chemistry* **65**, 765-769.

Bai, Z.-Q., Lin, X., Wang, Y., Wang, J., Zhou, X., Yang, B., Liu, J., Yang, X., Wang, Y., and Liu, Y. **(2014)**. New phenyl derivatives from endophytic fungus *Aspergillus flavipes* AIL8 derived of mangrove plant *Acanthus ilicifolius*. *Fitoterapia* **95**, 194-202.

Balagurunathan, R., and Radhakrishnan, M. **(2007)**. Exploiting the less explored-Microbial Endophytes. *Adv Biotechnol* **6**, 20-3.

Bao, J., Luo, J.-F., Qin, X.-C., Xu, X.-Y., Zhang, X.-Y., Tu, Z.-C., and Qi, S.-H. **(2014)**. Dihydrothiophene-condensed chromones from a marine-derived fungus *Penicillium oxalicum* and their structure–bioactivity relationship. *Bioorganic and Medicinal Chemistry Letters* **24**, 2433-2436.

Bao, J., Sun, Y.-L., Zhang, X.-Y., Han, Z., Gao, H.-C., He, F., Qian, P.-Y., and Qi, S.-H. **(2013)**. Antifouling and antibacterial polyketides from marine gorgonian coral-associated fungus *Penicillium sp.* SCSGAF 0023. *Journal of Antibiotics* **66**, 219-223.

Bara, R., Aly, A. H., Pretsch, A., Wray, V., Wang, B., Proksch, P., and Debbab, A. **(2013a)**. Antibiotically active metabolites from *Talaromyces wortmannii*, an endophyte of *Aloe vera*. The *Journal of Antibiotics* **66**, 491-493.

Bara, R., Aly, A. H., Wray, V., Lin, W., Proksch, P., and Debbab, A. **(2013b)**. Talaromins A and B, new cyclic peptides from the endophytic fungus *Talaromyces wortmannii*. *Tetrahedron Letters* **54**, 1686-1689.

Bara, R., Zerfass, I., Aly, A. H., Goldbach-Gecke, H., Raghavan, V., Sass, P., Mándi, A., Wray, V., Polavarapu, P. L., Pretsch, A., Lin, W., Kurtán, T., Debbab, A., Brötz-Oesterhelt, H., and Proksch, P. **(2013c)**. Atropisomeric Dihydroanthracenones as Inhibitors of Multiresistant *Staphylococcus aureus*. *Journal of Medicinal Chemistry* **56**, 3257-3272.

Barrow, C. J., and Sun, H. H. **(1994)**. Spiroquinazoline, a Novel Substance P Inhibitor with a New Carbon Skeleton, Isolated from *Aspergillus flavipes*. *Journal of Natural Products* **57**, 471-476.

Barton, D., and Sutherland, J. **(1965)**. 329. The nonadrides. Part I. Introduction and general survey. *Journal of the Chemical Society (Resumed)*, 1769-1772.

Barton, D., Gondinho, L., and Sutherland, J. **(1965a)**. 331. The nonadrides. Part III. The absolute configuration of glauconic and glaucanic acids. *Journal of the Chemical Society (Resumed)*, 1779-1786.

Barton, D., Jackman, L., Rodriguez-Hahn, L., and Sutherland, J. **(1965b)**. 330. The nonadrides. Part II. The constitutions of glauconic and glaucanic acids. *Journal of the Chemical Society (Resumed)*, 1772-1778.

Bazes, A., Silkina, A., Douzenel, P., Faÿ, F., Kervarec, N., Morin, D., Berge, J.-P., and Bourgougnon, N. **(2009)**. Investigation of the antifouling constituents from the brown alga *Sargassum muticum* (Yendo) Fensholt. *Journal of Applied Phycology* **21**, 395-403.

Benjamin, C. R. **(1955)**. Ascocarps of *Aspergillus* and *Penicillium*. *Mycologia* **47**, 669-687.

Benyhe, S. **(1994)**. Morphine: new aspects in the study of an ancient compound. *Life Sciences* **55**, 969-979.

Berdy, J. **(2005)**. Bioactive microbial metabolites. *Journal of Antibiotics* **58**, 1-26.

Bergmann, W., and Stempien Jr, M. F. **(1957)**. Contributions to the Study of Marine Products. XLIII. The Nucleosides of Sponges. V. The Synthesis of Spongosine1. *The Journal of Organic Chemistry* **22**, 1575-1577.

Berthod, A., Liu, Y., Bagwill, C., and Armstrong, D. W. **(1996)**. Facile liquid chromatographic enantioresolution of native amino acids and peptides using a teicoplanin chiral stationary phase. *Journal of Chromatography A* **731**, 123-137.

Besitulo, A. D., Sarma, V. V., and Hyde, K. D. **(2002)**. Mangrove fungi from Siargao Island, Philippines. *Fungi in Marine Environments*, **7**, 267-283.

Bessa, L. J., Barbosa-Vasconcelos, A., Mendes, Â., Vaz-Pires, P., and da Costa, P. M. **(2014)**. High prevalence of multidrug-resistant *Escherichia coli* and *Enterococcus spp*. in river water, upstream and downstream of a wastewater treatment plant. *Journal of Water and Health* **12**, 426-435.

Bessa, L. J., Palmeira, A., Gomes, A. S., Vasconcelos, V., Sousa, E., Pinto, M., and Martins da Costa, P. **(2015)**. Synergistic Effects between thioxanthones and oxacillin against methicillin-resistant *Staphylococcus aureus*. *Microbial Drug Resistance* **21**, 404-415.

Bhadury, P., Mohammad, B. T., and Wright, P. C. **(2006)**. The current status of natural products from marine fungi and their potential as anti-infective agents. *Journal of Industrial Microbiology and Biotechnology* **33**, 325-337.

Bhatnagar, I., and Kim, S.-K. **(2010)**. Immense essence of excellence: marine microbial bioactive compounds. *Marine Drugs* **8**, 2673-2701.

Blunt, J. W., and Munro, M. H. **(2007)**. Dictionary of marine natural products with CD-ROM, CRC Press.

Blunt, J. W., Copp, B. R., Hu, W.-P., Munro, M. H., Northcote, P. T., and Prinsep, M. R. **(2009)**. Marine natural products. *Natural Product Reports* **26**, 170-244.

Blunt, J. W., Copp, B. R., Keyzers, R. A., Munro, M. H., and Prinsep, M. R. **(2014)**. Marine natural products. *Natural Product Reports* **31**, 160-258.

Blunt, J. W., Copp, B. R., Keyzers, R. A., Munro, M., and Prinsep, M. R. **(2013)**. Marine natural products. *Natural Product Reports* **30**, 237-323.

Blunt, J. W., Copp, B. R., Munro, M. H. G., Northcote, P. T., and Prinsep, M. R. **(2005)**. Marine natural products. *Natural Product Reports* **22**, 15-61.

Bodanszky, M. **(2012)**. Principles of peptide synthesis. Springer Science and Business Media.

Borel, J. F., Feurer, C., Magnee, C., and Stähelin, H. **(1977)**. Effects of the new anti-lymphocytic peptide cyclosporin A in animals. *Immunology* **32**, 1017-1025.

Brakhage, A. A., and Langfelder, K. **(2002)**. Menacing mold: the molecular biology of *Aspergillus fumigatus*. *Annual Reviews in Microbiology* **56**, 433-455.

Bringmann, G., Gulder, T. A., Lang, G., Schmitt, S., Stöhr, R., Wiese, J., Nagel, K., and Imhoff, J. F. **(2007)**. Large-scale biotechnological production of the antileukemic marine natural product sorbicillactone A. *Marine Drugs* **5**, 23-30.

Bugni, T. S., and Ireland, C. M. **(2004)**. Marine-derived fungi: a chemically and biologically diverse group of microorganisms. *Natural Product Reports* **21**, 143-163.

Bulama, J., Dangoggo, S., Halilu, M., Tsafe, A. I., and Hassan, S. **(2014)**. Isolation and Characterization of Palmitic Acid from Ethyl Acetate Extract of Root Bark of *Terminalia Glaucescens*. *Chemistry and Materials Research* **6**, 140-143.

Butler, M. S. **(2004)**. The role of natural product chemistry in drug discovery. *Journal of Natural Products* **67**, 2141-2153.

Buttachon, S., Chandrapatya, A., Manoch, L., Silva, A., Gales, L., Bruyère, C., Kiss, R., and Kijjoa, A. **(2012)**. Sartorymensin, a new indole alkaloid, and new analogues of tryptoquivaline and fiscalins produced by *Neosartorya siamensis* (KUFC 6349). *Tetrahedron* **68**, 3253-3262.

Cantrell, C. L., Rajab, M. S., Franzblau, S. G., Fronczek, F. R., and Fischer, N. H. **(1999)**. Antimycobacterial ergosterol-5, 8-endoperoxide from *Ajuga remota*. *Planta Medica* **65**, 732-734.

Capon, R. J., Skene, C., Stewart, M., Ford, J., O'Hair, R. A. J., Williams, L., Lacey, E., Gill, J. H., Heiland, K., and Friedel, T. **(2003)**. Aspergillicins A-E: five novel depsipeptides from the marine-derived fungus *Aspergillus carneus*. *Organic and Biomolecular Chemistry* **1**, 1856-1862.

Carter, G. T. **(2011)**. Natural products and Pharma 2011: Strategic changes spur new opportunities. *Natural Product Reports* **28**, 1783-1789.

Chaeprasert, S., Piapukiew, J., Whalley, A. J., and Sihanonth, P. **(2010)**. Endophytic fungi from mangrove plant species of Thailand: their antimicrobial and anticancer potentials. *Botanica Marina* **53**, 555-564.

Chaillan, F., Le Flèche, A., Bury, E., Phantavong, Y. h., Grimont, P., Saliot, A., and Oudot, J. **(2004)**. Identification and biodegradation potential of tropical aerobic hydrocarbon-degrading microorganisms. *Research in Microbiology* **155**, 587-595.

Chen, B.-Y., Wang, Z., Ying, Y.-M., Jiang, L.-X., Zhan, Z.-J., Wang, J.-L., and Zhang, W. **(2014)**. Neofipiperzine D, a new prenylated indole alkaloid metabolite of the fungus *Neosartorya fischeri*. *Journal of Chemical Research* **38**, 539-541.

Chen, G., Zhu, Y., Wang, H.-Z., Wang, S.-J., and Zhang, R.-Q. **(2007)**. The metabolites of a mangrove endophytic fungus, *Penicillium thomi*. *Journal of Asian Natural Products Research* **9**, 159-164.

Chen, L., and GU, Q.-Q. **(2010)**. Study on the antitumor metabolites of a sponge-derived fungus, *Aspergillus repens*. *Periodical of Ocean University of China* **40**, 69-71.

Chen, X., Si, L., Liu, D., Proksch, P., Zhang, L., Zhou, D., and Lin, W. **(2015)**. Neoechinulin B and its analogues as potential entry inhibitors of influenza viruses, targeting viral hemagglutinin. *European Journal of Medicinal Chemistry* **93**, 182-195.

Cheng, Z. S., Pan, J. H., Tang, W. C., Chen, Q. J., and Lin, Y. C. **(2009)**. Biodiversity and biotechnological potential of mangrove-associated fungi. *Journal of Forestry Research* **20**, 63-72.

Chooi, Y.-H., Fang, J., Liu, H., Filler, S. G., Wang, P., and Tang, Y. **(2013)**. Genome Mining of a Prenylated and Immunosuppressive Polyketide from Pathogenic Fungi. *Organic Letters* **15**, 780-783.

Clark, A. M. **(1996)**. Natural products as a resource for new drugs. *Pharmaceutical Research* **13**, 1133-1141.

Cole, R., and Cox, R. **(1981)**. Handbook of Toxic Fungal Metabolites. Academic Press INC.

Cragg, G. M. **(1998)**. Paclitaxel (Taxol®): a success story with valuable lessons for natural product drug discovery and development. *Medicinal Research Reviews* **18**, 315-331.

Cragg, G. M., and Newman, D. J. **(2005a)**. International collaboration in drug discovery and development from natural sources. *Pure and Applied Chemistry* **77**, 1923-1942.

Cragg, G. M., and Newman, D. J. **(2005b)**. Plants as a source of anti-cancer agents. *Journal of Ethnopharmacology* **100**, 72-79.

Cragg, G. M., Grothaus, P. G., and Newman, D. J. **(2009)**. Impact of natural products on developing new anti-cancer agents. *Chemical Reviews* **109**, 3012-3043.

Cragg, G. M., Newman, D. J., and Snader, K. M. **(1997)**. Natural products in drug discovery and development. *Journal of Natural Products* **60**, 52-60.

Der Marderosian, A., and Beutler, J. **(2002)**. Oregano, in The Review of Natural Products.

Dethoup, T., Manoch, L., Kijjoa, A., Pinto, M., Gales, L., Damas, A. M., Silva, A. M., Eaton, G., and Herz, W. **(2007)**. Merodrimanes and other constituents from *Talaromyces thailandiasis*. *Journal of Natural Products* **70**, 1200-1202.

Dewapriya, P., Prasad, P., Damodar, R., Salim, A. A., and Capon, R. J. **(2017)**. Talarolide A, a Cyclic Heptapeptide Hydroxamate from an Australian Marine Tunicate-Associated Fungus, *Talaromyces sp*. (CMB-TU011). *Organic Letters* **19**, 2046-2049.

Dias, D. A., Urban, S., and Roessner, U. **(2012)**. A historical overview of natural products in drug discovery. *Metabolites* **2**, 303-336.

Dickson, M., and Gagnon, J. P. **(2004)**. Key factors in the rising cost of new drug discovery and development. *Nature Reviews Drug Discovery* **3**, 417-429.

Ding, H.-E., Yang, Z.-D., Sheng, L., Zhou, S.-Y., Li, S., Yao, X.-J., Zhi, K.-K., Wang, Y.-G., and Zhang, F. **(2015)**. Secovironolide, a novel furanosteroid scaffold with a five-membered B ring from the endophytic fungus *Talaromyces wortmannii* LGT-4. *Tetrahedron Letters* **56**, 6754-6757.

Domsch, K. H., Gams, W., and Anderson, T.-H. **(1980)**. Compendium of soil fungi. Volume 1, Academic Press (London) Ltd.

Dong, Y., Lin, J., Lu, X., Zheng, Z., Ren, X., Zhang, H., He, J., and Yang, J. **(2009)**. Cathepsin B Inhibitory Tetraene Lactones from the Fungus *Talaromyces wortmannii*. *Helvetica Chimica Acta* **92**, 567-574.

Dong, Y., Yang, J., Zhang, H., Lin, J., Ren, X., Liu, M., Lu, X., and He, J. **(2006)**. Wortmannilactones A− D, 22-Membered Triene Macrolides from *Talaromyces wortmannii*. *Journal of Natural Products* **69**, 128-130.

Dossena, A., Marchelli, R., and Pochini, A. **(1974)**. New metabolites of *Aspergillus amstelodami* related to the biogenesis of neoechinulin. *Journal of the Chemical Society, Chemical Communications*, 771-772.

Dossena, A., Marchelli, R., and Pochini, A. **(1975)**. Neoechinulin D, a new isoprenylated dehydrotryptophyl metabolite from *Aspergillus amstelodami*. *Experientia* **31**, 1249-1249.

Du, F.-Y., Li, X., Li, X.-M., Zhu, L.-W., and Wang, B.-G. **(2017)**. Indolediketopiperazine alkaloids from *Eurotium cristatum* EN-220, an endophytic fungus Isolated from the marine alga *sargassum thunbergii*. *Marine Drugs* **15**, 24.

Du, F.-Y., Li, X.-M., Li, C.-S., Shang, Z., and Wang, B.-G. **(2012)**. Cristatumins A–D, new indole alkaloids from the marine-derived endophytic fungus *Eurotium cristatum* EN-220. *Bioorganic and Medicinal Chemistry Letters* **22**, 4650-4653.

Du, F.-Y., Li, X.-M., Song, J.-Y., Li, C.-S., and Wang, B.-G. **(2014)**. Anthraquinone derivatives and an orsellinic acid ester from the marine alga-derived endophytic fungus *Eurotium cristatum* EN-220. *Helvetica Chimica Acta* **97**, 973-978.

Du, L., Zhu, T., Liu, H., Fang, Y., Zhu, W., and Gu, Q. **(2008)**. Cytotoxic polyketides from a marine-derived fungus *Aspergillus glaucus*. *Journal of Natural Products* **71**, 1837-1842.

Dumontet, C., and Jordan, M. A. **(2010)**. Microtubule-binding agents: a dynamic field of cancer therapeutics. *Nature Reviews Drug discovery* **9**, 790-803.

Eamvijarn, A., Gomes, N. M., Dethoup, T., Buaruang, J., Manoch, L., Silva, A., Pedro, M., Marini, I., Roussis, V., and Kijjoa, A. **(2013)**. Bioactive meroditerpenes and indole alkaloids from the soil fungus *Neosartorya fischeri* (KUFC 6344), and the marine-derived fungi *Neosartorya laciniosa* (KUFC 7896) and *Neosartorya tsunodae* (KUFC 9213). *Tetrahedron* **69**, 8583-8591.

Eamvijarn, A., Kijjoa, A., Bruyère, C., Mathieu, V., Manoch, L., Lefranc, F., Silva, A., Kiss, R., and Herz, W. **(2012)**. Secondary metabolites from a culture of the fungus *Neosartorya pseudofischeri* and their in vitro cytostatic activity in human cancer cells. *Planta Medica* **78**, 1767-1776.

El-Beih, A. A., Kawabata, T., Koimaru, K., Ohta, T., and Tsukamoto, S. **(2007)**. Monodictyquinone A: A new antimicrobial anthraquinone from a sea urchin-derived fungus *Monodictys sp*. *Chemical and Pharmaceutical Bulletin* **55**, 1097-1098.

Fang, W., Lin, X., Zhou, X., Wan, J., Lu, X., Yang, B., Ai, W., Lin, J., Zhang, T., and Tu, Z. **(2014)**. Cytotoxic and antiviral nitrobenzoyl sesquiterpenoids from the marine-derived fungus *Aspergillus ochraceus* Jcma1F17. *Medicinal Chemistry Communications* **5**, 701-705.

Farnsworth, N. R., Akerele, O., Bingel, A. S., Soejarto, D. D., and Guo, Z. **(1985)**. Medicinal plants in therapy. *Bulletin of the World Health Organization* **63**, 965-981.

Faulkner, D. J. **(2000a)**. Highlights of marine natural products chemistry (1972–1999). *Natural Product Reports* **17**, 1-6.

Faulkner, D. J. **(2000b)**. Marine pharmacology. *Antonie van Leeuwenhoek* **77**, 135-145.

Feher, M., and Schmidt, J. M. **(2003)**. Property distributions: differences between drugs, natural products, and molecules from combinatorial chemistry. *Journal of Chemical Information and Computer Sciences* **43**, 218-227.

Firn, R. D., and Jones, C. G. **(2000)**. The evolution of secondary metabolism–a unifying model. *Molecular Microbiology* **37**, 989-994.

Firsova, D., Mahajan, N., Solanki, H., Morrow, C., and Thomas, O. P. **(2017)**. Current Status and Perspectives in Marine Biodiscovery. In *Bioprospecting*. Springer **16**, 29-50.

Flewelling, A. J., Currie, J., Gray, C. A., and Johnson, J. A. **(2015)**. Endophytes from marine macroalgae: promising sources of novel natural products. *Current Science (00113891)* **109**, 88-111.

Frisvad, J. C., Rank, C., Nielsen, K. F., and Larsen, T. O. **(2009)**. Metabolomics of *Aspergillus fumigatus*. *Medical Mycology* **47**, S53-S71.

Frisvad, J. C., Yilmaz, N., Thrane, U., Rasmussen, K. B., Houbraken, J., and Samson, R. A. **(2013)**. *Talaromyces atroroseus*, a new species efficiently producing industrially relevant red pigments. *PloS one* **8**, e84102.

Fu, C. G., Yang, D. Z., Zhou, Y. S., Yu, T. H., Zhang, F., and Yao, J. X. **(2016a)**. Two new compounds, deacetylisowortmins A and B, isolated from an endophytic fungus, *Talaromyces wortmannii* LGT-4. *Natural Product Research* **30**, 1623-1627.

Fu, G.-C., Yang, Z.-D., Zhou, S.-Y., Li, X.-M., Yu, H.-T., Yao, X.-J., Fang, J.-G., Shu, Z.-M., Xue, H.-Y., and Wang, Y.-G. **(2016b)**. Wortmannines A–C, three novel wortmannin derivatives with an unusual five-membered B ring from the endophytic fungus *Talaromyces wortmannii* LGT-4. *Tetrahedron Letters* **57**, 4608-4611.

Fujimoto, H., Negishi, E., Yamaguchi, K., Nishi, N., and Yamazaki, M. **(1996)**. Isolation of New Tremorgenic Metabolites from an Ascomycete, *Corynascus setosus*. *Chemical and Pharmaceutical Bullentin* **44**, 1843-1848.

Gamal-Eldeen, A. M., Abdel-Lateff, A., and Okino, T. **(2009)**. Modulation of carcinogen metabolizing enzymes by chromanone A; a new chromone derivative from algicolous marine fungus *Penicillium sp*. *Environmental Toxicology and Pharmacology* **28**, 317-322.

Gao, J., León, F., Radwan, M. M., Dale, O. R., Husni, A. S., Manly, S. P., Lupien, S., Wang, X., Hill, R. A., Dugan, F. M., Cutler, H. G., and Cutler, S. J. **(2011)**. Benzyl derivatives with in vitro binding affinity for human opioid and cannabinoid receptors from the fungus *Eurotium repens*. *Journal of Natural Products* **74**, 1636-1639.

Gao, J., Radwan, M. M., León, F., Wang, X., Jacob, M. R., Tekwani, B. L., Khan, S. I., Lupien, S., Hill, R. A., Dugan, F. M., Cutler, H. G., and Cutler, S. J. **(2012)**. Antimicrobial and antiprotozoal activities of secondary metabolites from the fungus *Eurotium repens*. *Medicinal Chemistry Research* **21**, 3080-3086.

Gardes, M., and Bruns, T. D. **(1993)**. ITS primers with enhanced specificity for basidiomycetes-application to the identification of mycorrhizae and rusts. *Molecular Ecology* **2**, 113-118.

Gerwick, W. H., and Fenner, A. M. **(2013)**. Drug discovery from marine microbes. *Microbial Ecology* **65**, 800-806.

Goel, R., Das, G. G., Ram, S., and Pandey, V. **(1991)**. Antiulcerogenic and anti-inflammatory effects of emodin, isolated from Rhamnus triquerta wall. *Indian Journal of Experimental Biology* **29**, 230-232.

Gomes, N. G. M. **(2014)**. Isolation, characterization and biological activity evaluation of bioactive compounds from marine sponge-associated Fungi.

Gomes, N. M., Bessa, L. J., Buttachon, S., Costa, P. M., Buaruang, J., Dethoup, T., Silva, A., and Kijjoa, A. **(2014)**. Antibacterial and antibiofilm activities of tryptoquivalines and meroditerpenes isolated from the marine-derived fungi *Neosartorya paulistensis*, *N. laciniosa*, *N. tsunodae*, and the soil fungi *N. fischeri* and *N. siamensis*. *Marine Drugs* **12**, 822-839.

Gomes, N. M., Dethoup, T., Singburaudom, N., Gales, L., Silva, A. M. S., and Kijjoa, A. **(2012)**. Eurocristatine, a new diketopiperazine dimer from the marine sponge-associated fungus *Eurotium cristatum*. *Phytochemistry Letters* **5**, 717-720.

Gould, B. S., and Raistrick, H. **(1934)**. Studies in the biochemistry of micro-organisms: The crystalline pigments of species in the *Aspergillus glaucus* series. *Biochemical Journal* **28**, 1640-1656.

Grabley, S., and Sattler, I. **(2003)**. Natural products for lead identification: nature is a valuable resource for providing tools. *In Modern methods of drug discovery*, Birkhäuser Basel **93**, 87-107.

Haefner, B. **(2003)**. Drugs from the deep: marine natural products as drug candidates. *Drug Discovery Today* **8**, 536-544.

Haibin, Y., Fang, L., and Naiyun, J. **(2016)**. Alkaloids from an algicolous strain of *Talaromyces sp.* Chinese Journal of Oceanology and Limnology* **34**, 367-371.

Halgren, T. A. **(1996)**. Merck molecular force field. I. Basis, form, scope, parameterization, and performance of MMFF94. *Journal of Computational Chemistry* **17**, 490-519.

Hamasaki, T., Nagayama, K., and Hatsuda, Y. **(1976)**. Structure of a new metabolite from *Aspergillus chevalieri*. *Agricultural and Biological Chemistry* **40**, 203-205.

Hammerschmidt, L., Wray, V., Lin, W., Kamilova, E., Proksch, P., and Aly, A. H. **(2012)**. New styrylpyrones from the fungal endophyte *Penicillium glabrum* isolated from *Punica granatum*. *Phytochemistry Letters* **5**, 600-603.

Harvey, A. L. **(1993)**. Drugs from natural products: pharmaceuticals and agrochemicals, E. Horwood.

Hawas, U. W., El-Beih, A. A., and El-Halawany, A. M. **(2012)**. Bioactive anthraquinones from endophytic fungus *Aspergillus versicolor* isolated from red sea algae. *Archives of Pharmacal Research* **35**, 1749-1756.

Hayashi, H., Oka, Y., Kai, K., and Akiyama, K. **(2012a)**. New Chrodrimanin Congeners, Chrodrimanins D-H, from YO-2 of *Talaromyces sp*. *Bioscience, Biotechnology, and Biochemistry* **76**, 1765-1768.

Hayashi, H., Oka, Y., Kai, K., and Akiyama, K. **(2012b)**. A New Meroterpenoid, Chrodrimanin C, from YO-2 of *Talaromyces sp*. *Bioscience, Biotechnology, and Biochemistry* **76**, 745-748.

He, J.-W., Liang, H.-X., Gao, H., Kuang, R.-Q., Chen, G.-D., Hu, D., Wang, C.-X., Liu, X.-Z., Li, Y., and Yao, X.-S. **(2014a)**. Talaflavuterpenoid A, a new nardosinane-type sesquiterpene from *Talaromyces flavus*. *Journal of Asian Natural Products Research* **16**, 1029-1034.

He, J.-W., Mu, Z.-Q., Gao, H., Chen, G.-D., Zhao, Q., Hu, D., Sun, J.-Z., Li, X.-X., Li, Y., Liu, X.-Z., and Yao, X.-S. **(2014b)**. New polyesters from *Talaromyces flavus*. *Tetrahedron* **70**, 4425-4430.

He, J.-W., Qin, D.-P., Gao, H., Kuang, R.-Q., Yu, Y., Liu, X.-Z., and Yao, X.-S. **(2014c)**. Two New Coumarins from *Talaromyces flavus*. *Molecules* **19**, 20880-20887.

Hill, R. A. **(2013)**. Marine natural products. *Annual Reports Section B (Organic Chemistry)* **109**, 146-166.

Hong, W.-H., Chang, T., and Daly, R. E. **(1986)**. Vidarabine. *Analytical Profiles of Drug Substances* **15**, 647-672.

Horie, Y., Abliz, P., Fukushima, K., Okada, K., and Gusmão, N. B. **(2001)**. *Neosartorya takakii*, a new species from soil in Brazil. *Mycoscience* **42**, 91-95.

Hu, G.-P., Yuan, J., Sun, L., She, Z.-G., Wu, J.-H., Lan, X.-J., Zhu, X., Lin, Y.-C., and Chen, S.-P. **(2011)**. Statistical research on marine natural products based on data obtained between 1985 and 2008. *Marine Drugs* **9**, 514-525.

Hu, Y., Chen, J., Hu, G., Yu, J., Zhu, X., Lin, Y., Chen, S., and Yuan, J. **(2015)**. Statistical research on the bioactivity of new marine natural products discovered during the 28 years from 1985 to 2012. *Marine Drugs* **13**, 202-221.

Hussain, H., Kock, I., Al-Harrasi, A., Al-Rawahi, A., Abbas, G., Green, I. R., Shah, A., Badshah, A., Saleem, M., and Draeger, S. **(2014)**. Antimicrobial chemical constituents from endophytic fungus *Phoma sp*. *Asian Pacific Journal of Tropical Medicine* **7**, 699-702.

Huyck, T. K., Gradishar, W., Manuguid, F., and Kirkpatrick, P. **(2011)**. Eribulin mesylate. *Nature Reviews Drug Discovery* **10**, 173-174.

Hyde, K. **(1988)**. Studies on the tropical marine fungi of Brunei. *Botanical Journal of the Linnean Society* **98**, 135-151.

Ishikawa, Y., Morimoto, K., and Hamasaki, T. **(1984)**. Flavoglaucin, a metabolite of *Eurotium chevalieri*, its antioxidation and synergism with tocopherol. *Journal of the American Oil Chemists' Society* **61**, 1864-1868.

Jabs, A., Weiss, M. S., and Hilgenfeld, R. **(1999)**. Non-proline cis peptide bonds in proteins. *Journal of Molecular Biology* **286**, 291-304.

Jayasuriya, H., Koonchanok, N. M., Geahlen, R. L., McLaughlin, J. L., and Chang, C.-J. **(1992)**. Emodin, a protein tyrosine kinase inhibitor from *Polygonum cuspidatum*. *Journal of Natural Products* **55**, 696-698.

Jayasuriya, H., Zink, D., Basilio, A., Vicente, F., Collado, J., Bills, G., Goldman, M. L., Motyl, M., Huber, J., and Dezeny, G. **(2009)**. Discovery and antibacterial activity of glabramycin A–C from *Neosartorya glabra* by an antisense strategy. *The Journal of Antibiotics* **62**, 265-269.

Jensen, P. R., and Fenical, W. **(2000)**. Marine microorganisms and drug discovery: current status and future potential. *In Drugs from the Sea*. Karger Publishers, 6-29.

Jin, L., Quan, C., Hou, X., and Fan, S. **(2016)**. Potential pharmacological resources: natural bioactive compounds from marine-derived fungi. *Marine Drugs* **14**, 76.

Jones, E. B. G. and K. D. Hyde **(1988).** Methods for the study of mangrove marine fungi. *Mangrove microbiology; role of microorganisms in nutrient cycling of mangrove soils and water*, 9-27.

Jones, E. G., and Pang, K.-L. **(2012)**. Marine Fungi: and Fungal-like Organisms, Walter de Gruyter.

Kaifuchi, S., Mori, M., Nonaka, K., Masuma, R., mura, S., and Shiomi, K. **(2015a)**. Ukulactone C, a new NADH-fumarate reductase inhibitor produced by *Talaromyces sp*. FKI-6713. *The Journal of General and Applied Microbiology* **61**, 57-62.

Kaifuchi, S., Mori, M., Nonaka, K., Masuma, R., Omura, S., and Shiomi, K. **(2015b)**. Sartorypyrone D: a new NADH-fumarate reductase inhibitor produced by *Neosartorya fischeri* FO-5897. *Journal of Antibiotics* **68**, 403-405.

Kalansuriya, P., Quezada, M., Espósito, B. P., and Capon, R. J. **(2017)**. Talarazines A–E: Noncytotoxic Iron(III) Chelators from an Australian Mud Dauber Wasp-Associated Fungus, *Talaromyces sp*. (CMB-W045). *Journal of Natural Products* **80**, 609-615.

Kamauchi, H., Kinoshita, K., Sugita, T., and Koyama, K. **(2016)**. Conditional changes enhanced production of bioactive metabolites of marine derived fungus *Eurotium rubrum*. *Bioorganic and Medicinal Chemistry Letters* **26**, 4911-4914.

Kanoh, K., Kohno, S., Asari, T., Harada, T., Katada, J., Muramatsu, M., Kawashima, H., Sekiya, H., and Uno, I. **(1997)**. (−)-Phenylahistin: A new mammalian cell cycle inhibitor produced by *Aspergillus ustus*. *Bioorganic and Medicinal Chemistry Letters* **7**, 2847-2852.

Kanokmedhakul, K., Kanokmedhakul, S., Suwannatrai, R., Soytong, K., Prabpai, S., and Kongsaeree, P. **(2011)**. Bioactive meroterpenoids and alkaloids from the fungus *Eurotium chevalieri*. *Tetrahedron* **67**, 5461-5468.

Kanokmedhakul, S., Kanokmedhakul, K., Phonkerd, N., Soytong, K., Kongsaeree, P., and Suksamrarn, A. **(2002)**. Antimycobacterial anthraquinone-chromanone compound and diketopiperazine alkaloid from the fungus *Chaetomium globosum* KMITL-N0802. *Planta Medica* **68**, 834-836.

Kelecom, A. **(2002)**. Secondary metabolites from marine microorganisms. *Anais da Academia Brasileira de Ciências* **74**, 151-170.

Kijjoa, A., and Sawangwong, P. **(2004)**. Drugs and cosmetics from the sea. *Marine Drugs* **2**, 73-82.

Kijjoa, A., Santos, S., Dethoup, T., Manoch, L., Almeida, A. P., Vasconcelos, M. H., Silva, A., Gales, L., and Herz, W. **(2011)**. Sartoryglabrins, analogs of ardeemins, from *Neosartorya glabra*. *Natural Product Communications* **6**, 807-812.

Kim, D.-H., Jung, S. J., Chung, I.-S., Lee, Y.-H., Kim, D.-K., Kim, S.-H., Kwon, B.-M., Jeong, T.-S., Park, M.-H., Seoung, N.-S., and Baek, N.-l. **(2005)**. Ergosterol Peroxide from Flowers of *Erigeron annuus* L. as an Anti-Atherosclerosis Agent. *Archives of Pharmacal Research* **28**, 541-545.

Kimura, T., Nishida, M., Kuramochi, K., Sugawara, F., Yoshida, H., and Mizushina, Y. **(2008)**. Novel azaphilones, kasanosins A and B, which are specific inhibitors of eukaryotic DNA polymerases β and λ from *Talaromyces sp*. *Bioorganic and Medicinal Chemistry* **16**, 4594-4599.

Kimura, Y., Hamasaki, T., Isogai, A., and Nakajima, H. **(1982a)**. Structure of aszonapyrone A, a new metabolite produced by *Aspergillus zonatus*. *Agricultural and Biological Chemistry* **46**, 1963-1965.

Kimura, Y., Hamasaki, T., Nakajima, H., and Isogai, A. **(1982b)**. Structure of aszonalenin, a new metabolite of *Aspergillus zonatus*. *Tetrahedron Letters* **23**, 225-228.

Kobayashi, J., and Tsuda, M. **(2004)**. Bioactive products from Okinawan marine micro-and macroorganisms. *Phytochemistry Reviews* **3**, 267-274.

Kobayashi, M., Uehara, H., Matsunami, K., Aoki, S., and Kitagawa, I. **(1993)**. Trichoharzin, a new polyketide produced by the imperfect fungus *Trichoderma harzianum* separated from the marine sponge *Micale cecilia*. *Tetrahedron Letters* **34**, 7925-7928.

Kobel, H., and Traber, R. **(1982)**. Directed biosynthesis of cyclosporins. *European Journal of Applied Microbiology and Biotechnology* **14**, 237-240.

Kohlmeyer, J. **(1984)**. Tropical marine fungi. *Marine Ecology* **5**, 329-378.

Kohlmeyer, J., and Kohlmeyer, E. **(1979)**. Marine mycology : the higher fungi Academic Press New York, USA.

Komai, S.-i., Hosoe, T., Itabashi, T., Nozawa, K., Okada, K., de Campos Takaki, G. M., Chikamori, M., Yaguchi, T., Fukushima, K., Miyaji, M., and Kawai, K.-i. **(2004)**. A new funicone derivative isolated from *Talaromyces flavus* IFM52668. *Journal of the Japanese Association of Mycotoxicology*. **54**, 15-19.

Koolen, H. H. F., Menezes, L. S., Souza, M. P., Silva, F. M. A., Almeida, F. G. O., Souza, A. Q. L. d., Nepel, A., Barison, A., Silva, F. H. d., Evangelista, D. E., and Souza, A. D. L. d. **(2013)**. Talaroxanthone, a novel xanthone dimer from the endophytic fungus *Talaromyces sp*. associated with *Duguetia stelechantha* (Diels) R. E. Fries. *Journal of the Brazilian Chemical Society* **24**, 880-883.

Kornsakulkarn, J., Thongpanchang, C., Lapanun, S., and Srichomthong, K. **(2009)**. Isocoumarin glucosides from the scale insect fungus *Torrubiella tenuis* BCC 12732. *Journal of Natural Products* **72**, 1341-1343.

Kozlovsky, A. G., Vinokurova, N. G., Adanin, V. M., Burkhardt, G., Dahse, H.-M., and Gräfe, U. **(2000)**. New diketopiperazine alkaloids from *Penicillium fellutanum*. *Journal of Natural Products* **63**, 698-700.

Kremsner, P. G., Winkler, S., Brandts, C., Neifer, S., Bienzel, U., and Graninger, W. **(1994)**. Clindamycin in combination with chloroquine or quinine is an effective therapy for uncomplicated Plasmodium falciparum malaria in children from Gabon. *Journal of Infectious Diseases* **169**, 467-470.

Kumar, M., Qadri, M., Sharma, P. R., Kumar, A., Andotra, S. S., Kaur, T., Kapoor, K., Gupta, V. K., Kant, R., Hamid, A., Johri, S., Taneja, S. C., Vishwakarma, R. A., Riyaz-Ul-Hassan, S., and Shah, B. A. **(2013)**. Tubulin inhibitors from an endophytic fungus isolated from *Cedrus deodara*. *Journal of Natural Products* **76**, 194-199.

Kuml, D., Dethoup, T., Buttachon, S., Singburaudom, N., Silva, A. M. S., and Kijjoa, A. **(2014)**. Spiculisporic acid E, a new spiculisporic acid derivative and ergosterol derivatives from the marine-sponge associated fungus *Talaromyces trachyspermus* (KUFA 0021). *Natural Product Communications* **9**, 1147-1150.

Kusari, S., Zühlke, S., and Spiteller, M. **(2009)**. An endophytic fungus from *Camptotheca acuminata* that produces camptothecin and analogues. *Journal of Natural Products* **72**, 2-7.

Lan, W.-J., Fu, S.-J., Xu, M.-Y., Liang, W.-L., Lam, C.-K., Zhong, G.-H., Xu, J., Yang, D.-P., and Li, H.-J. **(2016)**. Five new cytotoxic metabolites from the marine fungus *Neosartorya pseudofischeri*. *Marine Drugs* **14**, 18.

Lebar, M. D., Heimbegner, J. L., and Baker, B. J. **(2007)**. Cold-water marine natural products. *Natural Product Reports* **24**, 774-797.

Lee, W.-Y., Park, Y.-K., Ahn, J.-K., Park, S.-Y., and Lee, H.-J. **(2005)**. Cytotoxic activity of ergosta-4, 6, 8 (14), 22-tetraen-3-one from the sclerotia of *Polyporus umbellatus*. *Bulletin of the Korean Chemical Society* **26**, 1464-1466.

Lee, Y. M., Kim, M. J., Li, H., Zhang, P., Bao, B., Lee, K. J., and Jung, J. H. **(2013).** Marine-derived *Aspergillus* species as a source of bioactive secondary metabolites. *Marine Biotechnology* **15**, 499-519.

Li, D. L., Li, X. M., Li, T. G., Dang, H. Y., and Wang, B. G. **(2008c)**. Dioxopiperazine alkaloids produced by the marine mangrove derived endophytic fungus *Eurotium rubrum*. *Helvetica Chimica Acta* **91**, 1888-1893.

Li, D.-L., Li, X.-M., and Wang, B.-G. **(2009)**. Natural anthraquinone derivatives from a marine mangrove plant-derived endophytic fungus *Eurotium rubrum*: structural elucidation and DPPH radical scavenging activity. *Journal of Microbiology and Biotechnology* **19**, 675-680.

Li, D.-L., Li, X.-M., Li, T.-G., Dang, H.-Y., and Wang, B.-G. **(2008b)**. Dioxopiperazine alkaloids produced by the marine mangrove derived endophytic fungus *Eurotium rubrum*. *Helvetica Chimica Acta* **91**, 1888-1893.

Li, D.-L., Li, X.-M., Li, T.-G., Dang, H.-Y., Proksch, P., and Wang, B.-G. **(2008a)**. Benzaldehyde derivatives from *Eurotium rubrum*, an endophytic fungus derived from the mangrove plant *Hibiscus tiliaceus*. *Chemical and Pharmaceutical Bulletin* **56**, 1282-1285.

Li, D.-L., Li, X.-M., Proksch, P., and Wang, B.-G. **(2010a)**. 7-O-Methylvariecolortide A, a new spirocyclic diketopiperazine alkaloid from a marine mangrove derived endophytic fungus, *Eurotium rubrum*. *Natural Product Communications* **5**, 1583-1586.

Li, F., Li, K., Li, X., and Wang, B. **(2011a)**. Chemical constituents of marine algal-derived endophytic fungus *Exophiala oligosperma* EN-21. *Chinese Journal of Oceanology and Limnology* **29**, 63-67.

Li, H., Huang, H., Shao, C., Huang, H., Jiang, J., Zhu, X., Liu, Y., Liu, L., Lu, Y., Li, M., Lin, Y., and She, Z. **(2011b)**. Cytotoxic norsesquiterpene peroxides from the endophytic fungus *Talaromyces flavus* Isolated from the mangrove plant *Sonneratia apetala*. *Journal of Natural Products* **74**, 1230-1235.

Li, J. W.-H., and Vederas, J. C. **(2009)**. Drug discovery and natural products: end of an era or an endless frontier? *Science* **325**, 161-165.

Li, J. Y., Sidhu, R. S., Ford, E., Long, D., Hess, W., and Strobel, G. **(1998)**. The induction of taxol production in the endophytic fungus-*Periconia sp* from Torreya grandifolia. *Journal of Industrial Microbiology and Biotechnology* **20**, 259-264.

Li, L.-Q., Yang, Y.-G., Zeng, Y., Zou, C., and Zhao, P.-J. **(2010b)**. A new azaphilone, kasanosin C, from an endophytic *Talaromyces sp*. T1BF. *Molecules* **15**, 3993-3997.

Li, X. D., Miao, F. P., Liang, X. R., and Ji, N. Y. **(2014)**. Meroterpenes from an algicolous strain of *Penicillium echinulatum*. *Magnetic Resonance in Chemistry* **52**, 247-250.

Li, X.-J., Zhang, Q., Zhang, A.-L., and Gao, J.-M. **(2012)**. Metabolites from *Aspergillus fumigatus*, an endophytic fungus associated with *Melia azedarach*, and their antifungal, antifeedant, and toxic activities. *Journal of Agricultural and Food Chemistry* **60**, 3424-3431.

Li, Y., Sun, K.-L., Wang, Y., Fu, P., Liu, P.-P., Wang, C., and Zhu, W.-M. **(2013)**. A cytotoxic pyrrolidinoindoline diketopiperazine dimer from the algal fungus *Eurotium herbariorum* HT-2. *Chinese Chemical Letters* **24**, 1049-1052.

Li, Y.-F., Wu, X.-B., Niaz, S.-I., Zhang, L.-H., Huang, Z.-J., Lin, Y.-C., Li, J., and Liu, L. **(2017)**. Effect of culture conditions on metabolites produced by the crinoid-derived fungus *Aspergillus ruber* 1017. *Natural Product Research* **31**, 1299-1304.

Liang, W.-L., Le, X., Li, H.-J., Yang, X.-L., Chen, J.-X., Xu, J., Liu, H.-L., Wang, L.-Y., Wang, K.-T., and Hu, K.-C. **(2014)**. Exploring the chemodiversity and biological activities of the secondary metabolites from the marine fungus *Neosartorya pseudofischeri*. *Marine Drugs* **12**, 5657-5676.

Lim, G., and Tan, T. **(1986)**. Mycological research in Singapore. *Proceedings: Plant Sciences* **96**, 335-341.

Liu, F., Cai, X.-L., Yang, H., Xia, X.-K., Guo, Z.-Y., Yuan, J., Li, M.-F., She, Z.-G., and Lin, Y.-C. **(2010)**. The bioactive metabolites of the mangrove endophytic fungus *Talaromyces sp*. ZH-154 isolated from Kandelia candel (L.) Druce. *Planta Medica* **76**, 185-189.

Liu, F., Li, Q., Yang, H., Cai, X. L., Xia, X. K., Chen, S. P., Li, M. F., She, Z. G., and Lin, Y. C. **(2009)**. Structure elucidation of three diphenyl ether derivatives from the mangrove endophytic fungus SBE-14 from the South China Sea. *Magnetic Resonance in Chemistry* **47**, 453-455.

Liu, J.-X., Zhang, J.-H., Li, H.-H., Lai, F.-J., Chen, K.-J., Chen, H., Luo, J., Guo, H.-C., Wang, Z.-H., and Lin, S.-Z. **(2012)**. Emodin induces Panc-1 cell apoptosis via declining the mitochondrial membrane potential. *Oncology reports* **28**, 1991-1996.

Liu, R., Zhu, W., Zhang, Y., Zhu, T., Liu, H., Fang, Y., and Gu, Q. **(2006)**. A new diphenyl ether from marine-derived fungus *Aspergillus sp*. BF-2. *Journal of Antibiotics* **59**, 362-365.

Liu, W.-C., Wang, Y.-Y., Liu, J.-H., Ke, A.-B., Zheng, Z.-H., Lu, X.-H., Luan, Y.-S., Xiu, Z.-L., and Dong, Y.-S. **(2016a)**. Wortmannilactones I–L, new NADH-fumarate reductase inhibitors, induced by adding suberoylanilide hydroxamic acid to the culture medium of *Talaromyces wortmannii*. *Bioorganic and Medicinal Chemistry Letters* **26**, 5328-5333.

Liu, W.-C., Yang, F., Zhang, R., Shi, X., Lu, X.-H., Luan, Y.-S., Xiu, Z.-L., and Dong, Y.-S. **(2016b)**. Production of polyketides with anthelmintic activity by the fungus *Talaromyces wortmannii* using one strain-many compounds (OSMAC) method. *Phytochemistry Letters* **18**, 157-161.

Liu, W.-H., Zhao, H., Li, R.-Q., Zheng, H.-B., and Yu, Q. **(2015)**. Polyketides and Meroterpenoids from *Neosartorya glabra*. *Helvetica Chimica Acta* **98**, 515-519.

Liu, X.-H., Miao, F.-P., Liang, X.-R., and Ji, N.-Y. **(2014a)**. Ergosteroid derivatives from an algicolous strain of *Aspergillus ustus*. *Natural Product Research* **28**, 1182-1186.

Liu, Z., Xia, G., Chen, S., Liu, Y., Li, H., and She, Z. **(2014b)**. Eurothiocin A and B, sulfur-containing benzofurans from a soft coral-derived fungus *Eurotium rubrum* SH-823. *Marine Drugs* **12**, 3669-3680.

Lynn, D. G., Phillips, N. J., Hutton, W. C., Shabanowitz, J., Fennell, D., and Cole, R. **(1982)**. Talaromycins: application of homonuclear spin correlation maps to structure assignment. *Journal of the American Chemical Society* **104**, 7319-7322.

Mahmoodian, A., and Stickings, C. **(1964)**. Studies in the biochemistry of micro-organisms. 115. Metabolites of *Penicillium frequentans* Westling: isolation of sulochrin, asterric acid,(+)-bisdechlorogeodin and two new substituted anthraquinones, questin and questinol. *Biochemical Journal* **92**, 369-378.

Manojlovic, N., Solujic, S., Sukdolak, S., and Krstic, L. **(2000)**. Isolation and antimicrobial activity of anthraquinones from some species of the lichen genus *Xanthoria*. *Journal-Serbian Chemical Society* **65**, 555-560.

Marchelli, R., Dossena, A., Pochini, A., and Dradi, E. **(1977)**. The structures of five new didehydropeptides related to neoechinulin, isolated from *Aspergillus amstelodami*. *Journal of the Chemical Society, Perkin Transactions 1*, 713-717.

Marine pharmacology. Available online: http://marinepharmacology.midwestern.edu/clinPipeline.htm (accessed on 21 June 2017).

Masi, M., Andolfi, A., Mathieu, V., Boari, A., Cimmino, A., Banuls, L. M. Y., Vurro, M., Kornienko, A., Kiss, R., and Evidente, A. **(2013)**. Fischerindoline, a pyrroloindole sesquiterpenoid isolated from *Neosartorya pseudofischeri*, with in vitro growth inhibitory activity in human cancer cell lines. *Tetrahedron* **69**, 7466-7470.

Matsunaga, H., Kamisuki, S., Kaneko, M., Yamaguchi, Y., Takeuchi, T., Watashi, K., and Sugawara, F. **(2015)**. Isolation and structure of vanitaracin A, a novel anti-hepatitis B virus compound from *Talaromyces sp*. *Bioorganic and Medicinal Chemistry Letters* **25**, 4325-4328.

Matsuzawa, T., Horie, Y., Abliz, P., Gonoi, T., and Yaguchi, T. **(2014)**. *Aspergillus huiyaniae* sp. nov., a teleomorphic species in sect. *Fumigati* isolated from desert soil in China. *Mycoscience* **55**, 213-220.

Mayer, A. M., Glaser, K. B., Cuevas, C., Jacobs, R. S., Kem, W., Little, R. D., McIntosh, J. M., Newman, D. J., Potts, B. C., and Shuster, D. E. **(2010)**. The odyssey of marine pharmaceuticals: a current pipeline perspective. *Trends in Pharmacological Sciences* **31**, 255-265.

Mayer, A. M., Rodríguez, A. D., Berlinck, R. G., and Fusetani, N. **(2011)**. Marine pharmacology in 2007–8: Marine compounds with antibacterial, anticoagulant, antifungal, anti-inflammatory, antimalarial, antiprotozoal, antituberculosis, and antiviral activities; affecting the immune and nervous system, and other miscellaneous mechanisms of action. *Comparative Biochemistry and Physiology Part C: Toxicology and Pharmacology* **153**, 191-222.

McChesney, J. D., Venkataraman, S. K., and Henri, J. T. **(2007)**. Plant natural products: back to the future or into extinction? *Phytochemistry* **68**, 2015-2022.

Mehbub, M. F., Lei, J., Franco, C., and Zhang, W. **(2014)**. Marine sponge derived natural products between 2001 and 2010: Trends and opportunities for discovery of bioactives. *Marine Drugs* **12**, 4539-4577.

Meng, L.-H., Du, F.-Y., Li, X.-M., Pedpradab, P., Xu, G.-M., and Wang, B.-G. **(2015)**. Rubrumazines A–C, indolediketopiperazines of the isoechinulin class from *Eurotium rubrum* MA-150, a fungus obtained from marine mangrove-derived Rhizospheric Soil. *Journal of Natural Products* **78**, 909-913.

Meng, L.-H., Mándi, A., Li, X.-M., Liu, Y., Kurtán, T., and Wang, B.-G. **(2016)**. Isolation, stereochemical study, and antioxidant activity of benzofuranone derivatives from a mangrove-derived fungus *Eurotium rubrum* MA-150. *Chirality* **28**, 581-584.

Mishra, B. B., and Tiwari, V. K. **(2011)**. Natural products: an evolving role in future drug discovery. *European Journal of Medicinal Chemistry* **46**, 4769-4807.

Molinari, G. **(2009)**. Natural products in drug discovery: present status and perspectives. *Pharmaceutical Biotechnology*, 13-27.

Molinski, T. F., Dalisay, D. S., Lievens, S. L., and Saludes, J. P. **(2009)**. Drug development from marine natural products. *Nature Reviews Drug Discovery* **8**, 69-85.

Mori, T., Inoue, Y., and Grimme, S. **(2006)**. Time dependent density functional theory calculations for electronic circular dichroism spectra and optical rotations of conformationally flexible chiral donor− acceptor dyad. *The Journal of Organic Chemistry* **71**, 9797-9806.

Morino, T., Nishimoto, M., Itou, N., and Nishikiori, T. **(1994)**. NK372135s, novel antifungal agents produced by *Neosartoria fischeri*. *The Journal of Antibiotics* **47**, 1546-1548.

Morino, T., Nishimoto, M., Masuda, A., Fujita, S., NISHIKIOR, T., and Saito, S. **(1995)**. NK374200, a novel insecticidal agent from *Taralomyces*, found by physico-chemical screening. *The Journal of Antibiotics* **48**, 1509-1510.

Murti, Y., and Agrawal, T. **(2010)**. Marine derived pharmaceuticals-development of natural health products from marine biodiversity. *International Journal of ChemTech Research* **2**, 2198-2217.

Nam, K. S., Jo, Y. S., Kim, Y. H., Hyun, J. W., and Kim, H. W. **(2001)**. Cytotoxic activities of acetoxyscirpenediol and ergosterol peroxide from *Paecilomyces tenuipes*. *Life Sciences* **69**, 229-237.

Nastrucci, C., Cesario, A., and Russo, P. **(2012)**. Anticancer drug discovery from the marine environment. *Recent Patents on Anti-Cancer Drug Discovery* **7**, 218-232.

Newberger, N. C., Ranzer, L. K., Boehnlein, J. M., and Kerr, R. G. **(2006)**. Induction of terpene biosynthesis in dinoflagellate symbionts of Caribbean gorgonians. *Phytochemistry* **67**, 2133-2139.

Newman, D. J., and Cragg, G. M. **(2004)**. Marine natural products and related compounds in clinical and advanced preclinical trials. *Journal of Natural Products* **67**, 1216-1238.

Newman, D. J., and Cragg, G. M. **(2007)**. Natural products as sources of new drugs over the last 25 years⊥. *Journal of Natural Products* **70**, 461-477.

Newman, D. J., and Cragg, G. M. **(2012)**. Natural products as sources of new drugs over the 30 years from 1981 to 2010. *Journal of Natural Products* **75**, 311-335.

Newman, D. J., and Cragg, G. M. **(2016)**. Natural products as sources of new drugs from 1981 to 2014. *Journal of Natural Prod*uct **79**, 629-661.

Newman, D. J., Cragg, G. M., and Battershill, C. N. **(2009)**. Therapeutic agents from the sea: biodiversity, chemo-evolutionary insight and advances to the end of Darwin's 200th year. *Diving and Hyperbaric Medicine* **39**, 216-225.

Newman, D. J., Cragg, G. M., and Snader, K. M. **(2003)**. Natural products as sources of new drugs over the period 1981− 2002. *Journal of Natural Products* **66**, 1022-1037.

Nicholson, B., Lloyd, G. K., Miller, B. R., Palladino, M. A., Kiso, Y., Hayashi, Y., and Neuteboom, S. T. **(2006)**. NPI-2358 is a tubulin-depolymerizing agent: in-vitro evidence for activity as a tumor vascular-disrupting agent. *Anti-Cancer Drugs* **17**, 25-31.

Noinart, J., Buttachon, S., Dethoup, T., Gales, L., Pereira, J. A., Urbatzka, R., Freitas, S., Lee, M., Silva, A., and Pinto, M. M. **(2017)**. A new ergosterol analog, a new bis-anthraquinone and anti-obesity activity of anthraquinones from the marine sponge-associated fungus *Talaromyces stipitatus* KUFA 0207. *Marine Drugs* **15**, 139.

Nonaka, K., Chiba, T., Suga, T., Asami, Y., Iwatsuki, M., Masuma, R., Omura, S., and Shiomi, K. **(2015)**. Coculnol, a new penicillic acid produced by a coculture of *Fusarium solani* FKI-6853 and *Talaromyces sp*. FKA-65. *Journal of Antibiotics* **68**, 530-532.

Nong, X.-H., Wang, Y.-F., Zhang, X.-Y., Zhou, M.-P., Xu, X.-Y., and Qi, S.-H. **(2014)**. Territrem and butyrolactone derivatives from a marine-derived fungus *Aspergillus terreus*. *Marine Drugs* **12**, 6113-6124.

Overy, D. P., Bayman, P., Kerr, R. G., and Bills, G. F. **(2014)**. An assessment of natural product discovery from marine (sensu strictu) and marine-derived fungi. *Mycology* **5**, 145-167.

Ozoe, Y., Kuriyama, T., Tachibana, Y., Harimaya, K., Takahashi, N., Yaguchi, T., Suzuki, E., Imamura, K.-i., and Oyama, K. **(2004)**. Isocoumarin derivative as a novel GABA receptor ligand from *Neosartorya quadricincta*. *Journal of Pesticide Science* **29**, 328-331.

Pang, K.-L., Sharuddin, S. S., Alias, S. A., Nor, N. A., and Awaluddin, H. H. **(2010)**. Diversity and abundance of lignicolous marine fungi from the east and west coasts of Peninsular Malaysia and Sabah (Borneo Island). *Botanica Marina* **53**, 515-523.

Parshikov, I. A., Miriyala, B., Muraleedharan, K. M., Avery, M. A., and Williamson, J. S. **(2006)**. Microbial transformation of artemisinin to 5-hydroxyartemisinin by *Eurotium amstelodami* and *Aspergillus niger*. *Journal of Industrial Microbiology and Biotechnology* **33**, 349-352.

Parvatkar, R. R., D'Souza, C., Tripathi, A., and Naik, C. G. **(2009)**. Aspernolides A and B, butenolides from a marine-derived fungus *Aspergillus terreus*. *Phytochemistry* **70**, 128-132.

Perdicaris, S., Vlachogianni, T., and Valavanidis, A. **(2013)**. Bioactive natural substances from marine sponges: new developments and prospects for future pharmaceuticals. *Natural Product Chemistry and Research* **1**, 2329-6836.

Petcher, T. J., Weber, H. P., and Rüegger, A. **(1976)**. Crystal and molecular structure of an iodo-derivative of the cyclic undecapeptide cyclosporin A. *Helvetica Chimica Acta* **59**, 1480-1488.

Pettit, G. R., Fujii, Y., Hasler, J. A., and Schmidt, J. M. **(1982)**. Isolation and characterization of palystatins AD. *Journal of Natural Products* **45**, 272-276.

Pettit, G. R., Kamano, Y., Herald, C. L., Tuinman, A. A., Boettner, F. E., Kizu, H., Schmidt, J. M., Baczynskyj, L., Tomer, K. B., and Bontems, R. J. **(1987)**. The isolation and structure of a remarkable marine animal antineoplastic constituent: dolastatin 10. *Journal of the American Chemical Society* **109**, 6883-6885.

Phattanawasin, P., Pojchanakom, K., Sotanaphun, U., Piyapolrungroj, N., and Zungsontiporn, S. **(2007)**. Weed growth inhibitors from *Aspergillus fischeri* TISTR 3272. *Natural Product Research* **21**, 1286-1291.

Phillips, N., Cole, R., and Lynn, D. **(1987)**. Talaromycins C, D, E, and F. *Tetrahedron Letters* **28**, 1619-1621.

Pinheiro, Â., Dethoup, T., Bessa, J., Silva, A. M., and Kijjoa, A. **(2012)**. A new bicyclic sesquiterpene from the marine sponge associated fungus *Emericellopsis minima*. *Phytochemistry Letters* **5**, 68-70.

Pitt, J., and Hocking, A. **(1997)**. Fungi and food spoilage, vol II. *Blackie Academic and Professional, London*.

Pomponi, S. A. **(1999)**. The bioprocess-technological potential of the sea. *Journal of Biotechnology* **70**, 5-13.

Proksa, B., Uhrin, D., Liptaj, T., and Šturdíková, M. **(1998)**. Neosartorin, an ergochrome biosynthesized by *Neosartorya fischeri*. *Phytochemistry* **48**, 1161-1164.

Prompanya, C., Dethoup, T., Bessa, L. J., Pinto, M. M., Gales, L., Costa, P. M., Silva, A., and Kijjoa, A. **(2014)**. New isocoumarin derivatives and meroterpenoids from the marine sponge-associated fungus *Aspergillus similanensis* sp. nov. KUFA 0013. *Marine Drugs* **12**, 5160-5173.

Prompanya, C., Dethoup, T., Gales, L., Lee, M., Pereira, J. A., Silva, A., Pinto, M. M., and Kijjoa, A. **(2016)**. New polyketides and new benzoic acid derivatives from the marine sponge-associated fungus *Neosartorya quadricincta* KUFA 0081. *Marine Drugs* **14**, 134.

Prompanya, C., Fernandes, C., Cravo, S., Pinto, M. M., Dethoup, T., Silva, A., and Kijjoa, A. **(2015)**. A new cyclic hexapeptide and a new isocoumarin derivative from the marine sponge-associated fungus *Aspergillus similanensis* KUFA 0013. *Marine Drugs* **13**, 1432-1450.

PubChem Substance. Available online: http//pubchem.ncbi.nlm.nih.gov/substance/185030170 (accessed on 25 April 2015).

Putra, M. Y., and Murniasih, T. **(2016)**. Marine soft corals as source of lead compounds for anti-inflammatories. *Journal of Coastal Life Medicine* **4**, 73-77.

Radjasa, O. K., Vaske, Y. M., Navarro, G., Vervoort, H. C., Tenney, K., Linington, R. G., and Crews, P. **(2011)**. Highlights of marine invertebrate-derived biosynthetic products: Their biomedical potential and possible production by microbial associants. *Bioorganic and Medicinal Chemistry* **19**, 6658-6674.

Rajachan, O.-a., Kanokmedhakul, K., Sanmanoch, W., Boonlue, S., Hannongbua, S., Saparpakorn, P., and Kanokmedhakul, S. **(2016)**. Chevalone C analogues and globoscinic acid derivatives from the fungus *Neosartorya spinosa* KKU-1NK1. *Phytochemistry* **132**, 68-75.

Rateb, M. E., and Ebel, R. **(2011)**. Secondary metabolites of fungi from marine habitats. *Natural Product Reports* **28**, 290-344.

Rauck, R. L., Wallace, M. S., Burton, A. W., Kapural, L., and North, J. M. **(2009)**. Intrathecal ziconotide for neuropathic pain: a review. *Pain Practice* **9**, 327-337.

Ren, H., Tian, L., Gu, Q., and Zhu, W. **(2006)**. Secalonic acid D; A cytotoxic constituent from marine lichen-derived fungus *Gliocladium sp*. T31. *Archives of Pharmacal Research* **29**, 59-63.

Rouhi, A. **(1995)**. Supply issues complicate trek of chemicals from sea to market. *Chemical and Engineering News* **73**, 42-44.

Rowinsky, E. K., Onetto, N., Canetta, R. M., and Arbuck, S. G. **(1992)**. Taxol: the first of the taxanes, an important new class of antitumor agents. *Seminars in Oncology* **19**, 646-662.

Rüegger, A., Kuhn, M., Lichti, H., Loosli, H. R., Huguenin, R., Quiquerez, C., and von Wartburg, A. **(1976)**. Cyclosporin A, ein immunsuppressiv wirksamer Peptidmetabolit aus *Trichoderma polysporum* (Link ex Pers.) Rifai. *Helvetica Chimica Acta* **59**, 1075-1092.

Sáiz-Jiménez, C., and Haider, K. M. **(1975)**. Synthesis of aromatic compounds by *Eurotium echinulatum* Delacr. *Anales de Edafología y Agrobiología* **34**, 931-941.

Sallam, L. A., El-Refai, A.-M. H., Hamdi, A.-H. A., El-Minofi, H. A., and Abd-Elsalam, I. S. **(2005)**. Studies on the application of immobilization technique for the production of cyclosporin A by a local strain of *Aspergillus terreus*. *The Journal of General and Applied Microbiology* **51**, 143-149.

Salomon, C. E., Magarvey, N. A., and Sherman, D. H. **(2004)**. Merging the potential of microbial genetics with biological and chemical diversity: an even brighter future for marine natural product drug discovery. *Natural Product Reports* **21**, 105-121.

Samson, R. A., and Pitt, J. I. **(2000)**. Integration of modern taxonomic methods for *Penicillium* and *Aspergillus* classification, CRC Press.

Samson, R. A., Hong, S., Peterson, S. W., Frisvad, J. C., and Varga, J. **(2007)**. Polyphasic taxonomy of *Aspergillus* section *Fumigati* and its teleomorph *Neosartorya*. *Studies in Mycology* **59**, 147-203.

Samuel, P., Prince, L., and Prabakaran, P. **(2017)**. Antibacterial activity of marine derived fungi collected from South East Coast of Tamilnadu, India. *Journal of Microbiology and Biotechnology Research* **1**, 86-94.

Schumacher, M., Kelkel, M., Dicato, M., and Diederich, M. **(2011)**. Gold from the sea: marine compounds as inhibitors of the hallmarks of cancer. *Biotechnology Advances* **29**, 531-547.

Sgarbi, D. B., Da Silva, A. J. R., Carlos, I. Z., Silva, C. L., Angluster, J., and Alviano, C. S. **(1997)**. Isolation of ergosterol peroxide and its reversion to ergosterol in the pathogenic fungus *Sporothrix schenckii*. *Mycopathologia* **139**, 9-14.

Shan, W., Wang, S., Ying, Y., Ma, L., and Zhan, Z. **(2014)**. Indole-benzodiazepine-2, 5-dione derivatives from *Neosartorya fischeri*. *Journal of Chemical Research* **38**, 692-694.

Shearer, C. A., Descals, E., Kohlmeyer, B., Kohlmeyer, J., Marvanová, L., Padgett, D., Porter, D., Raja, H. A., Schmit, J. P., and Thorton, H. A. **(2007)**. Fungal biodiversity in aquatic habitats. *Biodiversity and Conservation* **16**, 49-67.

Sheldrick, G. M. **(2008)**. A short history of SHELX. *Acta Crystallographica Section A: Foundations of Crystallography* **64**, 112-122.

Shimada, A., Kusano, M., Takeuchi, S., Fujioka, S., Inokuchi, T., and Kimura, Y. **(2002)**. Aspterric acid and 6-hydroxymellein, inhibitors of pollen development in *Arabidopsis thaliana*, produced by *Aspergillus terreus*. *Zeitschrift für Naturforschung C* **57**, 459-464.

Simoes, R. R., Aires-de-Sousa, M., Conceiçao, T., Antunes, F., da Costa, P. M., and de Lencastre, H. **(2011)**. High prevalence of EMRSA-15 in Portuguese public buses: a worrisome finding. *PLoS One* **6**, e17630.

Slack, G. J., Puniani, E., Frisvad, J. C., Samson, R. A., and Miller, J. D. **(2009)**. Secondary metabolites from *Eurotium* species, *Aspergillus calidoustus* and *A. insuetus* common in Canadian homes with a review of their chemistry and biological activities. *Mycological Research* **113**, 480-490.

Smetanina, O., Kalinovskii, A., Khudyakova, Y. V., Slinkina, N., Pivkin, M., and Kuznetsova, T. **(2007)**. Metabolites from the marine fungus *Eurotium repens*. *Chemistry of Natural Compounds* **43**, 395-398.

Sorra, K., Chang, C.-F., Pusuluri, S., Mukkanti, K., Laiu, M.-C., Bao, B.-Y., Su, C.-H., and Chuang, T.-H. **(2012)**. Synthesis and cytotoxicity testing of new amido-substituted triazolopyrrolo [2, 1-c] [1, 4] benzodiazepine (PBDT) derivatives. *Molecules* **17**, 8762-8772.

Sridhar, K. R. **(2004)**. Mangrove fungi in India. *Current Science* **86**, 1586-1587.

Staats, P. S., Yearwood, T., Charapata, S. G., Presley, R. W., Wallace, M. S., Byas-Smith, M., Fisher, R., Bryce, D. A., Mangieri, E. A., and Luther, R. R. **(2004)**. Intrathecal ziconotide in the treatment of refractory pain in patients with cancer or AIDS: a randomized controlled trial. *The Journal of the American Medical Association* **291**, 63-70.

Stephens, P. J., and Harada, N. **(2010)**. ECD cotton effect approximated by the Gaussian curve and other methods. *Chirality* **22**, 229-233.

Stolk, A. C., and Samson, R. A. **(1972).** *The genus Talaromyces: studies on Talaromyces and related genera II*. Baarn: Centraalbureau voor Schimmelcultures.

Strobel, G. A., Ford, E., Li, J., Sears, J., Sidhu, R. S., and Hess, W. **(1999)**. *Seimatoantlerium tepuiense* gen. nov., a unique epiphytic fungus producing taxol from the Venezuelan Guyana. *Systematic and Applied Microbiology* **22**, 426-433.

Strobel, G., Stierle, A., Stierle, D., and Hess, W. **(1993)**. *Taxomyces andreanae*, a proposed new taxon for a bulbilliferous hyphomycete associated with Pacific yew (Taxus brevifolia). *Mycotaxon* **47**, 71-80.

Strobel, G., Yang, X., Sears, J., Kramer, R., Sidhu, R. S., and Hess, W. **(1996)**. Taxol from *Pestalotiopsis microspora*, an endophytic fungus of *Taxus wallachiana*. *Microbiology* **142**, 435-440.

Sudek, S., Lopanik, N. B., Waggoner, L. E., Hildebrand, M., Anderson, C., Liu, H., Patel, A., Sherman, D. H., and Haygood, M. G. **(2007)**. Identification of the putative bryostatin polyketide synthase gene cluster from "*Candidatus* Endobugula sertula", the uncultivated microbial symbiont of the marine bryozoan Bugula neritina. *Journal of Natural Products* **70**, 67-74.

Sun, T., Zou, J., Chen, G., Hu, D., Wu, B., Liu, X., Yao, X., and Gao, H. **(2017)**. A set of interesting sequoiatones stereoisomers from a wetland soil-derived fungus *Talaromyces flavus*. *Acta Pharmaceutica Sinica B* **7**, 167-172.

Sun, T.-Y., Kuang, R.-Q., Chen, G.-D., Qin, S.-Y., Wang, C.-X., Hu, D., Wu, B., Liu, X.-Z., Yao, X.-S., and Gao, H. **(2016)**. Three pairs of new isopentenyl dibenzo [b,e] oxepinone enantiomers from *Talaromyces flavus*, a wetland soil-derived fungus. *Molecules* **21**, 1184.

Sun, X.-P., Xu, Y., Cao, F., Xu, R.-F., Zhang, X.-L., and Wang, C.-Y. **(2014)**. Isoechinulin-type alkaloids from a soft coral-derived fungus *Nigrospora oryzae*. *Chemistry of Natural Compounds* **50**, 1153-1155.

Sundari, R. V., S; Yusoff, M; Jones, EBG **(2010)**. Observations on tropical arenicolous marine fungi on driftwood from Malaysia and Singapore. *Botanica Marina* **53**, 327–333.

Tabata, Y., Ikegami, S., Yaguchi, T., Sasaki, T., Hoshiko, S., Sakuma, S., SfflN-YAtt, K., and SETO, H. **(1999)**. Diazaphilonic Acid, a new azaphilone with telomerase inhibitory activity. *The Journal of Antibiotics* **52**, 412-414.

Takeuchi, M., Nakajima, M., T. Ogita, Inukai, M., Kodama, K., K. Furuya, NAGAKIn, H., and HANEISHIm, T. **(1989)**. Fosfonochlorin*, A new antibiotic with spheroplast forming activity. *The Journal of Antibiotics* **42** 198-205.

Tan, Q.-W., Ouyang, M.-A., Shen, S., and Li, W. **(2012)**. Bioactive metabolites from a marine-derived strain of the fungus *Neosartorya fischeri*. *Natural Product Research* **26**, 1402-1407.

Taylor, M. W., Hill, R. T., Piel, J., Thacker, R. W., and Hentschel, U. **(2007)**. Soaking it up: the complex lives of marine sponges and their microbial associates. *The International Society for Microbial Ecology Journal* **1**, 187-190.

Thakur, N. L., and Thakur, A. N. **(2006)**. Marine Biotechnology: an overview. *Indian Journal of Biotechnology* **5**, 263-268.

Thatoi, H., Behera, B. C., and Mishra, R. R. **(2013)**. Ecological role and biotechnological potential of mangrove fungi: a review. *Mycology* **4**, 54-71.

Thomas, X. **(2009)**. Chemotherapy of acute leukemia in adults. *Expert Opinion on Pharmacotherapy* **10**, 221-237.

Tomikawa, T., Shin-Ya, K., Furihata, K., Kinoshita, T., Miyajima, A., Seto, H., and Hayakawa, Y. **(2000)**. Rasfonin, a new apoptosis inducer in ras-dependent cells from *Talaromyces sp*. *The Journal of Antibiotics* **53**, 848-850.

Verweij, J. **(2009)**. Soft Tissue Sarcoma Trials: One Size No Longer Fits All. *Journal of Clinical Oncology* **27**, 3085-3087.

Visagie, C. M., Hirooka, Y., Tanney, J. B., Whitfield, E., Mwange, K., Meijer, M., Amend, A. S., Seifert, K. A., and Samson, R. A. **(2014)**. *Aspergillus*, *Penicillium* and *Talaromyces* isolated from house dust samples collected around the world. *Studies in Mycology* **78**, 63-139.

Wakana, D., Hosoe, T., Itabashi, T., Nozawa, K., Okada, K., de Campos Takaki, G., Yaguchi, T., Fukushima, K., and Kawai, K. **(2006)**. Isolation of isoterrein from *Neosartorya fischeri*. *Mycotoxins (Japan)* **56**, 3-6.

Wang, W., Zhu, T., Tao, H., Lu, Z., Fang, Y., Gu, Q., and Zhu, W. **(2007b)**. Two new cytotoxic quinone type compounds from the halotolerant fungus *Aspergillus variecolor. Journal of Antibiotics* **60**, 603-607.

Wang, W.-L., Lu, Z.-Y., Tao, H.-W., Zhu, T.-J., Fang, Y.-C., Gu, Q.-Q., and Zhu, W.-M. **(2007a)**. Isoechinulin-type alkaloids, variecolorins A-L, from halotolerant *Aspergillus variecolor*. *The Journal of Natural Products* **70**, 1558-1564.

Wani, M. C., Taylor, H. L., Wall, M. E., Coggon, P., and McPhail, A. T. **(1971)**. Plant antitumor agents. VI. Isolation and structure of taxol, a novel antileukemic and antitumor agent from *Taxus brevifolia*. *Journal of the American Chemical Society* **93**, 2325-2327.

White, T. J., Bruns, T., Lee, S., and Taylor, J. **(1990)**. Amplification and direct sequencing of fungal ribosomal RNA genes for phylogenetics. *PCR protocols: A Guide to Methods and Applications* **18**, 315-322.

Wijesekara, I., Zhang, C., Van Ta, Q., Vo, T.-S., Li, Y.-X., and Kim, S.-K. **(2014)**. Physcion from marine-derived fungus *Microsporum sp*. induces apoptosis in human cervical carcinoma HeLa cells. *Microbiological Research* **169**, 255-261.

Wijkman, N. **(1931)**. Über einige neue, durch Schimmelpilze gebildete Substanzen. *European Journal of Organic Chemistry* **485**, 61-73.

Wong, S.-M., Musza, L. L., Kydd, G. C., Kullnig, R., Gillum, A. M., and Cooper, R. **(1993)**. Fiscalins. New substance p inhibitors produced by the fungus *Neosartorya fischeri*. Taxonomy, fermentation, structures, and biological properties. *The Journal of Antibiotics* **46**, 545-553.

Wu, B., Ohlendorf, B., Oesker, V., Wiese, J., Malien, S., Schmaljohann, R., and Imhoff, J. F. **(2015)**. Acetylcholinesterase inhibitors from a marine fungus *Talaromyces sp*. strain LF458. *Marine Biotechnology* **17**, 110-119.

Xie, X.-S., Fang, X.-W., Huang, R., Zhang, S.-P., Wei, H.-X., and Wu, S.-H. **(2016)**. A new dimeric anthraquinone from endophytic *Talaromyces sp*. YE3016. *Natural Product Research* **30**, 1706-1711.

Yamazaki, M., Fujimoto, H., and Okuyama, E. **(1978)**. Structure determination of six fungal metabolites, tryptoquivaline E, F, G, H, I and J from *Aspergillus fumigatus*. *Chemical and Pharmaceutical Bulletin* **26**, 111-117.

Yamazaki, M., Okuyama, E., and Maebayashi, Y. **(1979)**. Isolation of some new tryptoquivaline-related metabolites from *Aspergillus fumigatus*. *Chemical and Pharmaceutical Bulletin* **27**, 1611-1617.

Yan, H. J., Li, X. M., Li, C. S., and Wang, B. G. **(2012)**. Alkaloid and anthraquinone derivatives produced by the marine-derived endophytic fungus *Eurotium rubrum*. *Helvetica Chimica Acta* **95**, 163-168.

Yang, X., Kang, M.-C., Li, Y., Kim, E.-A., Kang, S.-M., and Jeon, Y.-J. **(2014)**. Anti-inflammatory activity of questinol isolated from marine-derived fungus *Eurotium amstelodami* in lipopolysaccharide-stimulated RAW 264.7 macrophages. *Journal of Microbiology and Biotechnology* **24**, 1346-1353.

Yang, Y.-C., Lim, M.-Y., and Lee, H.-S. **(2003)**. Emodin isolated from Cassia obtusifolia (Leguminosae) seed shows larvicidal activity against three mosquito species. *Journal of Agricultural and Food Chemistry* **51**, 7629-7631.

Yap, T. A., Carden, C. P., and Kaye, S. B. **(2009)**. Beyond chemotherapy: targeted therapies in ovarian cancer. *Nature Reviews Cancer* **9**, 167-181.

Yarden, O. **(2014)**. Fungal association with sessile marine invertebrates. *Frontiers in Microbiology* **5**, 228.

Yauan, G., Wahlqvist, M., He, G., Yang, M., and Li, D. **(2006)**. Natural products and anti-inflammatory activity. *Asia Pacific Journal of Clinical Nutrition* **15**, 143-152.

Yilmaz, N., Visagie, C. M., Houbraken, J., Frisvad, J. C., and Samson, R. A. **(2014)**. Polyphasic taxonomy of the genus *Talaromyces*. *Studies in Mycology* **78**, 175-341.

Yim, T., Kanokmedhakul, K., Kanokmedhakul, S., Sanmanoch, W., and Boonlue, S. **(2014)**. A new meroterpenoid tatenoic acid from the fungus *Neosartorya tatenoi* KKU-2NK23. *Natural Product Research* **28**, 1847-1852.

Yin, W.-B., Grundmann, A., Cheng, J., and Li, S.-M. **(2009)**. Acetylaszonalenin Biosynthesis in *Neosartorya fischeri*: Identificatin of the biosynthetic gene cluster by genomic mining and functional proof of the genes by biochemical investigation. *Journal of Biological Chemistry* **284**, 100-109.

Yoshida, E., Fujimoto, H., Baba, M., and YamazakI, M. **(1995)**. Four new chlorinated azaphilones, helicusins A-D, closely related to 7-epi-sclerotiorin, from an ascomycetous fungus, *Talaromyces helicus*. *Chemical and Pharmaceutical Bulletin* **43**, 1307-1310.

You, F., Han, T., Wu, J.-z., Huang, B.-k., and Qin, L.-p. **(2009)**. Antifungal secondary metabolites from endophytic *Verticillium sp*. *Biochemical Systematics and Ecology* **37**, 162-165.

You, M., Liao, L., Hong, S. H., Park, W., Kwon, D. I., Lee, J., Noh, M., Oh, D.-C., Oh, K.-B., and Shin, J. **(2015)**. Lumazine peptides from the marine-derived fungus *Aspergillus terreus*. *Marine Drugs* **13**, 1290-1303.

Yu, G., Zhou, G., Zhu, M., Wang, W., Zhu, T., Gu, Q., and Li, D. **(2016)**. Neosartoryadins A and B, fumiquinazoline alkaloids from a mangrove-derived fungus *Neosartorya udagawae* HDN13-313. *Organic Letters* **18**, 244-247.

Yuill, J. L. **(1934)**. The acids produced from sugar by a *Penicillium* parasitic upon *Aspergillus niger*. *Biochemical Journal* **28**, 222-227.

Zainuddin, N., Alias, S. A., Lee, C. W., Ebel, R., Othman, N. A., Mukhtar, M. R., and Awang, K. **(2010)**. Antimicrobial activities of marine fungi from Malaysia. *Botanica Marina* **53**, 507-513.

Zang, Y., Genta-Jouve, G. g., Escargueil, A. E., Larsen, A. K., Guedon, L., Nay, B., and Prado, S. **(2016)**. Antimicrobial Oligophenalenone Dimers from the Soil Fungus *Talaromyces stipitatus*. *Journal of Natural Products* **79**, 2991-2996.

Zang, Y., Genta-Jouve, G., Sun, T. A., Li, X., Didier, B., Mann, S., Mouray, E., Larsen, A. K., Escargueil, A. E., and Nay, B. **(2015)**. Unexpected talaroenamine derivatives and an undescribed polyester from the fungus *Talaromyces stipitatus* ATCC10500. *Phytochemistry* **119**, 70-75.

Zhai, M.-M., Li, J., Jiang, C.-X., Shi, Y.-P., Di, D.-L., Crews, P., and Wu, Q.-X. **(2016)**. The Bioactive Secondary Metabolites from *Talaromyces species*. *Natural Products and Bioprospecting* **6**, 1-24.

Zhang, A., and Demain, A. L. **(2005)**. Natural Products. *Drug Discovery and Therapeutical Medicine.* 382 p.

Zhang, A.-L., Liu, L.-P., Wang, M., and Gao, J.-M. **(2007)**. Bioactive ergosterol derivatives isolated from the fungus *Lactarius hatsudake*. *Chemistry of Natural Compounds* **43**, 637-638.

Zhang, C.-C., Ding, S.-S., Shi, W.-S., Cao, F., Zhu, H.-J., and Wen, M.-L. **(2017)**. A new quinolinone from freshwater lake-derived fungus *Myrothecium verrucaria*. *Natural Product Research* **31**, 99-103.

Zhang, M., Wang, W.-L., Fang, Y.-C., Zhu, T.-J., Gu, Q.-Q., and Zhu, W.-M. **(2008)**. Cytotoxic alkaloids and antibiotic nordammarane triterpenoids from the marine-derived fungus *Aspergillus sydowi*. *Journal of Natural Products* **71**, 985-989.

Zhang, P., Li, X. M., Wang, J. N., and Wang, B. G. **(2015)**. Oxepine-containing diketopiperazine alkaloids from the algal-derived endophytic fungus *Paecilomyces variotii* EN-291. *Helvetica Chimica Acta* **98**, 800-804.

Zhang, P., Li, X., and Wang, B.-G. **(2016)**. Secondary metabolites from the marine algal-derived endophytic fungi: chemical diversity and biological activity. *Planta Medica* **82**, 832-842.

Zhang, P., Mandi, A., Li, X.-M., Du, F.-Y., Wang, J.-N., Li, X., Kurtan, T., and Wang, B.-G. **(2014)**. Varioxepine A, a 3 H-oxepine-containing alkaloid with a new oxa-cage from the marine algal-derived endophytic fungus *Paecilomyces variotii*. *Organic Letters* **16**, 4834-4837.

Zhao, Y.-Y., Zhao, Y., Zhang, Y.-M., Lin, R.-C., and Sun, W.-J. **(2009)**. Qualitative and quantitative analysis of the diuretic component ergone in *Polyporus umbellatus* by HPLC with fluorescence detection and HPLC-APCI-MS/MS. *Die Pharmazie-An International Journal of Pharmaceutical Sciences* **64**, 366-370.

Zheng, Z. Z., Shan, W. G., Wang, S. L., Ying, Y. M., Ma, L. F., and Zhan, Z. J. **(2014)**. Three new prenylated diketopiperazines from *Neosartorya fischeri*. *Helvetica Chimica Acta* **97**, 1020-1026.

Zhi, K.-K., Yang, Z.-D., Zhou, S.-Y., Yao, X.-J., Li, S., and Zhang, F. **(2016)**. A new furanosteroid from *Talaromyces sp*. lgt-4, a fungal endophyte isolated from *Tripterygium wilfordii*. *Natural Product Research* **30**, 2137-2141.

Zhou, L. N., Zhu, T. J., Cai, S. X., Gu, Q. Q., and Li, D. H. **(2010)**. Three new indole-containing diketopiperazine alkaloids from a deep-ocean sediment derived fungus *Penicillium griseofulvum*. *Helvetica Chimica Acta* **93**, 1758-1763.

Zhou, X., Hu, Y., Tian, Y., and Hu, X. **(2009)**. Effect of N-trimethyl chitosan enhancing the dissolution properties of the lipophilic drug cyclosporin A. *Carbohydrate Polymers* **76**, 285-290.

Zhou, X., Lin, X., Ma, W., Fang, W., Chen, Z., Yang, B., and Liu, Y. **(2014)**. A new aromatic amine from fungus *Pestalotiopsis vaccinii*. *Phytochemistry Letters* **7**, 35-37.

Zou, X., Li, Y., Zhang, X., Li, Q., Liu, X., Huang, Y., Tang, T., Zheng, S., Wang, W., and Tang, J. **(2014)**. A new prenylated indole diketopiperazine alkaloid from *Eurotium cristatum*. *Molecules* **19**, 17839-17847.

APPENDICES

APPENDIX I

NMR SPECTRA OF THE ISOLATED NEW COMPOUNDS

APPENDIX I. NMR SPECTRA OF THE ISOLATED NEW COMPOUNDS

1.1 Sartorenol (NTK 12)

1.1.1. ^{1}H NMR spectrum ($CDCl_3$, 300.13 MHz)

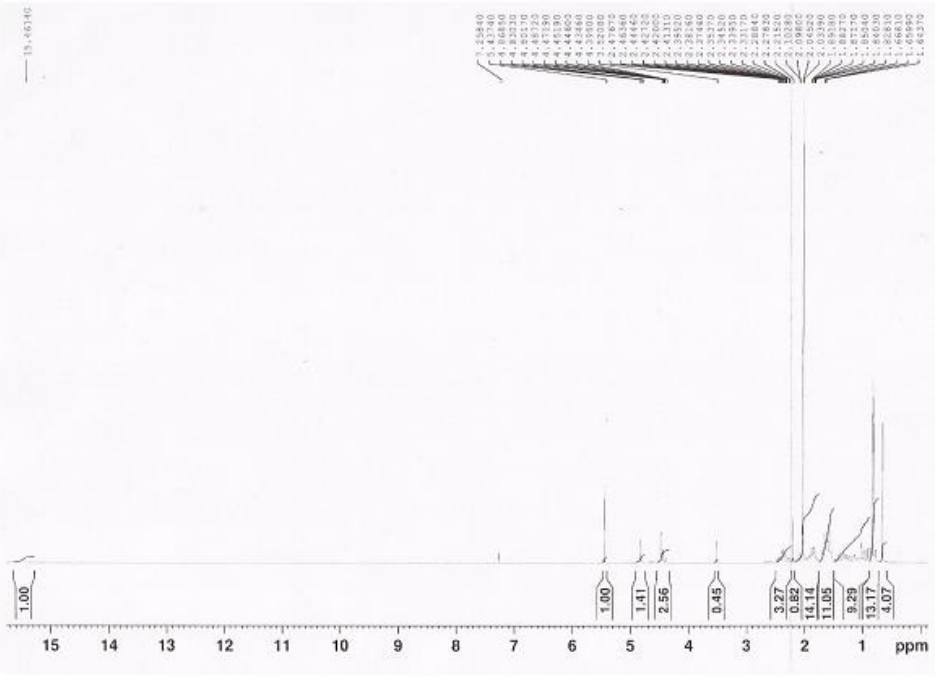

1.1.2. ^{13}C NMR spectrum ($CDCl_3$, 75.47 MHz)

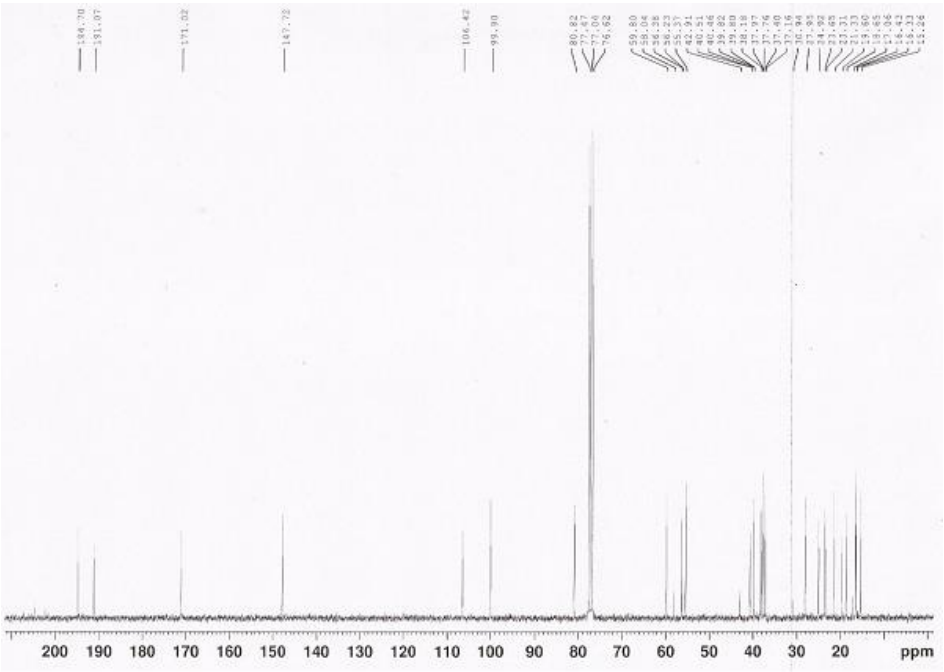

1.2 Takakiamide (NTK4/NG 7)

1.2.1. ^{1}H NMR spectrum ($CDCl_3$, 300.13 MHz)

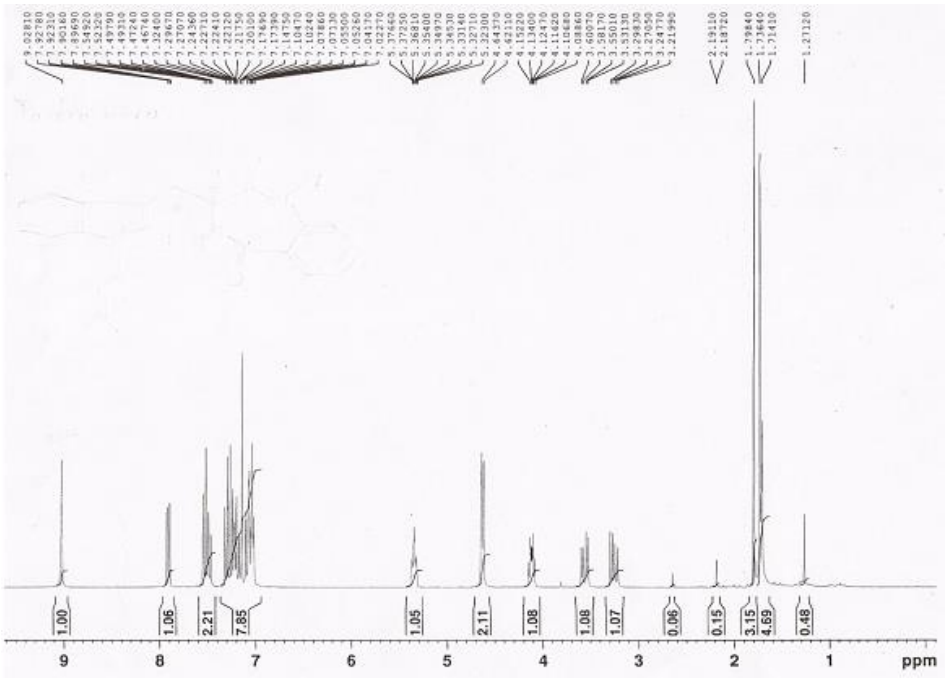

1.2.2. ^{13}C NMR spectrum ($CDCl_3$, 75.47 MHz)

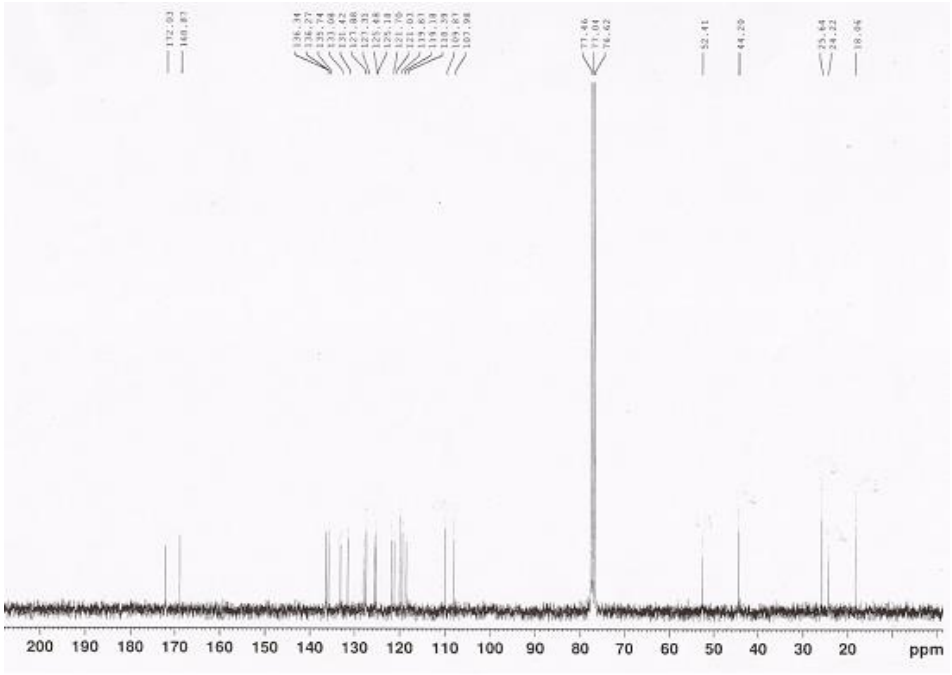

1.3 Tryptoquivaline U (NTK 9)

1.3.1. ^{1}H NMR spectrum (DMSO, 300.13 MHz)

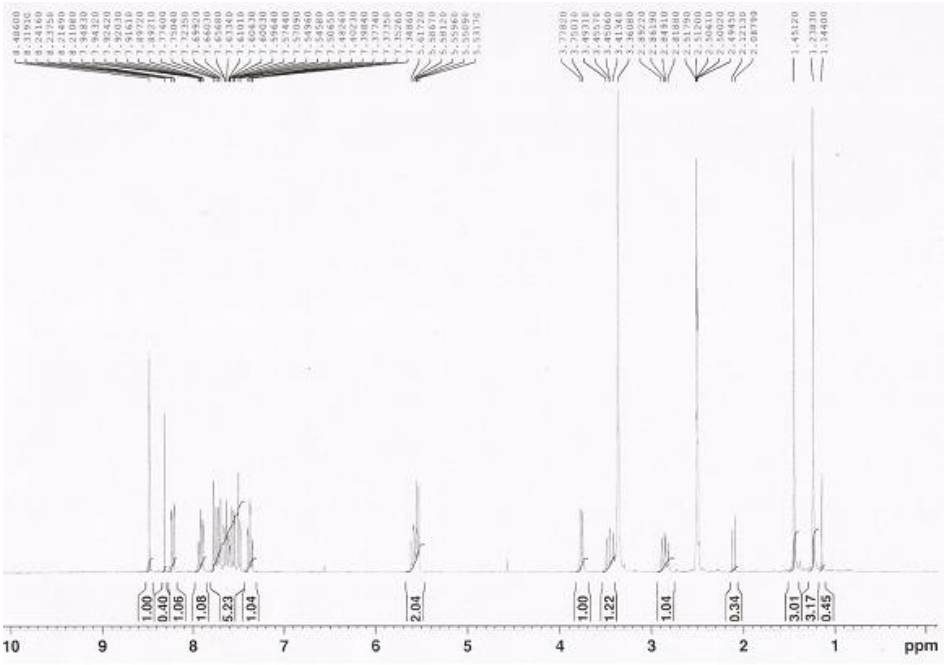

1.3.2. ^{13}C NMR spectrum (DMSO, 75.47 MHz)

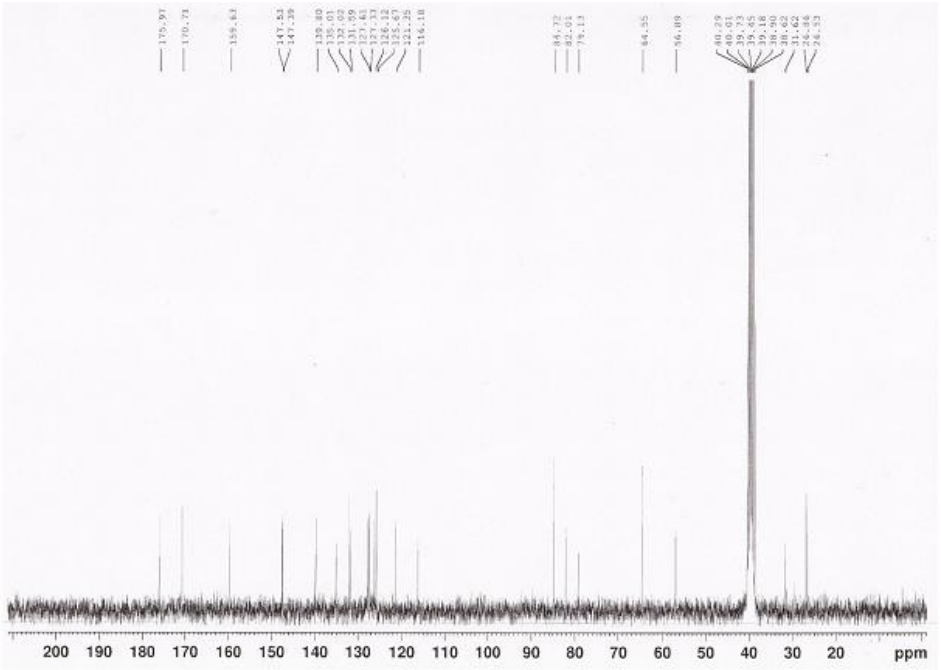

1.4 Sartoryglabramide A (NG 8)

1.4.1. ^{1}H NMR spectrum (DMSO, 500.13 MHz)

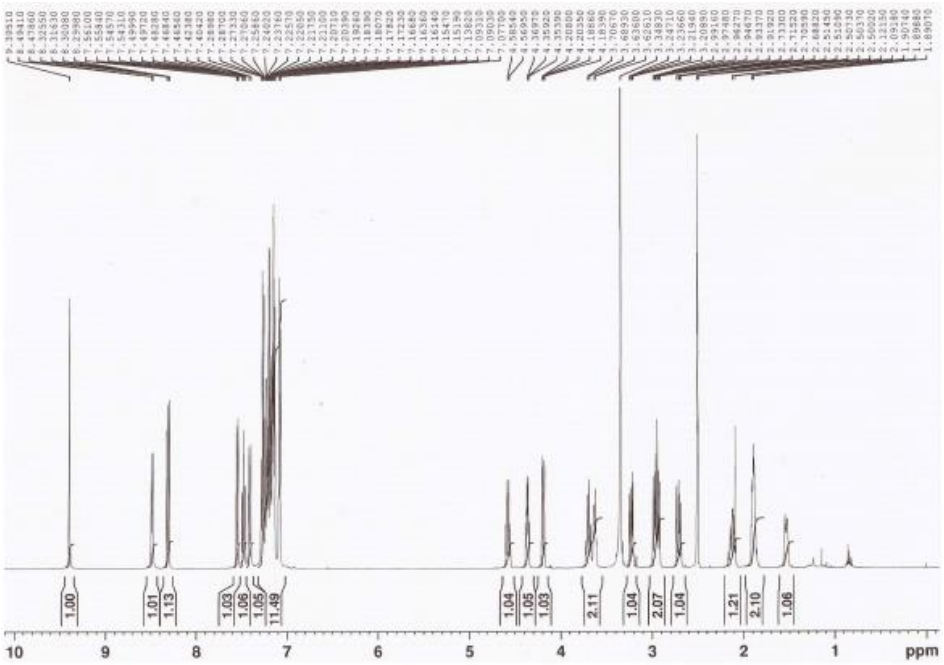

1.4.2. ^{13}C NMR spectrum (DMSO, 125.77 MHz)

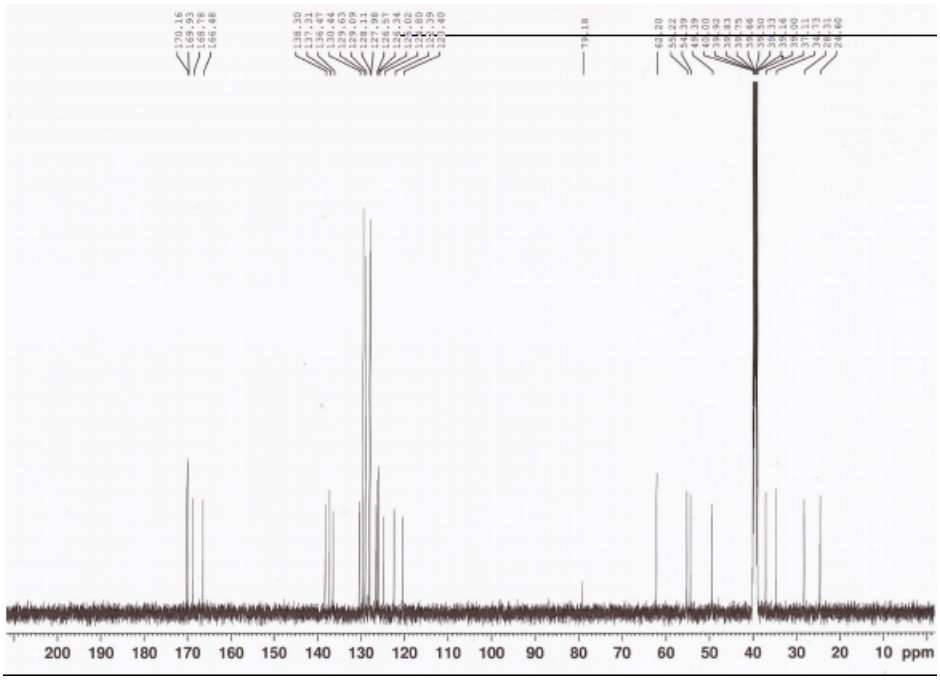

1.5 Sartoryglabramide B (NG 9)

1.5.1. ^{1}H NMR spectrum (DMSO, 500.13 MHz)

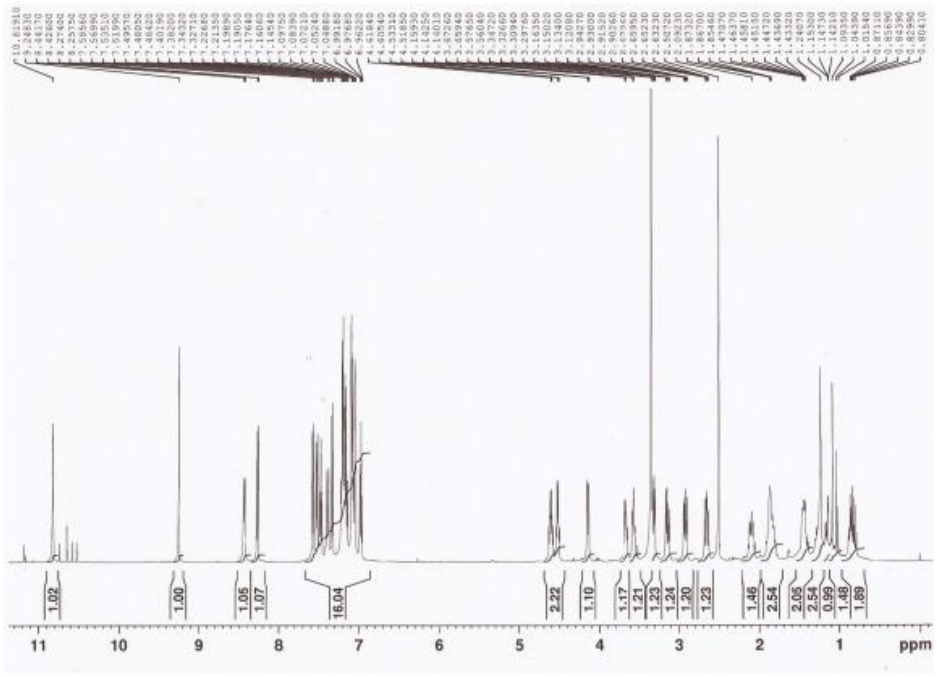

1.5.2. ^{13}C NMR spectrum (DMSO, 125.77 MHz)

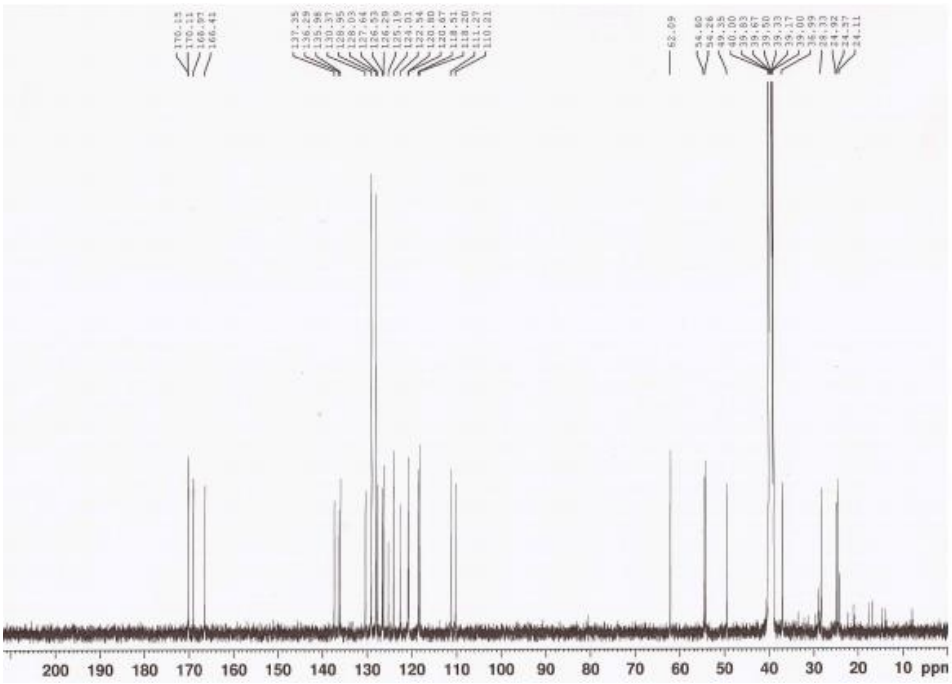

1.6 Fellutanine A epoxide (NG 11)

1.6.1. ^{1}H NMR spectrum (DMSO, 300.13 MHz)

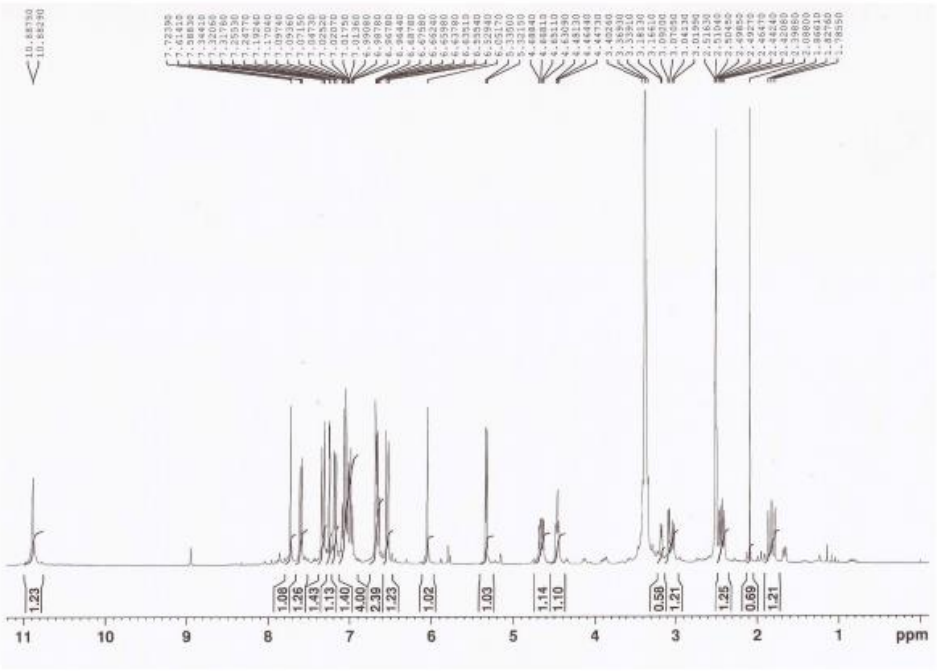

1.6.2. ^{13}C NMR spectrum (DMSO, 75.47 MHz)

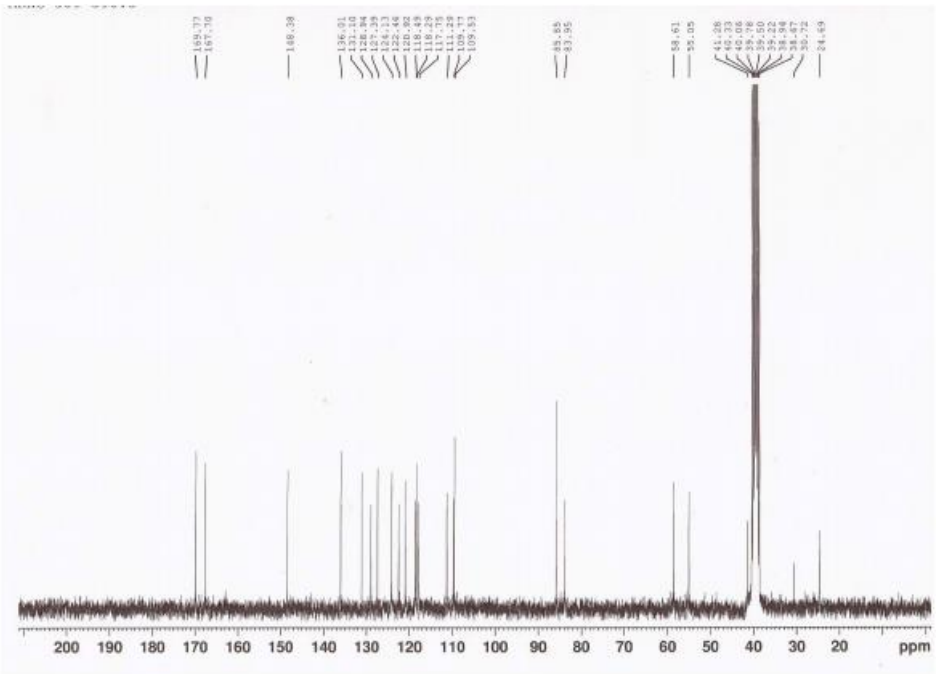

1.7 Acetylquestinol (EC 7)

1.7.1. ^{1}H NMR spectrum of acetylquestinol (**EC 7**) (DMSO, 300.13 MHz)

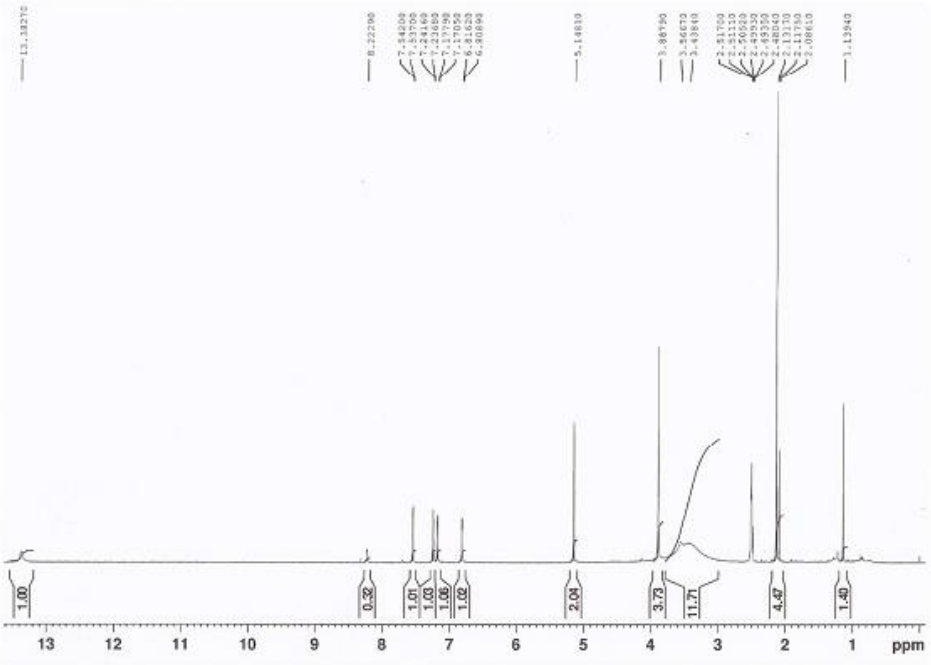

1.7.2. ^{13}C NMR spectrum of acetylquestinol (**EC 7**) (DMSO, 75.47 MHz)

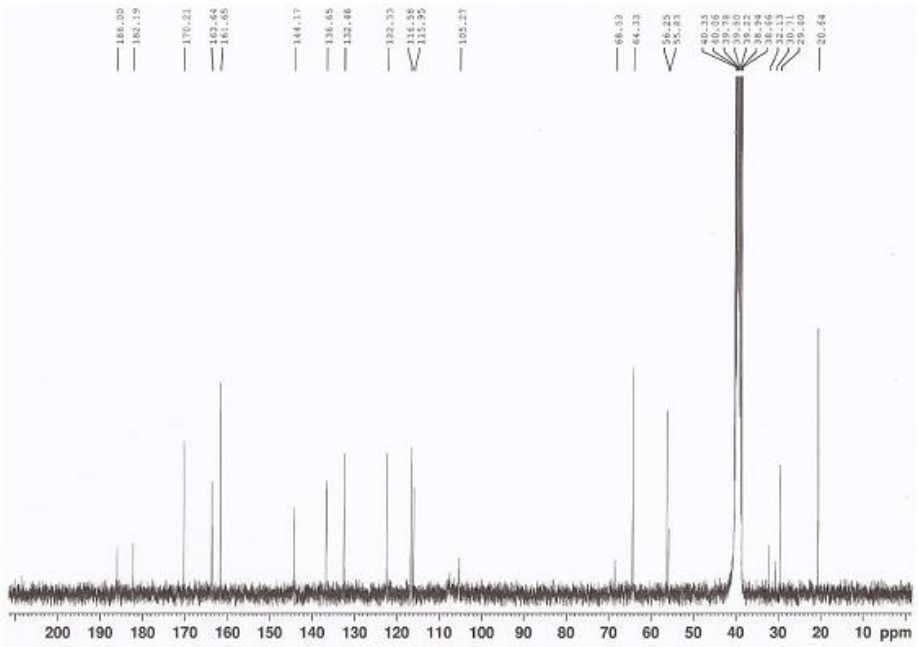

1.8 2-(2-Methyl-3-en-2-yl)-1*H*-indole-3-carbaldehyde (EC 8)

1.8.1. ^{1}H NMR spectrum ($CDCl_3$, 300.13 MHz)

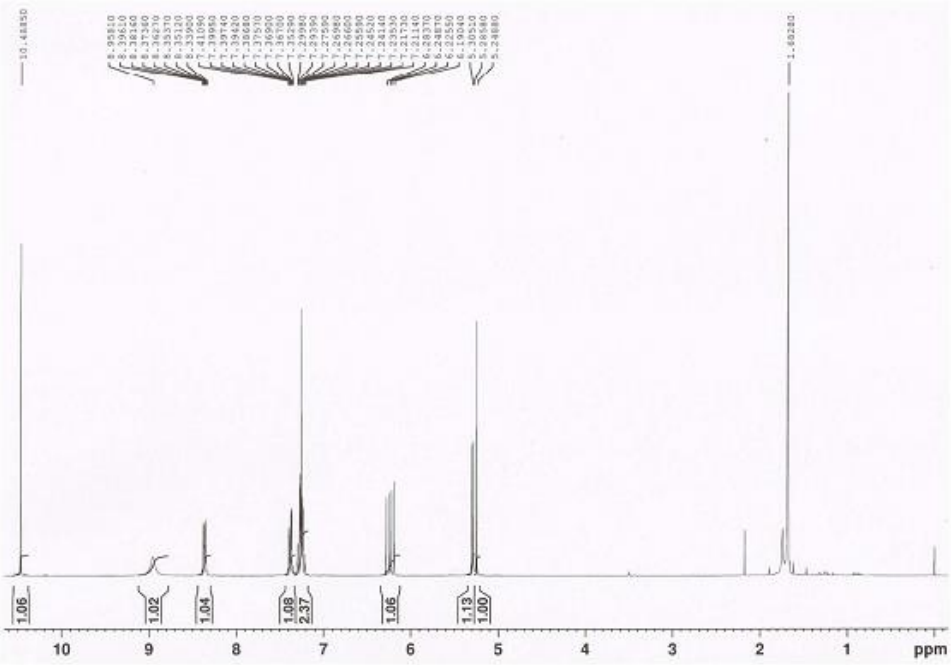

1.8.2. ^{1}H NMR spectrum ($CDCl_3$, 75.47 MHz)

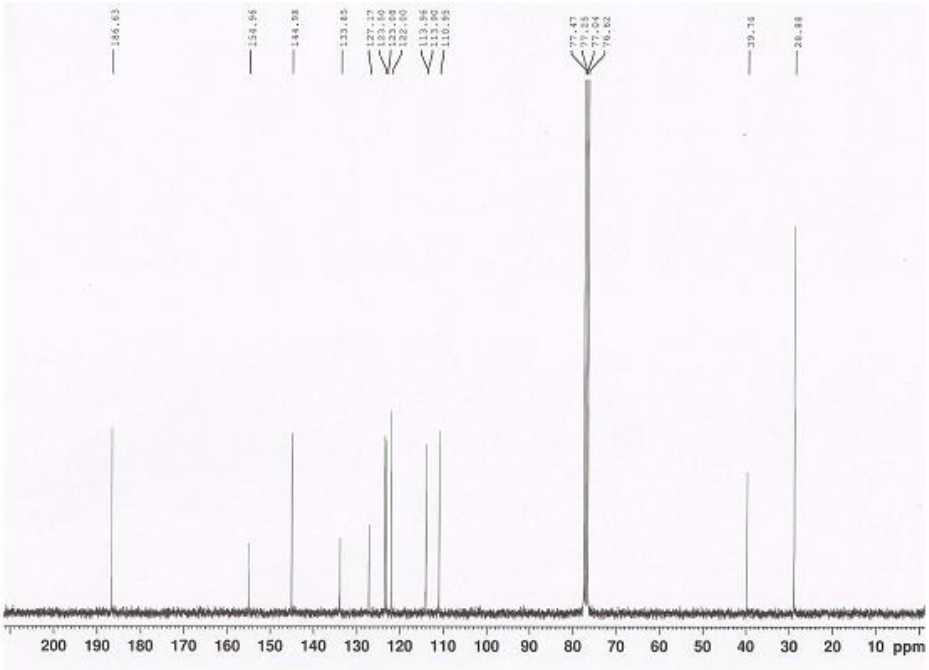

1.92-(2, 2-dimethylcyclopropyl)-1*H*-indole-3-carbaldehyde (EC 9)

1.9.1. ^{1}H NMR spectrum ($CDCl_3$, 300.13 MHz)

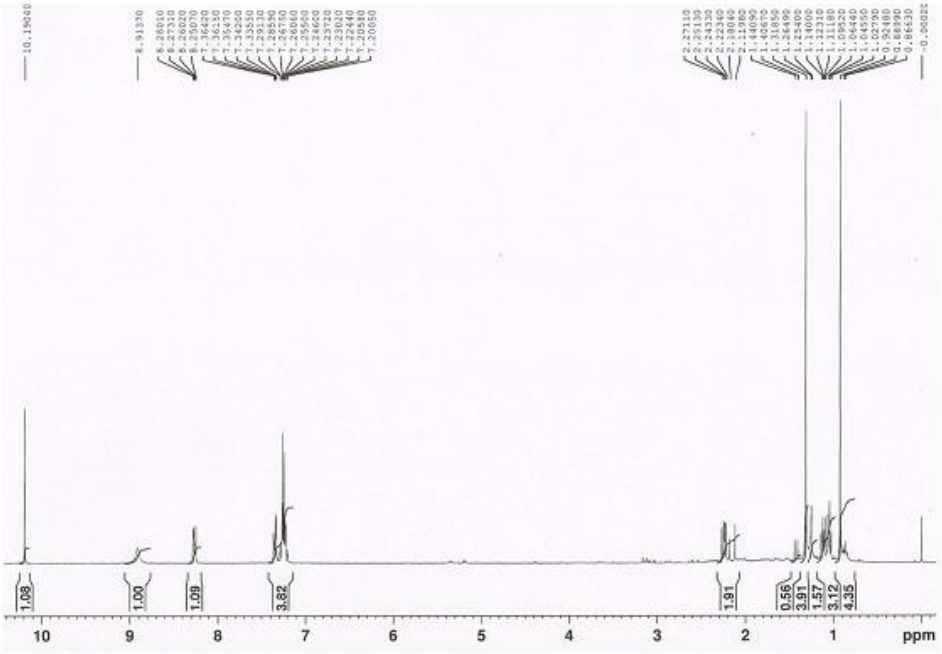

1.9.2. ^{1}H NMR spectrum ($CDCl_3$, 75.47 MHz)

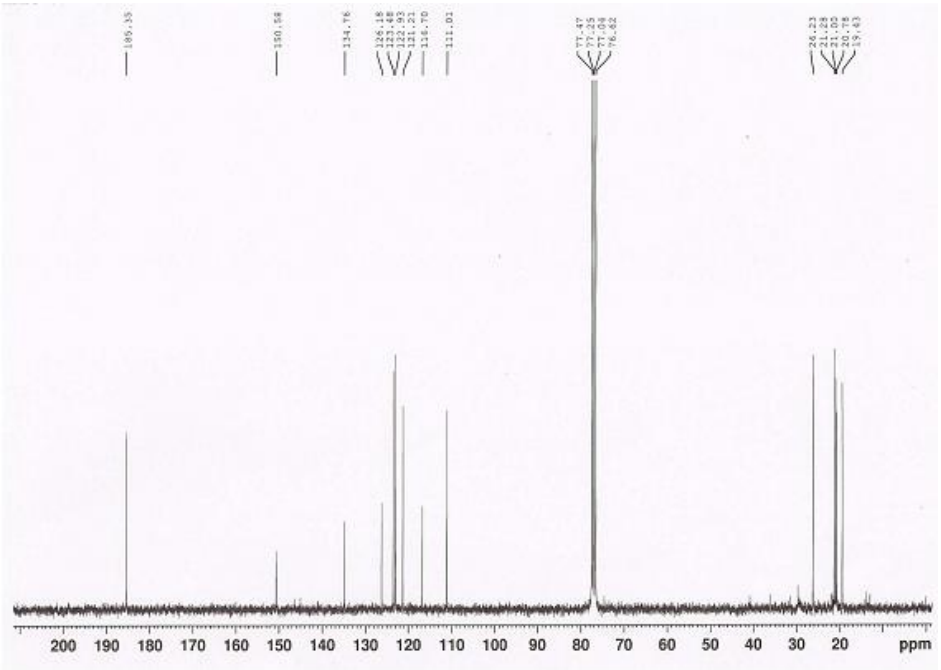

1.10 2-(2, 2-dimethylbut-3enoyl) amino-benzoic acid (EC 10)

1.10.1. ^{1}H NMR (DMSO, 300.13 MHz)

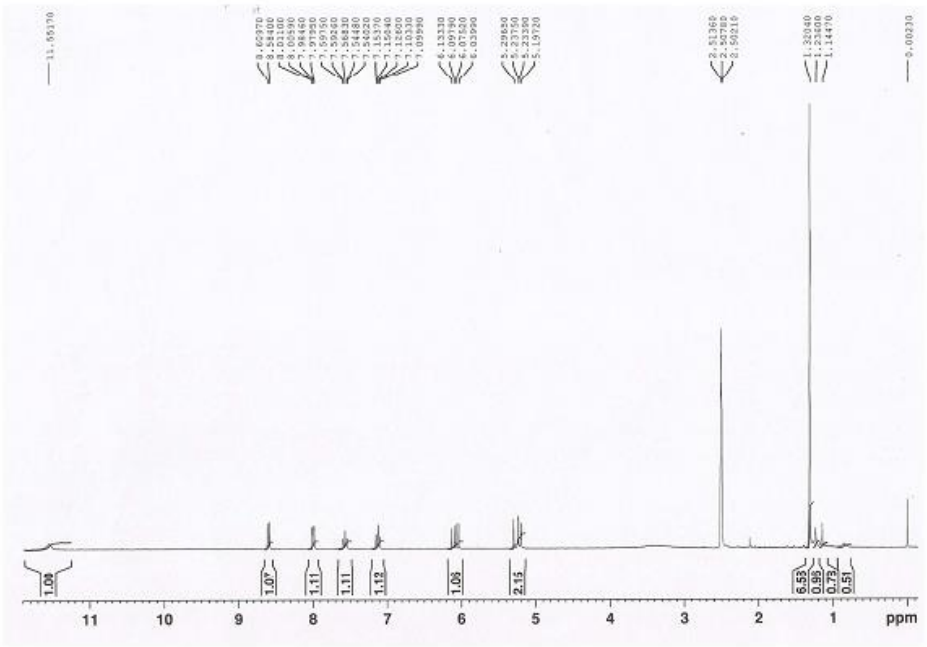

1.10.2. ^{13}C NMR spectrum (DMSO, 75.47 MHz)

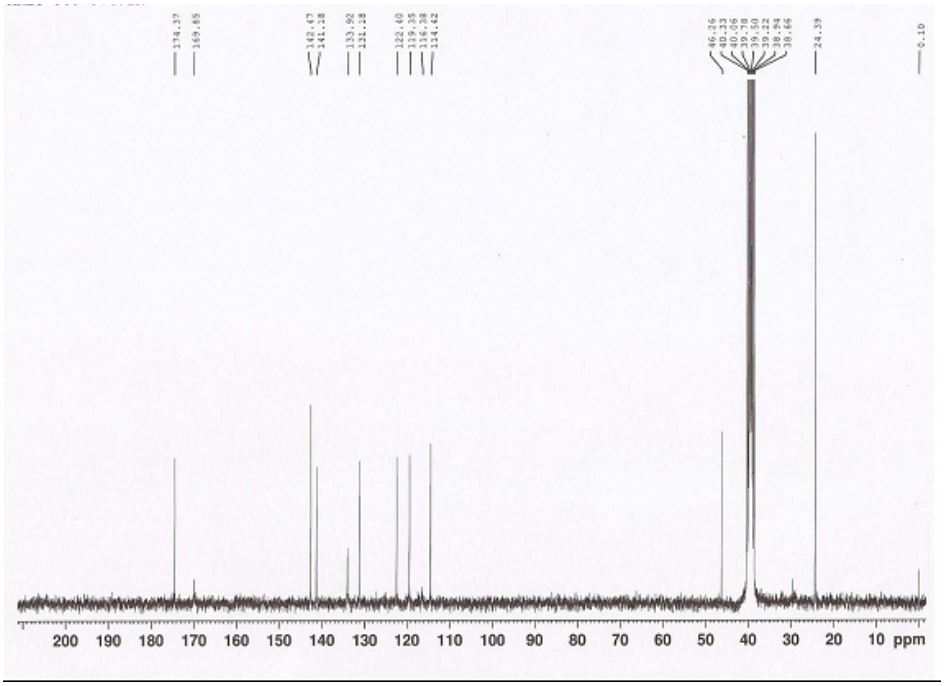

1.11 6, 8-dihydroxy-3(2*R*-hydroxypropyl)-7-methyl-1*H*-isochromen-1-one (EC 11)

1.11.1. ^{1}H NMR spectrum (DMSO, 300.13 MHz)

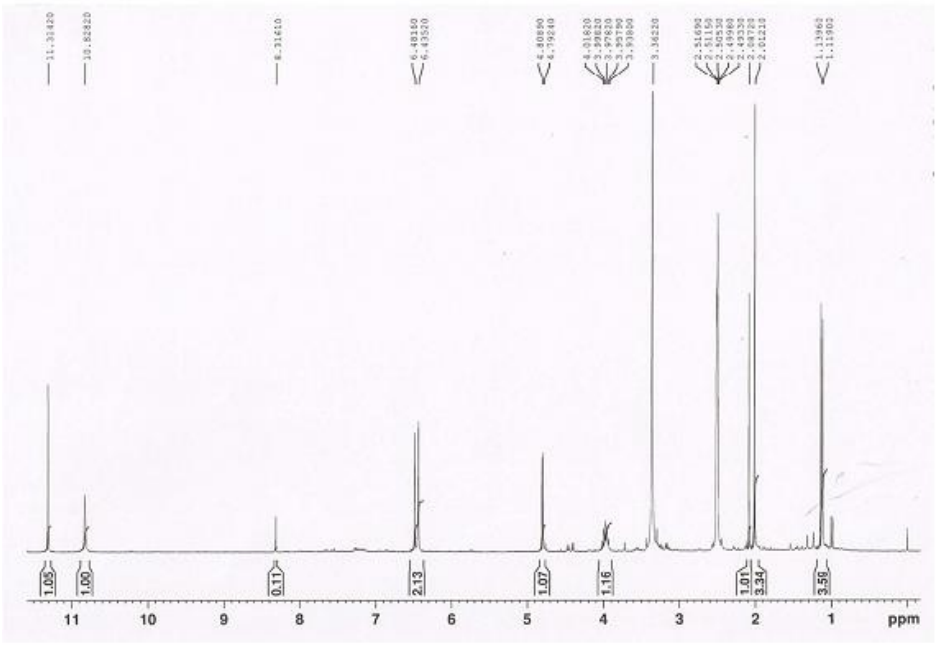

1.11.2. ^{13}C NMR spectrum (DMSO, 75.47 MHz)

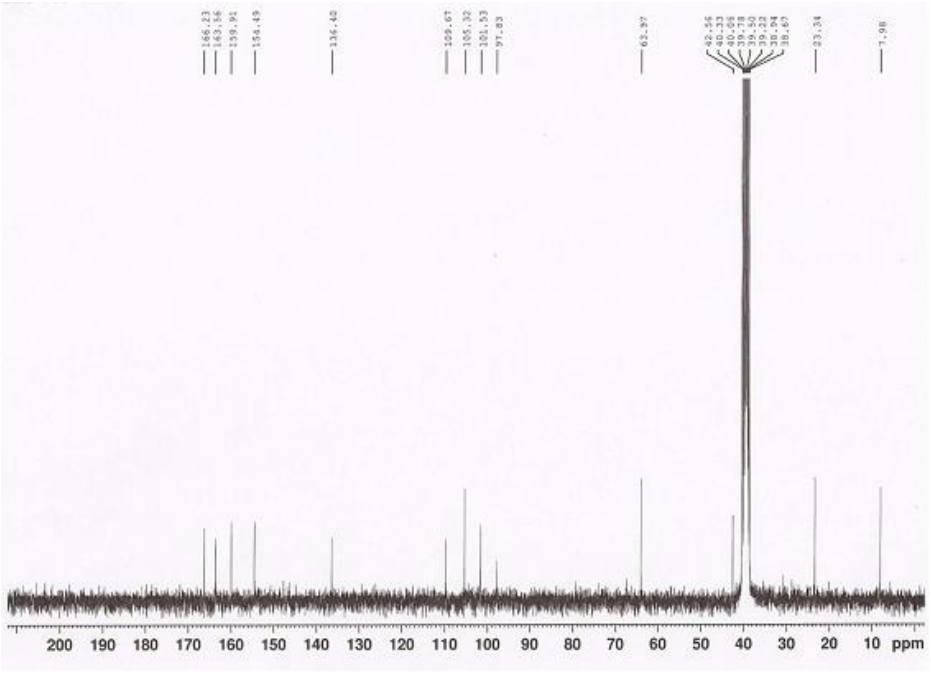

APPENDIX I. NMR SPECTRA OF THE ISOLATED NEW COMPOUNDS

APPENDIX II

Zin, W. W. M., Buttachon, S., Buaruang, J., Gales, L., Pereira, J. A., Pinto, M. M., Silva, A., and Kijjoa, A. **(2015)**. A new meroditerpene and a new tryptoquivaline analog from the algicolous fungus *Neosartorya takakii* KUFC 7898. *Marine Drugs* **13**, 3776-3790. Doi:10.390/md13063776.

Mar. Drugs **2015**, *13*, 3776-3790; doi:10.3390/md13063776

OPEN ACCESS

marine drugs

ISSN 1660-3397

www.mdpi.com/journal/marinedrugs

Article

A New Meroditerpene and a New Tryptoquivaline Analog from the Algicolous Fungus *Neosartorya takakii* KUFC 7898

War War May Zin [1,2], Suradet Buttachon [1,2], Jamrearn Buaruang [3], Luís Gales [1,4], José A. Pereira [1], Madalena M. M. Pinto [2,5], Artur M. S. Silva [6] and Anake Kijjoa [1,2,*]

1 ICBAS—Instituto de Ciências Biomédicas Abel Salazar, Universidade do Porto, Rua de Jorge Viterbo Ferreira, 228, 4050-313 Porto, Portugal; E-Mails: wwmzin.chem.yu@gmail.com (W.W.M.Z.); nokrari_209@hotmail.com (S.B.); lgales@ibmc.up.pt (L.G.); jpereira@icbas.up.pt (J.A.P.)

2 Interdisciplinary Centre of Marine and Environmental Research (CIIMAR), Rua dos Bragas 289, 4050-313 Porto, Portugal; E-Mail: madalena@ff.up.pt

3 Division of Environmental Science, Faculty of Science, Ramkhamhaeng University, Bangkok 10240, Thailand; E-Mail: jbuaruang@ru.mail.go.th

4 Instituto de Biologia Molecular e Celular (IBMC), Universidade do Porto, Rua de Jorge Viterbo Ferreira, 228, 4050-313 Porto, Portugal

5 Laboratório de Química Orgânica, Departamento de Ciências Químicas, Faculdade de Farmácia, Universidade do Porto, Rua de Jorge Viterbo Ferreira, 228, 4050-313 Porto, Portugal

6 Departamento de Química & QOPNA, Universidade de Aveiro, 3810-193 Aveiro, Portugal; E-Mail: artur.silva@ua.pt

* Author to whom correspondence should be addressed; E-Mail: ankijjoa@icbas.up.pt; Tel.: +351-220428331; Fax: +351-220428090.

Academic Editor: Alejandro Mayer

Received: 29 April 2015 / Accepted: 4 June 2015 / Published: 15 June 2015

Abstract: A new meroditerpene sartorenol (**1**), a new natural product takakiamide (**2**) and a new tryptoquivaline analog (**3**) were isolated, together with nine known compounds, including aszonapyrone A, chevalone B, aszonalenin, acetylaszonalenin, 3′-(4-oxoquinazolin-3-yl) spiro[1*H*-indole-3,5′-oxolane]-2,2′-dione, tryptoquivalines L, F and H, and the isocoumarin derivative, 6-hydroxymellein, from the ethyl acetate extract of the culture of the algicolous fungus *Neosartorya takakii* KUFC 7898. The structures of the new compounds were established based on 1D and 2D NMR spectral analysis, and, in the case of sartorenol (**1**) and tryptoquivaline U (**3**), X-ray analysis was used to confirm their structures and to determine the absolute configuration of their stereogenic carbons. Compounds **1**, **2**

and **3** were evaluated for their antimicrobial activity against Gram-positive and Gram-negative bacteria, and multidrug-resistant isolates from the environment; however, none exhibited antibacterial activity (MIC > 256 mg/mL). The three new compounds did not show any quorum sensing inhibition in the screening protocol based on the pigment production by *Chromobacterium violaceum* (ATCC 31532).

Keywords: *Neosartorya takakii*; meroditerpene; sartorenol; tryptoquivaline U; aszonapyrone A; chevalone B; aszonalenin; 6-hydroxymellein

1. Introduction

In recent years, marine-derived fungi have been demonstrated to be a rich and promising source of novel anticancer, antibacterial, antiplasmodial, anti-inflammatory, and antiviral agents [1]. To date, more than one thousand unique molecular structures have been discovered from marine-derived fungi. Several reviews on marine fungi [2–4] have shown that a variety of secondary metabolites isolated from marine-derived fungi had not been produced by terrestrial fungi, and these metabolites possibly act as a chemical defense, enabling marine-derived fungi to survive competition with native microorganisms [5]. Thus, marine-derived fungi, which successfully fostered their armamentarium against bacterial competitors for millions of years, can be considered as a potential source of antibiotics.

In our ongoing pursuit of new natural products with antibacterial activity produced by marine-derived fungi of the genera *Neosartorya* and *Aspergillus*, we have investigated the secondary metabolites of a Thai collection of *Neosartorya takakii* KUFC 7898, isolated from the marine macroalga *Amphiroa* sp., collected from Samaesarn Island in the Gulf of Thailand. The ethyl acetate extract of its culture yielded, in addition to the previously reported aszonapyrone A [6], chevalone B [7,8], aszonalenin [6], acetylaszonalenin [6], 3′-(4-oxoquinazolin-3-yl) spiro[1*H*-indole-3,5′-oxolane]-2,2′-dione [9], tryptoquivalines L, F and H [9], and 6-hydroxymellein [10], three new compounds including a meroditerpene sartorenol (**1**), a prenylated indole alkaloid takakiamide (**2**), and a new tryptoquivaline analog, which we have named tryptoquivaline U (**3**) (Figure 1). Compounds **1**–**3** were screened for their antibacterial activity against Gram-positive and Gram-negative bacteria, and multidrug-resistant isolates from the environment as well as for their quorum sensing inhibitory activity.

2. Results and Discussion

Compound **1** was isolated as white crystals (mp, 122–123 °C) and its molecular formula $C_{27}H_{42}O_4$ was established on the basis of the (+)-HRESIMS *m*/*z* 431.3175 $[M + H]^+$ (calculated 431.3161), indicating seven degrees of unsaturation. The IR spectrum showed absorption bands for hydroxyl (3393 cm^{-1}), conjugated ketone carbonyl (1645 cm^{-1}), ester carbonyl (1728 cm^{-1}), and olefin (1558, 1540 cm^{-1}) groups. The ^{13}C NMR, DEPT and HSQC spectra (Table 1, Supplementary Figures S3 and S4) exhibited the signals of one conjugated ketone carbonyl (δ_C 194.7), one ester carbonyl (δ_C 171.0), two quaternary sp^2 (δ_C 147.7 and 191.1), one methine sp^2 (δ_C 99.9), one methylene sp^2 (δ_C 106.4), three quaternary sp^3 (δ_C 37.4, 37.8, 39.8), one oxymethine sp^3 (δ_C 80.8), three methine sp^3 (δ_C 55.4, 56.4 and 59.8), eight methylene

sp^3 (δ_C 18.7, 19.6, 23.3, 23.6, 37.2, 38.0, 38.2 and 40.5) and six methyl (δ_C 15.3, 16.3, 16.4, 21.3, 24.9 and 28.0) carbons. The ^{1}H NMR spectrum (Table 1, Supplementary Figure S1) revealed the presence of one hydrogen-bonded hydroxyl group of an enol at δ_H 15.47, s, two exocyclic methylene protons at δ_H 4.84, brs and 4.50, brs, one olefinic proton at δ_H 5.45, s, and the protons of six methyl groups at δ_H 0.69, s, 0.83, s, 0.84, s, 0.86, s, 2.05, s (integrating for two methyls). Except for the enolic hydroxyl group, the olefinic proton and the conjugated ketone carbonyl (δ_C 194.7), the ^{1}H and ^{13}C data (Table 1, Supplementary Figures S1 and S3) revealed the presence of a perhydrophenanthrene moiety, similar to that of aszonapyrone A [6]. Like aszonapyrone A, the acetoxyl group on C-3 of compound **1** was β, as was evidenced by the coupling constants of H-3 (δ_H 4.48, dd, J = 10.9, 4.6 Hz). Another portion of the molecule, which consists of $C_6H_9O_2$, was identified as (4*Z*)-5-hydroxy-3-oxohex-4-enyl group due to the HMBC correlations (Table 1, Supplementary Figure S5) of H_3-20 (δ_H 2.05, s) to C-18 (δ_C 99.9) and C-19 (δ_C 191.1), of H-18 (δ_H 5.45, s) to C-16 (δ_C 37.2), C-17 (δ_C 194.7), C-19 (δ_C 191.1) and C-20 (δ_C 24.9), as well as the NOESY correlation (Supplementary Figure S6) between H-18 and H_3-20. That C-15 of the (4*Z*)-5-hydroxy-3-oxohex-4-enyl group was connected to C-14 of the perhydrophenanthrene moiety was supported by the correlations between H-14 (δ_H 1.59, m) and H-15 (δ_H1.86, m) in the COSY spectrum (Table 1, Supplementary Figure S2), as well as by the HMBC correlation of H_2-15 to C-13 (δ_C 147.7). The structure and stereochemistry of compound **1** were unambiguously determined by X-ray analysis (Figure 2), and the absolute configurations of C-3, C-5, C-8, C-9, C-10 and C-14 were identified as 3*S*, 5*R*, 8*R*, 9*R*, 10*R* and 14*S*, respectively. Since **1** is a new compound, we have named it sartorenol.

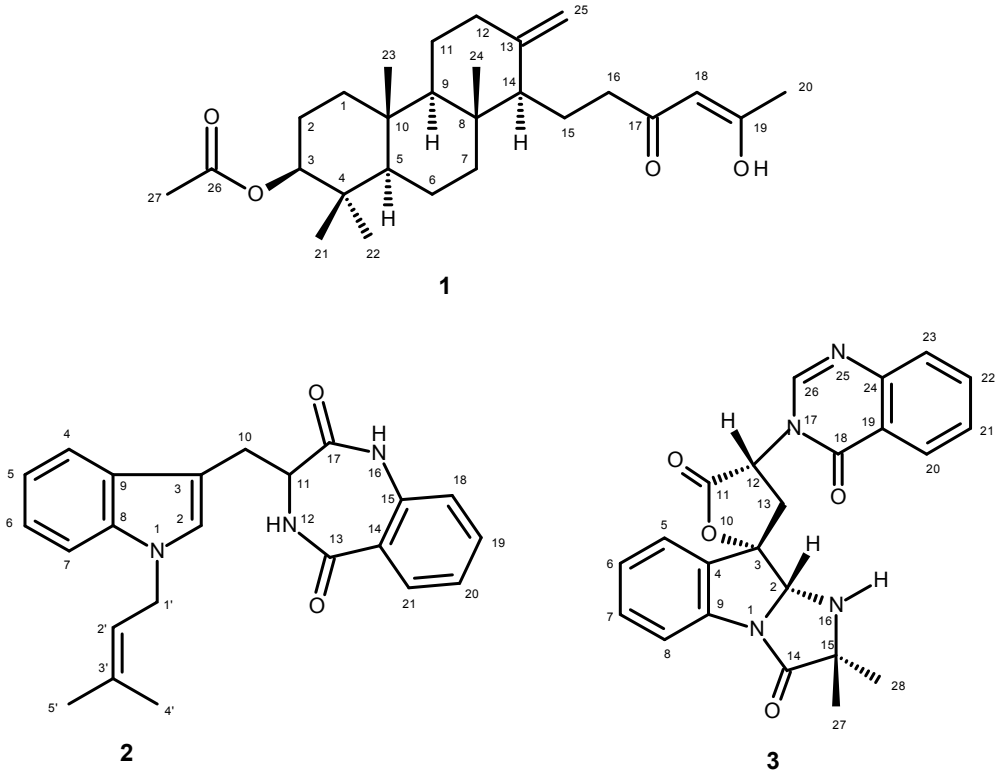

Figure 1. New secondary metabolites isolated from the ethyl acetate extract of the culture of *N. takakii* KUFC 7898.

Table 1. ^{1}H and ^{13}C NMR ($CDCl_3$, 300.13 MHz and 75.47 MHz) and HMBC assignment for **1**.

Position	δ_C, Type	δ_H, (*J* in Hz)	COSY	HMBC
1	38.2, CH_2	1.05, m	H-2	
2	23.3, CH_2	1.65, m	H-1, 3	
		1.33, dd (12.9, 4.2)	H-1, 3	C-4
3	80.8, CH	4.48, dd (10.9, 4.6)	H-2	C-1, 4, 21, 22
4	37.8, C	-		
5	55.4, CH	0.91, dd (12.0, 2.2)	H-6	
6	18.7, CH_2	1.62, m	H-5	
		1.14, m		
7	40.5, CH_2	1.18, dd (12.5, 3.6)		
		1.88, m		
8	39.8, C	-		
9	59.8, CH	1.02, dd (12.3, 2.6)		
10	37.4, C	-		
11	23.6, CH_2	1.70, m		
12	38.0, CH_2	2.38, m		
		1.92, m		C-14, 25
13	147.7, C	-		
14	56.4, CH	1.59, m	H-15	
15	19.6, CH_2	1.86, m	H-14, 16	C-13
16	37.2, CH_2	2.08, m	H-15	
17	194.7, CO	-		
18	99.9, CH	5.45, s		C-16, 17, 19, 20
19	191.1, C	-		
20	24.9, CH_3	2.05, s		C-18, 19
21	16.3, CH_3	0.83, s		C-3, 4, 5, 22
22	28.0, CH_3	0.86, s		C-3, 4, 5, 21
23	16.4, CH_3	0.84, s		C-1, 5, 9, 10
24	15.3, CH_3	0.69, s		C-7, 8, 9, 14
25a	106.4, CH_2	4.84, brs		C-12, 14
b		4.50, brs		C-12, 13, 14
26	171.0, CO	-		
27	21.3, CH_3	2.05, s		C-26
OH-19		15.47, s		

The biosynthetic pathway of sartorenol (**1**) resembles those proposed for aszonapyrone A and sartorypyone A [6], which is hypothesized as originating from a reaction of the triketide derivative (**II**) with GPP oxide (**III**) to form the meroditerpene intermediate (**IV**). Cyclization, hydrolysis of the CoA ester and enolization of the side chain give the intermediate (**V**). Decarboxylation of the side chain and acetylation of the hydroxyl group of the perhydrophenanthrene moiety would finally lead to the formation of sartorenol (**1**) (Figure 3).

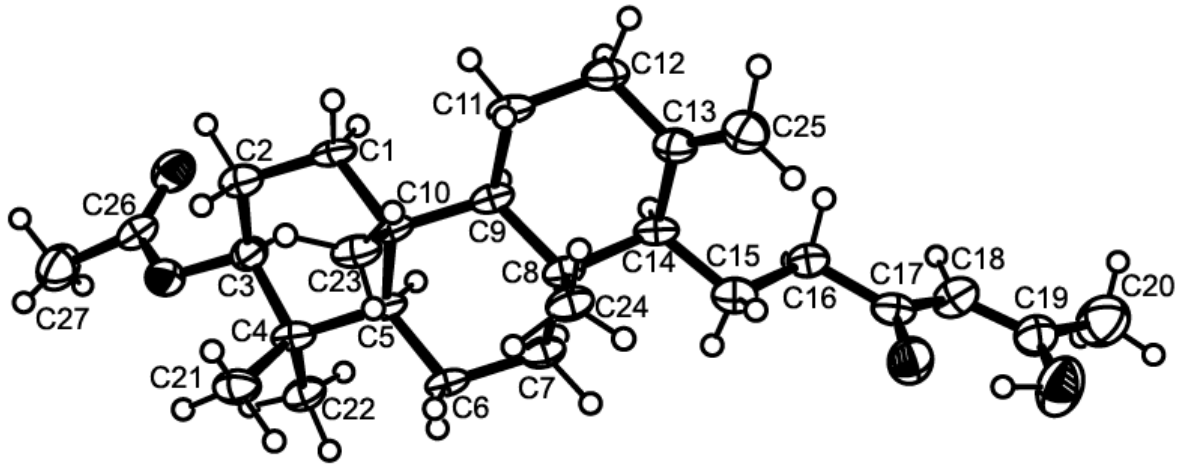

Figure 2. Ortep view of sartorenol (**1**).

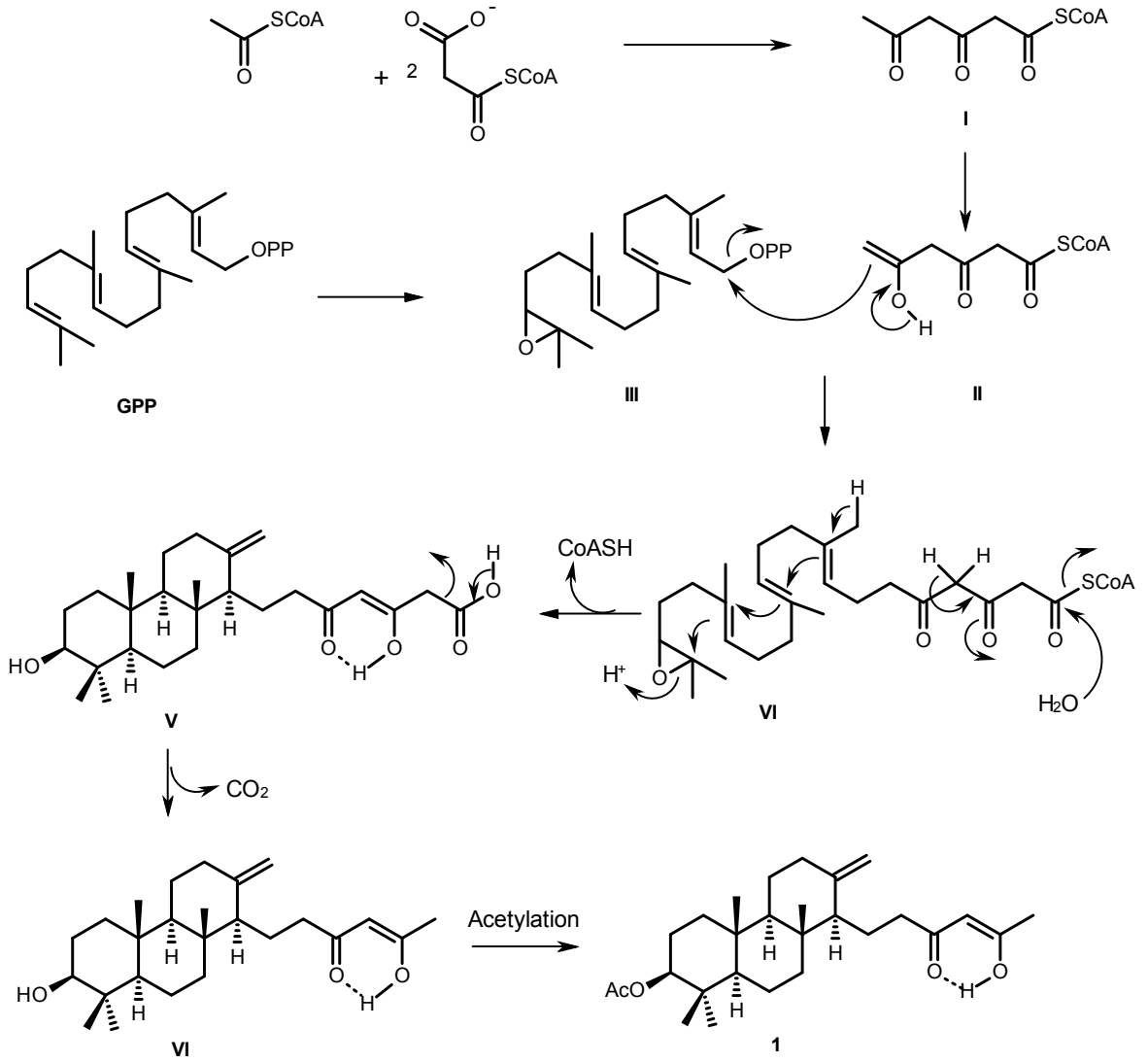

Figure 3. Proposed biogenesis of sartorenol (**1**).

Compound **2** was isolated as white solid (mp, 182–183 °C), and its molecular formula $C_{23}H_{23}N_3O_2$ was established on the basis of the (+)-HRESIMS *m*/*z* 374.1876 $[M + H]^+$ (calculated for $C_{23}H_{24}N_3O_2$, 374.1869), indicating fourteen degrees of unsaturation. The IR spectrum showed absorption bands for amine (3214 cm^{-1}), amide carbonyls (1688, 1654 cm^{-1}), aromatic (3057, 1579 cm^{-1}) and olefin (1607, 1468 cm^{-1}) groups. The ^{13}C NMR, DEPTs and HSQC spectra (Table 2, Supplementary Figures S9 and S10) revealed the presence of two amide carbonyls (δ_C172.0 and 168.9), six quaternary sp^2 (δ_C 136.4, 136.3, 135.7, 127.9, 125.5, 108.0), ten methine sp^2 (δ_C 133.1, 131.4, 127.3, 125.2, 121.7, 121.0, 119.9, 119.2, 118.4, 109.9), one methine sp^3 (δ_C 52.4), two methylene sp^3 (δ_C 44.2 and 22.4) and two methyl (δ_C 25.6 and 18.1) carbons. The coupling system of the aromatic protons, observed in the COSY spectrum (Table 2, Supplementary Figure S8), indicated the presence of two 1,2-disubstituted benzene rings. That one of the 1,2-disubstituted benzene rings was part of the 3,4-dihydro-1*H*-1,4-benzodiazepine-2,5-dione was supported by the HMBC cross peaks (Table 2, Supplementary Figure S11) of the singlet of the amine proton at δ_H 9.03 (NH-16) to C-11 (δ_C 52.4) and C-14 (δ_C 125.5), of H-21 (δ_H 7.91, dd, J = 8.0, 1.5 Hz) to C-13 (δ_C 168.9), as well as by the COSY cross peaks (Table 2, Supplementary Figure S8) observed between NH-12 (δ_H 7.03, brd, J = 5.5 Hz) and H-11 (δ_H 4.12, dt, J = 8.3, 5.5 Hz). That another 1,2-disubstituted benzene ring belonged to the indole moiety of the molecule was substantiated by the HMBC cross peaks (Table 2, Supplementary Figure S11) of H-2 (δ_H 7.15, s) to C-3 (δ_C 108.0), C-8 (δ_C 136.3) and C-9 (δ_C 127.9). The presence of the 3-methylbuten-2-yl moiety was corroborated by cross peaks of H-1′ (δ_H 4.63, d, J = 6.8 Hz) to H-2′ (δ_H 5.35, m), CH_3-4′ (δ_H 1.74, s) and CH_3-5′ (δ_H 1.80, s) protons in the COSY spectrum, as well as by the HMBC cross peaks of CH_3-4′ (1.74, s) and CH_3-5′ (1.80, s) protons to C-2′ (δ_C 119.9) and C-3′ (δ_C 136.4). Since the HMBC spectrum showed cross peaks of H-1′ to C-2 (δ_C 127.3) and C-8 (δ_C 136.3), the 3-methylbuten-2-yl moiety was linked to the indole nitrogen. That the indole moiety was linked to the 3,4-dihydro-1*H*-1,4-benzodiazepine-2,5-dione by a methylene bridge, through C-3 of the former and C-11 of the latter, was evidenced by the COSY correlations of H_2-10 (δ_H 3.57, dd, J = 15.2, 5.5 Hz and 3.26, dd , J = 15.2, 8.3 Hz) to H-11 (δ_H 4.12, dt, J = 8.3, 5.5 Hz), as well as by the HMBC cross peaks of H_2-10 to C-2, C-3 (δ_C 108.0) and C-17 (δ_C 172.0).

A literature search revealed that the compound (3*S*)-3-[1-(3-methylbut-2-enyl)indol-3-yl]-3, 4-dihydro-1*H*-1,4-benzodiazepine-2,5-dione (PubChem SID 185030170), whose flat structure is the same as that of compound **2**, was reported as a product of Angene Chemical (AGN-PC-069E9V) [11]. Although the absolute configuration of its C-11 is reported as *S*, there is neither $^1H/^{13}C$ NMR nor optical rotation data available for this compound in the PubChem Substance website. Since compound **2** did not provide suitable crystals for X-ray diffraction, it was not possible to determine the absolute configuration of C-11 with certainty. Thus, an attempt was made to combine the data from the NOESY spectrum, scalar coupling constants and molecular mechanics simulations.

Table 2. ^{1}H and ^{13}C NMR (DMSO, 300.13 MHz and 75.47 MHz) and HMBC assignment for **2**.

Position	δ_C, Type	δ_H, (*J* in Hz)	COSY	HMBC
2	127.3, CH	7.15, s		C-3, 8, 9
3	108.0, C	-		
4	118.4, CH	7.54, d (7.8)	H-5	C-3, 6, 8
5	119.2, CH	7.08, ddd (7.8, 7.8, 0.7)	H-4, 6	C-7, 9
6	121.7, CH	7.20, ddd (7.8, 7.8, 0.7)	H-5, 7	C-4, 8
7	109.9, CH	7.31, d (7.8)	H-6	C-5, 9
8	136.3, C	-		
9	127.9, C	-		
10	22.4, CH_2	3.57, dd (15.2, 5.5)	H-11	C-2, 3, 17
		3.26, dd (15.2, 8.3)	H-11	C-2, 3, 17
11	52.4, CH	4.12, dt (8.3, 5.5)	H-10, NH-12	
13	168.9, CO	-		
14	125.5, C	-		
15	135.7, C	-		
17	172.0, CO			
18	121.0, CH	7.06, d (8.0)	H-19	C-14, 20
19	133.1, CH	7.50, ddd (8.0, 8.0, 1.5)	H-18, 20	C-15, 21
20	125.2, CH	7.24, dd (8.0, 8.0)	H-19, 21	C-14, 18
21	131.4, CH	7.91, dd (8.0, 1.5)	H-20	C-13, 19, 15
1′	44.2, CH_2	4.63, d (6.8)	H-2′	C-2, 2′, 3′
2′	119.9, CH	5.35, m	H-1′, 4′, 5′	
3′	136.4, C	-		
4′	25.6, CH_3	1.74, s	H-1′, 2′	C-2′, 3′, 5′
5′	18.1, CH_3	1.80, s	H-1′, 2′	C-2′, 3′, 5′
NH-12		7.03, d (5.5)	H-11	
NH-16		9.03, s		C-11, 14

The NOESY spectrum (Supplementary Figure S12) exhibited correlations of H-11 to H-4, NH-12 and NH-16. A stochastic conformational search using MMFF force field models of the C-11 stereoisomers of compound **2**, performed with ChemBio3D Ultra 14.0 using the MMFF force field with application's default parameters [12] showed a somewhat flat energy landscape concerning the spatial relative positions of the two cyclic regions of the molecule. The rotational freedom around the two carbon-carbon single bonds of C-10, on which compound **2** whole conformations hinge, precludes any clear differentiation between the two stereoisomers since both C-11*R* and C-11*S* stereoisomers yield lowest energy conformations that explain the observed NOESY cross-peaks as well as the ^{1}H scalar coupling constants measured. Regardless of the stereoisomer, the gas-phase least energetic conformers of compound **2** show almost equal steric energy for the two major conformations (half-chair) of the amide ring. Figure 4 shows the C-11*R* stereoisomer as an example: (a) H-11 is in the equatorial and (b) H-11 is in the axial position. The major difference resides in the dihedral angle between H-11 and NH-12, which is approximately 0° for the equatorial and 110° for the axial position of H-11 relative to the ring. The observed scalar coupling of 5.5 Hz between the two protons may be interpreted as an average value between their extreme relative positions, suggesting that the two conformations exchange rapidly at room temperature. The observed NOESY correlation between H-11 and NH-16 does not allow

us to positively decide for any of the two amide ring conformations since the distances between the two protons in the molecular mechanics models are very close, *i.e.*, 4.0 Å for the equatorial H-11, and 3.6 Å for the axial H-11. Therefore, the constant exchange between the two conformations of the amide ring is the most probable case.

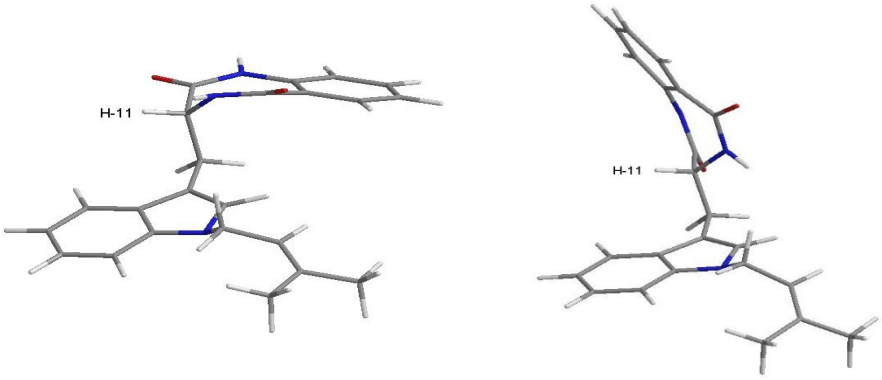

(**a**) (**b**)

Figure 4. Conformations of C-11*R* stereoisomer of compound **2** obtained by simulation performed with ChemBio3D Ultra 14.0; (**a**) conformer with H-11 in equatorial position; (**b**) conformer with H-11 in axial position.

However, the co-occurrence of compound **2** with aszonalenin and acetylaszonalenin in this extract suggested that they should be derived from the same biosynthetic pathways. Thus, it is probable that the absolute configuration of C-11 of compound **2** is the same as that of the corresponding carbons of aszonalenin and acetylaszonalenin, *i.e.*, 11*R*. Thus, compound **2** is a new natural product and we have named it takakiamide.

Compound **3** was isolated as white crystals (mp, 208–209 °C), and its molecular formula $C_{23}H_{21}N_4O_4$ was established on the basis of the $[M + H]^+$ peak at *m/z* 417.1563 (calculated 417.1563) in the (+)-HRESIMS. The ^1H and ^{13}C NMR spectra of compound **3** (Table 3, Supplementary Figures S13 and S15) resembled those of tryptoquivaline L [9]. The ^{13}C NMR, DEPT and HSQC spectra (Table 3, Supplementary Figures S15 and S16) displayed signals of three carbonyls (δ_C 176.0, 170.7, 159.6), four quaternary sp^2 (δ_C 147.5, 139.8, 132.0, 121.4), nine methine sp^2 (δ_C 147.4, 135.0, 131.6, 127.6, 127.3, 126.1, 125.7, 125.7, 116.2), two quaternary sp^3 (δ_C 84.7 and 64.6), two methine sp^3 (δ_C 82.0 and 56.9), one methylene sp^3 (δ_C 31.6) and two methyl (δ_C 26.9 and 26.5) carbons. The ^1H NMR and COSY spectra (Table 3, Supplementary Figures S13 and S14) revealed the presence of two 1,2-disubstituted benzene rings of the *gem*-dimethyl imidazoindolone ring system and quinazolin-4(3*H*)-one moiety as well as the protons of the five-membered spirolactone ring, similar to those of tryptoquivaline L [9]. However, contrary to tryptoquivaline L, H-2 of compound **3** appeared as a doublet at δ_H 5.55 (J = 8.4 Hz) instead of a singlet at δ_H 5.25 [9]. Moreover, the COSY spectrum exhibited a correlation between H-2 signal and a doublet at δ_H 3.76 (J = 8.4 Hz). Consequently, this signal was attributed to NH-16. Interestingly, both CH_3-27 (δ_C 26.5) and CH_3-28 (δ_C 26.9) resonated at higher chemical shift values than their counterparts in tryptoquivaline L (δ_C 16.4 and 22.8) while C-15 exhibited lower chemical shift value (δ_C 64.6) than the corresponding carbon (δ_C 70.0) of tryptoquivaline L [9]. Thus, the only difference between the structure

of compound **3** and that of tryptoquivaline L is the presence of a hydrogen atom on N-16 instead of a hydroxyl group. This was supported by the molecular formula of compound **3** ($C_{23}H_{20}N_4O_4$), which has one oxygen atom less than that of tryptoquivaline L. In order to verify if the stereochemistry of compound **3** is the same as that of tryptoquivaline L, X-ray analysis of compound **3** was performed. The ORTEP diagram of compound **3** (Figure 5) showed unambiguously that the absolute configurations of C-2, C-3 and C-12 are *S*, *S* and *R*, the same as that of the corresponding carbons of tryptoquivaline L. Since compound **3** is a new analog of tryptoquivalines, and in accordance with the names given to the tryptoquivaline series, we have named compound **3** tryptoquivaline U.

Table 3. ^{1}H and ^{13}C NMR (DMSO, 300.13 MHz and 75.47 MHz) and HMBC assignment for tryptoquivaline U (**3**).

Position	δ_C, Type	δ_H, (*J* in Hz)	COSY	HMBC
2	82.0, CH	5.55, d (8.4)	NH-16	C-13, 14
3	84.7, C	-		
4	132.0, C	-		
5	125.7, CH	7.71, d (7.3)	H-6	C-7, 9
6	125.7, CH	7.38, ddd (7.5, 7.5, 1.2)	H-5, 7	C-4, 8
7	131.6, CH	7.57, ddd (8.1, 7.7, 1.2)	H-6, 8	C-5, 9
8	116.2, CH	7.49, d (7.2)	H-7	C-4, 6
9	139.8, C	-		
11	170.7, CO	-		
12	56.9, CH	5.58, dd (10.8, 9.1	H-13	C-3, 11, 13, 18, 26
13	31.6, CH_2	2.86, dd (12.9, 9.1)	H-12	C-2, 4, 11, 12
		3.45, dd (12.9, 11.2)	H-12	C-2, 3, 4, 12
14	176.0, CO	-		
15	64.6, C	-		
16	-	3.76, d (8.4)	H-2	C-2, 3, 14, 15, 26, 27
18	159.6, CO	-		
19	121.4, C	-		
20	126.1, CH	8.23, dd (8.0, 1.2)	H-21	C-18, 22, 24
21	127.6, CH	7.63, ddd (7.6, 7.6, 1.0)	H-20, 22	C-19, 23
22	135.0, CH	7.92, ddd (8.2, 8.2, 1.5)	H-21, 23	C-20, 24
23	127.3, CH	7.76, d (7.7)	H-22	C-19, 21
24	147.5, C	-		
26	147.4, CH	8.49, s		C-12, 18, 24
27	26.5, CH_3	1.45, s		C-14, 15, 28
28	26.9, CH_3	1.24, s		C-14, 15, 27

Since we have previously found that the meroditerpenes aszonapyrone A and sartorypyrone A, isolated from the culture of *N. fischeri* KUFC 6344, exhibited potent antibacterial activity as well as synergism with antibiotics against the Gram-positive multidrug-resistant strains [7], we also evaluated sartorenol (**1**), takakiamide (**2**) and tryptoquivaline U (**3**) for their antibacterial activity against four reference strains (*Staphylococcus aureus*, *Bacillus subtillis*, *Escherichia coli* and *Pseudomonas aeruginosa*), as well as the environmental multidrug-resistant isolates, according to the previously described method [7]. The results showed that none of the tested compounds exhibited relevant antibacterial activity, *i.e.*, their

MIC values are higher than 256 mg/mL. These compounds were also tested for their capacity to inhibit a quorum sensing by the screening protocol based on the pigment production by *Chromobacterium violaceum* ATCC 31532 [13] and none of them showed a quorum sensing inhibitory activity.

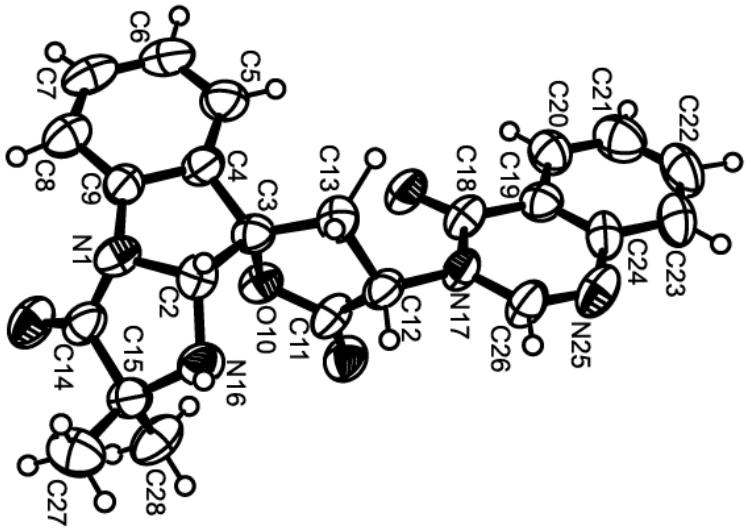

Figure 5. Ortep view of tryptoquivaline U (**3**).

3. Experimental Section

3.1. General Procedure

Melting points were determined on a Bock monoscope and are uncorrected. Optical rotations were measured on an ADP410 Polarimeter (Bellingham + Stanley Ltd., Tunbridge Wells, Kent, UK). Infrared spectra were recorded in a KBr microplate in a FTIR spectrometer Nicolet iS10 from Thermo Scientific (Waltham, MA, USA) with Smart OMNI-Transmission accessory (Software 188 OMNIC 8.3). UV spectra were taken in $CHCl_3$ and were recorded on a Varian CARY 100 spectrophotometer. ^{1}H and ^{13}C-NMR spectra were recorded at ambient temperature on a Bruker AMC instrument (Bruker Biosciences Corporation, Billerica, MA, USA) operating at 300.13 and 75.4 MHz, respectively. High-resolution mass spectra were measured with a Waters Xevo QToF mass spectrometer (Waters Corporations, Milford, MA, USA) coupled to a Waters Aquity UPLC system. A Merck (Darmstadt, Germany) silica gel GF254 was used for preparative TLC, and a Merck Si gel 60 (0.2–0.5 mm) was used for analytical chromatography.

3.2. Extraction and Isolation

The strain KUFC 7898 was isolated from the alga *Amphiroa* sp., which was collected from Samaesarn Island in the Gulf of Thailand, Chonburi Province, in September 2011. The alga was washed with 0.06% sodium hypochlorite solution for 1 min, followed by sterilized seawater three times. The alga was dried on sterile filter paper, cut into small pieces (5 × 5 mm) and placed on a malt extract agar (MEA) medium containing 70% seawater and incubated at 28 °C for 5–7 days. The fungus was identified as *Neosartorya takakii*, by Leka Manoch (Department of Plant Pathology, Faculty of Agriculture, Kasetsart University, Bangkok, Thailand), based on morphological characteristics such as colony growth rate and growth

pattern on standard media, namely Czapek's agar (CZA), Czapek yeast autolysate agar (CYA) and malt extract agar (MEA). Microscopic characteristics including size, shape, ornamentation of ascospores and *Aspergillus takakii* anamorph were examined under light and scanning electron microscopes [14]. This identification was supported by sequence analysis of the β-tubulin, calmodulin and actin genes as described in the previous report [15]. *Neosartorya takakii* was also confirmed by analysis sequence of the internal transcribed spacer (ITS) gene. Briefly, 2–15 mg of mycelia was ground in liquid nitrogen. DNA was extracted using the DNeasy™ Plant Mini Kit (QIAGEN, Hilden, Germany) according to the manufacturer's instructions. The entire nuclear ITS regions were amplified with the primers: ITS1F-5′ [16] and ITS4-3′ [17]. PCR reactions were conducted on Thermal Cycler and the amplification process consisted of initial denaturation at 95 °C for 5 min, 34 cycles at 95 °C for 1 min (denaturation), at 55 °C for 1 min (annealing) and at 72 °C for 1.5 min (extension), followed by final extension at 72 °C for 10 min. PCR products were cleaned using QIAquick PCR Purification Kit (QIAGEN, Hilden, Germany), then examined by Agarose gel electrophoresis (1% agarose with 1× TBE buffer) and visualized under UV light after staining with ethidium bromide. DNA sequencing analyses were carried out by Macrogen Inc. (Seoul, South Korea). The sequences were compared using the NCBI nucleotide BLAST program (http://www.ncbi.nlm.nih.gov/BLAST) for identification [18]. The pure cultures were deposited as KUFC 7898 at Kasetsart University Fungal Collection, Department of Plant Pathology, Faculty of Agriculture, Kasetsart University, Bangkok, Thailand, and also as MMERU 03 at Microbes Marine Environment Research Unit, Division of Environmental Science, Faculty of Science, Ramkhamhaeng University, Bangkok, Thailand.

The fungus was cultured for one week at 28 °C in 10 Petri dishes (i.d. 90 mm) containing 25 mL of MEA with 70% seawater per dish. Fifty 1000 mL Erlenmeyer flasks, each containing rice (200 g), water (30 mL), and seawater (70 mL), were autoclaved, inoculated with five mycelia plugs of *N. takakii* and incubated at 28 °C for 30 days, after which the moldy rice was macerated in ethyl acetate (15 L total) for 10 days and then filtered. The two layers were separated using a separating funnel and the ethyl acetate solution was concentrated under reduced pressure to yield 83.5 g of crude ethyl acetate extract which was dissolved in 500 mL of $CHCl_3$ and then washed with 5% $NaHCO_3$ aqueous solution (2 × 300 mL) and H_2O (3 × 300 mL). The organic layers were combined and dried with anhydrous Na_2SO_4, filtered and evaporated under reduced pressure to give 53.8 g of the crude chloroform extract, which was applied on a column of silica gel (420 g), and eluted with mixtures of petrol–$CHCl_3$ and $CHCl_3$–Me_2CO, 250 mL fractions were collected as follows: Frs 1–40 (petrol–$CHCl_3$, 1:1), 41–82 (petrol–$CHCl_3$, 3:7), 83–197 (petrol–$CHCl_3$, 1:9), 198–321 ($CHCl_3$–Me_2CO, 9:1), and 322–460 ($CHCl_3$-Me_2CO, 7:3). Frs 198–203 were combined (1.57 g) and applied over a column chromatography of silica gel (35 g) and eluted with mixtures of petrol–$CHCl_3$, $CHCl_3$–Me_2CO and Me_2CO, 200 mL sub-fractions were collected as follows; sfrs 1–80 (petrol-$CHCl_3$, 1:1), 81–110 (petrol–$CHCl_3$, 3:7), 111–138 (petrol–$CHCl_3$, 1:9), 139–150 ($CHCl_3$–Me_2CO, 9:1), and 151–154 (Me_2CO). Sfrs 27–33 were combined (80.3 mg) and recrystallized in MeOH to give 26.7 mg of sartorenol (**1**). Sfrs 34–70 were combined (498 mg) and purified by TLC (silica gel G_{254}, $CHCl_3$–Me_2CO–HCO_2H, 9.5:0.5:0.1) to give an additional 18.2 mg of sartorenol (**1**). Sfrs 71–90 were combined (179.0 mg) and purified by TLC (silica gel G_{254}, $CHCl_3$–Me_2CO–HCO_2H, 9.5:0.5:0.1) to give chevalone B (33.6 mg) [7]. Sfrs 91–112 were combined (78.4 mg) and purified by TLC (silica gel G_{254}, $CHCl_3$–Me_2CO–HCO_2H, 9.5:0.5:0.1) to yield additional 2.7 mg of chevalone B. Frs 204–209 were combined (2.08 g) was recrystallized in MeOH to give aszonalenin (586.0 mg) [6],

and the mother liquor was combined with frs 210–212 (1.53 g) and applied over a column chromatography of silica gel (35 g) and eluted with mixtures of petrol–$CHCl_3$, $CHCl_3$–Me_2CO and Me_2CO, wherein 200 mL sub-fractions were collected as follows: sfrs 1–25 (petrol–$CHCl_3$, 1:1), 26–120 (petrol–$CHCl_3$, 3:7). Sfrs 69–105 were combined (150.2 mg) and purified by TLC (silica gel G_{254}, $CHCl_3$–Me_2CO–HCO_2H, 9.5:0.5:0.1) to give 6-hydroxymellein (5 mg) [10]. Frs 213–224 were combined (626 mg) and crystallized in MeOH to give aszonapyraone A (230 mg) [6]. Frs 262–267 were combined (573.4 mg) and purified by TLC (silica gel G_{254}, $CHCl_3$–Me_2CO–HCO_2H, 8:2:0.1) to give 20.5 mg of takakiamide (**2**) and 91.3 mg of acetylaszonalenin [6]. Frs 268–283 were combined (1.03 g) and recrystallized in MeOH to give acetylaszonalenin (115.1 mg). Frs 325–334 were combined (2.95 g) and recrystallized in MeOH to give tryptoquivaline L (0.98 g) [9]. Frs 335–342 were combined (6.06 g) and recrystallized in MeOH to give tryptoquivaline H (259.5 mg) [9]. Frs 343–348 were combined (281 mg) and crystallized in MeOH to give 3′-(4-oxoquinazolin-3-yl) spiro[1*H*-indole-3,5′-oxolane]-2,2′-dione (24.9 mg) [9]. Frs 356–390 were combined (1.15 g) and purified by TLC (silica gel G_{254}, $CHCl_3$–Me_2CO–HCO_2H, 7:3:0.1) to give 16.5 mg of tryptoquivaline U (**3**) and 3.9 mg tryptoquivaline F [9]. Frs 391–400 were combined (125.3 mg) and recrystallized in MeOH to give 8.6 mg of tryptoquivaline F [9].

3.2.1. Satorenol (**1**)

White crystal, Mp 122–123 °C (petrol-$CHCl_3$); $[\alpha]_D^{20}$ −18 (*c* 0.02, $CHCl_3$); λ_{max} (log ε) 228 (4.41), 275 (3.99); IR (KBr) ν_{max} 3393, 2932, 2850, 1728, 1645, 1558, 1540, 1418, 1251 cm^{-1}; ^1H and ^{13}C NMR (see Table 1); HRESIMS *m*/*z* 431.3175 $(M + H)^+$ (calculated for $C_{27}H_{43}O_4$, 431.3161).

3.2.2. Takakiamide (**2**)

White solid, Mp 182–183 °C (petrol/$CHCl_3$); $[\alpha]_D^{20}$ −213 (*c* 0.06, $CHCl_3$); IR (KBr) ν_{max} 3214, 3057, 2924, 2851, 1688, 1654, 1607, 1579, 1481, 1468, 1334, 1255 cm^{-1}; ^1H and ^{13}C NMR (see Table 2); HRESIMS *m*/*z* 374.1876 $(M + H)^+$ (calculated for $C_{23}H_{24}N_3O_2$, 374.1869).

3.2.3. Tryptoquivaline U (**3**)

White crystals, Mp 208–209 °C (petrol/$CHCl_3$); $[\alpha]_D^{20}$ −196 (*c* 0.01, $CHCl_3$); IR (KBr) ν_{max} 3363, 2924, 2852, 1775, 1710, 1662, 1607, 1473, 1384, 1260, 1199 cm^{-1}; ^1H and ^{13}C NMR (see Table 3); HRESIMS 417.1563 $(M + H)^+$ (calculated for $C_{23}H_{21}N_4O_4$, 417.1563).

*3.3. X-Ray Crystal Structure of Sartorenol (**1**)*

Crystals were orthorhombic, space group $P2_12_12_1$, cell volume 2449.73(12) $Å^3$ and unit cell dimensions *a* = 5.99830(16) Å, *b* =13.1349(3) Å and *c* = 31.0931(11) Å (uncertainties in parentheses). There are four molecules per unit cell with calculated density of 1.170 g/cm^{-3}. Diffraction data were collected at 110 K with a Gemini PX Ultra equipped with CuK_α radiation (λ = 1.54184 Å). The structure was solved by direct methods using SHELXS-97 and refined with SHELXL-97 [19]. Carbon and oxygen were refined anisotropically. Hydrogen atoms bound to the carbon atom C20 were placed at their idealized positions using appropriate *HFIX* instructions in SHELXL, and included in subsequent refinement cycles. All other hydrogen atoms were directly found from difference Fourier maps and were refined freely

with isotropic displacement parameters. The refinement converged to *R* (all data) = 9.51% and wR_2 (all data) = 17.76%. Full details of the data collection and refinement and tables of atomic coordinates, bond lengths and angles, and torsion angles have been deposited with the Cambridge Crystallographic Data Centre (CCDC 1060934).

*3.4. X-Ray Crystal Structure of Tryptoquivaline U (**3**)*

Crystals were triclinic, space group P1, cell volume 501.08(12) $Å^3$ and unit cell dimensions *a* = 5.3913(7) Å, *b* =9.8891(15) Å and *c* = 9.9063(13) Å and angles α = 84.939(11)°, β = 75.732(11)° and γ = 78.452(12)° (uncertainties in parentheses). There is one molecule per unit cell with calculated density of 1.380 g/cm^{-3}. Diffraction data were collected at 293 K with a Gemini PX Ultra equipped with CuK_α radiation (λ = 1.54184 Å). The structure was solved by direct methods using SHELXS-97 and refined with SHELXL-97 [16]. Carbon and oxygen were refined anisotropically. Hydrogen atoms bound to carbon atoms C-5, C-6, C-20 and C-23 were placed at their idealized positions using appropriate *HFIX* instructions in SHELXL, and included in subsequent refinement cycles. All other hydrogen atoms were directly found from difference Fourier maps and were refined freely with isotropic displacement parameters. The refinement converged to *R* (all data) = 10.88% and wR_2 (all data) = 30.04%. The absolute structure was established with confidence (flack *x* parameter 0.03(11)). Full details of the data collection and refinement and tables of atomic coordinates, bond lengths and angles, and torsion angles have been deposited with the Cambridge Crystallographic Data Centre (CCDC 1060935).

4. Conclusions

N. takakii has been previously isolated from a soil sample; however, this is the first report of the secondary metabolites from a marine-derived strain of this species. Besides the indole alkaloids aszonalenin; acetylaszonalenin; and tryptoquivalines L, H, and F, and the meroditerpene aszonapyrone A, which are common among the members of this genus, a new tryptoquivaline analog (trytoquivaline U), a new meroditerpene with an uncommon side chain containing an enol function (sartorenol), a prenylated indole alkaloid (takakiamide) and the previously reported isocoumarin derivative (6-hydroxymellein) were also produced by the culture of the marine-derived *N. takakii* KUFC 7898. Although sartorenol, takakiamide and tryptoquivaline U did not exhibit any antibacterial activity against the Gram-positive (*Staphylococcus aureus* ATCC 25923 and *Bacillus subtilis* ATCC 6633) and Gram-negative (*Escherichia coli* ATCC 25922 and *Pseudomonas aeruginosa* ATCC 27853) bacteria as well as methicillin-resistant *S. aureus* (MRSA) and vancomycin-resistant Enterococci (VRE) from the environment in our assay protocol, it does not mean that these new metabolites do not have other interesting biological activities. Thus, these new metabolites should be explored in other bioassay protocols so that their potential can be further discovered.

Acknowledgments

This work was partially supported by the Project MARBIOTECH (reference NORTE-07-0124-FEDER-000047) within the SR&TD Integrated Program MARVALOR—Building research and innovation capacity for improved management and valorization of marine resources, supported by the Programa Operacional Regional do Norte (ON.2—O Novo Norte) and by the European Regional Development Fund, and also by FCT—Fundação para a Ciência e a Tecnologia under the project under the project CEQUIMED-PEst-OE/SAU/UI4040/2014, FEDER funds through the COMPETE program under the project FCOMP-01-0124-FEDER-011057. We thank Michael Lee of the Department of Chemistry, Leicester University (UK) for providing the HRESIMS. W.W. May Zin thanks the Lotus Unlimited Project under the ERASMUS MUNDUS ACTION 2-EU-Asia Mobility Project for a PhD's scholarship. We thank Júlia Bessa and Sara Cravo for technical support.

Author Contributions

War War May Zin and Suradet Buttachon performed isolation, purification and structure elucidation of the compounds; Jamrearn Buaruang performed isolation, identification and cultivation of the fungus as well as preparation of the crude extract; Luís Gales provided X-ray crystallographic data; José A. Pereira performed conformational analysis using ChemBio3D Ultra 14.0; Artur M.S. Silva provided NMR spectra; Madalena M.M. Pinto and Anake Kijjoa conceived and designed the research and wrote the paper.

Conflicts of Interest

The authors declare no conflict of interest.

References

1. Damare, S.; Singh, P.; Raghukumar, S. Biotechnology of Marine Fungi. In *Biology of Marine Fungi*; Raghukumar, C., Ed.; Springer: Heidelberg, Germany, 2012, pp. 277–297.
2. Bugni, T.S.; Ireland, C.M. Marine-derived fungi: A chemically and biologically diverse group of microorganisms. *Nat. Prod. Rep.* **2004**, *21*, 143–163.
3. Saleem, M.; Ali, M.S.; Hussain, S.; Jabbar, A.; Ashraf, M.; Lee, Y.S. Marine natural products of fungal origin. *Nat. Prod. Rep.* **2007**, *24*, 1142–1152.
4. Rateb, M.E.; Ebel, R. Secondary metabolites of fungi from marine habitats. *Nat. Prod. Rep.* **2011**, *28*, 290–344.
5. Fenical W.; Jensen, P R. Marine microorganisms: A new biomedical resource. In *Marine Biotechnology*; Attaway, D.H., Zaborsky, O.R., Eds.; Plenum Press: New York, NY, USA, 1993; Volume 1, pp. 2419–2457.
6. Eamvijarn, A.; Gomes, N.M.; Dethoup, T.; Buaruang, J.; Manoch, L.; Silva, A.; Pedro, M.; Marini, I.; Roussis, V.; Kijjoa, A. Bioactive meroditerpenes and indole alkaloids from the soil fungus *Neosartorya fischeri* (KUFC 6344), and the marine-derived fungi *Neosartorya laciniosa* (KUFC 7896) and *Neosartorya tsunodae* (KUFC 9213). *Tetrahedron* **2013**, *69*, 8583–8591.

7. Gomes, N.M.; Bessa, L.J.; Buttachon, S.; Costa, P.M.; Buaruang, J.; Dethoup, T.; Silva, A.M.S.; Kijjoa, A. Antibacterial and Antibiofilm Activities of Tryptoquivalines and Meroditerpenes Isolated from the Marine-Derived Fungi *Neosartorya paulistensis*, *N. laciniosa*, *N. tsunodae*, and the Soil Fungi *N. fischeri* and *N. siamensis*. *Mar. Drugs* **2014**, *12*, 822–839.
8. Kanokmedhakul, K.; Kanokmedhakul, S.; Suwannatrai, R.; Soytong, K.; Prabpai, S.; Kongsaeree, P. Bioactive meroterpenoids and alkaloids from the fungus *Eurotium chevalieri. Tetrahedron* **2011**, *67*, 5461–5468.
9. Buttachon, S.; Chandrapatya, A.; Manoch, L.; Silva, A.; Gales, L.; Bruyére, C.; Kiss, R.; Kijjoa, A. Sartorymensin, a new indole alkaloid, and new analogues of tryptoquivaline and fiscalins produced by *Neosartorya siamensis* (KUFC 6349). *Tetrahedron* **2012**, *68*, 3253–3262.
10. Shimada, A.; Kusano, M.; Takeuchi, S.; Fujioka, S.; Inokuchi, T.; Kimura, Y. Aspterric acid and 6-hydroxymellein, inhibitors of pollen development in Arabidopsis thaliana, produced by *Aspergillus terreus*. *Z. Naturforsch.* **2002**, *57*, 459–464.
11. PubChem Substance. Available online: http://pubchem.ncbi.nlm.nih.gov/substance/185030170 (accessed on 25 April 2015).
12. Halgren, T.A. Merck molecular force field. I. Basis, form, scope, parameterization, and performance of MMFF94. *J. Comp. Chem.* **1996**, *17*, 490–519.
13. McLean, R.J.C.; Pearson, L.S., III; Fuqua, C. A simple screening protocol for the identification of quorum signal antagonists. *J. Microbiol. Methods* **2004**, *58*, 351–360.
14. Horie, Y.; Abliz, P.; Fukushima, K.; Okada, K.; Gusmão, N.B. *Neosartorya takakii*, a new species from soil in Brazil. *Mycoscience* **2001**, *42*, 91–95.
15. Matsuzawa, T.; Horie, Y.; Abliz, P.; Gonoi, T.; Yaguchi, T. *Aspergillus huiyaniae* sp. nov., a teleomorphic species in sect. Fumigati isolated from desert soil in China. *Mycoscience* **2014**, *55*, 213–220.
16. Gardes, M.; Bruns, T.D. ITS primers with enhanced specificity for Basidiomycetes—Application to the identification of mycorrhizae and rusts. *Mol. Ecol*. **1993**, *2*, 113–118.
17. White, T.J.; Bruns, T.; Lee, S.; Taylor, J. Amplification and direct sequencing of fungal ribosomal RNA genes for phylogenetics. In *PCR Protocols: A Guide to Methods and Applications*; Innis, M.A., Gelfand, D.H., Sninsky, J.J., White; T.J., Eds.; Academic Press: New York, NY, USA, 1990; pp. 315–322.
18. Altschul, S.F.; Madden, T.L.; Schäffer, A.A.; Zhang, J.; Zhang, Z.; Miller, W.; Lipman, D.J. Gapped BLAST and PSI-BLAST: A new generation of protein database search programs. *Nucleic Acids Res*. **1997**, *25*, 3389–3402.
19. Sheldrick, G.M. A short history of SHELX. *Acta Cryst.* **2008**, *A64*, 112–122.

APPENDIX III

Zin, W. W. M., Prompanya, C., Buttachon, S., and Kijjoa, A. **(2016)**. Bioactive secondary metabolites from a Thai collection of soil and marine-derived fungi of the genera *Neosartorya* and *Aspergillus*. *Current Drug Delivery* **13**, 378-388.

.

Current Drug Delivery, 2016, *13*, 378-388

Bioactive Secondary Metabolites from a Thai Collection of Soil and Marine-Derived Fungi of the Genera *Neosartorya* and *Aspergillus*

War War May Zin, Chadaporn Prompanya, Suradet Buttachon and Anake Kijjoa*

ICBAS-Instituto de Ciências Biomédicas Abel Salazar and Interdisciplinary Centre of Marine and Environmental Research (CIIMAR), Universidade do Porto, Rua de Jorge Viterbo Ferreira, 228, 4050-313 Porto, Portugal

A. Kijjoa

Abstract: ***Background***: Fungi are microorganisms which can produce interesting secondary metabolites with structural diversity. Although terrestrial fungi have been extensively investigated for their bioactive secondary metabolites such as antibiotics, marine-derived fungi have only recently attracted attention of Natural Products chemists.

Methods: Our group has been working on the secondary metabolites produced by the cultures of the fungi of the genera *Neosartorya* and *Aspergillus*, collected from soil and marine environments from the tropical region for the purpose of finding new leads for anticancer and antibacterial drugs.

Results: This review covers only the secondary metabolites of four soil and six marine-derived species of *Neosarorya* as well as a new species of marine-derived *Aspergillus*, investigated by our group. In total, we have isolated fifty three secondary metabolites which can be categorized as polyketides (two), isocoumarins (six), terpenoids (two), meroterpenes (fourteen), alkaloids (twenty eight) and cyclic peptide (one). The anticancer and antibacterial activities of these fungal metabolites are also discussed.

Conclusion: Among fifty three secondary metabolites isolated, only the alkaloid eurochevalierine and the cadinene sesquiterpene, isolated from the soil fungus *N. pseudofisheri*, showed relevant *in vitro* cytostatic activity against glioblastoma (U373) and non-small cell lung cancer (A549) cell lines while the meroditerpene aszonapyrone A exhibited strong antibacterial activity against multidrug-resistant Gram-positive bacteria and also strong antibiofilm activity in these isolates.

Keywords: Antibacterial, antibiofilm, anticancer, marine-derived fungi, secondary metabolites, soil fungi.

Received: May 28, 2015 **Revised: July 30, 2015** **Accepted: August 14, 2015**

1. INTRODUCTION

The potential of marine natural products has attracted attention of many researchers in the past few decades. Since the marine environment presents different physical and chemical conditions from the land, it can be an extraordinary reservoir of bioactive compounds, many of which possess unique and interesting structural characteristics which are not found in terrestrial counterparts [1]. Since natural products and their synthetically modified derivatives have been extensively developed for clinical use for the treatment of almost all human diseases, especially in anti-infective and oncology areas, research on chemistry of marine natural products has experienced a tremendous boost due to the need for compounds with bioactivity and possible therapeutic applications [2]. Recently, researchers have focused more of their attention on marine-derived fungi as a source of interesting bioactive compounds since many consider them as one of the still untapped resources for new and biologically relevant chemical entities [3]. Moreover, through established culture methods, they can produce quantity of compounds needed for medicinal chemistry development, clinical trials and even marketing.

On the other hand, the two major important areas of the pharmaceutical industries are anticancer and anti-infective drugs. It is widely recognized that cancer is a constant and major problem of the human population. Since epidemiological evidence shows that current treatment of cancer with chemotherapy and surgery are still far from ideal, more research is necessary to find new drugs that are more effective and have less side-effect than those currently used in chemotherapy as an alternative. One of these approaches is to look for new chemical entities which can be potential for the development of cancer chemotherapeutic agents *via* genetic mining from the marine environment [4]. Since natural products from terrestrial environments and their derivatives have traditionally been a major source of new anticancer agents [5], it is no wonder that marine-derived fungi can be a potential source of anticancer compounds. Curiously, even though fungal metabolites have been found to exhibit a variety of the *in vitro* anticancer properties such as pro-apoptotic, antiproliferative, anti-angiogenic and anti-migratory effects through different pathways, no single fungi-derived compound has been approved as an anticancer drug so far [6].

On the other hand, the infectious diseases are the second major cause of death worldwide and the third leading cause

*Address correspondence to this author at the Instituto de Ciências Biomédicas Abel Salazar, Universidade do Porto, Rua de Jorge Viterbo Ferreira, 228, 4050-313 Porto, Portugal; Tel: ++351-2-2042-8331; Fax: +351-2-204-8090; E-mail: ankijjoa@icbas.up.pt

1875-5704/16 $58.00+.00

of death in developed countries [7]. It is also recognized that more and more bacterial infections cannot be controlled by a current standard treatment, and more often than not, they are very difficult or even impossible to treat. As the resistance to multiple antibiotics is spreading throughout the world, the therapy failure and rising treatment costs, especially in the hospital environment, are becoming a great concern. At the same time, the use of antibiotics is proved to be the cause of resistance development which ultimately limits the efficacy and life span of every antibiotic [8]. Although resistance can be slowed down by using appropriate antibiotic, it will by no means prevent it. Thus, only the continuing discovery and development of new antibiotics can help tackle this problem [8]. Since antibiotics are the third largest segment of the pharmaceutical drug market, it becomes obvious that there is an urgent need for novel antibacterial agents which do not exhibit cross-resistance to the currently used antibiotics. From the evolutionary point of view, natural products are considered as promising lead structures, especially for antibacterial drugs [9]. Microorganisms evolved sustainable defense strategies to modulate competitors and aggressors based on the coevolution of their secondary metabolites with their corresponding targets in bacteria [8]. In this perspective, microorganisms, especially fungi, which successfully produced secondary metabolites as their vital armamentarium in the persistent fight for space and resources against bacterial competitors for millions of years, can be considered as promising target organisms for antibiotics production. Therefore, besides terrestrial fungi, marine-derived fungi can be considered potential source for new antibiotics.

2. THE GENUS NEOSARTORYA

Fungi belonging to the genus *Neosartorya* are a teleomorphic or sexual state of *Aspergillus* section *Fumigati*. While the *Aspergillus* species produce only conidiospores, *Neosartorya* species produce both a sexual state with ascospores, and an asexual state with conidiospores [10]. Recently, this nomenclature has suffered a great extent of modification since the distinct morphological features from fungal sexual stages had let to a dual nomenclature permitting separate names for anamorphs of fungi with a pleomorphic lifecycle, which caused ambiguity regarding the correct and unequivocal taxonomic classification of several fungal species. The fact that an increasing number of mycologists recognizing the urgent need for a transition to a single-name nomenclatural system for fungi had resulted in the preparation of the "Amsterdam Declaration on Fungal Nomenclature", under the auspices of the International Commission on the Taxonomy of Fungi (ICTF) during the symposium "One Fungus = One Name" held in Amsterdam in April 2011 [11]. The discontinuance of the dual nomenclature system was later approved and adopted in the 18th International Botanical Congress in Melbourne in July 2011, during which the Vienna edition of the "International Code of Botanical Nomenclature" was replaced by the "International Code of Nomenclature for algae, fungi and Plants (The Melbourne Code) published in December 2012. According to the Melbourne Code, after 1st January 2013, one fungus can have only one name [11, 12]. Therefore, only the genus name *Aspergillus* is used for both sexual and asexual states after this rule was established. However, the genus name *Neosartorya* is still used for the fungi which had already been taxonomically classified before the new rule was in force. In this case, a teleomorphic state of a new species of *Aspergillus* we have recently isolated was named *Aspergillus similanensis* KUFA 0013 instead of *Neosartorya similanensis*.

3. SECONDARY METABOLITES FROM THE CULTURES OF SOIL AND MARINE-DERIVED STRAINS OF *NEOSARTORYA* AND *ASPERGILLUS*

Aspergillus section *Fumigati* and its teleomorph *Neosartorya* include many important species because they can be pathogenic or allergenic to man as well as causing food spoilage and producing mycotoxins. Certain species are also found to produce interesting bioactive secondary metabolites that can be considered potential for drug development [13]. Although *Aspergillus* species are known to produce several bioactive secondary metabolites including indole alkaloids with unique structural features such as prenylated indole derivatives [14, 15], quinazolinone containing indole derivatives such as the tryptoquivalines [16-21] and pyrazinoquinazolinone containing indole derivatives such as the fumiquinazolines [22, 23], there were only few reports on the studies of secondary metabolites from *Neosartorya* species. For these reasons, together with our interest in bioactive secondary metabolites from microorganisms with potential biotechnological applications, we have investigated four *Neosartorya* species collected from soil in Thailand (*N. glabra* KUFC 6311, *N. pseudofisheri* KUFC 6422, *N. siamensis* KUFC 6349 and *N. fischeri* KUFC 6344) and six marine-derived species of *Neosartorya,* i.e. *N. paulistensis* KUFC 7898 (isolated from a marine sponge *Chondrilla australiensis*), *N. laciniosa* KUFC 7896 (isolated from a diseased coral *Porites lutea*), *N. spinosa* KUFC 8104 (isolated from a marine sponge *Dedronephthya* sp.), *N. tsunodae* KUFC 9213 (isolated from a marine sponge *Aka coralliphaga*), *N. siamensis* KUFA 0017 (isolated from a sea fan *Rumphella* sp.) and *N. takakii* KUFC 7898 (isolated from a marine alga *Amphiroa* sp.), as well as the previously unidentified marine-derived *Aspergillus similanensis* KUFA 0013 (isolated from a marine sponge *Rhabdermia* sp.). The compounds isolated from the cultures of these soil and marine-derived *Neosartorya* species can be categorized into the following classes:

3.1. Polyketides (Fig. 1)

Only two polyketides were isolated from the soil fungi of the genus *Neosartorya* in our investigation. 3'-Hydroxy-5'-methylphenyl-2,4-dihydroxy-6-methylbenzoate (**1**) was isolated from the culture of *N. pseudofisheri* KUFC 6422 [24], while 2,4-dihydroxy-3-methylacetophenone (**2**) was obtained from the ethyl acetate extract of the culture of *N. siamensis* KUFC 6349 [25].

3.2. Isocoumarins (Fig. 2)

Reticulol (**3**) and four new hydroxylated isocoumarins, including 6,8-dihydroxy-3-methylisocoumarin (**4**), similanpyrone A (**5**), similanpyrone B (**6**) and similanpyrone C (**7**) were isolated from the ethyl acetate extract of the culture of *A. similanensis* KUFA 0013, isolated from the marine sponge *Rhabdermia* sp, which was collected from the Similan Islands,

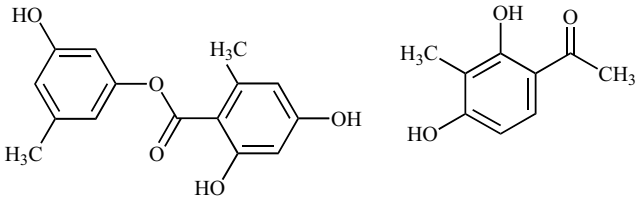

1 **2**

Fig. (1). Structures of 3'-Hydroxy-5'-methylphenyl-2,4-dihydroxy-6-methylbenzoate (**1**) and 2,4-dihydroxy-3-methylacetophenone (**2**).

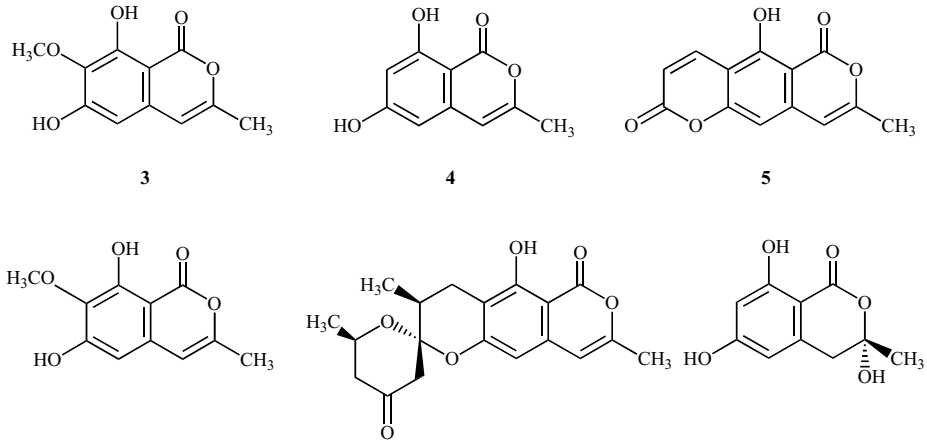

3 **4** **5**

6 **7** **8**

Fig. (2). Structures of isocoumarins isolated from the cultures of *A. similanensis* KUFA 0013 and *N. takakii* KUFC 7898.

in Southern Thailand [26, 27]. The structures of the new compounds were established by an extensive analysis of 1D and 2D NMR (^{1}H, ^{13}C NMR, DEPT, COSY, HSQC, HMBC and NOESY) as well as by High Resolution Mass Spectrometry (HRMS) technique. The ethyl acetate extract of the culture of *N. takakii* KUFC 7898, isolated from a marine alga *Amphiroa* sp., yielded the previously reported 6-hydroxymellein (**8**) [28].

3.3. Terpenoids (Fig. 3)

The cadinene sesquiterpene (**9**) was isolated only from the ethyl acetated extract of the culture of *N. pseudofisheri* KUFC 6422 while the fungal steroid helvolic acid (**10**) was isolated from the cultures of the soil fungus *N. fischeri* KUFC 6344 [24] as well as from the marine-derived *N. tsunodae* KUFC 9213 [29].

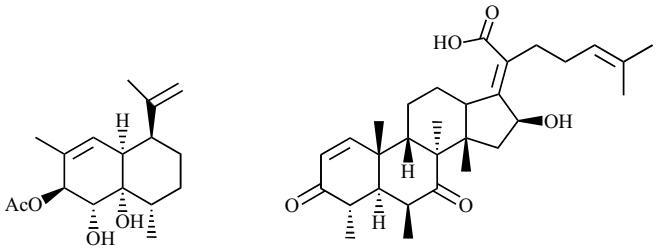

9 **10**

Fig. (3). Structures of cadinene sesquiterpene (**9**) and helvolic acid (**10**).

3.4. Meroterpenoids

3.4.1. Pyripyropenes (Fig. 4)

Pyripyropene A (**11**) was isolated from the culture of *N. pseudofisheri* KUFC 6422 [24]. Pyripyropene E (**12**), two new pyripyropene derivatives: pyripyropenes S and T (**13** and **14**), and a structurally related meroterpene S14-95 (**15**) were isolated from the culture of *A. similanensis* KUFA 0013 [26, 27].

3.4.2. Meroditerpenes (Fig. 5)

Aszonapyrone A (**16**) was isolated from the cultures of *N. fischeri* KUFC 6344 and the marine-derived *N. laciniosa* KUFC 7896 [29] as well as *N. takakii* KUFC 7898 [28], while aszonapyrone B (**17**) was only found in the culture of *N. laciniosa* KUFC 7896 [29]. A new aszonapyrone analog, sartorypyrone C (**18**), was isolated only from the culture of the marine-derived *N. paulistensis* KUFC 7897 [30] Interestingly, while chevalone B (**19**) was isolated from the cultures of both soil (KUFC 6349) and marine-derived *N. siamensis* (KUFA 0017) [25], *N. takakii* KUFC 7898 [28] and *A. similanensis* KUFA 0013 [26], chevalone C (**20**) was found in the cultures of both soil and marine-derived *N. siamensis* (KUFC 6349 and KUFA 0017) and a marine-derived *A. similanensis* KUFA 0013 [26]. While a new chevalone derivative, chevalone E (**21**), was isolated only from the culture of *A. similanensis* KUFA 0013 [26], a new chevalone analog, sartotypyrone B [**23**] was found only in the extract of *N. tsunodae* KUFC 9213 [29]. On the other hand, a new monocyclic meroditerpene, sartorypyrone A (**22**) was isolated from the culture of *N. fischeri* KUFC 6344 [29]. Recently,

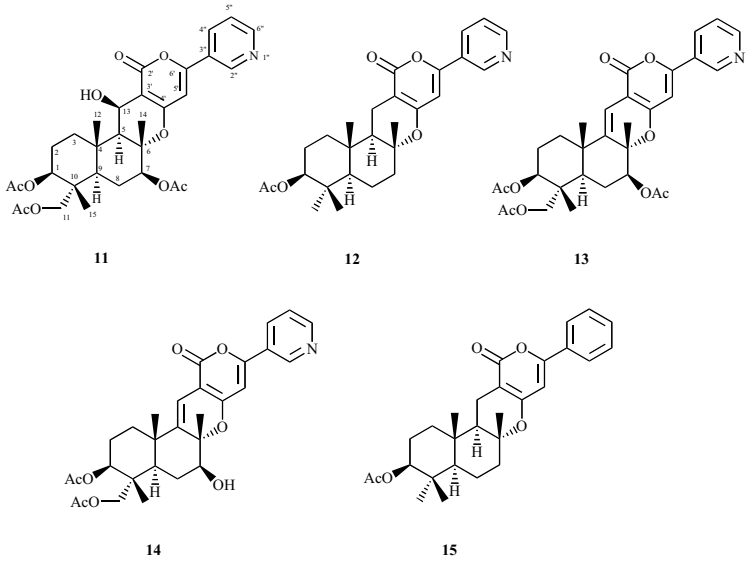

Fig. (4). Structures of pyripyropenes A (**11**), E (**12**), S (**13**), T (**14**) and S14-95 (**15**).

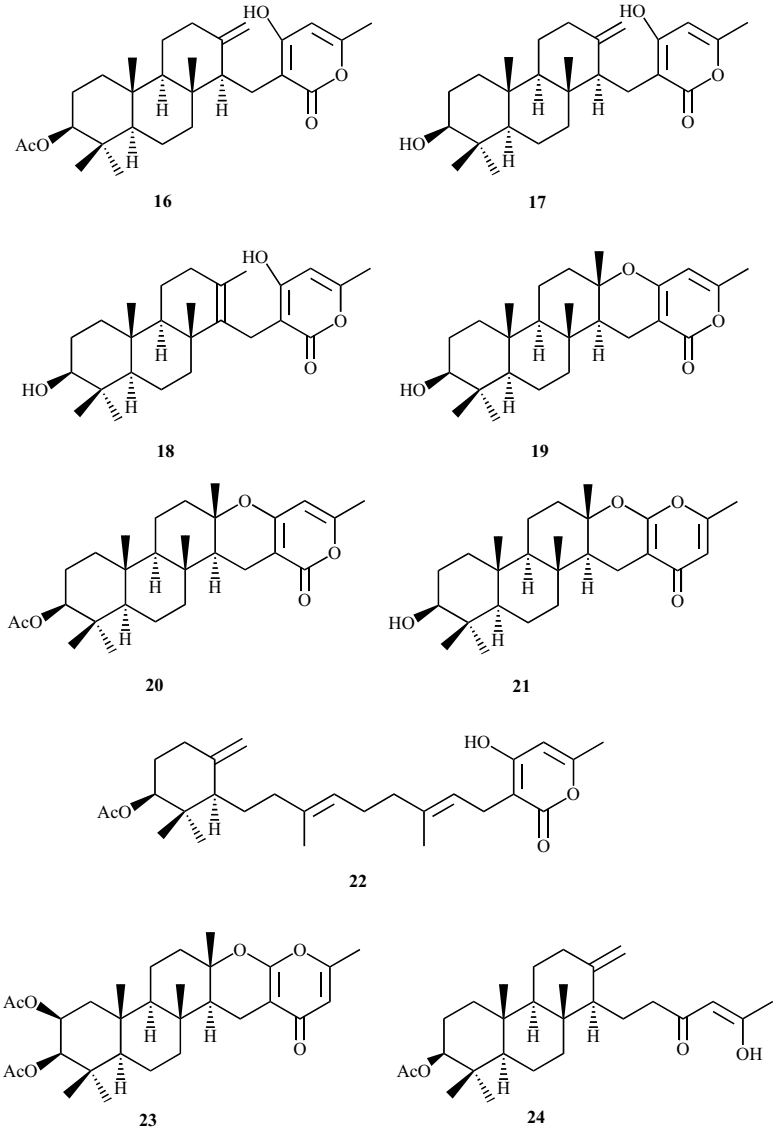

Fig. (5). Structure of meroditerpenes isolated from soil and marine-derived *Neosartorya* species.

we have reported isolation of a new tricyclic meroditerpene with an enolic side chain which we have named sartorenol (**24**) from the culture of the marine-derived *N. takakii* [28].

3.5. Alkaloids

3.5.1. Alkaloids Derived from Phenylalanine (Fig. **6**)

Eurochevalierine (**25**), a sesquiterpene containing alkaloid, previously isolated from the culture of the fungus *Eurotium chevalieri* [31], was isolated together with a previously reported brasiliamide B (**26**) and a new 1,4-diacetyl-2,5-dibenzylpiperazine-3,7"-oxide (**27a** and **27b**) from the culture of *N. pseudofisheri* KUFC 6422 [24]. The conformations of brasiliamide B (**26**) and 1,4-diacetyl-2,5-dibenzylpiperazine-3,7"-oxide (**27a** and **27b**) were studied using the ^{1}H chemical shift values and NOESY correlations [24].

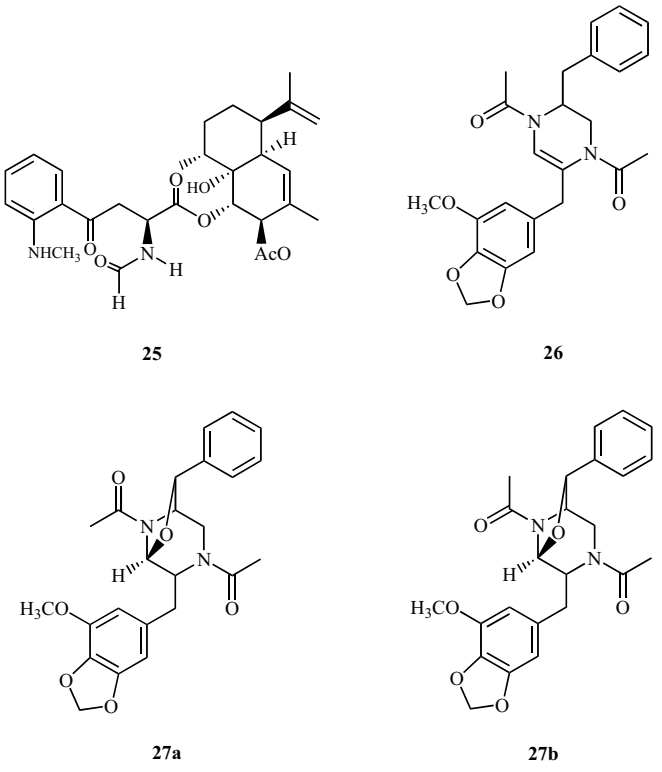

Fig. (6). Structure of eurochevalierine (**25**), brasiliamide B (**26**) and 1,4-diacetyl-2,5-dibenzylpiperazine-3,7"-oxide (**27a** and **27b**).

3.5.2. Prenylated Indole Alkaloids (Fig. **7**)

The culture of *N. fischeri* KUFC 6344 yielded aszonalenin (**28**), acetylaszonalenin (**29**), 1-formyl -5-hydroxyaszonalenin (**30**), and 13-oxofumitremorgin (**31**) [29], while the culture of *N. spinosa* KUFC 8104 furnished aszonalenin (**28**) and acetylaszonalenin (**29**). Aszonalenin (**28**) and acetylaszonalenin (**29**) were also isolated, together with a new natural product takakiamide (**32**), from the culture of *N. takakii* KUFC 7898 [28]. On the other hand, only the culture of *N. glabra* KUFC 6311 produced the ardeemin analogs: sartoryglabrins A (**33**), B (**34**) and C (**35**) [32].

3.5.3. Quinazolinone Containing Indole Alkaloids (Fig. **8**)

The new indole alkaloid pseudofisherine (**36**) was isolated from the culture of *N. pseudofisheri* KUFC 6422 [24]. Although the structure of pseudofisherine (**36**) resembles that of a cytotoxic alkaloid chaetominine, produced by an endophytic fungus *Chaetomium* sp. IFB-E015 [33], the stereochemistry of C-8 and C-15 of pseudofisherine (**36**) is opposite to that of the corresponding carbons of chaetominine. A new hexacyclic indole alkaloid containing a quinazolinone ring system, sartorymensin (**37**), was isolated from the culture of the soil fungus *N. siamensis* KUFC 6349 [25], and the absolute configuration of its stereogenic carbons was determined by X-ray analysis. Interestingly, sartorymensin (**37**) was not detected in the culture of the marine-derived strain of *N. siamensis* KUFA 0017.

3.5.4. Tryptoquivaline Derivatives (Fig. **9**)

Tryptoquivalines are a class of indole alkaloids containing the quinazolinone moiety connected to the *6-5-5* imidazoindolone ring system through a five-membered spirolactone. Several analogs of tryptoquivaline were isolated from both soil and marine-derived *Neosartorya* species. While tryptoquivalines F (**40**) and H (**41**) were found only in the cultures of *N. siamensis* (KUFC 6349 and KUFA 0017), *N. paulistensis* KUFC 7898 [29] and *N. takakii* KUFC 7898 [28], tryptoquivaline L (**42**) was isolated from the cultures of both soil and marine-derived *N. siamensis* (KUFC 6349 and KUFA 0017) [25], *N. paulistensis* KUFC 7898, *N. laciniosa* KUFC 7896 [30], *N. spinosa* KUFC 8104 and *N. takakii* KUFC 7898 [28]. Interestingly, although both soil and marine-derived *N. siamensis* (KUFC 6349 and KUFA 0017) produced tryptoquivaline (**38**) and a new tryptoquivaline derivative, trytoquivaline O (**43**), only the marine strain produced nortryptoquivaline (**39**).

The cultures of *N. laciniosa* KUFC 7896 and *N. takakii* KUFC 7898 also produced new tryptoquivaline analogs, respectively, tryptoquivalines T (**44**) [29] and U (**45**) [28]. A structurally related natural product, 3'-(4-oxoquinazolin-3-yl)spiro [1H-indole-3,5'-oxolane]-2,2'-dione (**46**) was also isolated from the cultures of *N. siamensis* (KUFC 6349 and KUFA 0017) [25], *N. laciniosa* KUFC 7896 [29], *N. spinosa* KUFC 8104 and *N. takakii* KUFC 7898 [28]. The absolute configuration of the stereogenic carbons of the new tryptoquivalines was determined unambiguously by X-ray analysis and the stereochemistry of the previously isolated analogs was also revised by X-ray analysis.

3.5.5. Fiscalin Derivatives (Fig. **10**)

Fiscalins are indole alkaloids with a pyrazinoquinazolinone ring system connected with the *6-5-5* imidazoindolone ring system by a methylene group. The culture of both soil and marine-derived *N. siamensis* (KUFC 6349 and KUFA 0017) were found to produce, besides the previously reported fiscalins A (**47**) and C (**51**), the new analogs *epi*-fiscalin A (**48**), neofiscalin A (**49**), *epi*-neofiscalin A (**50**) and *epi*-fiscalin C (**52**) [25]. The stereochemistry of the stereogenic carbons (C-3, C-14, C-19, C-20, and C-22) of these compounds was unequivocally established by X-ray analysis.

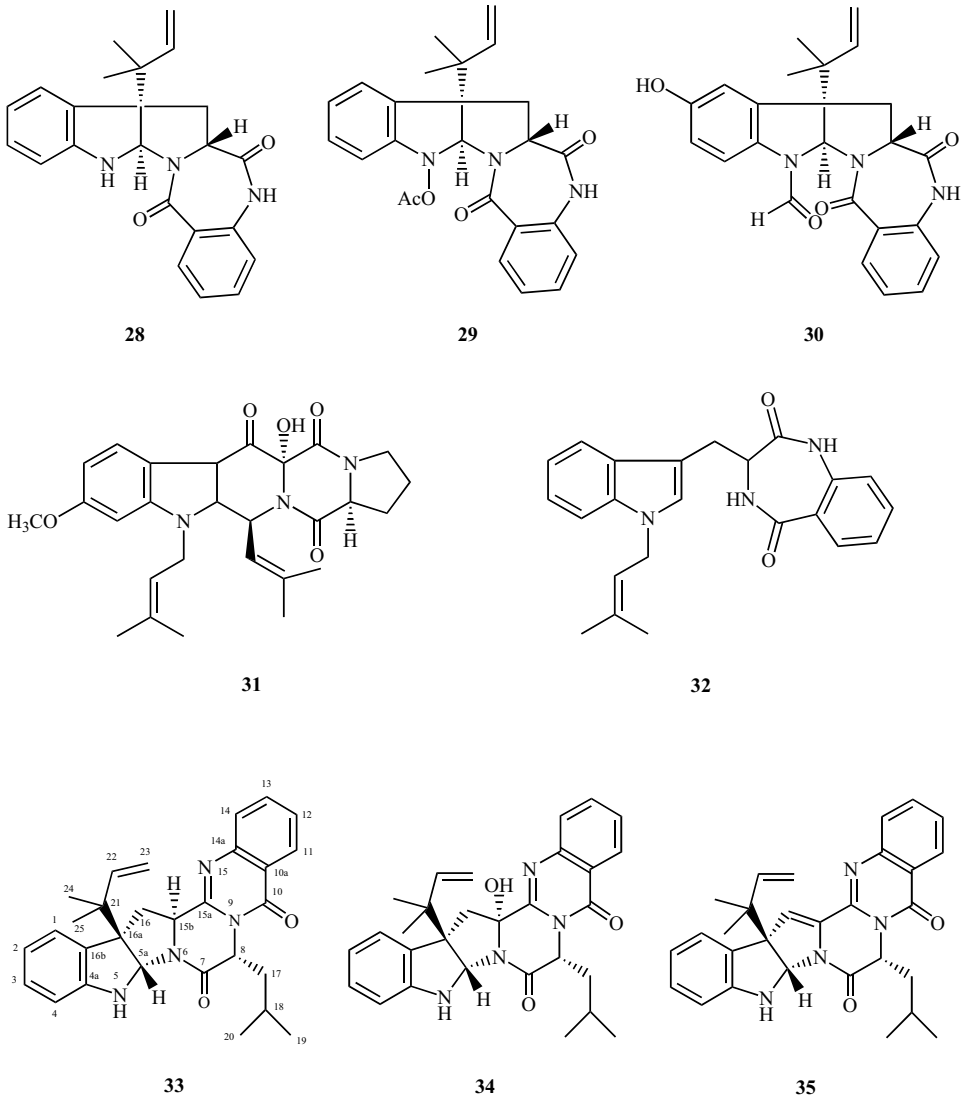

Fig. (7). Structures of the prenylated indole alkaloids aszonalenin (**28**), acetylaszonalenin (**29**), 1-formyl -5-hydroxyaszonalenin (**30**), 13-oxofumitremorgin (**31**), takakiamide (**32**) and sartoryglabrins A (**33**), B (**34**) and C (**35**).

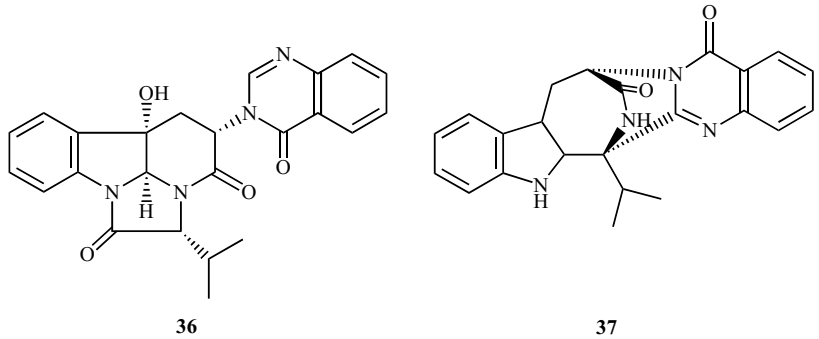

Fig. (8). Structures of the quinazolinone containing indole alkaloids pseudofisherine (**36**) and sartorymensin (**37**).

3.6. Cyclopeptides (Fig. 11)

Similanamide (**53**), a new cyclic hexapeptide, was isolated from the culture of *A. similanensis* KUFA 0013 [27]. The structure of the compound was determined, by HRMS and extensive analysis of their 1D and 2D NMR as well as by a chiral HPLC analysis of the acid hydrolysate by co-injection with D and L amino acids standards, as *cyclo* (anthranilic acid-L-Val-D-Leu-L-Ala-*N*-methyl-L-Leu-D-pipecolic acid).

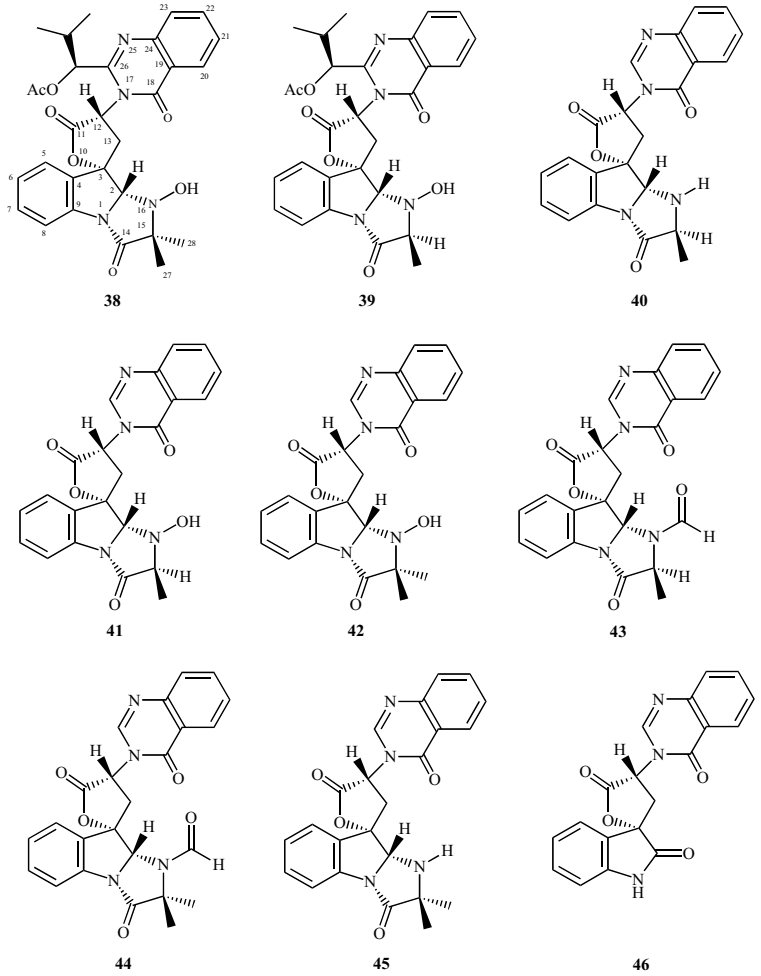

Fig. (9). Structures of tryptoquivaline derivatives.

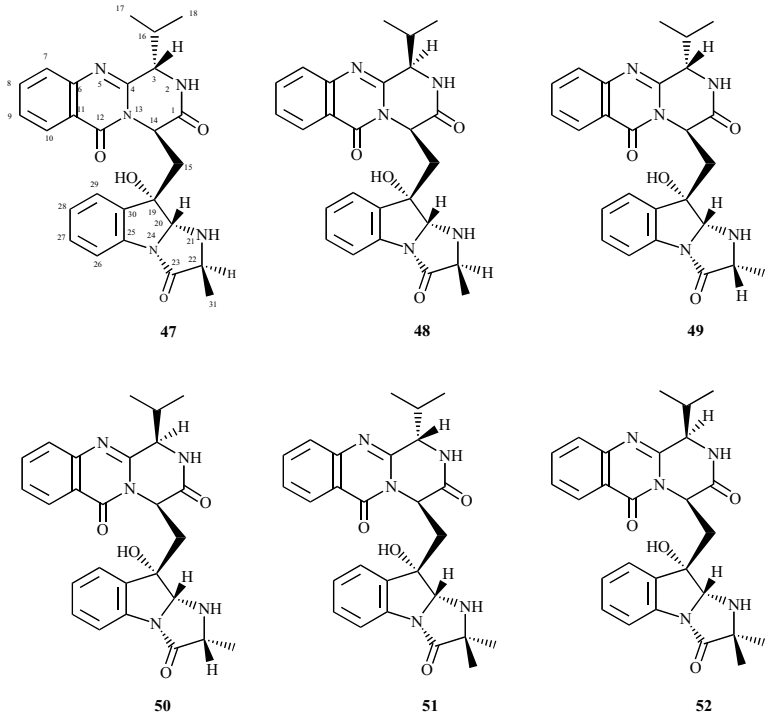

Fig. (10). Structure of fiscalin derivatives.

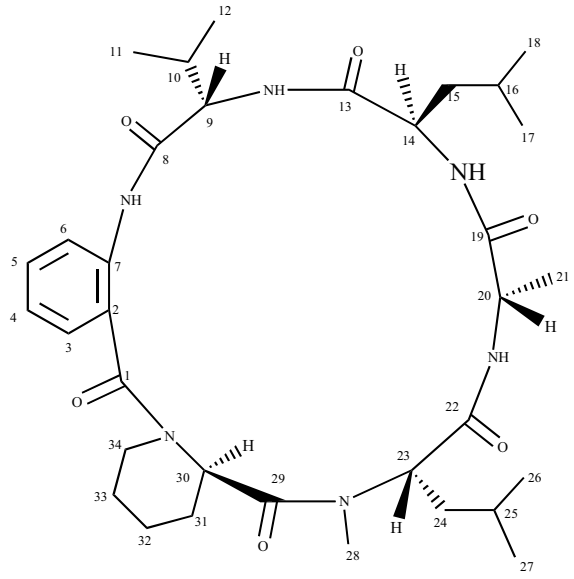

53

Fig. (11). Structure of similanamide (**53**).

4. BIOLOGICAL ACTIVITIES

Although the secondary metabolites isolated from the fungi of the genera *Neosartorya* and *Aspergillus* exhibited a myriad of biological and pharmacological activities, we have evaluated only their capacity to inhibit *in vitro* growth of some human cancer cell lines, as well as antibacterial activity since the main goal of our research is to search for lead compounds for anticancer and antibacterial drugs.

4.1. Anticancer Activity

The fact that 15b-β-hydroxy-5-*N*-acetylardeemin, an ardeemin analog isolated from the fungus *Aspergillus fischeri* var. *brasiliensis*, was able to reverse multiple drug resistance in tumor cells [34-36], together with the similarity of the structures of sartoryglabrins A (**33**), B (**34**), and C (**35**), isolated from the culture of *N. glabra* KUFC 6311, with those of the ardeemins, has motivated us to evaluate the *in vitro* growth inhibitory activity of sartoryglabrins A (**33**), B (**34**), and C (**35**) against the MCF-7 (breast adenocarcinoma), NCI-H460 (non-small cell lung cancer) and A375-C5 (melanoma) human tumor cell lines by using the protein binding dye SRB method. Sartoryglabrin A (**33**) was found to exhibit a strong growth inhibitory activity against MCF-7 cell line (GI_{50} = 27.0 ± 0.57 μM) and a weak activity against NCI-H460 cell line (GI_{50} = 84.0 ± 2.1 μM) but inactive against the A375-C5 cell line, at the highest concentration tested (GI_{50} >150 μM). On the contrary, sartoryglabrin B (**34**) exhibited a moderate growth inhibitory activity against MCF-7 cell line (GI_{50} = 53.0 ± 4.7 μM), but inactive (GI_{50} >150 μM) against both NCI-H460 and A375-C5 cell lines. These results suggested that sartoryglabrin B (**34**) was not cytotoxic since it was only active against the MCF-7 cell line. Therefore, sartoryglabrin B (**34**) may be considered as an interesting scaffold for further anticancer drug development [32]. On the other hand, sartoryglabrin C (**35**) exhibited moderate growth inhibitory activity against MCF-7 cell line (GI_{50} = 44.0 ± 7.2 μM) and weak inhibitory activity against NCI-H460 (GI_{50} = 82.3 ± 5.6 μM) and A375-C5 (GI_{50} = 108.0 ± 7.7 μM) cell lines [32].

3”-Hydroxy-5’-methylphenyl-2,4-dihydroxy-6-methylbenzoate (**1**), the cadinene sesquiterpene (**9**), pyripyropene A (**11**), and the alkaloids eurochevalierine (**25**), 1,4-diacetyl-2,5-dibenzylpiperazine-3,7”-oxide (**27a** and **27b**) and pseudofischerine (**36**), isolated from the culture of the soil fungus *N. pseudofisheri* KUFC 6422, were assayed, together with the the widely used anticancer drugs etoposide and carboplatin, for their growth inhibitory activity against six human cancer cell lines, i.e. Hs683 (glioblastoma), U373 (glioblastoma), A546 (non-small cell lung cancer), MCF-7 (breast cancer), OE21 (esophageal cancer), SKMEL28 (melanoma), by the MTT colorimetric method [24]. Interestingly, eurochevalierine (**25**) was found to have an *in vitro* anticancer activity in the range of etoposide and carboplatin while the cadinene sesquiterpene (**9**), whose activity was similar to carboplatin, was found to be less active than eurochevalierine (**25**). On the contrary, pyripyropene A (**11**), 1,4-diacetyl-2,5-dibenzylpiperazine-3,7”-oxide (**27a** and **27b**) and pseudofischerine (**36**) were inactive in all cell lines at the highest concentration tested. Furthermore, observation of the global cell growth by the computer-assisted phase-contrast microscopy, over a 72 hours period, revealed that 50 μM of eurochevalierine (**25**) was able to reduce growth of the human glioblastoma cells (U373) by 65% and of the non-small cell lung cancer cells (A549) by 50%. These data revealed that eurochevalierine (**25**) is not cytotoxic, but instead cytostatic which was able to overcome the intrinsic resistance of the two cancer cell lines to pro-apoptotic stimuli. Moreover, the lack of cytotoxicity of eurochevalierine (**25**) was also confirmed by flow cytometry analysis. Contrary to the positive control narciclasine which induced marked pro-apoptotic effects in human apoptosis-sensitive PC-3 prostate cancer cells, eurochevalierine (**25**) did not exhibit any pro-apoptotic effects in the human U373 glioblastoma and A549 non-small cell lung cancer cells. Furthermore, flow cytometry analysis also demonstrated that eurochevalierine (**25**) did not modify cell cycle kinetic such as distribution of cells into the G1, S and G2 phases of the cell cycle of these two cell lines. Additionally, determination of the percentages of mitosis under control and treatment with eurochevalierine (**25**) by quantitative videomicroscopy revealed that treatment with eurochevalierine (**25**) caused a significant decrease in the percentage of the mitotic cells in both human U373 glioblastoma and A549 non-small cell lung cancer cells. Therefore, we have concluded that the inhibition of mitotic rates by eurochevalierine (**25**) was responsible for its cytostatic effects [24].

Similarly, the indole alkaloids sartorymensin (**37**), tryptoquivaline (**38**), tryptoquivalines F (**40**), H (**41**), L (**42**), O (**43**), and 3’-(4-oxoquinazolin-3-yl) spiro [1H-indole-3,5’-oxolane]-2,2’-dione (**46**), isolated from the culture of *N. siamensis* KUFC 6349, were evaluated for their *in vitro* growth inhibitory activity on the human U373 and Hs683 glioblastoma, the A549 non-small cell lung cancer, the MCF-7 breast cancer, and the SKMEL-28 melanoma cell lines by MTT colorimetric assay [25]. However, only sartorymensin (**37**)

exhibited moderate *in vitro* growth inhibitory activity on these five cancer cell lines with the mean of IC_{50} = 44 μM [25].

The prenylated indole alkaloids aszonalenin (**28**), acetylaszonalenin (**29**), 1-formyl-5-hydroxyaszonalenin (**30**), and 13-oxofumitremorgin (**31**), isolated from the culture of *N. fisheri* KUFC 6344, were also evaluated for their *in vitro* growth inhibitory activity on the MCF-7 (breast adenocarcinoma), NCI-H460 (non-small cell lung cancer) and A375-C5 (melanoma) human tumor cell lines by the protein binding dye SRB method. Although 13-oxofumitremorgin (**31**) exhibited a weak growth inhibitory activity against all the three cell lines, with GI_{50}= 115.0 ± 20.0 μM, 123.3 ± 11.5 μM, 68.6 ± 12.9 μM, respectively, for MCF-7, NCI-H460 and A375-C5, aszonalenin (**28**), acetylaszonalenin (**29**) and 1-formyl -5-hydroxyaszonalenin (**30**) were inactive in all the cell lines at the highest concentration tested (>150 μM) [29].

The meroditerpenes aszonapyrones A (**16**) and B (**17**), isolated from the culture of *N. laciniosa* KUFC 7896, as well as sartorypyrone B (**23**), isolated from the culture of *N. tsunodae* KUFC 9213, were also assayed for their *in vitro* growth inhibitory activity against MCF-7, NCI-H460 and A375-C5 human tumor cell lines by the protein binding dye SRB method. Aszonapyrone A (**16**) was found to be the most active, showing strong growth inhibitory activity against the three cell lines, with GI_{50}= 13.6 ± 0.9 μM, 11.6 ± 1.5 μM, 10.2 ± 1.2 μM, respectively for MCF-7, NCI-H460 and A375-C5, while sartorypyrone B (**23**), which possesses a monocyclic diterpene core, also exhibited strong growth inhibitory activity, although less than that of aszonapyrone A (**16**), with GI_{50}= 17.8 ± 7.4 μM, 20.5 ± 2.4 μM and 25.0 ± 4.4 μM, for MCF-7, NCI-H460 and A375-C5 respectively. Interestingly, aszonapyrone B (**17**) whose structure corresponds to 3-deacetyl aszonapyrone A, was inactive in all the cell lines at the highest concentration tested [29].

4.2. Antibacterial Activity

The meroditerpenes aszonapyrones A (**16**) and B (**17**), chevalones B (**19**), C (**20**) and E (**21**), sartorypyrones A (**22**), B (**23**), and C (**18**), together with pyripyropenes E (**12**) and S (**13**), S14-95 (**15**), tryptoquivalines F (**40**), H (**41**), L (**42**) and 3'-(4-oxoquinazolin-3-yl) spiro[1H-indole-3,5'-oxolane]-2,2'-dione (**46**), were tested for antibacterial activity against Gram-positive (*Staphylococcus aureus* ATCC 25923 and *Bacillus subtilis* ATCC 6633) and Gram-negative (*Escherichia coli* ATCC 25922 and *Pseudomonas aeruginosa* ATCC 27853) bacteria, as well as the multidrug-resistant isolates from the environment [30]. Neither of the indole alkaloids, i.e. tryptoquivalines F (**40**), H (**41**), L (**42**) and 3'-(4-oxoquinazolin-3-yl) spiro[1H-indole-3,5'-oxolane]-2,2'-dione (**46**), nor pyripyropene derivatives exhibited antibacterial activity. However, within the meroditerpene group, only aszonapyrone A (**16**) and sartorypyrone A (**22**) showed significant MIC values against Gram-positive bacteria. While aszonapyrone A (**16**) showed the MIC values of 8 μg/mL against *S. aureus* ATCC 25923 and *B. subtilis* ATCC 6633, sartorypyrone A (**22**) showed the MIC values of 32 and 64 μg/mL, respectively against both reference strains. Moreover, aszonapyrone A (**16**) was also active against both *S. aureus* MRSA and *Enterrococcus* spp. VRE isolates. On the contrary, sartorypyrone A (**22**) was not active against both strains in the range of concentrations tested [30].

Synergism study by the disc diffusion method revealed that there was a small synergistic association between all the compounds tested and the antibiotics to which a multidrug-resistant *E. coli* was resistant. However, only few compounds showed synergism against the *S. aureus* MRSA and *E. faecium* VRE isolates. It was observed that only the combination of aszonapyrone A (**16**) with the antibiotics produced the biggest halo, while sartorypyrone A (**22**) only showed an increase in the inhibition halo of the antibiotics against *S. aureus* MRSA, and, in a small extent, against *E. faecium* VRE. Curiously, both chevalones C (**20**) and E (**21**) were found to display a synergistic effect with antibiotic against the multidrug-resistant isolates in spite of the fact that they did not exhibit antibacterial activity at the highest concentration tested (MIC > 256 μg/mL) when tested alone. By using the Checkerboard method [37] to evaluate the synergistic effect of aszonapyrone A (**16**) and sartorypyrone A (**22**) with the antibiotics, it was found that the combination effect of aszonapyrone A (**16**) with oxacillin against MRSA isolates, as well as with ampicillin against VRE isolates, was not different (ΣFIC > 0.5). Since aszonapyrone A (**16**) was found to decrease the MIC of each antibiotic tested, it may be considered to exert partial synergism. On the contrary, the association of aszonapyrone A (**16**) with vancomycin displayed clearly the synergistic effect (ΣFIC < 0.5) against the VRE isolates tested. It was found also that the combination of sartorypyrone A (**22**) with oxacillin and ampicillin against MRSA isolates was also indifferent (ΣFIC > 0.5).

Using the biomass quantification method [38] to evaluate the effect of aszonapyrone A (**16**) and sartorypyrone A (**22**), at different concentrations, on the biofilm formation of *S. aureus* ATCC 25923, *B. subtilis* ATCC 6633, *S. aureus* MRSA and *E. faecalis* VRE, revealed that no biofilm was formed in all the tested strains in the presence of aszonapyrone A (**16**) and sartorypyrone A (**22**) at 2 x MIC and MIC concentrations. However, it was found that both *S. aureus* ATCC 25923 and *S. aureus* MRSA produced more biofilm than in the control in the presence of aszonapyrone A (**16**) at a sub-inhibitory concentration, i.e. 1/2 x MIC. Interestingly, in the presence of sartorypyrone A (**22**) at 1/2 x MIC, a significantly higher amount of biofilm was produced by *S. aureus* ATCC 25923 than in the control.

The results obtained revealed that the antibacterial activity of the meroditerpenes tested is related to their structural features. For this series of meroditerpenes, the presence of a free 4-hydroxy-6-methyl-2*H*-pyran-2-one ring on C-15 as well as of the β-acetoxyl group on C-4 of the perhydrophenanthrene ring system is required for their antibacterial activity [30].

The isocoumarins reticulol (**3**), 6, 8-dihydroxy-3-methylisocoumarin (**4**), similanpyrone A (**5**), similanpyrone B (**6**) and similanpyrone C (**7**), together with the cyclohexapeptide similanamide (**53**), isolated from the culture of *A. similanensis* KUFA 0013, were also tested for their antibacterial activity. However, none of these compounds was found to exhibit any significant activity on the reference and multidrug-resistant strains of bacteria at the highest concentration tested [26, 27].

CONCLUSION

Soil and marine-derived fungi continue to be an important source of interesting secondary metabolites with unique structural feature. Although the terrestrial fungi have been more intensively investigated for their bioactive secondary metabolites, the marine-derived counterparts have just recently emerged as an interesting source of bioactive compounds. Fungi of the genera *Neosartorya* and *Aspergillus* continue to be a prolific source of bioactive secondary metabolites. With new culture methods and advancement in biotechnology techniques, these fungi can be a very promising source for biotechnological applications. Although many of the secondary metabolites isolated from the fungi of these genera, both terrestrial and marine strains, exhibited neither the *in vitro* growth inhibitory activity on the human cancer cell lines nor antibacterial activities in our test systems, it is by no means to conclude that these compounds do not have other interesting biological functions. Thus, it is necessary to test these compounds in more bioassay systems so that their potential can be duly exploited.

CONFLICT OF INTEREST

The authors confirm that this article content has no conflict of interest.

ACKNOWLEDGEMENTS

This work was partially supported by Structured Program of R&D&I INNOVMAR - Innovation and Sustainability in the Management and Exploitation of Marine Resources, reference NORTE-01-0145-FEDER-000035, Research Line NOVELMAR – Novel marine products with biotechnological applications, supported by the Northern Regional Operational Programme (NORTE2020), through the European Regional Development Fund (ERDF).

PATIENT CONSENT

Declared none.

REFERENCES

[1] Kijjoa, A.; Sawangwong, P. Drugs and cosmetics from the sea. *Mar. Drugs*, **2004**, *2*, 73-82.

[2] Montaser, R., Luesch, H. Marine natural products: a new wave of drugs? *Fut. Med Chem.*, **2011**, *3*, 1475-1489.

[3] Rateb, M.E.; Ebel, R. Secondary metabolites of fungi from marine habitats. *Nat. Prod. Rep*., **2011**, *28*, 290-344.

[4] Indumathy, S.; Dass, C. R. Finding chemo: the search for marine-based pharmaceutical drugs active against cancer. *J. Pharm. Pharmacol.*, **2013**, *65*, 1280-1301.

[5] Bhanot, A.; Sharma, R. Noolvi, M. N. Natural sources as potential anti-cancer agents: A review. *Int. J. Phytomed.*, **2001**, *3*, 9-26.

[6] Evidente, A.; Kornienko, A.; Cimmino, A.; Andolfi, A.; Florence Lefranc, F.; Mathieu, V.; Kiss, R. Fungal metabolites with anticancer activity. *Nat. Prod. Rep*.**, 2014**, *31*, 617-627.

[7] Nathan, C. Antibiotics at the crossroads. *Nature*, **2004**, *431*, 899-902.

[8] Von Nussbaum, F.; Brands, M.; Hinzen, B.; Weigand, S., Häbich, D. Antibacterial natural products in medicinal chemistry-exodus or revival. *Angew. Chem. Int. Ed*., **2006**, 5072-5129.

[9] Firn, R.D.; Jones, C. G. Natural products – a simple model to explain chemical diversity. *Nat. Prod. Rep*., **2003**, *20*, 382-391.

[10] Frisvad, J.C.; Rank, C.; Nielsen, K. F.; Larsen, T.O. Metabolomics of *Aspergillus fumigatus*. *Med. Mycol*., **2009**, *47*, S53-S71.

[11] Hawkswoth, D. L. A new dawn for the naming of fungi: impacts of decisions made in Melbourne in July 2011 on the future publication and regulation of fungal names. *MycoKeys*, **2011**, *1*, 7-20.

[12] McNeill, J.; Turland, N. J.; Anna M. Monro, A. M.; Brendan J. Lepschi, B. J. XVIII International Botanical Congress: Preliminary mail vote and report of congress action on nomenclature proposals. *Taxon.*, **2011**, *60*, 1507-1520.

[13] Hong, S-B.; Shin, H-D.; Hong, J.; Jens C. Frisvad, Per V. Nielsen, János Varga, Robert A. Samson. New taxa of *Neosartorya* and *Aspergillus* in *Aspergillus* section Fumigati. *Anton. Leeuwen.*, **2008**, *93*, 87-98.

[14] Li, S.M. Prenylated indole derivatives from fungi: structure diversity, biological activities, biosynthesis and chemoenzymatic synthesis. *Nat. Prod. Rep*., **2010**, *27*, 57-78.

[15] Ge, H. M.; Peng, H.; Guo, Z.K.; Cui, J. T.; Song, Y. C.; Tan, R. X. Bioactive alkaloids from the plant endophytic fungus *Aspergillus terreus*. *Planta Med*., **2010**, *76*, 822-824.

[16] Clardy, J.; Springer, J. P.; Büchi, J.; Matsuo, K.; Wightman, R. J. Tryptoquivaline and tryptoquivalone, two tremorgenic metabolites of *Aspergillus clavatus*. *Am. Chem. Soc*., **1975**, *97*, 663-665.

[17] Büchi, J.; Luk, K. C.; Kobbe, B.; Townsend, J. M. Four new mycotoxins from *Aspergillus clavatus* related to tryptoquivaline. *J. Org. Chem*., **1977**, *42*, 244-246.

[18] Yamazaki, M.; Fujimoto, H.; Okuyama, E. Structure of tryptoquivaline C (FTC) and D (FTD). Novel fungal metabolites from *Aspergillus fumigatus Chem. Pharm. Bull*., **1977**, *25*, 2554-2560.

[19] Yamazaki, M.; Fujimoto, H.; Okuyama, E. Structure determination of six fungal metabolites, tryptoquivaline E, F, G, H, I and J from *Aspergillus fumigatus Chem. Pharm. Bull*., **1978**, *26*, 111-117.

[20] Yamazaki, M.; Okuyama, E.; Maebayashi, Y. Isolation of some new tryptoquivaline-related metabolites from *Aspergillus fumigatus*. *Chem. Pharm. Bull*., **1979**, *27*, 1611-1617.

[21] Springer, J. P. The absolute configuration of nortryptoquivaline. *Tetrahedron Lett.*, **1979**, *4*, 339-342.

[22] Numata, A.; Takahashi, C.; Matsushita, T.; Miyamoto, T.; Kawai, K.; Usami, Y.; Matsumura, E.; Inoue, M.; Ohishi, H.; Shingu, T. Fumiquinazolines, novel metabolites of a fungus isolated from a saltfish. *Tetrahedron Lett.,* **1992**, *33*, 1621-1624.

[23] Takahashi, C.; Matsushita, T.; Doi, M.; Minoura, K.; Shingu, T.; Kumeda, Y.;Numata, A. Fumiquinazolines A–G, novel metabolites of a fungus separated from a *Pseudolabrus* marine fish. *J. Chem. Soc., Perkin Trans.,* **1995**, *1*, 2345-2353.

[24] Eamvijarn, A.; Kijjoa, A.; Bruyère, C.; Mathieu, V.; Manoch, L.; Lefranc, F.; Silva, A.; Kiss, R., Herz, W. Secondary metabolites from a culture of the fungus *Neosartorya pseudofischeri* and their *in vitro* cytostatic activity in human cancer cells. *Planta Med*., **2012**, *78*, 1767-1776.

[25] Buttachon, S.; Chandrapatya, A.; Manoch, L.; Silva, A.; Gales, L.; Bruyére, C., Kiss, R.; Kijjoa, A. Sartorymensin, a new indole alkaloid, and new analogues of tryptoquivaline and fiscalins produced by *Neosartorya siamensis* (KUFC 6349). *Tetrahedron*, **2012**, *68*, 3253-3262.

[26] Prompanya, C.; Dethoup, T.; Bessa, L. J.; Pinto, M. M. M.; Gales, L.; Costa, P. M.; Silva, A.M. S.; Kijjoa, A. New isocoumarin derivatives and meroterpenoids from the marine sponge-associated fungus *Aspergillus similanensis* sp. nov. KUFA 0013. *Mar. Drugs*, **2014**, *12*, 5160-5173.

[27] Prompanya, C.; Fernandes, C.; Cravo, S.; Pinto, M.M.M., Dethoup, T.; Artur, M.S. Silva, A.M.S.; Kijjoa, A.; A new cyclic hexapeptide and a new isocoumarin derivative from the marine sponge-associated fungus *Aspergillus similanensis* KUFA 0013. *Mar. Drugs*, **2015**, *13*, 1432-1450.

[28] Zin, W.W.M.; Buttachon, S., Buaruang, J., Gales, L.; Pereira, J.A., Pinto, M.M.M.; Silva, A.M.S.; Kijjoa, A. A new meroditerpene and a new tryptoquivaline analog from the algicolous fungus *Neosartorya takakii* KUFC 7898. *Mar. Drugs*, **2015**, *13*, 3776-3790.

[29] Eamvijarn, A.; Gomes, N. M.; Dethoup, T.; Buaruang, J.; Manoch,L.; Silva, A.; Pedro, M., Ioulia Marini, Roussis, V.; Kijjoa, A. Bioactive meroditerpenes and indole alkaloids from the soil fungus *Neosartorya fischeri* (KUFC 6344) and the marine-derived fungi *Neosartorya laciniosa* (KUFC 7896) and *Neosartorya tsunodae* (KUFC 9213). *Tetrahedron*, **2013**, *69*, 8583-8591.

[30] Gomes, N. M.; Bessa, L. J.; Buttachon, B.; Costa, P. M.; Buaruang, J.; Dethoup, T.; Silva, A.M.S.; Kijjoa, A. Antibacterial and antibiofilm activity of tryptoquivalines and meroditerpenes from marine-deived fungi *Neosartorya paulistensis, N. laciniosa*, N. *tsunodae*, and the soil fungi *N. fischeri* and *N. siamensis*. *Mar. Drugs*, **2014**, *12*, 822-839.

[31] Kanokmedhakul, K.; Kanokmedhakul, S.; Suwannatrai, R., Soytong, K., Prabpai, S., Kongsaeri, P. Bioactive meroterpenoids and alkaloids from the fungus *Eurotium chevalieri*. *Tetrahedron*, **2011**, *67*, 5461-5468.

[32] Kijjoa, A.; Santos, S.; Dethoup, T.; Manoch, L.; Almeida, A. P.; Vasconcelos, M. H., Silva, A.; Gales, L.; Werner Herz, W. Sartoryglabrins, analogs of the ardeemins from *Neosartorya glabra*. *Nat. Prod. Commun*., **2011**, *6*, 807-812.

[33] Jiao, R. H., Xu, S., Liu, J.Y.; Ge, H. M.; Ding, H.; Xu, C.; Zhu, H. L., Tan, R. X. Chaetominine. A cytotoxic alkaloid produced by endophytic *Chaetomium* sp. IFB-E015. *Org. Lett*., **2006**, *8*, 820-826.

[34] Karwowski, J. P.; Jackson, M.; Rasmussen, R. R., Humphrey, P. E., Poddig, J. P.; Kohl, W. L.; Cherr, M. H.; Kadam, S.; McAlpine, J. B. 5-*N*-Acetylardeemin, a novel heterocyclic compound which reverses multiple drug resistance in tumor cells. I. Taxonomy and fermentation of the producing organism and biological activity. *J. Antibiot.*, **1993**, *46*, 374-379.

[35] Hochlowski, J.E.; Mullally, M.M.; Spanton, S.G.; Whittern, D.N.; Preston, H.; McAlpine, J.B. 5-*N*-Acetylardeemin, a novel heterocyclic compound which reverses multiple drug resistance in tumor cells. II. Isolation and elucidation of the structure of 5-N-acetylardeemin and two congeners. *J. Antibiot*., **1993**, *46*, 380-386.

[36] Chou, T.C.; Depew, K.M.; Zheng, Y.H.; Safer, M.L.; Chan, D., Helfridch, B.; Zatorska, D.; Zartoski, A.; Bornmann, W. G.; Danishefsky, S.J. Reverseal of anticancer multiple resistance by the ardeemins. *PNAS*, **1998**, *95*, 8369-8374.

[37] Odds, F.C. Synergy, antagonism, and what the chequerboard puts between them. *J. Antimicrob. Chemother*., **2003**, *52*, doi: 10.1093/jac/dkg301.

[38] Johnson, S.A.; Goddard, P. A.; Iliffe, C.; Timmins, B.; Rickard, A. H.; Robson, G.; Handley, R. S.; Comparative susceptibility of resident and transient hand bacteria to para-chloro-meta-xylenol and triclosan. *J. Appl. Microbiol*., **2002**, *93*, 336-344.

APPENDIX IV

Zin, W. W. M., Buttachon, S., Dethoup, T., Fernandes, C., Cravo, S., Pinto, M. M., Gales, L., Pereira, J. A., Silva, A., and Sekeroglu, N. **(2016)**. New cyclotetrapeptides and a new diketopiperzine derivative from the marine sponge-associated fungus *Neosartorya glabra* KUFA 0702. *Marine Drugs* **14**, 136. Doi:10.390/md14070136.

marine drugs

MDPI

Article

New Cyclotetrapeptides and a New Diketopiperzine Derivative from the Marine Sponge-Associated Fungus *Neosartorya glabra* KUFA 0702

War War May Zin [1,2], Suradet Buttachon [1,2], Tida Dethoup [3], Carla Fernandes [2,4], Sara Cravo [2,4], Madalena M. M. Pinto [2,4], Luís Gales [1,5], José A. Pereira [1], Artur M. S. Silva [6], Nazim Sekeroglu [7] and Anake Kijjoa [1,2,*]

1 *ICBAS*—Instituto de Ciências Biomédicas Abel Salazar, Universidade do Porto, Rua de Jorge Viterbo Ferreira, 228, 4050-313 Porto, Portugal; wwmzin.chem.yu@gmail.com (W.W.M.Z.); nokrari_209@hotmail.com (S.B.); lgales@ibmc.up.pt (L.G.); jpereira@icbas.up.pt (J.A.P.)
2 Interdisciplinary Centre of Marine and Environmental Research (CIIMAR), Rua dos Bragas 289, 4050-313 Porto, Portugal; cfernandes@ff.up.pt (C.F.); scravo@ff.up.pt (S.C.); madalena@ff.up.pt (M.M.M.P.)
3 Department of Plant Pathology, Faculty of Agriculture, Kasetsart University, 10240 Bangkok, Thailand; agrtdd@ku.ac.th
4 Laboratório de Química Orgânica, Departamento de Ciências Químicas, Faculdade de Farmácia, Universidade do Porto, Rua de Jorge Viterbo Ferreira, 228, 4050-313 Porto, Portugal
5 Instituto de Biologia Molecular e Celular (IBMC), Universidade do Porto, Rua de Jorge Viterbo Ferreira, 228, 4050-313 Porto, Portugal
6 Departamento de Química & QOPNA, Universidade de Aveiro, 3810-193 Aveiro, Portugal; artur.silva@ua.pt
7 Medicinal and Aromatic Plant Programme, Plant and Animal Sciences Department, Vocational School, Kilis Aralık University, 79000 Kilis, Turkey; nsekeroglu@gmail.com
* Correspondence: ankijjoa@icbas.up.pt; Tel.: +351-220-428-331; Fax: +351-220-428-090

Academic Editor: Orazio Taglialatela-Scafati
Received: 17 June 2016; Accepted: 15 July 2016; Published: 20 July 2016

Abstract: Two new cyclotetrapeptides, sartoryglabramides A (**5**) and B (**6**), and a new analog of fellutanine A (**8**) were isolated, together with six known compounds including ergosta-4, 6, 8 (14), 22-tetraen-3-one, ergosterol 5, 8-endoperoxide, helvolic acid, aszonalenin (**1**), (3*R*)-3-(1*H*-indol-3-ylmethyl)-3,4-dihydro-1*H*-1,4-benzodiazepine-2,5-dione (**2**), takakiamide (**3**), (11a*R*)-2,3-dihydro-1*H*-pyrrolo[2,1-*c*][1,4]benzodiazepine-5,11(10*H*,11a*H*)-dione (**4**), and fellutanine A (**7**), from the ethyl acetate extract of the culture of the marine sponge-associated fungus *Neosartorya glabra* KUFA 0702. The structures of the new compounds were established based on extensive 1D and 2D spectral analysis. X-ray analysis was also used to confirm the relative configuration of the amino acid constituents of sartoryglabramide A (**5**), and the absolute stereochemistry of the amino acid constituents of sartoryglabramide A (**5**) and sartoryglabramides B (**6**) was determined by chiral HPLC analysis of their hydrolysates by co-injection with the D- and L- amino acids standards. Compounds **1**–**8** were tested for their antibacterial activity against Gram-positive (*Escherichia coli* ATCC 25922) and Gram-negative (*Staphyllococus aureus* ATCC 25923) bacteria, as well as for their antifungal activity against filamentous (*Aspergillus fumigatus* ATCC 46645), dermatophyte (*Trichophyton rubrum* ATCC FF5) and yeast (*Candida albicans* ATCC 10231). None of the tested compounds exhibited either antibacterial (MIC > 256 μg/mL) or antifungal activities (MIC > 512 μg/mL).

Keywords: *Neosartorya glabra*; marine-derived fungus; *Mycale* sp.; cyclotetrapeptides; sartoryglabramides A and B; diketopiperazines; fellutanine A epoxide

1. Introduction

Although the chemical constituents of the fungi of the genus *Neosartorya*, a teleomorphic state of *Aspergillus* section *Fumigatus*, have not previously been intensively investigated [1], there are currently three reports on the secondary metabolites and their biological activities of *Neosartorya glabra* (Fennell & Raper) Kozakiewicz. Jayasuriya et al. first described isolation of three new antibacterial bicyclic lactones, glabramycins A–C, from *N. glabra* isolated from a soil sample collected from Candamia, Spain, by antisense screening [2]. However, it is only very recently that the synthesis and revision of the relative configuration of glabramycin B were achieved [3]. Kijjoa et al. described isolation of three new reverse prenylated indole derivatives, sartoryglabrins A–C, and their in vitro growth inhibitory activity against three human cancer cell lines, from the Thai collection of a soil-derived *N. glabra* [4]. Recently, Liu et al. reported isolation of two new polyketides, neosarphenols A and B, together with six known polyketides and two known meroterpenoids, from the crude ethyl acetate extract of *N. glabra* CGMCC 32286 [5]. During our ongoing search for bioactive secondary metabolites from members of the genus *Neosartorya* and our pursuit for natural antibiotics from marine-derived fungi, we have investigated the secondary metabolites of a Thai collection of *N. glabra* KUFA 0702, isolated from the marine sponge *Mycale* sp., collected from the coral reef at Samaesarn Island in the Gulf of Thailand. The ethyl acetate extract of its culture furnished three new compounds including two new cyclotetrapeptides, sartoryglabramides A (**5**) and B (**6**), and a new analog of fellutanine A (**8**), in addition to the previously reported ergosta-4,6,8 (14), 22-tetraen-3-one [6], ergosterol 5, 8-endoperoxide [7], helvolic acid [8], aszonalenin (**1**) [9], (3*R*)-3-(1*H*-indol-3-ylmethyl)-3, 4-dihydro-1*H*-1,4-benzodiazepine-2,5-dione (**2**) [10], takakiamide (**3**) [11], (11a*R*)-2,3-dihydro-1*H*-pyrrolo[2,1-*c*][1,4]benzodiazepine-5,11(10*H*,11a*H*)-dione (**4**) [12], and fellutanine A (**7**) [13,14] (Figure 1). Compounds **1**–**8** were tested for their antibacterial activity against Gram-positive (*Escherichia coli* ATCC 25922) and Gram-negative (*Staphyllococus aureus* ATCC 25923) bacteria, as well as for their antifungal activity against filamentous (*Aspergillus fumigatus* ATCC 46645), dermatophyte (*Trichophyton rubrum* ATCC FF5) and yeast (*Candida albicans* ATCC 10231).

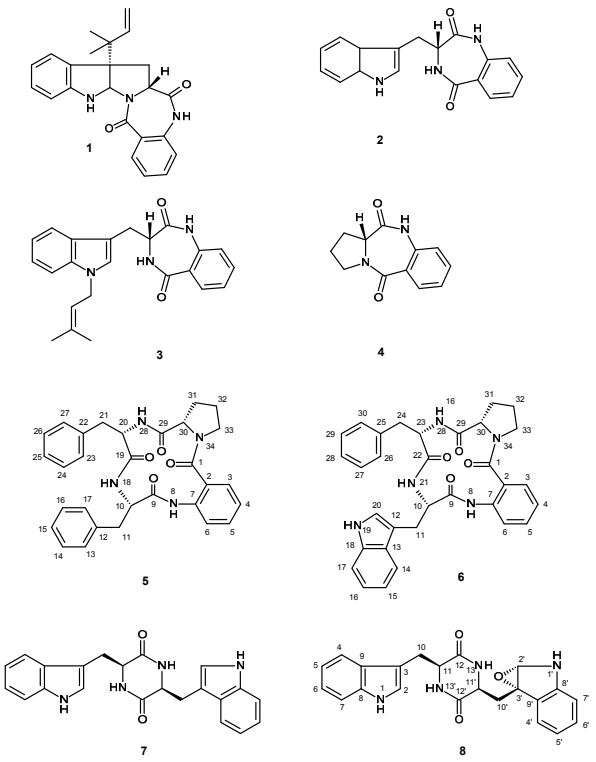

Figure 1. Secondary metabolites isolated from the ethyl acetate extract of the culture of *N. glabra* KUFA 0702.

2. Results and Discussion

Compound **5** was isolated as white crystals (mp, 146–148 °C), and its molecular formula $C_{30}H_{30}N_4O_4$ was established on the basis of the (+)-HRESIMS m/z 511.2365 $[M + H]^+$, indicating eighteen degrees of unsaturation. The IR spectrum showed absorption bands for amine (3447 cm^{-1}), amide carbonyl (1655 cm^{-1}) and aromatic (1622, 1587, and 1526 cm^{-1}). The ^{13}C NMR (Supplementary Materials, Figure S10), DEPTs and HSQC spectra (Table 1, Supplementary Materials, 12) revealed the presence of four amide carbonyls (δ_C 170.2, 169.9, 168.8, 166.5), four quaternary sp^2 (δ_C 138.3, 137.3, 136.5, 124.8), fourteen methine sp^2 [δ_C 130.4, 129.6 (2C), 129.1 (2C), 128.1 (2C), 128.0 (2C), 126.6, 126.3, 126.0, 122.4, 120.4], three methine sp^3 (δ_C 62.2, 55.2, 54.4), and five methylene sp^3 (δ_C 49.4, 37.1, 34.7, 28.3, 24.6). The ^1H NMR spectrum (Table 1, Supplementary Materials, Figure S9) revealed three NH signals at δ_H 9.40, s, 8.49, d (J = 7.8 Hz) and 7.41, d (J = 9.8 Hz), the signals of four aromatic protons of anthranilic acid at δ_H 8.31, dd (J = 7.9, 0.5 Hz, H-6), 7.55, dd (J = 7.7, 1.3 Hz, H-3), 7.48, ddd (J = 7.9, 7.9, 1.4 Hz, H-5) and 7.16, dd (J = 7.9, 7.7 Hz, H-4) [15]. The anthranilic acid residue was linked to the phenylalanine residue, through the amino group of the former and the carboxyl group of the latter, since the HMBC spectrum (Supplementary Materials, Figure S12) showed correlations of the NH signal at δ_H 9.40, s (NH-8) to the carbonyl carbon at δ_C 168.8 (C-9), C-2 (δ_C 124.8), C-6 (δ_C 120.4), of the methine proton at δ_H 4.36, ddd (J = 8.4, 7.8, 5.3 Hz, H-10) to C-9, C-11 (δ_C 34.7), C-12 (δ_C 138.3), of the methylene protons at δ_H 2.97, dd (J = 13.9, 8.4 Hz, H-11a) and 3.23, dd (J = 13.9, 5.3 Hz, H-11b) to C-9, C-10 (δ_C 55.2), C-12, C-13/C-17 (δ_C 129.6). The COSY spectrum also showed correlation (Supplementary Materials, Figure S11) of H-10 to H_2-11 of this phenylalanine residue (Table 1 and Figure 2). That this phenylalanine residue (Phe-I) was linked to another phenylalanine residue (Phe-II) was corroborated by the COSY correlation of H-10 to the proton doublet at δ_H 8.49, d (J = 7.8 Hz, NH-18), as well as by the HMBC correlations of NH-18 to C-10 and the carbonyl carbon at δ_C 169.9 (C-19), of the methine proton signal at δ_H 4.58, ddd (J = 9.8, 8.9, 7.3 Hz, H-20) to C-19, C-21 (δ_C 37.1), C-22 (δ_C 137.3), of the methylene proton signals at δ_H 2.71, dd (J = 13.5, 8.9 Hz, H-21a)/2.94 dd (J = 13.5, 7.3 Hz, H-21b) to C-22, C-19, C-20 (δ_C 54.4), and C-23/C-27 (δ_C129.1) (Table 1 and Figure 2). This was further supported by the COSY correlations of H-20 to H_2-21 and the proton doublet at δ_H 7.41 (J = 9.8 Hz, NH-28). The existence of the proline residue was evidenced not only by the COSY correlations of the double doublet at δ_H 4.20 (J = 9.8, 2.3 Hz, H-30; δ_C 62.2) to the multiplets at δ_H 1.54 and 2.12 (H_2-31, δ_C 28.3), of the multiplet at δ_H 1.89 (H_2-32; δ_C 24.6) to H_2-31 and the double doublet at δ_H 3.70 (J = 17.6, 9.6 Hz, H-33a; δ_C 49.4) and a multiplet at δ_H 3.63 (H-33b; δ_C 49.4) but also by the HMBC correlations of H-30 to the carbon signals at δ_C 170.2 (CO-29), δ_C 28.3 (C-31) and δ_C 24.6 (C-32), and of H-33a to C-30 (δ_C 62.2), C-32, of H_2-31 to C-29 and C-30, respectively (Table 1 and Figure 2). That the proline residue was connected to the Phe-II residue, through the carbonyl of the former and the amino group of the latter, was corroborated by the HMBC correlation of NH-28 to CO-29. Since there are only three NH signals, the nitrogen of the pyrrolidine ring of the proline residue was linked to the carbonyl group (C-1) of anthranilic acid. This was corroborated by the HMBC correlations of H-3 to CO-1 (δ_C 166.5), and of NH-8 to C-2 (δ_C 124.8) and C-6 (δ_C 120.4) (Table 1 and Figure 2). Therefore, combining this information, it was possible to conclude that **5** was cyclo (anthranilic acid-Phe-Phe-Pro).

Table 1. ^1H and ^{13}C NMR (DMSO, 500 MHz and 125 MHz) and HMBC assignment for **5**.

	Position	δ_C, Type	δ_H, (J in Hz)	COSY	HMBC
Anthranilic acid	1	166.5, C	-		
	2	124.8, C	-		
	3	126.6, CH	7.55, dd (7.7, 1.3)	H-4	C-1, 5, 7
	4	122.4, CH	7.16, dd (7.9, 7.7)	H-3, 5	C-2, 6
	5	130.4, CH	7.48, ddd (7.9, 7.9, 1.4)	H-4, 6	C-3, 7
	6	120.4, CH	8.31, dd (7.9, 0.5)	H-5	C-2, 4
	7	136.5, C	-		
	NH-8	-	9.40, s	-	C-2, 6, 9

Table 1. *Cont.*

	Position	δ_C, Type	δ_H, (*J* in Hz)	COSY	HMBC
Phe-I	9	168.8, CO	-		
	10	55.2, CH	4.36, ddd (8.4, 7.8, 5.3)	H-11, NH-21	C-9, 11, 12
	11a	34.7, CH_2	2.97, dd (13.9, 8.4)	H-10, 11b	C-9, 10, 12, 13, 17
	b		3.23, dd (13.9, 5.3)	H-10, 11a	C-9, 10, 12, 13, 17
	12	138.3, C	-		
	13	129.6, CH	7.08, dd (7.4, 1.4)	H-14	C-11, 15, 17
	14	128.0, CH	7.19, dd (7.4, 7.4)	H-14, 15	C-12, 16
	15	126.0, CH	7.18, dd (7.4, 7.4)	H-14, 16	C-13, 17
	16	128.0, CH	7.19, dd (7.4, 7.4)	H-15, 17	C-12, 14
	17	129.6, CH	7.08, dd (7.4, 1.4)	H-16	C-11, 13, 15
	NH-18	-	8.49, d (7.8)	H-20	C-10, 19
Phe-II	19	169.9, CO	-		
	20	54.4, CH	4.58, ddd (9.8, 8.9, 7.3)	H-21a, b	C-19, 21, 22
	21a	37.1, CH_2	2.71, dd (13.5, 8.9)	H-21b, 20	C-19, 20, 22, 23, 27
	b		2.94, dd (13.5, 7.3)	H-21a, 20	C-19, 20, 22, 23, 27
	22	137.3, C	-		
	23	129.1, CH	7.14, dd (7.4, 1.4)	H-24	C-25, 27
	24	128.1, CH	7.27, dd (7.4, 7.4)	H-23, 25	C-22, 26
	25	126.3, CH	7.23, dd (7.4, 7.4)	H-24, 26	C-23, 27
	26	128.1, CH	7.27, dd (7.4, 7.4)	H-25, 27	C-22, 24
	27	129.1, CH	7.14, dd (7.4, 1.4)	H-26	C-23, 25
	NH-28	-	7.41, d (9.8)	H-20	C-19, 20, 29
Pro	29	170.2, CO	-		
	30	62.2, CH	4.20, dd (9.8, 2.3)	H-31a, b	C-29, 31, 32
	31a	28.3, CH_2	1.54, m	H-30, 31b	-
	b		2.12, m	H-30, 31a	C-29, 30
	32	24.6, CH_2	1.89, m	H-31a, b, 32a, b	
	33a	49.4, CH_2	3.70, dd (17.6, 9.6)	H-32, 33b	C-30, 32
	b		3.63, m	H-32, 33a	
	N-34	-	-		

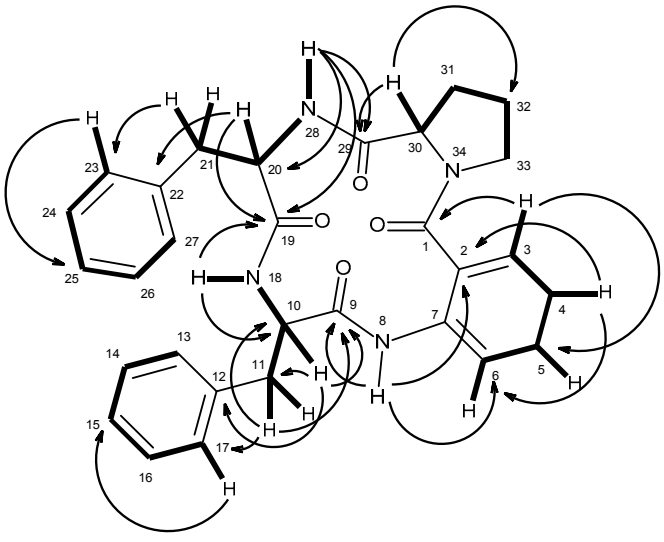

Figure 2. Key COSY (—) and HMBC (→) correlations of compound **5**.

Since **5** was obtained as a suitable crystal for X-ray diffraction, the stereochemistry of its amino acid residues was tentatively determined by X-ray analysis, and the ORTEP view shown in Figure 3 revealed that Phe-I, Phe-II and Pro have the same relative configuration. However, since the flack *x* parameter (0.3) did not guarantee the absolute confidence of the absolute configurations, the stereochemistry of the amino acid residues of **5** was confirmed by a chiral HPLC analysis of its acidic hydrolysate,

using appropriate D- and L-amino acid standards, according to the previously described method [15]. The enantioseparations of the standard amino acids were successfully performed with the Chirobiotic T column under reversed-phase elution conditions [16]. The elution order of the enantiomers of all the standards amino acids was confirmed by injecting the solutions of the enantiomeric mixtures and then each enantiomer separately at a flow rate of 1 mL/min (Supplementary Materials, Table S1). As predicted, the D-enantiomer was always more strongly retained than the corresponding L-enantiomer on Chirobiotic column [16]. The retention times (t_R min) for standards amino acids, using MeOH: H_2O (80:20 *v*/*v*) as mobile phase, at a flow rate of 1.0 mL/min, and with UV detection set at 210 nm, were L-Phe (3.8) and D-Phe (5.0), L-Pro (6.7) and D-Pro (20.1). Based on mix HPLC analyses of the acidic hydrolysate with standard D- and L-amino acids (co-injection) (Supplementary Materials, Figure S27 and Table S1), compound **5** was elucidated as cyclo (anthranilic acid-L-Phe-L-Phe-L-Pro). Since compound **5** is a new compound, we have named it sartoryglabamide A.

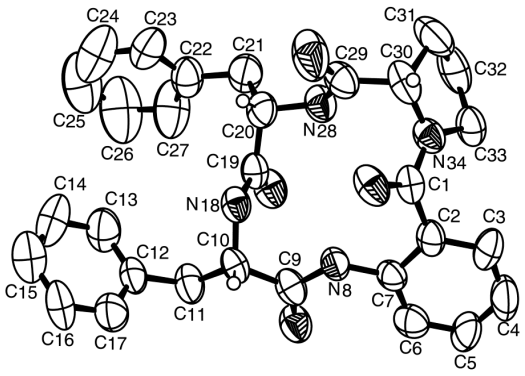

Figure 3. Ortep view of compound **5**.

Compound **6**, which was also isolated as white solid (mp, 190–192 °C), exhibited the $[M + H]^+$ peak at *m*/*z* 550.2501 [(+)-HRESIMS], corresponding to $C_{32}H_{32}N_5O_4$ (calcd. 550.2454). Therefore, the molecular formula $C_{32}H_{31}N_5O_4$ was attributed to compound **6**, which indicated twenty degrees of unsaturation. Like compound **5**, the IR spectrum of **6** showed absorption bands for amine (3417 cm^{-1}), amide carbonyl (1649 cm^{-1}) and aromatic (3058, 1620, 1588, 1526 cm^{-1}). With some exceptions, the general features of the ^1H and ^{13}C spectra of compound **6** resembled those of **5**. The ^{13}C NMR (Supplementary Materials, Figure S15), DEPTs and HSQC spectra (Table 2, Supplementary Materials, Figure S17) displayed signals of four carbonyls (δ_C 170.2, 170.1, 169.0, 166.4), six quaternary sp^2 (δ_C 137.4, 136.3, 136.0, 127.7, 125.2, 110.2), fourteen methine sp^2 [δ_C 130.4, 129.0 (2C), 128.1 (2C), 126.5, 126.3, 124.0, 122.6, 120.8, 120.7, 118.5, 118.2, and 111.3], three methine sp^3 (δ_C 62.1, 54.6, 54.3), and five methylene sp^3 (δ_C 49.4, 37.0, 28.3, 24.9, 24.6). Unlike compound **5**, the ^1H NMR spectrum of **6** (Table 2, Supplementary Materials, Figure S15), exhibited four NH signals at δ_H 10.82, d (*J* = 1.8 Hz), 9.25, s, 8.42, d (*J* = 7.9 Hz) and 7.38, d (*J* = 10.0 Hz). Similar to compound **5**, the presence of the proline residue was corroborated by the presence of the coupling system of the protons from H-33 to H_2-36 [(δ_H 4.15, dd, *J* = 9.0, 2.0 Hz, H-33; δ_C 62.1), δ_H 1.45 m and 2.09, m (H_2-34; δ_C 28.3), δ_H 1.86 m (H_2-35; δ_C 24.6), and δ_H 3.55 m and 3.67, m (H_2-36; δ_C 49.4)] as well as by the HMBC correlation of H-33 to the carbonyl carbon at δ_C 170.2 (C-32), while the presence of the phenylalanine residue was supported by the coupling system from H_2-24 (δ_H 2.66, dd, *J* = 13.6, 10.0 Hz, and 2.92, dd, *J* = 13.6, 6.4 Hz; δ_C 37.0) through H-23 (δ_H 4.61, ddd, *J* = 10.0, 10.0, 6.4 Hz; δ_C 54.6) to NH-31 (δ_H 7.38, d, *J* = 10.0 Hz), as observed in the COSY spectrum, as well as by the HMBC correlations from H-23 to C-24 (δ_C 37.0) and C-25 (δ_C 137.4), of H_2-24 to C-23 (δ_C 54.6), C-25, C-26/30 (δ_C 129.0)(Table 2 and Figure 4). Like compound **5**, the HMBC correlation of the amine proton at δ_H 7.38, d (*J* = 10 Hz, NH-31) to C-32 confirmed the linkage of the carbonyl group of the proline residue (C-32) to the amino group of the phenylalanine residue (N-31). Similarly, the nitrogen of the pyrrolidine ring of the proline residue (N-37) was linked

to the carbonyl group of anthranilic acid (C-1, δ_C 166.4). That one of the phenyl residues of **5** was replaced by a tryptophan residue in **6** was substantiated by the presence of the indole system, which was characterized by the coupling system of H-14 (δ_H 7.58, d, *J* = 7.9 Hz, δ_C 118.5) through H-17 (δ_H 7.34, d, *J* = 8.0 Hz, δ_C 111.3), as observed in the COSY spectrum (Table 2 and Figure 4, Supplementary Materials, Figure S16), and also by the HMBC correlations from NH-19 (δ_H 10.82, brs) to C-12 (δ_C 110.2), C-13 (δ_C 127.7), C-18 (δ_C 136.0) and C-20 (δ_C 124.0) (Table 2 and Figure 4, Supplementary Materials, Figure S18), as well as of the ethylamino moiety, as evidenced by the coupling system from H_2-11 (δ_H 3.14, dd, *J* = 14.7, 6.7 Hz and 3.32 dd, *J* = 14.7, 5.9 Hz; δ_C 24.9) through H-10 (δ_H 4.52, ddd, *J* = 7.9, 6.7, 5.9 Hz; δ_C 54.3) to NH-21 (8.42, d, *J* = 7.9 Hz) (Table 2 and Figure 4). That the tryptophan residue was linked to the phenylalanine residue, through the amino group of the former and the carbonyl group of the latter, was corroborated by the HMBC correlations of NH-21 to the carbonyl carbons at δ_C 170.1 (C-22) and 169.0 (C-9), as well as of H-10 to C-9, C-11, C-12 and C-22. Finally, the amino group of the anthranilic acid residue was linked to the carbonyl group of the tryptophan residue was supported by the HMBC correlations of NH-8 (δ_H 9.25, s) to C-2 (δ_C 125.2), C-6 (δ_C 120.7) and C-9. Therefore, **6** was identified as cyclo (anthranilic acid-Trp-Phe-Pro).

Table 2. ^{1}H and ^{13}C NMR (DMSO, 500 MHz and 125 MHz) and HMBC assignment for **6**.

	Position	δ_C, Type	δ_H, (*J* in Hz)	COSY	HMBC
Anthranilic acid	1	166.4, CO	-		
	2	125.2, C	-		
	3	126.5, CH	7.53, d (7.6)	H-4	C-1, 5, 7
	4	122.6, CH	7.16, dd (7.6, 7.6)	H-3, 5	C-2, 6
	5	130.4, CH	7.48, ddd (8.3, 7.6)	H-4, 6	C-3, 7
	6	120.7, CH	8.27, d (8.3)	H-5	C-2, 4
	7	136.3, C	-		
	NH-8	-	9.25, s		C-2, 6, 9
Trp	9	169.0, CO	-		
	10	54.3, CH	4.52, ddd (7.9, 6.7, 5.9)	H-11, NH-21	C-9, 11, 12, 22
	11a	24.9, CH_2	3.32, dd (14.7, 5.9)	H-10, 11b	C-9, 10, 12, 13, 20
	b		3.14, dd (14.7, 6.7)	H-10, 11a	C-9, 10, 12, 13, 20
	12	110.2, C	-		
	13	127.7, C	-		
	14	118.5, CH	7.58, d (7.9)	H-15	C-16, 18
	15	118.2, CH	6.98, dd (7.9, 7.5)	H-14, 16	C-13, 17
	16	120.8, CH	7.06, dd (8.0, 7.5)	H-15, 17	C-14, 18
	17	111.3, CH	7.34, d (8.0)	H-16	C-13, 15
	18	136.0, C	-		
	NH-19	-	10.82, brs	H-20	C-12, 13, 18, 20
	20	124.0, CH	7.04, d (1.8)	NH-19	C-13
	NH-21	-	8.42, d (7.9)	H-10	C-9, 22
Phe	22	170.1, CO	-		
	23	54.6, CH	4.61, ddd (10.0, 10.0, 6.4)	H-24a, b	C-24, 32
	24a	37.0, CH_2	2.66, dd (13.6, 10.0)	H-23, 24b	C-22, 23, 25, 26, 30
	b		2.92, dd (13.6, 6.4)	H-23, 24a	C-22, 23, 25, 26, 30
	25	134.4, C	-		
	26	129.0, CH	7.10, dd (7.7, 1.0)	H-27	C-25
	27	128.1, CH	7.20, m	H-26, 28	C-25
	28	126.3, CH	7.18, m	H-27, 29	
	29	128.1, CH	7.20, m	H-28, 30	C-28
	30	129.0, CH	7.10, dd (7.7, 1.0)	H-29	C-25
	NH-31	-	7.38, d (10.0)	H-23	C-32
Pro	32	170.2, CO	-		
	33	62.1, CH	4.15, dd (9.0, 1.2)	H-34a, b	C-32
	34a	28.3, CH_2	1.45, m	H-33, 34b	
	b		2.09, m	H-33, 34a	
	35	24.6, CH_2	1.86, m	H-34a,b, 36a, b	
	36a	49.4, CH_2	3.55, m	H-35, 36b	
	b		3.67, m	H-35, 36a	
	N-37	-	-		

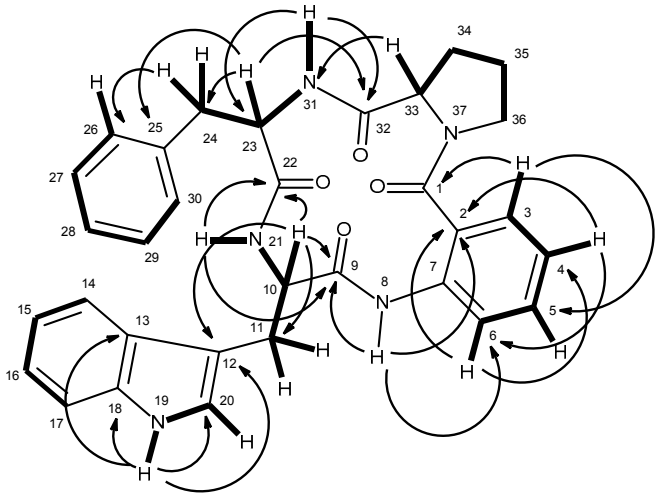

Figure 4. Key COSY (—) and HMBC (→) correlations of compound **6**.

The absolute stereochemistry of the amino acid residues of compound **6** was also determined by chiral HPLC analysis of its acidic hydrolysate, using appropriate D- and L-amino acids standards. The retention times (t_R min) for standards amino acids, using MeOH: H_2O (80:20 *v*/*v*) as mobile phase, at a flow rate of 1.0 mL/min, and with UV detection set at 210 nm, were L-Phe (3.8) and D-Phe (5.0), L-Pro (6.7) and D-Pro (20.1), L-Trp (4.5) and D-Trp (5.2). Based on mix HPLC analyses of the acidic hydrolysate with standard D- and L-amino acids (co-injection) (Supplementary Materials, Figure S28, Table S1), compound **6** was elucidated as cyclo (anthranilic acid-L-Trp-L-Phe-L-Pro). Since compound **6** is also a new compound, we have named it sartoryglabamide B.

Compound **8** was isolated as pale yellow viscous mass, and its molecular formula $C_{22}H_{20}N_4O_3$ was established on the basis of the (+)-HRESIMS *m*/*z* 389.1626 $[M + H]^+$, indicating fifteen degrees of unsaturation. The IR spectrum showed absorption bands for amine (3420 cm^{-1}), amide carbonyl (1649 cm^{-1}) and aromatic (1418 cm^{-1}). The ^{13}C NMR (Supplementary Materials, Figure S22), DEPTs and HSQC spectra (Table 3, Supplementary Materials, Figure S25) revealed the presence of two amide carbonyls (δ_C 169.8 and 167.7), five quaternary sp^2 (δ_C 148.4, 136.0, 131.1, 127.4, 109.5), nine methine sp^2 (δ_C 128.9, 124.1, 122.5, 120.9, 118.5, 118.3, 117.8, 111.3, 109.8), one oxygen bearing quaternary sp^3 (δ_C 85.9), one oxygen bearing methine sp^3 (δ_C 84.0), two methine sp^3 (δ_C 58.6, 55.1) and two methylene sp^3 (δ_C 41.3, 24.7). The ^1H NMR spectrum (Table 3, Supplementary Materials, Figure S21), exhibited, besides four NH signals at δ_H 10.88, brd (*J* = 1.4 Hz), 7.72, brs, 6.68, brs, and 6.05, s, and, in conjunction with the COSY and HSQC spectra (Table 3, Supplementary Materials, Figures S23 and S24), the proton signals of two 1,2-disubstituted benzene rings at δ_H 7.60, d (*J* = 7.9 Hz, H-4; δ_C 118.5), 7.33, d (*J* = 7.9 Hz, H-7, δ_C 111.3), 7.07, ddd (*J* = 7.9, 7.9, 1.1 Hz, H-6, δ_C 120.9), 6.99, ddd (*J* = 7.9, 7.9, 0.5 Hz, H-5, δ_C 118.3), and at δ_H 7.18, d (*J* = 7.4 Hz, H-4′; δ_C 122.5), 7.05, ddd (*J* = 7.8, 7.4, 1.3 Hz, H-6′, δ_C 128.9), 6.61, ddd (*J* = 7.8, 7.4, 0.5 Hz, H-5′, δ_C 117.8) and 6.54, d (*J* = 7.8 Hz, H-7′, δ_C 109.8). That one of the 1,2-disubstituted benzene rings was part of the indole moiety was corroborated by the HMBC correlations of H-4 to C-3 (δ_C 109.5), C-6 (δ_C 120.9) and C-8 (δ_C 136.0), of the amine proton at δ_H 10.88, brd (*J* = 1.4 Hz, NH-1) to C-2 (δ_C 124.1), C-3, C-8, C-9 (δ_C 127.4), and of H-2 (δ_H 7.25, d, *J* = 2.3 Hz) to C-3 and C-9 (Table 3 and Figure 5). The presence of a 2,5-disubstituted 1,4-diketopiperazine was supported by the HMBC correlations of NH-13′ (δ_H 7.72, brs) to the carbonyl at δ_C 167.7 (C-12), the methine carbons at δ_C 58.6 (C-11′) and δ_C 55.1 (C-11) and the methylene carbon at δ_C 24.7 (C-10), of NH-13 (δ_H 6.05, s) to the methylene carbon at δ_C 41.3 (C-10′), of H-11 (δ_H 4.46, t, *J* = 5.1 Hz) to C-10 and C-12, of H-11′ (δ_H 4.66, dd, *J* = 11.6, 6.7 Hz) to C-10′ and C-12′. Moreover, the COSY correlations of H-11 to H_2-10 (δ_H 3.06, dd, *J* = 15.7, 6.5 Hz and 3.40, m), and of H-11′ to H_2-10′ (δ_H 1.83, dd, *J* = 13.0, 11.6 Hz and 2.43, dd, *J* = 13.0, 6.7 Hz) (Table 3 and Figure 5) confirmed

that the substituents on C-11 and C-11′ are methylene groups. The indole ring system was connected to the 1, 4-diketopiperazine moiety through CH_2-10 since the HMBC spectrum exhibited correlations of H-11 to C-3, and of H-10 to C-9 (Table 3, Figure 5, Supplementary Materials, Figure S25). The second 1,2-disubstituted benzene ring was part of the 2,3-disubstituted 2,3-dihydro-1*H*-indole ring system since the HMBC spectrum showed correlations of NH-1′ (δ_H 6.68,d, J = 4.1 Hz) to the oxygenated sp^3 quaternary carbon at δ_C 85.9 (C-3′) and to the quaternary aromatic carbon at δ_C 131.1 (C-9′), and also of H-2′ (δ_H 5.33, d, J = 4.1 Hz,) to C-3′. Since the HMBC spectrum showed correlations of H-2′ to C-10′, as well as of H-10′ to C-3′, it was concluded that the 2, 3-disubstituted 2, 3-dihydro-1*H*-indole ring system was linked to the 1, 4-diketopiperazine moiety through CH_2-10′. As all of the ^{1}H and ^{13}C data so far mentioned accounted only for $C_{22}H_{20}N_4O_2$, which is one oxygen atom less than the molecular formula, the epoxide functionality was placed between C-2′ and C-3′.

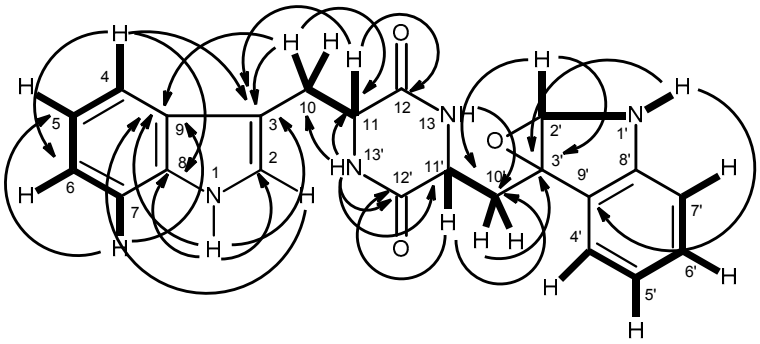

Figure 5. Key COSY (—) and HMBC (→) correlations of compound **8**.

Table 3. ^{1}H and ^{13}C NMR (DMSO, 300 and 75 MHz), HMBC assignment and NOESY for **8**.

Position	δ_C, type	δ_H, (J in Hz)	COSY	HMBC	NOESY
2	124.1, CH	7.25, d (2.3)	NH-1	C-3, 9	H-10a, 11 (str), NH-13′
3	109.5, C	-			
4	118.5, CH	7.60, d (7.9)	H-5	C-3, 6, 8	H-10a, 11 (str)
5	118.3, CH	6.99, ddd (7.9, 7.9, 0.5)	H-4, 6	C-7, 9	
6	120.9, CH	7.07, ddd (7.9, 7.9, 1.1)	H-5, 7	C-4, 8	
7	111.3, CH	7.33, d (7.9)	H-6	C-5, 9	
8	136.0, C	-			
9	127.4, C	-			
10a	24.7, CH_2	3.06, dd (15.7, 6.5)	H-10b, 11	C-3, 9, 11, 12	H-4, 10b, 11, NH-13′
b		3.40, m	H-10a, 11	C-3, 9, 11, 12	H-10a
11	55.1, CH	4.46, t (5.1)	H-10a, 10b	C-3, 10, 12	H-2, 4, 10a, 11′, NH-13′
12	167.7, CO	-			
2′	84.0, CH	5.33, d (4.1)	NH-1′	C-3′, 10′	H-11, NH-13, NH-1′ (str)
3′	85.9, C	-			
4′	122.5, CH	7.18, d (7.4)	H-5′	C-6′, 8′	NH-13
5′	117.8, CH	6.61, ddd (7.8, 7.4, 0.5)	H-4′, 6′	C-7′, 9′	
6′	128.9, CH	7.05, ddd (7.8, 7.8, 1.3)	H-5′, 7′	C-4′, 8′	
7′	109.8, CH	6.54, d (7.8)	H-6′	C-5′, 9′	
8′	148.4, C	-			
9′	131.1, C	-			
10′a	41.3, CH_2	1.83, dd (13.0, 11.6)	H-10′b, 11	C-11′, 12′	H-10′b
b		2.43, dd (13.6, 6.7)	H-10′a, 11	C-3′	H-10′a, 11′
11′	58.6, CH	4.66, dd (11.6, 6.7)	H-10′a, 10b	C-10′, 12′	H-11, 2′, 10′b
12′	169.8, CO	-			
NH-1	-	10.88, brd (1.4)	H-2	C-2, 3, 8, 9	H-2, 4
NH-1′	-	6.68, d (4.1)	H-2′	C-3′, 9′	
NH-13	-	6.05, s	-	C-10′	H-2′, 4′
NH-13′	-	7.72, brs	-	C-10, 11, 11′, 12	H-10a (str), 11 (str), H-2

Since compound **8** was obtained as pale yellow viscous mass, its stereochemistry could not be determined by X-ray crystallography. However, as compounds **8** was isolated together with fellutanine A (**7**) [13,14], it is reasonable to assume that the stereochemistry of C-11 and C-11′ of both compounds are the same. Like compounds **1–3, 5** and **6**, fellutanine A (**7**) and compound **8** must be derived from the same biosynthetic precursor, i.e., L-tryptophan. Consequently, the absolute configurations of C-11 and C-11′ of fellutanine A (**7**) and compound **8** are presumed to be *S*. In an effort to unravel the stereochemistry of C-11, C-11′, and the epoxide bearing carbons (C-2′ and C-3′) of compound **8**, the NOESY experiments and molecular dynamic simulations were carried out. The NOESY spectrum of compound **8** (Table 3 and Figure 6, Supplementary Materials, Figure S26) exhibited correlations of H-11 to H-2, H-4, H-10a, H-11′, NH-13′, therefore confirming the *cis*-relation between H-11 and H-11′. Since the coupling constant between H-11 and H-10a is 6.5 Hz, H-10a must be in an equatorial and H-11 in axial positions in the major conformation. On the other hand, H-11′ exhibited only correlations to H-11 and H-10′b (δ_H 2.43, dd, J = 13.0, 6.7 Hz), and H-2′, but not with H-10′a (δ_H 1.83, dd, J = 13.0, 11.6 Hz) and NH-13, while H-2′ gave correlations to only H-11′ and NH-13, but not to H-10′a or 10′b. The values of the coupling constants of H-11′ to H-10′a (J = 11.6 Hz) and to H-10′b ((J = 6.7 Hz) indicated that H-11′ and H-10′a are "*anti*", while H-11′ and H-10′b are "gauche". These data indicated that H-2′ is in the same face as H-11′ and points to the opposite direction from H-10′a/10′b. However, these correlations do not allow us to determine the stereochemistry of the epoxide. Surprisingly, the NOESY spectrum also shows strong correlation of H-4′ to NH-13.

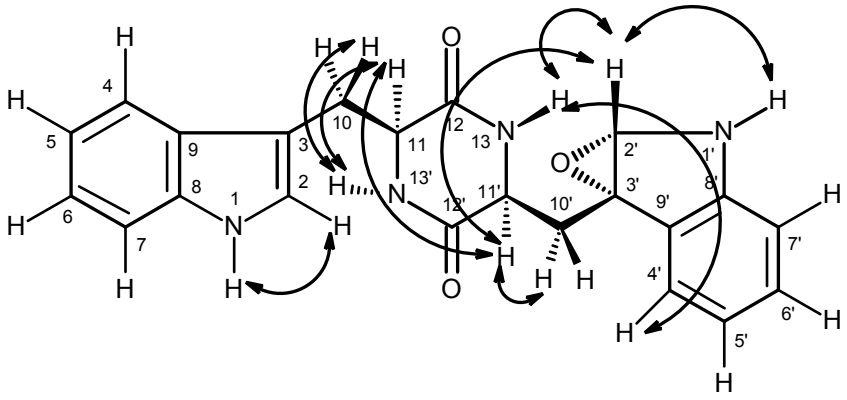

Figure 6. Key NOESY (↔) correlations of compound **8**.

Furthermore, a strong NOESY cross-peak between H-11 and H-11′ of compound **8**, and in conjunction with conformational search, molecular dynamics and ab initio molecular modeling, showed that both amide bonds in the diketopiperazine ring are cis and that both amino acids have the same stereochemistry for their α-carbons. This type of six-membered ring is thermodynamically stable because resonance compensates for the extra energy of the amide cis configurations [17], when compared to the more normal trans configuration. Nevertheless, cis peptide bonds occur naturally even in linear biological proteins [18]. NOESY cross-peaks and molecular modeling also aided the assignment of the absolute configurations to the epoxide carbon atoms of **8**. The minimal energy conformations for the *R*/*R* and *S*/*S* models are presented in Figure 7, showing how the epoxide oxygen points outwards in both cases for minimal repulsion. Conformational analysis was based mainly on the combinations of the three staggered conformations for C-10′/C-11′ bond and two for the C-3′/C-10′ bond. These six conformers differ by less than 7 kcal/mol (RHF/6-21G total energy), independently of the configuration of the epoxide. Of all the conformations, the most stable conformation of the 2′*S*/3′*S* epoxide actually explains simultaneously the observed NOESY correlations of H-4′ to NH-13 and of H-2′ to H-11′ (Table 3 and Figure 6, Supplementary Materials, Figure S26). On the other hand, none of the *R*/*R* conformations justifies the NOESY data without assuming unreasonable spin-diffusion. The assignment of the *S*/*S* isomer for the epoxide carbons of **8** has to assume, however, that there

is a spin-diffusion during the mixing time; otherwise, given the proposed structure for **8**, it would not be possible to explain also the H-2′/H-13 NOESY cross-peak. The proximities H-4′/NH-13 and H-2′/H-11′ are physically incompatible with direct H-2′/H-13 NOE proximity. The fact that H-2′/H-11′/NH-13 form a coupled dipolar spin system is perhaps an explanation for the very week H-11′/NH-13 NOESY cross-peak (Table 3 and Figure 6, Supplementary Materials, Figure S26), which is expected to be strong unless some polarization transfer is at play between the three spins.

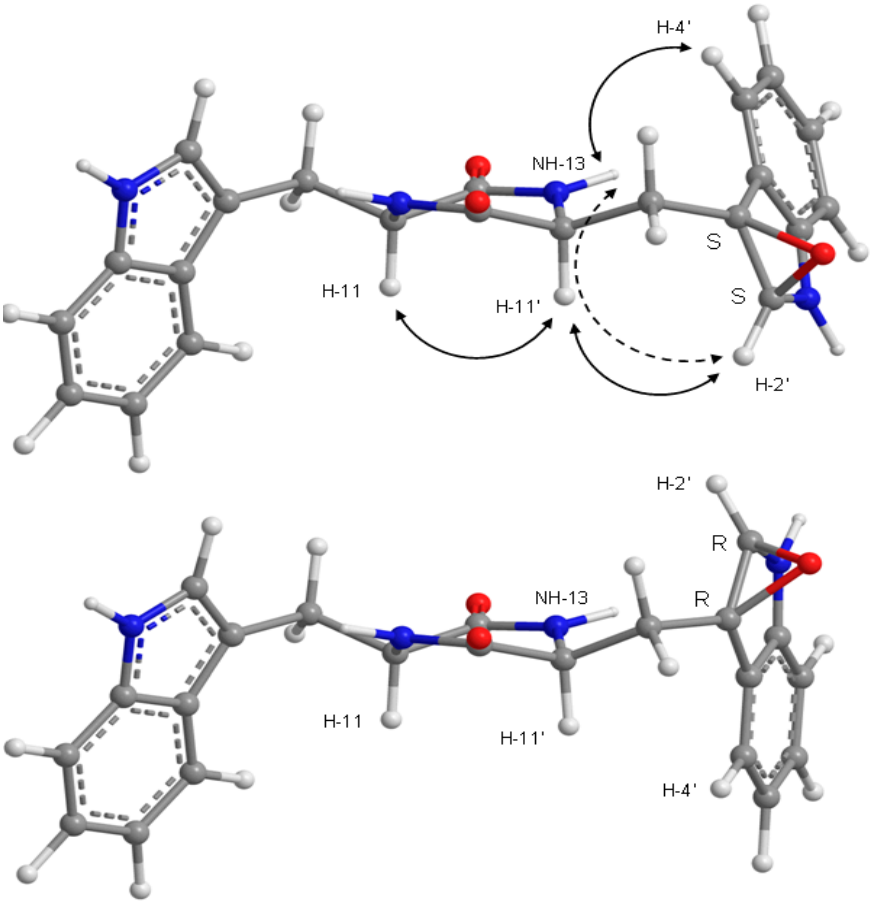

Figure 7. The two possible epoxide configurations for **8** in their lowest RHF/6-21G total energy conformation. Solid lines indicate direct NOESY correlations, explained by the *S*/*S* stereoisomer and not by the *R*/*R*. The discontinuous line shows how spin diffusion gives rise to an H-2′/NH-13 NOESY cross-peak.

Taking all of the evidence together, the structure of compound **8** was proposed as fellutanine A 2′*S*, 3′*S*-epoxide. To the best of our knowledge, compound **8** is also a new compound.

Compounds **1**–**8** were tested for their antibacterial activity against Gram-positive (*Escherichia coli* ATCC 25922) and Gram-negative (*Staphyllococus aureus* ATCC 25923) bacteria, as well as for their antifungal activity against filamentous (*Aspergillus fumigatus* ATCC 46645), dermatophyte (*Trichophyton rubrum* ATCC FF5) and yeast (*Candida albicans* ATCC 10231), according to the previously described protocols [19,20]; however, none of the tested compounds exhibited either antibacterial (MIC > 256 μg/mL) or antifungal activities (MIC > 512 μg/mL).

3. Experimental Section

3.1. General Procedure

Melting points were determined on a Bock monoscope and are uncorrected. Optical rotations were measured on an ADP410 Polarimeter (Bellingham + Stanley Ltd., Tunbridge Wells, Kent, UK). Infrared spectra were recorded in a KBr microplate in a FTIR spectrometer Nicolet iS10 from Thermo Scientific (Waltham, MA, USA) with Smart OMNI-Transmission accessory (Software 188 OMNIC 8.3). ^{1}H and ^{13}C NMR spectra were recorded at ambient temperature on a Bruker AMC instrument (Bruker Biosciences Corporation, Billerica, MA, USA) operating at 300.13 or 500.13 MHz, and 75.4 or 125.8 MHz, respectively. High resolution mass spectra were measured with a Waters Xevo QToF mass spectrometer (Waters Corporations, Milford, MA, USA) coupled to a Waters Aquity UPLC system. A Merck (Darmstadt, Germany) silica gel GF_{254} was used for preparative TLC, and a Merck Si gel 60 (0.2–0.5 mm) was used for column chromatography.

3.2. Extraction and Isolation

The strain KUFA 0702 was isolated from the marine sponge *Mycale* sp., which was collected, by scuba diving at a depth of 15–20 m, from the coral reef at Samaesarn Island (12°34′36.64″ N 100°56′59.69″ E) in the Gulf of Thailand, Chonburi Province, in February 2015. The sponge was washed with 0.06% sodium hypochlorite solution for 1 min, followed by sterilized seawater 3 times, and then dried on sterile filter paper, cut into small pieces (5 × 5 mm), and placed on a malt extract agar (MEA) medium containing 70% seawater and 300 mg/L of streptomycin sulfate. After incubation at 28 °C for 7 days, the hyphal tips were transferred onto a slant MEA and maintained as pure culture for further identification. The fungus was identified as *Neosartorya glabra* (Fennell & Raper) Kozak based on morphological characteristics such as colony growth rate and growth pattern on standard media, namely Czapek's agar, Czapek yeast autolysate agar and malt extract agar. Microscopic characteristics including size, shape and ornamentation of ascospores were examined under light and scanning electron microscopes. This identification was supported by sequence analysis of the β-tubulin, calmodulin and actin genes as described in the previous report [21]. *Neosartorya glabra* was also confirmed by sequence analysis of the internal transcribed spacer (ITS) gene, according the procedure previously described by us [11]. Its gene sequences were deposited in GenBank with accession numbers KU955860. The pure cultures were deposited as KUFA 0702 at Kasetsart University Fungal Collection, Department of Plant Pathology, Faculty of Agriculture, Kasetsart University, Bangkok, Thailand. The fungus was cultured for one week at 28 °C in 5 Petri dishes (i.d. 90 mm) containing 15 mL of potato dextrose agar. In order to obtain the mycelial suspension, the mycelial plugs were transferred to two 500 mL Erlenmeyer flasks containing 250 mL of potato dextrose broth, and then incubated on a rotary shaker at 150 rpm at 28 °C for 7 days. Forty 1000-mL Erlenmeyer flasks, each containing 300 g of cooked rice, were autoclaved at 121 °C for 15 min, and then inoculated with 25 mL of mycelial suspension of *N. glabra*, and incubated at 28 °C for 30 days, after which the moldy rice was macerated in ethyl acetate (20 L total) for 7 days, and then filtered with filter paper. The ethyl acetate solution was concentrated under reduced pressure to yield 98.2 g of crude ethyl acetate extract, which was dissolved in 1000 mL of $CHCl_3$, and then washed with H_2O (3 × 500 mL). The organic layers were combined and dried with anhydrous Na_2SO_4, filtered and evaporated under reduced pressure to give 71.2 g of the crude chloroform extract, which was applied on a column of silica gel (420 g), and eluted with mixtures of petrol-$CHCl_3$ and $CHCl_3$–Me_2CO, 250 mL fractions were collected as follows: Frs 1-80 (petrol–$CHCl_3$, 1:1), 81-144 (petrol–$CHCl_3$, 3:7), 145-201 (petrol–$CHCl_3$, 1:9), 202-356 ($CHCl_3$–Me_2CO, 9:1), 357-398 ($CHCl_3$–Me_2CO, 7:1), and 399-410 (Me_2CO). Frs 85-105 were combined (2.04 g) and purified by TLC (silica gel G_{254}, $CHCl_3$–Petrol–EtOAc–HCO_2H, 8:1:1:0.01) to give 11 mg of ergosta-4,6,8 (14), 22-tetraen-3-one. Fr 207 (1.14 g) was applied over a column chromatography of Sephadex LH-20 (10 g) and eluted with MeOH and a mixture of MeOH: CH_2Cl_2 (1:1), wherein 20 mL subfractions were collected as follows: sfrs 1–90 (MeOH), and 91–145

(MeOH: CH_2Cl_2, 1:1). Sfrs 53–61 were combined (19.5 mg) and recrystallized in MeOH to give 16.8 mg of ergosterol 5,8-endopeoxide. Sfrs 62-90 were combined (53.2 mg) and purified by TLC (silica gel G_{254}, $CHCl_3$-Petrol-EtOAc-HCO_2H, 8:1:1:0.01) to give 11.2 mg of **1**. Frs 206–212 were combined (4.88 g) and applied over a column chromatography of Si gel (45 g) and eluted with mixture of petrol–$CHCl_3$, $CHCl_3$–Me_2CO and Me_2CO, wherein 100 mL subfractions were collected as follows: sfrs 1–51 (petrol–$CHCl_3$, 1:1), 52-107 (petrol–$CHCl_3$, 3:7), 108–164 (petrol–$CHCl_3$, 1:9), 165–190 ($CHCl_3$–Me_2CO, 9.5:0.5), 191–310 ($CHCl_3$–Me_2CO, 9:1). Sfrs 83–164 were combine (53.4 mg) and recrystallized in MeOH to give 27.6 mg of ergosterol 5,8-endopeoxide. Sfr 166 (38.8 mg) was recrystallized in Me_2CO to give 8.7 mg of **1**. Frs 213–245 were combined (3.61 g) and applied over a column chromatography of Sephadex LH-20 (10 g) and eluted with MeOH, wherein 60 sfrs of 20 mL were collected. Sfrs 31–51 were combined and purified by TLC (silica gel G_{254}, $CHCl_3$–Me_2CO–HCO_2H, 4:1:0.01) to give 9.7 mg of **3** and 13.1 mg of **4**. Frs 246–257 were combined (1.44 g) and recrystallized in MeOH to give 23.7 mg of helvolic acid. Frs 273–287 were combined (621.0 mg) and purified by TLC (silica gel G_{254}, $CHCl_3$–Me_2CO–HCO_2H, 7:3:0.03) to give 12.1 mg of helvolic acid and 32.3 mg of **5**. Frs 363–373 were combined (1.26 g) and applied over a column chromatography of Sephadex LH-20 (10 g) and eluted with MeOH, wherein 60 subfractions of 20 mL were collected. Sfrs 22–54 were combined (91.2 mg) and purified by TLC (silica gel G_{254}, $CHCl_3$–Me_2CO–HCO_2H, 9.5:0.5:0.03) to give 14.7 mg of **6** and 10 mg of **2**. Frs 374–398 were combined (1.37 g) and purified by TLC (silica gel G_{254}, $CHCl_3$–Me_2CO–HCO_2H, 3:2:0.03) to give 32.8 mg of **8**. Frs 403–405 were combined (2.49 g) and applied over a column chromatography of Sephadex LH-20 (10 g) and eluted with MeOH, wherein 112 sfrs of 20 mL were collected. Sfrs 90–112 were combined (24.9 mg) and purified by TLC (silica gel G_{254}, $CHCl_3$–Me_2CO–HCO_2H, 9.5:0.5:0.03) to give 20.7 mg of **7**.

3.2.1. Satoryglabramide A (**5**)

White crystal, mp 146–148 °C ($CHCl_3$-Me_2CO); $[\alpha]_D^{20}$ +34.6 (*c* 0.06, Me_2CO); IR (KBr) ν_{max} 3447, 3060, 3028, 2920, 2850, 1655, 1622, 1587, 1526, 1453, 1415, 1300, 1261, 1173 cm^{-1}; ^1H and ^{13}C NMR (see Table 1); HRESIMS *m*/*z* 511.2365 $(M + H)^+$ (calculated for $C_{30}H_{31}N_4O_4$, 511.2345).

3.2.2. Satoryglabramide B (**6**)

White solid, mp 190–192 °C ($CHCl_3$–Me_2CO); $[\alpha]_D^{20}$ +42.8 (*c* 0.05, Me_2CO); IR (KBr) ν_{max} 3417, 3058, 2924, 2852, 1649, 1620, 1588, 1526, 1454, 1418, 1302, 1263, 1101 cm^{-1}; ^1H and ^{13}C NMR (see Table 2); HRESIMS *m*/*z* 550.2501 $(M + H)^+$ (calculated for $C_{32}H_{32}N_5O_4$, 550.2454).

3.2.3. Fellutanine A Epoxide (**8**)

Pale yellow viscous mass; $[\alpha]_D^{20}$ +13.9 (*c* 0.07, Me_2CO); IR (KBr) ν_{max} 3420, 2922, 1649, 1416, 1188, 1047, 1025, 996 cm^{-1}; ^1H and ^{13}C NMR (see Table 3); HRESIMS *m*/*z* 389.1626 $(M + H)^+$ (calculated for $C_{22}H_{21}N_4O_3$, 389.1614).

*3.3. X-ray Crystal Structure of Sartoryglabramide A (**5**)*

A single crystal of sartoryglabamide A was mounted on a cryoloop using paratone. X-ray diffraction data was collected at room temperature with a Gemini PX Ultra equipped with CuK_α radiation (λ = 1.54184 Å). The crystal was orthorhombic, space group $P2_12_12_1$, cell volume 5459.8(2) $Å^3$ and unit cell dimensions *a* = 15.1792(3) Å, *b* = 18.7674(5) Å and *c* = 19.1659(3) Å (uncertainties in parentheses). There are two molecules per unit cell with calculated density of 1.242 g/cm^3. The structure was solved by direct methods using SHELXS-97 and refined with SHELXL-97 [22]. Carbon, nitrogen and oxygen atoms were refined anisotropically. Hydrogen atoms were either placed at their idealized positions using appropriate HFIX instructions in SHELXL and included in subsequent refinement cycles or were directly found from difference Fourier maps and were refined freely with isotropic displacement parameters. The refinement converged to R (all data) = 10.02%

and wR2 (all data) = 15.26%. The absolute structure could not be established with confidence (flack *x* parameter 0.3(4)).

Full details of the data collection and refinement and tables of atomic coordinates, bond lengths and angles, and torsion angles have been deposited with the Cambridge Crystallographic Data Centre (CCDC 1483750).

*3.4. Amino Acids Analysis of Acidic Hydrolysate of Sartoryglabramide A (**5**) and Sartoryglabramide B (**6**)*

3.4.1. Acid Hydrolysis

The stereochemistry of the amino acids was determined by analysis of the acidic hydrolysate from **5** and **6**. Compound **5** or **6** (5.0 mg) was dissolved in 6 N HCl (5 mL) and heated at 110 °C, in a furnace, for 24 h in a sealed glass tube. After cooling to room temperature, the solution was dried under N_2 for 24 h, reconstituted in MeOH for HPLC-MS (200 µL), filtered through a 4 mm PTFE Syringe Filter F2504-4 of 0.2 µm pore size (Thermo Scientific, Mumbai, India), and then analyzed by HPLC equipped with a chiral column.

3.4.2. Chiral HPLC Analysis

The HPLC system consisted of Shimadzu LC-20AD pump, equipped with a Shimadzu DGV-20A5 degasser, a Rheodyne 7725i injector fitted with a 20 µL loop, and a SPD-M20A DAD detector (Kyoto, Japan). Data acquisition was performed using Shimadzu LCMS Lab Solutions software, version 3.50 SP2. The chiral column used in this study was Chirobiotic T (15 cm × 4.6 mm I.D., particle size 5 µm) manufactured by ASTEC (Whippany, NJ, USA). The mobile phase composition was MeOH: H_2O (80:20 *v*/*v*), all were LC-MS grade solvents obtained from Sigma-Aldrich Co. (St. Louis, MO, USA). The flow rate was 1.0 mL/min and the UV detection wavelength was 210 nm. Analyses were performed at room temperature in an isocratic mode. All standards of pure amino acid enantiomers were purchased from Sigma-Aldrich Co. (St. Louis, MO, USA). The elution order of the enantiomers of all the standards amino acids was confirmed by injecting the solutions of enantiomeric mixtures, and then each enantiomer separately. Working solutions of single enantiomeric amino acids were prepared by dissolution in MeOH at the concentration of 1 mg/mL (10 µL sample injection), while the enantiomeric mixtures were prepared by mixing equal aliquots of each enantiomer (20 µL sample injection). Mix HPLC analyses of the acidic hydrolysate with standard amino acids (co-injection) confirmed the stereochemistry of the amino acids of **5** and **6**.

3.4.3. Molecular Mechanics Conformation Analysis of Fellutanine A Epoxide (**8**)

Molecular simulations for structure **8** were carried out in ChemBio3D Ultra 14 (Perkin-Elmerm, Waltham, MA, USA). Stochastic and dihedral driver conformational search, with MMFF force field energy minimization, was done for both *S*/*S* and *R*/*R* isomers of **8**, followed by ab initio RHF/6-21G energy re-minimization of the lowest energy conformations using CS GAMESS interfaced by ChemBio3D. The PCM solvent model for DMSO was used on the ab initio minimizations.

4. Conclusions

Although there are few reports of the constituents of *N. glabra*, this is the first study of the secondary metabolites from the marine-derived strain of this fungus. It is interesting to point out that even though some common fungal metabolites previously isolated from other members of this and related genera, such as ergosta-4,6,8 (14), 22-tetraen-3-one, ergosterol 5,8-endoperoxide, helvolic acid, aszonalenin, takakiamide, (3*R*)-3-(1*H*-indol-3-ylmethyl)-3,4-dihydro-1*H*-1,4-benzodiazepine-2,5-dione (**2**) and fellutanine A (**7**), compound **4** was only described as a synthetic intermediate obtained by cyclocondensation of L-proline with isatoic acid anhydride [12]. Moreover, this is the first report on isolation of the cyclopeptides (sartoryglabramides A and B) from the genus *Neosartorya*. In addition, despite the fact that compounds **1**–**8** did not exhibit antimicrobial activities in our assay protocols,

it does not mean that they do not possess any other relevant biological activities. It is also worth mentioning that several cyclopeptides have been shown to possess antifungal and antibacterial activities, however, their potencies depend on the stereochemical configurations of the amino acids constituents [23]. Therefore, it is not surprising that the stereochemistry of the amino acids constituents of both sartoryglabramides A (**5**) and B (**6**) could play an important role in their (lack of) antimicrobial activities. Therefore, it is necessary to further examine the isolated metabolites in other target-based assay protocols.

Supplementary Materials: The supplementary materials are available online at www.mdpi.com/1660-3397/14/7/136/s1.

Acknowledgments: This work was developed in the Natural Products Research Laboratory of the Department of Chemistry, Instituto de Ciências Biomédicas Abel Salazar (ICBAS) of the University of Porto, and partially supported through national funds provided by FCT—Foundation for Science and Technology and European Regional Development Fund (ERDF) and COMPETE, under the projects PEst-C/MAR/LA0015/2013, PTDC/MAR-BIO/4694/2014 as well as by the project INNOVMAR—Innovation and Sustainability in the Management and Exploitation of Marine Resources (reference NORTE-01-0145-FEDER-000035, within Research Line NOVELMAR/INSEAFOOD/ECOSERVICES), supported by North Portugal Regional Operational Programme (NORTE 2020), under the PORTUGAL 2020 Partnership Agreement, through the European Regional Development Fund (ERDF)". We thank Michael Lee of the Department of Chemistry, Leicester University (UK) for providing the HRESIMS. War War May Zin thanks the Lotus Unlimited Project under the ERASMUS MUNDUS ACTION 2-EU-Asia Mobility Project for a Ph.D. scholarship. We thank Júlia Bessa for technical support.

Author Contributions: A.K. and M.P. conceived, designed the experiments; W.W.M.Z. performed isolation, purification and structure elucidation of the compounds; S.B. participated in structure elucidation of the compounds; T.D. collected, identified, cultured the fungus and prepared the extract; L.G. performed X-ray analysis; J.P. performed molecular mechanics conformation analysis; A.S. provided NMR spectra; C.F. and S.C. performed chiral HPLC analyses of the amino acids; N.S. participated in discussion of the results; A.K. wrote the paper.

Conflicts of Interest: The authors declare no conflict of interest.

References

1. Zin, W.W.; Prompanya, C.; Buttachon, S.; Kijjoa, A. Bioactive secondary metabolites from a Thai collection of soil and marine-derived fungi of the genera *Neosartorya* and *Aspergillus*. *Curr. Drug Deliv.* **2016**, *13*, 378–388. [PubMed]
2. Jayasuriya, H.; Zink, D.; Basilio, A.; Vicente, F.; Collado, J.; Bills, G.; Goldman, M.L.; Motyl, M.; Huber, J.; Dezeny, G.; et al. Discovery and antibacterial activity of glabramycin A–C from *Neosartorya glabra* by an antisense strategy. *J. Antibiot.* **2009**, *62*, 265–269. [CrossRef] [PubMed]
3. Ishigami, K.; Yamamoto, M.; Watanabe, H. Synthesis and revision of the relative configuration of glabramycin B. *Tetrahedron Lett.* **2016**, *56*, 6290–6293. [CrossRef]
4. Kijjoa, A.; Santos, S.; Dethoup, T.; Manoch, L.; Almeida, A.P.; Vasconcelos, M.H.; Silva, A.; Gales, L.; Herz, W. Sartoryglabrins, analogs of ardeemins, from *Neosartorya glabra*. *Nat. Prod. Comm.* **2011**, *6*, 1–6.
5. Liu, W.-H.; Zhao, H.; Li, R.-Q.; Zheng, H.-B.; Yu, Q. Polyketides and meroterpenoids from *Neosartorya glabra*. *Helv. Chim. Acta* **2015**, *98*, 515–519. [CrossRef]
6. Kobayashi, M.; Krishna, M.M.; Ishida, K.; Anjaneyulu, V. Marine sterols. XXII. Occurrence of 3-oxo-4,6,8(14)-triunsaturated steroids in the sponge *Dysidea herbacea*. *Chem. Pharm. Bull.* **1992**, *40*, 72–74. [CrossRef]
7. Cantrell, C.L.; Franzblau, S.G.; Fischer, N.H. Antimycobacterial plant terpenoids. *Planta Med.* **2001**, *67*, 685–694. [CrossRef] [PubMed]
8. Fujimoto, H.; Negishi, E.; Yamaguchi, K.; Nishi, N.; Yamazaki, M. Isolation of new tremorgenic metabolites from an ascomycete *Corynascus setosus*. *Chem. Pharm. Bull.* **1996**, *44*, 1843–1848. [CrossRef]
9. Eamvijarn, A.; Gomes, N.M.; Dethoup, T.; Buaruang, J.; Manoch, L.; Silva, A.; Pedro, M.; Marini, I.; Roussis, V.; Kijjoa, A. Bioactive meroditerpenes and indole alkaloids from the soil fungus *Neosartorya fischeri* (KUFC 6344), and the marine-derived fungi *Neosartorya laciniosa* (KUFC 7896) and *Neosartorya tsunodae* (KUFC 9213). *Tetrahedron* **2013**, *69*, 8583–8591. [CrossRef]

10. Yin, W.B.; Grundmann, A.; Cheng, J.; Li, S.M. Acetylaszonalenin biosynthesis in *Neosartorya fischeri*: Identification of the biosynthetic gene cluster by genomic mining and functional proof of the genes by biochemical investigation. *J. Biochem. Chem.* **2009**, *284*, 100–109. [CrossRef] [PubMed]
11. Zin, W.W.; Buttachon, S.; Buaruang, J.; Gales, L.; Pereira, J.A.; Pinto, M.M.; Silva, A.M.S.; Kijjoa, A. A new meroditerpene and a new tryptoquivaline analog from the algicolous fungus *Neosartorya takakii* KUFC 7898. *Mar. Drugs* **2015**, *13*, 3776–3790. [CrossRef] [PubMed]
12. Sorra, K.; Chang, C.-F.; Pusuluri, S.; Mukkanti, K.; Laiu, M.-C.; Bao, B.-Y.; Su, C.-H.; Chuang, T.-H. Synthesis and cytotoxicity testing of new amido-substituted triazolopyrrol[2,1-*c*][1,4]benzodiazepine (PBDT) derivatives. *Molecules* **2012**, *17*, 8762–8772. [CrossRef] [PubMed]
13. Kozlovsky, N.G.; Vinokurova, N.G.; Adanin, V.M.; Burkhardt, G.; Hans-Martin Dahse, H.-M.; Gräfe, U. New diketopiperazine alkaloids from *Penicillium fellutanum*. *J. Nat. Prod.* **2000**, *63*, 698–700. [CrossRef] [PubMed]
14. Qureshi, A.; Salvá, J.; Harper, M.K.; Faulkner, D.J. New cyclic peroxides from the Philippine sponge *Plakinastrella* sp. *J. Nat. Prod.* **2001**, *64*, 553–554. [CrossRef]
15. Prompanya, C.; Fernandes, C.; Cravo, S.; Pinto, M.M.M.; Dethoup, T.; Silva, A.M.S.; Kijjoa, A. A new cyclic hexapeptide and a new isocoumarin derivative from the marine sponge-associated fungus *Aspergillus similanensis* KUFA 0013. *Mar. Drugs* **2015**, *13*, 1432–1450. [CrossRef] [PubMed]
16. Berthod, A.; Liu, Y.; Bagwill, C.; Armstrong, D.W. Facile liquid chromatographic enantioresolution of native amino acids and peptides using a teicoplanin chiral stationary phase. *J. Chromatogr. A* **1996**, *731*, 123–127. [CrossRef]
17. Bodanszky, M. Principles of Peptide Synthesis. In *Reactivity and Structure: Concepts in Organic Chemistry*; Springer Science & Business Media: New York, NY, USA, 2012; Volume 16, p. 218.
18. Jabs, A.; Weiss, M.S.; Hilgenfeld, R. Non-proline cis peptide bonds in proteins. *J. Mol. Biol.* **1999**, *286*, 291–304. [CrossRef] [PubMed]
19. Gomes, N.M.; Bessa, L.J.; Buttachon, S.; Costa, P.M.; Buaruang, J.; Dethoup, T.; Silva, A.M.S.; Kijjoa, A. Antibacterial and antibiofilm activities of tryptoquivalines and meroditerpenes isolated from the marine-derived fungi *Neosartorya paulistensis*, *N. laciniosa*, *N. tsunodae*, and the soil fungi *N. fischeri* and *N. siamensis*. *Mar. Drugs* **2014**, *12*, 822–839. [CrossRef] [PubMed]
20. Wattanadilok, R.; Sawangwong, P.; Rodrigues, C.; Cidade, H.; Pinto, M.; Pinto, E.; Silva, A.; Kijjoa, A. Antifungal activity evaluation of the constituents of *Haliclona baeri* and *H. cymaeformis*, collected from the Gulf of Thailand. *Mar. Drugs* **2007**, *5*, 40–51. [CrossRef] [PubMed]
21. Matsuzawa, T.; Horie, Y.; Abliz, P.; Gonoi, T.; Yaguchi, T. *Aspergillus huiyaniae* sp. nov., a new teleomorphic species in *Aspergillus* section *Fumigati* isolated from desert soil in China, and described using polyphasic approach. *Mycoscience* **2014**, *55*, 213–220. [CrossRef]
22. Sheldrick, G.M. A short history of SHELX. *Acta Cryst.* **2008**, *64*, 112–122. [CrossRef] [PubMed]
23. Xu, L.; Meng, W.; Cao, C.; Wang, J.; Shan, W.; Wang, Q. Antibacterial and antifungal compounds from marine fungi. *Mar. Drugs* **2015**, *13*, 3497–3515. [CrossRef] [PubMed]

APPENDIX V

Zin, W. W. M., Buttachon, S., Dethoup, T., Pereira, J. A., Gales, L., Inácio, Â., Costa, P. M., Lee, M., Sekeroglu, N., and Silva, A. M. **(2017)**. Antibacterial and antibiofilm activities of the metabolites isolated from the culture of the mangrove-derived endophytic fungus *Eurotium chevalieri* KUFA 0006. *Phytochemistry* **141**, 86-97. Doi.org/10.1016/j.phytochem.2017.05.015.

Phytochemistry 141 (2017) 86–97

Contents lists available at ScienceDirect

Phytochemistry

journal homepage: www.elsevier.com/locate/phytochem

Antibacterial and antibiofilm activities of the metabolites isolated from the culture of the mangrove-derived endophytic fungus *Eurotium chevalieri* KUFA 0006

War War May Zin [a, b], Suradet Buttachon [a, b], Tida Dethoup [c], José A. Pereira [a, b], Luís Gales [a, d], Ângela Inácio [b], Paulo M. Costa [a, b], Michael Lee [e], Nazim Sekeroglu [f], Artur M.S. Silva [g], Madalena M.M. Pinto [b, h], Anake Kijjoa [a, b, *]

[a] ICBAS-Instituto de Ciências Biomédicas Abel Salazar, Rua de Jorge Viterbo Ferreira, 228, 4050-313, Porto, Portugal
[b] Interdisciplinary Centre of Marine and Environmental Research (CIIMAR), Terminal de Cruzeiros do Porto de Lexões, Av. General Norton de Matos s/n, 4450-208, Matosinhos, Portugal
[c] Department of Plant Pathology, Faculty of Agriculture, Kasetsart University, Bangkok, 10240, Thailand
[d] Instituto de Biologia Molecular e Celular (IBMC), Universidade do Porto, Rua de Jorge Viterbo Ferreira, 228, 4050-313, Porto, Portugal
[e] Department of Chemistry, University of Leicester, University Road, Leicester, LE 7 RH, UK
[f] Medicinal and Aromatic Plant Programme, Plant and Animal Sciences Department, Vocational School, Kilis 7 Aralık University, 79000, Kilis, Turkey
[g] Departamento de Química & QOPNA, Universidade de Aveiro, 3810-193, Aveiro, Portugal
[h] Laboratório de Química Orgânica, Departamento de Ciências Químicas, Faculdade de Farmácia, Universidade do Porto, Rua de Jorge Viterbo Ferreira, 228, 4050-313, Porto, Portugal

ARTICLE INFO

Article history:
Received 9 March 2017
Received in revised form
5 May 2017
Accepted 27 May 2017
Available online 3 June 2017

Keywords:
Eurotium chevalieri
Trichocomaceae
Prenylated indoles
Isochromone
Anthraquinones
Diketopiperazines
Mangrove-derived fungus
Antibacterial activity
Antibiofilm

ABSTRACT

Five previously undescribed metabolites, including acetylquestinol, two prenylated indole 3-carbaldehyde derivatives, an anthranilic acid derivative and an isochromone derivative, were isolated, in addition to eleven known compounds: palmitic acid, ergosterol 5,8-endoperoxide, emodin, physcion, questin, questinol, (11*S*, 14*R*)-cyclo(tryptophylvalyl), preechinulin, neoechinulin E, echinulin and eurocristatine, from the culture of the endophytic fungus *Eurotium chevalieri* KUFA 0006. The structures of the previously undescribed compounds were established based on an extensive 1D and 2D NMR spectral analysis as well as HRMS and IR data. In case of 2-(2, 2-dimethylcyclopropyl)-1*H*-indole-3-carbaldehyde and 6, 8-dihydroxy-3-(2*S*-hydroxypropyl)-7-methylisochromone, the absolute configurations of their stereogenic carbons were established based on comparison of their experimental and calculated ECD spectra. All the compounds, except for palmitic acid and ergosterol 5, 8-endoperoxide, were evaluated for their antibacterial and antibiofilm activities against two Gram-positive and two Gram-negative bacteria, as well as multidrug-resistant isolates from the environment. Emodin not only exhibited moderate antibacterial activity against the Gram-positive bacteria but also showed strong synergistic association with oxacillin against MRSA *Staphylococcus aureus*.

1. Introduction

The fungi of the genus *Eurotium* (Family Trichocomaceae) have shown to produce a variety of interesting bioactive specialised metabolites (Smetanina et al., 2007; Li et al., 2008a, 2008b). For this reason we have previously investigated these metabolites from the culture of the marine-sponge associated fungus *Eurotium cristatum* KUFC 7356 and their *in vitro* anticancer activity during our research program of biodiscovery of novel bioactive metabolites from marine-derived fungi (Almeida et al., 2010; Gomes et al., 2012). On the other hand, it is well recognized that mangrove-derived

* Corresponding author. ICBAS-Instituto de Ciências Biomédicas Abel Salazar, Rua de Jorge Viterbo Ferreira, 228, 4050-313, Porto, Portugal.
E-mail addresses: wwmzin.chem.yu@gmail.com (W.W. May Zin), nokrari_209@hotmail.com (S. Buttachon), tdethoup@yahoo.com (T. Dethoup), jpereira@icbas.up.pt (J.A. Pereira), lgales@ibmc.up.pt (L. Gales), angelainacio@gmail.com (Â. Inácio), pmcosta@icbas.up.pt (P.M. Costa), ml34@leicester.ac.uk (M. Lee), nsekeroglu@gmail.com (N. Sekeroglu), artur.silva@ua.pt (A.M.S. Silva), madalena@ff.up.pt (M.M.M. Pinto), ankijjoa@icbas.up.pt (A. Kijjoa).

http://dx.doi.org/10.1016/j.phytochem.2017.05.015
0031-9422/

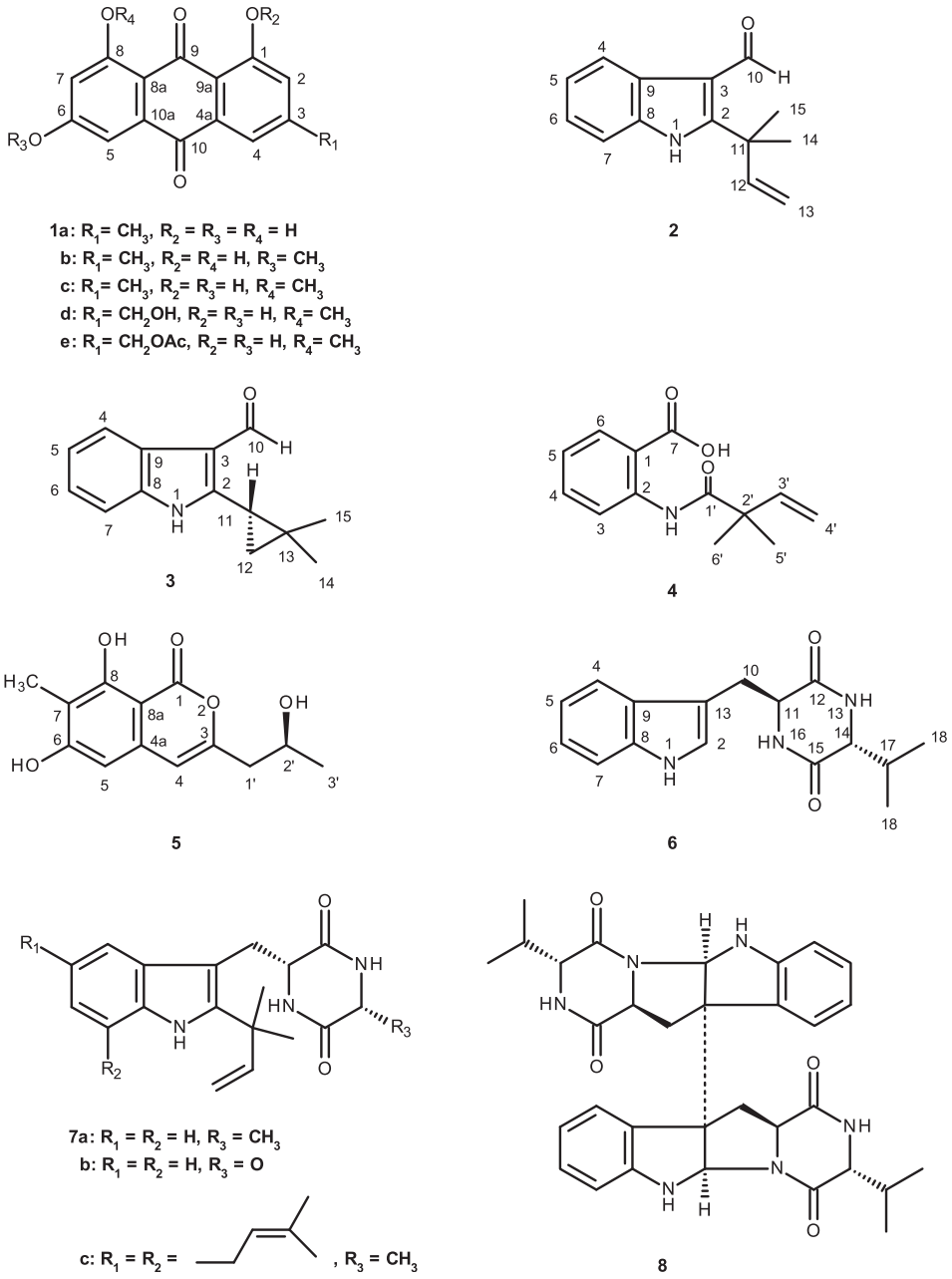

Fig. 1. Specialised metabolites from the culture of *Eurotium chevalieri* KUFA 0006.

endophytic fungi are promising sources of structurally unprecedented natural products and drug leads with an amazing array of bioactivities (Debbab et al., 2013). Combining these concepts with the objective to search for antibiotics from marine-derived fungi, we have decided to investigate if the endophytic strain of *Eurotium chevalieri* L. Mangin, isolated from the mangrove tree, could produce different specialised metabolites from the previously investigated soil-derived strain (Kanokmedhakul et al., 2011) as well as to find new compounds with antibacterial activity. The ethyl acetate extract of *E. chevalieri* KUFA 0006, isolated from the inner twig of *Rhizophora mucronata* Poir, which was collected in the Eastern Seaboard of Thailand, furnished five previously undescribed metabolites including the anthraquinone derivative acetylquestinol (**1e**), two prenylated indole 3-carbaldehydes (**2**, **3**), an anthranilic acid derivative (**4**) and an isochromone derivative (**5**), along with palmitic acid, ergosterol 5,8-endoperoxide (Cantrell et al., 2001), four previously described anthraquinones: emodin (**1a**) (Bao et al., 2013), physcion (**1b**) (Anke et al., 1980), questin (**1c**) (Li et al., 2009), questinol (**1d**) (Bao et al., 2013), and the previously reported diketopiperazine derivatives: echinulin (**7c**) (Smetanina et al., 2007), neoechinulin E (**7b**) (Li et al., 2008a), preechinulin (**7a**) (Aoki et al., 2010), (11*R*, 14*S*)-3-(1*H*-indol-3ylmethyl) 6-isopropyl-2, 5-piperazinedione (**6**) and eurocristatine (**8**) (Gomes et al., 2012) (Fig. 1).

All the isolated compounds, except palmitic acid and ergosterol 5, 8-endoperoxide, were tested for their antibacterial activity against two Gram-positive (*Staphylococcus aureus* ATCC 25923 and *Enterococcus faecalis* ATCC 29212) and two Gram-negative (*Escherichia coli* ATCC 25922 and *Pseudomonas aeruginosa* ATCC 27853) bacteria as well as multidrug-resistant isolates from the

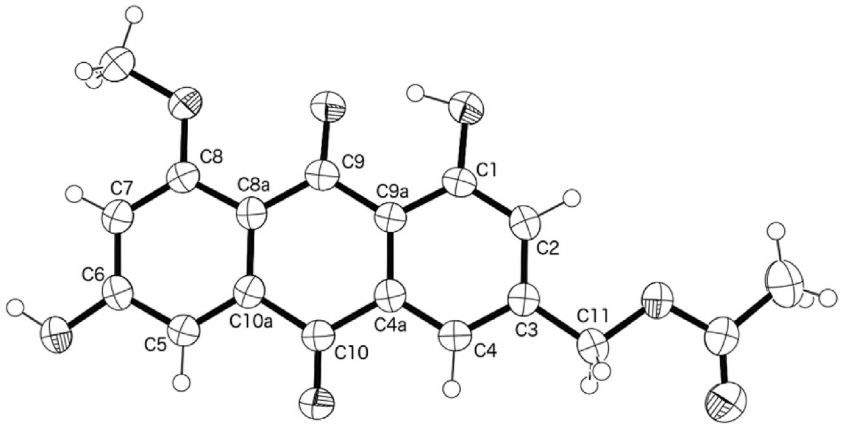

Fig. 2. Ortep view of compound **1e**.

environment. The tested compounds were also investigated for their capacity to inhibit biofilm formation in the reference strains of *S. aureus*, *E. faecalis* and *E. coli*. The potential synergism between the tested compounds and the clinically used antibiotics was also evaluated against multidrug-resistant bacteria: methicillin-resistant *S. aureus* (MRSA), vancomycin-resistant enterococci (VRE) and extended-spectrum beta- lactamases *E. coli* (ESBL).

2. Results and discussion

The structures of palmitic acid, ergosterol 5,8-endoperoxide, emodin (**1a**), physcion (**1b**), questin (**1c**), questinol (**1d**), echinulin (**7c**), neoechinulin E (**7b**), preechinulin (**7a**) and eurocristatine (**8**) were elucidated by analysis of their ^{1}H, ^{13}C NMR spectra and HRMS data, as well as by comparison of their spectral data to those reported in the literature.

Compound **1e** was isolated as yellow crystal (mp 101-103 °C) and its molecular formula was determined as $C_{18}H_{14}O_7$, based on the (+)-HRESIMS *m/z* 343.0814 $[M+H]^+$ (calculated 343.0818), indicating twelve degrees of unsaturation. The IR spectrum showed absorption bands for hydroxyl (3442 cm^{-1}), ester (1749 cm^{-1}), conjugated carbonyl (1631 cm^{-1}) and aromatic (1588 cm^{-1}) groups. The ^{13}C NMR spectrum exhibited seventeen carbon signals which, based on DEPTs and HSQC spectra, can be classified as two conjugated ketone carbonyls (δ_C 186.0 and 182.2), one ester carbonyl (δ_C 170.2), eight quaternary sp^2 [δ_C 163.6, 161.7 (2C), 144.2, 136.7, 132.5, 116.0, 111.8], four methine sp^2 (δ_C 122.3, 116.6, 107.5, 105.3), one methylene sp^3 (δ_C 64.3), one methoxy (δ_C 56.3) and one methyl (δ_C 20.6) groups. The ^{1}H NMR spectrum, together with the COSY spectrum, exhibited two pairs of *meta*-coupled aromatic protons at δ_H 7.24, d (J = 1.5 Hz)/δ_H 7.54, d (J = 1.5 Hz) and δ_H 7.17, d (J = 2.2 Hz)/δ_H 6.81, d (J = 2.2 Hz), a broad singlet of a hydrogen-bonded phenolic hydroxyl at δ_H 13.38, an aromatic methoxyl singlet at δ_H 3.89, a singlet of two magnetically equivalent oxymethylene protons at δ_H 5.15 and a methyl singlet at δ_H 2.13. The ^{1}H and ^{13}C NMR general features of **1e** suggested that it is a 1,3,6,8-tetrasubsituted 9,10-anthraquinone, similar to questinol (Bao et al., 2013). The presence of the acetoxyl group (δ_H 2.13/δ_C 20.6; δ_C 170.2) together with the higher frequency oxymethylene protons at δ_H 5.15 (δ_C 64.3) led to the conclusion that the structure of **1e** was acetylquestinol, which was confirmed by the X-ray analysis as shown in the ORTEP view (Fig. 2). Literature search revealed that, although questinol was isolated from several sources (Bao et al., 2013; Yang et al., 2014), this is the first report on isolation of acetylquestinol.

The concomitant isolation of questinol (**1d**) and acetylquestinol (**1e**) from the ethyl acetate extract of this fungus could raise the prospect of acetylquestinol (**1e**) being originated from questinol (**1d**) during the extraction process. However, this hypothesis seems to be improbable since many natural products with the acetoxyl group have been isolated from many extracts other than ethyl acetate extract. Moreover, the extraction condition is not vigorous enough to promote a nucleophilic substitution of a strong base (OMe) of ethyl acetate by a primary hydroxyl group in questinol (**1d**). On the contrary, acetyl CoA from the biosynthetic pool is the most probable acetylating agent.

Compound **2** was isolated as yellow crystal (mp 162–164 °C) and its molecular formula $C_{14}H_{15}NO$ was determined based on the (+)-HRESIMS *m/z* 214.1236 $[M+H]^+$ (calculated 214.1232), indicating eight degrees of unsaturation. The IR spectrum showed absorption bands for amine (3242 cm^{-1}), carbonyl (1735 cm^{-1}), aromatic (1583 cm^{-1}) and olefin (1622 cm^{-1}) groups. The ^{13}C NMR spectrum (Table 1) exhibited thirteen carbon signals which, in combination with DEPTs and HSQC spectra, can be categorized as one aldehyde carbonyl (δ_C 186.6), four quaternary sp^2 (δ_C 155.0, 133.9, 127.2, 113.9), five methine sp^2 (δ_C 145.0, 123.5, 123.1, 122.0, 111.0), one methylene sp^2 (δ_C 114.0), one quaternary sp^3 (δ_C 39.0) and two methyl (δ_C 28.9) groups. The ^{1}H NMR and COSY spectra (Table 1) revealed the presence of four aromatic protons of a 1, 2-disubstituted benzene ring at δ_H 8.37, dd (J = 7.4, 2.0 Hz, H-4), δ_H 7.38, dd (J = 7.4, 2.0 Hz, H-7), δ_H 7.27, ddd (J = 7.4, 7.4, 2.0 Hz, H-5) and δ_H 7.24, ddd (J = 7.4, 7.4, 2.0 Hz, H-6), three olefinic protons of the vinyl group at δ_H 6.24, dd (J = 17.5, 11.0 Hz, H-12), 5.27, d (J = 11.0 Hz, H-13b), 5.28, d (J = 17.5, Hz, H-13a), in addition to a singlet of an aldehyde proton at δ_H 10.49 (H-10), a broad singlet of NH group at δ_H 8.96 (NH-1) and a singlet of two methyl groups at δ_H 1.68 (Me-14, 15). The HMBC spectrum (Table 1) showed correlations from H-4 to C-8 (δ_C 133.9), from H-5 and H-7 to C-9 (δ_C 127.2), from H-6 to C-8 as well as from the aldehyde proton (H-10) to C-3 (δ_C 113.9) and C-9, suggesting the existence of a 3-carbaldehyde indole moiety. Moreover, the HMBC spectrum also showed correlations from H-12 to C-11 (δ_C 39.8), from H-13a/13b and H_3-14/15 to C-11 and C-12 (δ_C 145.0), indicating the presence of the 2-methyl-3-en-2-yl substituent. As both H-12 and H_3-14/15 also showed HMBC cross peaks to C-2 (δ_C 155.0), the 2-methyl-3-en-2-yl substituent was placed on C-2. Taking into account the ^{1}H and ^{13}C chemical shift values and their correlations, the structure of **2** was established as 2-(2-methyl-3-en-2-yl)-1*H*-indole-3-carbaldehyde. Literature search revealed that **2** has never been reported previously.

Compound **3** is an isomer of **2** since it has the same molecular formula ($C_{14}H_{15}NO$) as **2**, as determined by the (+)-HRESIMS *m/z* 214.1239 $[M+H]^+$ (calculated 214.1232). The IR spectrum showed

Table 1
^{1}H and ^{13}C NMR ($CDCl_3$, 300.13 MHz and 75.4 MHz) of **2** and **3**.

Position	**2**				**3**			
	δ_C, type	δ_H, (J in Hz)	COSY	HMBC	δ_C, type	δ_H, (J in Hz)	COSY	HMBC
1	–	8.96, brs	–	–	–	8.91, s	–	
2	155.0, C	–			150.6, C		–	
3	113.9, C	–			116.7, C		–	
4	122.0, CH	8.37, dd (7.4, 2.0)	H-5	C-6, 8	121.2, CH	8.26, dd (7.5, 2.0)	H-5	C-6, 8
5	123.1, CH	7.27, ddd (7.4, 7.4, 2.0)	H-4, 6	C-7, 9	122.9, CH	7.26, ddd (7.5, 7.5, 2.0)	H-4, 6	C-7, 9
6	123.5, CH	7.24, ddd (7.4, 7.4, 2.0)	H-5, 7	C-4, 8	123.5, CH	7.23, ddd (7.5, 7.5, 2.0)	H-5, 7	C-4, 8
7	111.0, CH	7.38, dd (7.4, 2.0)	H-6	C-5, 9	111.0, CH	7.35, dd (7.5, 2.0)	H-6	C-5, 9
8	133.9, C	–			134.8, C	–		
9	127.2, C	–			126.2, C	–		
10	186.6, CHO	10.49, s	–	C-3, 9	185.4, CHO	10.19, s		C-3, 9
11	39.8, C	–			21.0, CH	2.25, dd (8.4, 5.9)	H-12a, 12b	C-13, 14, 15
12a	145.0, CH	6.24, dd (17.5, 11.0)	H-13a, 13b	C-2, 11	19.4, CH_2	1.12, dd (8.4, 5.1)	H-11, 12b	C-2, 11
b		–				1.05, dd (5.7, 5.7)	H-11, 12a	C-2, 11, 14
13a	114.0, CH_2	5.27, d (11.0)	H-12	C-11, 12	20.8, C	–		
b		5.28, d (17.5)	H-12	C-11, 12				
14	28.9, CH_3	1.68, s	–	C-2, 11, 12, 15	26.2, CH_3	1.32, s		C-11, 15
15	28.9, CH_3	1.68, s	–	C-2, 11, 12, 14	21.3, CH_3	0.92, s		C-11, 15

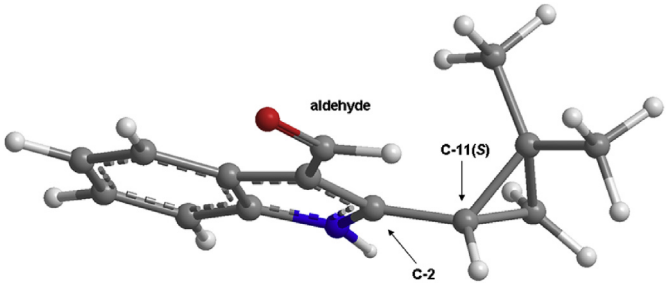

Fig. 3. The most stable conformation of **3** (C-11*S*), representing a fraction of around 90% of all four main conformations. In this visualization, the aldehyde is the nearest group and the rings are viewed from below.

also absorption bands for amine (3252 cm^{-1}), carbonyl (1768 cm^{-1}), aromatic (1583, 1558 cm^{-1}), and olefin (1633 cm^{-1}) groups. The general features of the ^{1}H and ^{13}C NMR spectra (Table 1) of **3** resemble those of **2**, revealing the presence of a 1*H*-indole-3-carbaldehyde moiety. This suggestion was supported by the HMBC correlations (Table 1) of the singlet of the aldehyde proton at δ_H 10.19 (H-10) to C-3 (δ_C 116.7) and C-9 (δ_C 126.2), from H-4 (δ_H 8.26, dd, $J = 7.5$, 2.0 Hz) to C-8 (δ_C 134.8), from H-5 (δ_H 7.26, ddd, $J = 7.5$, 7.5, 2.0 Hz) and H-7 (δ_H 7.35, dd, $J = 7.5$, 2.0 Hz) to C-9 (δ_C 126.2), and from H-6 (δ_H 7.23, ddd, $J = 7.5$, 7.5, 2.0 Hz) to C-8. That the substituent on C-2 was the 2, 2-dimethylcyclopropyl group was substantiated by the presence of two tertiary methyls (δ_H 1.32, s/δ_C 26.2, Me-14, and δ_H 0.92, s/δ_C 21.3, Me-15), one methylene sp^3 (δ_H 1.05, dd, $J = 5.7$, 5.7 Hz and 1.12, dd, $J = 8.4$, 5.1 Hz/δ_C 19.4, C-12), one methine proton (δ_H 2.25, dd, $J = 8.4$, 5.7 Hz/δ_C 21.0, C-11) and one quaternary sp^3 carbon (δ_C 20.8, C-13) as well as by the HMBC correlations from H_3-14 and H_3-15 to C-11, from H_2-12 to C-2, C-11 and C-14, as well as from H-11 to C-13 and C-14. Therefore, the structure of **3** was established as (2, 2-dimethylcyclopropyl)-1*H*-indole-3-carbaldehyde.

Since **3** was isolated as a yellowish viscous liquid, the stereochemistry of C-11 could not be determined by X-ray analysis. Therefore, the absolute configuration of C-11 of **3** was determined by comparison of the experimental electronic circular dichroism (ECD) spectrum with the calculated ECD spectra. In order to perform ECD calculations, conformational analysis by dihedral driver search and MM2 minimization was carried out which resulted in four main conformations, of which the most populated is represented in Fig. 3 (11*S* enantiomer). The other three conformations resulted from rotating the aldehyde and/or the C-2/C-11 bond by 180°. Each conformation was energetically optimized using APFD/6-311 + G (2d, p) model chemistry and the IEFPCM model of solvation for chloroform. The Gibbs energies thereby obtained were used to determine the populations of each conformation by Boltzmann weighing at 298 K (Mori et al., 2006). The conformation shown in Fig. 3 represents 89.5% of all conformers and was therefore solely used to calculate ECD spectra (Fig. 4) for the C-11*S* enantiomer, which superimposed on the experimental spectrum. ECD transitions calculations used the same model chemistry as the energy minimization but with the time-dependent (TD) method. The experimentally observed negative Cotton effects (242 nm, $\Delta\varepsilon = -1.4\ M^{-1}\ cm^{-1}$ and 280 nm, $\Delta\varepsilon = -0.7\ M^{-1}\ cm^{-1}$) fit well the calculated spectrum. Therefore, the absolute configuration of C-11 is determined to be *S*. To the best of our knowledge, the structure of **3** has not yet been reported so far.

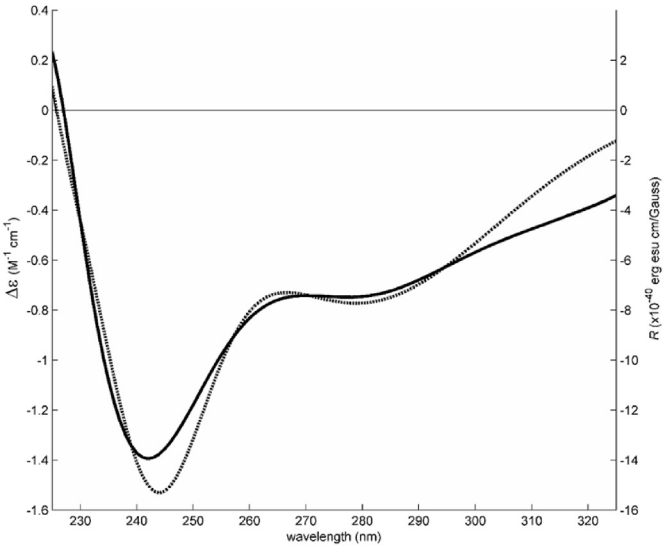

Fig. 4. Experimental (solid, left axis) and simulated (dotted, right axis) ECD spectra of **3** (C-11*S*) in chloroform. A line broadening of 0.4 eV was applied to calculated rotatory strengths. The experimental data exhibit two minima around 242 nm ($\Delta\varepsilon = -1.4\ M^{-1}\ cm^{-1}$) and 280 nm ($\Delta\varepsilon = -0.7\ M^{-1}\ cm^{-1}$) that are well matched by the calculated data.

Compound **4** was also isolated as yellow viscous liquid. The (+)-HRESIMS exhibited the *m/z* at 234.1132 $(M + H)^+$, corresponding to $C_{13}H_{16}NO_3$ (calculated 234.1130). Therefore, the molecular formula of **4** is $C_{13}H_{15}NO_3$, indicating seven degree of unsaturation. The IR spectrum showed absorption bands for amine (3421 cm^{-1}), hydroxyl (3253 cm^{-1}), conjugated carbonyl (1696 cm^{-1}), amide carbonyl (1670 cm^{-1}), aromatic (1606, 1586 cm^{-1}) and olefin (1636 cm^{-1}) groups. The ^{13}C NMR spectrum (Table 2) exhibited twelve carbon signals which can be classified, according to DEPTs and HSQC spectra, as two carbonyl (δ_C 174.4 and 169.9), two quaternary sp^2 (δ_C 141.2, 116.4), five methine sp^2 (δ_C 142.5, 133.9, 131.2, 122.4, 119.4), one methylene sp^2 (δ_C 114.4), one quaternary sp^3 (δ_C 46.3) and two tertiary methyl (δ_C 24.4) groups. The ^1H NMR spectrum (Table 2), in combination with COSY and HSQC spectra, exhibited the signals of aromatic protons of the 1, 2-disubsituted benzene ring at δ_H 8.60, d (J = 7.8 Hz, H-3; δ_C 119.4), 8.00, dd (J = 7.8, 1.5 Hz, H-6; δ_C 131.2), 7.57, ddd (J = 7.8, 7.8, 1.5 Hz, H-4; δ_C 133.9), 7.13, ddd (J = 7.8, 7.8, 1.5 Hz, H-5; δ_C 122.4), three vinyl proton signals at δ_H 6.09, dd (J = 17.4, 10.6 Hz, H-3'; δ_C 142.5), 5.27, d (J = 17.4 Hz, H-4'a; δ_C 114.4) and 5.22, d (J = 10.6 Hz, H-4'b; δ_C 114.4) and a methyl singlet at δ_H 1.32 (Me-5′, 6′, δ_C 24.4), in addition to a broad singlet of the hydroxyl group at δ_H 11.55. The HMBC spectrum (Table 2), exhibited correlations from the methyl singlet of Me-5'/6′ to the quaternary sp^3 carbon at δ_C 46.3 (C-2′), the olefinic carbon at δ_C 142.5 (C-3′) and the carbonyl carbon at δ_C 174.4 (C-1′), from H-4'a and H-4'b to C-2′ and C-3′, as well as from H-3′ to C-2′ and C-5'/6′, revealing the existence of a 2, 2-dimethylbut-3-enoyl moiety. Additionally, the HMBC spectrum also exhibited correlations from H-6 to C-2 (δ_C 141.2) and C-7 (δ_C 169.9), and from H-3 to C-1 (δ_C 116.4), confirming the presence of the anthranilic acid moiety. Taking together the NMR data and its molecular formula, the structure of **4** was established as 2[(2, 2-dimethylbut-3-enoyl)amino]benzoic acid. Literature search revealed that **4** has never been previously reported.

Compound **5** was also isolated as yellow viscous liquid and its molecular formula $C_{13}H_{14}O_5$ was determined based on the (+)-HRESIMS *m/z* 251.0900 $[M+H]^+$ (calculated 251.0919), indicating seven degrees of unsaturation. The IR spectrum showed absorption bands for hydroxyl (3443 cm^{-1}), a conjugated ester carbonyl (1671 cm^{-1}), aromatic (1540, 1507 cm^{-1}) and olefin (1623 cm^{-1}) groups. The ^{13}C NMR spectrum (Table 2) exhibited thirteen carbon signals which can be categorized, according to the DEPTs and HSQC spectra, into one conjugated ester carbonyl (δ_C 166.2), six quaternary sp^2 (δ_C 163.6, 159.9, 154.5, 136.4, 109.7, 97.8), three of which are oxygen bearing, two methine sp^2 (δ_C 105.4 and 101.5), one oxygen bearing methine sp^3 (δ_C 64.0), one methylene sp^3 (δ_C 42.6), and two methyl (δ_C 23.4 and δ_C 8.0) groups. The ^1H NMR spectrum (Table 2) revealed the presence of two phenolic hydroxyl groups (δ_H 11.31, s and 10.83, brs), one of which is hydrogen-bonded (δ_H 11.31, s), one aromatic (δ_H 6.44, s; δ_C 101.5, s), one olefinic (δ_H 6.48, s; δ_C 105.3, s), one secondary hydroxyl (δ_H 4.80, d, J = 4.5 Hz), one oxygen-bearing methine multiplet (δ_H 3.98; δ_H 64.0), one methylene multiplet (δ_H 2.52; δ_C 42.6), one tertiary methyl (δ_H 2.01, s, δ_C 8.0) and one secondary methyl (δ_H 1.13, d, J = 6.2 Hz; δ_C 23.4) groups. That **5** was a 6, 8-dihydroxy-7-methyl isochromone derivative was corroborated by HMBC correlations (Table 2) from the hydrogen-bonded phenolic hydroxyl at δ_H 11.31, s (OH-8) to the aromatic carbons at δ_C159.9 (C-8), 97.8 (C-8a), 109.7 (C-7), from the tertiary methyl singlet at δ_H 2.01, s (H_3-9) to C-7, C-8 and C-6 (δ_C163.6), from the singlet at δ_H 6.44 (H-5) to C-6, C-7, C-8a and C-4 (δ_C105.3), and from the singlet at δ_H 6.48, s (H-4) to C-5 (δ_C101.5), C-8a and C-3 (δ_C154.5). The presence of the 2-hydroxypropyl moiety was substantiated by COSY correlations from the methylene multiplet at δ_H 2.52 (H_2-1′) to the hydroxymethine multiplet at δ_H 3.98 (H_2-2′), from the secondary methyl doublet at δ_H 1.13 (J = 6.2 Hz, H_3-3′) to H_2-2′, as well as by the HMBC correlations (Table 2) from the hydroxyl doublet at δ_H 4.80 (J = 4.5 Hz, OH-2′) to C-1' (δ_C 42.6), C-2' (δ_C 64.0), CH_3-3' (δ_C 23.4), from H_3-3′ to C-1'. That the 2-hydroxypropyl substituent was on C-3 of the isochromone nucleus was supported by the HMBC correlations from H-4 to C-1′ as well as from H-1' to C-3 and C-4. Therefore, the structure of **5** was established as 6, 8-dihydroxy-3-(2-hydroxypropyl)-7-methyl-1*H*-isochromen-1-one.

Since **5** could not be obtained as a suitable crystal for X-ray analysis, the absolute configuration of C-2′ was established by comparison of the calculated and experimental ECD spectra. Conformational analysis of **5** by dihedral driver search and MM2 minimization resulted in eighteen main conformations, and the most populated conformation is represented in Fig. 5. The other seventeen conformations resulted from rotating the C-3'/C-2′, C-1'/

Table 2
^1H and ^{13}C NMR (DMSO, 300.13 MHz and 75.4 MHz) and HMBC assignment for **4** and **5**.

Position	**4**				**5**			
	δ_C, type	δ_H, (J in Hz)	COSY	HMBC	δ_C, type	δ_H, (J in Hz)	COSY	HMBC
1	116.4, C	–			166.2, CO	–		
2	141.2, C	–			–			
3	119.4 CH	8.60, d (7.8)	H-4	C-1, 5	154.5, C	–		
4	133.9, CH	7.57, ddd (7.8, 7.8, 1.5)	H-3, 5	C-2, 6	105.3, CH	6.48, s	–	C-3, 5, 8a, 1′
4a	–	–			136.4, C	–		
5	122.4, CH	7.13, ddd (7.8, 7.8, 1.5)	H-4, 6	C-1, 3	101.5, CH	6.44, s		C-4, 6, 7, 8a
6	131.2, CH	8.00, dd (7.8, 1.5)	H-5	C-2, 4, 7	163.6, C	–		
7	169.9, CO	–			109.7, C	–		
8	–				159.9, C	–		
8a	–				97.8, C	–		
9	–				8.0, CH_3	2.01, s	–	C-6, 7, 8
1′	174.4, CO	–			42.6, CH_2	2.51, m	H-2′	C-3, 4, 2′
2′	46.3, C	–			64.0, CH	3.98, m	OH-2′, H_3-3′	
3′	142.5, CH	6.09, dd (17.4, 10.6)	H-4'a, 4'b	C-2′, 5′, 6′	23.4, CH_3	1.13, d (6.2)	H-2′	C-1′, 2′
4'a	114.4, CH_2	5.27, d (17.4)	H-3′	C-2′, 3′				
b		5.22, d (10.6)	H-3′	C-2′, 3′				
5′	24.4, CH_3	1.32, s	–	C-1′, 2′, 3′, 6′				
6′	24.4, CH_3	1.32, s	–	C-1′, 2′, 3′, 5′				
OH-6					–	10.83, brs	–	C-6, 7
HO-7	–	11.55, brs						
OH-8					–	11.31, s	–	C-7, 8, 8a
OH-2′					–	4.80, d (4.5)	H-2′	C-1′, 2′, 3′

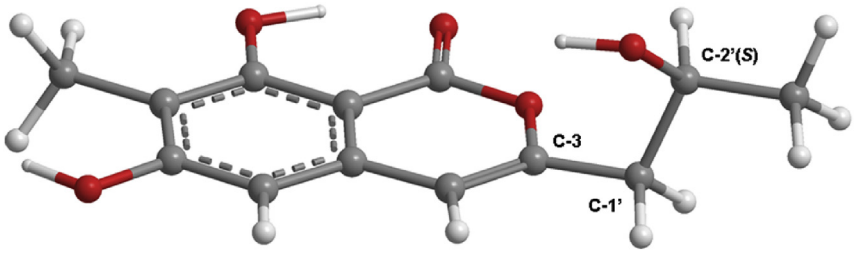

Fig. 5. Most stable conformation of **5** (C-2′*S*), representing a fraction of around 35% of all the 18 conformations considered. The next most stable conformation represents a fraction of around 13% of all conformations and is obtained by rotating the hydroxyl group in C-2′ 120° towards the viewer. In this visualization, the carbonyl group points away from the viewer and the rings are viewed diagonally from above.

C-2′ and C-2′/OH bonds by 180°, 120° and 120° steps, respectively. Each conformation was energetically optimized in Gaussian using APFD/6-311 + G(2d,p) model chemistry and IEFPCM model of solvation for methanol. The Gibbs energies thereby obtained were used to determine the populations of each conformation by Boltzmann weighing of the energies at 298 K (Mori et al., 2006). The ECD transitions for each conformation were calculated also in Gaussian using the same model chemistry as the energy minimization but with the time-dependent (TD) method. Line broadening was performed for the eighteen sets of transitions and a weighted sum enabled to obtain the calculated spectrum in Fig. 6. As can be seen, the experimentally obtained ECD spectrum, with negative Cotton effects (217 nm, $\Delta\varepsilon = -2.3\ M^{-1}\ cm^{-1}$), also in Fig. 6, fits well the calculated spectrum. Therefore, the absolute configuration of C-2′ is 2′*S*. To the best of our knowledge, **5** is a new natural product.

Finally, compound **6** was isolated as white crystal (mp 270-271 °C). Analysis of the ^{1}H, ^{13}C NMR and (+)-HRESIMS data allowed to establish its structure as 3-(1*H*-indol-3-yethyl)-6-isopropyl-2,5-piperazinedione or cyclo(tryptophylvalyl). Literature survey revealed that both 11*S*, 14*R* and 11*S*, 14*S* forms have been previously reported. While the 11*S*, 14*R* form [mp 278-280 °C; $[\alpha]_D$ −15 ($c = 1$, DMF)] was isolated from *Aspergillus chevalieri*, the 11*S*, 14*S* form [mp 294–298 °C; $[\alpha]_D$ −98 ($c = 1$, DMF)] was reported from *Phoma lingam* (Blunt and Munro, 2007). Since the specific rotation of **6**, determined in acetone, was levorotatory ($[\alpha]_D$ −187, c = 0.02, acetone), it was not possible to determine unequivocally the absolute configuration of C-11 and C-14. However, since **6** was obtained in a suitable crystal, an X-ray diffraction was performed. The ORTEP view of **6** (Fig. 7) showed clearly that the absolute configuration of C-11 and C-14 are 11*S* and 14*R*, respectively.

Biosynthetically, compounds **1**–**8** are derived from different biosynthetic pathways. The biosynthesis of the prenylated indole derivatives, including diketopiperazine derivatives, has been reviewed by Li (2010).

The previously undescribed prenylated indole derivatives **2** and **3** are proposed to derive from L-tryptophan as shown in Fig. 8.

Oxidative deamination of L-Trp produces indole pyruvic acid (**I**) which, after oxidative decarboxylation, gives rise to indole acetaldehyde (**II**). Oxidation of indole acetaldehyde (**II**) gives indole acetic acid (**III**) which, after oxidative decarboxylation, leads to a formation of indole 3-carbaldehyde (**IV**). Prenylation of **IV** by different prenyltransferase enzymes gives rise to the reverse prenylated indole 3-carbaldehyde (**2**) and the prenylated 3-carbaldehyde (**V**). Cyclization of the prenyl sidechain of **V** leads to a formation of **3**.

The biosynthesis of anthraquinones has been extensively investigated and recently reviewed (Fouillaud et al., 2016). The biogenesis of **5**, from the acetate pathway, is summarized in Fig. 9. Condensation of acetyl CoA (**VI**) with five units of malonyl CoA (**VII**) gives a hexaketide intermediate (**VIII**) which, after cyclization and methylation (by SAM), forms an intermediate **IX**. Enolization of **IX** leads to a formation of an isochromone (**X**) which, after stereospecific reduction of the ketone function in the side chain, gives rise to **5**.

Compounds **1**–**8** (Fig. 1) were tested for their antibacterial activity against Gram-positive and Gram-negative bacteria, and their minimum inhibitory concentration (MIC) for the reference strains and environmental multidrug-resistant isolates were determined. In the range of concentrations tested, only emodin (**1a**) exhibited

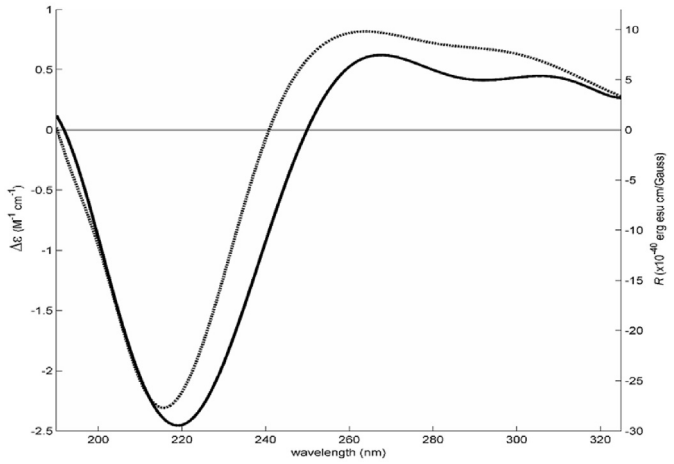

Fig. 6. Experimental (solid, right axis) and simulated (dotted, left axis) ECD spectra of **5** (C-2′*S*) in methanol. The calculated spectral line results from the Boltzmann weighing of rotatory strengths of all 18 conformations of the compound with a gaussian line broadening of 0.3 eV. The experimental data exhibit a negative, deep minimum at 217 nm ($\Delta\varepsilon = -2.3\ M^{-1}\ cm^{-1}$) and two smaller positive maxima at 260 nm ($\Delta\varepsilon = 0.8\ M^{-1}\ cm^{-1}$) and 295 nm ($\Delta\varepsilon = 0.7\ M^{-1}\ cm^{-1}$) that are well matched by the calculated data.

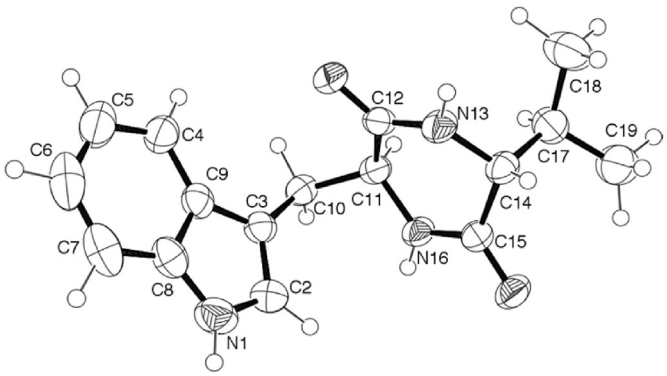

Fig. 7. Ortep view of **6**.

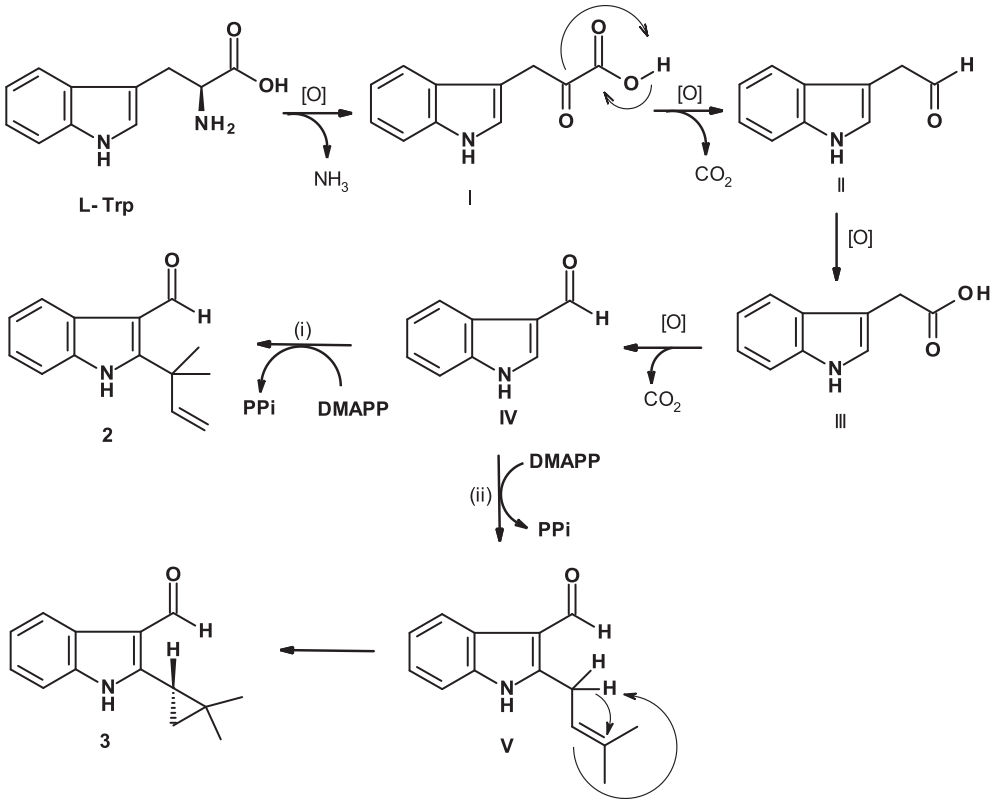

Fig. 8. Proposed biogenesis of **2** and **3**.

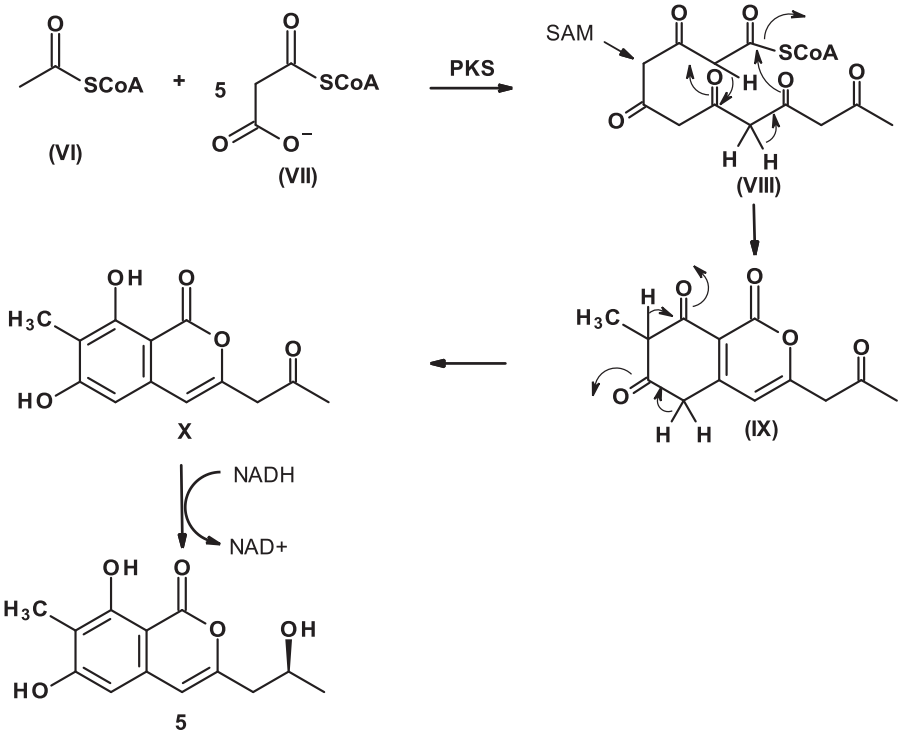

Fig. 9. Proposed biogenesis of **5**.

antibacterial activity against Gram-positive bacteria, with MIC values of 32 and 64 μg/mL for *S. aureus* ATCC 25923 and *E. faecalis* ATCC 29212, respectively (Table 3). None of the compounds were active against either Gram-negative bacteria or methicillin-resistant *S. aureus* (MRSA) and vancomycin-resistant enterococci (VRE). Since emodin (**1a**) did not exhibit the bactericidal effect

Table 3
Antimicrobial activity, expressed in μg/mL, of emodin (**1a**) against reference strains and multidrug-resistant isolates.

	E. coli ATCC 25922	*P. aeruginosa* ATCC 27853	*E. faecalis* ATCC 29212	*S. aureus* ATCC 25923	*E. coli SA/2* (ESBL)	*E. faecalis* B3/101 (VRE)	*S. aureus* 66/1 (MRSA)
MIC	>64	>64	64	32	>64	>64	>64
MBC	>64	>64	>64	>64	>64	>64	>64

MIC, minimum inhibitory concentration; MBC, minimum bactericidal concentration; ESBL, extended- spectrum beta-lactamases; VRE, vancomycin-resistant enterococci; MRSA, methicillin-resistant *Staphylococcus aureus*.

against any of the tested strains, its minimum bactericidal concentration (MBC) was not determined.

The efficacy of **1**–**8** in preventing biofilm formation was also evaluated in the reference strains. Compounds that showed a statistically significant reduction (one sample *t*-test) of biofilm formation are shown in Table 4. For emodin (**1a)**, three concentrations, i.e. 2 x MIC, MIC and ½ x MIC, were tested against *S. aureus* ATCC 25923. For the rest of the compounds, the highest concentration that did not inhibit bacterial growth was used since it was not possible to determine their MIC. Questinol (**1d**), acetylquestinol (**1e**), **3**, **5**, **6**, **7b** and **8** were found to cause a significant reduction in biofilm production by *E. coli* ATCC 25922. On the other hand, emodin (**1a**), physcion (**1b**), **2** and **3** showed inhibition of biofilm production in *S. aureus* ATCC 25923. Emodin (**1a)** not only showed maximum inhibitory effects but also interfered with the biofilm production even at the sub-inhibitory concentration. Interestingly, **3**, which is the most effective in inhibiting biofilm formation in *E. coli* ATCC 25922, also caused nearly 80% reduction of the biofilm production in *S. aureus* ATCC 25923. On the other hand, only physcion (**1b**) causes a reduction of biofilm formation in *E. faecalis* ATCC 29212.

Compounds **1**–**8** were also investigated for their potential synergy with clinically relevant antibiotics on the multidrug-resistant isolates by a disk diffusion method. The results revealed that some of the tested compounds exhibited a small to moderate synergistic association with antibiotics, depending on the multidrug-resistant strain. When tested alone, none of the compounds showed inhibition against the three multidrug-resistant strains. However, in combination with cefotaxime (CTX) in the impregnated disks, emodin (**1a**), physcion (**1b**), questinol (**1d**), **2**, **5**, **7b** and **7c** produced a small synergistic association as evidenced by a small increase in the inhibition zone when compared with the halo of inhibition produced by CTX alone in the ESBL *E. coli* strain SA/2. On the other hand, all the compounds induced a weak or moderate increase in the halo of partial inhibition of vancomycin (VAN) in VRE *E. faecalis* B3/101, when compared with VAN alone. Interestingly, only emodin (**1a)** produced a synergistic effect with oxacillin (OX) against MRSA *S. aureus* 66/1, increasing the halo of inhibition zone from zero (when treated with OX alone) to 11 mm when tested in combination. These results were also confirmed by determining the MICs of each antibiotic for the respective strain, in the presence of a fixed concentration (the highest concentration that did not inhibit the growth of the three multidrug-resistant strains) of each compound. The combination of CTX with **7c** resulted in a four-fold decrease in the MIC of CTX, i.e. from 256 μg/mL of CTX alone to 64 μg/mL of the combination, when tested against ESBL *E. coli* SA/2. The combination of VAN with emodin (**1a**) resulted in a four-fold decrease (from 512 μg/mL to 128 μg/mL) in MIC of VAN against VRE *E. faecalis* B3/101 when compared to VAN alone. Contrary to what was observed by the disk diffusion method, the combination of OX with emodin (**1a**) against the MRSA *S. aureus* 66/1 did not result in a decrease in the MIC of OX.

3. Conclusions

The culture of the endophytic strain *E. chevalieri* KUFA 0006, isolated from the twig of the mangrove plant *Rhizophora mucronata* Poir., was found to produce different secondary metabolites from those previously reported from the soil-derived strain of *E. chevalieri*. Besides polyhydroxy anthraquinones and diketopiperazine derivatives, which were commonly isolated from other species of *Eurotium*, two new prenylated indole 3-carbaldehydes, a new isochromone derivative and a new anthranilic acid derivative were isolated from this endophytic strain, however, no meroditerpenes were detected. Except for emodin (**1a**), neither of the isolated metabolites exhibited antibacterial activity against the reference strains of Gram-positive (*Staphylococcus aureus* ATCC 25923 and *Enterococcus faecalis* ATCC 29212) and Gram-negative (*Escherichia coli* ATCC 25922 and *Pseudomonas aeruginosa* ATCC 27853) bacteria as well as multidrug-resistant isolates from the environment. Interestingly, some of these compounds have a capacity to inhibit biofilm formation in *S. aureus* ATCC 25923 (Gram-

Table 4
Percentage of biofilm formation for compounds that showed antibiofilm activity, after 24 h incubation.

Compound	Concentration (μg/mL)	Biofilm biomass (% of control)		
		E. coli ATCC 25922	*E. faecalis* ATCC 29212	*S. aureus* ATCC 25923
CTX	0.031	1.0 ± 1.4*** (MIC)	–	–
1a	64	–	–	15.4 ± 20.4* (2XMIC)
1a	32	–	–	21.1 ± 30.2* (MIC)
1a	16	–	–	74.5 ± 2.6* (1/2 MIC)
1b	16	–	39.1 ± 16.0*	60.3 ± 27.9*
1d	64	56.1 ± 14.3*	–	–
1e	64	50.6 ± 17.6*	–	–
2	64	–	–	21.1 ± 11.5**
3	64	23.7 ± 24.8*	–	21.8 ± 18.9*
5	64	57.6 ± 8.1*	–	–
6	64	59.6 ± 16.2*	–	–
7b	64	54.0 ± 17.4*	–	–
8	64	67.1 ± 10.2*	–	–

Data are shown as Mean ± SD of 3 independent experiments. One-sample *t*-test: $^{*}p < 0.05$ and $^{**}p < 0.01$, significantly different from 100%.
MIC, minimum inhibitory concentration.

positive) and *E. coli* ATCC 25922 (Gram-negative). Moreover, all of the tested metabolites also exhibited synergistic association with vancomycin against the multidrug-resistant VRE *E. faecalis* B3/101. In particular, the anthraquinones emodin (**1a**) and physcion (**1b**), and the two new prenylated indole carbaldehydes (**2** and **3**) are found to significantly inhibit the production of biofilm in *S. aureus* ATCC 25923. Additionally, emodin (**1a**) also showed strong synergism with the antibiotic oxacillin against the MRSA *S. aureus* 66/1. Therefore, fungal anthraquinones can represent an interesting group of compounds for further development as arsenal against multidrug-resistant bacteria.

4. Experimental section

4.1. General experimental procedures

Melting points were determined on a Bock monoscope and are uncorrected. Optical rotations were measured on an ADP410 Polarimeter (Bellingham + Stanley Ltd., Tunbridge Wells, Kent, UK). Infrared spectra were recorded in a KBr microplate in a FTIR spectrometer Nicolet iS10 from Thermo Scientific (Waltham, MA, USA) with Smart OMNI-Transmission accessory (Software 188 OMNIC 8.3). ^{1}H and ^{13}C NMR spectra were recorded at ambient temperature on a Bruker AMC instrument (Bruker Biosciences Corporation, Billerica, MA, USA) operating at 300.13 and 75.4 MHz, respectively. High resolution mass spectra were measured with a Waters Xevo QToF mass spectrometer (Waters Corporations, Milford, MA, USA) coupled to a Waters Aquity UPLC system. A Merck (Darmstadt, Germany) silica gel GF_{254} was used for preparative TLC, and a Merck Si gel 60 (0.2–0.5 mm) was used for column chromatography.

4.2. Fungal material

The strain KUFA 0006 was isolated from a healthy twig of *Rhizophora mucronata* Poir., which was collected at Kung Krabaen Bay Royal Development Study Center (altitude 12°311′7.92″ N, 101°54′01.06″E), Chanthaburi Province, Eastern Thailand, in July 2010. The twig was washed with running tap water, air died in a laminar hood, cut into pieces of 1 cm and then sterilized with 70% ethanol for 5 min, followed by sterile distilled water for three times. The surface of sterilized twig was blotted dry on a sterilized filter paper under aseptic condition, and transversely cut to 1–2 mm slices using a sterile razor blade, and then placed in Petri dishes containing potato dextrose agar (PDA) amended with streptomycin sulphate (300 mg/L). The dishes were incubated at room temperature and the mycelia emerged from plant tissues were observed daily. The hyphal tips of the mycelia were then transferred to PDA slants using a sterile needle and maintained as pure culture for further identification. The fungus was identified as *Eurotium chevalieri* L. Mangin (Family Trichocomaceae) on the basis of morphological characteristics such as colony growth rate and growth pattern on standard media, namely Czapek's agar, Czapek yeast autolysate agar and malt extract agar as well as on the microscopic characteristics including size, shape and ornamentation of ascospores observed under light and scanning electron microscopes. The identification was also confirmed by molecular techniques. The internal transcribed spacer (ITS) region of rRNA of the fungus was amplified using ITS primers (ITS 1 and ITS 4) as described previously by us (May Zin et al., 2015). Its gene sequence was deposited at GenBank with the accession number KX431211, and the pure cultures were deposited at Kasetsart University Fungal Collection, Department of Plant Pathology, Faculty of Agriculture, Kasetsart University, Bangkok, Thailand.

4.3. Extraction and isolation

Forty 1000 mL Erlenmeyer flasks, each containing 200 g of cooked white rice and 100 mL of water containing 20% sucrose, were autoclaved at 121 °C for 15 min and then inoculated with ten mycelial plugs of *E. chevalieri* KUFA 0006, and incubated at 28 °C for 40 days. Each flask, containing the moulded rice, was added 500 mL of EtOAc and the content was left to macerate for 7 days and then filtered. The EtOAc solution was concentrated under reduced pressure to yield 79 g of dark brown viscous mass of crude EtOAc extract which was dissolved in 1000 mL of $CHCl_3$, and then washed with H_2O (3 × 500 mL). The organic layers were combined and dried with anhydrous Na_2SO_4, filtered and evaporated under reduced pressure to give 75 g of the crude chloroform extract, which was applied on a column of silica gel (770 g), and eluted with mixtures of petrol-$CHCl_3$ and $CHCl_3$-Me_2CO, wherein 250 mL fractions were collected as follows: Frs 1–450 (petrol-$CHCl_3$, 1:1), 451–518 (petrol-$CHCl_3$, 3:7), 519–726 (petrol-$CHCl_3$, 1:9), 727–1000 ($CHCl_3$-Me_2CO, 9:1), 1001–1192 ($CHCl_3$-Me_2CO, 7:3). Frs 72–85 were combined (605.5 mg) and recrystallized in MeOH to give 27.3 mg of physcion (**1b**)(Anke et al., 1980). Frs 250–294 were combined (919.1 mg) and precipitated in MeOH to give 31.3 mg of palmatic acid. Frs 365–368 were combined (94.3 mg) and precipitated in petroleum ether to give 10.7 mg of 2-(2-methyl-3-en-2-yl)-1*H*-indole-3-carbaldehyde (**2**). Frs 369–398 were combined (453.6 mg) and purified by TLC (Silica gel G_{254}, $CHCl_3$-Me_2CO-HCO_2H 9.5:0.5:0.01) to give 10.6 mg of ergosterol 5, 8-endoperoxide (Cantrell et al., 2001). Frs 652–708 were combined (157.0 mg) and purified by TLC (Silica gel G_{254}, $CHCl_3$-Me_2CO-HCO_2H 9.5:0.5:0.01) to give 25.1 mg of 2-(2, 2-dimethylcyclopropyl)-1*H*-indole-3-carbaldehyde (**3**). Frs 734–738 were combined (166.2 mg) and applied on a Sephadex LH-20 column (10 g) and eluted with MeOH and a mixture with MeOH:CH_2Cl_2 (1:1), wherein 20 mL subfractions (sfrs) were collected as follows: Sfrs 1–56 (MeOH) and 57–68 (MeOH:CH_2Cl_2, 1:1). Sfrs 48–56 were combined (15.0 mg) and purified by TLC (Silica gel G_{254}, $CHCl_3$-Me_2CO-HCO_2H 9.5:0.5:0.01) to give 10.2 mg of emodin (**1a**) (Bao et al., 2013). Frs 756–770 were combined (155.7 mg) and applied on a Sephadex LH-20 column (10 g) and eluted with MeOH, wherein 60 subfractions of 20 mL were collected. Sfrs 42–60 were combined (28.2 mg) and purified by TLC (Silica gel G_{254}, $CHCl_3$-Me_2CO-HCO_2H 9:1:0.01) to give 23.3 mg of questin (**1c**) (Li et al., 2009). Frs 801–815 were combined (371.5 mg) and applied on a Sephadex LH-20 column (10 g) and eluted with MeOH wherein 68 subfractions of 20 mL were collected. Sfrs 34–48 were combined (29.4 mg) and purified by TLC (Silica gel G_{254}, $CHCl_3$-Me_2CO-HCO_2H 9:1:0.01) to give 23.8 mg of acetylquestinol (**1e**). Frs 860–874 were combined (59.8 mg) and purified by TLC (Silica gel G_{254}, $CHCl_3$-Me_2CO-HCO_2H 9:1:0.01) to give 10 mg of 2 [(2, 2-dimethylbut-3-enoyl)amino]benzoic acid (**4**), 10.2 mg of echinulin (**7c**) (Smetanina et al., 2007) and 38.2 mg of neoechinulin E (**7b**) (Li et al., 2008a). Frs 919–945 were combined (439.1 mg) and purified by TLC (Silica gel G_{254} $CHCl_3$-Me_2CO-HCO_2H 9.5:0.5:0.01) to give 10 mg of 6, 8-dihydroxy-3-(2*S*-hydroxypropyl)-7-methyl-1*H*-isochromen-1-one (**5**). Frs 1004–1010 were combined (456.9 mg) and purified by TLC (Silica gel G_{254}, $CHCl_3$-MeOH-HCO_2H 9.5:0.5:0.01) to give 23.3 mg of questinol (**1d**) (Bao et al., 2013). Frs 1032–1049 were combined (1.34 g) and applied on a Sephadex LH-20 column (10 g) and eluted with MeOH: CH_2Cl_2 (1:1), wherein 73 subfractions of 20 mL were collected. Sfrs 29–42 were combined (84.4 mg) and purified by TLC (Silica gel G_{254}, $CHCl_3$-MeOH-HCO_2H 9.5:0.5:0.01) to give 11.9 mg of eurocristatine (**8**) (Gomes et al., 2012), 15.1 mg of preechinulin (**7a**) (Aoki et al., 2010) and 20.3 mg of (11*S*, 14*R*) - 3-(1*H*-indol-3ylmethyl) 6-isopropyl-2, 5-piperazinedione (**6**).

Acetylquestinol (**1e**). Yellow crystal; mp 101–103 °C; IR (KBr) υ_{max} 3442, 2922, 1749, 1631, 1588, 1466, 1379, 1352, 1264 cm^{-1}; ^1H NMR (DMSO, 300.13 MHz): 13.38, brs (OH-1), 7.54, d (J = 1.5 Hz; H-4), 7.24, d (J = 1.5 Hz; H-2), 7.17, d (J = 2.2 Hz; H-5), 6.81, d (J = 2.2 Hz; H-7), 5.15, s (H_2-11), 3.89, s (OMe), 2.13, s (CH_3, OAc); ^{13}C NMR (DMSO, 75.4 MHz): 186.0 (C-9), 182.2 (C-10), 170.2 (CO, OAc), 163.6 (C-8), 161.7 (C-1), 161.1 (C-6), 144.2 (C-3), 136.7 (C-10a), 132.5 (C-4a), 122.3 (C-2), 116.0 (C-9a), 111.8 (C-8a), 107.5 (C-5), 105.3 (C-7), 64.3 (C-11), 56.3 (OMe), 20.6 (CH_3, OAc); (+)-HRESIMS m/z 343.0814 $[M+H]^+$ (calcd for $C_{18}H_{15}O_7$, 343.0818).

2-(2-Methyl-3-en-2-yl)-1*H*-indole-3-carbaldehyde (**2**). Yellow crystal; mp 162-164 °C; IR (KBr) υ_{max} 3242, 2972, 2928, 1735, 1622, 1583, 1453, 1381, 1274 cm^{-1}; For ^1H and ^{13}C spectroscopic data ($CDCl_3$, 300.13 and 75.4 MHz), see Table 1; (+)-HRESIMS m/z 214.1236 $[M+H]^+$ (calcd for $C_{14}H_{16}NO$, 214.1232).

2-(2, 2-Dimethylcyclopropyl)-1*H*-indole-3-carbaldehyde (**3**). Yellow viscous liquid. $[\alpha]^{20}_D$ + 68 (*c* 0.04, $CHCl_3$); IR (KBr) υ_{max} 3252, 2923, 1768, 1633, 1583, 1558, 1463, 1376, 1239; For ^1H and ^{13}C spectroscopic data ($CDCl_3$, 300.13 and 75. MHz), see Table 1; (+)-HRESIMS m/z 214.1239 $[M+H]^+$ (calcd for $C_{14}H_{16}NO$, 214.1232).

2[(2, 2-Dimethylbut-3-enoyl)amino]benzoic acid (**4**). Yellow viscous liquid. IR (KBr) υ_{max} 3421, 3253, 2927, 1696, 1670, 1636, 1606, 1586, 1522, 1448, 1385, 1295, 1259 cm^{-1}; For ^1H and ^{13}C spectroscopic data (DMSO, 300.13 and 75.4 MHz), see Table 2; (+)-HRESIMS m/z 234.1132 $[M+H]^+$ (calcd for $C_{13}H_{16}NO_3$, 234.1130).

6, 8-Dihydroxy-3-(2*S*-hydroxypropyl)-7-methyl-1H-isochromen-1-one (**5**). Yellow viscous liquid. $[\alpha]^{20}_D$ - 88 (*c* 0.07, Me_2CO); IR (KBr) υ_{max} 3443, 2921, 2254, 1671, 1623, 1540, 1507, 1455 cm^{-1}; For ^1H and ^{13}C spectroscopic data (DMSO, 300.13 and 75.4 MHz), see Table 2; (+)-HRESIMS m/z 251.0900 $[M+H]^+$ (calcd for $C_{13}H_{15}O_5$, 251.0919).

(11S, 14R) - 3-(1*H*-indol-3-yllmethyl)-6-isopropyl-2, 5-piperazinedione (**6**). White crystal; mp 270-271 °C; $[\alpha]^{20}_D$ - 187 (*c* 0.02, Me_2CO); ^1H NMR (DMSO, 300.13 MHz): 10.88, brs (NH-1), 8.03, brs (NH-16), 7.86, brs (NH-13), 7.60, d (J = 7.5 Hz; H-4), 7.32, d (J = 7.5 Hz; H-7), 7.08, d (J = 2.3 Hz, H-2), 7.04, ddd (J = 7.5, 7.5, 1.0 Hz; H-6), 6.95, ddd (J = 7.5, 7.5, 1.0 Hz; H-5), 4.13, brt (J = 3.9 Hz, H-11), 3.27, dd (J = 14.5, 4.4 Hz, H-10a), 3.04, m (2H, H-10b, 14), 2.03, m (H-17), 0.82, d (J = 7.1, H_3-19), 0.77, d (J = 6.8, H_3-18). ^{13}C NMR (DMSO, 75.4 MHz): 168.1 (CO-12), 167.1 (CO-15), 135.8 (C-8), 127.7 (C-9), 124.5 (C-2), 120.8 (C-6), 118.9 (C-4), 118.3 (C-5), 111.1 (C-7), 108.5 (C-3), 59.1 (C-14), 54.7 (C-11), 31.5 (C-17), 28.4 (C-10), 18.2 (Me-18), 16.6 (Me-19). (+)-HRESIMS m/z 286.1575 $[M+H]^+$ (calcd for $C_{16}H_{20}N_3O_2$, 286.1556).

4.4. Electronic circular dichroism (ECD)

ECD spectra were obtained in a Jasco J-815 CD spectropolarimeter with a 1 mm cuvette; Savitsky-Golay noise reduction was applied when necessary. Dihedral driver and MM2 minimizations were done in Chem3D Ultra (Perkin-Elmer Inc.). All other minimizations and spectral calculations were performed with Gaussian (Gaussian Inc.) at the APFD/6-311 + G(2d,p) level (Austin et al., 2012) with IEFPCM solvation model. The simulated spectral lines were obtained by summation of Gaussian curves, as recommended in Stephens and Harada (2010). ECD spectra for all conformations were added using Boltzmann weights derived from its minimal energies (Mori et al., 2006).

4.5. X-ray crystal structure of **1e** and **6**

Diffraction data were collected at 293 K with a Gemini PX Ultra equipped with CuK_α radiation (λ = 1.54184 Å). The structures were solved by direct methods using SHELXS-97 and refined with SHELXL-97 (Sheldrick, 2008). Carbon, nitrogen and oxygen atoms were refined anisotropically. Hydrogen atoms were directly found from difference Fourier maps and were refined freely with isotropic displacement parameters. Full details of the data collection and refinement and tables of atomic coordinates, bond lengths and angles, and torsion angles have been deposited with the Cambridge Crystallographic Data Center.

Acetylquestinol (**1e**). Crystals were monoclinic, space group $P2_1/c$, cell volume 1470.45(19) $Å^3$ and unit cell dimensions a = 4.4939(3) Å, b = 29.533(2) Å and c = 11.0898(9) Å and angle β = 92.503(7)° (uncertainties in parentheses). The refinement converged to R (all data) = 7.65% and wR_2 (all data) = 14.76%. CCDC 1532709.

(11*S*, 14*R*)-cyclo(tryptophylvalyl) (**6**). Crystals were monoclinic, space group $P2_1$, cell volume 748.51(4) $Å^3$ and unit cell dimensions a = 6.10326(16) Å, b = 13.4265(4) Å and c = 9.4770(3)Å angle β = 105.457(3)°. The refinement converged to R (all data) = 3.32% and wR_2 (all data) = 8.01%. The flack x parameter was refined with SHELXL-97 to yield 0.1(3). CCDC 1532719.

4.6. Antibacterial activity bioassays

4.6.1. Bacterial strains and growth conditions

Two Gram-positive (*Staphylococcus aureus* ATCC 25923 and *Enterococcus faecalis* ATCC 29212) and two Gram-negative (*Escherichia coli* ATCC 25922 and *Pseudomonas aeruginosa* ATCC 27853) reference strains were used. Multidrug-resistant bacterial strains isolated from public buses (MRSA *S. aureus* 66/1) (Simões et al., 2011), river water (VRE *E. faecalis* B3/101) (Bessa et al., 2014), and a clinical isolate (ESBL *E. coli* SA/2) were also used. Frozen stocks of all strains were grown in Mueller-Hinton agar (MH-BioKar diagnostics, Allone, France) at 37 °C. Bacteria were subcultured in MH agar and incubated overnight at 37 °C in order to obtain fresh cultures for each assay.

4.6.2. Antimicrobial susceptibility testing

The minimum inhibitory concentration (MIC) for each compound was determined by the broth microdilution method according to the recommendations of the Clinical and Laboratory Standards Institute (CLSI) (CLSI, 2015). With the exception of **1b**, 10 mg/mL stock solutions of each compound were prepared in dimethylsulfoxide (DMSO- Applichem GmbH, Darmstadt, Germany). For **1b** (which was less soluble in DMSO than the other compounds), a stock solution of 1 mg/mL was prepared. Two-fold serial dilutions of concentrated stock solutions were prepared in Mueller-Hinton broth 2 (MHB2-Sigma-Aldrich, St. Louis, MO, USA). The range of concentrations tested was 0.016–16 μg/mL in the case of **1b**, and 0.062–64 μg/mL for all other compounds. The highest concentration tested was chosen in order to maintain DMSO in-test concentration below 1%, as recommended by the CLSI (CLSI, 2015). At this concentration, DMSO did not affect the bacterial growth. Cefotaxime (CTX), ranging from 0.031 to 16 μg/mL, was used as a control. Purity check and colony counts of the inoculum suspensions were also evaluated in order to ensure that the final inoculum density closely approximates the intended number (5×10^5 CFU/mL). The MIC was determined as the lowest concentration at which no visible growth was observed. The minimum bactericidal concentration (MBC) was assessed by spreading 10 μL of culture collected from wells showing no visible growth on MH agar plates. The MBC was determined as the lowest concentration at which no colonies grew after 16–18 h incubation at 37 °C. These assays were performed in duplicate.

4.6.3. Biofilm formation inhibition assay

The effect of all compounds on biofilm formation was evaluated

using crystal violet staining as described previously (Gomes et al., 2014). Briefly, the highest concentration tested in the MIC assay was added to bacterial suspensions of 1×10^6 CFU/mL prepared in Tryptic Soy broth (TSB-BioKar diagnostics, Allonne, France). When it was possible to determine a MIC, three concentrations were tested: 2 x MIC, MIC, and ½ x MIC. A control without any compound as well as a negative control (TSB alone) were included. CTX was used as a positive control. The stabilized biofilm mass was quantified after 24 h incubation at 37 °C. The samples were quantified calorimetrically at 595 nm on an iMark™ microplate spectrophotometer (Bio-Rad Laboratories, Hercules, CA, USA). The background absorbance (TSB without inoculum) was subtracted from the absorbance of each sample and the data are presented as percentage of control. Three independent experiments were performed in triplicate for each experimental condition.

4.6.4. Antibiotic synergy testing

In order to evaluate the combined effect of the compounds and clinically relevant antimicrobial drugs, a screening was conducted using the disk diffusion method, as described previously (Gomes et al., 2014; Bessa et al., 2015). A set of antibiotic disks (Oxoid, Basingstoke, UK) to which the isolates were resistant was selected: cefotaxime (CTX, 30 μg) for *E. coli* SA/2, oxacillin (OX, 1 μg) for *S. aureus* 66/1, and vancomycin (VAN, 30 μg) for *E. faecalis* B3/101. Antibiotic disks alone (controls) and antibiotic disks impregnated with 15 μg of each compound were placed on MH agar plates seeded with the respective bacteria. Sterile 6 mm blank paper disks (Oxoid, Basingstoke, UK) impregnated with 15 μg of each compound alone were also tested. A blank disk with DMSO was used as a negative control. MH inoculated plates were incubated for 18–20 h at 37 °C. Potential synergism was recorded when the halo of the antibiotic disk impregnated with a compound was greater than the halo of the antibiotic or compound-impregnated blank disk alone.

The potential synergy between the compounds and clinically relevant antibiotics was also evaluated by determining the antibiotic MIC in the presence of each compound. Briefly, MIC of CTX, OX and VAN (Sigma-Aldrich, St. Louis, MO, USA) for the respective multidrug-resistant strains was determined in the presence of the highest concentration of each compound tested that did not affect bacterial growth when the compound was tested alone. The antibiotic tested was serially diluted whereas the concentration of each compound was fixed. In the case of **1b**, the concentration used was 16 μg/mL. For all other compounds the concentration used was 64 μg/mL. Antibiotic MICs were determined as described above.

Conflicts of interest

The authors declare no conflict of interest.

Acknowledgements

This work was partially supported by national funds provided by FCT- Foundation for Science and Technology and European Regional Development Fund (ERDF) and COMPETE, under the projects PEst-C/MAR/LA0015/2013, PTDC/MAR-BIO/4694/2014 as well as by the project INNOVMAR - Innovation and Sustainability in the Management and Exploitation of Marine Resources (reference NORTE-01-0145-FEDER-000035, within Research Line NOVELMAR/INSEA-FOOD/ECOSERVICES), supported by North Portugal Regional Operational Programme (NORTE 2020), under the PORTUGAL 2020 Partnership Agreement, through the European Regional Development Fund (ERDF)". W. W. May Zin thanks the Lotus Unlimited Project under the ERASMUS MUNDUS ACTION 2-EU-Asia Mobility Project for a PhD's scholarship. We thank Mrs. Júlia Bessa and Ms. Sara Cravo for technical support.

Appendix A. Supplementary data

Supplementary data related to this article can be found at http://dx.doi.org/10.1016/j.phytochem.2017.05.015.

References

Almeida, A.P., Dethoup, T., Singburaudom, N., Lima, R., Vasconcelos, M.H., Pinto, M., Kijjoa, A., 2010. The *in vitro* anticancer activity of the crude extract of the sponge-associated fungus *Eurotium cristanum* and its secondary metabolites. J. Nat. Pharm. 1, 25–29.

Anke, H., Kolthoum, I., Zähner, H., Laatsch, H., 1980. Metabolic products of microorganisms 185. The anthraquinones of the *Aspergillus glaucus* group. I. Occurrence, isolation, identification and antimicrobial activity. Arch. Microbiol. 126, 223–230.

Aoki, Toshiaki, Ohnishi, Kensuke, Kimoto, Masaaki, Fujieda, Satoshi, Kuramochi, Kouji, Takeuchi, Toshifumi, Nakazaki, Atsuo, Watanabe, Nobuo, Sugawara, Fumio, Arai, Takao, Kobayashi, Susumu, 2010. Synthesis and neuroprotective action of optically pure neoechinulin a and its analogs. Pharmaceuticals 3 (4), 1063–1069.

Austin, Amy, Petersson, George A., Frisch, Michael J., Dobek, Frank J., Scalmani, Giovanni, Throssell, Kyle, 2012. A density functional with spherical atom dispersion terms. J. Chem. Theory Comput. 8 (12), 4989–5007.

Bao, Jie, Sun, Yu-Lin, Zhang, Xiao-Yong, Han, Zhuang, Gao, Hai-Chun, He, Fei, Qian, Pei-Yuan, Qi, Shu-Hua, 2013. Antifouling and antibacterial polyketides from marine gorgonian coral-associated fungus Penicillium sp. SCSGAF 0023. J. Antibiot. 66 (4), 219–223.

Bessa, L.J., Barbosa-Vasconcelos, A., Mendes, A., Vaz-Pires, P., Martins da Costa, P., 2014. High prevalence of multidrug-resistant *Escherichia coli* and *Enterococcus* spp. in river water, upstream and downstream of a wastewater treatment plant. J. Water Health 12, 426–435.

Bessa, L.J., Palmeira, A., Gomes, A.S., Vasconcelos, V., Sousa, E., Pinto, M., Martins da Costa, P., 2015. Synergistic effects between thioxanthones and oxacillin against methicillin-resistant *Staphylococcus aureus*. Microb. Drug Resist 21, 404–415.

Blunt, J.W., Munro, M.H.G., 2007. Dictionary of Marine Natural Products with CD-ROM. Chapman and Hall/CRC, p. C-1080.

Cantrell, C.L., Franzblau, S.G., Fischer, N.H., 2001. Antimycobacterial plant terpenoids. Planta Med. 67, 685–694.

Clinical and laboratory Standards Institute, 2015. Methods for Dilution Antimicrobial Susceptibility Tests for Bacteria that Grow Aerobically. Approved Standard -10th ed. Document M07–A10.CLSI, Wayne, PA, USA.

Debbab, Abdessamad, Aly, Amal H., Proksch, Peter, 2013. Mangrove derived fungal endophytes – a chemical and biological perception. Fungal Divers. 61 (1), 1–27.

Fouillaud, M., Venkatachalam, M., Girard-Valenciennes, E., Caro, Y., Dufossé, L., 2016. Anthraquinones and derivatives from marine-derived fungi: structural diversity and selected biological activities. Mar. Drugs 14, 64. http://dx.doi.org/10.3390/md14040064.

Gomes, N.M., Dethoup, T., Singburaudom, N., Gales, L., Silva, A.M.S., Kijjoa, A., 2012. Eurocristatine, a new diketopiperazine dimer from the marine sponge-associated fungus *Eurotium cristatum*. Phytochem. Lett. 5, 717–720.

Gomes, N.M., Bessa, L.J., Buttachon, S., Costa, P.M., Buaruang, J., Dethoup, T., Silva, A.M.S., Kijjoa, A., 2014. Antibacterial and antibiofilm activities of tryptoquivalines and meroditerpenes isolated from the marine-derived fungi *Neosartorya paulistensis*, *N. laciniosa*, *N. tsunodae*, and the soil fungi *N. fischeri* and *N. siamensis*. Mar. Drugs 12, 822–839.

Kanokmedhakul, K., Kanokmedhakul, S., Suwannatrai, R., Soytong, K., Prabpai, S., Kongsaeree, P., 2011. Bioactive meroterpenoids and alkaloids from the fungus *Eurotium chevalieri*. Tetrahedron 67, 5461–5468.

Li, D.L., Li, X.M., Li, T.G., Dang, H.Y., Wang, B.G., 2008a. Dioxopiperazine alkaloids produced by the marine mangrove derived endophytic fungus *Eurotium rubrum*. Helv. Chim. Acta 91, 1888–1893.

Li, D.L., Li, X.M., Li, T.G., Dang, H.Y., Proksch, P., Wang, B.G., 2008b. Benzaldehyde derivatives from *Eurotium rubrum*, an endophytic fungus derived from the mangrove plant *Hibiscus tiliaceus*. Chem. Pharm. Bull. 56, 1282–1285.

Li, D.L., Li, X.M., Wang, B.G., 2009. Natural anthraquinone derivatives from a marine mangrove plant-derived endophytic fungus *Eurotium rubrum*: structural elucidation and DPPH radical scavenging activity. J. Microbiol. Biotechnol. 19, 675–680.

Li, Sh-M., 2010. Prenylated indole derivatives from fungi: structure diversity, biological activities, biosynthesis and chemoenzymatic synthesis. Nat. Prod. Rep. 27, 57–78.

May Zin, W.W., Buttachon, S., Buaruang, J., Gales, L., Pereira, J.A., Pinto, M.M.M., Silva, A.M.S., Kijjoa, A., 2015. A new Meroditerpene and a aew tryptoquivaline analog from the algicolous fungus *Neosartorya takakii* KUFC 7898. Mar. Drugs 13, 3776–3790.

Mori, Tadashi, Inoue, Yoshihisa, Grimme, Stefan, 2006. Time dependent density functional theory calculations for electronic circular dichroism spectra and optical rotations of conformationally flexible chiral Donor–Acceptor dyad. J. Org. Chem. 71 (26), 9797–9806.

Sheldrick, G.M., 2008. A short history of SHELX. Acta Cryst. A64, 112–122.

Simões, Roméo Rocha, Aires-de-Sousa, Marta, Conceição, Teresa, Antunes, Filipa, da Costa, Paulo Martins, de Lencastre, Hermínia, 2011. High prevalence of EMRSA-15 in Portuguese public buses: a worrisome finding. PLoS ONE 6 (3), e17630.
Smetanina, O.F., Kalinovskii, A.I., Khudyakova, Y.V., Slinkina, N.N., Pivkin, M.V., Kuznetsova, T.A., 2007. Metabolites from the marine fungus *Eurotium repens*. Chem. Nat. Compd. 43, 395–398.
Stephens, P.J., Harada, N., 2010. ECD Cotton effect approximated by the Gaussian curve and other methods. Chirality 22, 229–233.
Yang, Xiudong, Kang, Min-Cheol, Li, Yong, Kim, Eun-A., Kang, Sung-Myung, Jeon, You-Jin, 2014. Anti-inflammatory activity of questinol isolated from marine-derived fungus Eurotium amstelodami in lipopolysaccharide-stimulated RAW 264.7 macrophages. J. Microbiol. Biotechnol. 24 (10), 1346–1353.